

Handbook of Experimental Pharmacology 190

Eric Beitz
Editor

Aquaporins



Springer

Handbook of Experimental Pharmacology

Volume 190

Editor-in-Chief

F. Hofmann, München

Editorial Board

J. Beavo, Seattle, WA

A. Busch, Berlin

D. Ganten, Berlin

J.-A. Karlsson, Singapore

M. Michel, Amsterdam

C.P. Page, London

W. Rosenthal, Berlin

Eric Beitz
Editor

Aquaporins

Contributors

P. Agre, J.C. Atkinson, B. Baum, D. Becker, E. Beitz, S. Beulshausen, H. Bhattacharjee, F. Bonté, M. Boury-Jamot, J.S. Brahim, J.M. Carbrey, A. Chepelinsky, C. Conrad, A.P. Cotrim, J. Daraspe, B. de Groot, C. Delporte, M. Dumas, A. Engel, R.A. Fenton, S. Flitsch, N. Fricke, J. Frøkiær, Y. Fujiyoshi, T. Funahashi, A. Geadkaew, C.M. Goldsmith, H. Grubmüller, R. Haddoub, T. Hibuse, J.S. Hub, G.G. Illei, K. Ishibashi, E. Klussmann, D. Krenc, T.-H. Kwon, T. Litman, S. Liu, N. Maeda, G. Manley, L. McCullagh, H.B. Møller, R. Mukhopadhyay, P.I. Nedvetsky, J. Nielsen, S. Nielsen, N. Nikolov, E. Perrier, A. Robin, B.P. Rosen, W. Rosenthal, M. Rützler, S. Sasaki, S. Schnebert, R. Søggaard, E. Sohara, J. Song, S. Stiver, D. Taguchi, T. Takeda, G. Tamma, R.J. Turner, S. Uchida, G. Valenti, J.-M. Verbavatz, A.S. Verkman, J. von Bülow, T. Walz, V. Wang, D. Wree, B. Wu, M. Yasui, Z. Zador, T. Zeuthen, C. Zheng

Editor

Prof. Dr. Eric Beitz
Universität Kiel
Pharmazeutisches Inst.
Gutenbergstr. 76
24118 Kiel
Germany
ebeitz@pharmazie.uni-kiel.de

ISBN 978-3-540-79884-2 e-ISBN 978-3-540-79885-9

Handbook of Experimental Pharmacology ISSN 0171-2004

Library of Congress Control Number: 2008932921

© 2009 Springer-Verlag Berlin Heidelberg

This work is subject to copyright. All rights are reserved, whether the whole or part of the material is concerned, specifically the rights of translation, reprinting, reuse of illustrations, recitation, broadcasting, reproduction on microfilm or in any other way, and storage in data banks. Duplication of this publication or parts thereof is permitted only under the provisions of the German Copyright Law of September 9, 1965, in its current version, and permission for use must always be obtained from Springer. Violations are liable to prosecution under the German Copyright Law.

The use of general descriptive names, registered names, trademarks, etc. in this publication does not imply, even in the absence of a specific statement, that such names are exempt from the relevant protective laws and regulations and therefore free for general use.

Product liability: The publisher cannot guarantee the accuracy of any information about dosage and application contained in this book. In every individual case the user must check such information by consulting the relevant literature.

Cover Design: WMXDesign GmbH, Heidelberg

Printed on acid-free paper

springer.com

Preface

Sophisticated fluid regulation systems are in place in mammalian organism to maintain basic vital and sensory functions. Such systems control body water homeostasis on a large scale that requires daily filtration and reabsorption of 180 l of fluid from the blood. At the same time, the volume and ional composition of fluids in compartments as tiny as the 40 μ l endolymphatic space of the sensory inner ear are meticulously adjusted. Despite early evidence for an inhabitable channel protein that facilitates water permeation at higher rates and with lower activation energy than the plain lipid bilayer, it was not before 1992 that water conductance of an aquaporin (AQP) was demonstrated by Peter Agre. Subsequently, in 2003, Peter Agre was awarded the Nobel Prize in Chemistry for the discovery of the aquaporins. Aquaporins constitute a large and ancient family comprising all kingdoms of life; 13 isoforms are expressed in mammals, i.e. AQP0–AQP12. Besides water-specific, orthodox aquaporins, there are aquaporins with a wider spectrum of permeants, such as glycerol, urea, and ammonia, the so-called aquaglyceroporins. Aquaporins strictly exclude the passage of ions including protons, with the remarkable exception of AQP6, which is permeated by nitrite, chloride, and other anions. Aquaporin expression is found throughout the body but follows a distinct tissue-specific and subcellular pattern with a high concentration in the kidney and in red blood cells. Malfunctions of aquaporins are associated with diseases such as nephrogenic diabetes insipidus and Sjögren's syndrome. Aquaporin water and solute permeability has been further implicated in lung and brain edema, obesity, tumor angiogenesis, and wound healing, to name just a few.

The aquaporin field has matured at an exceptionally fast pace and we are at the verge of developing serious strategies to therapeutically modulate aquaporin function directly or via regulatory networks. Key prerequisites are available today (1) a considerable (and growing) number of aquaporin crystal structures for the rational design of inhibitory molecules, (2) elaborate molecular dynamics simulation techniques for theoretical analyses of selectivity mechanisms and docking experiments, (3) comprehensive data on aquaporin immunohistochemistry, (4) aquaporin knock-out animals for physiological studies, and (5) assay systems for compound library screenings. The structure of this volume on aquaporins follows the points laid out

above and thus covers the developments from basic research to potential pharmacological use. Situated between pharmacology textbooks and recent scientific papers, this book provides a timely overview for readers from the fundamental as well as the applied disciplines.

I am grateful to more than 70 colleagues for their positive response to my inquiry and for the contribution of excellent chapters. All the chapters in this volume have been reviewed by leaders in the respective fields. They have taken great care to provide the latest information in a comprehensive and appealing manner, as illustrated by the large number of high-quality figures. Please note that the electronic version of the book contains colored figures. It is a special honor that Nobel Laureate Peter Agre has contributed the introduction – together with Jennifer M. Carbrey – outlining the history, current status, and future potential of aquaporin research. I cannot close without acknowledging and thanking our Desk Editor, Susanne Dathe. She has been an indispensable driving-force behind the project.

Kiel, Germany

Eric Beitz

Contents

Introduction	1
Discovery of the Aquaporins and Development of the Field	3
Jennifer M. Carbrey and Peter Agre	
Part I Aquaporin Protein Structure and Selectivity Mechanisms	
The AQP Structure and Functional Implications	31
Thomas Wspalz, Yoshinori Fujiyoshi, and Andreas Engel	
Dynamics and Energetics of Permeation Through Aquaporins. What do we Learn from Molecular Dynamics Simulations?	57
Jochen S. Hub, Helmut Grubmüller, and Bert L. de Groot	
In Vitro Analysis and Modification of Aquaporin Pore Selectivity	77
Eric Beitz, Dana Becker, Julia von Bülow, Christina Conrad, Nadine Fricke, Amornrat Geadkaew, Dawid Krenc, Jie Song, Dorothea Wree, and Binghua Wu	
Part II Aquaporin Function in Mammalian Water Homeostasis	
Aquaporins in the Kidney	95
Tae-Hwan Kwon, Jakob Nielsen, Hanne B. Møller, Robert A. Fenton, Søren Nielsen, and Jørgen Frøkiær	
Regulation of Aquaporin-2 Trafficking	133
Pavel I. Nedvetsky, Grazia Tamma, Sven Beulshausen, Giovanna Valenti, Walter Rosenthal, and Enno Klussmann	
Role of Aquaporin-4 in Cerebral Edema and Stroke	159
Zsolt Zador, Shirley Stiver, Vincent Wang, and Geoffrey T. Manley	

Aquaporins as Potential Drug Targets for Meniere’s Disease and its Related Diseases	171
Taizo Takeda and Daizo Taguchi	
Aquaporins in Secretory Glands and their Role in Sjögren’s Syndrome ..	185
Christine Delporte	
Part III Aquaporin Glycerol Permeability in Mammalian Physiology	
Skin Aquaporins: Function in Hydration, Wound Healing, and Skin Epidermis Homeostasis	205
Mathieu Boury-Jamot, Jean Daraspe, Frédéric Bonté, Eric Perrier, Sylvianne Schnebert, Marc Dumas, and Jean-Marc Verbavatz	
Function of Aquaporin-7 in the Kidney and the Male Reproductive System	219
Eisei Sohara, Shinichi Uchida, and Sei Sasaki	
Role of Aquaporin-7 and Aquaporin-9 in Glycerol Metabolism; Involvement in Obesity	233
Norikazu Maeda, Toshiyuki Hibuse, and Tohru Funahashi	
New Members of Mammalian Aquaporins: AQP10–AQP12	251
Kenichi Ishibashi	
Part IV Aquaporin Functions Apart from Water and Glycerol Transport	
Structural Function of MIP/Aquaporin 0 in the Eye Lens; Genetic Defects Lead to Congenital Inherited Cataracts	265
Ana B. Chepelinsky	
pH Regulated Anion Permeability of Aquaporin-6	299
Masato Yasui	
Aquaglyceroporins and Metalloid Transport: Implications in Human Diseases	309
Hiranmoy Bhattacharjee, Barry P. Rosen, and Rita Mukhopadhyay	
Ammonia and Urea Permeability of Mammalian Aquaporins	327
Thomas Litman, Rikke Sjøgaard, and Thomas Zeuthen	
Knock-Out Models Reveal New Aquaporin Functions	359
Alan S. Verkman	
Part V Towards Therapeutic Use of Aquaporins	
Design, Synthesis and Assaying of Potential Aquaporin Inhibitors	385
Rose Haddoub, Michael Rützler, Aélig Robin, and Sabine L. Flitsch	

Aquaporin-1 Gene Transfer to Correct Radiation-Induced Salivary Hypofunction 403
Bruce J. Baum, Changyu Zheng, Ana P. Cotrim, Linda McCullagh,
Corinne M. Goldsmith, Jaime S. Brahim, Jane C. Atkinson, R. James Turner,
Shuying Liu, Nikolay Nikolov, and Gabor G. Illei

Index 419

Contributors

Peter Agre Department of Molecular Microbiology and Immunology, Johns Hopkins Malaria Research Institute, Johns Hopkins Bloomberg School of Public Health, Room E5146, 615 North Wolfe Street, Baltimore, MD 21205, pagre@jhsph.edu

Jane C. Atkinson Molecular Physiology and Therapeutics Branch and Clinical Research Core, National Institute of Dental and Craniofacial Research, NIH, Bethesda, MD 20892, USA

Bruce Baum Building 10, Room 1N113, MSC-1190, GTTB/NIDCR/NIH, 10 Center Drive, Bethesda, MD 20892-1190, USA, bbaum@dir.nidcr.nih.gov

Dana Becker Department of Pharmaceutical Chemistry, University of Kiel, Gutenbergstrasse 76, 24118 Kiel, Germany

Eric Beitz Pharmaceutical Chemistry, University of Kiel, Gutenbergstrasse 76, 24118 Kiel, Germany, ebeitz@pharmazie.uni-kiel.de

Sven Beulshausen Leibniz-Institut für Molekulare Pharmakologie (FMP), Campus Berlin-Buch, 13125 Berlin, Germany

Hiranmoy Bhattacharjee Department of Biochemistry and Molecular Biology, Wayne State University, School of Medicine, Detroit, MI 48201, USA

Frédéric Bonté LVMH-Recherche, F-45800 St Jean de Braye, France

Mathieu Boury-Jamot IBITEC-S and CNRS URA 2096, CEA-Saclay F-91191 Gif-sur-Yvette and LRA17V, University Paris-Sud 11, F-91400 Orsay, France

Jaime S. Brahim Molecular Physiology and Therapeutics Branch and Clinical Research Core, National Institute of Dental and Craniofacial Research, NIH, Bethesda, MD 20892, USA

Jennifer M. Carbrey Department of Cell Biology, Duke University School of Medicine, DUMC Box 102143, Durham, NC 27710, USA

Ana Chepelinsky Laboratory of Molecular and Developmental Biology, National Eye Institute, National Institutes of Health, 7 Memorial Drive, MSC 0704, Building 7, Room 105, Bethesda, MD 20892-0704, USA, abc@helix.nih.gov

Christina Conrad Department of Pharmaceutical Chemistry, University of Kiel, Gutenbergstrasse 76, 24118 Kiel, Germany

Ana P. Cotrim Molecular Physiology and Therapeutics Branch and Clinical Research Core, National Institute of Dental and Craniofacial Research, NIH, Bethesda, MD 20892, USA

Jean Daraspe IBITEC-S and CNRS URA 2096, CEA-Saclay F-91191 Gif-sur-Yvette and LRA17V, University Paris-Sud 11, 91400 Orsay, France

Bert de Groot Max Planck Institute for Biophysical Chemistry, Computational Biomolecular Dynamics Group, Am Fassberg 11, 37077 Göttingen, Germany, bgroot@gwdg.de

Christine Delporte Laboratory of Biological Chemistry and Nutrition, Bat G/E, CP611, Université Libre de Bruxelles, 808 Route de Lennik, 1070 Brussels, Belgium, cdelport@ulb.ac.be

Marc Dumas LVMH-Recherche, F-45800 St Jean de Braye, France

Andreas Engel Maurice E. Müller Institute for Microscopy, Biozentrum, University of Basel, Klingelbergstrasse 50/70, 4056 Basel, Switzerland, andreas.engel@unibas.ch

Robert A. Fenton Water and Salt Research Center, Institute of Anatomy, University of Aarhus, 8000 Aarhus C, Denmark
Department of Biochemistry and Cell Biology, School of Medicine, Kyungpook National University, Taegu 700-422, Korea

Sabine Flitsch School of Chemistry, Manchester Interdisciplinary Biocentre (MIB), 131 Princess Street, Manchester M1 7DN, UK, sabine.flitsch@manchester.ac.uk

Nadine Fricke Department of Pharmaceutical Chemistry, University of Kiel, Gutenbergstrasse 76, 24118 Kiel, Germany

Jørgen Frøkiær Water and Salt Research Center, Institute of Anatomy, University of Aarhus, 8000 Aarhus C, Denmark
Department of Biochemistry and Cell Biology, School of Medicine, Kyungpook National University, Taegu 700-422, Korea

Y. Fujiyoshi Department of Biophysics, Kyoto University, Oiwake, Kitashirakawa, Sakyo-ku, Kyoto 606-8502, Japan

Tohru Funahashi Department of Metabolic Medicine, Graduate School of Medicine, Osaka University, 2-2-B5 Yamada-oka, Suita, Osaka 565-0871, Japan

Amornrat Geadkaew Department of Pharmaceutical Chemistry,
University of Kiel, Gutenbergstrasse 76, 24118 Kiel, Germany

Corinne M. Goldsmith Molecular Physiology and Therapeutics Branch and
Clinical Research Core, National Institute of Dental and Craniofacial Research,
NIH, Bethesda, MD 20892, USA

Helmut Grubmüller Department of Theoretical and Computational Biophysics,
Max-Planck-Institute for Biophysical Chemistry, Am Fassberg 11,
37077 Göttingen, Germany

R. Haddoub Manchester Interdisciplinary Biocentre (MIB) & The School of
Chemistry, University of Manchester, 131 Princess Street, M1 7DN
Manchester, UK

Toshiyuki Hibuse Department of Metabolic Medicine, Graduate School of
Medicine, Osaka University, 2-2-B5 Yamada-oka, Suita, Osaka 565-0871, Japan

Jochen S. Hub Computational Biomolecular Dynamics Group,
Max-Planck-Institute for Biophysical Chemistry, Am Fassberg 11, 37077
Göttingen, Germany

Gabor G. Illei Molecular Physiology and Therapeutics Branch and Clinical
Research Core, National Institute of Dental and Craniofacial Research, NIH,
Bethesda, MD 20892, USA

Kenichi Ishibashi Molecular Biology, Clinical research Center, Chiba-east
Hospital, 673 Nitona, Chuuo-ku, Chiba 260-8712, Japan,
kishiba@nitona.hosp.go.jp
Department of Medical Physiology, Meiji Pharmaceutical University, 2-522-1
Noshio, Kiyose, Tokyo 204-8588 Japan, kishiba@my-pharm.ac.jp

Enno Klussmann Leibniz-Institut für Molekulare Pharmakologie,
Robert-Rössle-Str. 10, 13125 Berlin, Germany, klussmann@fmp-berlin.de

Dawid Krenc Department of Pharmaceutical Chemistry, University of Kiel,
Gutenbergstrasse 76, 24118 Kiel, Germany

Tae-Hwan Kwon Water and Salt Research Center, Institute of Anatomy,
University of Aarhus, 8000 Aarhus C, Denmark Department of Biochemistry and
Cell Biology, School of Medicine, Kyungpook National University,
Taegu 700-422, Korea

Thomas Litman Exiqon A/S, Department of Biomarker Discovery,
Bygstubben 16, 2950 Vedbæk, Denmark

Shuying Liu Molecular Physiology and Therapeutics Branch and Clinical
Research Core, National Institute of Dental and Craniofacial Research, NIH,
Bethesda, MD 20892, USA

Norikazu Maeda Department of Internal Medicine and Molecular Science, Graduate School of Medicine, Osaka University, 2-2-B5 Yamada-oka, Suita, Osaka 565-0871, Japan, nmaeda@imed2.med.osaka-u.ac.jp

Geoffrey Manley Department of Neurosurgery, University of California, San Francisco, CA 94143, USA, manley@itsa.ucsf.edu

Linda McCullagh Molecular Physiology and Therapeutics Branch and Clinical Research Core, National Institute of Dental and Craniofacial Research, NIH, Bethesda, MD 20892, USA

Hanne B. Møller Water and Salt Research Center, Institute of Anatomy, University of Aarhus, 8000 Aarhus C, Denmark
Department of Biochemistry and Cell Biology, School of Medicine, Kyungpook National University, Taegu 700-422, Korea

Rita Mukhopadhyay Department of Biochemistry and Molecular Biology, Wayne State University School of Medicine, 4351 Scott Hall, 540 East Canfield Avenue, Detroit, MI 48201, USA, rmukhopa@med.wayne.edu

Pavel I. Nedvetsky Leibniz-Institut für Molekulare Pharmakologie (FMP), Campus Berlin-Buch, 13125 Berlin, Germany
Department of Molecular Pharmacology and Cell Biology, Charité – Universitätsmedizin Berlin, Germany

Jakob Nielsen Water and Salt Research Center, Institute of Anatomy, University of Aarhus, 8000 Aarhus C, Denmark
Department of Biochemistry and Cell Biology, School of Medicine, Kyungpook National University, Taegu 700-422, Korea

Søren Nielsen The Water and Salt Research Center, Institute of Anatomy, Building 233/234, University of Aarhus, 8000 Aarhus, Denmark, sn@ana.au.dk

Nikolay Nikolov Molecular Physiology and Therapeutics Branch and Clinical Research Core, National Institute of Dental and Craniofacial Research, NIH, Bethesda, MD 20892, USA

Eric Perrier LVMH-Recherche, F-45800 St Jean de Braye, France

A. Robin Manchester Interdisciplinary Biocentre (MIB) & The School of Chemistry, University of Manchester, 131 Princess Street, M1 7DN Manchester, UK

Barry P. Rosen Department of Biochemistry and Molecular Biology, Wayne State University, School of Medicine, Detroit, MI 48201, USA

Walter Rosenthal Leibniz-Institut für Molekulare Pharmakologie (FMP), Campus Berlin-Buch, 13125 Berlin, Germany
Department of Molecular Pharmacology and Cell Biology, Charité – Universitätsmedizin Berlin, Germany

M. Rützler The Water and Salt Research Centre, Institute of Anatomy, Aarhus University, 8000 Aarhus C, Denmark

Sei Sasaki Department of Nephrology, Tokyo Medical and Dental University, Tokyo 113-8519, Japan, ssasaki.kid@tmd.ac.jp

Sylvianne Schnebert LVMH-Recherche, 45800 St Jean de Braye, France

Rikke Søgaard Nordic Centre for Water Imbalance Related Disorders, Institute of Cellular and Molecular Medicine, The Panum Institute, Blegdamsvej 3C, University of Copenhagen, 2200N, Denmark

Eisei Sohara Department of Nephrology, Graduate School of Medicine, Tokyo Medical and Dental University, Tokyo, Japan

Jie Song Department of Pharmaceutical Chemistry, University of Kiel, Gutenbergstrasse 76, 24118 Kiel, Germany, ebeitz@pharmazie.uni-kiel.de

Shirley Stiver Department of Neurological Surgery, University of California, San Francisco, 1001 Potrero Avenue, Room 101, San Francisco, CA 94110, USA
The Brain and Spinal Injury Center, 1001 Potrero Avenue, Room 101, San Francisco, CA 94110, USA

Daizo Taguchi c/o AG Loewenheim, HNO-Klinik, Elfriede-Aulhorn-Str.5, 72076 Tuebingen, Germany, taguchident@aol.com

Taizo Takeda Department of Otolaryngology, Kochi Medical School, Kohasu, Oko-cho, Nankoku Kochi 783-8505, Japan

Grazia Tamma Dipartimento di Fisiologia Generale ed Ambientale, University of Bari, Via Amendola 165/A, 70126 Bari, Italy

R. James Turner Molecular Physiology and Therapeutics Branch, National Institute of Dental and Craniofacial Research, NIH, Bethesda, MD 20892, USA

Shinichi Uchida Department of Nephrology, Graduate School of Medicine, Tokyo Medical and Dental University, Tokyo, Japan

Giovanna Valenti Dipartimento di Fisiologia Generale ed Ambientale, University of Bari, Via Amendola 165/A, 70126 Bari, Italy

Jean-Marc Verbavatz Service de Biophysique des fonctions membranaires, DBJC/SBFM, Bâtiment 532, CEA/Saclay, 91191 Gif-sur-Yvette Cedex, France, jean-marc.verbavatz@cea.fr

Alan S. Verkman 1246 Health Sciences East Tower, Cardiovascular Research Institute, University of California, San Francisco, CA 94143-0521, USA, verkman@itsa.ucsf.edu, <http://www.ucsf.edu/verklab>

Julia von Bülow Dept. of Pharmaceutical Chemistry, University of Kiel, Gutenbergstrasse 76, 24118 Kiel, Germany

T. Walz Department of Cell Biology, Harvard Medical School, 240 Longwood Avenue, Boston, MA 02115, USA

Vincent Wang Department of Neurological Surgery, University of California, San Francisco, 1001 Potrero Avenue, Room 101, San Francisco, CA 94110, USA
Brain and Spinal Injury Center, University of California, San Francisco, 1001 Potrero Avenue, Room 101, San Francisco, CA 94110, USA

Dorothea Wree Department of Pharmaceutical Chemistry, University of Kiel, Gutenbergstrasse 76, 24118 Kiel, Germany

Binghua Wu Department of Pharmaceutical Chemistry, University of Kiel, Gutenbergstrasse 76, 24118 Kiel, Germany

Masato Yasui Department of Pharmacology School of Medicine, Keio University, 35 Shinanomachi, Shinjuku-ku, Tokyo 160-8582 Japan, myasui@sc.itc.keio.ac.jp

Zsolt Zador Department of Neurological Surgery, University of California, San Francisco, 1001 Potrero Avenue, Room 101, San Francisco, CA 94110, USA
The Brain and Spinal Injury Center, University of California, San Francisco, 1001 Potrero Avenue, Room 101, San Francisco, CA, USA

Thomas Zeuthen Nordic Centre for Water Imbalance Related Disorders, Department of Medical Physiology, Panum Institute, University of Copenhagen, 2200 N, Denmark, tzeuthen@mfi.ku.dk

Changyu Zheng Molecular Physiology and Therapeutics Branch and Clinical Research Core, National Institute of Dental and Craniofacial Research, NIH, Bethesda, MD 20892, USA

Introduction

Discovery of the Aquaporins and Development of the Field

Jennifer M. Carbrey and Peter Agre

Contents

1	Discovery of the Aquaporins	4
1.1	Early Studies of Water Transport	4
1.2	Discovery of Aquaporin 1	5
2	Solute Transport	7
2.1	Glycerol and Urea	8
2.2	Anions	8
2.3	Ammonia and Hydrogen Peroxide	8
2.4	Arsenite and Antimonite	9
2.5	CO ₂ and NO Gases	9
3	Aquaporin Regulation	10
3.1	Regulation of Permeability	10
3.2	Regulation of Subcellular Localization	11
4	Physiological Roles of Aquaporins	13
4.1	Mammalian Aquaporins	14
4.2	Mammalian Aquaglyceroporins	18
	References	20

Abstract The study of water transport began long before the molecular identification of water channels with studies of water-permeable tissues. The discovery of the first aquaporin, AQP1, occurred during experiments focused on the identity of the Rh blood group antigens. Since then the field has expanded dramatically to study aquaporins in all types of organisms. In mammals, some of the aquaporins transport only water. However, there are some family members that collectively transport a diverse set of solutes. The aquaporins can be regulated by factors that affect channel permeability or subcellular localization. An extensive set of studies examines the physiological role of many of the mammalian aquaporins. However, much is still to be discovered about the physiological role of this membrane protein family.

P. Agre (✉)

Department of Molecular Microbiology and Immunology, Johns Hopkins Malaria Research Institute, Johns Hopkins Bloomberg School of Public Health, Room E5146, 615 North Wolfe Street, Baltimore, MD 21205
pagre@jhsp.edu

Abbreviations

ADH	Antidiuretic hormone
P_f	Coefficient of osmotic water permeability
AQP1	Aquaporin 1
NPA	Asparagine–proline–alanine
CO ₂	Carbon dioxide
NO	Nitric oxide
AVP	Arginine-vasopressin
NDI	Nephrogenic diabetes insipidus

1 Discovery of the Aquaporins

The discovery of the aquaporins, although serendipitous, was possible only through the contributions of many researchers over several decades.

1.1 Early Studies of Water Transport

The first studies of water transport began with the observation that certain amphibian tissues, such as the skin or bladder that are functionally similar to the collecting duct of mammalian kidneys, are more permeable to water than other tissues. Hans Ussing and his colleagues observed that amphibian skin is particularly permeable to water (reviewed in Ussing 1965). This idea was expanded upon when other groups observed, with the electron microscope, structures in amphibian bladder that they presumed to be water channels. These protein aggregates became more numerous under conditions when water permeability was increased in the tissue (reviewed in Kachadorian et al. 2000). The idea of the water permeability of a tissue being regulated by the localization of the putative water channels began with the *shuttle hypothesis*. Protein aggregates were observed in vesicles when the water reabsorption by the tissue was low (diuresis) and in the plasma membrane when the water reabsorption was high (antidiuresis) (Wade et al. 1981).

Red blood cells were also known to be highly permeable to water. A.K. Solomon and his colleagues observed water transport in red blood cells with low Arrhenius activation energy, indicating that the movement of water was due to a pore in the membrane (reviewed in Solomon 1968). Further studies by Robert Macey and colleagues revealed that the water permeability of red blood cells could be inhibited by HgCl₂ and that the inhibition could be reversed with chemical reducing agents. Taken together, these studies suggested that water transport occurs through a protein that has free sulfhydryl groups that are accessible to mercury (reviewed in Macey 1984).

Several groups tried different strategies to determine the molecular identity of the water channels. Many groups tried examining known channels and carriers for water transport (reviewed in van Os et al. 1994). William Harris and colleagues radioactively labeled proteins on the apical surface of toad bladder exposed to antidiuretic hormones (ADH) and compared those proteins to ones labeled without ADH in an attempt to find the protein that was specifically localized on the plasma membrane in response to ADH (Harris et al. 1988). Expression cloning was attempted using mRNA from various tissues that were injected into *Xenopus laevis* oocytes to see if there was an increase in water permeability (Zhang et al. 1990). Radiation inactivation was used to correctly predict a water channel of approximately 30 kDa based on the amount of radiation needed to inactivate water channel activity in renal brush border membranes (van Hoek et al. 1991). Working under difficult conditions in Romania, a series of red cell membrane proteins was radiolabeled with an organomercurial inhibitor of water transport (Benga et al. 1986). Unfortunately, using these approaches the molecular identity of the aquaporins was not revealed.

1.2 Discovery of Aquaporin 1

The first water channel, AQP1, was identified during a search for the identity of the Rh blood group antigens. One of the Rh antigens was isolated from radiolabeled red blood cell membranes using hydroxylapatite chromatography and was found to be about 32 kDa (Agre et al. 1987; Saboori et al. 1988). The protein did not stain well with Coomassie stain. When silver reagent was used to detect the protein, another protein of 28 kDa was detected. It was initially thought that the 28-kDa protein was a proteolytic fragment of the 32-kDa protein until an antibody specific for the 28-kDa protein did not bind to the 32-kDa protein. Further characterization of the 28-kDa protein determined that it was not related to the 32-kDa protein (Denker et al. 1988) and that it had several physical properties similar to a membrane channel. As a result, the 28-kDa protein was temporarily named *CHIP28*, acronym for *channel-like integral protein of 28 kDa* (Smith and Agre 1991). On the basis of its localization in red blood cells, in the brush border of renal proximal tubules, and in the descending thin limb of the loop of Henle, John C. Parker, a membrane physiologist at the University of North Carolina at Chapel Hill, first suggested that CHIP28 may be the water channel that was yet to be identified (Parker and Agre, personal discussions, 1990).

The cDNA that encodes CHIP28 was cloned from an erythroid library and found to be similar to other gene sequences from a microbe and plants that had not yet been functionally characterized (Preston and Agre 1991). The first evidence that CHIP28 was a water channel came by expressing the protein in *Xenopus laevis* oocytes. Oocytes had been used to express and study other transport proteins (Hediger et al. 1987). Erich Windhager at Cornell Medical School was first to suggest that oocytes would be useful to study water transport due to their particularly low water permeability. When oocytes expressing CHIP28 were placed into dilute

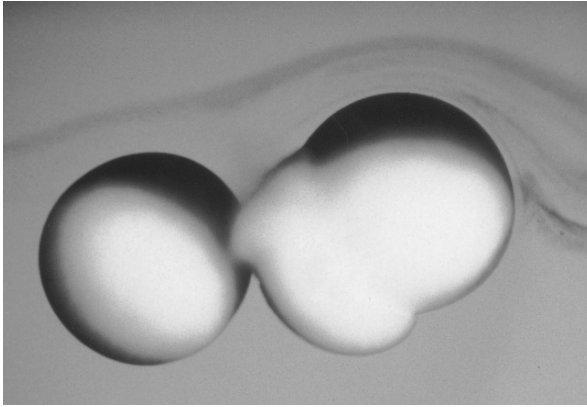


Fig. 1 Swelling and rupture of *Xenopus* oocyte expressing AQP1 (*right*) vs. water-injected control oocyte (*left*). Both oocytes were in dilute buffer. Reproduced with permission from Preston et al. (1992)

Modified Barth's solution (70 mosM instead of 200 mosM), they rapidly swelled and exploded. Control oocytes swelled negligibly (Preston et al. 1992) (Fig. 1). The CHIP28-expressing oocytes had a coefficient of osmotic water permeability (P_f) that was 20-fold higher than that of the control oocytes. In addition, the Arrhenius activation energy of the CHIP28 oocytes was lower than that of the control oocytes and comparable to water transport in native membranes as observed before. The water permeability of the CHIP28 oocytes was inhibited by 1 mM HgCl_2 and reversed by a reducing agent. This again was predicted from previous studies with water-permeable tissues (reviewed in Macey 1984). To rule out that CHIP28 was just activating a water channel endogenous to oocytes, purified CHIP28 was reconstituted into membrane proteoliposomes. The presence of CHIP28 raised the water permeability of the proteoliposomes 50-fold but urea and protons were not transported. It was estimated that 3×10^9 water molecules per second pass through a single CHIP28 subunit (Zeidel et al. 1992, 1994).

As more CHIP28 homologs were identified, the name *aquaporin* was proposed for the family of water channels (Agre et al. 1993). The name of CHIP28 was changed to Aquaporin 1 (AQP1).

AQP1 has been well characterized in many respects and in many ways is prototypical of most of the aquaporins that are found in microorganisms, plants, and mammals. Studies in red blood cells predicted that AQP1 exists in the membrane as a homotetramer and that most of the polypeptide spans the membrane with the N- and C-termini projecting into the cytoplasm (Smith and Agre 1991). Further studies with negative staining electron microscopy of cells expressing AQP1 and proteoliposomes revealed an oligomer calculated to be a tetramer (Verbavatz et al. 1993).

Previous studies with the lens MIP protein, now referred to as AQP0, predicted that there were six membrane-spanning domains (Gorin et al. 1984). This was confirmed for AQP1 with experiments that inserted an epitope at different locations

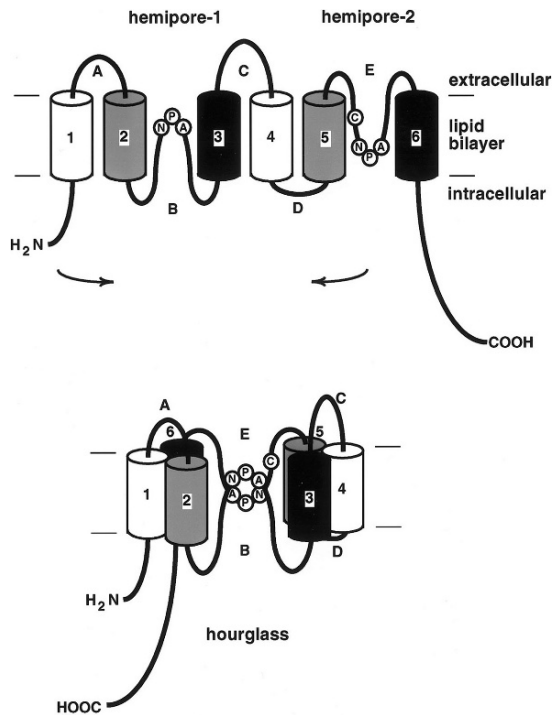


Fig. 2 Schematic diagram of AQP1 monomer in the proposed hourglass structure. (*Top*) Two repeats of three membrane-spanning domains are arranged so that they are obversely symmetric. Loops B and E fold back into the membrane. (*Bottom*) When loops B and E join in the membrane, they form a single water pore and form an hourglass-like structure. Reproduced with permission from Jung et al. 1994

throughout the polypeptide. The side of the membrane the epitope resided on was determined by proteolysis and antibodies to the epitope. The orientation of the helices in the membrane led to the realization that the two halves of the polypeptide are obversely symmetric. It was proposed that the two highly conserved NPA (asparagine-proline-alanine) motifs are juxtaposed in the bilayer causing AQP1 to resemble an hourglass (Jung et al. 1994) (Fig. 2). This overall structure of AQP1 has been confirmed by high-resolution structures of AQP1 and other aquaporins (Murata et al. 2000, Fu et al. 2000, Sui et al. 2001, Savage et al. 2003, Gonen et al. 2005).

2 Solute Transport

Permeation of aquaporins represents diffusion through a neutral pore driven by an osmotic gradient. Some aquaporins transport only water. However, some aquaporins have a physiological role that involves transporting other solutes.

2.1 *Glycerol and Urea*

Some aquaporin family members, referred to as *aquaglyceroporins*, transport glycerol and other uncharged solutes in addition to water. The aquaglyceroporins can be distinguished from aquaporins based on amino acid sequence alignments (Borgnia et al. 1999). The first mammalian aquaglyceroporin to be cloned, AQP3, is permeable to glycerol and water (Echevarria et al. 1994, Ishibashi et al. 1994, Ma et al. 1994). AQP7 and AQP10 transport water, glycerol, and urea when expressed in *Xenopus* oocytes (Ishibashi et al. 1997, Ishibashi et al. 2002). AQP9 transports water, glycerol, and urea, but also is permeable to a wide range of other solutes in oocytes (Tsukaguchi et al. 1998).

2.2 *Anions*

One member of the mammalian aquaporin family, AQP6, is unique because the channel transports anions and is only slightly permeable to water. AQP6 is permeable to a wide range of anions, but it is most permeable to nitrate (Ikeda et al. 2002). In addition, the water and anion permeability of AQP6 is gated by either Hg^{2+} or by low pH (Yasui et al. 1999a). The residues that are important for anion permeability of AQP6 were determined. When an asparagine residue in AQP6, which resides where two helices of the pore cross, was changed to a glycine (as in all other members), AQP6 became permeable to water but no longer permeable to anions. The bulkier residue in the spot where two helices cross provides instability that in the case of AQP6 results in anion permeability (Liu et al. 2005).

It should be noted that Andrea Yool and colleagues have proposed that AQP1 may also conduct ions in special circumstances (Boassa et al. 2006).

2.3 *Ammonia and Hydrogen Peroxide*

Ammonia is a nitrogen source for plants and a waste product of metabolism in animals. The first aquaporins shown to transport ammonia were mammalian AQP8 and three aquaporins from wheat roots (Jahn et al. 2004). These aquaporins share residues in one of the narrow portions of the pore. The ammonia permeability of AQP8 was shown to exclude ammonium ions and protons using purified protein in planar bilayers (Saparov et al. 2007). Evidence suggests that aquaglyceroporins from certain parasites transport ammonia as well (Zeuthen et al. 2006).

Hydrogen peroxide is a reactive oxygen species that may be used in cellular signaling. Out of 24 plant and mammalian aquaporins tested, only AQP8 and two aquaporins from *Arabidopsis* were found to transport hydrogen peroxide (Bienert et al. 2007). In mammals, there is not yet a clear physiological role for ammonia or hydrogen peroxide transport by AQP8 (Yang et al. 2006).

2.4 Arsenite and Antimonite

Arsenite and antimonite are trivalent versions of the toxic metalloids, arsenic and antimony, that can be transported by some aquaglyceroporins. The *E. coli* aquaglyceroporin, GlpF, and the *S. cerevisiae* aquaglyceroporin, Fps1p, were the first membrane proteins shown to transport antimonite and arsenite (Sanders et al. 1997; Wysocki et al. 2001). Mammalian aquaglyceroporins, AQP7 and AQP9, have also been shown to transport antimonite and arsenite (Liu et al. 2002). The amount of aquaglyceroporin expression has been shown to affect the tolerance of a human lung adenocarcinoma cell line as well as a human leukemia cell line for arsenite or antimonite (Lee et al. 2006; Bhattacharjee et al. 2004). The protozoan parasite, *Leishmania*, also expresses an aquaglyceroporin. Antimonite and arsenite are used to treat leishmaniasis. Disruption of one of the alleles of the aquaglyceroporin in *L. major* caused the parasite to be ten-fold more resistant to treatment with antimonite (Gourbal et al. 2004). Arsenic contamination of drinking water is an enormous problem in the Ganges Delta region of India and Bangladesh. At the same time, arsenic and antimony are used to treat some parasitic infections and some types of leukemia. Fully understanding the roles of the aquaglyceroporins in antimonite and arsenite transport may be of therapeutic or toxicologic significance.

2.5 CO₂ and NO Gases

AQP1 has been proposed by Walter Boron and colleagues to be permeated by the gases, carbon dioxide (CO₂) and nitric oxide (NO). AQP1 expressed in oocytes or reconstituted into proteoliposomes has been used to study water channel transport of CO₂. In both systems, carbonic anhydrase was present to convert the CO₂ into H₂CO₃ thereby reducing the pH inside the oocytes or proteoliposomes (Nakhoul et al. 1998, Prasad et al. 1998). Oocytes expressing AQP1 transported CO₂ 40% faster than control oocytes (Nakhoul et al. 1998). In proteoliposomes containing AQP1, water permeability and CO₂ permeability were increased four-fold and were inhibited by mercury (Prasad et al. 1998). Whether the CO₂ permeability of AQP1 is potent enough to be physiologically relevant in mammals is still in discussion. In AQP1 null mice, a lack of AQP1 did not affect the permeability of red blood cells or the lung to CO₂ (Yang et al. 2000). However, in human AQP1 null red blood cells, CO₂ permeability was reduced by 60% compared with wild-type cells in studies using ¹⁸O₂ to measure the exchange of CO₂ and HCO₃⁻ across the membrane (Endeward et al. 2006).

A number of experiments suggest that AQP1 is permeable to NO. Nitric oxide is a gas that is important in vasodilation of blood vessels and as a signaling molecule. Expressing AQP1 in cultured cells increased the permeability of the cells to NO by almost four-fold. In addition, AQP1 proteoliposomes were over three-fold more permeable to NO than control liposomes (Herrera et al. 2006). Consistent with a role in the NO-induced dilatation of blood vessels, AQP1 is expressed in the endothelial

cells and the smooth muscle cells lining the walls of vessels. Rings of tissue were taken from the aortas of wild type and AQP1 null mice. When they were exposed to acetylcholine that increases NO production in the tissue, the AQP1 null rings exhibited reduced dilation. NO entry into vascular smooth muscle cells taken from AQP1 null mice was reduced by 62% compared with wild-type mice (Herrera and Garvin 2007). The relative physiological importance of the gas transport of AQP1 vs. the water transport activities is yet to be determined.

3 Aquaporin Regulation

Several examples indicate that expression of aquaporins may be regulated. However, there are few examples of regulation of channel permeability or subcellular localization.

3.1 Regulation of Permeability

Several aquaporins have permeabilities that are regulated in some way. However, in most cases the physiological purpose or relevance of the gating or regulation is unknown.

3.1.1 AQP6

Perhaps the most striking example of mammalian aquaporin permeability regulation is AQP6, which is permeable to anions and expressed in intracellular vesicles in α -intercalated cells in the kidney (Yasui et al. 1999a; Yasui et al. 1999b). Exposing AQP6-expressing oocytes to 300- μ M HgCl₂ increased water permeability over five-fold and increased ion conductance more than six-fold. Two cysteine residues in AQP6 were shown to be important for the Hg²⁺ gating of AQP6 (Yasui et al. 1999a). Hg²⁺ is unlikely to be the natural activator of AQP6. The expression of AQP6 in acid-secreting cells of the kidney suggests that pH could be the physiological activator of AQP6. A shift to pH 4.0 increased the water permeability of AQP6 expressing oocytes by more than two-fold and ion conductance by more than three-fold (Yasui et al. 1999a). The physiological role of AQP6 gating is still under investigation, but a role in urinary acid secretion is suspected.

3.1.2 AQP3

AQP3 is an aquaglyceroporin that can be inhibited by low pH, copper, and nickel. The water and glycerol permeability of AQP3-expressing oocytes was completely inhibited at pH 5.6 and lower (Zeuthen and Klaerke 1999). Under neutral pH

conditions, Ni^{2+} reduces AQP3 permeability by more than 50% in cells transfected with AQP3-GFP (Zelenina et al. 2003). Cu^{2+} also inhibits water and glycerol permeability in cultured cells to a similar extent as Ni^{2+} . The inhibition is specific for certain divalent cations as there was no inhibition with Pb^{2+} or Zn^{2+} (Zelenina et al. 2004). The inhibition of AQP3 glycerol permeability by copper and nickel has been confirmed in studies of human red blood cells (Liu et al., unpublished data). It is not clear if the inhibition of AQP3 is important physiologically.

3.1.3 AQP0

AQP0 is expressed in lens fiber cells and has relatively low water permeability (Gorin et al. 1984; Mulders et al. 1995). As with AQP3, divalent cations may also play a role in AQP0 water permeability. Ni^{2+} and Zn^{2+} increase AQP0 water permeability in oocytes two-fold (Nemeth-Cahalan et al. 2007). Lowering the pH of AQP0-expressing oocytes from 7.5 to 6.5 resulted in about a two-fold increase in the water permeability of AQP0. In addition, lowering internal Ca^{2+} concentration or inhibiting calmodulin increased AQP0 water permeability (Nemeth-Cahalan and Hall 2000). Similar increases in water permeability with pH and Ca^{2+} were seen in lens fiber cells (Varadaraj et al. 2005). Since the pH and Ca^{2+} concentration throughout the layers of the lens differ, it is possible that the water permeability of AQP0 also varies among the layers of the lens in a physiologically significant manner (Mathias et al. 1991; Baldo et al. 2002).

3.2 Regulation of Subcellular Localization

Adjusting the water permeability of a tissue is accomplished by regulating the subcellular localization of the aquaporin in only a few notable cases.

3.2.1 AQP2

AQP2 in the collecting duct of the kidney is the most striking and well-studied example of the cell controlling water permeability using the subcellular localization of the aquaporin. AQP2 is expressed by principal cells that are located toward the end of the nephron in the connecting tubule and collecting duct (Fushimi et al. 1993; Nielsen et al. 1993a). Most urinary water is reabsorbed before the filtrate arrives at the collecting duct. However, this last segment is where the body controls water permeability based on the short-term needs of the individual. The hormone arginine-vasopressin (AVP) is released from the pituitary during dehydration when more water needs to be reabsorbed from the filtrate. The AVP binds receptors in the principal cells that cause an increase in cAMP, which activates protein kinase A. AQP2 resides in storage vesicles in the principal cells and is phosphorylated by the activated protein kinase A (Fushimi et al. 1997, Katsura et al. 1997). If at least

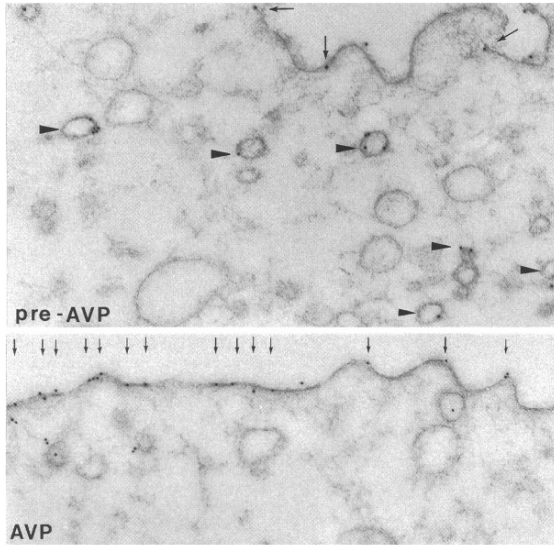


Fig. 3 Immunogold electron microscopy of AQP2 in principal cells of renal collecting duct. (*Top*) Localization of AQP2 mostly to intracellular vesicles in an unstimulated state. (*Bottom*) After treatment with AVP AQP2 is localized predominantly in the plasma membrane. Reproduced with permission from Nielsen et al. (1995a)

three of the AQP2 polypeptides in a tetramer are phosphorylated then the AQP2 is translocated to the apical plasma membrane of the principal cell (Kamsteeg et al. 2000, Van Balkom et al. 2002) (Fig. 3). When the vasopressin levels drop, AQP2 is ubiquitinated, which leads to endocytosis, degradation of AQP2, and a reduction in the water permeability of the apical plasma membrane (Kamsteeg et al. 2006).

3.2.2 AQP1

Other aquaporins have been shown in special situations to be regulated by their localization in the cell. AQP1 is expressed in cholangiocytes, the cells that line bile ducts and secrete water in response to the hormone secretion (Nielsen et al. 1993b). When cholangiocytes were stimulated with secretin there was an increase in the amount of AQP1 on the plasma membrane and a decrease in the amount of intracellular AQP1 (Marinelli et al. 1997). When rats were treated with colchicine, a drug that disassembles microtubules, secretin-stimulated AQP1 movement to the plasma membrane and bile flow was inhibited (Marinelli et al. 1999).

3.2.3 AQP5

AQP5 is expressed in the exocrine portions of the pancreas, lacrimal, and salivary glands presumably to add water to the proteinaceous secretions (Nielsen et al.

1997a). When rat parotid gland slices were exposed to acetylcholine for 1 min, which stimulates saliva production, the amount of AQP5 in the apical membrane vs. intracellular increased more than two-fold as measured by differential centrifugation and immunoblotting. A Ca^{2+} ionophore could also induce the trafficking of AQP5, suggesting that the process is mediated by Ca^{2+} (Ishikawa et al. 1998). Human salivary gland cells transfected to express AQP5 were exposed to a Ca^{2+} ionophore, and AQP5 trafficked from an intracellular location to the plasma membrane as observed by immunofluorescence. The translocation of AQP5 was blocked by pretreatment with colchicine, a microtubule inhibitor (Tada et al. 1999). To examine the trafficking of AQP5 *in vivo*, immunofluorescence and immunoelectron microscopy were used to examine the localization of AQP5 in rat salivary glands after secretion was stimulated or inhibited. Under both conditions, the majority of AQP5 was localized to the apical plasma membrane of acinar and intercalated duct cells suggesting that AQP5 may not traffic in salivary glands *in vivo* (Gresz et al. 2004). However, in cells of the larger interlobular ducts of rat parotid gland, AQP5 was localized to intracellular vesicles and trafficked to the plasma membrane in response to muscarinic stimulation or a calcium ionophore (Ishikawa et al. 2005). These apparent discrepancies are unresolved. Thus, AQP5 may be regulated by trafficking in only a subset of tissues or cells.

3.2.4 AQP8

AQP8 is expressed in pancreatic acinar cells and in the liver, among other tissues in the digestive tract (Ma et al. 1997b; Koyama et al. 1997). In the pancreas, AQP8 is localized to both the apical membrane and intracellular vesicles by immunoelectron microscopy (Hurley et al. 2001). In isolated rat hepatocytes, AQP8 was localized intracellularly until the cells were stimulated with cAMP, when AQP8 is trafficked to the plasma membrane (Garcia et al. 2001). Immunoelectron microscopic analyses of the rat liver revealed AQP8 in intracellular vesicles and the portion of the plasma membrane that forms the bile canaliculi (Calamita et al. 2001). Hepatocytes isolated as a two-cell couplet retain their polarity. In such couplets, AQP8 was localized intracellularly and then trafficked specifically to the canalicular plasma membrane after stimulation with cAMP (Huebert et al. 2002). The trafficking of AQP8 can also be stimulated in hepatocytes by glucagon, which is known to increase intracellular cAMP (Gradilone et al. 2003). It is still unknown if AQP8 is phosphorylated in response to increased intracellular cAMP levels similar to AQP2.

4 Physiological Roles of Aquaporins

The physiological roles of aquaporins have been well characterized for some aquaporins using various aquaporin null mice and a few human studies. However, there is still much to be discovered about the roles of this membrane protein family in mammalian physiology.

4.1 Mammalian Aquaporins

Despite the fact that all of the mammalian aquaporins transport water, they have diverse roles in the different tissues in which they are expressed.

4.1.1 AQP0

AQP0 is expressed exclusively in the lens fiber cells of the eye (Gorin et al. 1984). Two mouse models of cataracts, the CAT and Lop mice, develop opacity of the lens of the eye as early as day 13–14 after gestation. The mutations responsible for the CAT and Lop mice phenotypes are known. CAT mice have a transposon that causes a splicing error in AQP0. Lop mice have an amino acid substitution that prevents AQP0 from trafficking to the plasma membrane (Shiels and Bassnett 1996). Two different mutations in AQP0 were identified in two human families with congenital cataracts (Berry et al. 2000). Two additional mutations in two unrelated families have been found more recently (Geyer et al. 2006; Gu et al. 2007). All four mutations identified so far are autosomal dominant. High-resolution structures of AQP0 have revealed lipid protein interactions (Gonen et al. 2005) and defective protein folding in AQP0 mutants with cataracts (Harries et al. 2004).

AQP0 can transport water, although to a lesser extent than most aquaporins, but there has also been a second role proposed for AQP0 in cell-to-cell adhesion. Liposomes containing purified AQP0 can aggregate (Dunia et al. 1987). Two-dimensional crystals of reconstituted AQP0 are double-layered. Using electron and atomic force microscopy the interactions responsible for the binding of the extracellular surfaces of AQP0 were revealed (Hasler et al. 1998, Fotiadis et al. 2000). The binding of AQP0 extracellular portions to one another may be important in lens fiber cell adhesion. It is not clear whether it is the contribution of AQP0 to cell adhesion or to water homeostasis or both that is crucial for maintaining lens transparency.

4.1.2 AQP1

AQP1 is expressed in many tissues and therefore plays a variety of roles in mammals. In the kidney, AQP1 is expressed in the endothelial cells of the vasa recta, the proximal tubule, and the thin descending limb of Henle (Denker et al. 1988, Nielsen et al. 1993c, Nielsen et al. 1995b). During water deprivation, AQP1 null mice are not able to concentrate their urine and as a result they have an increase in serum osmolality compared with wild-type mice (Ma et al. 1998). Further studies of the AQP1 null mice conclude that the lack of AQP1 results in reduced proximal tubule and thin descending limb water permeability (Schnermann et al. 1998, Chou et al. 1999). In the descending vasa recta, AQP1 is believed to be important in the water transport that is needed for countercurrent exchange (Pallone et al. 2000). Humans lacking AQP1 also have a urinary concentrating deficiency when deprived of water (King et al. 2001).

In the lung, AQP1 is expressed in the endothelial cells of the capillaries where gas exchange occurs (Nielsen et al. 1993b). AQP1 null mice are protected from lung edema resulting from an increase in pulmonary artery pressure (Bai et al. 1999). In studies of AQP1 null patients, the control subjects responded to the intravenous infusion of 3 L of saline with a 44% increase in the airway wall thickness while the AQP1 null human patients had no increase (King et al. 2002) (Fig. 4). Although the AQP1 deficiency was protective in mice and humans when excess fluid came from the vasculature, it is probable that AQP1 is important in other situations such as lung fluid reabsorption at the time of birth (King et al. 1996, Umenishi et al. 1996).

AQP1 also has important functions in the eye and the central nervous system. AQP1 is expressed in nonpigmented ciliary epithelium and in the endothelial cells

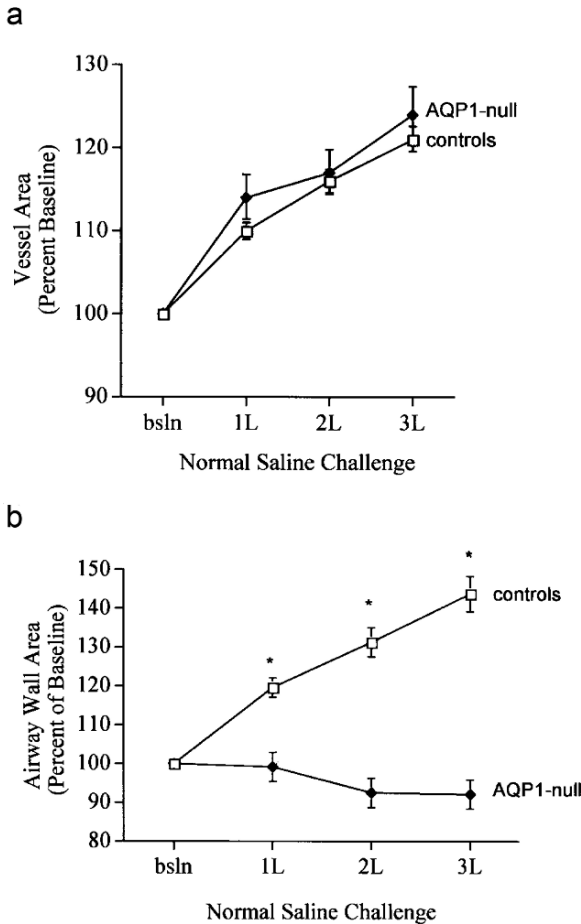


Fig. 4 Study of the response of AQP1 null subjects and control subjects to infusion of saline. (a) Vessel area in the lung increased during infusion of saline in the AQP1 null subjects and control subjects. (b) Airway wall thickness increased in response to saline infusion in control subjects but did not increase in AQP1 null subjects. Reproduced with permission from King et al. (2002)

of the trabecular meshwork of the anterior chamber (Nielsen et al. 1993b). The ciliary epithelium produces aqueous fluid for the eye. AQP1 null mice have reduced intraocular pressure and aqueous fluid production. However, there was no significant difference in the rate of aqueous fluid leaving the eye (Zhang et al. 2002). In the brain, AQP1 is expressed in choroid plexus on the apical membrane of the epithelium exposed to cerebrospinal fluid in the ventricles (Nielsen et al. 1993b). Intracranial pressure was reduced by over 50% in AQP1 null mice compared with wild-type mice. Cerebrospinal fluid production was also reduced in the AQP1 null mice. After a targeted injury to the brain, the AQP1 null mice had a lower intracranial pressure and improved survival compared with wild-type mice (Oshio et al. 2005). In both the eye and the choroid plexus, AQP1 is important for fluid accumulation but not fluid depletion.

Alan Verkman and colleagues have proposed that AQP1 may also be involved in cell migration. Tumors grown in AQP1 null mice grew more slowly and contained fewer blood vessels than tumors from wild-type mice or AQP3 null mice. Endothelial cells cultured from AQP1 null mice migrated more slowly than wild-type endothelial cells, which could explain the lack of vessels and angiogenesis in the tumors. Cells made to express AQP1 or AQP4 were able to migrate more quickly (Saadoun et al. 2005a). AQP1 may play a role in protrusion formation in migrating cells. The relevance to AQP1 in humans is unclear, since AQP1 null humans are not known to suffer decreased angiogenesis and at least one is known to have died of cancer (Agre unpublished).

4.1.3 AQP2

AQP2 is expressed in the connecting tubule and collecting duct of the kidney and traffics to the plasma membrane in response to arginine-vasopressin (AVP) to increase water permeability and conserve water for the organism (Fushimi et al. 1993, Nielsen et al. 1993a). Human patients with autosomal recessive nephrogenic diabetes insipidus (NDI) had a mutation in *AQP2* (Deen et al. 1994). Many more patients with various mutations in *AQP2* have been found since (reviewed in Fujiwara and Bichet 2005). Mice expressing an *AQP2* gene with a mutation that causes NDI in humans have a severe urine concentrating defect. These mice are affected just a few days after birth and die by 6 days of age unless supplemental fluids are given (Yang et al. 2001). Mice deficient for AQP2 in the collecting duct but still expressing AQP2 in the connecting tubule survive to adulthood, but with reduced body weight and produced ten-fold greater urine volumes with reduced osmolality compared with wild-type mice (Rojek et al. 2006).

4.1.4 AQP4

Most of the studies of AQP4 physiological function examine its role in the central nervous system. AQP4 is expressed in the collecting duct of the kidney (Terris et al.

1995). However, AQP4 null mice have only a minor urine concentrating defect after water deprivation (Ma et al. 1997a). In the brain, AQP4 is expressed in the end-feet of astroglial cells that form the blood–brain barrier and the glial limiting membrane as well as in ependymal cells that line the ventricles (Nielsen et al. 1997b, Rash et al. 1998). AQP4 null mice are protected from cytotoxic brain edema, which occurs when water is taken up from the interstitial portion of the brain into the cells. Temporary loss of AQP4 from neocortex was observed after transient arterial occlusion (Frydenlund et al. 2006). Cytotoxic edema can occur during hyponatremia or cerebral ischemia (Kimelberg 1995, Papadopoulos and Verkman 2007). AQP4 null mice had reduced mortality or better neurological outcome in cytotoxic brain edema arising from intraperitoneal water injection, bacterial meningitis, or cerebral artery occlusion compared with wild-type mice (Manley et al. 2000, Papadopoulos and Verkman 2005). This was confirmed in alpha-syntrophin null mice that have a mislocalization of AQP4 so that it is not expressed at the blood–brain barrier (Amiry-Moghaddam et al. 2004). AQP4 null mice are more sensitive to vasogenic edema, which occurs when there is a breach of the blood–brain barrier and fluid enters the brain from the vasculature. Vasogenic edema can occur from brain tumors or abscesses (Papadopoulos and Verkman 2007). AQP4 null mice had increased intracranial pressure and neurological deterioration compared with wild-type mice during intraparenchymal fluid infusion, freeze-injury, and brain tumor edema (Papadopoulos et al. 2004). AQP4 is important for eliminating vasogenic edema.

Under normal conditions, AQP4 in astrocytes may play a role in migration and neural excitability. Astroglial cells from AQP4 null mice had reduced migration in culture compared with wild-type cells. There was also reduced astroglial migration to the site of a cortical stab injury in AQP4 null mice (Saadoun et al. 2005b). There are signs of decreased neural excitability in AQP4 null mice. They have an increased seizure threshold and duration (Binder et al. 2004, Binder et al. 2006). This may be explained if AQP4 is needed for efficient potassium ion clearance from the extracellular space after neuronal activity. In alpha-syntrophin null mice that have a mislocalization of AQP4, potassium clearance was prolonged two-fold (Amiry-Moghaddam et al. 2003). This was confirmed in AQP4 null mice (Binder et al. 2006). The human relevance of AQP4 was established in epileptogenic hippocampus (Eid et al. 2005).

4.1.5 AQP5

AQP5 is expressed in the exocrine portions of the pancreas, lacrimal, and salivary glands and in the lung and eye (Nielsen et al. 1997a, Hamann et al. 1998). AQP5 null mice show reduced perinatal survival and altered salivary function (Krane et al. 2001b). Of the three aquaporins expressed in the salivary glands, AQP5 null mice have the most dramatic phenotype in saliva formation with a 60% reduction in saliva production and saliva that was viscous and hypertonic (Ma et al. 1999). There was a similar decrease in fluid secretion by upper airway submucosal glands from

AQP5 null mice (Song and Verkman 2001). This may be of importance in lung bronchoconstriction and asthma (Krane et al. 2001a). There was no effect on the tear production of the AQP5 null mice (Moore et al. 2000). The number of active sweat glands after stimulation was reduced in one set of experiments with AQP5 null mice (Nejsum et al. 2002) but not with different AQP5 null mice (Song et al. 2002). AQP5 in mice seems to play an important role in some secretion events and a more subtle role in other cases. In humans, abnormal trafficking of AQP5 has been described in the lacrimal and salivary glands of some patients with Sjögren's syndrome (Tsubota et al. 2001, Steinfeld et al. 2001) whereas reduced AQP1 expression in surrounding myocytes has been described in other patients (Beroukas et al. 2002).

4.2 Mammalian Aquaglyceroporins

The physiological roles of the aquaglyceroporins have been more difficult to ascertain, in part because the understanding of the role of glycerol in mammals is incomplete.

4.2.1 AQP3

AQP3 is expressed in the collecting duct of the kidney, airway epithelia, secretory glands, and skin (Ecelbarger et al. 1995, Frigeri et al. 1995, Nielsen et al. 1997a, Matsuzaki et al. 1999). Mice lacking AQP3 are unable to properly concentrate their urine mostly because AQP2 expression is reduced in AQP3 null mice (Ma et al. 2000). In addition, AQP4 and Na,K-ATPase expression are also reduced in the kidney collecting duct of AQP3 null mice (Kim et al. 2005). It is not known why the lack of AQP3 in the kidney affects the expression of other transport proteins.

In the skin, AQP3 is expressed in keratinocytes in the basal layer of the epidermis (Matsuzaki et al. 1999). Water and glycerol permeability of the epidermis is reduced in AQP3 null mice. In addition, the stratum corneum, or the most superficial layer of cells that are derived from keratinocytes, have reduced water content and a reduced water holding capacity in the AQP3 null mice (Ma et al. 2002). A dramatic three-fold reduction in glycerol content of the stratum corneum was observed in the AQP3 null mice, which explains the reduced water holding capacity. Further studies revealed reduced skin hydration, elasticity, and wound healing capability (Hara et al. 2002). The role of glycerol was confirmed when either systemic or topical glycerol replacement was shown to reverse all of the effects of the lack of AQP3 in mouse skin (Hara and Verkman 2003). Beauty products are now being marketed with claims that AQP3 expression is increased in sun-exposed skin (Christian Dior).

4.2.2 AQP7

The physiological role of AQP7 in adipose tissue has been extensively studied. When triglycerides are broken down in adipocytes, free fatty acids and glycerol are released into the circulation. The free fatty acids can be taken up by tissues for energy. Glycerol is taken up by the liver for gluconeogenesis. AQP7 null mice have a lower plasma glycerol concentration than wild-type mice. After prolonged fasting, the AQP7 mice had a smaller increase of plasma glycerol and a lower blood glucose concentration than wild-type mice (Maeda et al. 2004). At maturity, the AQP7 null mice had a 3.7-fold increase in body fat that comes from enlarged adipocytes. The AQP7 null adipocytes contain more glycerol and triglycerides (Hara-Chikuma et al. 2005). Another group found the same adult-onset obesity and found that the AQP7 null mice became insulin resistant after being fed a high-fat and high-sucrose diet. In addition there was increased glycerol kinase enzymatic activity that the authors propose is responsible for the increased storage of triglycerides in the adipocytes of the AQP7 null mice (Hibuse et al. 2005). AQP7 is being investigated in human subjects. One study compared AQP7 transcript abundance in the adipose tissue of two groups of patients. Both groups had the same daily fat intake and physical activity level but one group was lean and the other was obese. Using microarray analysis and real-time PCR to quantitate mRNA, the obese individuals had a lower amount of AQP7 transcript (Marrades et al. 2006). In a Japanese study one patient was identified who had a homozygous mutation in AQP7. During exercise in the AQP7 null individual, there was no increase in plasma glycerol even though there was an increase in blood noradrenaline levels, which in control patients stimulates triglyceride hydrolysis and glycerol release from adipose (Kondo et al. 2002). While the AQP7 null individual was not described as being overweight, protecting factors including nutritional benefits from eating a traditional Japanese diet may be involved.

4.2.3 AQP9

AQP9 is expressed in the liver where it is proposed to play a role in glycerol uptake for gluconeogenesis during fasting (Ishibashi et al. 1998, Carbrey et al. 2003). Plasma concentrations of glycerol and triglycerides were slightly increased in AQP9 null mice. When AQP9 null mice were mated with leptin-resistant diabetic mice, the double mutants had dramatically increased plasma glycerol levels and reduced blood glucose levels after fasting (Rojek et al. 2007). Mouse red blood cells express AQP9 in contrast to human and rat red blood cells that express AQP3. Red blood cells from AQP9 null mice have dramatically reduced glycerol permeability but the water permeability remains unchanged (Liu et al. 2007). The physiological role for AQP9 in red blood cells is not clear.

Red blood cells are invaded during malarial infection. Glycerol has been shown to be used by *Plasmodium*, the parasite that causes malaria, for lipid biogenesis and as an energy source (Vial et al. 1989, Daily et al. 2007). For the parasite to gain access to glycerol, the glycerol must cross the red blood cell plasma membrane, the

parasitophorous vacuolar membrane that surrounds all of the parasites, and the parasite plasma membrane. When the gene encoding the aquaglyceroporin in *Plasmodium berghei*, a mouse malaria parasite, was disrupted the parasites grew more slowly in mice, which allowed the mice to survive longer (Promeneur et al. 2007). AQP9 null mice infected with *Plasmodium berghei* survived longer during the initial phase of the infection compared with wild-type mice (Liu et al. 2007). Glycerol seems to be important for maximal *Plasmodium* growth and virulence. This approach may be exploited in the search for new pathways for potential therapeutic intervention.

References

- Agre P, Saboori AM, Asimos A, Smith BL (1987) Purification and partial characterization of the M_r 30,000 integral membrane protein associated with the erythrocyte Rh(D) antigen. *J Biol Chem* 262:17497–17503
- Agre P, Sasaki S, Chrispeels MJ (1993) Aquaporins, a family of membrane water channels. *Am J Physiol* 265:F461
- Amiry-Moghaddam M, Williamson A, Palomba M, Eid T, de Lanerolle NC, Nagelhus EA, Adams ME, Froehner SC, Agre P, Ottersen OP (2003) Delayed K^+ clearance associated with aquaporin-4 mislocalization: phenotypic defects in brains of alpha-syntrophin-null mice. *Proc Natl Acad Sci USA* 100:13615–13620
- Amiry-Moghaddam M, Xue R, Haug FM, Neely JD, Bhardwaj A, Agre P, Adams ME, Froehner SC, Mori S, Ottersen OP (2004) Alpha-syntrophin deletion removes the perivascular but not the endothelial pool of aquaporin-4 at the blood–brain barrier and delays the development of brain edema in an experimental model of acute hyponatremia. *FASEB J* 18:542–544
- Bai C, Fukuda N, Song Y, Ma T, Matthay MA, Verkman AS (1999) Lung fluid transport in aquaporin-1 and aquaporin-4 knockout mice. *J Clin Invest* 103:555–561
- Baldo GJ, Gao J, Sun X, Mathias R (2002) Intracellular Ca^{2+} concentration gradient within the lens. *Invest Ophthalmol Vis Sci* 43:3539
- Benga G, Popescu O, Pop VI, Holmes RP (1986) *p*-(Chloromercuri)benzenesulfonate binding by membrane proteins and the inhibition of water transport in human erythrocytes. *Biochemistry* 25:1535–1538
- Beroukas D, Hiscock J, Gannon BJ, Jonsson R, Gordon TP, Waterman SA (2002) Selective down-regulation of aquaporin-1 in salivary glands in primary Sjögren's syndrome. *Lab Invest* 82:1547–1552
- Berry V, Francis P, Kaushal S, Moore A, Bhattacharya S (2000) Missense mutations in MIP underlie autosomal dominant 'polymorphic' and lamellar cataracts linked to 12q. *Nat Genet* 25:15–17
- Bhattacharjee H, Carbrey J, Rosen BP, Mukhopadhyay R (2004) Drug uptake and pharmacological modulation of drug sensitivity in leukemia by AQP9. *Biochem Biophys Res Commun* 322:836–841
- Bienert GP, Møller AL, Kristiansen KA, Schulz A, Møller IM, Schjoerring JK, Jahn TP (2007) Specific aquaporins facilitate the diffusion of hydrogen peroxide across membranes. *J Biol Chem* 282:1183–1192
- Binder DK, Oshio K, Ma T, Verkman AS, Manley GT (2004) Increased seizure threshold in mice lacking aquaporin-4 water channels. *Neuroreport* 15:259–262
- Binder DK, Yao X, Zador Z, Sick TJ, Verkman AS, Manley GT (2006) Increased seizure duration and slowed potassium kinetics in mice lacking aquaporin-4 water channels. *Glia* 53:631–636
- Boassa D, Stamer WD, Yool AJ (2006) Ion channel function of aquaporin-1 natively expressed in choroid plexus. *J Neurosci* 26:7811–7819

- Borgnia M, Nielsen S, Engel A, Agre P (1999) Cellular and molecular biology of the aquaporin water channels. *Annu Rev Biochem* 68:425–458
- Calamita G, Mazzone A, Bizzoca A, Cavalier A, Cassano G, Thomas D, Svelto M (2001) Expression and immunolocalization of the aquaporin-8 water channel in rat gastrointestinal tract. *Eur J Cell Biol* 80:711–719
- Carbrey JM, Gorelick-Feldman DA, Kozono D, Praetorius J, Nielsen S, Agre P (2003) Aquaglyceroporin AQP9: solute permeation and metabolic control of expression in liver. *Proc Natl Acad Sci USA* 100:2945–2950
- Chou CL, Knepper MA, Hoek AN, Brown D, Yang B, Ma T, Verkman AS (1999) Reduced water permeability and altered ultrastructure in thin descending limb of Henle in aquaporin-1 null mice. *J Clin Invest* 103:491–496
- Daily JP, Scanfled D, Pochet N, Le Roch K, Plouffe D, Kamal M, Sarr O, Mboup S, Ndir O, Wypij D, Levasseur K, Thomas E, Tamayo P, Dong C, Zhou Y, Lander ES, Ndiaye D, Wirth D, Winzeler EA, Mesirov JP, Regev A (2007) Distinct physiological states of *Plasmodium falciparum* in malaria-infected patients. *Nature* 450:1091–1095
- Deen PM, Verdijk MA, Knoers NV, Wieringa B, Monnens LA, van Os CH, van Oost BA (1994) Requirement of human renal water channel aquaporin-2 for vasopressin-dependent concentration of urine. *Science* 264:92–95
- Denker BM, Smith BL, Kuhajda FP, Agre P (1988) Identification, purification, and characterization of a novel M_r 28,000 integral membrane protein from erythrocytes and renal tubules. *J Biol Chem* 263:15634–15642
- Dunia I, Manenti S, Rousselet A, Benedetti EL (1987) Electron microscopic observations of reconstituted proteoliposomes with the purified major intrinsic membrane protein of eye lens fibers. *J Cell Biol* 105:1679–1689
- Ecelbarger CA, Terris J, Frindt G, Echevarria M, Marples D, Nielsen S, Knepper MA (1995) Aquaporin-3 water channel localization and regulation in rat kidney. *Am J Physiol* 269:F663–F672
- Echevarria M, Windhager EE, Tate SS, Frindt G (1994) Cloning and expression of AQP3, a water channel from medullary collecting duct of rat kidney. *Proc Natl Acad Sci USA* 91:10997–11001
- Eid T, Lee TS, Thomas MJ, Amiry-Moghaddam M, Bjørnsen LP, Spencer DD, Agre P, Ottersen OP, de Lanerolle NC (2005) Loss of perivascular aquaporin 4 may underlie deficient water and K^+ homeostasis in the human epileptogenic hippocampus. *Proc Natl Acad Sci USA* 102:1193–1198
- Endeward V, Musa-Aziz R, Cooper GJ, Chen LM, Pelletier MF, Virkki LV, Supuran CT, King LS, Boron WF, Gros G (2006) Evidence that aquaporin 1 is a major pathway for CO_2 transport across the human erythrocyte membrane. *FASEB J* 20:1974–1981
- Fotiadis D, Hasler L, Muller DJ, Stahlberg H, Kistler J, Engel A (2000) Surface tongue-and-groove contours on lens MIP facilitate cell-to-cell adherence. *J Mol Biol* 300:779–789
- Frigeri A, Gropper M, Turck CW, Verkman AS (1995) Immunolocalization of the mercurial-insensitive water channel and glycerol intrinsic protein in epithelial cell plasma membranes. *Proc Natl Acad Sci USA* 92:4328–4331
- Frydenlund DS, Bhardwaj A, Otsuka T, Mylonakou MN, Yasumura T, Davidson KG, Zeynalov E, Skare O, Laake P, Haug FM, Rash JE, Agre P, Ottersen OP, Amiry-Moghaddam M (2006) Temporary loss of perivascular aquaporin-4 in neocortex after transient middle cerebral artery occlusion in mice. *Proc Natl Acad Sci USA* 103:13532–13536
- Fu D, Libson A, Miercke LJ, Weitzman C, Nollert P, Krucinski J, Stroud RM (2000) Structure of a glycerol-conducting channel and the basis for its selectivity. *Science* 290:481–486
- Fujiwara TM, Bichet DG (2005) Molecular biology of hereditary diabetes insipidus. *J Am Soc Nephrol* 16:2836–2846
- Fushimi K, Uchida S, Hara Y, Hirata Y, Marumo F, Sasaki S (1993) Cloning and expression of apical membrane water channel of rat kidney collecting tubule. *Nature* 361:549–552
- Fushimi K, Sasaki S, Marumo F (1997) Phosphorylation of serine 256 is required for cAMP-dependent regulatory exocytosis of the aquaporin-2 water channel. *J Biol Chem* 272:14800–14804

- Garcia F, Kierbel A, Larocca MC, Gradilone SA, Splinter P, LaRusso NF, Marinelli RA (2001) The water channel aquaporin-8 is mainly intracellular in rat hepatocytes, and its plasma membrane insertion is stimulated by cyclic AMP. *J Biol Chem* 276:12147–12152
- Geyer DD, Spence MA, Johannes M, Flodman P, Clancy KP, Berry R, Sparkes RS, Jonsen MD, Isenberg SJ, Bateman JB (2006) Novel single-base deletional mutation in major intrinsic protein (MIP) in autosomal dominant cataract. *Am J Ophthalmol* 141:761–763
- Gonen T, Cheng Y, Sliz P, Hiroaki Y, Fujiyoshi Y, Harrison SC, Walz T (2005) Lipid-protein interactions in double-layered two-dimensional AQP0 crystals. *Nature* 438:633–638
- Gorin MB, Yancey SB, Cline J, Revel JP, Horwitz J (1984) The major intrinsic protein (MIP) of the bovine lens fiber membrane. *Cell* 39:49–59
- Gourbal B, Sonuc N, Bhattacharjee H, Legare D, Sundar S, Ouellette M, Rosen BP, Mukhopadhyay R (2004) Drug uptake and modulation of drug resistance in *Leishmania* by an aquaglyceroporin. *J Biol Chem* 279:31010–31017
- Gradilone SA, Garcia F, Huebert RC, Tietz PS, Larocca MC, Kierbel A, Carreras FI, LaRusso NF, Marinelli RA (2003) Glucagon induces the plasma membrane insertion of functional aquaporin-8 water channels in isolated rat hepatocytes. *Hepatology* 37:1435–1441
- Gresz V, Kwon TH, Gong H, Agre P, Steward MC, King LS, Nielsen S (2004) Immunolocalization of AQP-5 in rat parotid and submandibular salivary glands after stimulation or inhibition of secretion in vivo. *Am J Physiol Gastrointest Liver Physiol* 287:G151–G161
- Gu F, Zhai H, Li D, Zhao L, Li C, Huang S, Ma X (2007) A novel mutation in major intrinsic protein of the lens gene (MIP) underlies autosomal dominant cataract in a Chinese family. *Mol Vis* 13:1651–1656
- Hamann S, Zeuthen T, la Cour M, Nagelhus E, Ottersen OP, Agre P, Nielsen S (1998) Aquaporins in complex tissues. III. Distribution of aquaporins 1–5 in human and rat eye. *Am J Physiol* 274:C1332–C1345
- Hara M, Verkman AS (2003) Glycerol replacement corrects defective skin hydration, elasticity, and barrier function in aquaporin-3-deficient mice. *Proc Natl Acad Sci USA* 100:7360–7365
- Hara M, Ma T, Verkman AS (2002) Selectively reduced glycerol in skin of aquaporin-3-deficient mice may account for impaired skin hydration, elasticity, and barrier recovery. *J Biol Chem* 277:46616–46621
- Hara-Chikuma M, Sohara E, Rai T, Ikawa M, Okabe M, Sasaki S, Uchida S, Verkman AS (2005) Progressive adipocyte hypertrophy in aquaporin-7-deficient mice: adipocyte glycerol permeability as a novel regulator of fat accumulation. *J Biol Chem* 280:15493–15496
- Harries WE, Akhavan D, Miercke LJ, Khademi S, Stroud RM (2004) The channel architecture of aquaporin 0 at a 2.2-Å resolution. *Proc Natl Acad Sci USA* 101:14045–14050
- Harris HW, Wade JB, Handler JS (1988) Identification of specific apical membrane polypeptides associated with the antidiuretic hormone-elicited water permeability increase in the toad urinary bladder. *Proc Natl Acad Sci USA* 85:1942–1946
- Hasler L, Walz T, Tittmann P, Gross H, Kistler J, Engel A (1998) Purified lens major intrinsic protein (MIP) forms highly ordered tetragonal two-dimensional arrays by reconstitution. *J Mol Biol* 279:855–864
- Hediger MA, Coady JM, Ikeda TS, Wright EM (1987) Expression cloning and cDNA sequencing of the Na⁺/glucose co-transporter. *Nature* 330:379–381
- Herrera M, Garvin JL (2007) Novel role of AQP-1 in NO-dependent vasorelaxation. *Am J Physiol Renal Physiol* 292:F1443–F1451
- Herrera M, Hong NJ, Garvin JL (2006) Aquaporin-1 transports NO across cell membranes. *Hypertension* 48:157–164
- Hibuse T, Maeda N, Funahashi T, Yamamoto K, Nagasawa A, Mizunoya W, Kishida K, Inoue K, Kuriyama H, Nakamura T, Fushiki T, Kihara S, Shimomura I (2005) Aquaporin 7 deficiency is associated with development of obesity through activation of adipose glycerol kinase. *Proc Natl Acad Sci USA* 102:10993–10998
- Huebert RC, Splinter PL, Garcia F, Marinelli RA, LaRusso NF (2002) Expression and localization of aquaporin water channels in rat hepatocytes. *J Biol Chem* 277:22710–22717

- Hurley PT, Ferguson CJ, Kwon TH, Anderson ML, Norman AG, Steward MC, Nielsen S, Case RM (2001) Expression and immunolocalization of aquaporin water channels in rat exocrine pancreas. *Am J Physiol Gastrointest Liver Physiol* 280:G701–G709
- Ikeda M, Beitz E, Kozono D, Guggino WB, Agre P, Yasui M (2002) Characterization of aquaporin-6 as a nitrate channel in mammalian cells. Requirement of pore-lining residue threonine 63. *J Biol Chem* 277:39873–39879
- Ishibashi K, Sasaki S, Fushimi K, Uchida S, Kuwahara M, Marumo F (1994) Molecular cloning and expression of a member of the aquaporin family with permeability to glycerol and urea in addition to water expressed at the basolateral membrane of kidney collecting duct cells. *Proc Natl Acad Sci USA* 91:6269–6273
- Ishibashi K, Kuwahara M, Gu Y, Kageyama Y, Tohsaka A, Suzuki F, Marumo F, Sasaki S (1997) Cloning and functional expression of a new water channel abundantly expressed in the testis permeable to water, glycerol, and urea. *J Biol Chem* 272:20782–20786
- Ishibashi K, Kuwahara M, Gu Y, Tanaka Y, Marumo F, Sasaki S (1998) Cloning and functional expression of a new aquaporin (AQP9) abundantly expressed in the peripheral leukocytes permeable to water and urea, but not to glycerol. *Biochem Biophys Res Commun* 244:268–274
- Ishibashi K, Morinaga T, Kuwahara M, Sasaki S, Imai M (2002) Cloning and identification of a new member of water channel (AQP10) as an aquaglyceroporin. *Biochim Biophys Acta* 1576:335–340
- Ishikawa Y, Eguchi T, Skowronski MT, Ishida H (1998) Acetylcholine acts on M3 muscarinic receptors and induces the translocation of aquaporin 5 water channel via cytosolic Ca^{2+} elevation in rat parotid glands. *Biochem Biophys Res Commun* 245:835–840
- Ishikawa Y, Yuan Z, Inoue N, Skowronski MT, Nakae Y, Shono M, Cho G, Yasui M, Agre P, Nielsen S (2005) Identification of AQP5 in lipid rafts and its translocation to apical membranes by activation of M3 mAChRs in interlobular ducts of rat parotid gland. *Am J Physiol Cell Physiol* 289:C1303–C1311
- Jahn TP, Møller AL, Zeuthen T, Holm LM, Klaerke DA, Mohsin B, Kühlbrandt W, Schjoerring JK (2004) Aquaporin homologues in plants and mammals transport ammonia. *FEBS Lett* 574:31–36
- Jung JS, Preston GM, Smith BL, Guggino WB, Agre P (1994) Molecular structure of the water channel through aquaporin CHIP: The hourglass model. *J Biol Chem* 269:14648–14654
- Kachadorian WA, Wade JB, DiScala VA (2000) Vasopressin: Induced structural changes in toad bladder luminal membrane. *J Am Soc Nephrol* 11:376–380
- Kamsteeg EJ, Heijnen I, van Os CH, Deen PM (2000) The subcellular localization of an aquaporin-2 tetramer depends on the stoichiometry of phosphorylated and nonphosphorylated monomers. *J Cell Biol* 151:919–930
- Kamsteeg EJ, Hendriks G, Boone M, Konings IB, Oorschot V, van der Sluijs P, Klumperman J, Deen PM (2006) Short-chain ubiquitination mediates the regulated endocytosis of the aquaporin-2 water channel. *Proc Natl Acad Sci USA* 103:18344–18349
- Katsura T, Gustafson CE, Ausiello DA, Brown D (1997) Protein kinase A phosphorylation is involved in regulated exocytosis of aquaporin-2 in transfected LLC-PK1 cells. *Am J Physiol Renal Physiol* 272:F816–F822
- Kim SW, Gresz V, Rojek A, Wang W, Verkman AS, Frøkiaer J, Nielsen S (2005) Decreased expression of AQP2 and AQP4 water channels and Na,K-ATPase in kidney collecting duct in AQP3 null mice. *Biol Cell* 97:765–778
- Kimelberg HK (1995) Current concepts of brain edema. Review of laboratory investigations. *J Neurosurg* 83:1051–1059
- King LS, Nielsen S, Agre P (1996) Aquaporin-1 water channel protein in lung: Ontogeny, steroid-induced expression, and distribution in rat. *J Clin Invest* 97:2183–2191
- King LS, Choi M, Fernandez PC, Cartron JP, Agre P (2001) Defective urinary-concentrating ability due to a complete deficiency of aquaporin-1. *N Engl J Med* 345:175–179
- King LS, Nielsen S, Agre P, Brown RH (2002) Decreased pulmonary vascular permeability in aquaporin-1 null humans. *Proc Natl Acad Sci USA* 99:1059–1063

- Kondo H, Shimomura I, Kishida K, Kuriyama H, Makino Y, Nishizawa H, Matsuda M, Maeda N, Nagaretani H, Kihara S, Kurachi Y, Nakamura T, Funahashi T, Matsuzawa Y (2002) Human aquaporin adipose (*AQPap*) gene. Genomic structure, promoter analysis and functional mutation. *Eur J Biochem* 269:1814–1826
- Koyama Y, Yamamoto T, Kondo D, Funaki H, Yaoita E, Kawasaki K, Sato N, Hatakeyama K, Kihara I (1997) Molecular cloning of a new aquaporin from rat pancreas and liver. *J Biol Chem* 272:30329–30333
- Krane CM, Fortner CN, Hand AR, McGraw DW, Lorenz JN, Wert SE, Towne JE, Paul RJ, Whitsett JA, Menon AG (2001a) Aquaporin 5-deficient mouse lungs are hyperresponsive to cholinergic stimulation. *Proc Natl Acad Sci USA* 98:14114–14119
- Krane CM, Melvin JE, Nguyen HV, Richardson L, Towne JE, Doetschman T, Menon AG (2001b) Salivary acinar cells from aquaporin 5-deficient mice have decreased membrane water permeability and altered cell volume regulation. *J Biol Chem* 276:23413–23420
- Lee TC, Ho IC, Lu WJ, Huang JD (2006) Enhanced expression of multidrug resistance-associated protein 2 and reduced expression of aquaglyceroporin 3 in an arsenic-resistant human cell line. *J Biol Chem* 281:18401–18407
- Liu K, Kozono D, Kato Y, Agre P, Hazama A, Yasui M (2005) Conversion of aquaporin 6 from an anion channel to a water-selective channel by a single amino acid substitution. *Proc Natl Acad Sci USA* 102:2192–2197
- Liu Y, Promeneur D, Rojek A, Kumar N, Frøkiaer J, Nielsen S, King LS, Agre P, Carbrey JM (2007) Aquaporin 9 is the major pathway for glycerol uptake by mouse erythrocytes, with implications for malarial virulence. *Proc Natl Acad Sci USA* 104:12560–12564
- Liu Z, Shen J, Carbrey JM, Mukhopadhyay R, Agre P, Rosen BP (2002) Arsenite transport by mammalian aquaglyceroporins AQP7 and AQP9. *Proc Natl Acad Sci USA* 99:6053–6058
- Ma T, Frigeri A, Hasegawa H, Verkman AS (1994) Cloning of a water channel homolog expressed in brain meningeal cells and kidney collecting duct that functions as a stilbene-sensitive glycerol transporter. *J Biol Chem* 269:21845–21849
- Ma T, Yang B, Gillespie A, Carlson EJ, Epstein CJ, Verkman AS (1997a) Generation and phenotype of a transgenic knockout mouse lacking the mercurial-insensitive water channel aquaporin-4. *J Clin Invest* 100:957–962
- Ma T, Yang B, Verkman AS (1997b) Cloning of a novel water and urea-permeable aquaporin from mouse expressed strongly in colon, placenta, liver, and heart. *Biochem Biophys Res Commun* 240:324–328
- Ma T, Yang B, Gillespie A, Carlson EJ, Epstein CJ, Verkman AS (1998) Severely impaired urinary concentrating ability in transgenic mice lacking aquaporin-1 water channels. *J Biol Chem* 273:4296–4299
- Ma T, Song Y, Gillespie A, Carlson EJ, Epstein CJ, Verkman AS (1999) Defective secretion of saliva in transgenic mice lacking aquaporin-5 water channels. *J Biol Chem* 274:20071–20074
- Ma T, Song Y, Yang B, Gillespie A, Carlson EJ, Epstein CJ, Verkman AS (2000) Nephrogenic diabetes insipidus in mice lacking aquaporin-3 water channels. *Proc Natl Acad Sci USA* 97:4386–4391
- Ma T, Hara M, Sougrat R, Verbavatz JM, Verkman AS (2002) Impaired stratum corneum hydration in mice lacking epidermal water channel aquaporin-3. *J Biol Chem* 277:17147–17153
- Macey RI (1984) Transport of water and urea in red blood cells. *Am J Physiol* 246:C195–C203
- Maeda N, Funahashi T, Hibuse T, Nagasawa A, Kishida K, Kuriyama H, Nakamura T, Kihara S, Shimomura I, Matsuzawa Y (2004) Adaptation to fasting by glycerol transport through aquaporin 7 in adipose tissue. *Proc Natl Acad Sci USA* 101:17801–17806
- Manley GT, Fujimura M, Ma T, Noshita N, Filiz F, Bollen AW, Chan P, Verkman AS (2000) Aquaporin-4 deletion in mice reduces brain edema after acute water intoxication and ischemic stroke. *Nat Med* 6:159–163
- Marinelli RA, Pham L, Agre P, LaRusso NF (1997) Secretin promotes osmotic water transport in rat cholangiocytes by increasing aquaporin-1 water channels in plasma membrane. *J Biol Chem* 272:12984–12988

- Marinelli RA, Tietz PS, Pham LD, Rueckert L, Agre P, LaRusso NF (1999) Secretin induces the apical insertion of aquaporin-1 water channels in rat cholangiocytes. *Am J Physiol Gastrointest Liver Physiol* 276:G280–G286
- Marrades MP, Milagro FI, Martinez JA, Moreno-Aliaga MJ (2006) Differential expression of aquaporin 7 in adipose tissue of lean and obese high fat consumers. *Biochem Biophys Res Commun* 339:785–789
- Mathias RT, Riquelme G, Rae JL (1991) Cell to cell communication and pH in the frog lens. *J Gen Physiol* 98:1085–1103
- Matsuzaki T, Suzuki T, Koyama H, Tanaka S, Takata K (1999) Water channel protein AQP3 is present in epithelia exposed to the environment of possible water loss. *J Histochem Cytochem* 47:1275–1286
- Moore M, Ma T, Yang B, Verkman AS (2000) Tear secretion by lacrimal glands in transgenic mice lacking water channels AQP1, AQP3, AQP4 and AQP5. *Exp Eye Res* 70:557–562
- Mulders SM, Preston GM, Deen PM, Guggino WB, van Os CH, Agre P (1995) Water channel properties of major intrinsic protein of lens. *J Biol Chem* 270:9010–9016
- Murata K, Mitsuoka K, Hirai T, Walz T, Agre P, Heymann JB, Engel A, Fujiyoshi Y (2000) Structural determinants of water permeation through aquaporin-1. *Nature* 407:599–605
- Nakhoul NL, Davis BA, Romero MF, Boron WF (1998) Effect of expressing the water channel aquaporin-1 on the CO₂ permeability of *Xenopus* oocytes. *Am J Physiol* 274:C543–C548
- Nejsum LN, Kwon TH, Jensen UB, Fumagalli O, Frøkiaer J, Krane CM, Menon AG, King LS, Agre PC, Nielsen S (2002) Functional requirement of aquaporin-5 in plasma membrane of sweat glands. *Proc Natl Acad Sci USA* 99:511–516
- Nemeth-Cahalan KL, Hall JE (2000) pH and calcium regulate the water permeability of aquaporin 0. *J Biol Chem* 275:6777–6782
- Nemeth-Cahalan KL, Kalman K, Froger A, Hall JE (2007) Zinc modulation of water permeability reveals that Aquaporin 0 functions as a cooperative tetramer. *J Gen Physiol* 130:457–464
- Nielsen S, DiGiovanni SR, Christensen EI, Knepper MA, Harris HW (1993a) Cellular and subcellular immunolocalization of vasopressin-regulated water channel in rat kidney. *Proc Natl Acad Sci USA* 90:11663–11667
- Nielsen S, Smith BL, Christensen EI, Agre P (1993b) Distribution of the aquaporin CHIP in secretory and resorptive epithelia and capillary endothelia. *Proc Natl Acad Sci USA* 90:7275–7279
- Nielsen S, Smith BL, Christensen EI, Knepper MA, Agre P (1993c) CHIP28 water channels are localized in constitutively water-permeable segments of the nephron. *J Cell Biol* 120:371–383
- Nielsen S, Chou CL, Marples D, Christensen EI, Kishore BK, Knepper MA (1995a) Vasopressin increases water permeability of kidney collecting duct by inducing translocation of aquaporin-CD water channels to plasma membrane. *Proc Natl Acad Sci USA* 92:1013–1017
- Nielsen S, Pallone TL, Smith B, Christensen EI, Agre P, Maunsbach AB (1995b) Aquaporin CHIP water channels in short and long loop descending thin limb and in descending vasa recta in rat kidney. *Am J Physiol* 268:F1023–F1037
- Nielsen S, King LS, Christensen BM, Agre P (1997a) Aquaporins in complex tissues. II. Subcellular distribution in respiratory and glandular tissues of rat. *Am J Physiol* 273:C1549–C1561
- Nielsen S, Nagelhus EA, Amiry-Moghaddam M, Bourque C, Agre P, Ottersen OP (1997b) Specialized membrane domains for water transport in glial cells: high-resolution immunogold cytochemistry of aquaporin-4 in rat brain. *J Neurosci* 17:171–180
- Oshio K, Watanabe H, Song Y, Verkman AS, Manley GT (2005) Reduced cerebrospinal fluid production and intracranial pressure in mice lacking choroid plexus water channel Aquaporin-1. *FASEB J* 19:76–78
- Pallone TL, Edwards A, Ma T, Silldorff EP, Verkman AS (2000) Requirement of aquaporin-1 for NaCl-driven water transport across descending vasa recta. *J Clin Invest* 105:215–222
- Papadopoulos MC, Verkman AS (2005) Aquaporin-4 gene disruption in mice reduces brain swelling and mortality in pneumococcal meningitis. *J Biol Chem* 280:13906–13912
- Papadopoulos MC, Verkman AS (2007) Aquaporin-4 and brain edema. *Pediatr Nephrol* 22:778–784
- Papadopoulos MC, Manley GT, Krishna S, Verkman AS (2004) Aquaporin-4 facilitates reabsorption of excess fluid in vasogenic brain edema. *FASEB J* 18:1291–1293

- Prasad GV, Coury LA, Finn F, Zeidel ML (1998) Reconstituted aquaporin 1 water channels transport CO₂ across membranes. *J Biol Chem* 273:33123–33126
- Preston GM, Agre P (1991) Isolation of the cDNA for erythrocyte integral membrane protein of 28 kilodaltons: Member of an ancient channel family. *Proc Natl Acad Sci USA* 88:11110–11114
- Preston GM, Carroll T, Guggino WB, Agre P (1992) Appearance of water channels in *Xenopus* oocytes expressing red cell CHIP28 protein. *Science* 256:385–387
- Promeneur D, Liu Y, Maciel J, Agre P, King LS, Kumar N (2007) Aquaglyceroporin PbAQP during intraerythrocytic development of the malaria parasite *Plasmodium berghei*. *Proc Natl Acad Sci USA* 104:2211–2216
- Rash JE, Yasumura T, Hudson CS, Agre P, Nielsen S (1998) Direct immunogold labeling of aquaporin-4 in square arrays of astrocyte and ependymocyte plasma membranes in rat brain and spinal cord. *Proc Natl Acad Sci USA* 95:11981–11986
- Rojek A, Führtbauer EM, Kwon TH, Frøkiaer J, Nielsen S (2006) Severe urinary concentrating defect in renal collecting duct-selective AQP2 conditional-knockout mice. *Proc Natl Acad Sci USA* 103:6037–6042
- Rojek AM, Skowronski MT, Führtbauer EM, Führtbauer AC, Fenton RA, Agre P, Frøkiaer J, Nielsen S (2007) Defective glycerol metabolism in aquaporin 9 (AQP9) knockout mice. *Proc Natl Acad Sci USA* 104:3609–3614
- Saadoun S, Papadopoulos MC, Hara-Chikuma M, Verkman AS (2005a) Impairment of angiogenesis and cell migration by targeted aquaporin-1 gene disruption. *Nature* 434:786–792
- Saadoun S, Papadopoulos MC, Watanabe H, Yan D, Manley GT, Verkman AS (2005b) Involvement of aquaporin-4 in astroglial cell migration and glial scar formation. *J Cell Sci* 118:5691–5698
- Saboori AM, Smith BL, Agre P (1988) Polymorphism in the M_r 32,000 Rh protein purified from Rh(D)-positive and -negative erythrocytes. *Proc Natl Acad Sci USA* 85:4042–4045.
- Sanders OI, Rensing C, Kuroda M, Mitra B, Rosen BP (1997) Antimonite is accumulated by the glycerol facilitator GlpF in *Escherichia coli*. *J Bacteriol* 179:3365–3367
- Saparov SM, Liu K, Agre P, Pohl P (2007) Fast and selective ammonia transport by aquaporin-8. *J Biol Chem* 282:5296–5301
- Savage DF, Egea PF, Robles-Colmenares Y, O'Connell JD III, Stroud RM (2003) Architecture and selectivity in aquaporins: 2.5 Å X-ray structure of aquaporin Z. *PLoS Biol* 1:334–340
- Schnermann J, Chou CL, Ma T, Traynor T, Knepper MA, Verkman AS (1998) Defective proximal tubular fluid reabsorption in transgenic aquaporin-1 null mice. *Proc Natl Acad Sci USA* 95:9660–9664
- Shiels A, Bassnett S (1996) Mutations in the founder of the MIP gene family underlie cataract development in the mouse. *Nature* 12:212–215
- Smith BL, Agre P (1991) Erythrocyte M_r 28,000 transmembrane protein exists as a multisubunit oligomer similar to channel proteins. *J Biol Chem* 266:6407–6415
- Solomon AK (1968) Characterization of biological membranes by equivalent pores. *J Gen Physiol* 51:S335–S364
- Song Y, Verkman AS (2001) Aquaporin-5 dependent fluid secretion in airway submucosal glands. *J Biol Chem* 276:41288–41292
- Song Y, Sonawane N, Verkman AS (2002) Localization of aquaporin-5 in sweat glands and functional analysis using knockout mice. *J Physiol* 541:561–568
- Steinfeld S, Cogan E, King LS, Agre P, Kiss R, Delporte C (2001) Abnormal distribution of aquaporin-5 water channel protein in salivary glands from Sjögren's syndrome patients. *Lab Invest* 81:143–148
- Sui H, Han BG, Lee JK, Walian P, Jap BK (2001) Structural basis of water-specific transport through the AQP1 water channel. *Nature* 414:872–878
- Tada J, Sawa T, Yamanaka N, Shono M, Akamatsu T, Tsumura K, Parvin MN, Kanamori N, Hosoi K (1999) Involvement of vesicle-cytoskeleton interaction in AQP5 trafficking in AQP5-gene-transfected HSG cells. *Biochem Biophys Res Commun* 266:443–447
- Terris J, Ecelbarger CA, Marples D, Knepper MA, Nielsen S (1995) Distribution of aquaporin-4 water channel expression within rat kidney. *Am J Physiol* 269:F775–F785

- Tsubota K, Hirai S, King LS, Agre P, Ishida N (2001) Defective cellular trafficking of lacrimal gland aquaporin-5 in Sjögren's syndrome. *Lancet* 357:688–689
- Tsukaguchi H, Shayakul C, Berger UV, Mackenzie B, Devidas S, Guggino WM, van Hoek AN, Hediger MA (1998) Molecular characterization of a broad selectivity neutral solute channel. *J Biol Chem* 273:24737–24743
- Umenishi F, Carter EP, Yang B, Oliver B, Matthay MA, Verkman AS (1996) Sharp increase in rat lung water channel expression in the perinatal period. *Am J Respir Cell Mol Biol* 15:673–679
- Ussing HH (1965) Transport of electrolytes and water across epithelia. *Harvey Lect* 59:1–30
- Van Balkom BWM, Savelkoul PJ, Markovich D, Hofman E, Nielsen S, van der Sluijs P, Deen PMT (2002) The role of putative phosphorylation sites in the targeting and shuttling of the aquaporin-2 water channel. *J Biol Chem* 277:41473–41479
- van Hoek AN, Hom ML, Luthjens LH, de Jong MD, Dempster JA, van Os CH (1991) Functional unit of 30-kDa for proximal tubule water channels as revealed by radiation inactivation. *J Biol Chem* 266:16633–16635
- van Os CH, Deen PMT, Dempster JA (1994) Aquaporins: water selective channels in biological membranes. *Biochim Biophys Acta* 1197:291–309
- Varadaraj K, Kumari S, Shiels A, Mathias RT (2005) Regulation of aquaporin water permeability in the lens. *Invest Ophthalmol Vis Sci* 46:1393–1402
- Verbavatz JM, Brown D, Sabolic I, Valenti G, Ausiello DA, van Hoek AN, Ma T, Verkman AS (1993) Tetrameric assembly of CHIP28 water channels in liposomes and cell membranes: a freeze-fracture study. *J Cell Biol* 123:605–618
- Vial HJ, Ancelin ML, Thuet MJ, Philippot JR (1989) Phospholipid metabolism in Plasmodium-infected erythrocytes: guidelines for further studies using radioactive precursor incorporation. *Parasitology* 98:351–357
- Wade JB, Stetson DL, Lewis SA (1981) ADH action: Evidence for a membrane shuttle mechanism. *Ann NY Acad Sci* 372:106–117
- Wysocki R, Chéry CC, Wawrzycka D, Van Hulle M, Cornelis R, Thevelein JM, Tamás MJ (2001) The glycerol channel Fps1p mediates the uptake of arsenite and antimonite in *Saccharomyces cerevisiae*. *Mol Microbiol* 40:1391–1401
- Yang B, Fukuda N, van Hoek A, Matthay MA, Ma T, Verkman AS (2000) Carbon dioxide permeability of aquaporin-1 measured in erythrocytes and lung of aquaporin-1 null mice and in reconstituted proteoliposomes. *J Biol Chem* 275:2686–2692
- Yang B, Gillespie A, Carlson EJ, Epstein CJ, Verkman AS (2001) Neonatal mortality in an aquaporin-2 knock-in mouse model of recessive nephrogenic diabetes insipidus. *J Biol Chem* 276:2775–2779
- Yang B, Zhao D, Solenov E, Verkman AS (2006) Evidence from knockout mice against physiologically significant aquaporin 8-facilitated ammonia transport. *Am J Physiol Cell Physiol* 291:C417–C423
- Yasui M, Hazama A, Kwon TH, Nielsen S, Guggino WB, Agre P (1999a) Rapid gating and anion permeability of an intracellular aquaporin. *Nature* 402:184–187
- Yasui M, Kwon TH, Knepper MA, Nielsen S, Agre P (1999b) Aquaporin 6: an intracellular vesicle water channel protein in renal epithelia. *Proc Natl Acad Sci USA* 96:5808–5813
- Zeidel ML, Ambudkar SV, Smith BL, Agre P (1992) Reconstitution of functional water channels in liposomes containing purified red cell CHIP28 protein. *Biochemistry* 31:7436–7440
- Zeidel ML, Nielsen S, Smith BL, Ambudkar SV, Maunsbach AB, Agre P (1994) Ultrastructure, pharmacologic inhibition, and transport-selectivity of aquaporin CHIP in proteoliposomes. *Biochemistry* 33:1606–1615
- Zelenina M, Bondar AA, Zelenin S, Aperia A (2003) Nickel and extracellular acidification inhibit the water permeability of human aquaporin-3 in lung epithelial cells. *J Biol Chem* 278:30037–30043
- Zelenina M, Tritto S, Bondar AA, Zelenin S, Aperia A (2004) Copper inhibits the water and glycerol permeability of aquaporin-3. *J Biol Chem* 279:51939–51943
- Zeuthen T, Klaerke DA (1999) Transport of water and glycerol in Aquaporin 3 is gated by H⁺. *J Biol Chem* 274:21631–21636

- Zeuthen T, Wu B, Pavlovic-Djuranovic S, Holm LM, Uzcategui NL, Duszenko M, Kun JF, Schultz JE, Beitz E (2006) Ammonia permeability of the aquaglyceroporins from *Plasmodium falciparum*, *Toxoplasma gondii* and *Trypanosoma brucei*. *Mol Microbiol* 61:1598–1608
- Zhang D, Vetrivel L, Verkman AS (2002) Aquaporin deletion in mice reduces intraocular pressure and aqueous fluid production. *J Gen Physiol* 119:561–569
- Zhang R, Logee KA, Verkman AS (1990) Expression of mRNA coding for kidney and red cell water channels in *Xenopus* oocytes. *J Biol Chem* 265:15375–15378

Part I
Aquaporin Protein Structure
and Selectivity Mechanisms

The AQP Structure and Functional Implications

Thomas Wspalz, Yoshinori Fujiyoshi, and Andreas Engel

Contents

1	Introduction	32
2	Mammalian and Plant AQP Subfamilies	33
2.1	Functional Characterization	36
3	The Structure of AQPs	37
3.1	The AQP Fold	38
3.2	The Structure of the Pore	38
3.3	Surface Structure of AQPs Involved in Membrane Junctions	41
4	Unsolved Riddles	45
4.1	AQP Trafficking	45
4.2	AQP Gating	48
4.3	Anion Transport	49
4.4	Gas Transport	50
5	Perspectives	51
	References	51

Abstract Progress in the structure determination of AQPs has led to a deep understanding of water and solute permeation by these small integral membrane proteins. The atomic structures now available have allowed the water permeation and exclusion of protons to be monitored by molecular dynamics simulations, and have provided a framework for assessing the water and solute permeation in great detail by site-directed mutations. In spite of this, further structural and molecular dynamics analyses are required to elucidate the basis for regulation as well as for gas permeation, processes that are still to be deciphered.

A. Engel (✉)

Maurice E. Müller Institute for Structural Biology, Biozentrum, University of Basel, 4056 Basel, Switzerland
andreas.engel@unibas.ch

E. Beitz (ed.), *Aquaporins*, Handbook of Experimental Pharmacology 190,
© Springer-Verlag Berlin Heidelberg 2009

31

1 Introduction

Aquaporins (AQPs) represent an ancient family of small (≈ 30 kDa) ubiquitous membrane channels that facilitate the permeation of water (aquaporins) and small, uncharged solutes (aquaglyceroporins) (Heymann and Engel 2000; Zardoya 2005). These proteins are present in all kingdoms of life, demonstrating their central role in maintaining normal physiology of all organisms. In unicellular organisms, such as archaea, bacteria, or yeast only a few aquaporin genes are present, encoding water channels and glycerol facilitators. However, more aquaporin genes are found in the genomes of multicellular organisms: *Arabidopsis thaliana* contains 38 putative AQP genes (Maurel 2007), while the human body expresses 13 aquaporins with specific organ, tissue, and cellular localization (Magni et al. 2006). Thus, different members of the AQP family are expected to function in virtually all physiological processes that involve water transport across the membrane.

Since the first demonstration of aquaporin-1 (AQP1) from human red blood cells as a *bona fide* water channel (Preston et al. 1992), more than 450 individual AQPs have been identified and many family members are being functionally and structurally studied. Early biophysical characterizations and sequence analysis of the major intrinsic protein (MIP; now known as AQP0) (Gorin et al. 1984) of lens fiber cell membranes and AQP1 (Preston and Agre 1991) indicated that these channels consist of six α -helical membrane-spanning segments and connecting loops of variable length. The intriguing homology between the first and second half of AQPs suggests an early gene duplication event. As a result of each half containing three transmembrane domains, the two halves must integrate in the membrane in opposite orientations, a basic structural property of the AQP membrane channels that relates to their internal pseudo two-fold symmetry. Another key feature concerns the long loops between helices 2 (H2) and H3 (loop B), and between H5 and H6 (loop E), which both bear the highly conserved Asn-Pro-Ala (NPA) motif, a hallmark of AQP sequences. Site-directed mutagenesis experiments on these loops led to the hour-glass model, predicting loops B and E to meet in the center of the membrane to form the channel (Jung et al. 1994). Over the last years the striking selectivity of these channels for the permeation of water or small solutes and the strict exclusion of protons came into the focus of research into AQPs. Apart from water and glycerol, a number of other permeants, including CO_2 , NO , H_2O_2 , NH_3 , $\text{As}(\text{OH})_3$, $\text{Sb}(\text{OH})_3$, and even $\text{Si}(\text{OH})_4$ have recently been shown to pass specific AQPs (Wu and Beitz 2007).

Electron crystallography of biologically active, two-dimensional (2D) crystals (Walz et al. 1994a) reconstituted from AQP1 in the presence of lipids provided a first low-resolution 3D structure of negatively stained preparations soon after the discovery of the water channel function (Walz et al. 1994b). Several groups used cryoelectron crystallography of unstained crystals to resolve the right-handed bundle of six α -helices at a resolution of 6–7 Å (Cheng et al. 1997; Walz et al. 1997), and as the resolution improved also the two half-helices of loop B and loop E (Mitsuoka et al. 1999). With a resolution of 4.5 Å the latter map allowed the fold of AQP1 to be predicted (de Groot et al. 2000). While steady progress in electron crystallography

eventually led to the first atomic model of AQP1 (Murata et al. 2000), the structure of the bacterial aquaglyceroporin GlpF was solved by X-ray crystallography almost at the same time (Fu et al. 2000) (Fig. 1). The subsequent X-ray structure of AQP1 at 2.2-Å resolution confirmed the model established by electron crystallography (Sui et al. 2001), and another AQP1 structure obtained by electron crystallography was published at the same time (Ren et al. 2001). Since then, the structures of several aquaporins and aquaglyceroporins have been solved, either by electron or by X-ray crystallography, the latter contributing the bulk of structural information (Savage et al. 2003; Harries et al. 2004; Lee et al. 2005; Tornroth-Horsefield et al. 2006) (Table 1). In contrast, electron crystallography is a less widely used and slower method, which has thus produced fewer structures than X-ray crystallography (Gonen et al. 2004a, 2005; Hiroaki et al. 2006). However, it has given structural information on the lipid–protein interactions for the lens water channel AQP0 at 1.9-Å resolution (Gonen et al. 2005), and has provided insight into the adhesive function of AQP0 (Gonen et al. 2004b, 2005), AQP4 (Hiroaki et al. 2006), and the plant water channel SoPIP2;1 (Kukulski et al. 2005). This progress in the structure determination of AQPs has provided the basis for a deep understanding of water and solute permeation by these small integral membrane proteins.

The atomic structures now available have made detailed molecular dynamics simulation possible (de Groot and Grubmuller 2005) (see chapter by ..., this volume), which allowed the water permeation and exclusion of protons to be monitored. In addition, these structures have given the framework for assessing the water and solute permeation in great detail by site-directed mutations (Beitz et al. 2004, 2006). In spite of this, further structural analyses are required to elucidate the basis for regulation as well as for gas and anion permeation, processes that are still to be deciphered. In this chapter we discuss both the progress in structure determination and the remaining open questions.

2 Mammalian and Plant AQP Subfamilies

Thirteen functionally and phylogenetically distinct members of the AQP family have been identified in mammals (AQP0–AQP12) on the basis of sequence homology to AQP1 (Zardoya 2005). Evolutionary comparison of mammalian AQP sequences classifies AQP0, AQP1, AQP2, AQP4, AQP5, AQP6, and AQP8 as members of the water-selective aquaporin subgroup, whereas AQP3, AQP7, AQP9, and AQP10 are evolutionarily grouped as aquaglyceroporins (Zardoya 2005; Gonen and Walz 2006; Gorelick et al. 2006). AQP11 and AQP12 are the most distantly related paralogs (Morishita et al. 2005). They share only 20% homology with AQP family members, belong to an AQP subfamily with divergent NPA boxes (Ishibashi 2006), and may constitute a third functionally distinct evolutionary branch of this channel protein superfamily (Gorelick et al. 2006; Morishita et al. 2005; Itoh et al. 2005).

Angiosperm plants possess about 35 different AQP genes (Kaldenhoff et al. 2008). Genome sequencing has identified 38 AQP genes in *Arabidopsis* (Johanson et al. 2001; Quigley et al. 2002), 33 in rice (Sakurai et al. 2005), and 36 AQP

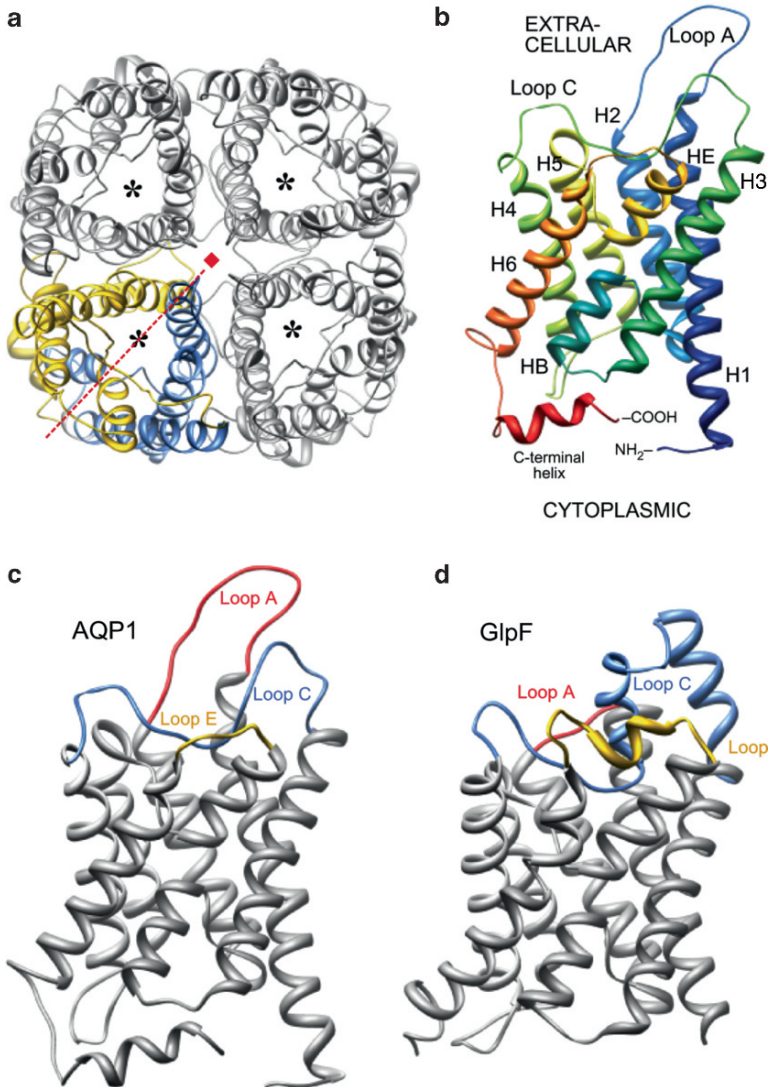


Fig. 1 The aquaporin fold. **(a)** Aquaporins and aquaglyceroporins exist as tetramers, which feature four independent pores (*). As result of a gene duplication, the monomer consists of two similar halves that are structurally related by a quasi two-fold symmetry with the symmetry axis running through the center of and parallel to the membrane (line). **(b)** The AQP1 monomer reveals the AQP fold, with H1, H2, HB, H3 forming the first half of the protein and H4, H5, HE, H6 the second half. Noteworthy are the two half-helices HB and HE that emanate from the center outward. **(c)** The extracellular surface of AQP1 exhibits a prominent loop A that connects the first and second part of the protein, and a short loop connecting HE with H6. **(d)** These features are much different in the glycerol facilitator GlpF. In contrast to AQP1, loop A is short and stretched. H3 is extended by a short helix pointing outward, forming part of loop C that contains a second helical stretch. Another distinct difference is the short helix that connects HE with H6 in GlpF, this connection being an unstructured short loop in AQP1.

Table 1 Atomic structures of AQPs

PDB ID	Protein	Organism	Function	Method & Resolution	Release date
1FQY	AQP1	Human	Water channel	EM, 3.8 Å	18-Oct-00
1FX8	GlpF	<i>E. coli</i>	Glycerol channel	X-ray, 2.2 Å	01-Nov-00
1IH5	AQP1	Human	Water channel	EM, 3.7 Å	25-Apr-01
1H6I	AQP1	Human	Water channel; refined	EM, 3.5 Å	13-Dec-01
1J4N	AQP1	Bovine	Water channel	X-ray, 2.2 Å	27-Mar-02
1LDA	GlpF; no glycerol	<i>E. coli</i>	Glycerol channel	X-ray, 2.8 Å	08-May-02
1LDF	GlpF	<i>E. coli</i>	Glycerol channel	X-ray, 2.1 Å	08-May-02
1LDI	GlpF; no glycerol	<i>E. coli</i>	Glycerol channel	X-ray, 2.7 Å	08-May-02
1RC2	AqpZ	<i>E. coli</i>	Water channel	X-ray, 2.5 Å	25-Nov-03
1YMG	AQP0	Bovine lens	Water channel	X-ray, 2.2 Å	08-Feb-05
2ABM	AqpZ	<i>E. coli</i>	Water channel	X-ray, 3.2 Å	20-Sep-05
2B6P	AQP0	Bovine lens	Water channel; open conform	X-ray, 2.4 Å	06-Dec-05
2EVU	AqpM	<i>Methanobacterium thermoauto- trophicum</i>	Water channel	X-ray, 2.3 Å	06-Dec-05
2F2B	AqpM	<i>Methanobacterium thermoauto- trophicum</i>	Water channel	X-ray, 1.7 Å	06-Dec-05
2B6O	AQP0	Bovine lens	Water channel	EM, 1.9 Å	06-Dec-05
1Z98	SoPIP2;1	Spinach	Water channel; closed conform	X-ray, 2.1 Å	20-Dec-05
2B5F	SoPIP2;1	Spinach	Water channel; open conform	X-ray, 3.9 Å	20-Dec-05
2D57	AQP4 AQP4M23	Human	Water channel	EM, 3.2 Å	31-Jan-06
2O9D	AqpZ; T183C	<i>E. coli</i>	Water channel	X-ray, 2.3 Å	13-Feb-07
2O9E	AqpZ; T183C, Hg	<i>E. coli</i>	Water channel	X-ray, 2.2 Å	13-Feb-07
2O9F	AqpZ; L170C	<i>E. coli</i>	Water channel	X-ray, 2.5 Å	13-Feb-07
2O9G	AqpZ; L170C, Hg	<i>E. coli</i>	Water channel	X-ray, 1.9 Å	13-Feb-07

isoforms in maize (Chaumont et al. 2001). Phylogenetically these proteins can be divided into four different subfamilies, which to some extent correspond to distinct subcellular localizations (Johanson et al. 2001; Quigley et al. 2002; Chaumont et al. 2001). AQPs preferentially inserted into the plasma membrane are called plasma membrane intrinsic proteins (PIPs) and those that integrate into the tonoplast are tonoplast intrinsic proteins (TIPs). PIPs are further subdivided into two phylogenetic subgroups, PIP1 and PIP2. At the sequence level, PIP1 group members have a longer N-terminal region and a shorter C-terminal region when compared with PIP2 group members (Chaumont et al. 2001), and PIP1 proteins exhibit no or very

low water channel activity compared with PIP2 proteins, when expressed in *Xenopus* oocytes. Because of their abundance, PIPs and TIPs represent central pathways for transcellular and intracellular water transport (Maurel 2007). NIP aquaporins were initially identified in nodulated roots of soybean where they are located in the peribacteroid membrane, which is a part of the plasma membrane (Niemietz and Tyerman 2000). NIPs are present in nonleguminous plants, where they have been localized in plasma and intracellular membranes (Ma et al. 2006; Mizutani et al. 2006; Takano et al. 2006). The small basic intrinsic proteins (SIP) define the fourth and least analyzed AQP subgroup in plants. They were first discovered by genome sequence analysis (Johanson and Gustavsson 2002) and are mostly localized in the endoplasmic reticulum (ER) (Ishikawa et al. 2005). In the past few years analysis of plant aquaporins *in planta* has provided further insight into function and localization. Emerging evidence suggests that PIPs are also located in organellar membranes, while TIPs can also be found in the plasma membrane. The large number of different AQP genes in plants is still enigmatic. It could indicate the contribution of different AQPs in the fine-tuning of water transport during changing environmental conditions and developmental stages or it could be related to different substrate properties of different AQP isoforms.

2.1 Functional Characterization

The osmotic water permeability of AQP family members can be characterized by expressing the candidate AQP cRNA in *Xenopus* oocytes and measuring cell volume changes upon hypotonic challenge (Preston et al. 1992). Likewise, solute (i.e., urea/glycerol) permeability can be determined by measuring solute uptake in isotonic solution. In some instances, AQP function has also been assessed in reconstituted proteoliposomes (Zeidel et al. 1992) and in vesicular 2D crystals (Walz et al. 1994a) or by expression in yeast (Lagree et al. 1998). Simultaneous measurement of water permeability and ion conductance was introduced by Pohl et al. (2001). Functionally, AQPs 0–10 support various levels of transmembrane water permeability. AQP0, AQP6, AQP9, and AQP10 show low water permeability compared with AQP1, AQP2, AQP3, AQP4, AQP5, AQP7, and AQP8. The water permeability of AQP0, AQP3, and AQP6 is affected by pH. AQP3, AQP7, AQP9, and AQP10 are also permeable to both urea and glycerol, whereas AQP8 has been reported to exhibit urea and ammonia permeability (Saparov et al. 2007). Interestingly, both AQP7 and AQP9 have been reported to facilitate arsenite uptake (Liu et al. 2002), and AQP6 functions as an anion channel, with permeability to nitrate and chloride (Ikeda et al. 2002; Yasui et al. 1999a,b). The membrane transport properties of AQP11 and AQP12 are currently unknown. While water transport of AQP11 has been demonstrated (Yakata et al. 2007), the transport properties of AQP12 remain unstudied because of the inability to obtain adequate plasma membrane expression in *Xenopus* oocytes (Itoh et al. 2005). In addition to transport of water and small solutes experimental evidence for the permeation of AQPs by CO₂ and other gas molecules has recently been presented.

A high or at least residual water activity has been observed with members of all four subclasses of plant AQPs (Takano et al. 2006; Ishikawa et al. 2005; Biela et al. 1999; Dean et al. 1999; Gerbeau et al. 1999). The water permeation in some plant AQPs was found to be regulated by phosphorylation, and/or by changes in pH. In addition, it has become increasingly clear that some of these proteins do not exhibit a strict specificity for water, but can transport a wide range of small neutral molecules, including CO₂, NO, H₂O₂, NH₃, As(OH)₃, Sb(OH)₃, and even Si(OH)₄. Recent experiments revealed mixed selectivity profiles for certain PIP, TIP, or NIP homologues, similar to those described for aquaglyceroporins in other organisms. The idea that the primary function of some of these homologues may not be restricted to water transport and may truly involve solute transport has found strong support only recently, with the identification of substrates of a real physiological significance for the plant. In particular, the involvement of plant AQPs in gas transport such as NH₃ and CO₂ has pointed to important roles for plant AQPs in nitrogen and carbon fixation (Holm et al. 2005; Jahn et al. 2004; Loque et al. 2005; Uehlein et al. 2003).

A less widely discussed function of some AQPs is their involvement in junctional structures (Engel et al. 2008). The most prominent example is AQP0, which plays a major role as an adhesion molecule in the stacking of lens fiber cells. Loss of this function causes loss of stacking order and thus a turbidity of the lens, commonly known as cataract (Shiels et al. 2001). Freeze-fracture electron microscopy of lens tissue has revealed the presence of orthogonal arrays, which belong to the 11–13-nm *thin lens junctions* (Costello et al. 1989) that assemble after proteolytic cleavage of AQP0. Orthogonal arrays of AQP4 have also been observed by freeze-fracture analysis of mouse kidney, skeletal muscle, and brain tissue, but their function has remained elusive (Verbavatz et al. 1997). The adhesive property of AQP4 arrays has only recently been recognized, and the tongue-into-groove packing arrangement of the two layers has been structurally resolved at atomic resolution (Hiroaki et al. 2006). A similar packing arrangement has also been found in double-layered 2D crystals of the plant AQP SoPIP2;1 (Kukulski et al. 2005).

3 The Structure of AQPs

All AQPs form tetramers with each monomer functioning as an independent pore (Fig. 1a). Initially, electron crystallography has contributed to the structural definition of AQPs, together with atomic force microscopy (AFM) that provided information on the structure and dynamics of AQP surfaces (Fotiadis et al. 2000; Fotiadis et al. 2001, 2002; Scheuring et al. 2002). Since then several atomic structures of AQPs have been resolved by X-ray and electron crystallography, including the mammalian aquaporins AQP0 (Harries et al. 2004; Gonen et al. 2004a, 2005), AQP1 (Murata et al. 2000; Sui et al. 2001; Ren et al. 2001; de Groot et al. 2001), and AQP4 (Hiroaki et al. 2006), the *E. coli* aquaglyceroporin GlpF (Fu et al. 2000, 2002) and orthodox aquaporin AQPZ (Savage et al. 2003; Savage and Stroud 2007), the

archaeobacterial AQP_M (Lee et al. 2005), and plant SoPIP₂;1 (Tornroth-Horsefield et al. 2006). In the following paragraphs we discuss the basic AQP fold, the structure of the channel, and specific features of the extracellular surfaces of specific AQPs that exhibit an adhesive function.

3.1 *The AQP Fold*

An AQP monomer is built from six transmembrane helices arranged in a right-handed helical bundle that provides the framework for the channel (Fig. 1b). The angle at which the transmembrane helices are oriented gives rise to funnel-shaped cytoplasmic and extracellular vestibules connected by the conduction pore. The latter is formed by loop B connecting H2 and H3, and loop E connecting H5 and H6, each comprising a short α -helical segment, called HB and HE. The first and second protein halves share a considerable sequence homology arising from an ancient gene duplication event. Each repeat contains three transmembrane helices and one short helix, and the repeats insert in opposite orientations in the lipid bilayer. Therefore, helices H1–H3, HB in the structure are related to H4–H6, HE by quasi two-fold symmetry in the plane of the membrane, a feature recognized throughout all AQPs. Loops B and E meet in the middle of the membrane, where the prolines belonging to the NPA motifs stack by van der Waals interactions to form a platform from which the helices HB and HE emanate toward the cytosolic and extracellular surfaces (Fig. 1b). Loop C comprising about 25 residues connects H3 and H4, i.e., the first and second half of the AQP, stretching across the extracellular surface of the protein. The stability of this fold is provided by a significant packing of helices, as well as by the tetramerization.

3.2 *The Structure of the Pore*

Despite the strict conservation of the canonical AQP fold essential differences were identified between aquaporins and aquaglyceroporins (Fig. 2a; see Gonen and Walz 2006 for a review on the structure of AQPs). Overall the conduction pores of AQPs are roughly 25-Å long and exhibit two sites interacting strongly with water, the constriction and the NPA motif (Fig. 2b). Permeating molecules are coordinated to the channel through a combination of backbone carbonyl and amino acid side-chain interactions, the amphipathic nature of the channel complementing the chemical nature of the conducted molecules. The narrowest constriction is located close to the extracellular pore mouth. In water-specific AQPs it is approximately 2.8 Å in diameter, i.e., identical to that of a water molecule, and about 3.4 Å in aquaglyceroporins matching the diameter of a carbon hydroxyl group of polyols such as glycerol. This constriction, referred to as aromatic residue/arginine (ar/R) constriction, is formed by four residues, i.e., Phe56, His180, Cys189, and Arg195 in AQP1

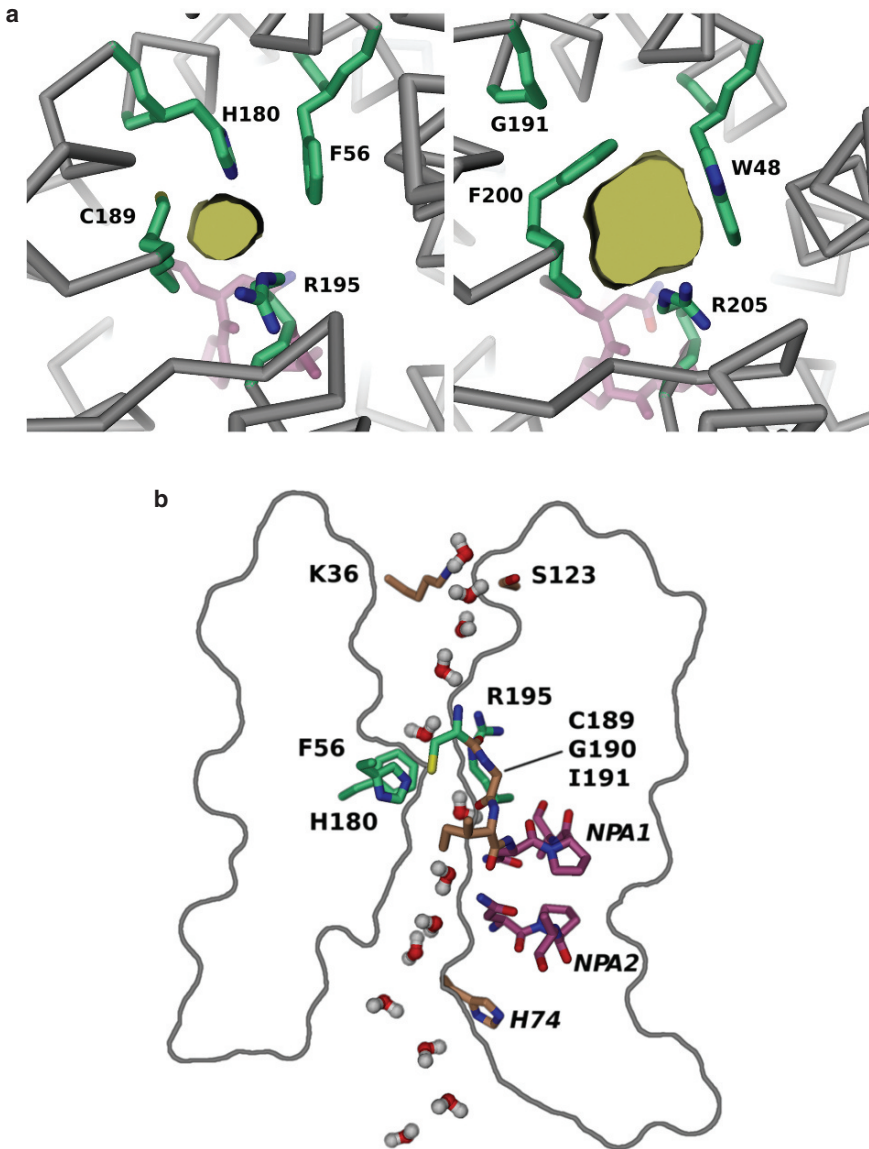


Fig. 2 The structures of the AQP1 and GlpF pore. **(a)** The principal constriction is distinctly smaller in aquaporins (*left*) than in aquaglyceroporins (*right*), yet the arginine is highly conserved in both channels. Aromatic residues are more prominent in aquaglyceroporins, and they serve as a greasy slide to facilitate passage of glycerol and other polyols. **(b)** In AQP1 the pore has a length of about 25 Å, and connects the extracellular with the cytosolic vestibules. Water molecules are from a snapshot of a molecular dynamics simulation (see de Groot and Grubmüller 2005), and reveal their tendency to orient in the electric field of the channel, with the hydrogen atoms preferentially oriented toward the extracellular (top half of the pore) or the cytosolic surface (bottom half of the pore). The graphical representations have been created with DINO (www.dino3d.org)

or Trp48, Gly191, Phe200, and Arg205 in GlpF (Fig. 2a). A histidine is typical for water-specific AQP, which together with the highly conserved arginine provides a hydrophilic edge in juxtaposition to an aromatic residue. The sulfhydryl group of a cysteine side chain extends into the pore and is the binding site for the AQP1-inhibitor HgCl_2 (Preston et al. 1993). The positively charged arginine is to some extent involved in proton exclusion because exchange to a valine residue results in a small but measurable proton leakage (Beitz et al. 2006). In GlpF, and essentially in all other aquaglyceroporins, the ar/R region is more hydrophobic than that of AQP1 due to the lack of the histidine and substitution of the cysteine by a second aromatic residue. The ladder of aromatic residues forms a *greasy slide* that allows GlpF to efficiently conduct glycerol, small linear polyols, and urea, but makes GlpF a less efficient water channel (Stroud et al. 2003).

A less narrow constriction is located at the center of the pore in the NPA region (Fig. 2b), but the interaction between water molecules and the protein is nevertheless prominent at this site. The two asparagines are the capping amino acids at the positive ends of helices HB and HE and act as hydrogen donors to the oxygen atoms of passing permeants. In addition, water that enters this region is reoriented by the dipoles of the emanating half helices HB and HE, such that hydrogen bonds between neighboring water molecules in the chain are disrupted. This mechanism was initially proposed to prevent the formation of a proton wire throughout the pore and thought to represent a major energy barrier for proton conductance (Murata et al. 2000). Subsequent molecular dynamics simulations combined with quantum mechanical calculations of proton hopping probabilities demonstrated that protons are excluded from the central region of the channel by a strong free energy barrier, resulting from the dipole moments of HB and HE (de Groot and Grubmuller 2005) (see also chapter by XX, this volume). In GlpF, a similar free energy barrier blocks proton permeation as well. Selectivity by size may also be of relevance in the NPA constriction, because almost all the aquaglyceroporins have two leucine residues opposite the two asparagines instead of a leucine and a phenylalanine in aquaporins (Heymann and Engel 2000). This combination results in a somewhat larger pore diameter that is suitable for solutes larger than water.

The remaining part of the AQP pore is lined by hydrophobic residues that expose main-chain carbonyl oxygens to the pore surface. These oxygens distribute as a ladder along one side of the pore and serve as hydrogen bond acceptor sites to efficiently funnel small hydrogen bond donor molecules, such as water, urea, or polyols, through the AQP channel. Formation of hydrogen bonds between the AQP protein and the permeant also compensates for the solvation energy cost when a molecule enters from the bulk solution into the pore.

It is instructive to follow as an example a water molecule during its transit through the pore of human AQP1 (Fig. 2b). At the extracellular side (top) the pore is relatively wide and water molecules interact mainly with the A and C loops through Lys36 and Ser123, respectively. The first strong interaction site is found in the (ar/R) constriction formed by the side chains of Arg195, His180, C180, and Phe56. Within this region, between loop E and helix E, the hydrophobic Phe56 side chain orients the water molecules such as to enforce strong hydrogen bonds to Arg195 and

His180. Further down the channel, the carbonyl groups of residues Ile191, Gly190, and Cys189 interact with the water molecules in the pore. The next strong interaction site for water with the protein is in the middle of the channel, with both asparagines of the NPA motifs on one side, and the hydrophobic side chains of Phe24, Val176, and Ile191 on the other. At this site water molecules rotate by 180° as the result of the electrostatic field produced by HB and HE. The pore widens toward the intracellular side (bottom), and water molecules interact only weakly with the pore. The main interaction sites are formed by the main-chain carbonyl groups of the residues following the second NPA motif, Gly72 and Ala73, and the side chain of His74. Since the channel is rather symmetric in its nature, water permeation occurs in both directions, with the water flux following the osmotic gradient.

The pore structure dictates the permeation rate and the specificity. Changes in this structure resulting from changes in the pH or from other external factors will change the flux of water or solutes, and is termed gating. Since the specificity of the pore is high, only small changes of a few or even a single residue are required to produce the gating phenomenon. Small changes of critical residues at the pore entrances may obstruct the pore as well. Therefore, high-resolution structures are required to identify gating mechanisms in AQPs.

3.3 Surface Structure of AQPs Involved in Membrane Junctions

The role of AQP0 in membrane junctions was recognized early, and reconstitution of purified AQP0 into liposomes showed that it caused the vesicles to cluster (Dunia et al. 1987). Moreover, orthogonal arrays observed by freeze-fracture electron microscopy and *thin lens junctions* were investigated in the late seventies (Kistler and Bullivant 1980). Once AQP1 was shown to be a water channel (Preston et al. 1992), functional studies on AQP0 shifted toward its channel characteristics (e.g. Mulders et al. 1995; Nemeth-Cahalan and Hall 2000). Interest in the adhesive properties of AQP0 reemerged when 2D crystallization experiments resulted in single-layered as well as double-layered crystals, which were analyzed by electron crystallography and AFM (Fotiadis et al. 2000; Hasler et al. 1998). Proteolytic cleavage appeared to induce AQP0-based junctions, because AQP0 exists as a full-length protein of 26 kDa in young fiber cells of the lens cortex, where junctions are rarely found. Older fiber cells buried deeper in the lens core exhibit more junctions than the cortex tissue, and some of the AQP0 in the lens core is proteolytically cleaved (e.g. Takemoto et al. 1986). This hypothesis was experimentally tested by in vitro proteolysis of purified protein as well as AQP0 2D arrays (Gonen et al. 2004a). When detergent-solubilized, full-length AQP0 (26 kDa) was treated with chymotrypsin, the resulting 22-kDa fragment eluted at a higher molecular weight from a sizing column than full-length AQP0, suggesting that cleaved AQP0 tetramers form pairs.

Double-layered 2D crystals produced with a mixture of full-length and proteolytically cleaved AQP0 isolated from the lens core made it possible to determine the structure of junctional AQP0 by electron crystallography, first at 3-Å resolution

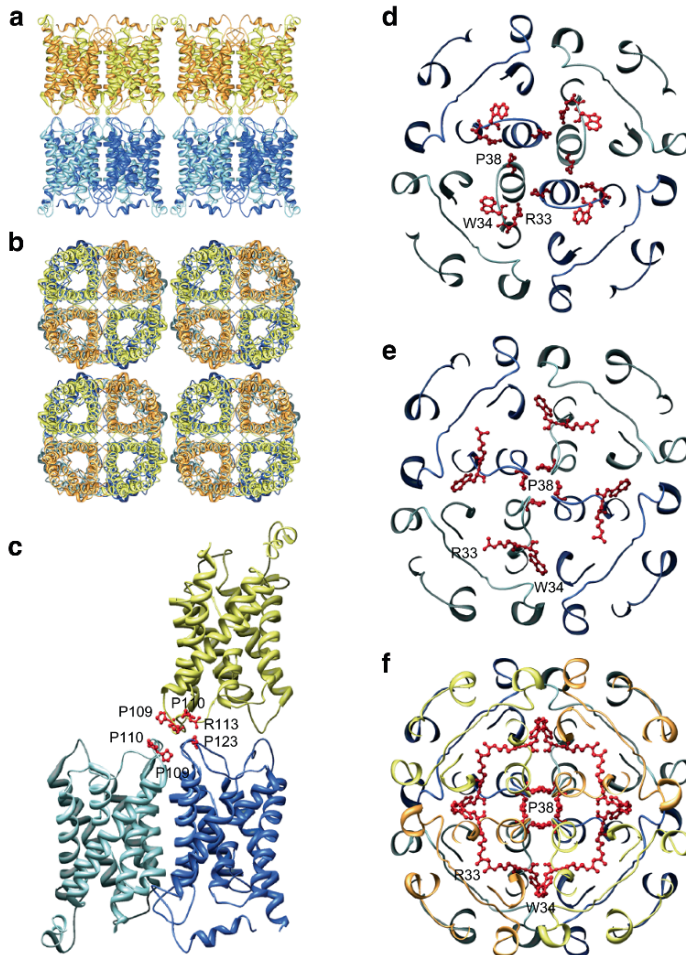


Fig. 3 The packing of AQP0 tetramers and their interaction in double-layered 2D crystals. **(a)** The view parallel to the membrane plane shows that the AQP0 tetramers in the two membrane layers are exactly in register. **(b)** The view perpendicular to the membrane plane shows that the water pores in interacting tetramers are lined up, although the channels are in a closed conformation in junctional AQP0. **(c)** Each subunit of an AQP0 tetramer in one membrane makes contact through loop C with two subunits of the interacting AQP0 tetramer in the other membrane. The proline-proline motif (Pro109 and Pro110) in loop C in the AQP0 monomer in the top layer makes interaction with the proline-proline motif in an AQP0 monomer in the bottom layer. In addition, Arg113 in loop C in the AQP0 monomer in the top layer makes interaction with Pro123 in loop C in another AQP0 monomer in the bottom layer. **(d)** Conformation of extracellular loop A in the X-ray structure of nonjunctional AQP0, in which Pro38 points away from the center of the tetramer, Trp34 lies above the pore and projects outward, and Arg33 is positioned in between two monomers. **(e)** Conformation of extracellular loop A in double-layered 2D crystals, in which Pro38 forms a rosette-like structure at the center of the tetramer, and the side chains of Arg33 and Trp34 have swapped positions (compare with panel **d**). **(f)** In the completed junction, residues Pro38, Arg33, and Trp34 interact with the corresponding residues from the opposing tetramer

(Gonen et al. 2004b) and then at 1.9-Å resolution (Gonen et al. 2005) (Fig. 3a, b). Besides a wealth of information on the protein–lipid interactions, and the closed conformation of AQP0, the structure of the junction formed between extracellular AQP0 surfaces was elucidated. The contacts formed by residues in loop C involve a Pro–Pro motif (Pro109 and Pro110), which is part of a one-turn helix (helix HC), and residues Arg113 and Pro123 (Fig. 3c). Although loop C is in a virtually identical conformation in junctional and nonjunctional AQP0 determined by X-ray crystallography, cleavage of the cytoplasmic tails seems to correlate with a rearrangement in loop A (Gonen et al. 2005). In the loop conformation of nonjunctional AQP0, Pro38 is at some distance from the center of the tetramer (Fig. 3d). In addition, Trp34 lies above the pore and projects outward, blocking the approach of a second tetramer, and Arg33 is positioned in between two monomers. In the junctional AQP0 tetramer, loop A has reconfigured, positioning Pro38 so that it can form a rosette-like structure at the center of the tetramer (Fig. 3e) and mediate a major junctional contact (Fig. 3f). The side chains of Arg33 and Trp34 also swap positions, so that Trp34 no longer interferes with the close approach of another tetramer. In the completed junction, all three residues interact with the corresponding residues from the opposing junction, all three residues interact with the corresponding residues from the opposing tetramer (Fig. 3f). Membranes isolated from the lens core were directly imaged with the AFM. The AFM tip was used to remove the top layer from junctional membrane patches, which made it possible to image the extracellular surface of AQP0 arrays (Buzhynskyy et al. 2007). The averaged surface topograph showed loop A to be at the same position as in the double-layered 2D crystals rather than at the position in the 3D crystals. Thus it is likely that the conformation of loop A is the cause for junction formation rather than being induced by the interaction with the tetramer in the adjoining membrane, which was removed by the AFM tip before imaging.

Similar to AQP0, AQP4 was found by freeze-fracture techniques to produce orthogonal arrays in murine kidneys, skeletal muscles, and brain (Verbavatz et al. 1997). These arrays were not present in AQP4 knock-out mice. Although a hypothetical role of AQP4 as an osmosensor was proposed (Venero et al. 1999), AQP4 had not been implicated in cell adhesion, and the interactions between AQP4 tetramers in adjoining membranes are apparently weak. However, they are sufficiently significant to dictate the formation of double-layered 2D crystals when reconstituting the AQP4 isoform M23, but not the AQP4 isoform M1. The latter isoform has a longer N-terminus, which apparently influences the fine structure of the AQP4 extracellular surface. The 3.2-Å structure revealed that AQP4 tetramers in the two membranes interact with each other through their extracellular surfaces (Fig. 4a) (Hiroaki et al. 2006). Rather than being exactly stacked, as in the case of AQP0, the AQP4 tetramers are shifted so that a tetramer in one membrane is at the center of four tetramers in the adjoining membrane (Fig. 4b). AQP4 features a short 3_{10} helix in extracellular loop C, helix HC, which contains the two residues, Pro139 and Val142, that mediate the interactions between opposing tetramers (Fig. 4c). In the 2D crystals each AQP4 tetramer interacts with four tetramers in the adjoining membrane, so that an orthogonal array would significantly enhance AQP4-mediated adhesion. To understand whether the double-layered 2D crystals were just a result of the *in vitro*

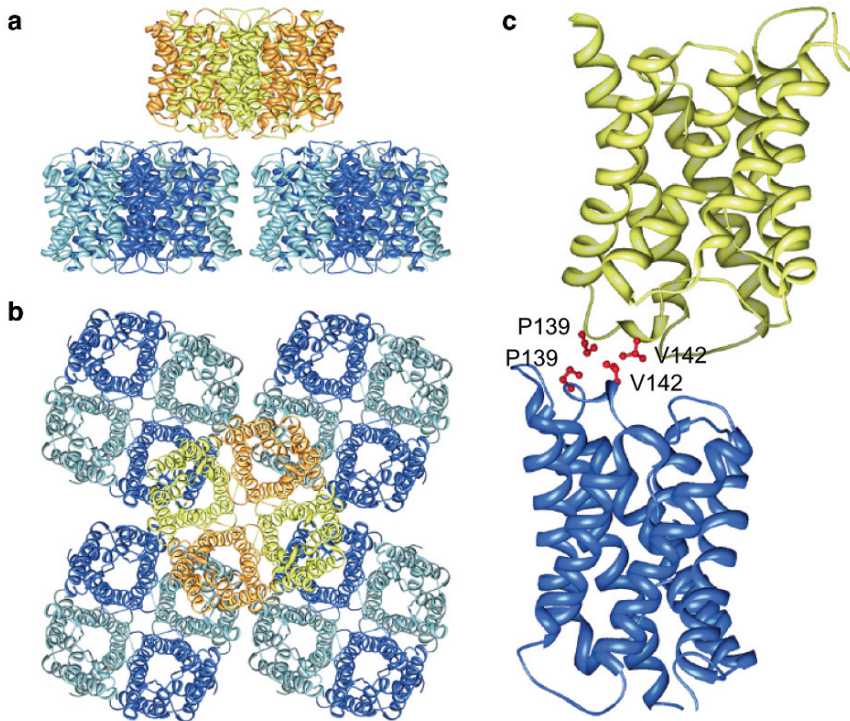


Fig. 4 The packing of AQP4 tetramers and their interaction in double-layered 2D crystals. **(a)** The view parallel to the membrane plane shows that the AQP4 tetramers in the two membrane layers are staggered. **(b)** The view perpendicular to the membrane plane shows that the entrances to the water pores in one membrane are partially obstructed by the four interacting tetramers in the other membrane. **(c)** Residues Pro139 and Val142 in extracellular loop C of AQP4 mediate the interactions between tetramers in the two adjoining membrane layers

2D crystallization of AQP4 or whether AQP4 could also form junctions *in vivo*, AQP4 was expressed in L-cells, a fibroblast cell line that does not express endogenous cell adhesion molecules. These cells showed some clustering, which was not observed when AQP1 was expressed (Hiroaki et al. 2006). Moreover, thin sections through the hypothalamus revealed large membrane junctions between glial lamellae with short stretches of separated membranes. Immunolabeling studies localized AQP4 to the separated membranes as well as to the junctional regions (Hiroaki et al. 2006). Together, these results suggest a possible role of AQP4 in junction formation *in vivo*, and provide an explanation for the involvement of AQP4 in osmoregulation (Venero et al. 1999). In the double-layered 2D crystals, the AQP4 molecules show a tight tongue-into-groove packing of their extracellular surfaces, which results in a partial blockage of the extracellular pore entrances (Fig. 4b). Formation of AQP4 junctions *in vivo* would thus potentially lead to a reduced water permeability of glial cell plasma membranes. Conversely, rapid water flow through the channels could drive the interacting membranes apart and thus resolve the junctions. As a result of

the characteristics of AQP4, glial cells expressing a high ratio of AQP4M1 would produce small AQP4 arrays providing weak adhesion between membranes, which would easily separate and be sensitive to small water flows resulting from small osmotic differences. Vice versa, glial cells expressing a high ratio of AQP4M23 would produce large AQP4 arrays providing stronger adhesion between membranes that would withstand larger water flows associated with larger osmotic differences.

A similar structure was observed upon 2D crystallization of the plant AQP SoPIP2;1 (Kukulski et al. 2005). The double-layered crystals with interacting extracellular surfaces exhibited a packing arrangement in which one tetramer of one layer interacts with four tetramers in the opposite layer, providing a tongue-and-groove fit of the extracellular surfaces (Fig. 5a). The overall architecture of the channel has a substantial similarity to AQP1, but some differences can be distinguished. The most salient difference is the length and straightness of H1, which appears to protrude farther out from the extracellular membrane surface than H1 of AQP1, and to point toward the four-fold axis of the tetramer. A corresponding alteration is found for H2, which is more tilted at its N terminus than H2 of AQP1. As a consequence, loop A connecting H1 and H2 is oriented toward the four-fold center of the tetramer in SoPIP2;1. All these features have recently been confirmed by a X-ray structure of *Spinacia oleracea* SoPIP2;1 (Tornroth-Horsefield et al. 2006). A tongue-and-groove packing arrangement in the double-layered 2D crystals results from the four extracellular ends of H1, which protrude into the opposite layer, filling the gap between adjacent tetramers. Therefore, the stability of the double-layered crystals might be the result of a contact between loops A from one layer with HE and/or H6 of the opposing layer (Fig. 5b). These results may suggest a physiological role of this specific surface interaction of SoPIP2;1 observed *in vitro*. The increase of the membrane surface upon stomata opening cannot be explained by stretching of the plasma membrane. It has to be attributed either to vesicles fusing with the plasma membrane or to plasma membrane invaginations being unfolded. Very fast cell volume changes necessitating vesicle fusion or unfolding of invaginations have been recorded for mesophyll protoplasts isolated from leaf tissue (Ramahaleo et al. 1999; Morillon et al. 2001; Moshelion et al. 2004). Immunogold electron microscopy has demonstrated PIP subfamily members to be associated with plasmalemmasomes, invaginations of the plasma membrane protruding into the cytosol toward the central vacuole of *Arabidopsis* mesophyll cells (Robinson et al. 1996). Therefore, it is possible that major integral proteins of the plasma membrane, such as AQPs, participate in interactions stabilizing membrane invaginations.

4 Unsolved Riddles

4.1 AQP Trafficking

Regulation of water flow in single cells and complex organisms is critical to establishing and maintaining normal physiology. AQPs are passive channels and water

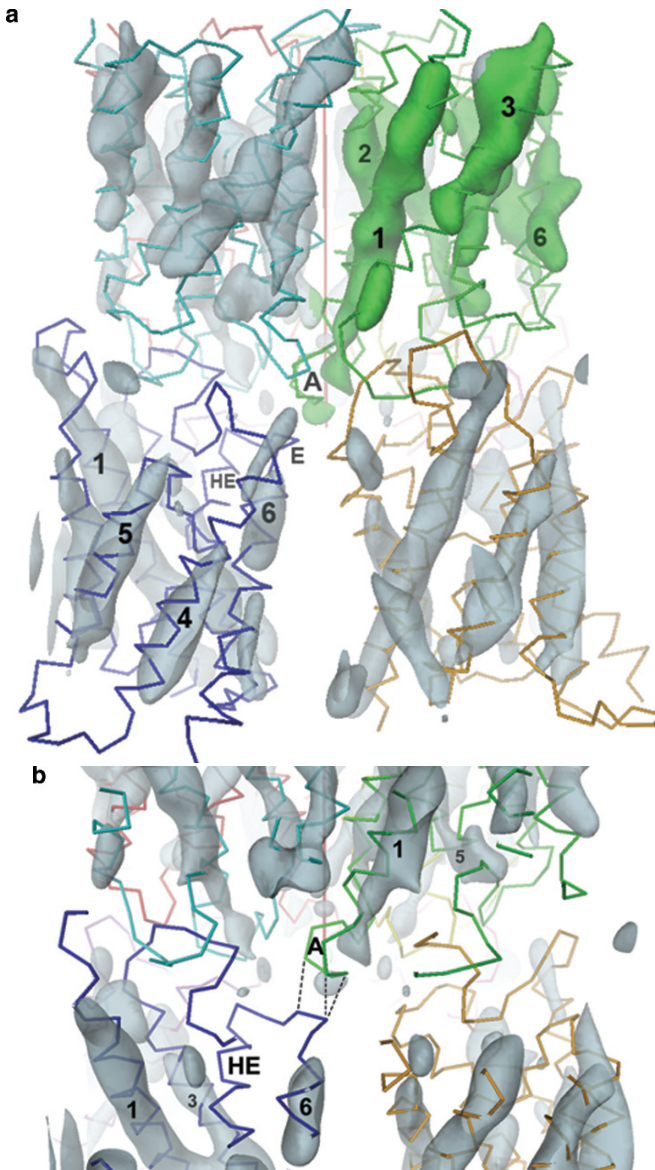


Fig. 5 The packing of SoPIP2;1 in double-layered 2D crystals is similar to that of AQP4 (see Fig. 4). The map calculated from electron micrographs has an in-plane resolution of 5 Å (Kukulski et al. 2005). The α -backbone of AQP1 has been fitted using a tool described previously (de Groot et al. 2000), and extending H1 (Kukulski et al. 2005). **(a)** The protrusion about the four-fold axis (vertical line) formed by the unusually long H1 fits into the depression about the four-fold axis between tetramers of the lower layer. **(b)** A closer view shows potential interaction sites between upper and lower layer: the loop between HE and H6 of the lower layer is in close proximity of loop A from the upper layer (indicated by dashed lines; C α backbone distance is about 5 Å in this model). The graphical representations have been created with DINO (www.dino3d.org)

permeation is driven by osmotic gradients – hence the water flow could be regulated by structural changes of the pore. Alternatively, the number of AQPs in the respective membranes could be controlled for water flux regulation. The latter is the case in the kidney, where at least six AQPs (AQP1, 2, 3, 4, 6, and 7) are known to be expressed (Nielsen et al. 2000) (see also chapter XX by, this volume). AQP1 is highly abundant in the proximal tubule and descending thin limb, and provides for the constitutive water reabsorption. At least three AQPs are expressed in the collecting duct, and they participate in vasopressin-regulated water reabsorption. AQP2 is the apical water channel of collecting duct principal cells, and is involved in short-term regulation of collecting duct water permeability by vasopressin. Collecting duct water reabsorption is also regulated on a long-term basis, predominantly through long-term regulation of AQP2 expression. AQP3 and AQP4 are both expressed in the basolateral plasma membranes of collecting duct principal cells and represent potential exit pathways for water reabsorbed via apical AQP2. Collecting ducts reabsorb about 10% of the 180 L of water being reabsorbed per 24 h by kidneys of a human body – underlining the importance of correct trafficking of AQP2 to and internalization from the apical membrane of collecting duct principal cells. Malfunctioning of this process leads to an imbalanced water reabsorption in the kidneys and is related to a variety of diseases (Nielsen et al. 2007; Robben et al. 2006).

AQP2 contains a consensus site for PKA phosphorylation in the cytoplasmic C-terminus (Ser256). PKA-mediated phosphorylation of Ser256 was shown to be critical for vasopressin-induced trafficking of AQP2 from intracellular vesicles to the plasma membrane. Antibodies that selectively recognize AQP2 phosphorylated at Ser256 labeled both the apical plasma membrane and vesicles, and it was demonstrated that V2 receptors play an important role in the regulation of Ser256 phosphorylation (Christensen et al. 2000). As a further proof that PKA phosphorylation/dephosphorylation of AQP2 is involved in the regulated trafficking of AQP2 to and from the plasma membrane, S256D and S256A AQP2 mutants were expressed in *Xenopus* oocytes. AQP2-S256D was transported to the plasma membrane, whereas AQP2-S256A was retained intracellularly. Coinjection of different ratios of AQP2-S256A and AQP2-S256D cRNAs revealed that at least three AQP2-S256D monomers in an AQP2 tetramer were required for its plasma membrane localization (Kamsteeg et al. 2000). Recent phosphoproteome analyses identified further phosphorylation sites, Ser261, Ser264, and Ser269 that also appear to affect AQP2 trafficking (Hoffert et al. 2006, 2007). In spite of this progress many questions about how phosphorylation/dephosphorylation of these sites regulate exocytic or endocytic events remain to be answered.

SNARE proteins (soluble NSF attachment protein receptors) play a key role in synaptic vesicle targeting, docking, and fusion. Are SNAREs involved in AQP2 trafficking? VAMP2, which is a vesicle SNARE, has been found associated with AQP2-bearing vesicles, and, recently, target SNAREs such as syntaxin-4 and SNAP23 have been identified in collecting duct principal cells, supporting the view that SNARE vesicle-targeting receptors may play a role in vasopressin regulation of AQP2 trafficking. Therefore, an enigmatic question concerns the structural platform

that interfaces pSer256-AQP2 tetramers to a vesicle SNARE, and to the trafficking machinery.

4.2 AQP Gating

The first indication of AQP gating came from studies of plant AQPs. Early experiments showed that the water channel activity of a TIP is regulated by phosphorylation (Maurel et al. 1995). Shortly afterward the phosphorylation of SoPIP2;1 of the spinach leaf plasma membrane (formerly called PM28A) was found to depend in vivo on the apoplastic water potential and in vitro on submicromolar concentrations of Ca^{2+} (Johansson et al. 1996). Subsequently, wild-type (wt) and mutant forms (S6A, S36A, S115A, S188A, S192A, S274A, and S115A/S274A) of SoPIP2;1 were expressed in *Xenopus* oocytes (Johansson et al. 1998). Swelling assays revealed differences in the osmotic water permeability of different oocytes, with minor variations among wt, S6A, S36A, S188A, S192A, and S274A, but a reduction of the permeability by 40% for mutants S115A and S115A/S274A. The same measurements were executed after incubation of the oocytes with the protein kinase inhibitor K252a. The results demonstrated a 30–40% reduction of the transport activity of wt and mutant S274A, whereas the mutants S115A and S115A/S274A were insensitive to K252a. Labeling of spinach leaves with ^{32}P -orthophosphate and subsequent sequencing of SoPIP2;1-derived peptides demonstrated that Ser274 is phosphorylated in vivo; however, phosphorylation of Ser115, a residue conserved among all plant plasma membrane AQPs, could not be demonstrated. From these experiments it was concluded that the water channel activity of SoPIP2;1 could be regulated by phosphorylation of two serine residues, Ser115 in loop B and Ser274 in the C-terminal region.

Other experiments showed that *Arabidopsis* plasma membrane (PM) vesicles isolated in the presence of chelators of divalent cations exhibited a Ca^{2+} and pH dependence in their water channel activity (Gerbeau et al. 2002). In these experiments, the water permeation was reduced by 50–60% compared with the unperturbed condition. Ca^{2+} was the most efficient inhibitor with an IC_{50} at 50–100 μM free Ca^{2+} . Water transport in purified PM vesicles was also reversibly blocked by H^+ , with an IC_{50} at pH 7.2–7.5, reaching the highest inhibition at pH 6.4. Thus, both Ca^{2+} and H^+ contribute to a membrane-delimited switch from active to inactive water channels in *Arabidopsis* PM that may allow coupling of water transport to cell signaling and metabolism.

A possible mechanism explaining the channel regulation by phosphorylation, pH changes, or Ca^{2+} was provided by the structure of *Spinacia oleracea* SoPIP2;1 in a closed conformation at 2.2-Å resolution and in an open state at 3.9-Å resolution (Tornroth-Horsefield et al. 2006). Gating appears to be related to conformational changes of loop D, which is four to seven residues longer for PIP subfamily members than for other AQPs. In the closed conformation loop D folds underneath the pore and occludes it, with the conserved Leu197 inserted into a cavity

near the entrance of the channel. In the open conformation, loop D is displaced by 16 Å to point outward and the N terminus of helix 5 extends a further half-turn into the cytoplasm relative to that of its closed conformation, thereby providing access to the pore. For understanding the pH-driven gating the conserved His193 residue in loop D needs to be considered. In the open conformation, His193 is not protonated and loop D is distal from the other cytoplasmic loop B. By contrast, the protonation of His193 allows interaction with an acidic residue of the N terminus, Asp28. This electrostatic interaction is assumed to drive a conformational change of loop D and closure of the pore by displacement of the hydrophobic side chain of Leu197 into the cytosolic pore mouth. Binding of divalent cations would also involve Asp28 and the adjacent acidic residue Glu31. Loop D would then be stabilized in the closed pore conformation through a network of H-bond and hydrostatic interactions, involving A118. In this model, phosphorylation of loop B, at Ser115, would disrupt this network of interactions and unlock loop D to allow the open conformation.

In spite of the beauty of this model, a number of observations suggest some caution. Mass spectroscopy on cyanogen bromide cleaved PvTIP3;1 heterologously expressed in *P. pastoris* revealed that PKA could only phosphorylate the N-terminal Ser7, and molecular modeling showed that the two other potential phosphorylation sites, Ser23 and Ser99, would be inaccessible to PKA (Daniels and Yeager 2005). Most recently, multiple phosphorylation sites at the C-terminal tail of *Arabidopsis thaliana* AtPIP2;1 were identified and found to have an influence on salt stress-induced trafficking of AtPIP2;1 (Prak et al. 2008). Thus, so far no experiment showed either Ser115 in SoPIP2;1 or a corresponding site in any other plant AQP to be phosphorylated, while phosphorylation in the C-terminal region was found to be related to trafficking, akin to that of AQP2. The two different SoPIP2;1 structures are from two different crystal forms with loop D in different local environments (Tornroth-Horsefield et al. 2006). The closed pore conformation was found under crystallization conditions that would have promoted the open form (pH 8), whereas the open conformation was from a crystal grown at pH 5.6, of the unphosphorylated SoPIP2;1, both conditions suggesting that the channel should be closed. Indeed, at this pH His193 is protonated, which according to the model should induce closing of the channel. Therefore, further functional and structural analyses are required to achieve a full understanding of phosphorylation-induced regulation.

4.3 Anion Transport

AQP6 was identified in acid-secreting α -intercalated cells in the renal collecting duct by immunoelectron and immunohistochemical microscopy. This channel is located predominantly in intracellular membrane vesicles in multiple types of renal epithelia, where it colocalizes alongside H^+ -ATPase (Yasui et al. 1999a,b). When expressed in *Xenopus* oocytes, AQP6 exhibits low basal water permeability, but when treated with the water channel inhibitor, Hg^{2+} , the water permeability of AQP6-expressing oocytes rapidly increases tenfold and is accompanied by ion con-

ductance. At pH values less than 5.5, anion conductance is rapidly and reversibly activated in AQP6-expressing oocytes, which suggests a role in the secretion of acid (Yasui et al. 1999a,b). Thus, while the primary sequence of AQP6 is closest to AQP2 and AQP5 (both inhibited by mercuric chloride), the structure of AQP6 must contain functionally important differences, which yet need to be unraveled.

4.4 Gas Transport

Early experiments in *Xenopus* oocytes indicated a remarkable CO₂ uptake that was induced by expressing AQP1 (Nakhoul et al. 1998). Although this report was heatedly debated, the issue of gas transport by AQPs remained. In another much discussed contribution, a CO₂ permeability comparable to that of human AQP1 was reported for the tobacco plasma membrane aquaporin NtAQP1 (Uehlein et al. 2003). It was further shown that NtAQP1 overexpression increases membrane permeability for CO₂ and water, and accelerates leaf growth. Therefore, the NtAQP1-related CO₂ permeability was concluded to be physiologically important under conditions where the CO₂ gradient across a membrane is small, as is the case between the atmosphere and the inside of a plant cell. More recently, the transport of ammonia/ammonium across AQP8 was assessed stoichiometrically (Saparov et al. 2007). Purified AQP8 was reconstituted into planar bilayers, and the exclusion of NH₄⁺ or H⁺ was established by ensuring a lack of current under voltage clamp conditions. The single channel water permeability coefficient measured was more than two-fold smaller than the single channel ammonia permeability. This permeability ratio suggested that electrically silent ammonia transport may be a major function of AQP8.

This controversially discussed issue has promoted an extensive set of molecular dynamics simulations that address the question of CO₂ permeation through human AQP1 (Hub and de Groot 2006) (see chapter by, this volumeXX). A barrier of $\approx 23 \text{ kJ mol}^{-1}$ in the ar/R constriction region of the water pore was obtained from the free energy profiles derived from the simulations. In contrast, a barrier of $\approx 4 \text{ kJ mol}^{-1}$ was found for a palmitoyl-oleoyl-phosphatidyl-ethanolamine lipid bilayer membrane, which has served as model bilayer for the simulations. From these results it is concluded that significant AQP1-mediated CO₂ permeation is to be expected only in membranes with a low intrinsic CO₂ permeability. In this work not only the water pore was studied, but the simulations also included the cavity about the fourfold axis of the tetramer. Two major barriers for CO₂ can be identified, one of $12 \pm 2 \text{ kJ mol}^{-1}$ at $z = 7.5 \text{ \AA}$ near the extracellular entrance to the central cavity. This aperture is surrounded by the four Val50 residues of the four monomers, forcing the CO₂ molecules to lose favorable interactions to neighboring water molecules. A second barrier of the same height is at a site where CO₂ is surrounded by the four Asp48 residues. In this case it is likely that CO₂ competes with water for hydrogen bonds to Asp48. Therefore, the free energy barrier for CO₂ permeation through the central cavity is significantly smaller than for the monomeric channel. However, HgCl₂, which abolishes water conduction through AQP1 also prevented

CO₂ permeation, arguing that water and CO₂ use the same pathway through aquaporins (Prasad et al. 1998; Blank and Ehmke 2003). A further and more detailed molecular dynamics analysis came to conclude that small hydrophobic solutes such as NO or CO₂ are expected to diffuse through the water channel of AQP1 at a very low rate, whereas they should do this at a 30 times higher rate through GlpF (Hub and de Groot 2008).

To elucidate the importance of AQPs for gas transport, site-directed mutations together with high-resolution structures and additional molecular dynamics simulations of the respective mutants would be required.

5 Perspectives

The availability of a large pool of information on structure and function of AQPs appears to be a solid basis to come to a full understanding of these highly specific, ancient channels. The gating of some AQPs remains to be further investigated, the anion conduction of AQP6 is an unsolved riddle, and the machinery for AQP trafficking to specific membranes is to be unveiled. Progress in structure determination fosters hopes that this will all be achieved relatively soon, and will provide a structural basis for future therapeutic strategies for AQP-related human diseases.

Acknowledgments This work has been supported by the Swiss National Science Foundation (SNF), the national center of competence in research (NCCR) of structural biology, SNF grant 3100A0-108299 to AE, EU grant 035995-2, the University of Basel and the Maurice E. Müller Foundation of Switzerland. Work on aquaporins in the Walz laboratory is supported by NIH grants R01 EY015107 and R01 GM082927. TW is an investigator of the Howard Hughes Medical Institute. The authors thank Bert de Groot for providing the coordinates of the single file on water molecules and Ansgar Philippsen for his help with Fig. 2 and Wanda Kukulski for Fig. 5.

References

- Beitz E, Pavlovic-Djuranovic S, Yasui M, Agre P, Schultz JE (2004) Molecular dissection of water and glycerol permeability of the aquaglyceroporin from *Plasmodium falciparum* by mutational analysis. *Proc Natl Acad Sci USA* 101:1153–1158
- Beitz E, Wu B, Holm LM, Schultz JE, Zeuthen T (2006) Point mutations in the aromatic/arginine region in aquaporin 1 allow passage of urea, glycerol, ammonia, and protons. *Proc Natl Acad Sci USA* 103:269–274
- Biela A, Grote K, Otto B, Hoth S, Hedrich R, Kaldenhoff R (1999) The *Nicotiana tabacum* plasma membrane aquaporin NtAQP1 is mercury-insensitive and permeable for glycerol. *Plant J* 18:565–570
- Blank ME, Ehmke H (2003) Aquaporin-1 and HCO₃⁽⁻⁾-Cl⁻ transporter-mediated transport of CO₂ across the human erythrocyte membrane. *J Physiol* 550:419–429
- Buzhynskyy N, Hite RK, Walz T, Scheuring S (2007) The supramolecular architecture of junctional microdomains in native lens membranes. *EMBO Rep* 8:51–55

- Chaumont F, Barrieu F, Wojcik E, Chrispeels MJ, Jung R (2001) Aquaporins constitute a large and highly divergent protein family in maize. *Plant Physiol* 125:1206–1215
- Cheng A, van Hoek AN, Yeager M, Verkman AS, Mitra AK (1997) Three-dimensional organization of a human water channel. *Nature* 387:627–630
- Christensen BM, Zelenina M, Aperia A, Nielsen S (2000) Localization and regulation of PKA-phosphorylated AQP2 in response to V(2)-receptor agonist/antagonist treatment. *Am J Physiol Renal Physiol* 278:F29–F42
- Costello MJ, McIntosh TJ, Robertson JD (1989) Distribution of gap junctions and square array junctions in the mammalian lens. *Invest Ophthalmol Vis Sci* 30:975–989
- Daniels MJ, Yeager M (2005) Phosphorylation of aquaporin PvTIP3;1 defined by mass spectrometry and molecular modeling. *Biochemistry* 44:14443–14454
- Dean RM, Rivers RL, Zeidel ML, Roberts DM (1999) Purification and functional reconstitution of soybean nodulin 26. An aquaporin with water and glycerol transport properties. *Biochemistry* 38:347–353
- de Groot BL, Grubmüller H (2005) The dynamics and energetics of water permeation and proton exclusion in aquaporins. *Curr Opin Struct Biol* 15:176–183
- de Groot BL, Heymann JB, Engel A, Mitsuoka K, Fujiyoshi Y, Grubmüller H (2000) The fold of human aquaporin 1. *J Mol Biol* 300:987–994
- de Groot BL, Engel A, Grubmüller H (2001) A refined structure of human aquaporin-1. *FEBS Lett* 504:206–211
- Dunia I, Manenti S, Rousselet A, Benedetti EL (1987) Electron microscopic observations of reconstituted proteoliposomes with the purified major intrinsic membrane protein of eye lens fibers. *J Cell Biol* 105:1679–1689
- Engel A, Fujiyoshi Y, Gonen T, Walz T (2008) Junction-forming aquaporins. *Curr Opin Struct Biol* 18:229–235
- Fotiadis D, Hasler L, Muller DJ, Stahlberg H, Kistler J, Engel A (2000) Surface tongue-and-groove contours on lens MIP facilitate cell-to-cell adherence. *J Mol Biol* 300:779–789
- Fotiadis D, Jenö P, Mini T, Wirtz S, Müller SA et al (2001) Structural characterization of two aquaporins isolated from native spinach leaf plasma membranes. *J Biol Chem* 276:1707–1714
- Fotiadis D, Suda K, Tittmann P, Jenö P, Philippsen A et al (2002) Identification and structure of a putative Ca²⁺-binding domain at the C terminus of AQP1. *J Mol Biol* 318:1381–1394
- Fu D, Libson A, Miercke LJ, Weitzman C, Nollert P et al (2000) Structure of a glycerol-conducting channel and the basis for its selectivity. *Science* 290:481–486
- Fu D, Libson A, Stroud R (2002) The structure of GlpF, a glycerol conducting channel. *Novartis Found Symp* 245:51–61; discussion 61–55, 165–168
- Gerbeau P, Guclu J, Ripoche P, Maurel C (1999) Aquaporin Nt-TiPA can account for the high permeability of tobacco cell vacuolar membrane to small neutral solutes. *Plant J* 18:577–587
- Gerbeau P, Amodeo G, Henzler T, Santoni V, Ripoche P, Maurel C (2002) The water permeability of *Arabidopsis* plasma membrane is regulated by divalent cations and pH. *Plant J* 30:71–81
- Gonen T, Walz T (2006) The structure of aquaporins. *Q Rev Biophys* 39:361–396
- Gonen T, Cheng Y, Kistler J, Walz T (2004a) Aquaporin-0 membrane junctions form upon proteolytic cleavage. *J Mol Biol* 342:1337–1345
- Gonen T, Sliz P, Kistler J, Cheng Y, Walz T (2004b) Aquaporin-0 membrane junctions reveal the structure of a closed water pore. *Nature* 429:193–197
- Gonen T, Cheng Y, Sliz P, Hiroaki Y, Fujiyoshi Y et al (2005) Lipid-protein interactions in double-layered two-dimensional AQP0 crystals. *Nature* 438:633–638
- Gorelick DA, Praetorius J, Tsunenari T, Nielsen S, Agre P (2006) Aquaporin-11: a channel protein lacking apparent transport function expressed in brain. *BMC Biochem* 7:14
- Gorin MB, Yancey SB, Cline J, Revel JP, Horwitz J (1984) The major intrinsic protein (MIP) of the bovine lens fiber membrane: characterization and structure based on cDNA cloning. *Cell* 39:49–59
- Harries WE, Akhavan D, Miercke LJ, Khademi S, Stroud RM (2004) The channel architecture of aquaporin 0 at a 2.2-Å resolution. *Proc Natl Acad Sci USA* 101:14045–14050

- Hasler L, Walz T, Tittmann P, Gross H, Kistler J, Engel A (1998) Purified lens major intrinsic protein (MIP) forms highly ordered tetragonal two-dimensional arrays by reconstitution. *J Mol Biol* 279:855–864
- Heymann JB, Engel A (2000) Structural clues in the sequences of the aquaporins. *J Mol Biol* 295:1039–1053.
- Hiroaki Y, Tani K, Kamegawa A, Gyobu N, Nishikawa K et al (2006) Implications of the aquaporin-4 structure on array formation and cell adhesion. *J Mol Biol* 355:628–639
- Hoffert JD, Pisitkun T, Wang G, Shen RF, Knepper MA (2006) Quantitative phosphoproteomics of vasopressin-sensitive renal cells: regulation of aquaporin-2 phosphorylation at two sites. *Proc Natl Acad Sci USA* 103:7159–7164
- Hoffert JD, Wang G, Pisitkun T, Shen RF, Knepper MA (2007) An automated platform for analysis of phosphoproteomic datasets: application to kidney collecting duct phosphoproteins. *J Proteome Res* 6:3501–3508
- Holm LM, Jahn TP, Moller AL, Schjoerring JK, Ferri D et al (2005) NH₃ and NH₄⁺ permeability in aquaporin-expressing *Xenopus* oocytes. *Pflugers Arch* 450:415–428
- Hub JS, de Groot BL (2006) Does CO₂ permeate through aquaporin-1? *Biophys J* 91:842–848
- Hub JS, de Groot BL (2008) Mechanism of selectivity in aquaporins and aquaglyceroporins. *Proc Natl Acad Sci USA* 105:1198–1203
- Ikeda M, Beitz E, Kozono D, Guggino WB, Agre P, Yasui M (2002) Characterization of aquaporin-6 as a nitrate channel in mammalian cells. Requirement of pore-lining residue threonine 63. *J Biol Chem* 277:39873–39879
- Ishibashi K (2006) Aquaporin subfamily with unusual NPA boxes. *Biochim Biophys Acta* 1758:989–993
- Ishikawa F, Suga S, Uemura T, Sato MH, Maeshima M (2005) Novel type aquaporin SIPs are mainly localized to the ER membrane and show cell-specific expression in *Arabidopsis thaliana*. *FEBS Lett* 579:5814–5820
- Itoh T, Rai T, Kuwahara M, Ko SB, Uchida S et al (2005) Identification of a novel aquaporin, AQP12, expressed in pancreatic acinar cells. *Biochem Biophys Res Commun* 330:832–838
- Jahn TP, Moller AL, Zeuthen T, Holm LM, Klaerke DA et al (2004) Aquaporin homologues in plants and mammals transport ammonia. *FEBS Lett* 574:31–36
- Johanson U, Gustavsson S (2002) A new subfamily of major intrinsic proteins in plants. *Mol Biol Evol* 19:456–461
- Johanson U, Karlsson M, Johansson I, Gustavsson S, Sjoval S et al (2001) The complete set of genes encoding major intrinsic proteins in *Arabidopsis* provides a framework for a new nomenclature for major intrinsic proteins in plants. *Plant Physiol* 126:1358–1369
- Johansson I, Larsson C, Ek B, Kjellbom P (1996) The major integral proteins of spinach leaf plasma membranes are putative aquaporins and are phosphorylated in response to Ca²⁺ and apoplastic water potential. *Plant Cell* 8:1181–1191
- Johansson I, Karlsson M, Shukla VK, Chrispeels MJ, Larsson C, Kjellbom P (1998) Water transport activity of the plasma membrane aquaporin PM28A is regulated by phosphorylation. *Plant Cell* 10:451–459
- Jung J, Preston G, Smith B, Guggino W, Agre P (1994) Molecular structure of the water channel through aquaporin CHIP. The hourglass model. *J Biol Chem* 269:14648–14654
- Kaldenhoff R, Carbo MR, Sans JF, Lovisollo C, Heckwolf M, Uehlein N (2008) Aquaporins and plant water balance. *Plant Cell Environ* 31:658–666
- Kamsteeg EJ, Heijnen I, van Os CH, Deen PM (2000) The subcellular localization of an aquaporin-2 tetramer depends on the stoichiometry of phosphorylated and nonphosphorylated monomers. *J Cell Biol* 151:919–930
- Kistler J, Bullivant S (1980) Lens gap junctions and orthogonal arrays are unrelated. *FEBS Lett* 111:73–78
- Kukulski W, Schenk AD, Johanson U, Braun T, de Groot BL et al (2005) The 5 Å structure of heterologously expressed plant aquaporin SoPIP2;1. *J Mol Biol* 350:611–616

- Lagree V, Pellerin I, Hubert JF, Tacnet F, Le Caherec F et al (1998) A yeast recombinant aquaporin mutant that is not expressed or mistargeted in *Xenopus* oocyte can be functionally analyzed in reconstituted proteoliposomes. *J Biol Chem* 273:12422–12426
- Lee JK, Kozono D, Remis J, Kitagawa Y, Agre P, Stroud RM (2005) Structural basis for conductance by the archaeal aquaporin AqpM at 1.68 Å. *Proc Natl Acad Sci USA* 102:18932–18937
- Liu Z, Shen J, Carbrey JM, Mukhopadhyay R, Agre P, Rosen BP (2002) Arsenite transport by mammalian aquaglyceroporins AQP7 and AQP9. *Proc Natl Acad Sci USA* 99:6053–6058
- Loque D, Ludewig U, Yuan L, von Wiren N (2005) Tonoplast intrinsic proteins AtTIP2;1 and AtTIP2;3 facilitate NH₃ transport into the vacuole. *Plant Physiol* 137:671–680
- Ma JF, Tamai K, Yamaji N, Mitani N, Konishi S et al (2006) A silicon transporter in rice. *Nature* 440:688–691
- Magni F, Sarto C, Ticozzi D, Soldi M, Bosso N et al (2006) Proteomic knowledge of human aquaporins. *Proteomics* 6:5637–5649
- Maurel C (2007) Plant aquaporins: novel functions and regulation properties. *FEBS Lett* 581:2227–2236
- Maurel C, Kado RT, Guern J, Chrispeels MJ (1995) Phosphorylation regulates the water channel activity of the seed-specific aquaporin α -TIP. *EMBO J* 14:3028–3035
- Mitsuoka K, Murata K, Walz T, Hirai T, Agre P et al (1999) The structure of aquaporin-1 at 4.5-Å resolution reveals short α -helices in the center of the monomer. *J Struct Biol* 128:34–43
- Mizutani M, Watanabe S, Nakagawa T, Maeshima M (2006) Aquaporin NIP2;1 is mainly localized to the ER membrane and shows root-specific accumulation in *Arabidopsis thaliana*. *Plant Cell Physiol* 47:1420–1426
- Morillon R, Lienard D, Chrispeels MJ, Lassalles JP (2001) Rapid movements of plants organs require solute-water cotransporters or contractile proteins. *Plant Physiol* 127:720–723
- Morishita Y, Matsuzaki T, Hara-chikuma M, Andoo A, Shimono M et al (2005) Disruption of aquaporin-11 produces polycystic kidneys following vacuolization of the proximal tubule. *Mol Cell Biol* 25:7770–7779
- Moshelion M, Moran N, Chaumont F (2004) Dynamic changes in the osmotic water permeability of protoplast plasma membrane. *Plant Physiol* 135:2301–2317
- Mulders SM, Preston GM, Deen PM, Guggino WB, van Os CH, Agre P (1995) Water channel properties of major intrinsic protein of lens. *J Biol Chem* 270:9010–9016
- Murata K, Mitsuoka K, Hirai T, Walz T, Agre P et al (2000) Structural determinants of water permeation through aquaporin-1. *Nature* 407:599–605.
- Nakhoul NL, Davis BA, Romero MF, Boron WF (1998) Effect of expressing the water channel aquaporin-1 on the CO₂ permeability of *Xenopus* oocytes. *Am J Physiol* 274:C543–C548
- Nemeth-Cahalan KL, Hall JE (2000) pH and calcium regulate the water permeability of aquaporin 0. *J Biol Chem* 275:6777–6782
- Nielsen S, Kwon TH, Frokiaer J, Knepper MA (2000) Key roles of renal aquaporins in water balance and water-balance disorders. *News Physiol Sci* 15:136–143
- Nielsen S, Kwon TH, Frokiaer J, Agre P (2007) Regulation and dysregulation of aquaporins in water balance disorders. *J Intern Med* 261:53–64
- Niemietz CM, Tyerman SD (2000) Channel-mediated permeation of ammonia gas through the peribacteroid membrane of soybean nodules. *FEBS Lett* 465:110–114
- Pohl P, Saparov SM, Borgnia MJ, Agre P (2001) Highly selective water channel activity measured by voltage clamp: analysis of planar lipid bilayers reconstituted with purified AqpZ. *Proc Natl Acad Sci USA* 98:9624–9629
- Prak S, Hem S, Boudet J, Viennois G, Sommerer N et al (2008) Multiple phosphorylations in the C-terminal tail of plant plasma membrane aquaporins. Role in sub-cellular trafficking of AtPIP2;1 in response to salt stress. *Mol Cell Proteomics* 7:1019–1030
- Prasad GV, Coury LA, Finn F, Zeidel ML (1998) Reconstituted aquaporin 1 water channels transport CO₂ across membranes. *J Biol Chem* 273:33123–33126
- Preston GM, Agre P (1991) Isolation of the cDNA for erythrocyte integral membrane protein of 28 kilodaltons: member of an ancient channel family. *Proc Natl Acad Sci USA* 88:11110–11114

- Preston GM, Carroll TP, Guggino WB, Agre P (1992) Appearance of water channels in *Xenopus* oocytes expressing red cell CHIP28 protein. *Science* 256:385–387
- Preston GM, Jung JS, Guggino WB, Agre P (1993) The mercury-sensitive residue at cysteine 189 in the CHIP28 water channel. *J Biol Chem* 268:17–20
- Quigley F, Rosenberg JM, Shachar-Hill Y, Bohnert HJ (2002) From genome to function: the *Arabidopsis* aquaporins. *Genome Biol* 3:RESEARCH0001
- Ramahaleo T, Morillon R, Alexandre J, Lassalles JP (1999) Osmotic water permeability of isolated protoplasts. Modifications during development. *Plant Physiol* 119:885–896
- Ren G, Reddy VS, Cheng A, Melnyk P, Mitra AK (2001) Visualization of a water-selective pore by electron crystallography in vitreous ice. *Proc Natl Acad Sci USA* 98:1398–1403
- Robben JH, Knoers NV, Deen PM (2006) Cell biological aspects of the vasopressin type-2 receptor and aquaporin 2 water channel in nephrogenic diabetes insipidus. *Am J Physiol Renal Physiol* 291:F257–F270
- Robinson DG, Sieber H, Kammerloher W, Schaffner AR (1996) PIP1 Aquaporins are concentrated in plasmalemmasomes of *Arabidopsis thaliana* mesophyll. *Plant Physiol* 111:645–649
- Sakurai J, Ishikawa F, Yamaguchi T, Uemura M, Maeshima M (2005) Identification of 33 rice aquaporin genes and analysis of their expression and function. *Plant Cell Physiol* 46: 1568–1577
- Saparov SM, Liu K, Agre P, Pohl P (2007) Fast and selective ammonia transport by aquaporin-8. *J Biol Chem* 282:5296–5301
- Savage DF, Stroud RM (2007) Structural basis of aquaporin inhibition by mercury. *J Mol Biol* 368:607–617
- Savage DF, Egea PF, Robles-Colmenares Y, O'Connell JD III, Stroud RM (2003) Architecture and selectivity in aquaporins: 2.5 Å X-ray structure of aquaporin Z. *PLoS Biol* 1:E72
- Scheuring S, Müller DJ, Stahlberg H, Engel HA, Engel A (2002) Sampling the conformational space of membrane protein surfaces with the AFM. *Eur Biophys J* 31:172–178.
- Shiels A, Bassnett S, Varadaraj K, Mathias R, Al-Ghoul K et al (2001) Optical dysfunction of the crystalline lens in aquaporin-0-deficient mice. *Physiol Genomics* 7:179–186
- Stroud RM, Miercke LJ, O'Connell J, Khademi S, Lee JK et al (2003) Glycerol facilitator GlpF and the associated aquaporin family of channels. *Curr Opin Struct Biol* 13:424–431
- Sui H, Han BG, Lee JK, Walian P, Jap BK (2001) Structural basis of water-specific transport through the AQP1 water channel. *Nature* 414:872–878
- Takano J, Wada M, Ludewig U, Schaaf G, von Wiren N, Fujiwara T (2006) The *Arabidopsis* major intrinsic protein NIP5;1 is essential for efficient boron uptake and plant development under boron limitation. *Plant Cell* 18:1498–1509
- Takemoto L, Takehana M, Horwitz J (1986) Covalent changes in MIP26K during aging of the human lens membrane. *Invest Ophthalmol Vis Sci* 27:443–446
- Tornroth-Horsefield S, Wang Y, Hedfalk K, Johanson U, Karlsson M et al (2006) Structural mechanism of plant aquaporin gating. *Nature* 439:688–694
- Uehlein N, Lovisollo C, Siefritz F, Kaldenhoff R (2003) The tobacco aquaporin NtAQP1 is a membrane CO₂ pore with physiological functions. *Nature* 425:734–737
- Venero JL, Vizuete ML, Ilundain AA, Machado A, Echevarria M, Cano J (1999) Detailed localization of aquaporin-4 messenger RNA in the CNS: preferential expression in periventricular organs. *Neuroscience* 94:239–250
- Verbavatz JM, Ma T, Gobin R, Verkman AS (1997) Absence of orthogonal arrays in kidney, brain and muscle from transgenic knockout mice lacking water channel aquaporin-4. *J Cell Sci* 110:2855–2860
- Walz T, Smith BL, Agre P, Engel A (1994a) The three-dimensional structure of human erythrocyte aquaporin CHIP. *EMBO J* 13:2985–2993
- Walz T, Smith BL, Zeidel ML, Engel A, Agre P (1994b) Biologically active 2-dimensional crystals of aquaporin CHIP. *J Biol Chem* 269:1583–1586
- Walz T, Hirai T, Murata K, Heymann JB, Mitsuoka K et al (1997) The three-dimensional structure of aquaporin-1. *Nature* 387:624–627
- Wu B, Beitz E (2007) Aquaporins with selectivity for unconventional permeants. *Cell Mol Life Sci* 64:2413–2421
- Yakata K, Hiroaki Y, Ishibashi K, Sohara E, Sasaki S et al (2007) Aquaporin-11 containing a divergent NPA motif has normal water channel activity. *Biochim Biophys Acta* 1768:688–693
- Yasui M, Hazama A, Kwon TH, Nielsen S, Guggino WB, Agre P (1999a) Rapid gating and anion permeability of an intracellular aquaporin. *Nature* 402:184–187

- Yasui M, Kwon TH, Knepper MA, Nielsen S, Agre P (1999b) Aquaporin-6: An intracellular vesicle water channel protein in renal epithelia. *Proc Natl Acad Sci USA* 96:5808–5813
- Zardoya R (2005) Phylogeny and evolution of the major intrinsic protein family. *Biol Cell* 97: 397–414
- Zeidel ML, Ambudkar SV, Smith BL, Agre P (1992) Reconstitution of functional water channels in liposomes containing purified red cell CHIP28 protein. *Biochemistry* 31:7436–7440

Dynamics and Energetics of Permeation Through Aquaporins. What Do We Learn from Molecular Dynamics Simulations?

Jochen S. Hub, Helmut Grubmüller, and Bert L. de Groot

Contents

1	Why Molecular Dynamics Simulations?	58
2	Water Permeates Through AQPs Along a Lattice of Protein-Water Hydrogen Bonds	58
2.1	Calculating Water Permeability Coefficients	61
2.2	Perfect Single-File Water Transport?	62
3	Protons Are Excluded by an Electrostatic Barrier	63
3.1	Origin of the Barrier: Protein Electric Field Vs. Desolvation Effects	65
4	Are Aquaporins Permeated by Gas?	65
5	Permeation of Uncharged Solutes Through Aquaporin Channels	68
5.1	Glycerol Permeation Through Aquaglyceroporin GlpF	68
5.2	Toward a General Understanding of Channel Selectivity	68
6	Summary and Concluding Remarks	73
	References	73

Abstract Aquaporins (AQPs) are a family of integral membrane proteins, which facilitate the rapid and yet highly selective flux of water and other small solutes across biological membranes. Molecular dynamics (MD) simulations contributed substantially to the understanding of the molecular mechanisms that underlie this remarkable efficiency and selectivity of aquaporin channels. This chapter reviews the current state of MD simulations of aquaporins and related aquaglyceroporins as well as the insights these simulations have provided. The mechanism of water permeation through AQPs and methods to determine channel permeabilities from simulations are described. Protons are strictly excluded from AQPs by a large electrostatic barrier and not by an interruption of the Grothuss mechanism inside the pore. Both the protein's electric field and desolvation effects contribute to this barrier. Permeation of apolar gas molecules such as CO₂ through AQPs is accompanied by a large energetic barrier and thus can only be expected in membranes with a low intrinsic gas permeability. Additionally, the insights from simulations into the mechanism of glycerol permeation through the glycerol facilitator GlpF from *E. coli*

B.L. de Groot (✉)

Computational Biomolecular Dynamics Group, Max-Planck Institute for Biophysical Chemistry, Am Fassberg 11, 37077 Göttingen, Germany
bgroot@gwdg.de

E. Beitz (ed.), *Aquaporins*, Handbook of Experimental Pharmacology 190,
© Springer-Verlag Berlin Heidelberg 2009

are summarized. Finally, MD simulations are discussed that revealed that the aromatic/arginine constriction region is generally the filter for uncharged solutes, and that AQP selectivity is controlled by a hydrophobic effect and steric restraints.

1 Why Molecular Dynamics Simulations?

Aquaporins (AQPs) facilitate water transport across biological membranes in response to an osmotic pressure (Preston et al. 1992). Compared with other biological processes, the translocation of water molecules by AQPs is extremely fast, on a nanosecond timescale (Zeidel et al. 1992). Remarkably, AQPs are also highly selective. Ions, in particular protons, are strictly excluded from AQPs, which ensures that electrochemical gradients across the membrane are maintained (Zeidel et al. 1994). Related aquaglyceroporins are permeated by larger solutes such as glycerol and/or urea whereas *ordinary* AQPs exclude any larger solutes. How can channels be efficient *and* highly selective at the same time?

High-resolution structures of AQPs have been determined by electron microscopy (Gonen et al. 2004; Murata et al. 2000) and X-ray diffraction experiments (Fu et al. 2000; Hiroaki et al. 2006; Lee et al. 2005; Savage et al. 2003; Sui et al. 2001; Törnroth-Horsefield et al. 2006). The structures provide invaluable insights in the molecular mechanisms acting in aquaporins. However, mostly static information was provided and we can therefore not observe aquaporins *at work*. So far, there is no experimental method of sufficient spatial and time resolution to monitor permeation through aquaporins on a molecular level. Molecular dynamics (MD) simulations therefore complement experiments by providing the progression of the biomolecular system at atomic resolution. Having all atomic coordinates as well as interaction energies and forces at hand, simulations yield insight into the physicochemical mechanisms (free energies, entropies, electrostatic forces, formation and rupture of hydrogen bonds, etc.), which drive biological processes such as permeation through aquaporins. The technique of MD simulations is sketched in Fig. 1.

During the last years, MD simulations of aquaporins have been a quite active field of research and provided (and still provide) remarkable insights into the function of these fascinating channels. This chapter overviews the current state of aquaporin simulations and shows how simulations reveal molecular mechanisms underlying the efficiency and selectivity of aquaporins, and thus explain biological function.

2 Water Permeates Through AQPs Along a Lattice of Protein-Water Hydrogen Bonds

High-resolution structures of aquaporin-1 (AQP1) (de Groot et al. 2001; Murata et al. 2000; Sui et al. 2001) and the bacterial glycerol facilitator GlpF (Fu et al. 2000) enabled atomistic *real-time* molecular dynamics (MD) simulations of spontaneous,

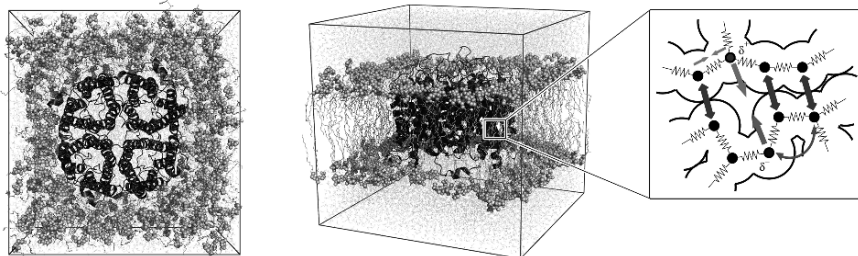


Fig. 1 Molecular dynamics simulations. Various kinds of interatomic forces act within macromolecules (here, an aquaporin tetramer). Forces arising from chemical bonds, here represented as springs, compel bound atoms into their equilibrium distances or equilibrium angles (thin arrows). Pauli repulsion (dark double arrows) prohibits atoms from penetrating through each other. Long-range interactions, particularly Coulomb interactions (thick light gray arrows) between partially charged atoms (δ^+ , δ^-), contribute significantly to the stability of a protein structure. All these interactions (and several others) determine the three-dimensional structure of a protein as well as the motion of each individual atom; they are therefore fully included within a molecular dynamics (MD) simulation. The movement of the atoms is calculated in classical approximation by numerical integration of Newton's equations of motion. This approximation holds at room temperature for many processes. Because the forces change rapidly with the changing atomic positions, all forces have to be repeatedly updated in small time steps (typically 10^{-15} s). Thus, 10^6 such integration steps simulate the movement of all atoms of the simulation system for the short time span of 1 ns. To date, the typical length of MD simulations is ≈ 100 ns, limited by the available computational resources.

full permeation events in aquaporins (de Groot and Grubmüller 2001; Tajkhorshid et al. 2002). It was found that both AQP1 and GlpF act as two-stage filters (de Groot and Grubmüller 2001). The first stage of the filter is located in the central part of the channel at the asparagine/proline/alanine (NPA) region; the second stage is located on the extracellular face of the channel in the aromatic/arginine (ar/R) constriction region (cf. Fig. 2). An independent simulation of GlpF (Tajkhorshid et al. 2002) using a different force field confirmed the crucial role of the NPA region; this had also been inferred from the fact that this motif is highly conserved (Heymann and Engel 2000; Jung et al. 1994). These simulation studies also suggested mutants that change the permeation characteristics in a predicted manner (Tajkhorshid et al. 2002).

The simulations also addressed the energetics of water permeation. Overall, the channels achieve their high water permeability through a fine-tuned *choreography* of hydrogen bonds (de Groot and Grubmüller 2001). Whenever and wherever bulk water-water hydrogen bonds have to be ruptured to allow the water molecule to *squeeze* through the narrow NPA or ar/R regions, the protein offers *replacement* interactions, which largely compensate for the energetic cost of water-water bond rupture (cf. Fig. 3b). This remarkable complementarity to bulk water lowers the activation barrier to a large extent and thus allows the high permeation rate, which is observed both experimentally and in simulations, despite the hydrophobic nature of the pore.

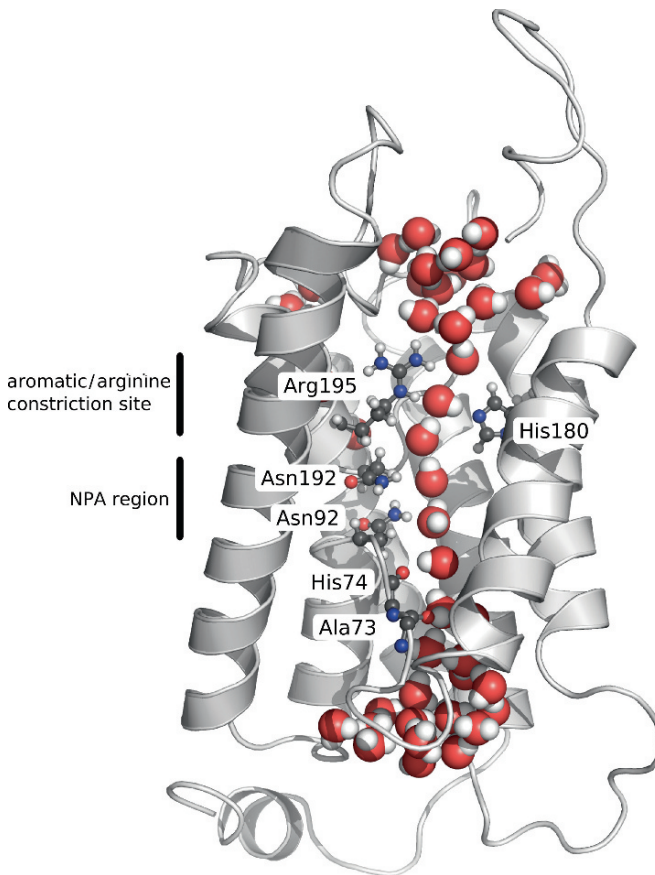


Fig. 2 Snapshot from an MD simulation of AQP1 showing a single file of water inside the AQP1 channel. Water molecules are shown as spheres, some water-interacting amino acid side chains are shown in ball-and-stick representation. As indicated by the black bar, the two conserved Asn-Pro-Ala (NPA) motifs are located at the end of the two half helices HB and HE. The asparagines of the NPA motifs form strong hydrogen bonds to permeating water molecules. Closer to the extracellular exit of the channel, the aromatic/arginine region (ar/R) forms the narrowest part of the channel (de Groot et al. 2001; Sui et al. 2001).

The simulations finally revealed a pronounced water dipole orientation pattern across the channel, with the NPA region as its symmetry center (de Groot and Grubmüller 2001). In the simulations, the water molecules were found to rotate by 180° on their path through the pore (Fig. 3a). By artificially switching off the electric dipoles of the half helices B and E, it was elegantly demonstrated that it is the electrostatic field generated by the helical macrodipoles that mainly determines the strict water dipole orientation (Tajkhorshid et al. 2002). The dipolar rotation does not allow the water file to form a continuous hydrogen bond network inside the pore.

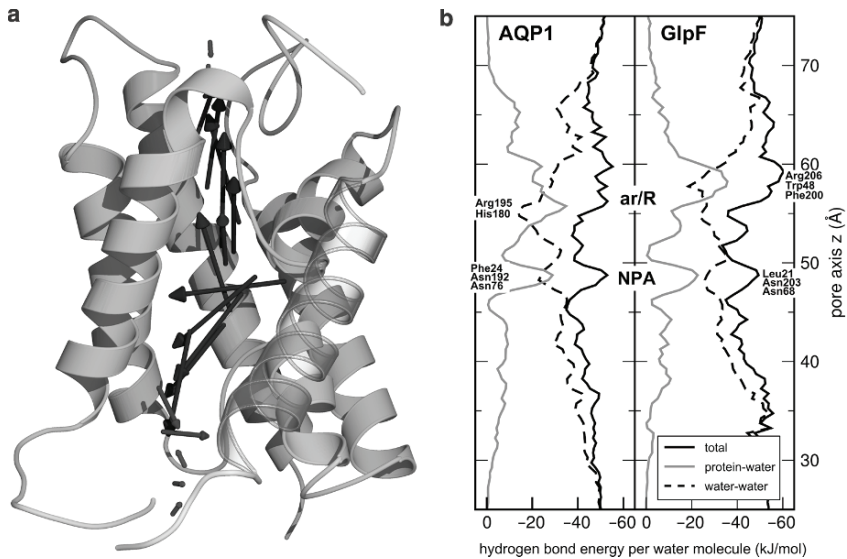


Fig. 3 (a) Bipolar orientation of water molecules inside the aquaporin-1 channel, as derived from MD simulations (de Groot and Grubmüller 2001). The water dipoles (black arrows) rotate by approximately 180° while permeating through the AQP1 pore. (b) Hydrogen bond energies per water molecule (solid black lines) in AQP1 (left) and GlpF (right). Protein–water hydrogen bonds (gray) compensate for the loss of water–water hydrogen bonds (dashed). The main protein–water interaction sites are the ar/R region and the NPA site, apparent from the maxima in the (absolute) protein–water hydrogen bond energies (gray).

This fact led to speculations (Tajkhorshid et al. 2002) that it is the water orientation that prevents the channel from proton leakage (see also next section).

2.1 Calculating Water Permeability Coefficients

MD simulations allow one to address aquaporin function in quantitative terms. Calculation of permeability coefficients and comparison with measured values (Engel and Stahlberg 2002) provide a very sensitive test of the simulations. The best-studied permeability coefficient is the *osmotic permeability* p_f . It can be defined from the net water flux j_w , which occurs in response to a difference in some solute concentration between the two water compartments ΔC_s . Then, p_f is given by (Finkelstein 1987)

$$j_w = p_f \Delta C_s \quad (1)$$

The calculation of p_f from MD simulation is not straightforward. The reason is the following: under equilibrium conditions (without any osmotic pressure) a large number of water molecules cross the channel as result of thermal fluctuations. These frequent spontaneous channel crossings occur equally often in both directions of the channel, yielding zero net flux. After applying an osmotic pressure, the number of

permeation events upward the chemical gradient is slightly reduced, yielding a net flux. The net flux is generally very small and is therefore difficult to detect against the large background of total channel crossings.

One strategy to overcome this problem is to apply a hydrostatic pressure instead of an osmotic pressure (Zhu et al. 2002). To generate a measurable net flux a very large pressure is however required, which, in turn, necessitates to artificially restrain the aquaporin in the simulation. Nevertheless, the obtained p_f is in good agreement to experiment.

An elegant alternative is to compute the nonequilibrium permeation coefficient p_f directly from equilibrium simulations. This approach is rigorous, because nonequilibrium quantities (such as transport coefficients) are closely related to equilibrium properties. Or more precisely, a thermodynamic system responds linearly to small external perturbations, and the response is quantitatively determined by equilibrium quantities of the system. This remarkable relation is referred to as *fluctuation dissipation theorem*. p_f , for example, is related to spontaneous permeation events under equilibrium.

Spontaneous hops of a single file of water have for the first time been used to determine the p_f of gramicidin-A (de Groot et al. 2002). The method rests on the assumption that the permeation rate is proportional to a Boltzmann factor $\exp(-\Delta G^\ddagger/k_B T)$ with an Arrhenius activation energy ΔG^\ddagger . (For an expanded derivation see Zhu et al. 2004b.) For AQP1, the method was reported to yield $p_f = 7.5 \times 10^{14} \text{ cm}^3 \text{ s}^{-1}$ (de Groot and Grubmüller 2001, 2005) or $7.1 \times 10^{14} \text{ cm}^3 \text{ s}^{-1}$ (Zhu et al. 2004b), in good agreement to experimental values of 3.2 to $11.7 \times 10^{14} \text{ cm}^3 \text{ s}^{-1}$ (Engel and Stahlberg 2002). More recently, a model has been proposed, which describes the motions of all water molecules in the pore by one collective coordinate (Zhu et al. 2004a). The diffusion of this collective coordinate is again related to p_f . The model has been successfully applied to a number of AQP channels, including mammalian AQP1 and AQP0 as well as the bacterial AQP-Z and GlpF (Hashido et al. 2005; Jensen and Mouritsen 2006). These studies found reasonable agreement to experimental p_f values for the water channels AQP1 and AQP-Z. The p_f of GlpF, however, was reported to be similar to the p_f of AQP-Z (Hashido et al. 2005), or even 2–3 times larger (Jensen and Mouritsen 2006), a finding which seems to contradict experiments (Borgnia and Agre 2001; Maurel et al. 1994). Further experiments and simulations are required to resolve this issue.

2.2 Perfect Single-File Water Transport?

The water permeation in AQPs is often referred to as *single-file* permeation. This picture may be supported by snapshots of MD simulations, which often display an ideal water file (compare Fig. 2). An idealized single-file structure requires, however, that no gaps between water molecules are present at any time, and that all water molecules in the channel move in a concerted fashion (Finkelstein 1987). In particular, water molecules must not interchange position. A number of MD stud-

ies have investigated to which extent this ideal picture actually holds. One strategy is to compare the osmotic permeability p_f to the diffusive permeability coefficient p_d . For a perfect single-file permeation $p_f/p_d = N + 1$, where N denotes the number of water binding sites inside the pore (or the average occupancy number if empty sites occur) (Finkelstein 1987). In AQP-Z p_f/p_d was found to be ≈ 12 , close to the number of water molecules inside the pore, whereas $p_f/p_d \approx 4$ was found for GlpF (Jensen and Mouritsen 2006). Hence, the single-file structure is more pronounced in the narrow pore of AQP-Z.

Recently, Hashido et al. proposed a method to determine to which extent (1) concerted water motion and (2) uncorrelated local diffusion contribute to the total p_f (Hashido et al. 2007). The analysis revealed that water-water correlations are particularly reduced around the NPA region and that p_f is affected by slow local diffusion in the narrow ar/R region.

Taken together, such studies indicate that the picture of single-file permeation is an idealized simplification of the real situation and it only partly describes the permeation through AQPs. Long-range correlations between water molecules are reduced by water-protein interactions, and water molecules occasionally interchange positions, in particular in wider AQP channels such as GlpF.

3 Protons Are Excluded by an Electrostatic Barrier

Proton conduction in bulk water proceeds via the Grotthuss mechanism (de Grotthuss 1806). Accordingly, protons are transferred between water molecules via hydrogen bonds and transient hydronium ions, Eigen and Zundel clusters. Necessarily, the water dipoles reorient during this process. The observation of interrupted hydrogen bonds along the water chain inside the AQP pore (de Groot and Grubmüller 2001), as well as the strict orientation of the water molecules (de Groot and Grubmüller 2001; Tajkhorshid et al. 2002), led to speculation that these effects interfere with the Grotthuss mechanism and thus preclude proton conduction through the channel. Because these *first-generation* studies were mainly aimed at – and succeeded in – explaining efficient water permeation, only (neutral) water molecules were considered and, hence, the aforementioned speculation about the mechanism of proton exclusion was based only on *indirect* evidence.

To obtain direct information, explicit treatments of excess protons and proton transfer reactions in *second-generation* simulations were required. Within only a few years, eight studies have been published, which explicitly address the energetics and dynamics of excess protons in the AQP channel (Burykin and Warshel 2003, 2004; Chakrabarti et al. 2004a, b; Chen et al. 2006; de Groot et al. 2003; Ilan et al. 2004; Kato et al. 2006). The applied methods are quite diverse, including classical electrostatics calculations (Chakrabarti et al. 2004b; de Groot et al. 2003; Jensen et al. 2003), Q-HOP proton transfer simulations (de Groot et al. 2003), semimicroscopic protein-dipole Langevin-dipole linear response approximation (PDL/D/S-LRA) calculations (Burykin and Warshel 2003; de Groot et al. 2003; Kato et al. 2006), umbrella MD simulations employing the PM6 dissociable water model

(Chakrabarti et al. 2004a, b), and steered (multistate) empirical valence bond proton transfer simulations (Chen et al. 2006; Ilan et al. 2004; Kato et al. 2006). Furthermore, the energetics of proton translocation have been computed for two different members of the aquaporin family, AQP1 and GlpF.

From these studies it became clear that the proton exclusion can *not* be explained from a discontinuous hydrogen bond network inside the channel, as inferred from the initial X-ray structures (Sui et al. 2001). Instead, if a proton is forced into the channel, remarkably high proton mobility through efficient Grotthuss transfers was observed throughout the channel, without any severe interruption (de Groot et al. 2003). These results contrast with the original picture of an interrupted proton wire. The water molecules inside the pore should in fact *not* be regarded as a static bipolar water column, with the water oxygen atoms pointed toward the channel center at any time. Instead, water molecules rotate inside the channel, and only the average water dipole is pointed toward the channel exits.

The consensus conclusion is that a large electrostatic barrier, rather than proton wire interruption effects, is the dominant mechanism of proton exclusion in aquaporins. From the free energy profile of proton translocation the barrier height was determined to approximately 25 kcal mol^{-1} (Chen et al. 2006; Kato et al. 2006), with the maximum of the profile being located in the NPA region (cf. Fig. 4). Accordingly, the presence of a proton wire has little influence on a hypothetical proton transport, because the protons could not *climb* the barrier, even if the proton wire was intact.

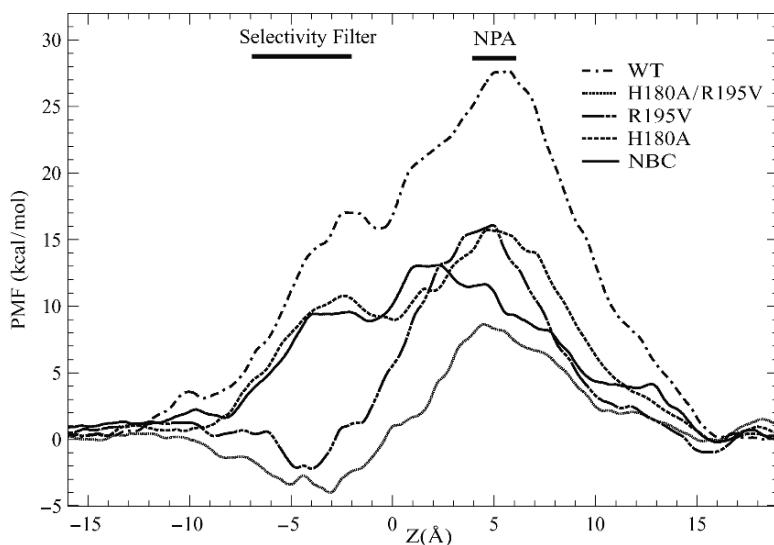


Fig. 4 Potentials of mean force (PMFs) for proton transfer through AQP1 (Chen et al. 2006). In the AQP1 wild type (WT, dotted-dashed curve), a large barrier of 28 kcal mol^{-1} prohibits any proton leakage. Switching off the dipoles of the half helices HB and HE (NBC, *no-backbone-charge*, solid curve) reduces the barrier substantially. Likewise, mutations in the aromatic/arginine region (here termed *selectivity filter*), such as R195V, H180A, R195V/H180A, reduce the barrier and may therefore cause proton leakage, as observed experimentally (Beitz et al. 2006).

3.1 Origin of the Barrier: Protein Electric Field Vs. Desolvation Effects

A question that has been lively discussed and that is not yet completely resolved is the origin of the electrostatic barrier. Two competing pictures have been suggested. First, electric field generated by the dipoles of the two AQP half helices HB and HE has been proposed to repel the protons from the NPA region (Chakrabarti et al. 2004b; de Groot et al. 2003). This picture implies that the bipolar water orientation is only a side effect of the electrostatic field in the pore (de Groot et al. 2003), and not the cause of proton exclusion.

Others studies emphasized desolvation effects as the origin of the electrostatic barrier (Burykin and Warshel 2003; Kato et al. 2006). In the highly dielectric ($\epsilon = 80$) bulk water, the proton is well solvated by surrounding water molecules. Upon moving the proton across the AQP pore, the solvation shell needs to be removed from the proton. Inside the pore, the hydronium ion is only partially solvated by few close water molecules, and the surrounding protein medium [$\epsilon \approx 4$ (Kato et al. 2006)] stabilizes the hydronium only to a fraction of the solvation in the bulk. Thus, a large energetic cost results for moving the hydronium from the water into the channel.

The controversy on the origin of the electrostatic barrier is mainly caused by the problem of how to *measure* the contributions of polar groups (mainly of the half helices) to the barrier. A common approach is to *switch off* the corresponding partial charges during the simulation (Chakrabarti et al. 2004a; Chen et al. 2006). After such an alchemical transformation, the protein atoms rearrange toward a new stable configuration. The protein may even become unstable, and artificial restraints may be required to keep the protein in its native structure. To which degree the rearrangement of protein atoms should be allowed by the simulation protocol seems somewhat unclear, but has an impact on the quantitative results (Kato et al. 2006). The most recent results indicate that 35–55% of the free energy barrier is generated by the dipoles of the half helices HB and HE (Chen et al. 2006; Kato et al. 2006), and the remaining part is caused by desolvation (compare Fig. 4).

4 Are Aquaporins Permeated by Gas?

It has been a long-standing question whether aquaporins also facilitate gas permeation. In particular, the role of AQP1 as a CO₂ channel has been a matter of lively debate ever since it has been reported that AQP1 increases the CO₂ permeability of *Xenopus* oocytes membranes (Nakhoul et al. 1998). By now, aquaporins have been reported to increase the CO₂ permeability of membranes of oocytes (Cooper and Boron 1998; Nakhoul et al. 1998), liposomes (Prasad et al. 1998), and red blood cells (Blank and Ehmke 2003; Endeward et al. 2006). Other studies did not report any impact of AQP1 on membrane CO₂ permeability (Yang et al. 2000). Moreover, a physiological role of AQP1 or AQP5 for CO₂ transport in the lung or

in the kidney has been questioned (Fang et al. 2002). Another process for which aquaporin-mediated CO₂ permeation has been suggested to play a physiological role is photosynthesis. It was shown that the leaf growth and the diffusion of CO₂ inside the leaves of tobacco plants were dependent on the level of NtAQP1 expression, an aquaporin homologous to human AQP1 (Uehlein et al. 2003). By now, this question is still not settled by experiments.

This controversy triggered MD simulations of CO₂ permeation through AQP1 (Hub and de Groot 2006). Potentials of mean force (PMFs) were computed of possible pathways for CO₂ across an AQP1 tetramer, embedded in a model membrane of pure POPE (1-palmitoyl-2-oleoyl-*sn*-glycero-3-phosphoethanolamine) (Fig. 5). The key finding was that CO₂ encounters a substantial barrier of approximately 23° kJ mol⁻¹ when permeating through the AQP1 water pore (Fig. 5, solid curve). The corresponding PMF for the central cavity of the AQP tetramer displays two barriers of only 13° kJ mol⁻¹, assuming that the cavity is not blocked by an ion or organic molecule. Hence, the central cavity is more likely to contribute to a CO₂ flux than the AQP1 water pores. A model POPE membrane, in contrast, was found to be highly permeable to CO₂ with barriers of only 4 kJ mol⁻¹ and a large membrane permeability of $P_f \approx 12 \text{ cm s}^{-1}$. AQP1 embedded in a membrane of POPE is therefore not expected to increase the CO₂ permeation. Therefore, AQP1 can be expected to play a physiological role only in membranes with a low intrinsic CO₂ permeability. Membranes with similar physicochemical characteristics to POPE are highly permeable to CO₂, rendering a physiological role for AQP1-mediated CO₂ permeation in such membranes unlikely.

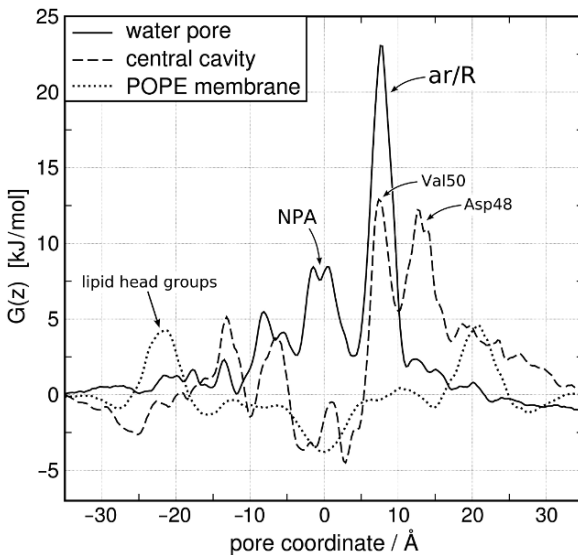


Fig. 5 Potentials of mean force $G(z)$ for CO₂ permeation along possible pathways across an AQP1 tetramer embedded in a bilayer of POPE: through the AQP1 water pore (black solid line), the tetrameric central cavity (dashed), and across the POPE lipid bilayer (dotted).

More recently, Wang et al. corroborated this picture (Wang et al. 2007) and showed that it holds qualitatively also to molecular oxygen. Like CO_2 , also O_2 might permeate through the apolar central cavity. Interestingly, a small apolar cavity located between neighboring AQP1 monomers was suggested to be permeable to O_2 . Compared with a membrane of POPE, however, the AQP1 pores are not expected to contribute substantially to O_2 permeation.

From the MD simulations it was possible to extract the molecular mechanism underlying the 23-kJ mol^{-1} barrier for CO_2 permeation through the AQP1 water pore (Hub and de Groot 2006). The main barrier is located in the ar/R region (cf. Fig. 5). The barrier has been proposed to originate from water-protein hydrogen bonds, mainly to Arg195. If no CO_2 molecule is present in the ar/R region, water forms hydrogen bonds to the guanidinium group of Arg195 (Fig. 6a, compare also Fig. 3b). Upon permeation of CO_2 through the narrow ar/R site these water-Arg195 hydrogen bonds are partially lost, leaving an energetically unfavorable configuration (Fig. 6b). Hence, since the ar/R site of AQP1 is both narrow and hydrophilic it generates a substantial barrier against permeation of the apolar CO_2 . This observation implies that the wider and more hydrophobic ar/R site of aquaglyceroporins is expected to be more permeable to CO_2 . Indeed, the main barrier for CO_2 permeation through the bacterial aquaglyceroporin GlpF was recently determined to be only 13.5 kJ mol^{-1} (Hub and de Groot 2008), close to the barrier for water permeation.

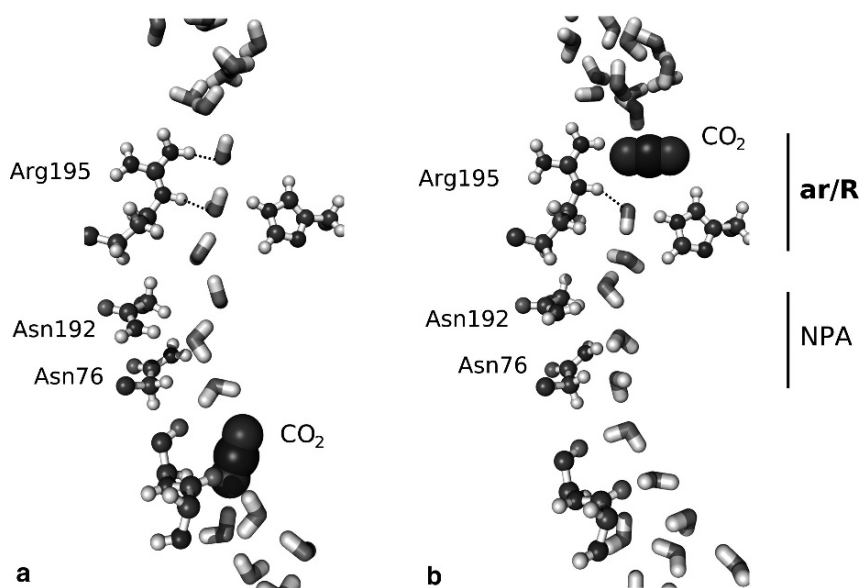


Fig. 6 Snapshots from a putative permeation event of a CO_2 molecule through the AQP1 water pore, as derived from MD simulations. Water molecules are shown as sticks, the CO_2 as dark spheres. (a) Water forms strong hydrogen bonds to the conserved arginine, as indicated by dotted lines. (b) Upon CO_2 permeation through the ar/R region, such water-Arg195 hydrogen bonds are (partially) lost, generating a substantial barrier against CO_2 permeation (cf. also Fig. 5).

5 Permeation of Uncharged Solutes Through Aquaporin Channels

5.1 Glycerol Permeation Through Aquaglyceroporin GlpF

The 2.2-Å-resolution structure of *E. coli* glycerol facilitator GlpF (Fu et al. 2000) opened the possibility to study the mechanism as well as the energetics of glycerol permeation through GlpF. The simulations revealed that glycerol is conducted via repeated formation and rupture of glycerol–protein hydrogen bonds (Jensen et al. 2001). Water is actively involved in this process as it competes with glycerol for hydrogen bonds to the protein. Using Jarzynski's equality, the potential of mean force (PMF) for glycerol permeation through GlpF was reconstructed from nonequilibrium simulations (Jensen et al. 2002). The PMF displayed a periplasmic vestibule of low energy, which was speculated to enhance the uptake of glycerol from the environment. The existence of this vestibule could however not be confirmed by more recent MD studies (Hénin et al. 2008; Hub and de Groot 2008).

Permeability measurements of chiral polyols have suggested that GlpF is stereoselective (Heller et al. 1980). Interestingly, the stereoselectivity has also been observed in MD simulations. The force that is required to pull glycerol through the ar/R region of GlpF depends on the orientation of the glycerol molecule inside the pore (Jensen et al. 2002). This effect is caused by the arrangement of potential hydrogen bond partners inside the channel: in the favorable orientation in the ar/R site, all three hydroxyl groups of glycerol are able to form hydrogen bonds to polar protein groups or to the nearby water molecules. In the unfavorable orientation, however, one hydroxyl group gets in close contact to the apolar side chain of Phe200, which accounts for an unfavorable configuration. Recently it has been suggested that different conformations of the two O–C–O torsional angles play a role in glycerol conduction through GlpF (Hénin et al. 2008). In these simulations, the probabilities for the two torsional angles to be in the *gauche* or *anti* state highly depend on the glycerol position along the channel. Hence, internal transitions of the glycerol molecule may be required for permeation.

5.2 Toward a General Understanding of Channel Selectivity

So far, 13 different AQP channels were identified in humans (Zardoya 2005). All AQPs are assumed to share a common fold and a number of conserved residues in the channel, such as the conserved NPA motifs and the arginine in the ar/R site (Heymann and Engel 2000). In spite of these remarkable similarities, 13 distinct AQPs have evolved, reflecting the need for tight control of membrane permeability for water and other solutes.

Fine-tuned differences between AQP family members in channel diameter and the arrangement of hydrogen bond partners may determine their permeabilities with respect to different solutes. However, the molecular mechanisms that determine the

AQPs' substrate specificities were poorly understood until recently. Therefore, a recent MD study investigated the selectivity of one member of each of the two AQP subfamilies, i.e., AQP1 as a representative for the AQP water channels, and *E. coli* GlpF as a member of the aquaglyceroporin family (Hub and de Groot 2008). Umbrella sampling simulations (Torrie and Valleau 1974) were employed to compute PMFs for the permeation of a number of solutes through AQP1 and GlpF (Fig. 7).

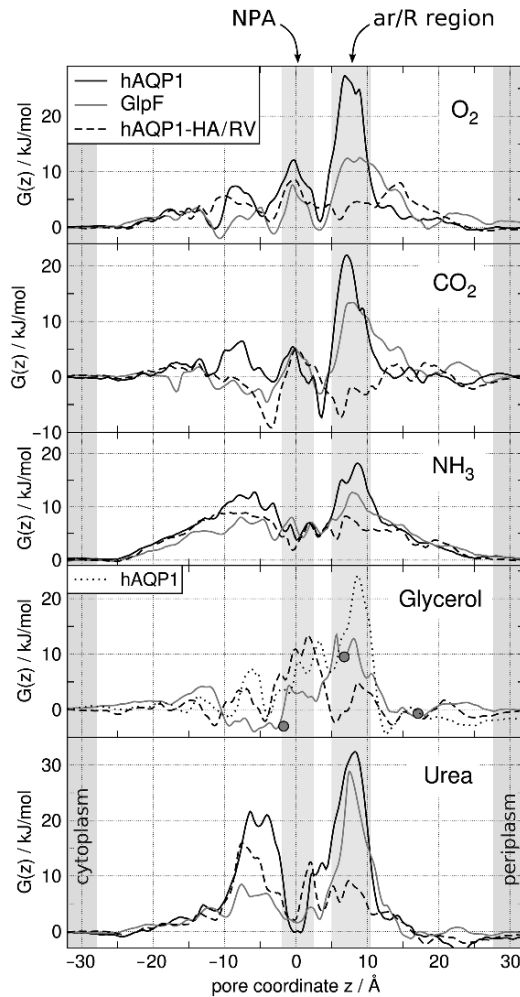


Fig. 7 Potentials of mean force $G(z)$ for the permeation of O_2 , CO_2 , NH_3 , glycerol, and urea through AQP1 (black solid curves) and GlpF (gray). The NPA site and the ar/R region are highlighted by gray bars. Note that the main barriers are located in the ar/R region, demonstrating its role for the selectivity of AQPs for uncharged solutes. The glycerol positions in the GlpF crystal structure are shown as small circles (Fu et al. 2000). The barrier against glycerol permeation through AQP1 (dotted line) may have been underestimated in the simulation protocol, see Hub and de Groot (2008) for details. Mutations in the ar/R region (dashed lines) have drastic effects on the main barrier and therefore on channel selectivity.

The considered solutes included O_2 , CO_2 , NH_3 , H_2O , glycerol, and urea, which differ substantially in hydrophobicity and size. All computed PMFs display a main barrier in the ar/R region, confirming its role as the selectivity filter for uncharged solutes. GlpF was found to be generally less selective than AQP1.

To address whether a solute is likely to permeate through a channel, the permeability of the channel must be compared with the permeability of the surrounding lipid bilayer. In terms of energetic barriers, permeation through the channel is only expected if the barrier for channel permeation is substantially lower than the barrier for permeation across the lipid bilayer. Therefore, PMFs for solute permeation through two model membranes, composed of pure POPC and pure POPE, respectively, have been computed from simulations (Hub and de Groot 2008). The PMFs for POPC are displayed in Fig. 8.

By comparing the AQP PMFs (Fig. 7) with the membrane PMFs (Fig. 8) a number of conclusions can be drawn. For example, membranes similar to POPE or POPC are rapidly permeated by apolar gas molecules such as O_2 and CO_2 . Neither AQP1 nor GlpF are expected to enhance the flux of O_2 or CO_2 in such membranes (compare previous section). AQP1 and GlpF could *potentially* be permeated by ammonia. However, only the barrier for NH_3 permeation through GlpF is substantially lower than the membrane barriers. Therefore, GlpF is expected to enhance NH_3 flux while AQP1 is not, in line with experimental findings (Holm et al. 2005).

It is illustrative to display permeation barriers as a function of the hydrophobicity of the permeating solute (Fig. 9). The plot demonstrates that the barrier height for the permeation of *small solutes* through AQP1 correlates with solute hydrophobicity (Fig. 9a). Larger solutes such as glycerol and urea are sterically excluded from

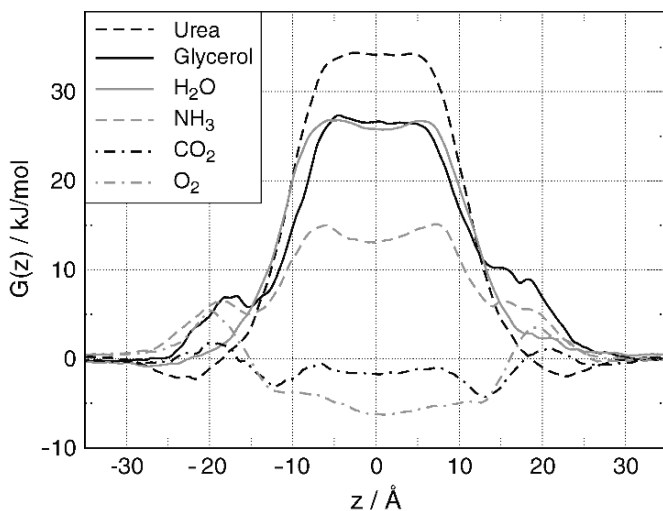


Fig. 8 Potentials of mean force for solute permeation through a membrane of POPC, as indicated in the legend. The membrane is highly permeable to apolar gas molecules such as O_2 and CO_2 , whereas urea, glycerol, and water require a channel for a rapid flux across the membrane.

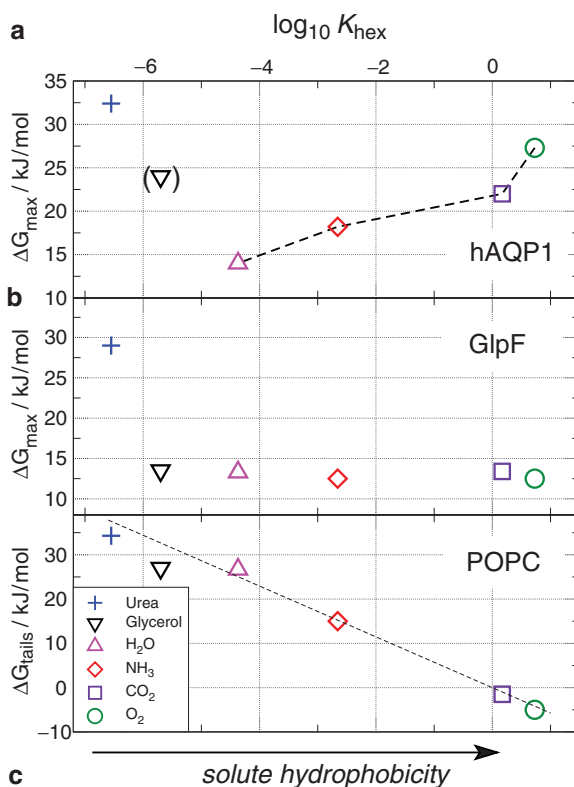


Fig. 9 Permeability as a function of solute hydrophobicity. The hexadecane–water partition coefficient K_{hex} is used as a measure for hydrophobicity. The main barrier height ΔG_{max} for solute permeation through AQP1 (a) and GlpF (b) vs. $\log_{10} K_{\text{hex}}$. AQP1 forms a filter against both hydrophobicity and size, whereas GlpF is permeable to all considered solutes except for urea (compare legend). (c) Solvation free-energy difference ΔG_{tails} between the solute in the bulk water and in the hydrophobic environment between the lipid tails. The measured energetic cost for moving the solute from water into hexadecane is shown for comparison as a dotted line.

AQP1. Taken together, the ar/R region of AQP1 can be considered as a filter that allows the permeation of small polar solutes. Note that this filter mechanism does not apply in GlpF (Fig. 9b). Its larger and more hydrophobic ar/R region allows the rapid permeation of all considered solutes except for urea.

As can be seen from Fig. 9, the permeation characteristics of AQP1 and GlpF are quite different. MD simulations revealed two molecular mechanisms underlying the different selectivities of AQP water channels and aquaglyceroporins. First, larger solutes such as glycerol are sterically excluded from narrow water pores such as AQP1 or *E. coli* AQP-Z (Hub and de Groot 2008; Wang et al. 2005), a finding that has already been suggested from the pore size of the crystal structures (Fu et al. 2000; Savage et al. 2003; Sui et al. 2001). Second, given a solute *fits* sterically through the pore, water–protein interactions play an important role in channel selectivity, in particular inside the ar/R region. When a small solute permeates

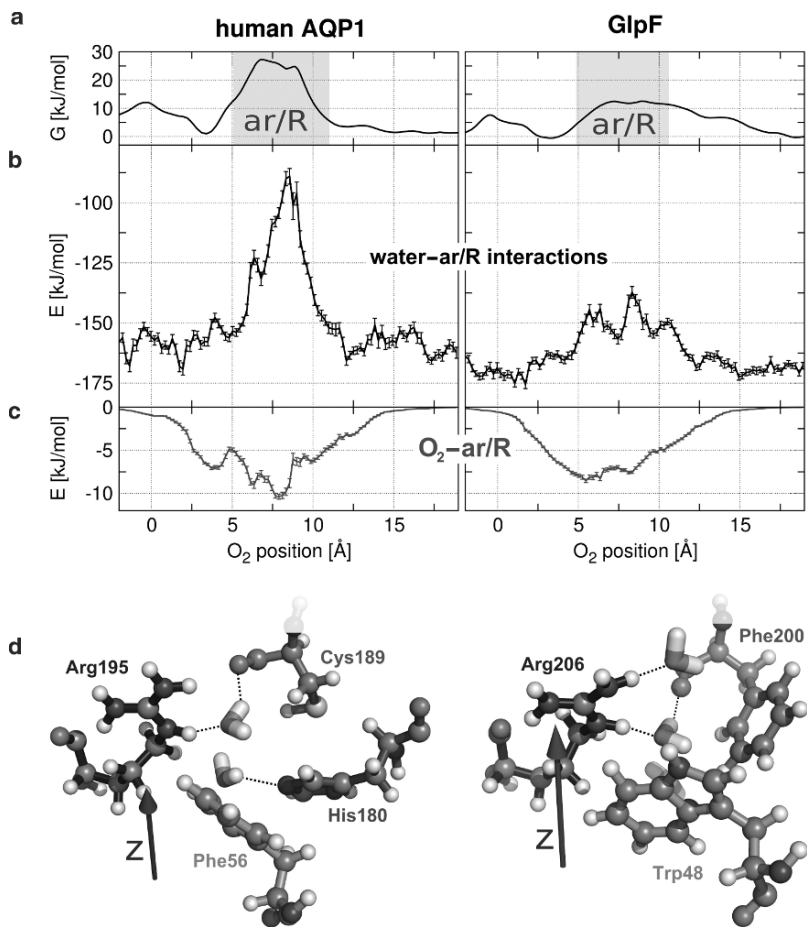


Fig. 10 Water–protein interactions as selectivity filter for aquaporins: analysis of interaction energies during a permeation event of O_2 through AQP1 (left) and GlpF (right). (a) PMFs for O_2 permeation through the ar/R regions of AQP1 and GlpF. (b) Interaction energies between water and the ar/R residues as a function of O_2 position. Water–protein interactions are reduced by $\approx 60 \text{ kJ mol}^{-1}$ during O_2 permeation through AQP1. (c) O_2 –protein interactions are weak ($\sim 10 \text{ kJ mol}^{-1}$) and cannot compensate for the loss of water–protein interaction. When O_2 permeates through GlpF (b, right), water–protein interactions are much less reduced than in AQP1, rendering a lower barrier for O_2 permeation through GlpF compared with AQP1. (d) Snapshots from MD simulations showing the ar/R regions of AQP1 and GlpF. Possible water–protein hydrogen bonds are indicated by dashed lines.

through the narrow and hydrophilic ar/R site of AQP1, water–protein interactions (mainly to the conserved arginine) are substantially reduced (cf. Fig. 10b, left) and replaced by solute–protein interactions (Fig. 10c). More hydrophilic the solutes interact more strongly with the polar groups in the ar/R region implying a lower cost to replace the water molecule. This hydrophobic effect leads to the correlation between solute hydrophobicity and barrier height in AQP1. The ar/R region of

aquaglyceroporins such as GlpF is wider and more hydrophobic (Fu et al. 2000). Therefore, water-protein interactions are hardly reduced upon permeation of small solutes through GlpF (Fig. 10b, right), rendering GlpF an efficient channel for small uncharged solutes. Taken together, water-pore interactions complemented by steric restraints emerge as the determinants underlying channel selectivity.

6 Summary and Concluding Remarks

Providing atomic coordinates and interaction energies at high time and spatial resolution, MD simulations have proved to be a powerful tool to investigate molecular mechanisms of solute and water permeation through AQP channels. Possible limitations of the applied force field and the simulation protocol as well as the need for comparison to experimental data should however be kept in mind. For many quantities, such as permeability coefficients, the agreement between simulation and experiment is favorable, providing a direct means of cross validation. Occasional but striking discrepancies – such as on the water permeability of GlpF – are expected to trigger further simulations *or* experiments that eventually resolve such issues.

Within only a few years, simulations enabled us to obtain a quite detailed understanding of aquaporin function. Water flux through AQPs may be roughly considered as single-file permeation, although interruptions of the single-file structure are quite frequent. The ordered water structure in the channel is ensured by the frequent arrangement of hydrogen bond partners along the pore, which also compensate for the loss of solvation when water molecules enter the channel. The dipoles of two half helices HB and HE generate an electrostatic field inside the pore, which makes the water dipoles rotate by 180° upon permeation. Protons are excluded from AQPs by a large electrostatic barrier, which has its maximum at the NPA site. The contributions of polar protein groups and of desolvation effects to the barrier are still a matter of debate.

The aromatic/arginine (ar/R) region is the selectivity filter for uncharged solutes. Small solutes are filtered through a hydrophobic effect. Whether and under which conditions AQPs facilitate gas, remains an intriguing question. For larger solutes such as glycerol, steric restraints combined with the arrangement of hydrogen bond donors and acceptors determine channel selectivity.

Acknowledgment This work was supported by EU grant no. LSHP-CT-2004–012189.

References

- Beitz E, Wu B, Holm LM, Schultz JE, Zeuthen T (2006) Point mutations in the aromatic/arginine region in aquaporin 1 allow passage of urea, glycerol, ammonia, and protons. *Proc Natl Acad Sci USA* 103:269–274
- Blank ME, Ehmke H (2003) Aquaporin-1 and HCO_3^- – Cl^- transporter-mediated transport of CO_2 across the human erythrocyte membrane. *J Physiol* 550:2:419–429

- Borgnia MJ, Agre P (2001) Reconstitution and functional comparison of purified GlpF and AqpZ, the glycerol and water channels from *Escherichia coli*. *Proc Natl Acad Sci USA* 98:2888–2893
- Burykin A, Warshel A (2003) What really prevents proton transport through aquaporin? Charge self-energy versus proton wire proposals. *Biophys J* 85:3696–3706
- Burykin A, Warshel A (2004) On the origin of the electrostatic barrier for proton transport in aquaporin. *FEBS Lett* 570:41–46
- Chakrabarti N, Roux B, Pomes R (2004a) Structural determinants of proton blockage in aquaporins. *J Mol Biol* 343:493–510
- Chakrabarti N, Tajkhorshid E, Roux B, Pomes R (2004b) Molecular basis of proton blockage in aquaporins. *Structure* 12:65–74
- Chen H, Wu Y, Voth GA (2006) Origins of proton transport behavior from selectivity domain mutations of the aquaporin-1 channel. *Biophys J* 90:L73–L75
- Cooper GJ, Boron WF (1998) Effect of PCMBs on CO₂ permeability of *Xenopus* oocytes expressing aquaporin 1 or its C189S mutant. *Am J Physiol* 275:C1481–C1486
- de Groot BL, Grubmüller H (2001) Water permeation across biological membranes: mechanism and dynamics of aquaporin-1 and GlpF. *Science* 294:2353–2357
- de Groot BL, Grubmüller H (2005) The dynamics and energetics of water permeation and proton exclusion in aquaporins. *Curr Opin Struct Biol* 15:176–183
- de Groot BL, Engel A, Grubmüller H (2001) A refined structure of human Aquaporin-1. *FEBS Lett* 504:206–211
- de Groot BL, Tieleman DP, Pohl P, Grubmüller H (2002) Water permeation through gramicidin A: desformylation and the double helix; a molecular dynamics study. *Biophys J* 82:2934–2942
- de Groot BL, Frigato T, Helms V, Grubmüller H (2003) The mechanism of proton exclusion in the aquaporin-1 water channel. *J Mol Biol* 333:279–293
- de Grothuss CJT (1806) Sur la décomposition de l'eau et des corps qu'elle tient en dissolution à l'aide de l'électricité galvanique. *Ann Chim LVIII*:54–74
- Endeward V, Musa-Aziz R, Cooper GJ, Chen L-M, Pelletier MF, Virkki LV, Supuran CT, King LS, Boron WF, Gros G (2006) Evidence that aquaporin 1 is a major pathway for CO₂ transport across the human erythrocyte membrane. *FASEB J* 20:1974–1981
- Engel A, Stahlberg H (2002) Aquaglyceroporins: channel proteins with a conserved core, multiple functions and variable surfaces. *Int. Rev. Cytol.* 215:75–104
- Fang X, Yang B, Matthay MA, Verkman AS (2002) Evidence against aquaporin-1-dependent CO₂ permeability in lung and kidney. *J Physiol* 542:63–69
- Finkelstein A (1987) Water movement through lipid bilayers, pores, and plasma membranes. Wiley, New York
- Fu D, Libson A, Miercke LJ, Weitzman C, Nollert P, Krucinski J, Stroud RM (2000) Structure of a glycerol-conducting channel and the basis for its selectivity. *Science* 290:481–486
- Gonen T, Sliz P, Kistler J, Cheng Y, Walz T (2004) Aquaporin-0 membrane junctions reveal the structure of a closed water pore. *Nature* 429:193–197
- Hashido M, Ikeguchi M, Kidera A (2005) Comparative simulations of aquaporin family: AQP1, AQPZ, AQP0 and GlpF. *FEBS Lett* 579:5549–5552
- Hashido M, Kidera A, Ikeguchi M (2007) Water transport in aquaporins: osmotic permeability matrix analysis of molecular dynamics simulations. *Biophys J* 93:373–385
- Heller KB, Lin EC, Wilson TH (1980) Substrate-specificity and transport-properties of the glycerol facilitator of *Escherichia coli*. *J Bacteriol* 144:274–278
- Hénin J, Tajkhorshid E, Schulten K, Chipot C (2008) Diffusion of glycerol through *Escherichia coli* aquaglyceroporin GlpF. *Biophys J* 94:832–839
- Heymann JB, Engel A (2000) Structural clues in the sequences of the aquaporins. *J Mol Biol* 295:1039–1053
- Hiroaki Y, Tani K, Kamegawa A, Gyobu N, Nishikawa K, Suzuki H, Walz T, Sasaki S, Mitsuoka K, Kimura K, Mizoguchi A, Fujiyoshi Y (2006) Implications of the aquaporin-4 structure on array formation and cell adhesion. *J Mol Biol* 355:625–639
- Holm LM, Jahn TP, Møller ALB, Schjøerring JK, Ferri D, Klaerke DA, Zeuthen T (2005) NH₃ and NH₄⁺ permeability in aquaporin-expressing *Xenopus* oocytes. *Pflügers Arch* 450:415–428

- Hub JS, de Groot BL (2006) Does CO₂ permeate through Aquaporin-1? *Biophys J* 91:842–848
- Hub JS, de Groot BL (2008) Mechanism of selectivity in aquaporins and aquaglyceroporins. *Proc Natl Acad Sci USA* 105:1198–1203
- Ilan B, Tajkhorshid E, Schulten K, Voth GA (2004) The mechanism of proton exclusion in aquaporin channels. *Proteins* 55:223–228
- Jensen MØ, Mouritsen OG (2006) Single-channel water permeabilities of *Escherichia coli* aquaporins AqpZ and GlpF. *Biophys J* 90:2270–2284
- Jensen MØ, Tajkhorshid E, Schulten K (2001) The mechanism of glycerol conduction in aquaglyceroporins. *Structure* 9:1083–1093
- Jensen MØ, Park S, Tajkhorshid E, Schulten K (2002) Energetics of glycerol conduction through aquaglyceroporin GlpF. *Proc Natl Acad Sci USA* 99:6731–6736
- Jensen MØ, Tajkhorshid E, Schulten K (2003) Electrostatic tuning of permeation and selectivity in aquaporin water channels. *Biophys J* 85:2884–2899
- Jung JS, Preston GM, Smith BL, Guggino WB, Agre P (1994) Molecular structure of the water channel through aquaporin CHIP – the hourglass model. *J Biol Chem* 269:14648–14654
- Kato M, Pislakov AV, Warshel A (2006) The barrier for proton transport in aquaporins as a challenge for electrostatic models: the role of protein relaxation in mutational calculations. *Proteins* 64:829–844
- Lee JK, Kozono D, Remis J, Kitagawa Y, Agre P, Stroud RM (2005) Structural basis for conductance by the archaeal aquaporin AqpM at 1.68 Å. *Proc Natl Acad Sci USA* 102:18932–18937
- Maurel C, Reizer J, Schroeder JI, Chrispeels MJ, Saier MH (1994) Functional characterization of the *Escherichia coli* glycerol facilitator, GlpF, in *Xenopus* oocytes. *J Biol Chem* 269:11869–11872
- Murata K, Mitsuoka K, Walz T, Agre P, Heymann JB, Engel A, Fujiyoshi Y (2000) Structural determinants of water permeation through aquaporin-1. *Nature* 407:599–605
- Nakhoul NL, Davis BA, Romero MF, Boron WF (1998) Effect of expressing the water channel aquaporin-1 on the CO₂ permeability of *Xenopus* oocytes. *Am J Physiol Cell Physiol* 274:C543–C548
- Prasad GVR, Coury LA, Finn F, Zeidel ML (1998) Reconstituted aquaporin 1 water channels transport CO₂ across membranes. *J Biol Chem* 273:33123–33126
- Preston GM, Carroll TP, Guggino WB, Agre P (1992) Appearance of water channels in *Xenopus* oocytes expressing red-cell CHIP28 protein. *Science* 256:385–387
- Savage DF, Egea PF, Robles-Colmenares Y, O'Connell JDI, Stroud RM (2003) Architecture and selectivity in aquaporins: 2.5 Å X-ray structure of aquaporin Z. *PLoS Biol.* 1:e72
- Sui H, Han B-G, Lee JK, Walian P, Jap BK (2001) Structural basis of water-specific transport through the AQP1 water channel. *Nature* 414:872–878
- Tajkhorshid E, Nollert P, Jensen MØ, Miercke LJW, O'Connell J, Stroud RM, Schulten K (2002) Control of the selectivity of the aquaporin water channel family by global orientational tuning. *Science* 296:525–530
- Törnroth-Horsefield S, Wang Y, Hedfalk K, Johanson U, Karlsson M, Tajkhorshid E, Neutze R, Kjellbom P (2006) Structural mechanism of plant aquaporin gating. *Nature* 439:688–694
- Torrie GM, Valleau JP (1974) Monte Carlo free energy estimates using non-Boltzmann sampling: application to the sub-critical Lennard-Jones fluid. *Chem Phys Lett* 28:578–581
- Uehlein N, Lovisollo C, Siefritz F, Kaldenhoff R (2003) The tobacco aquaporin NtAQP1 is a membrane CO₂ pore with physiological functions. *Nature* 425:734–737
- Wang Y, Schulten K, Tajkhorshid E (2005) What makes an aquaporin a glycerol channel? A comparative study of AqpZ and GlpF. *Structure* 13:1107–1118
- Wang Y, Cohen J, Boron WF, Schulten K, Tajkhorshid E (2007) Exploring gas permeability of cellular membranes and membrane channels with molecular dynamics. *J Struct Biol* 157: 534–544
- Yang B, Fukuda N, van Hoek A, Matthay MA, Ma T, Verkman AS (2000) Carbon dioxide permeability of aquaporin-1 measured in erythrocytes and lung of aquaporin-1 null mice and in reconstituted proteoliposomes. *J Biol Chem* 275:2686–2692
- Zardoya R (2005) Phylogeny and evolution of the major intrinsic protein family. *Biol Cell* 97: 397–414

- Zeidel ML, Ambudkar SV, Smith BL, Agre P (1992) Reconstitution of functional water channels in liposomes containing purified red-cell CHIP28 protein. *Biochemistry* 31:7436–7440
- Zeidel ML, Nielsen S, Smith BL, Ambudkar SV, Maunsbach AB, Agre P (1994) Ultrastructure, pharmacological inhibition, and transport selectivity of aquaporin channel-forming integral protein in proteoliposomes. *Biochemistry* 33:1606–1615
- Zhu F, Tajkhorshid E, Schulten K (2002) Pressure-induced water transport in membrane channels studied by molecular dynamics. *Biophys J* 83:154–160
- Zhu F, Tajkhorshid E, Schulten K (2004a) Collective diffusion model for water permeation through microscopic channels. *Phys Rev Lett* 93:224501
- Zhu F, Tajkhorshid E, Schulten K (2004b) Theory and simulation of water permeation in aquaporin-1. *Biophys J* 86:50–57

In Vitro Analysis and Modification of Aquaporin Pore Selectivity

Eric Beitz, Dana Becker, Julia von Bülow, Christina Conrad, Nadine Fricke, Amornrat Geadkaew, Dawid Krenc, Jie Song, Dorothea Wree, and Binghua Wu

Contents

1	Introduction	78
2	Quantitative Assays of Water and Solute Flux	79
2.1	Xenopus laevis Oocytes	79
2.2	Secretory Yeast Vesicles and Proteoliposomes	81
2.3	Mammalian Cells	82
3	Phenotypic Assays	82
3.1	Leishmania	82
3.2	Yeast	83
4	Modification of Aquaporin Pore Selectivity	85
4.1	General Aquaporin Pore Layout	86
4.2	Point Mutations in the Ar/R Constriction of AQP1	87
4.3	Water and Solute Permeability	87
4.4	Ammonia Permeability	88
4.5	Proton Exclusion	89
5	Conclusion	89
	References	90

Abstract Aquaporins enable the passage of a diverse set of solutes besides water. Many novel aquaporin permeants, such as antimonite and arsenite, silicon, ammonia, and hydrogen peroxide, have been described very recently. By the same token, the number of available aquaporin sequences has rapidly increased. Yet, sequence analyses and structure models cannot reliably predict permeability properties. Even the contribution to pore selectivity of individual residues in the channel layout is not fully understood. Here, we describe and discuss established in vitro assays for water and solute permeability. Measurements of volume change due to flux along osmotic or chemical gradients yield quantitative biophysical data, whereas phenotypic growth assays can hint at the relevance of aquaporins in the physiological

E. Beitz (✉)

Department of Pharmaceutical Chemistry, University of Kiel, Gutenbergstrasse 76, 24118 Kiel, Germany
ebeitz@pharmazie.uni-kiel.de

setting of a certain cell. We also summarize data on the modification of pore selectivity of the prototypical water-specific mammalian aquaporin-1. We show that replacing residues in the pore constriction region allows ammonia, urea, glycerol, and even protons to pass the aquaporin pore.

1 Introduction

The bursting of *Xenopus laevis* oocytes in a hypotonic bath was the Eureka moment of aquaporin (AQP) research. It functionally proved osmotic water permeability of the red cell and kidney CHIP28 protein, later termed AQP1 (Preston et al. 1992). This now classical – though still commonly used – in vitro assay, together with reconstitution of the protein in liposomes, were indispensable tools for the determination of the Arrhenius activation energy of water permeation (Zeidel et al. 1992), estimation of the permeation rate, and analysis of aquaporin inhibition by mercurials (Preston et al. 1993). The obtained data immediately confirmed that aquaporins account for the so-far unexplained high water permeability of erythrocytes and certain epithelia (Solomon et al. 1983; Verkman 1989).

Later, permeability for small, uncharged solutes, such as glycerol and urea, was shown by the oocyte swelling assay and other in vitro experiments leading to the functional division of the aquaporin protein family into water-specific, orthodox aquaporins, and aquaglyceroporins (Ishibashi et al. 1994; Zardoya 2005). Coefficients of water (P_f or L_p) and solute (P_{solute}) permeability are now routinely measured to functionally categorize novel aquaporins. In vitro assays further revealed that the list of aquaporin permeants is not complete with water, urea, and glycerol (plus somewhat longer polyols), but also includes carbonyl compounds (Pavlovic-Djuranovic et al. 2006), antimonite/arsenite (Wysocki et al. 2001; Liu et al. 2002; Gourbal et al. 2004), silicon (Ma et al. 2006), ammonia (Holm et al. 2005; Zeuthen et al. 2006; Saparov et al. 2007), hydrogen peroxide (Bienert et al. 2007) and, in the case of AQP6, even anions such as nitrite and chloride (Yasui et al. 1999).

Current questions on the inner workings and intramolecular regulation mechanisms of aquaporins are addressed using in vitro analyses of specific aquaporin mutants. Where are filters located that allow aquaporins to select between different permeants? How do aquaporins exclude protons and other ions? How is osmotic and pH-dependent pore gating of certain mammalian, plant, and yeast aquaporins accomplished? Today, prediction of such selectivity and regulation mechanisms is a domain of molecular dynamics computer simulations and quantum mechanical calculations (de Groot and Grubmüller 2005; Chen et al. 2006). Yet, real-world in vitro measurements are needed to complement in silico data or to challenge theoretical models (Beitz et al. 2006).

Aquaporins are also becoming the focus of the pharmaceutical sciences. Their physiological and pathophysiological relevance and the consequent desire to therapeutically modulate cell water permeability (Beitz and Schultz 1999; Castle 2005; Jeyaseelan et al. 2006; Frigeri et al. 2007) started the search for small molecule aquaporin inhibitors (Brooks et al. 2000; Detmers et al. 2006; Huber et al. 2007;

Huber et al. 2008). This calls for industry-style high-throughput assay systems that allow for rapid screening of large compound libraries.

Aquaporin assay systems range from living cells, i.e., bacteria (Hubert et al. 2005; Mallo and Ashby 2006), yeast (Luyten et al. 1995; Jahn et al. 2004; Beitz et al. 2006; Pettersson et al. 2006), and mammalian cells (Solenov et al. 2004; Gao et al. 2005), via preparations of cell organelles (Laizé et al. 1995; Calamita et al. 2006), to artificial proteoliposomes (Zeidel et al. 1992; Borgnia and Agre 2001) and even planar lipid membranes (Saparov et al. 2001). Depending on the nature of the assay, information is gained about the biophysical properties or on the physiological relevance of an aquaporin if the survival of cells depends on its function. This chapter discusses quantitative and phenotypic aquaporin assays for various permeants as well as mutations of the prototypical water-specific AQP1 that modify pore selectivity.

2 Quantitative Assays of Water and Solute Flux

Quantification of water flux through aquaporins requires a two-compartment system in which an osmotic gradient can be rapidly established. The sudden disturbance in equilibrium will drive water across the dividing membrane to revert the system to equal osmolality. Resulting flow rates depend on the number of aquaporins as well as their permeability properties, and are monitored by the volume change over time. Permeability for osmotically active solutes can be similarly analyzed by creating a chemical gradient between compartments with equal osmolality. The solute flow will then generate an osmotic disturbance leading to secondary water flow and volume change. In either case, i.e., water or solute permeability assays, the magnitude and time scale of the volume change dictate the method to be used for monitoring (see Table 1).

2.1 *Xenopus laevis* Oocytes

Oocytes of the South African claw frog *Xenopus laevis* have been used in physiology research laboratories for decades. Due to their large diameter (≈ 1.2 mm; Table 1),

Table 1 Dimensions of the compartments used in osmotic aquaporin swelling/shrinking assays and resulting observation time frames

Compartment	Diameter (cm)	Surface (cm ²)	Volume (cm ³)	Surface/volume (cm ⁻¹)	Swelling time (s)
<i>Xenopus</i> oocytes	1.2×10^{-1}	5.3×10^{-1} (true surface)	9×10^{-4}	5.9×10^2	100
Yeast, red cells	10^{-3}	3×10^{-6}	5×10^{-10}	6×10^3	10
Bacteria	10^{-4}	3×10^{-8}	5×10^{-13}	6×10^4	1
Vesicles, liposomes	10^{-5}	3×10^{-10}	5×10^{-16}	6×10^5	0.1

easy handling and culturing, and the possibility to express eukaryotic membrane proteins by simply injecting in vitro generated cRNA, *Xenopus* oocytes have become a standard tool in transmembrane transport studies. Particularly advantageous for studying aquaporins is their low intrinsic water permeability. In nature, this property warrants survival of the oocytes in the hypotonic environment of a freshwater pond. In vitro, as an assay system, it ensures a low background water flux resulting in reasonable signal-to-noise ratios.

One to four days prior to the assay, cRNA (5 ng in 50 nl) encoding an aquaporin is injected, and the oocyte is incubated in isotonic medium for protein expression and insertion into the plasma membrane (Preston et al. 1992). Swelling is then initiated by abruptly placing the oocyte in diluted medium exposing it to an inward directed osmotic gradient, usually in the range of 100–150 mOsm. Under these conditions, the oocyte will swell up to 40% within 1–2 min and eventually burst (Fig. 1a). The volume increase is calculated from the increase of the area covered by the oocyte as documented by a video camera via a microscope (Fig. 1b). To test for solute permeability, sodium chloride from the incubation medium is isotonicly replaced by the test solute to generate an inward directed chemical gradient (Hansen et al. 2002). Oocyte swelling due to solute influx and the secondary entry of water can reach

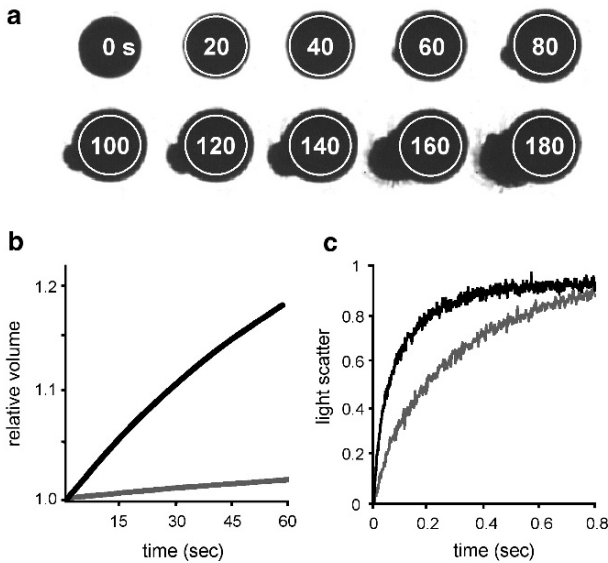


Fig. 1 Osmotic aquaporin swelling assay systems using *Xenopus laevis* oocytes or proteoliposomes. (a) Image series of a swelling and bursting *Xenopus* oocyte under hypotonic conditions (140 mOsm gradient) taken every 20 s for 3 min. The white circle denotes the area of the oocyte at time 0 s. (b) Relative volume increase of the oocyte shown in (a) (black curve) compared to a non-expressing control oocyte (gray curve). (c) Increase of light scattering due to volume change of liposomes in a stopped-flow machine. Shown are curves for proteoliposomes carrying purified human AQP2 (black curve) and for pure liposomes (gray curve). The steeper black curve indicates more rapid water flux

approximately the same rate as in osmotic assays. The actual solute permeability coefficient of aquaglyceroporins, however, is usually at least two orders of magnitude lower ($P_{\text{solute}} < 1 \mu\text{m s}^{-1}$) than the water permeability coefficient of orthodox aquaporins ($P_f \approx 50\text{--}200 \mu\text{m s}^{-1}$). Water permeability of non-expressing oocytes is $10\text{--}20 \mu\text{m s}^{-1}$, whereas permeability for glycerol and other solutes is hardly detectable.

Besides employing swelling assays to follow solute uptake into cells, one can also use radioactively labeled compounds, if available, and determine the intracellular accumulation of the nuclides, after certain time points, in a scintillation counter (Beitz et al. 2006). This method provides a direct measure of the uptake rather than an estimate via indirect osmotic effects.

Interindividual differences between the oocytes, i.e., slight variances in size, shape, or aquaporin expression levels, call for several repetitions (5–10 or more), in order to minimize error. In principle, the oocyte system can also be used for the determination of the Arrhenius activation energy, which requires measurements at different temperatures. This is, however, rather tedious due to the multiple replications that are needed for significant statistics. Such biophysical parameters can be obtained more easily in a stopped-flow machine using vesicle preparations or artificial proteoliposomes carrying the aquaporin to be studied.

2.2 Secretory Yeast Vesicles and Proteoliposomes

With diameters of only 50–200 nm, vesicles and liposomes are located at the opposite end of the scale as compared with *Xenopus* oocytes (Table 1). Consequently, the compartment volumes are dramatically different, i.e., $\approx 9 \times 10^{-4} \text{cm}^3$ for the oocytes and $\approx 5 \times 10^{-16} \text{cm}^3$ for the liposomes. When calculating the surface-to-volume ratios, liposomes and oocytes differ by 3–4 orders of magnitude. This difference explains why the swelling or shrinkage of liposomes in an osmotic gradient is complete within 10–100 ms (Fig. 1c; Zeidel et al. 1992; Borgnia and Agre 2001) instead of several minutes, as in the case of oocytes (Fig. 1b; Preston et al. 1992). Clearly, a rapid data sampling system is required to monitor the process.

Practically, a stopped-flow machine is used, in which small volumes (50–200 μl) of a vesicle suspension and an osmotically different solution are injected into an observation cuvette. Dead time should be around 1 ms. Osmotic water flow then changes the vesicle diameter that is monitored by quantification of the light scattering intensity. Short assay times and small sample sizes allow for multiple repetitions of the measurements. Temperature control, e.g., for the determination of the activation energy, is easily accomplished by bathing the machine parts that hold the test suspension/solution and the cuvette in a thermostat.

Test vesicles can be obtained from a mutant yeast strain expressing a temperature sensitive *Sec6*-protein (Laizé et al. 1995). Under non-permissive conditions, the mutation results in a cytosolic accumulation of secretory vesicles. When an aquaporin is heterologously expressed in this yeast strain, it will be present in these vesicles

together with multiple other endogenous membrane proteins. This particulate fraction can be collected by centrifugation and can be directly used for assaying. If a pure system is wished or required, one needs to engage in a more time-consuming procedure that involves purification of the aquaporin protein and functional reconstitution in proteoliposomes (Zeidel et al. 1992).

Besides vesicles, whole-cell water and solute permeability has also been analyzed in stopped-flow light scattering assays (Table 1), e.g., of erythrocytes (Mathai et al. 1996; Liu et al. 2007), yeast protoplasts (Pettersson et al. 2006), and even bacteria (Hubert et al. 2005) with aquaporin deletions or aquaporins carrying point mutations. This showed, for instance, that the erythrocytes of Colton null individuals that fully lack AQP1 have 87% reduced water permeability (Mathai et al. 1996) and glycerol influx into erythrocytes of AQP9 knockout mice is significantly slower by 85% than into wild-type cells (Liu et al. 2007).

2.3 Mammalian Cells

Mammalian aquaporins can also be analyzed in their typical cellular environment using primary cell cultures (Solenov et al. 2004) or expression systems (Gao et al. 2005). Changes in fluorescence intensity after an osmotic challenge are then correlated to cellular water permeability coefficients. The possibility to automate fluorescence measurements in stably transfected cells allows for high-throughput setups in which large libraries of small compounds can be screened for aquaporin inhibitors. However, a breakthrough has not yet been achieved (see Part V of this volume).

3 Phenotypic Assays

The biophysical assays described above provide valuable quantitative data and accurately describe permeability properties of aquaporins on a molecular level. They cannot answer, however, whether the found parameters are relevant in the physiological setting of a cell. Here, a phenotypic readout, such as cell growth or even cell survival, is needed to appreciate the role of an aquaporin under normal conditions and in certain stress situations.

3.1 *Leishmania*

The identification process of an aquaglyceroporin as a major pathway for trivalent antimony in human-pathogenic *Leishmania* parasites illustrates the quality of the phenotypic assay approach (Gourbal et al. 2004). Antimonials are still the first-line treatment for leishmaniasis. Antimony is therapeutically applied as Sb(V), in

the form of sodium stibogluconate or meglumine antimonate. In the parasite's cytosol, pentavalent antimony is reduced to Sb(III) to form the active compound. The aquaglyceroporin LmAQP1 was shown to be directly linked to antimonial resistance of *Leishmania major* parasites, probably by facilitating Sb(OH)₃ release (Gourbal et al. 2004). Evidence came from a naturally selected antimonial-resistant *Leishmania* strain in which the LmAQP1 gene was strongly overexpressed. The role and physiological relevance of LmAQP1 was analyzed in in vitro cultures of *Leishmania* in a reversed setup, i.e., parasites were treated directly with the reduced Sb(III) form. Indeed, loss of the LmAQP1 gene as a result of targeted gene disruption rendered the parasites ten times more resistant to externally applied Sb(III) by prohibiting the uptake, whereas overexpression of the gene led to sensitization of the parasites to external Sb(III). Here, the EC₅₀ was even shifted by two orders of magnitude to lower concentrations. This is clear evidence that LmAQP1 permeability for trivalent antimony is physiologically relevant in *Leishmania* parasites as a drug resistance pathway.

3.2 Yeast

The yeast system is particularly well suited for designing phenotypic growth or cell toxicity assays due to a long list of advantageous factors and available tools, e.g., the ease of generating gene disruptions, the possibility to express mammalian membrane proteins, usability of a wealth of nutritional selection markers, rapid growth, etc. Phenotypic yeast assays for glycerol, ammonia (or methylamine), arsenite/antimonite, and hydrogen peroxide permeability have been described.

Yeast cells rapidly and accurately adjust the internal glycerol concentration in order to compensate for osmotic imbalances between the cytosol and the environment. They express an aquaglyceroporin, Fps1, which has the ability to open and close the channel in an osmotically regulated fashion (Luyten et al. 1995). Under hyperosmotic conditions, the channel closes to retain the intracellular glycerol; additionally, glycerol is metabolically produced to reach adequate concentration levels. In turn, under hypotonic conditions, the Fps1 channel opens and releases glycerol into the medium, whereas glycerol biosynthesis ceases. Point mutations in the N- and C-terminus of Fps1 revealed that both termini mediate channel gating because the yeast lost its ability to adapt to osmotic changes, as seen by reduced growth (Karlgrén et al. 2004).

This phenotype can be exploited for functional assays of aquaglyceroporins. Yeast growth is unaffected in hypertonic medium even in the absence of Fps1, i.e., a Δ fps1 knockout strain, because the cells need to retain internal glycerol and would have closed the channel anyway (Fig. 2a, upper two rows). If a functional, unregulated aquaglyceroporin, e.g., the *Plasmodium falciparum* aquaglyceroporin PfAQP (Hansen et al. 2002), is heterologously expressed under these conditions, the cells will leak glycerol, cannot adapt to the osmotic conditions, and will stop growing (Fig. 2a, bottom row). The phenotype becomes even clearer in yeast, where enzymes

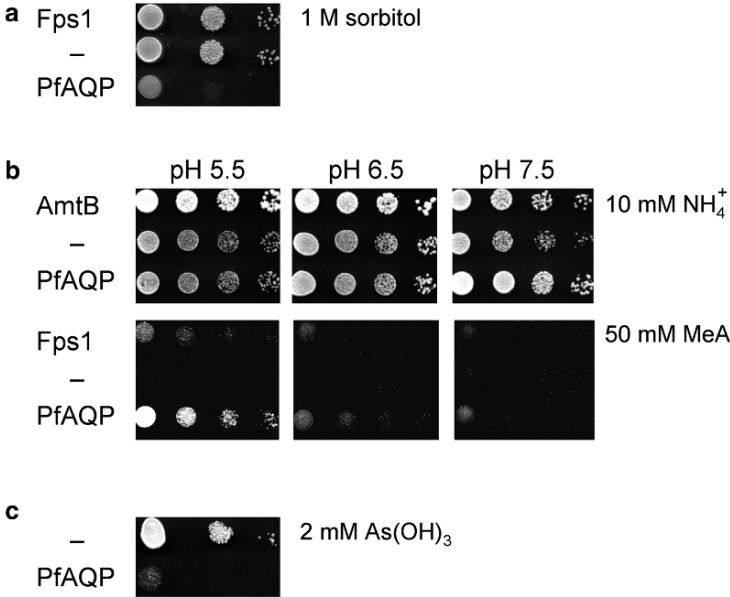


Fig. 2 Yeast-based phenotypic aquaporin assays for various solutes. **(a)** Glycerol release from yeast cells. The cells were grown in 1 M glycerol liquid medium and then plated on solid medium containing 1 M of impermeable sorbitol instead of glycerol, to establish a large outward gradient for glycerol. Cells that express regulated Fps1 grow as well as cells without the endogenous aquaglyceroporin, because the Fps1 pore will close under hypertonic conditions (*upper two rows*). Cells that express the unregulated aquaglyceroporin from *Plasmodium falciparum* (PfAQP) show reduced growth due to glycerol leakage and consequent osmotic stress. **(b)** Permeability assays for ammonia (Δ mep1–3 strain; *upper panel*) and methylamine (Δ fps1 strain; *lower panel*) at pH 5.5–7.5. Uptake of ammonia is facilitated pH-independently by expression of an ammonium transporter (AmtB, *positive control*) or pH-dependently by PfAQP with highest rates at neutral pH, i.e., at higher concentrations of uncharged ammonia. Diffusion of ammonia across the cell membrane is depicted by high background growth (*middle row*). Background is close to zero when cell growth depends upon the release of toxic methylamine (*lower panel, middle row*). Aquaporins with methylamine permeability (Fps1 and PfAQP) sustain cell growth in the acidic range according to the larger outward gradient of the uncharged form. **(c)** Permeability for arsenite, As(OH)₃. Aquaporins that facilitate the influx of toxic arsenite into the cells lead to reduced growth (PfAQP) compared to cells lacking the endogenous Fps1

of the glycerol biosynthesis pathway (*gpd1* and *gpd2*) are deleted in addition to the *Fps1* gene (Karlgrén et al. 2005).

Phenotypic yeast aquaporin assays are the more useful when the permeant, e.g., ammonia, is not osmotically active, because here osmotic swelling assays using *Xenopus* oocytes or liposomes would not work. Yeast, however, requires uptake of ammonia as a nitrogen source for cell proliferation and can therefore be used as an assay system (Jahn et al. 2004). In yeast, three ammonium transporters, Mep1–3, facilitate ammonium uptake very efficiently and pH-independently. A respective triple knockout can only grow when alternative pathways exist, such as a heterologously expressed ammonia-permeable aquaporin, e.g., human AQP8, plant

TIP2;1 (Jahn et al. 2004) or PfAQP (Fig. 2b, *upper panel*; Zeuthen et al. 2006). The growth rate will be pH-dependent decreasing toward acidic pH, because aquaporins only conduct the uncharged ammonia form and not the protonated ammonium ion (pK_a 9.25). The readout in this assay is not always convincing due to high background growth in the control cells (Fig. 2b, *upper panel*), hence a variant based on the cytotoxic ammonia derivative methylamine was established (Beitz et al. 2006).

Methylamine is a chemical analog of ammonia, with high toxicity for yeast cells. Similar to ammonia, it exists in two forms, i.e., the uncharged methylamine form and the protonated, charged methylammonium form. The latter prevails in the physiological pH-range due to a pK_a of 10.64 of the compound. The more acidic the pH, the farther is the chemical equilibrium shifted to charged methylammonium. Yeast cells take up methylammonium via the aforementioned Mep 1–3 ammonium transporters, resulting in an intracellular accumulation and inhibition of proliferation if the endogenous aquaglyceroporin is knocked out (Δ fps1 strain; Fig. 2b, *lower panel*). However, functional expression of a methylamine-conducting aquaglyceroporin, such as the endogenous yeast Fps1, *Escherichia coli* GlpF, or PfAQP, rescues the cells when grown in an acidic medium (Fig. 2b, *lower panel*; Wu et al. 2007). For instance, a gradient from cytosolic pH 7.2 to pH 5.5 in the external medium establishes an outward gradient for uncharged methylamine that renders PfAQP expressing yeast \approx 100 times more resistant (Zeuthen et al. 2006).

Yeast knockout strains have also been used for arsenite and antimonite uptake assays similar to the *Leishmania* system (Fig. 2c; Wysocki et al. 2001) and for phenotypic hydrogen peroxide permeability assays (Bienert et al. 2007). The yeast cells in the latter assays lack a transcription factor that renders them more sensitive to oxidative stress than wild-type cells. Uptake of hydrogen peroxide via aquaporins can then be analyzed by monitoring cell growth where high permeability for hydrogen peroxide is indicated by suppressed growth (Bienert et al. 2007).

This selection of aquaporin in vitro assays shows their wide application range. It should be mentioned that several other techniques have been employed to characterize more special permeability properties, such as for carbon dioxide leading to pH-shifts in the presence of carbonic anhydrase activity (Uehlein et al. 2003) and for the wide field of ion permeability using electrophysiology approaches (Yasui et al. 1999; Saparov et al. 2001; Holm et al. 2005; Beitz et al. 2006).

4 Modification of Aquaporin Pore Selectivity

With such diverse and complementary tools at hand, we set out to analyze, in vitro, which pore residues define selectivity for water, solutes, and protons in the prototypical, water-specific AQP1 (Beitz et al. 2006). For these studies, it was particularly helpful that the general layout of the aquaporin channels was well established due to the availability of several atomic structures of water-specific aquaporins, e.g., AQP1 (Sui et al. 2001), and aquaglyceroporins, e.g., *E. coli* GlpF (Fu et al. 2000). For more details than presented in this section, see the two preceding chapters.

4.1 General Aquaporin Pore Layout

All aquaporins form tetramers with an independent water pore in each monomer (Gonen and Walz 2006). Each monomer spans the membrane six times, and is further characterized by two short helices that only dip into the membrane and meet in the center of the channel. Two almost invariable Asn-Pro-Ala (NPA) motifs stabilize the stacking of the short helices and form a constriction, i.e., the so-called NPA region. The two asparagines are the capping amino acids at the positive ends of the short helices and act as hydrogen donors to the oxygen atoms of passing permeants. It is discussed that in this region (a) water is re-oriented such that hydrogen bonds between neighboring molecules in the water chain are disrupted, preventing the formation of a proton wire throughout the pore, and (b) a major energy barrier for proton conductance is formed due a strong positive electrostatic field (de Groot and Grubmüller 2005).

The major part of the aquaporin pore is lined by hydrophobic residues that contribute a ladder of main-chain carbonyl oxygens to the inner pore surface. These oxygen atoms serve as hydrogen bond acceptors and probably compensate for the energy cost of hydrogen bond breakage when a molecule is isolated from the bulk solution at the pore mouth.

The narrowest pore constriction is located close to the extracellular entrance (Fig. 3a, b). In water-specific aquaporins, it is 2.8 Å in diameter, perfectly matching a water molecule, whereas aquaglyceroporins accommodate larger molecules, such as glycerol and urea, due to a wider constriction of at least 3.4 Å. This constriction is referred to as the aromatic/arginine (ar/R) constriction and is formed by four residues, i.e., Phe56, His180, Cys189, and Arg195 in human AQP1 (Fig. 3b), and Trp48, Gly191, Phe200, and Arg205 in *E. coli* GlpF (Fig. 3a). A histidine is typical for water specific aquaporins, which, together with the highly conserved arginine, provides strong hydrophilicity. In GlpF, and essentially in all other aquaglyceroporins, the ar/R region is more hydrophobic due to the lack of the

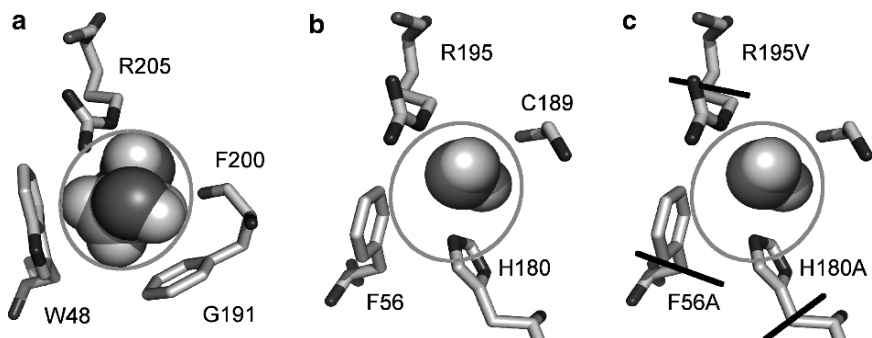


Fig. 3 Layout of the aromatic/arginine (ar/R) region of the *E. coli* aquaglyceroporin GlpF (a), the human water-specific AQP1 (b) and generated mutants of AQP1 (c). The circumference of a glycerol molecule is indicated by the oval; the black bars in (c) mark the length of the alanine and valine side chains in the AQP1 mutants

histidine and substitution of the cysteine by a second aromatic residue; there are also aquaglyceroporins carrying aliphatic residues as the lipophilic moieties (Beitz 2005).

4.2 Point Mutations in the ar/R Constriction of AQP1

In many respects, mammalian AQP1 is the best-characterized water channel. Besides numerous physiological studies, permeability assays have shown its water specificity; further, over the years, the atomic channel structure has been obtained and improved down to 2.2 Å resolution (Sui et al. 2001). We asked whether pore specificity is indeed defined in the ar/R constriction and whether it is possible to modify solute permeability of AQP1 by systematic replacement of residues in the region (Beitz et al. 2006). The mutations aimed at increasing the diameter, changing the shape, and reducing polarity at this site. We replaced, alone or in combinations, Phe56 and His180 with the smaller alanine and Arg195 with valine (Fig. 3c). Mutation of Arg195 to valine (R195V) removed a positive charge, elongated the pore shape, and enlarged the pore area almost threefold. Removal of the imidazole ring (H180A) deleted a putative protonation site and, similar to the R195V mutation, shaped and enlarged the pore, but in the opposite direction. Combination of both mutations (H180A/R195V) led to a flat pore shape that was strongly elongated in one direction, but hardly any wider than the wild-type pore in the other dimension. Here, the bulky aromatic Phe56 is restrictive. Consequently, replacement of Phe56 (F56A) widened the ar/R constriction dramatically, forming a more round pore shape. Despite the major impact on the protein structure in *Xenopus* oocytes as well as in yeast cells, expression levels of all mutants appeared to equal the wild-type AQP1 as shown by Western blotting using a specific antiserum.

4.3 Water and Solute Permeability

In the *Xenopus* oocyte swelling assay, all AQP1 mutants passed water at similar rates as the wild-type channel (Table 2). Even the Arrhenius activation energy for water permeation of 5 kcal mol⁻¹ was unchanged compared with wild-type AQP1. Considering the pronounced differences in polarity in the mutant ar/R constrictions, especially in the H180A/R195V mutant, this came as quite a surprise and shows firstly, that hydrophilic residues at the pore mouth are not required for efficient water permeability and secondly, that formation of hydrogen bonds with the ladder of carbonyl oxygens suffices to compensate for energy costs of bulk water isolation.

Water permeability was unaltered, but would the generated changes in shape and diameter allow larger solutes to pass? Isosmotic oocyte swelling assays with urea and glycerol (Table 2) showed that the single mutants AQP1-R195V and AQP1-H180A were impermeable. The double mutants AQP1-F56A/H180A and AQP1-H180A/R195V, however, were excellently permeated by urea. Glycerol

Table 2 Permeability of AQP1 wild-type and the mutants H180A, R195V, H180A/R195V, and F56A/H180A for water, urea, glycerol, ammonia, and protons (Beitz et al. 2006)

	AQP1	AQP1-HA	AQP1-RV	AQP1-HA/RV	AQP1-FA/HA
Water (L_p) ($\mu\text{m s}^{-1}$)	0.61 ± 0.07 (0.04 ± 0.01 in control)	0.84 ± 0.11	0.54 ± 0.05	0.62 ± 0.09	0.78 ± 0.09
Urea (P_{urea}) ($\mu\text{m s}^{-1}$)	0	0	0	0.13 ± 0.02	0.50 ± 0.15
Glycerol (P_{gly}) ($\mu\text{m s}^{-1}$)	0	0	0	0	0.34 ± 0.06
Ammonia (I_{H^+} at 5 mM NH_4Cl , pH 7.4) (nA)	8.70 ± 2.45 (equal to control)	96.20 ± 15.76	61.20 ± 16.30	58.70 ± 5.98	107.06 ± 16.85
Protons (I_{H^+} at pH 5.6) (nA)	0.65 ± 0.35 (equal to control)	0.60 ± 0.28	3.45 ± 0.48	8.60 ± 2.05	2.15 ± 0.29

permeability was seen only in AQP1-F56A/H180A and was clearly lower than that for urea. Elongation of the carbon chain to four methylhydroxyl groups, i.e., erythritol, had already abolished passage. This indicates that the ar/R constriction is indeed a major filter region in AQP1, limiting solute permeability by size. However, additional pore regions must exist that, although being wide enough for urea, restrict passage of larger solutes, such as glycerol. Theoretical analyses of the AQP1 mutants have very recently confirmed the findings *in silico* (Hub and de Groot 2008).

4.4 Ammonia Permeability

The requirements of an aquaporin pore layout that permits ammonia passage are far less clear. AQP1 effectively excludes ammonia, whereas other aquaporins, such as plant TIP2;1 and human AQP8, have been reported to conduct ammonia (Jahn et al. 2004; Holm et al. 2005). How can these channels discriminate between water and ammonia? Size exclusion cannot account for the selectivity against ammonia, because it has the same dimension as a water molecule and a dipole moment close to that of water (1.5 vs. 1.8 Debye). The most obvious difference lies in the number of hydrogen bond acceptor sites (two in water vs. one in ammonia), donor sites (two in water vs. three in ammonia), and the greater lipophilicity of ammonia. At the ar/R constriction of TIP2;1 and of AQP8, the position of the histidine is switched to that of phenylalanine in AQP1, resulting in a more hydrophobic edge in juxtaposition to the positive pore arginine. The AQP1 mutants described above are also more hydrophobic than the wild-type channel, providing a suitable system to ask whether the reduced polarity of the AQP1 mutants would enable ammonia or its derivative methylamine to pass.

Both phenotypic yeast assays, i.e., ammonia uptake in the $\Delta\text{mep1-3}$ strain as well as methylamine release using the Δfps1 strain, showed growth-sustaining

permeability of all generated AQP1 mutants, whereas yeast cells expressing the wild-type channel did not survive and therefore did not conduct physiologically meaningful amounts of ammonia or methylamine (Beitz et al. 2006). As expected, yeast growth was pH-dependent, indicating that only the uncharged forms of ammonia and methylamine passed the mutant aquaporins.

These findings were confirmed by an independent electrophysiological setup using *Xenopus* oocytes (Beitz et al. 2006). Yet, uncharged ammonia molecules are electroneutral, and the influx into oocytes cannot be measured directly with electrodes. However, inside the oocyte at pH 7.4, about 99% of the entering ammonia molecules get protonated in the process of establishing the pH-dependent chemical equilibrium. The oocytes will not tolerate a shift in internal pH, and a secondary proton influx is initiated through an as yet undefined transport entity that is measurable as a whole-cell inward current. In a range of pH 5.6–8.4 (corresponding to ammonia concentrations of 1.12 μ M to 1.12 mM), the AQP1 variants carrying an H180A mutation showed particularly high ammonia permeability (Table 2).

4.5 Proton Exclusion

In the case of AQP1 H180A/R195V toward more acidic pH, i.e., at lower availability of ammonia, an unexpected increase of the inward current was detected (Beitz et al. 2006). This indicated an ammonia-independent pH-effect. When the pH-shift experiments were repeated in the absence of ammonia, the pH-induced currents were still observed (Table 2). The currents were inward directed in the acidic range and outward in the alkaline range, with a reversal pH of 7.0 clearly calling for proton permeability of the AQP1 mutant. The AQP1 R195V mutant also showed some, although weaker, proton leakage, whereas the wild-type channel was impermeable. This established the ar/R constriction as a part of the proton exclusion mechanism of AQP1, which was not predicted before in silico. Subsequently adapted theoretical models based on the AQP1 ar/R mutants led to the same conclusion (Chen et al. 2006). Calculation of the proton flux rate of AQP1 H180A/R195V gave approximately 50 protons per channel per second, i.e., a rather low value, three orders of magnitude smaller than that of typical proton channels (Beitz et al. 2006). The major proton barrier may, therefore, indeed reside in the NPA region at the pore center. If, however, one considers the high copy number of aquaporin channels in a cell membrane (up to 200,000 in a red cell), this supporting proton barrier at the ar/R region seems physiologically relevant.

5 Conclusion

Today there are numerous assay systems in place for the characterization of aquaporin permeability properties. They yield quantitative biophysical parameters or show the impact of aquaporin function on the phenotype of living cells under certain

conditions. We are looking at a rapidly growing number of novel aquaporin sequences that are produced by genome sequencing. Many of those depict low similarity to prototypical channels, and theoretical deliberations alone cannot clarify their functionality. Hence, *in vitro* assays are instrumental to establish their function, to identify novel physiological permeants, and to analyze gating mechanisms and selectivity filters. Here, iteration between *in silico* and *in vitro* methods will provide optimal advancement. The continuous improvement of established assays and the installation of novel test systems mirror an increasing diversification in the field and will progressively reveal the complex relations between water, solutes, and their conducting channels.

References

- Beitz E (2005) Aquaporins from pathogenic protozoan parasites: structure, function and potential for chemotherapy. *Biol Cell* 97:373–383
- Beitz E, Schultz JE (1999) The mammalian aquaporin water channel family: a promising new drug target. *Curr Med Chem* 6:457–467
- Beitz E, Wu B, Holm LM, Schultz JE, Zeuthen T (2006) Point mutations in the aromatic/arginine region in aquaporin 1 allow passage of urea, glycerol, ammonia, and protons. *Proc Natl Acad Sci U S A* 103:269–274
- Bienert GP, Møller AL, Kristiansen KA, Schulz A, Møller IM, Schjoerring JK, Jahn TP (2007) Specific aquaporins facilitate the diffusion of hydrogen peroxide across membranes. *J Biol Chem* 282:1183–1192
- Borgnia MJ, Agre P (2001) Reconstitution and functional comparison of purified GlpF and AqpZ, the glycerol and water channels from *Escherichia coli*. *Proc Natl Acad Sci U S A* 98:2888–2893
- Brooks HL, Regan JW, Yool AJ (2000) Inhibition of aquaporin-1 water permeability by tetraethylammonium: involvement of the loop E pore region. *Mol Pharmacol* 57:1021–1026
- Calamita G, Gena P, Meleleo D, Ferri D, Svelto M (2006) Water permeability of rat liver mitochondria: a biophysical study. *Biochim Biophys Acta* 1758:1018–1024
- Castle NA (2005) Aquaporins as targets for drug discovery. *Drug Discov Today* 10:485–493
- Chen H, Wu Y, Voth GA (2006) Origins of proton transport behavior from selectivity domain mutations of the aquaporin-1 channel. *Biophys J* 90:L73–L75
- de Groot BL, Grubmüller H (2005) The dynamics and energetics of water permeation and proton exclusion in aquaporins. *Curr Opin Struct Biol* 15:176–183
- Detmers FJ, de Groot BL, Müller EM, Hinton A, Konings IB, Sze M, Flitsch SL, Grubmüller H, Deen PM (2006) Quaternary ammonium compounds as water channel blockers. Specificity, potency, and site of action. *J Biol Chem* 281:14207–14214
- Frigeri A, Nicchia GP, Svelto M (2007) Aquaporins as targets for drug discovery. *Curr Pharm Des* 13:2421–2427
- Fu D, Libson A, Miercke LJ, Weitzman C, Nollert P, Krucinski J, Stroud RM (2000) Structure of a glycerol-conducting channel and the basis for its selectivity. *Science* 290:481–486
- Gao J, Yu H, Song Q, Li X (2005) Establishment of HEK293 cell line expressing green fluorescent protein-aquaporin-1 to determine osmotic water permeability. *Anal Biochem* 342:53–58
- Gonen T, Walz T (2006) The structure of aquaporins. *Q Rev Biophys* 39:361–396
- Gourbal B, Sonuc N, Bhattacharjee H, Legare D, Sundar S, Ouellette M, Rosen BP, Mukhopadhyay R (2004) Drug uptake and modulation of drug resistance in *Leishmania* by an aquaglyceroporin. *J Biol Chem* 279:31010–31017
- Hansen M, Kun JF, Schultz JE, Beitz E (2002) A single, bi-functional aquaglyceroporin in blood-stage *Plasmodium falciparum* malaria parasites. *J Biol Chem* 277:4874–4882

- Holm LM, Jahn TP, Møller AL, Schjoerring JK, Ferri D, Klaerke DA, Zeuthen T (2005) NH_3 and NH_4^+ permeability in aquaporin-expressing *Xenopus* oocytes. *Pflügers Arch* 450:415–428
- Hub JS, de Groot BL (2008) Mechanism of selectivity in aquaporins and aquaglyceroporins. *Proc Natl Acad Sci U S A* 105:1198–1203
- Huber VJ, Tsujita M, Yamazaki M, Sakimura K, Nakada T (2007) Identification of arylsulfonamides as aquaporin 4 inhibitors. *Bioorg Med Chem Lett* 17:1270–1273
- Huber VJ, Tsujita M, Kwee IL, Nakada T (2008) Inhibition of aquaporin 4 by antiepileptic drugs. *Bioorg Med Chem* (in press)
- Hubert JF, Duchesne L, Delamarche C, Vaysse A, Gueuné H, Raguénès-Nicol C (2005) Pore selectivity analysis of an aquaglyceroporin by stopped-flow spectrophotometry on bacterial cell suspensions. *Biol Cell* 97:675–686
- Ishibashi K, Sasaki S, Fushimi K, Uchida S, Kuwahara M, Saito H, Furukawa T, Nakajima K, Yamaguchi Y, Gojōbori T, Marumo F (1994) Molecular cloning and expression of a member of the aquaporin family with permeability to glycerol and urea in addition to water expressed at the basolateral membrane of kidney collecting duct cells. *Proc Natl Acad Sci U S A* 91:6269–6273
- Jahn TP, Møller AL, Zeuthen T, Holm LM, Klaerke DA, Mohsin B, Kühlbrandt W, Schjoerring JK (2004) Aquaporin homologues in plants and mammals transport ammonia. *FEBS Lett* 574:31–36
- Jeyaseelan K, Sepramaniam S, Armugam A, Wintour EM (2006) Aquaporins: a promising target for drug development. *Exp Opin Ther Targets* 10:889–909
- Karlgren S, Filipsson C, Mullins JG, Bill RM, Tamás MJ, Hohmann S (2004) Identification of residues controlling transport through the yeast aquaglyceroporin Fps1 using a genetic screen. *Eur J Biochem* 271:771–779
- Karlgren S, Pettersson N, Nordlander B, Mathai JC, Brodsky JL, Zeidel ML, Bill RM, Hohmann S (2005) Conditional osmotic stress in yeast: a system to study transport through aquaglyceroporins and osmotic stress signaling. *J Biol Chem* 280:7186–7193
- Laizé V, Rousselet G, Verbavatz JM, Berthonaud V, Gobin R, Roudier N, Abrami L, Ripoché P, Tacnet F (1995) Functional expression of the human CHIP28 water channel in a yeast secretory mutant. *FEBS Lett* 373:269–2674
- Liu Z, Shen J, Carbrey JM, Mukhopadhyay R, Agre P, Rosen BP (2002) Arsenite transport by mammalian aquaglyceroporins AQP7 and AQP9. *Proc Natl Acad Sci U S A* 99:6053–6058
- Liu Y, Promeneur D, Rojek A, Kumar N, Frøkiaer J, Nielsen S, King LS, Agre P, Carbrey JM (2007) Aquaporin 9 is the major pathway for glycerol uptake by mouse erythrocytes, with implications for malarial virulence. *Proc Natl Acad Sci U S A* 104:12560–12564
- Luyten K, Albertyn J, Skibbe WF, Prior BA, Ramos J, Thevelein JM, Hohmann S (1995) Fps1, a yeast member of the MIP family of channel proteins, is a facilitator for glycerol uptake and efflux and is inactive under osmotic stress. *EMBO J* 14:1360–1371
- Ma JF, Tamai K, Yamaji N, Mitani N, Konishi S, Katsuhara M, Ishiguro M, Murata Y, Yano M (2006) A silicon transporter in rice. *Nature* 440:688–691
- Mallo RC, Ashby MT (2006) AqpZ-mediated water permeability in *Escherichia coli* measured by stopped-flow spectroscopy. *J Bacteriol* 188:820–822
- Mathai JC, Mori S, Smith BL, Preston GM, Mohandas N, Collins M, van Zijl PC, Zeidel ML, Agre P (1996) Functional analysis of aquaporin-1 deficient red cells. The Colton-null phenotype. *J Biol Chem* 271:1309–1313
- Pavlovic-Djuranovic S, Kun JF, Schultz JE, Beitz E (2006) Dihydroxyacetone and methylglyoxal as permeants of the *Plasmodium aquaglyceroporin* inhibit parasite proliferation. *Biochim Biophys Acta* 1758:1012–1017
- Pettersson N, Hagström J, Bill RM, Hohmann S (2006) Expression of heterologous aquaporins for functional analysis in *Saccharomyces cerevisiae*. *Curr Genet* 50:247–255
- Preston GM, Carroll TP, Guggino WB, Agre P (1992) Appearance of water channels in *Xenopus* oocytes expressing red cell CHIP28 protein. *Science* 256:385–387
- Preston GM, Jung JS, Guggino WB, Agre P (1993) The mercury-sensitive residue at cysteine 189 in the CHIP28 water channel. *J Biol Chem* 268:17–20

- Saparov SM, Kozono D, Rothe U, Agre P, Pohl P (2001) Water and ion permeation of aquaporin-1 in planar lipid bilayers. Major differences in structural determinants and stoichiometry. *J Biol Chem* 276:31515–31520
- Solenov E, Watanabe H, Manley GT, Verkman AS (2004) Sevenfold-reduced osmotic water permeability in primary astrocyte cultures from AQP-4-deficient mice, measured by a fluorescence quenching method. *Am J Physiol Cell Physiol* 286:C426–C432
- Saparov SM, Liu K, Agre P, Pohl P (2007) Fast and selective ammonia transport by aquaporin-8. *J Biol Chem* 282:5296–5301
- Solomon AK, Chasan B, Dix JA, Lukacovic MF, Toon MR, Verkman AS (1983) The aqueous pore in the red cell membrane: band 3 as a channel for anions, cations, nonelectrolytes, and water. *Ann N Y Acad Sci* 414:97–124
- Sui H, Han BG, Lee JK, Walian P, Jap BK (2001) Structural basis of water-specific transport through the AQP1 water channel. *Nature* 414:872–878
- Uehlein N, Lovisololo C, Siefritz F, Kaldenhoff R (2003) The tobacco aquaporin NtAQP1 is a membrane CO₂ pore with physiological functions. *Nature* 425:734–737
- Verkman AS (1989) Mechanisms and regulation of water permeability in renal epithelia. *Am J Physiol* 257:C837–C850
- Wu B, Altmann K, Barzel I, Krehan S, Beitz E (2008) A yeast based phenotypic screen for aquaporin inhibitors. *Pflügers Arch – Eur J Physiol* 456:717–720
- Wysocki R, Chéry CC, Wawrzycka D, Van Hulle M, Cornelis R, Thevelein JM, Tamás MJ (2001) The glycerol channel Fps1p mediates the uptake of arsenite and antimonite in *Saccharomyces cerevisiae*. *Mol Microbiol* 40:1391–1401
- Yasui M, Hazama A, Kwon TH, Nielsen S, Guggino WB, Agre P (1999) Rapid gating and anion permeability of an intracellular aquaporin. *Nature* 402:184–187
- Zardoya R (2005) Phylogeny and evolution of the major intrinsic protein family. *Biol Cell* 97:397–414
- Zeidel ML, Ambudkar SV, Smith BL, Agre P (1992) Reconstitution of functional water channels in liposomes containing purified red cell CHIP28 protein. *Biochemistry* 31:7436–7440
- Zeuthen T, Wu B, Pavlovic-Djuranovic S, Holm LM, Uzategui NL, Duszenko M, Kun JF, Schultz JE, Beitz E (2006) Ammonia permeability of the aquaglyceroporins from *Plasmodium falciparum*, *Toxoplasma gondii* and *Trypanosoma brucei*. *Mol Microbiol* 61:1598–1608

Part II
Aquaporin Function in Mammalian Water
Homeostasis

Aquaporins in the Kidney*

Tae-Hwan Kwon, Jakob Nielsen, Hanne B. Møller, Robert A. Fenton,
Søren Nielsen, and Jørgen Frøkiær*

Contents

1	Introduction	95
2	Expression and Function of Aquaporins in the Kidney	96
3	Vasopressin Regulation of Kidney Aquaporins	100
3.1	Exocytosis and Endocytosis of AQP2: Role of Phosphorylation	101
3.2	Other Signal Transduction Pathways Involved in Vasopressin Regulation of AQP2 Trafficking	105
4	Dysregulation of Renal Aquaporins in Water Balance Disorders	108
4.1	Urinary Concentrating Defects	109
4.2	Acquired Forms of Nephrogenic Diabetes Insipidus	110
4.3	Lithium-Induced NDI	111
4.4	Electrolytes Abnormality (Hypokalemia and Hypercalcemia)	115
4.5	Ureteral Obstruction	116
4.6	Acute and Chronic Renal Failure	117
5	Conditions Associated with Water Retention	118
5.1	Congestive Heart Failure	118
5.2	Hepatic Cirrhosis	119
5.3	Experimental Nephrotic Syndrome	120
5.4	SIADH and Vasopressin Escape	120
	References	121

1 Introduction

The kidneys are the major determinants of body water and electrolyte composition. Thus, comprehending the mechanisms of water transport is essential to understanding mammalian kidney physiology and water balance. Because of its importance

J. Frøkiær (✉)

Water and Salt Research Center, Institute of Clinical Medicine, University of Aarhus, DK-8200 Aarhus N, Denmark
jf@ki.au.dk

* This chapter is an update of previous detailed reviews (Nielsen et al. 2002, 2007, 2008b, c; Rojek et al. 2008).

to human health, water permeability has been particularly well characterized in the mammalian kidney (Knepper and Burg 1983). Approximately, 180L day^{-1} of glomerular filtrate is generated in an average adult human; more than 90% of this is constitutively reabsorbed by the highly water-permeable proximal tubules and descending thin limbs of Henle's loop. The ascending thin limbs and thick limbs are relatively impermeable to water and empty into renal distal tubules and ultimately into the collecting ducts. The collecting ducts are extremely important clinically in water-balance disorders, because they are the chief site of regulated water reabsorption. Basal epithelial water permeability in collecting duct principal cells is low, but the water permeability can become exceedingly high when stimulated with arginine vasopressin (AVP, also known as antidiuretic hormone (ADH)). In this regard, the toad urinary bladder behaves like the collecting duct, and it has served as an important model of vasopressin-regulated water permeability. Stimulation of this epithelium with vasopressin produces an increase in water permeability in the apical membrane, which coincides with the redistribution of intracellular particles to the cell surface (Kachadorian et al. 1975, 1977; Wade and Kachadorian 1988). These particles were believed to contain water channels. The discovery of aquaporin-1 (AQP1) by Agre and colleagues (Preston et al. 1992; Preston and Agre 1991; Smith and Agre 1991) explained the long-standing biophysical question of how water specifically crosses biological membranes, and these studies led to the identification of a whole new family of membrane proteins, the aquaporin water channels. At present, at least eight aquaporins are expressed at distinct sites in the kidney, and four members of this family (AQP1-4) have been demonstrated to play pivotal roles in the physiology and pathophysiology for renal regulation of body water balance. In the present review, we will focus on regulation of renal aquaporins and in particular how regulation of AQP2 takes place. In addition, a number of inherited and acquired conditions characterized by urinary concentration defects as well as common diseases associated with severe water retention are discussed with relation to the role of aquaporins in regulation and dysregulation of renal water transport.

2 Expression and Function of Aquaporins in the Kidney

Thirteen mammalian aquaporins are now known (Agre et al. 2002; Nielsen et al. 2002, 2008b; Rojek et al. 2008), and they can be classified into three major subtypes, which are mainly determined by their transport capabilities: (a) the classical aquaporins (AQP1, -2, -4, and -5), which are known to transport only water and thus serve essential roles in transcellular water transport, (b) aquaglyceroporins (AQP3, -7, -9, and -10), which are permeated by small uncharged molecules in addition to water, and (c) unorthodox aquaporins (AQP6, -8, -11, and -12), whose function is currently being elucidated. Of the known aquaporins, eight (AQP1, -2, -3, -4, -6, -7, -8, -11) are expressed in mammalian kidney (Table 1).

AQP1 protein (Agre et al. 1993; Preston et al. 1992; Preston and Agre 1991) is highly expressed in proximal tubules and descending thin limbs of kidney

Table 1 Aquaporins in the kidney

AQP	Localization (renal)	Subcellular Distribution	Regulation	Localization (extrarenal)
AQP1	S2, S3 segments of proximal tubules	Apical and basolateral plasma membranes	Glucocorticoids (peribronchiolar capillary endothelium) Vasopressin stimulates short-term exocytosis and long-term biosynthesis	Multiple tissues, including capillary endothelia, choroids plexus, ciliary and lens epithelium, etc. Epididymis
AQP2	Collecting duct principal cells	Intracellular vesicles, apical plasma membrane	Vasopressin stimulates long-term exocytosis and long-term biosynthesis	
AQP3	Collecting duct principal cells	Basolateral plasma membrane	Vasopressin stimulates long-term biosynthesis	Multiple tissues, including airway basal epithelia, conjunctiva, colon
AQP4	Collecting duct principal cells	Basolateral plasma membrane	Dopamine, protein kinase C	Multiple tissues, including central nervous system astroglia, ependyma, airway surface epithelia Unknown
AQP6	Collecting duct intercalated cells	Intracellular vesicles	Rapidly gated	
AQP7	S3 proximal tubules	Apical plasma membrane	Insulin (adipose tissue)	Multiple tissues, including adipose tissue, testis, and heart
AQP8	Proximal tubule, collecting duct cells	Intracellular domains	Unknown	Multiple tissues, including gastrointestinal tract, testis, and airways
AQP11	Proximal tubule	Intracellular domains	Unknown	Multiple tissues, including liver, testes, and brain

AQP aquaporin

(Nielsen et al. 1993c; Sabolic et al. 1992). AQP1 is also present in capillary endothelia (Nielsen et al. 1993b, 1995c), including the renal vasa recta. In addition, AQP1 is present in multiple water-permeable epithelia in the body (Bondy et al. 1993; Brown et al. 1993a; Gresz et al. 2001; Hasegawa et al. 1994a; Lai et al. 2001; Nielsen et al. 1993b; Stamer et al. 1994). The critical role of AQP1 in urinary concentration has been highlighted in studies using transgenic mice with knockout of the *AQP1* gene (Ma et al. 1998). These mice were polyuric and had a reduced urinary concentrating capacity. The polyuria and impaired urinary concentration seen in AQP1 null mice could be explained by two mechanisms: impaired near isosmolar water reabsorption by proximal tubule and reduced medullary hypertonicity resulting from impaired countercurrent multiplication and exchange (Pallone et al. 2003; Verkman 2008). Consistent with this, isolated perfused proximal tubules and descending thin limbs had an 80 and 90% reduction in osmotic water permeability, respectively, illustrating an important role of AQP1 in water transport across these tubule segments (Schnermann et al. 1998). Moreover, these studies also emphasized the important role of transcellular rather than paracellular water transport in these tubule segments.

Soon after AQP1 was discovered to be a water channel, AQP2 was identified in renal collecting duct (Fushimi et al. 1993), where it is regulated by vasopressin and is involved in multiple clinical disorders (Kwon et al. 2001; Loonen et al. 2008; Nielsen et al. 2002, 2007; Schrier 2008). AQP2 is expressed in principal cells of the cortical, outer, and inner medullary collecting ducts and is abundant both in the apical plasma membrane and subapical vesicles (Nielsen et al. 1993a). AQP2 is the primary target for vasopressin regulation of collecting duct water permeability (Nielsen et al. 1995a; Sabolic et al. 1995; Yamamoto et al. 1995). This conclusion was established from studies showing a direct correlation between AQP2 expression and collecting duct water permeability in rats (Nielsen et al. 1995a) and in studies demonstrating that humans with mutations in the *AQP2* gene (Deen et al. 1994a; Loonen et al. 2008) or rats with 95% reduction in AQP2 expression have profound nephrogenic diabetes insipidus (Christensen et al. 2006; Kwon et al. 2000; Marples et al. 1995a). As described later, body water balance is regulated both by short-term and long-term mechanisms, and it is now clear that AQP2 plays a fundamental role in both. Consistent with this, lack of functional AQP2 expression by generation of *AQP2* gene knockout mice (Rojek et al. 2006) produces a severe concentration defect, resulting in postnatal death. Morphological changes including renal medullary atrophy and dilation of the collecting ducts are also observed in these mice. Generation of *AQP2* $-/-$ knockouts selectively in the collecting ducts, but not in the connecting tubule segments, rescues mice from the lethal phenotype (Rojek et al. 2006). However, body weight, urinary production, and the response to water deprivation are still severely impaired. This indicates an essential role of AQP2 in the renal tubular water reabsorption in both the connecting tubule segment and in the entire collecting duct.

AQP3 was identified in kidney and other tissues and was found to be permeated by glycerol and water (Echevarria et al. 1994; Ishibashi et al. 1994; Ma et al. 1994). In the kidney AQP3 is localized in the basolateral plasma membranes of connecting tubule cells, collecting duct principal cells, and inner medullary collecting

duct cells (Coleman et al. 2000; Ecelbarger et al. 1995; Ishibashi et al. 1997b). AQP3 is expressed in the same cells as the vasopressin-regulated water channel AQP2 and is thought to mediate the basolateral exit of water that enters apically via AQP2. AQP3-deficient mice were shown to be severely polyuric (Ma et al. 2000), demonstrating that basolateral membrane water transport can also become a rate-limiting factor for water reabsorption. Moreover, urinary osmolality is reduced in AQP3 $-/-$ mice and they fail to respond appropriately to dDAVP, thus presenting with a urinary concentrating defect (Ma et al. 2000). Interestingly, AQP3 is not abundant in the cytoplasm, and there is no clear evidence for the short-term regulation of AQP3 by vasopressin-induced trafficking. However, AQP3 mRNA and protein expression are both upregulated by long-term stimulation of vasopressin, which is seen during water deprivation or vasopressin infusion (Ecelbarger et al. 1995; Ishibashi et al. 1997b; Murillo-Carretero et al. 1999; Terris et al. 1996). In addition, sodium restriction or aldosterone infusion in normal and Brattleboro rats greatly increases the abundance of AQP3, while AQP3 abundance is markedly reduced during aldosterone deficiency, suggesting a direct effect of aldosterone on collecting duct AQP3 expression (Kwon et al. 2002).

AQP4, a HgCl₂-insensitive water channel, is most abundantly expressed in brain and is present in kidney collecting duct (Coleman et al. 2000; Frigeri et al. 1995; Hasegawa et al. 1994b; Terris et al. 1995). Although AQP3 and AQP4 are basolateral water channels, they are distributed differently along the collecting duct system, with the greatest abundance of AQP3 in cortical and outer medullary collecting ducts and the greatest abundance of AQP4 in inner medullary collecting duct (Terris et al. 1995). AQP4 is also found in basolateral membranes of proximal tubule S3 segments, although only in mice (Van Hoek et al. 2000). Using freeze fracture electron microscopy, orthogonal arrays of intramembrane particles (OAP) were present in the basolateral membranes of the proximal tubule S3 segment in AQP4 $+/+$, but not in AQP4 $-/-$ mice (Van Hoek et al. 2000). AQP4 appears to be regulated by PKC and dopamine, where stimulation by these factors decreases water permeability in AQP4-transfected cells (Zelenina et al. 2002). Targeted disruption of AQP4 in mice results in a 75% reduction in the osmotic water permeability of the inner medullary collecting duct (Chou et al. 1998). However, phenotypically the AQP4 $-/-$ mice appeared grossly normal, presenting with a very mild urinary concentrating defect (Ma et al. 1997). In double AQP3 $-/-$ /AQP4 $-/-$ knockout mice, urinary concentrating ability was slightly more impaired than that in the AQP3 $-/-$ mice (Ma et al. 2000), suggesting an important role of AQP3 in urinary concentration. It should also be noted that the localization of AQP2 in basolateral membranes in both the connecting tubule and inner medullary collecting duct raises the possibility that the observed effect is partly compensated by this mechanism (Christensen et al. 2003).

AQP6 was found to be localized in the subapical vesicles within intercalated cells of collecting duct, where it is coexpressed with the V-type H⁺-ATPase (Yasui et al. 1999a, 1999b). AQP6 appears functionally distinct from other known aquaporins. Oocyte expression studies have revealed low water permeability of AQP6 during basal conditions, while in the presence of HgCl₂ a rapid increase in water

permeability and ion conductance is observed (Yasui et al. 1999a). Additionally, reductions in pH (below 5.5) quickly and reversibly increase anion conductance and water permeability in AQP6 expressing oocytes (Yasui et al. 1999a). Subsequent studies have shown that the channel is permeable to halides with the highest permeability to NO_3^- (Ikeda et al. 2002), while the ionic selectivity becomes less specific after the addition of HgCl_2 (Hazama et al. 2002). Moreover, when Asn60, a residue unique in mammalian AQP6, is converted to glycine, a highly conserved residue in other mammalian aquaporins, anionic permeability is abolished and osmotic water permeability is increased during basal conditions (Liu et al. 2005).

AQP7 is permeated by water and glycerol (Ishibashi et al. 1997a). AQP7 mRNA is abundantly expressed in the kidney (Ishibashi et al. 1997a; Kuriyama et al. 1997). Immunohistochemical studies in mouse and rat have localized AQP7 to the brush border of the proximal tubule S3 segment (Ishibashi et al. 2000; Nejsum et al. 2000), where AQP7 is colocalized with AQP1. AQP7 null mice have reduced water permeability in the proximal tubule brush border membrane (Sohara et al. 2005), whereas they do not exhibit a urinary concentrating defect or water balance abnormality since AQP1 is the major water transport pathway in the proximal tubule. AQP8 is a water channel found in intracellular domains of the proximal tubule and the collecting duct cells (Elkjaer et al. 2001); however, its function remains unclear. AQP11 is found in the cytoplasm of renal proximal tubule cells (Morishita et al. 2005). The exact function is not established, although deletion of the *AQP11* gene produces a severe phenotype with renal vacuolization and cyst formation (Morishita et al. 2005).

3 Vasopressin Regulation of Kidney Aquaporins

AQP2 has evoked the largest clinical interest, because it is expressed in principal cells of renal collecting duct, where it is the primary target for short-term regulation of collecting duct water permeability (Nielsen et al. 1995a; Sabolic et al. 1995; Yamamoto et al. 1995). AQP2 and AQP3 also are regulated either directly or indirectly by vasopressin through long-term effects that alter the abundance of these water-channel proteins in collecting duct cells (DiGiovanni et al. 1994; Ecelbarger et al. 1995; Lankford et al. 1991; Nielsen et al. 1993a; Terris et al. 1996). Water permeability in the collecting duct is regulated by two modes: short- and long-term regulation. Both involve regulation of the AQP2 water channel. Short-term regulation is the widely recognized process by which vasopressin rapidly increases water permeability of principal cells by binding to vasopressin V2-receptors in the basolateral membranes, a response measurable within 5–30 min after increasing the peritubular vasopressin concentration (Kuwahara and Verkman 1989; Wall et al. 1992). It is believed that vasopressin, acting through a cyclic adenosine monophosphate (cAMP) cascade, causes intracellular AQP2 vesicles to fuse with the apical plasma membrane, which increases the number of water channels in the apical plasma membrane (Fig. 1a–g). Long-term regulation of collecting duct water permeability is seen when circulating vasopressin levels are increased for 24 h or more, resulting in an

increase in the maximal water permeability of the collecting duct epithelium (Lankford et al. 1991). This response is a consequence of an increase in the abundance of AQP2 water channels per cell in the collecting duct (DiGiovanni et al. 1994; Nielsen et al. 1993a), apparently due to increased transcription of the *AQP2* gene (Fig. 1h).

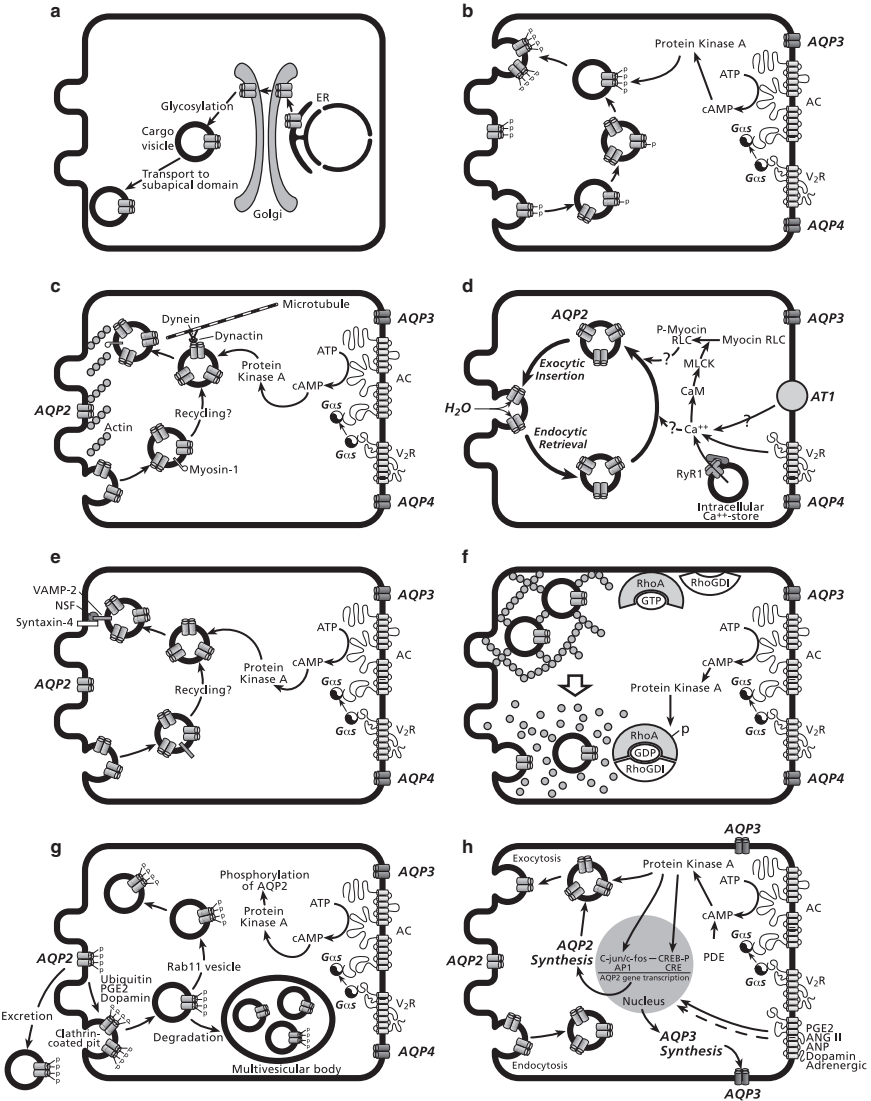
Multiple studies with affinity-purified polyclonal antibodies to AQP2 have unequivocally established that AQP2 is specifically involved in the vasopressin-induced increases of renal collecting duct water permeability. Soon after isolation of the AQP2 cDNA and generation of specific antibodies (Fushimi et al. 1993), immunoperoxidase microscopy and immunoelectron microscopy clearly demonstrated that principal cells within renal collecting ducts contain abundant AQP2 in the apical plasma membranes and in subapical vesicles (DiGiovanni et al. 1994; Nielsen et al. 1993a). These studies strongly supported the *shuttle hypothesis* originally proposed more than a decade earlier (Kachadorian et al. 1975). This hypothesis proposed that water channels can shuttle between an intracellular reservoir in subapical vesicles and the apical plasma membrane, and that vasopressin alters water permeability by regulating the shuttling process (Wade et al. 1981). Shuttling of AQP2 was directly demonstrated in isolated perfused tubule studies (Nielsen et al. 1995a). In these studies, water permeability of isolated perfused collecting ducts was measured before or after stimulation with vasopressin, and the tubules were fixed directly for immunoelectron microscopic examination. Vasopressin stimulation resulted in a markedly decreased immunogold labeling of intracellular AQP2 accompanied by a fivefold increase in the appearance of AQP2 immunogold particles in the apical plasma membrane. This redistribution was associated with an increase in osmotic water permeability of similar magnitude. These findings were reproduced in vivo by injecting rats with vasopressin, which also caused redistribution of AQP2 to the plasma membrane of collecting duct principal cells (Marples et al. 1995b; Sabolic et al. 1995). In contrast to the effect of vasopressin treatment, removal of vasopressin led to a reappearance of AQP2 in intracellular vesicles and a decline in osmotic water permeability in the isolated perfused collecting duct system (Nielsen et al. 1995a). Moreover, the offset response to vasopressin has been examined in vivo by acute treatment of rats with vasopressin- V_2 -receptor antagonist (Christensen et al. 1998; Hayashi et al. 1994) or acute water loading (to reduce endogenous vasopressin levels (Saito et al. 1997)). These treatments (both reducing vasopressin action) resulted in a prominent internalization of AQP2 from the apical plasma membrane to intracellular subapical vesicles, further underscoring the role of AQP2 trafficking in the regulation of collecting duct water permeability and the reversibility of AQP2 trafficking to the plasma membrane.

3.1 Exocytosis and Endocytosis of AQP2: Role of Phosphorylation

The accumulation of AQP2 on the apical plasma membrane is a balance between regulated exocytosis and endocytosis. Both processes occur continuously, and their relative rates are regulated to effect changes in water permeability. Numerous studies

have shown that actin, microfilaments, and motorproteins are all involved to some degree in translocation of AQP2 to the plasma membrane (see review Fenton and Moeller 2008) in addition to the role of phosphorylation in regulation of AQP2 trafficking.

Within the AQP2 amino acid sequence, there are several putative phosphorylation sites for different kinases including PKA, PKC, PKG, Golgi casein kinase, and casein kinase II. The role of PKA-induced phosphorylation in AQP2 trafficking has been extensively studied and will be described in detail later, but it is important to



consider that in addition to cAMP pathways, cGMP pathways may be involved in AQP2 translocation. The AQP2 carboxyl-terminal tail is a target for phosphorylation by PKG, and both nitric oxide and atrial natriuretic peptide induce AQP2 trafficking to the plasma membrane, without a resultant rise in intracellular cAMP (Bouley et al. 2000). Currently, it is not clear whether PKG directly phosphorylates AQP2, or whether the effects observed are mediated by a subsequent activation of PKA.

Binding of AVP to the type II vasopressin receptor of the kidney collecting duct (Fenton et al. 2007) results in activation of G-coupled proteins and a subsequent rise in intracellular cAMP (Fig. 1). This results in recruitment of PKA to AQP2-containing vesicles by PKA-anchoring proteins (AKAPs) (Klussmann et al. 1999). AKAP 18 delta and AQP2 colocalize in intracellular vesicles (Henn et al. 2004), making this the most likely isoform to mediate this event. Additionally, rolipram-mediated inhibition of the cAMP-specific phosphodiesterase-4D (PDE4D) increases AKAP-tethered PKA activity in AQP2-bearing vesicles and enhances AQP2 trafficking (Stefan et al. 2007), suggesting that a compartmentalized cAMP-dependent

Fig. 1 Regulation of AQP2 trafficking (Panels a–h) and expression (Panel g) in collecting duct principal cells. (a) AQP2 is synthesized in the endoplasmic reticulum (ER) and transported via the Golgi apparatus and cargo vesicles to the subapical plasma membrane domain. (b) Vasopressin binding to basolateral G-protein-linked V2 receptor stimulates adenylyl cyclase (AC); cyclic adenosine monophosphate (cAMP) activates protein kinase A to phosphorylate AQP2 in intracellular vesicles; phosphorylated AQP2 is exocytosed to the apical plasma membrane, resulting in increased apical membrane water permeability. (c) Overview of cytoskeletal elements, which may be involved in AQP2-trafficking. AQP2-containing vesicles may be transported along microtubules by dynein/dynactin. The cortical actin web may act as a barrier to fusion with the plasma membrane. (d) Intracellular calcium signaling and AQP2-trafficking. Increases in intracellular Ca^{2+} concentration may arise from stimulation of the V2 receptor. The existence and potential role of other receptors and pathways, e.g., VACM-1, in Ca^{2+} mobilization is still uncertain. The downstream targets of the calcium signal are unknown and conflicting data exist on the importance of a rise in intracellular Ca^{2+} for the hydroosmotic response to vasopressin. (e) Vesicle targeting receptors and AQP2-trafficking. AQP2 vesicles dock at the apical membrane by association of VAMP-2 with syntaxin-4 targets in the presence of NSF. The exact role of these remains to be established. (f) Changes in the actin cytoskeleton associated with AQP2-trafficking to the plasma membrane. Inactivation of RhoA by phosphorylation and increased formation of RhoA–RhoGDI complexes seem to control the dissociation of actin fibers seen after vasopressin stimulation. (g) Endocytic retrieval of AQP2 can be initiated by removal of AVP or favoured by prostaglandin E2 (PGE2) or dopamine. Ubiquitination of AQP2 in the plasma membrane is proposed to play a role in the endocytotic events. Endocytosis of AQP2 occurs in clathrin-coated pits via a phosphatidylinositol 3-kinase (PI3-kinase)-dependent mechanism. After membrane retrieval, AQP2 is transported to early endosomes (EE), recycling vesicles, or to multivesicular bodies (MVB) that may be targeted for proteasomal degradation. (h) Specifically cAMP participates in the long-term regulation of AQP2 by increasing the levels of the catalytic subunit of PKA in the nuclei, which is thought to phosphorylate transcription factors such as CREB-P (cyclic AMP responsive element binding protein) and C-Jun/c-Fos. Binding of these factors are thought to increase gene transcription of AQP2 resulting in synthesis of AQP2 protein, which in turn enters the regulated trafficking system. In parallel AQP3 and AQP4 synthesis and trafficking to the basolateral plasma membrane takes place. Importantly AQP2 regulation can be modified by a number of hormones including dopamine, ANP, PGE2, and adrenergic hormones. See text for details. *Gs* GTP-binding protein, *ATP* adenosine triphosphate, *P* phosphorylation, *V2R* Vasopressin-V2-receptors, *AC* adenylyl cyclase, *PKA* cAMP and protein kinase A. Redrawn and modified from Nielsen et al. (2001)

signal transduction pathway consisting of anchored PDE4D, AKAP18delta, and PKA plays an essential role in AQP2 trafficking.

PKA recruitment to AQP2-containing vesicles results in phosphorylation of AQP2. The most well-defined and extensively studied phosphorylated residue of AQP2 is serine 256 (S256), which has been shown to be critical for vasopressin-induced cell-surface accumulation of AQP2 (Fushimi et al. 1997; Katsura et al. 1996). pS256-AQP2 is localized both in the plasma membrane and intracellularly (Christensen et al. 2000), indicating that even in low-circulating vasopressin states it is constitutively phosphorylated. AVP stimulation results in translocation of pS256-AQP2 to the apical plasma membrane where AQP2 exists as a tetramer, with at least three monomers in an AQP2 tetramer being phosphorylated (Kamsteeg et al. 2000). Although the majority of studies of pS256-AQP2 have been performed in cell-culture models or oocytes, the phenotype of a mouse strain with an amino-acid substitution at S256 (S to L) preventing phosphorylation is congenital progressive hydronephrosis due to major polyuria (McDill et al. 2006). Phosphoproteomics studies have determined that in addition to S256, AQP2 is further phosphorylated on residues S261, S264, and S269 (Hoffert et al. 2006) in response to AVP stimulation. Immunolocalization studies suggest that these phosphorylated forms are localized to different intracellular compartments (Fenton et al. 2008; Hoffert et al. 2007). The precise role that these additional phosphorylation sites play remains undefined, but it has been suggested that AVP induces a dynamic effect on the phosphorylation status of AQP2 and as such defines its subcellular distribution (Fenton et al. 2008).

Although phosphorylation of AQP2 is essential for cell surface expression, it remains unclear as to how phosphorylation of AQP2 actually causes trafficking. One possibility is that phosphorylation of AQP2 directly influences an interaction between AQP2-containing vesicles and the cell cytoskeleton, microtubules, or accessory cross-linking proteins. Indeed, S256 is important for a direct interaction of AQP2 with 70-kDa heat-shock proteins and, ultimately, the AQP2 shuttle (Lu et al. 2007). Alternatively, phosphorylation could prevent endocytosis of AQP2, leading to accumulation at the cell surface.

In addition to PKA, there is evidence that other kinases and PKA-independent mechanisms are involved in AQP2 translocation. For example, S256 is also a substrate for Golgi casein kinase 2, which is required for the Golgi transition of AQP2 (Procino et al. 2003). Additionally, the phosphatase inhibitor okadaic acid induces increased AQP2 abundance at the cell surface even in the presence of the PKA inhibitor H89, and S256A AQP2 mutants (that lack S256 phosphorylation) are able to accumulate at the cell surface after treatment with cholesterol depleting agents (Lu et al. 2004).

Retrieval of AQP2 from the plasma membrane is a dynamic process. During endocytosis, AQP2 accumulates in clathrin-coated pits before being internalized via a clathrin-mediated process (Bouley et al. 2006; Lu et al. 2004; Russo et al. 2006) (Fig. 1g). Internalization of AQP2 is not dependent on its phosphorylation state. For example, both prostaglandin E2 and dopamine can promote removal of AQP2 from the cell surface without altering the phosphorylation state of AQP2 (Nejsum et al. 2005; Tamma et al. 2003). Furthermore, PKC activation mediates AQP2 endocytosis

independent of phosphorylation state (van Balkom et al. 2002). Once internalized, AQP2 is retrieved to EEA1-positive early endosomes via a phosphatidylinositol-3-kinase-dependent mechanism before being transferred to Rab11-positive storage vesicles (Tajika et al. 2004). Following AVP restimulation, AQP2 may be recycled to the apical plasma membrane, a process that is thought to involve the protein Rab11 (Barile et al. 2005; Tajika et al. 2005). Ubiquitination is important for endocytosis of AQP2 (Kamsteeg et al. 2006). AQP2 is polyubiquitinated at the plasma membrane on a single residue (K270), resulting in internalization of AQP2, transport to multivesicular bodies (MVBs), and subsequent proteasomal degradation. A proportion of AQP2 that is internalized to MVBs can be excreted into the urine as exosomes (Pisitkun et al. 2004).

3.2 Other Signal Transduction Pathways Involved in Vasopressin Regulation of AQP2 Trafficking

The signal transduction pathways have been described thoroughly in previous reviews (Knepper et al. 1994; Nielsen et al. 2002). Prostaglandin E₂ (PGE₂) has been known to inhibit vasopressin-induced water permeability by reducing cAMP levels. Zelenina et al. (Zelenina et al. 2000) investigated the effect of PGE₂ on PKA phosphorylation of AQP2 in kidney papilla, and the results suggest that the action of prostaglandins is associated with retrieval of AQP2 from the plasma membrane, but that this appears to be independent of AQP2 phosphorylation by PKA (Zelenina et al. 2000). Angiotensin II-induced activation of protein kinase C could be, at least in part, also involved in the AQP2 trafficking/expression (Kwon et al. 2005; Lee et al. 2007). Phosphorylation of other cytoplasmic or vesicular regulatory proteins may also be involved. These issues remain to be investigated directly.

3.2.1 Involvement of the Cytoskeleton and Ca²⁺ in AQP2 Trafficking

The cytoskeleton has been known to be involved in the AQP2 trafficking in kidney collecting duct. In particular, the microtubular network has been implicated in this process, since chemical disruption of microtubules inhibits the increase in permeability both in the toad bladder and in the mammalian collecting duct (Phillips and Taylor 1989, 1992). Thus, AQP2 vesicles may be transported along microtubules on their way to the apical plasma membrane. The microtubule-based motor protein dynein and the associated protein Arp1, which is part of the protein complex dynactin, were found by immunoblotting to be among the proteins associated with AQP2 vesicles from rat inner medulla. Immunoelectron microscopy further supported the presence of both AQP2 and dynein on the same vesicles (Marples et al. 1998). Moreover, both vanadate (nonspecific inhibitor of ATPases) and EHNA (specific inhibitor of dynein) inhibit the antidiuretic response in toad bladder (de Sousa and Grosso 1979; Marples et al. 1996a) and kidney

collecting duct (Shaw and Marples 2005). Thus, it is likely that dynein may drive the microtubule-dependent delivery of AQP2-containing vesicles to the apical plasma membrane. Actin filaments are also involved in the hydrosmotic response (DiBona 1983; Ding et al. 1991; Kachadorian et al. 1979; Muller et al. 1984; Pearl and Taylor 1983; Wade and Kachadorian 1988). Recently evidence was provided that the myosin light chain kinase (MLCK) pathway, through calmodulin-mediated calcium activation of MLCK, leads to phosphorylation of myosin regulatory light chain and nonmuscle myosin 2 motor activity (Chou et al. 2004). Studies in isolated perfused rat inner medullary collecting ducts showed that the MLCK-inhibitors ML-7 and ML-9 reduce the vasopressin-induced increase in water permeability (Chou et al. 2004), indicating that MLCK may be a downstream target for the vasopressin-induced Ca^{2+} signal.

The intracellular Ca^{2+} concentration has been shown to increase upon stimulation of isolated perfused rat inner medullary collecting ducts with vasopressin or dDAVP (Star et al. 1988). These observations have been followed by a number of studies of the role of the Ca^{2+} in the vasopressin-induced increase in water permeability. Vasopressin or 8-4-chlorophenylthio-cAMP induced a marked increase in intracellular $[\text{Ca}^{2+}]$ in isolated perfused IMCD, and BABTA blocked the rise in intracellular $[\text{Ca}^{2+}]$ and cocontaminantly lead to inhibition of the vasopressin-induced increase in tubular water permeability (Chou et al. 2000). Moreover blocking calmodulin with W7 or trifluoperazine also inhibited the effect of vasopressin on tubular water permeability and inhibited the vasopressin-induced AQP2 plasma membrane targeting in primary cultured IMCD cells (Chou et al. 2000). Removing Ca^{2+} from both bath and lumen in isolated perfused tubules did not affect the vasopressin-induced Ca^{2+} signal, indicating that Ca^{2+} was released from an intracellular source. This was further supported by the observations that ryanodine inhibited the Ca^{2+} signal in perfused IMCDs and inhibited AQP2 accumulation in the plasma membrane in primary cultured IMCD cells. In addition, RyR1 ryanodine receptor was localized to rat IMCD by immunohistochemistry (Chou et al. 2000). Ryanodine receptors are generally known to mediate a positive feedback and release Ca^{2+} from intracellular stores in response to an initial rise in intracellular $[\text{Ca}^{2+}]$. Thus, it is likely that another mechanism is responsible for the initialization of the rise in intracellular $[\text{Ca}^{2+}]$. Further studies revealed that vasopressin or dDAVP elicited oscillations in intracellular $[\text{Ca}^{2+}]$ in isolated perfused rat IMCD (Yip 2002). The results on isolated perfused IMCDs indicate that an intracellular increase in $[\text{Ca}^{2+}]$ is an obligate component of the vasopressin response leading to increased AQP2 expression in the apical plasma membrane. However, it should be mentioned that there is a discrepancy between the results from primary cultured IMCD cells (Lorenz et al. 2003) and isolated perfused IMCD tubules (Chou et al. 2000) with regard to the role of intracellular $[\text{Ca}^{2+}]$ in vasopressin-induced AQP2 trafficking. Consistent with this, Lorenz et al. (2003) demonstrated that AQP2 shuttling is evoked neither by AVP-dependent increase of $[\text{Ca}^{2+}]$ nor AVP-independent increase of $[\text{Ca}^{2+}]$ in primary cultured IMCD cells from rat kidney, although clamping of intracellular $[\text{Ca}^{2+}]$ below resting levels inhibits AQP2 exocytosis. Further studies are required to clarify this discrepancy, which may be related to altered

expression levels of vasopressin receptors and/or AQP2, or other elements in the AQP2 trafficking system.

3.2.2 Mechanism of AQP2 Trafficking by Targeting Receptors

The mechanism by which AQP2 vesicles are targeted to the apical plasma membrane and the mechanism by which cAMP controls docking and fusion of vesicles is a current area of active investigation. Considerable insight into this problem has been obtained from previous studies of regulated exocytosis of synaptic vesicles, which involve the actions of multiple proteins (Bajjalieh and Scheller 1995; Sollner et al. 1993). Vesicle-targeting receptors (often referred to as *SNAREs*) are believed to induce specific interaction of vesicles with membrane sites; vesicle targeting receptors associated chiefly with translocating vesicles are known as *VAMPs* (vesicle associated membrane proteins, also referred to as *synaptobrevins*), and *synaptotagmins*. Two other families of membrane proteins are believed to serve as receptors in target membranes: the *syntaxins* and SNAP-25 homologues. Several of these SNAREs have been found in renal collecting duct (Barile et al. 2005; Franki et al. 1995; Harris et al. 1994; Inoue et al. 1998; Kishore et al. 1998; Liebenhoff and Rosenthal 1995; Mandon et al. 1996, 1997; Nielsen et al. 1995b). Syntaxins are 30- to 40-kDa integral membrane proteins. Syntaxins have a one bilayer-spanning domain near the C-terminus, so the majority of the protein resides in the cytoplasm. Syntaxins are widely distributed among mammalian tissues. It has been established that syntaxin-4 is expressed in the mammalian collecting duct by studies using polyclonal antibodies raised to conjugated peptides specific for individual syntaxins, and this has been confirmed by RT-PCR (Mandon et al. 1996). Immunolocalization studies have demonstrated that syntaxin-4 is predominantly located in the apical plasma membrane of collecting duct principal cells, where AQP2 is targeted in response to vasopressin.

VAMPs are believed to induce specific docking of vesicles by interacting directly with syntaxins in the target plasma membrane (Fig. 1e). Although their primary amino acid sequences are not related to syntaxins, VAMPs also have a single bilayer spanning domain near the C-terminus, and the majority of the protein resides in the cytoplasm. Three VAMP isoforms were initially identified (Sudhof et al. 1993): VAMP-1, VAMP-2, and VAMP-3 (also referred to as *cellubrevin*), and subsequently several additional homologues have been cloned (Advani et al. 1998). VAMP-2 and VAMP3 have been localized in principal cells of renal collecting duct (Franki et al. 1995; Harris et al. 1994; Inoue et al. 1998; Kishore et al. 1998; Liebenhoff and Rosenthal 1995; Mandon et al. 1996, 1997; Nielsen et al. 1995b). Double-labeling immunoelectron microscopy revealed that AQP2 and VAMP-2 reside in the same intracellular vesicles in collecting duct principal cells (Nielsen et al. 1995b). Furthermore, AQP2 vesicles isolated by differential centrifugation were found to contain VAMP-2 (Harris et al. 1994; Liebenhoff and Rosenthal 1995).

Several putative vesicle-targeting proteins are known to reside in collecting duct principal cells. VAMP-2 resides in AQP2 intracellular vesicles, and syntaxin-4 resides in the apical plasma membrane. In vitro binding assays have documented that VAMP-2 binds syntaxin-4 with high affinity, but VAMP-2 has not been shown to

interact with syntaxin-3 or syntaxin-2 (Calakos et al. 1994; Pevsner et al. 1994). Thus, VAMP-2 and syntaxin-4 are likely participants in the targeting of AQP2 vesicles to the apical plasma membrane; however, a functional role for these targeting proteins remains to be formally demonstrated. A third SNARE protein, SNAP-23, also has been identified in principal cells of the collecting duct (Inoue et al. 1998). Although considered a target-membrane SNARE (t-SNARE), SNAP-23 is present both in AQP2-containing vesicles and in the apical plasma membrane of principal cells. The VAMP-2, syntaxin-4, and SNAP-23 may potentially form a complex with the *N*-ethylmaleimide-sensitive factor (NSF). Finally, synaptotagmin VIII, a calcium-insensitive homologue, was identified in collecting duct principal cells (Kishore et al. 1998).

Recently, LC-MS/MS-based proteomic analysis of immunisolated AQP2-containing intracellular vesicles from rat inner medullary collecting duct revealed that AQP2-containing vesicles are heterogeneous and that intracellular AQP2 resides chiefly in endosomes, trans-Golgi network, and rough endoplasmic reticulum (Barile et al. 2005). Vasopressin-stimulated exocytosis of AQP2 vesicles involves several steps including (1) translocation of vesicles from a diffuse distribution throughout the cell to the apical region of the cell, (2) translocation of AQP2 across the apical part of the cell composed of a dense filamentous actin network, (3) priming of vesicles for docking, (4) docking of vesicles, and (5) fusion of vesicles with the apical plasma membrane. Theoretically each of these steps could be target for regulation by vasopressin. If the SNARE proteins are involved in the vasopressin-induced trafficking of AQP2 to the apical plasma membrane, the regulatory mechanism might involve selective phosphorylation of one of the SNARE proteins or an ancillary protein that binds to them, possibly via protein kinase A or calmodulin-dependent kinase II. Although the SNARE proteins are recognized as potential targets for phosphorylation (Foster et al. 1998; Risinger and Bennett 1999; Shimazaki et al. 1996), there is presently no evidence for the phosphorylation in the collecting duct. As noted earlier, however, AQP2 itself appears to be a target for PKA-mediated phosphorylation at a serine in position 256 (Kuwahara et al. 1995). The phosphorylation does not modify the single channel water permeability of AQP2 (Lande et al. 1996) and instead the phosphorylation is believed to play a critical role in regulation of AQP2 trafficking to the plasma membrane (Fushimi et al. 1997; Katsura et al. 1997). The establishment of a role for these SNARE proteins in regulated trafficking of AQP2 will most likely depend on the preparation of targeted knockouts for each of these genes in the collecting duct.

4 Dysregulation of Renal Aquaporins in Water Balance Disorders

Aquaporins have been demonstrated to play a key role in the pathophysiology of a variety of water balance disorders. This section updates previous detailed reviews with regard to the critical role of AQP2 in water balance disorders (Kwon et al. 2001; Nielsen et al. 1999, 2000, 2002, 2007, 2008c).

4.1 Urinary Concentrating Defects

4.1.1 Inherited Forms of Diabetes Insipidus

The importance of AQP2 for urinary concentration was first demonstrated in a study by Deen et al. (Deen et al. 1994a). Chromosome 12q13 harbors the human *AQP2* gene (GenBank accession number z29491) (Deen et al. 1994b; Sasaki et al. 1994). The *AQP2* gene comprises four exons distributed over ~5 kb of genomic DNA and three introns (Deen et al. 1994a, 1994b; Sasaki et al. 1994). The 1.5-kb mRNA encodes a protein of 271 amino acids. Deen et al. (Deen et al. 1994a) found mutated and nonfunctional AQP2 in patients with very severe nephrogenic diabetes insipidus (non-X-linked NDI). The patient appeared to carry two point mutations in the *AQP2* gene, one resulting in substitution of a cysteine for arginine 187 (R187C) in the third extracellular loop of the AQP2 and the other resulting in substitution of a proline for serine 216 (S216P) in the sixth transmembrane domain (Deen et al. 1994a). Subsequently, it was demonstrated that Brattleboro rats, which are vasopressin-deficient and have extreme polyuria and therefore have central diabetes insipidus, have reduced expression of AQP2 and very low AQP2 levels in the apical plasma membrane (DiGiovanni et al. 1994; Promeneur et al. 2000; Yamamoto et al. 1995).

There are two significant inherited forms of diabetes insipidus (DI): central and nephrogenic. In central (or neurogenic) DI, normal vasopressin production is impaired. Central DI (CDI) is rarely hereditary in man, but usually occurring as a consequence of head trauma or diseases in the hypothalamus or pituitary gland. The Brattleboro rat provides an excellent model of this condition. These animals have a total or near-total lack of vasopressin production (Valtin and Schroeder 1964). Consequently, Brattleboro rats have substantially decreased expression levels of vasopressin-regulated AQP2 compared with the parent strain (Long Evans), and the AQP2 deficit was reversed by chronic vasopressin infusion, suggesting that patients lacking vasopressin are likely to have decreased AQP2 expression (DiGiovanni et al. 1994). The subsequent work showing that expression of AQP3 is also regulated by vasopressin implies that the expression levels of these water channels will also be decreased in patients with CDI. However, the most important denominator is the deficiency of AQP2 trafficking to the apical membrane. These deficits are likely to be the most important causes of the polyuria from which these patients of CDI suffer, which will be reversed by the desmopressin treatment. The second form of DI is called nephrogenic DI (NDI), and is caused by the inability of the kidney to respond to vasopressin stimulation. The most common hereditary cause (95% of the cases) is an X-linked disorder associated with mutations of the vasopressin V2 receptor making the collecting duct cells insensitive to vasopressin (Bichet 1996). The human gene that encodes for the V2 receptor (*AVPR2*) is located in chromosome region Xq28 and has three exons and two small introns (Birnbaumer et al. 1992; Seibold et al. 1992). The sequences of the cDNA predict a polypeptide of 371 amino acids with 7 transmembrane, 4 extracellular, and 4 cytoplasmic domains (Bichet 2008; Fujiwara and Bichet 2005; Mouillac et al. 1995). X-linked NDI is generally a rare disease in which the affected male patients do not concentrate

their urine, whereas female individuals are not likely to be affected. However, heterozygous females can show variable degrees of polyuria because of skewed X-chromosome inactivation (Bichet 2008; Fujiwara and Bichet 2005). The incidence of X-linked NDI among male individuals was reported to be ~ 8.8 in 1,000,000 male live births in Quebec (Arthus et al. 2000). To date, 193 putative disease-causing *AVPR2* mutations have been reported in 307 NDI families: there are 95 missense, 18 nonsense, 46 frameshift deletion or insertion, 7 inframe deletion or insertion, 4 splice-site, 22 large deletion mutations, and one complex mutation (Bichet 2008) (<http://www.medicine.mcgill.ca/nephros>). Ninety five of these 193 mutations are missense mutations likely to be misfolded, trapped in the endoplasmic reticulum, and unable to reach the basolateral plasma membrane. Although there is no direct evidence, it is likely that this form of NDI will be associated with decreased expression of AQP2, since the cells are unable to respond to circulating vasopressin. This will compound the lack of AQP2 trafficking. Consistent with this, urinary AQP2 levels are very low in patients with X-linked NDI (Deen et al. 1996; Kanno et al. 1995). However, since the amount of AQP2 in the urine appears to be determined largely by the response of the collecting duct cells to vasopressin (Wen et al. 1999) rather than their content of AQP2, the data must be interpreted with caution with respect to predicting AQP2 expression levels.

More rarely (5% of the cases), patients with hereditary NDI have mutations in the *AQP2* gene. Of these more than 90% are reported with autosomal recessive NDI. Since these patients manifest a severe form of diabetes insipidus, the critical role of AQP2 in renal water conservation was established. To date, 39 mutations have been reported in *AQP2* gene and, among them 32 mutations are involved in recessive NDI (Loonen et al. 2008). Nearly all the mutations in autosomal recessive NDI are found in the region encoding the AQP2 segment between the first and the last transmembrane domain. In contrast, seven mutations of *AQP2* gene have been described as autosomal dominant NDI and all mutations in dominant NDI are found in the coding region of the C-terminal tail of AQP2, which has a critical role in AQP2 trafficking to the apical plasma membrane. Thus, AQP2 mutants in dominant NDI are sorted to other subcellular locations in the cells than wt-AQP2 (de Mattia et al. 2004; Kamsteeg et al. 2003; Kuwahara et al. 2001; Marr et al. 2002; Mulders et al. 1998; Procino et al. 2003). Patients with autosomal dominant mutations of *AQP2* gene are likely to demonstrate more mild clinical manifestations than those with recessive form (Kamsteeg et al. 2001, 2003; Loonen et al. 2008; Marr et al. 2002): (1) in the dominant NDI, polyuria and polydipsia become apparent in the second half of the first year, whereas in recessive NDI the symptoms are already present at birth; and (2) some patients with dominant NDI respond to dDAVP administration or dehydration by showing a transient increase in urine concentration.

4.2 Acquired Forms of Nephrogenic Diabetes Insipidus

In contrast to the rare inherited forms of diabetes insipidus (central and nephrogenic), acquired forms of NDI are much more common. A series of studies has

been aimed at testing whether reduced expression and apical targeting of AQP2 might play a role in these polyuric conditions. For this purpose, several classic experimental protocols were used.

4.3 Lithium-Induced NDI

Lithium has been widely used for treating bipolar affective mood disorders (Timmer and Sands 1999). However, chronic lithium treatment also induces decreased AQP2 and AQP3 expression in the collecting duct (Kwon et al. 2000; Marples et al. 1995a), resulting in a pronounced vasopressin-resistant polyuria and inability to concentrate urine (i.e., nephrogenic diabetes insipidus) (Christensen et al. 1985; Kwon et al. 2000; Marples et al. 1995a). Lithium-induced polyuria is observed in approximately 20–30% of lithium-treated patients (approximately 1 in 1,000 of the population receives lithium treatment), and affected patients and experimental animals typically show a slow recovery of urinary concentrating ability when treatment is discontinued (Boton et al. 1987; Christensen et al. 2004). Lithium is almost exclusively excreted by the kidney (Radomski et al. 1950) and is reabsorbed by mechanisms similarly to sodium. Approximately 75% of the filtered lithium is reabsorbed by the termination of the cortical thick ascending limb in the loop of Henle (see review by Nielsen et al. 2008b). During conditions of restricted sodium intake significant lithium reabsorption also occurs in the connecting tubule and collecting duct, which is thought to be mediated by the amiloride-sensitive epithelial sodium channel ENaC. Thus, ENaC appears to play a central role in the development of lithium-induced NDI (see review by Nielsen et al. 2008b).

The progressive polyuria induced by chronic lithium-treatment in rats is associated with a parallel downregulation of both total protein expression of AQP2 and AQP3 and decreased apical trafficking of the vasopressin-regulated AQP2. The AQP2 protein and mRNA expression in kidney cortex and medulla decreased to below ~30% of controls within 28 days of treatment (Christensen et al. 2004; Kwon et al. 2000; Laursen et al. 2004; Marples et al. 1995a; Nielsen et al. 2003). A recent *in vivo* study using the collecting duct-derived mpkCCDC14 cells indicated that decreased AQP2 protein expression is likely due to decreased AQP2 mRNA transcription while AQP2 protein stability was unchanged (Li et al. 2006). Immunohistochemistry has shown that the AQP2 downregulation in the kidney cortex predominantly occurs in the cortical collecting duct (Fig. 2) while the connecting tubule appears to be less affected by lithium (Nielsen et al. 2006). Moreover, quantitative immunohistochemical analysis showed that lithium caused a cellular reorganization with a decreased fraction of AQP2 and AQP3 expressing principal cells relative to H⁺-ATPase expressing intercalated cells, which may also play an important role for the lithium-induced polyuria (Christensen et al. 2004, 2006) (Fig. 2). In addition to decreased overall cellular AQP2 expression quantitative immunoelectron microscopy demonstrated the marked reduction of AQP2 in the apical plasma membrane as well as in the intracellular vesicles in rat inner medullary collecting duct

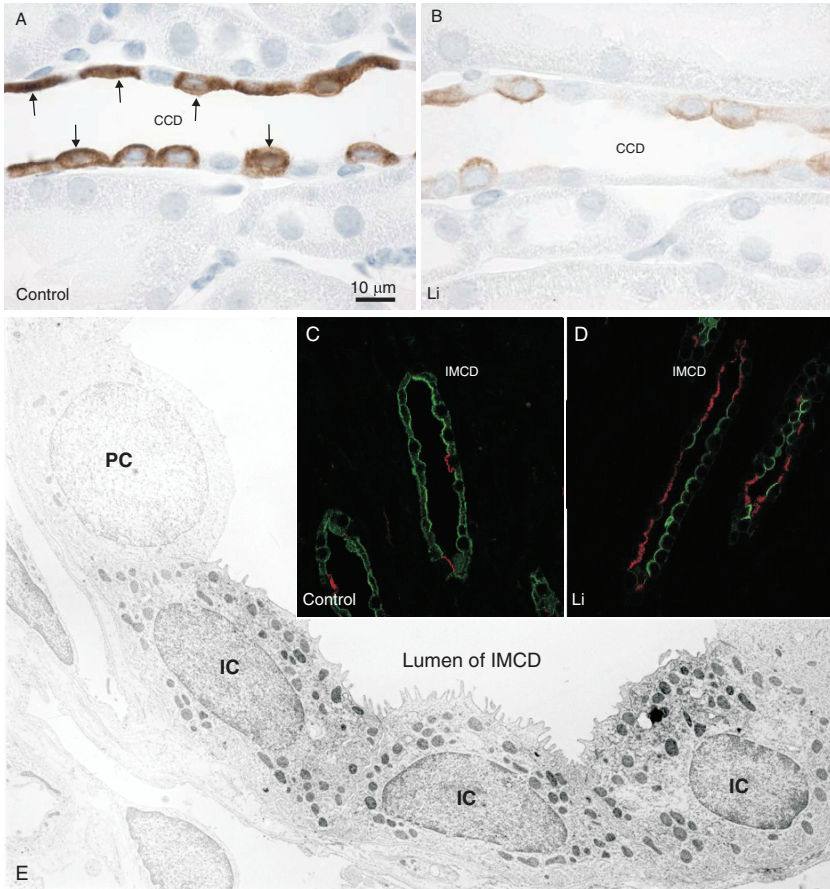


Fig. 2 Downregulation of AQP2 and cellular reorganization and composition in collecting duct of lithium-treated rats. Immunoperoxidase labeling of AQP2 in tissue section of kidney cortex of control rats (**a**) and rats treated with lithium for 4 weeks (**b**). In control rats strong AQP2 labeling was present in the apical plasma membrane domain (*arrows*) and dispersed within the cytoplasm in the principal cells of the cortical collecting duct (CCD). In the lithium-treated rats the AQP2 labeling in both the apical plasma membrane domain and cytoplasm of the principal cells of the cortical collecting duct was drastically decreased (**b**) compared with control rats. To illustrate altered fraction of principal cells and intercalated cells fluorescent double-labeling was performed with polyclonal anti-AQP2 antibody (using a relatively high concentration; *green*) and monoclonal anti- H^+ -ATPase antibody (*red*) in the proximal part of inner medulla; IM-1) from control rats (**c**) and lithium-treated rats (**d**). In both cortex (not shown) and IM-1 an increased density of H^+ -ATPase positive cells was observed after lithium treatment (**d**) as compared with controls (**c**). Immunoelectron microscopy of the inner medulla from lithium-treated rats shows three adjacent H^+ -ATPase positive intercalated cells, which are highly unusual in the normal rat kidney (**e**). Modified from (**a** and **b**) Nielsen et al. (2006), (**c** and **d**) Christensen et al. (2004), and (**e**) Kim et al. (2003)

principal cells (Marple et al. 1995a). Similarly the AQP3 expression in the basolateral plasma membrane was reduced as demonstrated by immunoblotting and immunoelectron microscopy (Kwon et al. 2000). The significance of the decreased

AQP2 and AQP3 in the collecting duct principal cells is underscored by the findings of similarly severe polyuria in the collecting duct-selective AQP2-deficient mice (Rojek et al. 2006) and *AQP3* gene-deficient mice (Ma et al. 2000).

Several attempts have been made to find useful therapies for both central and nephrogenic diabetes insipidus, and it is well established that thiazide and amiloride can have profound antidiuretic effects in patients with DI including lithium-induced NDI (Bedford et al. 2008; Crawford and Kennedy 1959). In rats with lithium-induced NDI the antidiuretic effect of thiazide and amiloride has been associated with increased AQP2 expression (Bedford et al. 2008; Kim et al. 2004a). Modulation of the renin–angiotensin–aldosterone system (RAAS) by captopril (an angiotensin-converting enzyme inhibitor) or spironolactone (a mineralocorticoid receptor blocker) also leads to decreased urine production in rats with diabetes insipidus (Henderson et al. 1979; Stamoutsos et al. 1981). We have shown that antidiuretic effect of spironolactone was associated with an increased apical AQP2 protein expression in the initial cortical collecting duct in both rats with lithium-induced NDI and vasopressin-deficient Brattleboro rats (Nielsen et al. 2006). In the same study we also showed that aldosterone infusion perturbed the polyuria in both lithium-treated rats and Brattleboro rats and that this is associated with decreased expression of AQP2 in the apical plasma membrane domain in connecting tubule and initial collecting duct (while the AQP2 expression in the basolateral plasma membrane domain was increased). The effect of aldosterone and spironolactone observed in both lithium-treated rats could not be explained by altered plasma lithium concentrations. In another series of studies we examined effect of modulating RAAS in normal rats. In sodium-restricted rats, receiving combined treatment with dDAVP and candesartan (an angiotensin II receptor antagonist) led to a blunted effect of dDAVP effect with decreased apical AQP2 targeting and increased urine production compared with rats treated with dDAVP alone (Kwon et al. 2005). On the other hand, combined treatment with dDAVP and aldosterone also blunted the effect of dDAVP with decreased apical (and increased basolateral) AQP2 and increased urine production compared with rats treated with dDAVP alone (de Seigneux et al. 2007). These results indicate that several pathways appear to modulate the response to vasopressin and aldosterone (and angiotensin II) with respect to AQP2 regulation both in normal and in polyuric rats (lithium-induced NDI and central DI). These studies indicate that angiotensin II and aldosterone receptors are likely to affect vasopressin signaling and that the effect of this may be more pronounced during states with altered vasopressin signaling (discussed in further detail in Nielsen et al. (2008b).

The mechanism responsible for the reduction in AQP2 expression is commonly thought to involve interference with the normal intracellular signaling of vasopressin (see review by Nielsen et al. 2008b). The normal vasopressin signaling is discussed earlier. The reduction in AQP2 and AQP3 expression may be induced by a lithium-dependent impairment in the production of cAMP by inhibition of the vasopressin-sensitive adenylate cyclase in collecting duct principal cells (Boton et al. 1987; Cogan et al. 1987; Cogan and Abramow 1986). The decreased cAMP production thus lead to a reduction in AQP2 and AQP3 expression as well as the

inhibition of AQP2 targeting to the apical plasma membrane in response to lithium treatment. This is consistent with the presence of a cAMP-responsive element in the 5'-untranslated region of the *AQP2* gene (Hozawa et al. 1996; Matsumura et al. 1997) and with the finding that mice with inherently low cAMP levels have decreased AQP2 expression (DI +/+ severe mouse) (Frokiær et al. 1999). The vasopressin signaling is also known to be modulated by prostaglandin E2 (PGE2) by attenuating the antidiuretic action of vasopressin on collecting duct water permeability by causing endocytic retrieval of AQP2 (see review by Nielsen et al. 2008b). In lithium-induced NDI urinary excretion of PGE2 is significantly increased in both humans and experimental animals (Hofer et al. 1992; Kotnik et al. 2005; Sugawara et al. 1988), and COX-2 inhibition has been shown to ameliorate lithium-induced polyuria and PGE2 excretion in COX-1 null mice (Rao et al. 2005). Lastly, in addition to vasopressin-dependent mechanisms there is evidence that nonvasopressin-mediated effects may play in AQP2 (and AQP3) regulation during lithium-induced NDI (Marples et al. 1995a; Umenishi et al. 2006).

To further explore the broad and significant effects of lithium we conducted combined proteomics and pathway analysis studies to identify novel candidate proteins and signaling mechanism affected by lithium (Nielsen et al. 2008a). Differential two-dimensional gel electrophoresis of protein isolated from IMCD combined with mass spectrometry identified 6 and 74 proteins with altered abundance compared with controls after 1 and 2 weeks of lithium treatment, respectively. Using bioinformatics analysis of the data indicated the protein changes were likely associated with changes in cellular functions affecting cell death, apoptosis, cell proliferation, and morphology. Consistent with these results, follow-up studies revealed that several signaling pathways involved in these cellular functions, including the PKB/Akt-kinase and the mitogen-activated protein kinases (MAPK) including ERK, JNK, and p38, were activated by lithium treatment. Activated PKB/Akt is a potential mediator of both JNK and P38 signaling pathways via activation of the apoptosis signal-regulating kinase 1 (ASK1), suggesting that these pathways may all be direct or indirect targets of lithium which leads to alteration in AQP2 and AQP3 expression.

The activation of PKB/Akt also indicated that the Wnt/beta-catenin (β -catenin) pathway, which regulates cellular proliferation, differentiation, and apoptosis, could be affected. The glycogen synthase kinase type 3 β (GSK3 β), which is also known to be inhibited by lithium (Klein and Melton 1996; Stambolic et al. 1996) plays a central role in this pathway and is inhibited by PKB/Akt. The GSK3 β phosphorylation (causing inactivation) was increased consistent with previous studies (Rao et al. 2005). In one of its many cellular functions, GSK3 β functions as a negative regulator of the Wnt/beta-catenin (β -catenin) pathway by phosphorylating β -catenin targeting it for degradation. Consistent with the increased phosphorylation (and inactivation of GSK3 β) β -catenin expression was increased and accumulated intracellularly after 2 weeks of lithium treatment compared with control rats (Nielsen et al. 2008a). When β -catenin is present intracellularly (during conditions with decreased GSK3 β activation) it serves as a nuclear transcription factor activating T-cell factor (TCF)-dependent transcription (Novak and Dedhar 1999). Interestingly mouse and rat *AQP2* gene 5' flanking regions contain the TCF consensus sites, and altered

Wnt/beta-catenin signaling could potentially play an important role in decreased AQP2 transcription in rats with lithium-induced NDI but potentially also in other conditions. Furthermore, TCF-dependent transcription has been demonstrated to regulate a number of proteins involved in cell-cycle entry and may also play a role in the principal cell proliferation observed with lithium treatment.

In addition to effects on the Wnt/beta-catenin pathway lithium-induced inhibition of GSK3 β has also been shown to increase PGE2 excretion (Rao et al. 2005). As discussed earlier the increased PGE2 may counteract vasopressin actions by causing endocytic retrieval of AQP2, resulting in impairing urinary concentrating ability (Zelenina et al. 2000).

4.4 Electrolytes Abnormality (Hypokalemia and Hypercalcemia)

It has also been demonstrated that hypokalemia and hypercalcemia, which are relatively common electrolyte disorders, are well-known causes of acquired NDI. Rat models of these conditions are valuable tools to study the molecular defects, and it was shown that both conditions are associated with downregulation of AQP2 expression and apical targeting. In these two conditions, however, the downregulation of AQP2 was much more modest, as was the polyuria, further supporting a role of AQP2 expression for the urinary concentration (Marples et al. 1996b; Wang et al. 2002b). Extracellular calcium-sensing receptor (CaSR), originally cloned from the bovine parathyroid gland (Brown et al. 1993b), has also been localized at the kidney tubular segments including collecting duct (Brown et al. 1993b; Riccardi et al. 1996, 1998). CaSR is a G-protein-coupled receptor and recent studies demonstrated that CaSR is involved in the signal transduction pathways that link urinary calcium levels to AQP2 expression and apical targeting in the collecting duct principal cells (Bustamante et al. 2008; Procino et al. 2004). Hypercalciuria, commonly seen in a condition of hypercalcemia, could impair AQP2 targeting and thus reduce urinary concentrating ability possibly by a functional cross-talk in signaling transduction between vasopressin signaling and CaSR signaling. However, further studies are still required to understand the underlying pathogenetic mechanisms fully. A calcium-dependent calpain activation was also proposed to modulate AQP2 expression levels through AQP2 proteolysis in hypercalcemia (Puliyanda et al. 2003). In addition to the AQP2 downregulation, both conditions also have been shown to be associated with downregulation of Na-K-2Cl cotransporter (NKCC2) in the thick ascending limb (Elkjaer et al. 2002; Wang et al. 2002a). Expression of NKCC2 in the thick ascending limb is known to be regulated by dDAVP (Kim et al. 1999; Kwon et al. 1999b), and hence this regulation could be significantly involved in the countercurrent multiplication system. Thus, downregulation of NKCC2 could reduce sodium and chloride reabsorption in the thick ascending limb and hence decreases medullary osmolality, also contributing to the polyuria and impaired urinary concentration in hypokalemia and hypercalcemia.

4.5 Ureteral Obstruction

A relatively common condition associated with long-term impaired urinary concentrating is obstruction of the urinary tract. Experimental bilateral obstruction of the ureters for 24 h was found to be associated with markedly reduced expression of AQP2, -3, -4, and -1 (Frokiaer et al. 1996; Li et al. 2001). In addition, BUO is associated with marked downregulation of key sodium transporters and urea transporters (Li et al. 2003). Following release of the obstruction, there is a marked polyuria during which period AQP2 and AQP3 levels remain downregulated up to 2 weeks after release providing an explanation at the molecular level for the observed postobstructive polyuria. In a number of studies BUO has been demonstrated to be associated with COX2 induction and cellular infiltration of the renal medulla (Cheng et al. 2004; Norregaard et al. 2005). Using specific COX2 inhibition to rats subjected to BUO it was demonstrated that this treatment prevents downregulation of AQP2 and several sodium transporters located to the proximal tubule and mTAL (Cheng et al. 2004; Norregaard et al. 2005). Moreover, specific inhibition of the AT1 receptor to rats subjected to BUO prevented downregulation of NaPi2 in the PT, BSC-1 in the mTAL, and AQP2 in the CD 3 days after release of BUO (Jensen et al. 2006), confirming that the renin-angiotensin system plays an important role for the pathophysiological changes in urinary tract obstruction.

In contrast to BUO conditions unilateral ureteral obstruction is not associated with changes in the absolute excretion of sodium and water since the nonobstructed kidney compensates for the reduced ability of the obstructed kidney to excrete solutes (Frokiaer et al. 1997; Li et al. 2001). These studies demonstrated a profound downregulation of AQP1, -2, -3, -4 and pAQP2 levels in the obstructed kidney, suggesting that local factors play a major role. Importantly, the role of PGs for regulation of AQP2 in response to urinary tract obstruction has been highlighted in a number of recent publications (Norregaard et al. 2005, 2006). Interestingly, it was demonstrated that treatment with a specific COX-2 inhibitor prevented downregulation of AQP2 and reduced the postobstructive polyuria indicating that COX-2 may be an important factor contributing to the impaired renal water and sodium handling in response to BUO (Norregaard et al. 2005). Moreover, the renin-angiotensin system is well known to be involved in the pathophysiological changes in renal function after obstruction of the ureter. In recent experiments it was demonstrated that candesartan treatment from the onset of obstruction attenuated the reduction in GFR and prevented the reduced abundance of AQP2, NaPi2, and NKCC2 coinciding with a reduction in the postobstructive polyuria (Jensen et al. 2006).

Congenital malformations of the kidney and urinary tract associated with ureteral obstruction account for a major proportion of renal insufficiency in infancy and childhood, but management of antenatally detected hydronephrosis is still debated (Shi et al. 2004b). To address this, the effect of neonatal partial unilateral ureter obstruction (PUUO) for 24 weeks was studied (Shi et al. 2004a, b). This resulted in a progressive decrease in RBF and a severe reduction in GFR in the obstructed kidney. The contralateral kidney counterbalanced the impairment of RBF and kidney growth. Obstruction was associated with severe hydronephrosis and obstructive

nephropathy, shown as a marked reduction in total kidney protein content. These changes were associated with a decreased abundance of Na–K–ATPase, consistent with a significant natriuresis from the obstructed kidney. The abundance of AQP1, AQP2, and AQP3 was also reduced, consistent with the reduced GFR and solute-free water reabsorption. Importantly, the results demonstrated that release after 4 weeks was associated with changes very similar to PUUO without release of obstruction. In contrast, release after 1 week of obstruction significantly attenuated the progressive reduction in RBF, and GFR was normal at 24 weeks of age. The development of hydronephrosis and obstructive nephropathy was prevented. Moreover, down-regulation of renal Na–K–ATPase and AQP1 and AQP3 was prevented, consistent with attenuation of the natriuresis and decreased solute-free water reabsorption in kidneys released 1 week after onset of neonatal PUUO (Shi et al. 2004a, b). Moreover, it has recently been demonstrated that treatment of neonatal rats subjected to PUUO at day 2 of life with candesartan prevented the reduction in RBF, GFR and dysregulation of AQP2 and Na–K–ATPase in response to congenital PUUO in rats, suggesting that AT1R blockade may protect the neonatally obstructed kidney against development of obstructive nephropathy (Topcu et al. 2007). These findings have been confirmed clinically by Valenti and coworkers, who demonstrated that children with severe unilateral hydronephrosis have reduced urinary AQP2 excretion levels (Murer et al. 2004). This suggests that urinary levels of AQP2 may be a useful biomarker for renal AQP2 levels. Importantly, decreased levels of urinary AQP2 excretion have also been demonstrated in various other significant clinical conditions with urinary concentrating defects, including nocturnal enuresis (Valenti et al. 2000, 2002).

4.6 Acute and Chronic Renal Failure

Acute and chronic renal failure is also an important clinical condition associated with polyuria and impaired urinary concentration. These are complex conditions and in both cases there is a wide range of glomerulotubular abnormalities that contribute to the overall renal dysfunction. Ischemia and reperfusion (I/R)-induced experimental acute renal failure (ARF) in rats is a model that is widely used. In this model there are structural alterations in renal tubule, in association with an impaired urinary concentration. ARF is complicated by defects of water and solute reabsorption in both the collecting duct and the proximal tubule (Hanley 1980; Tanner et al. 1973; Venkatachalam et al. 1978). Using an isolated tubule microperfusion model, water reabsorption in both the proximal tubule and the cortical collecting duct was significantly impaired following ischemia (Hanley 1980), and no differences were found in either basal or vasopressin-induced cAMP levels in the outer or inner medulla in rats with ARF (Anderson et al. 1982). The results support the view that there are defects in the collecting duct water reabsorption. Consistent with these findings, it was demonstrated that AQP2 and AQP3 expression in the collecting duct as well as AQP1 expression in the proximal tubule are

significantly decreased in ARF (Fernandez-Llama et al. 1999a; Kwon et al. 1999a). The decreased levels of AQPs were associated with impaired urinary concentration in rats with oliguric and nonoliguric ARF. Interestingly, reduced expression of AQP1, AQP2, and AQP3 and impaired urinary concentration ability were attenuated significantly by cotreatment with alpha-melanocyte-stimulating hormone (α -MSH), which is an anti-inflammatory cytokine that inhibits both neutrophil and nitric oxide pathways (Kwon et al. 1999a). Recently it was also demonstrated that hemorrhagic shock-induced acute renal failure is associated with decreased expression of collecting duct water channel AQP2 and AQP3 (Gong et al. 2003). And erythropoietin treatment (single or combined with α -MSH) in rats with I/R-induced ARF, which is known to prevent caspase-3, -8, and -9 activation in vivo and reduces apoptotic cell death (Sharples et al. 2004), prevents or reduces the urinary concentrating defects and the downregulation of AQP expression levels (Gong et al. 2004).

Patients with advanced chronic renal failure (CRF) have urine that remains hypotonic to plasma despite the administration of supramaximal doses of vasopressin (Tannen et al. 1969). This vasopressin-resistant hyposthenuria specifically implies abnormalities in collecting duct water reabsorption in CRF patients. Previous studies demonstrated virtual absence of V_2 receptor mRNA in the inner medulla of CRF rat kidneys (Teitelbaum and McGuinness 1995), providing evidence for significant defects in the collecting duct water reabsorption in response to vasopressin. Consistent with these observations, AQP2 and AQP3 expression was downregulated in the collecting duct, and decreased AQP2 expression was unchanged despite long-term dDAVP infusion in a rat model of 5/6 nephrectomy (Kwon et al. 1998).

5 Conditions Associated with Water Retention

5.1 Congestive Heart Failure

Retention of sodium and water is a common and clinically important complication of congestive heart failure (CHF). Two studies have examined the changes in renal AQP expression in rats with CHF induced by ligation of the left coronary artery to test if upregulation of AQP2 expression and targeting may play a role in the water retention in CHF (Nielsen et al. 1997; Xu et al. 1997). Both studies demonstrated that renal water retention in severe CHF in rats is associated with dysregulation of AQP2 in the renal collecting duct principal cells involving both an increase in the AQP2 expression and a marked redistribution of AQP2 to the apical plasma membrane (Nielsen et al. 1997; Xu et al. 1997). Rats with severe CHF had significantly elevated left ventricular end-diastolic pressures (LVEDP) and had reduced plasma sodium concentrations (Nielsen et al. 1997). Immunoblotting revealed a threefold increase in AQP2 expression compared with sham-operated animals. These changes were associated with elevated LVEDP or hyponatremia, since animals with normal LVEDP and plasma sodium did not have increased AQP2 levels compared with

sham-operated controls (Nielsen et al. 1997). Furthermore, this study showed an increased plasma membrane targeting, providing an explanation for the increased permeability of the collecting duct and an increase in water reabsorption. This may provide an explanation for excess free water retention in severe CHF and for the development of hyponatremia. In parallel, the other study showed upregulation of both AQP2 protein and AQP2 mRNA levels in kidney inner medulla and cortex in rats with CHF (Xu et al. 1997). These rats had significantly decreased cardiac output and, importantly, increased plasma vasopressin levels. Furthermore, in this study administration of V2 antagonist OPC 31260 was associated with a significant increase in diuresis, a decrease in urine osmolality, a rise in plasma osmolality, and a significant reduction in AQP2 protein and AQP2 mRNA levels compared with untreated rats with CHF. Consistent with this, treatment of V2 receptor antagonist in human patients with heart failure is associated with a dose-related increase in water excretion and a decrease in urinary AQP2 excretion (Martin et al. 1999). Moreover, V2 receptor antagonist treatment (tolvaptan (OPC-41061)) in patients with CHF increases urine volume, decreases edema, and normalizes serum sodium levels in patients with hyponatremia, compared with placebo-treated group (Gheorghiade et al. 2003).

5.2 *Hepatic Cirrhosis*

Hepatic cirrhosis is another chronic condition associated with water retention. It has been suggested that an important pathophysiological factor in the impaired ability to excrete water could be increased levels of plasma vasopressin. However, unlike CHF, the changes in expression of AQP2 protein levels vary considerably between different experimental models of hepatic cirrhosis. Several studies have examined the changes in renal AQP expression in rats with cirrhosis induced by common bile duct ligation (CBDL) (Fernandez-Llama et al. 1999b; Jonassen et al. 1998, 2000). The rats displayed impaired vasopressin-regulated water reabsorption despite normal plasma vasopressin levels. Consistent with this, semiquantitative immunoblotting showed a significant decrease in AQP2 expression in rats with hepatic cirrhosis (Fernandez-Llama et al. 1999b; Jonassen et al. 1998). In addition, the expression levels of AQP3 and AQP4 were downregulated in CBDL rats. This may predict a reduced water permeability of the collecting duct in this model (Fernandez-Llama et al. 1999b), hence renal water reabsorption in the collecting duct is decreased in rats with compensated liver cirrhosis. In contrast, Fujita et al. (Fujita et al. 1995) demonstrated that hepatic cirrhosis induced by intraperitoneal administration of carbon tetrachloride (CCl₄) was associated with a significant increase in both AQP2 protein levels and AQP2 mRNA expression. Interestingly, AQP2 mRNA expression correlated with the amount of ascites, suggesting that AQP2 may play a role in the abnormal water retention followed by the development of ascites in hepatic cirrhosis (Asahina et al. 1995). In a different model of CCl₄-induced cirrhosis, using CCl₄ inhalation, AQP2 expression was not increased (Fernandez-Llama et al. 2000). There was, however, evidence for increased trafficking of AQP2 to the plasma membrane,

consistent with the presence of elevated levels of vasopressin in the plasma. Interestingly, there was a marked increase in AQP3 expression that is likely to be due to increased vasopressin levels. The pattern of increased AQP3 expression without upregulation of AQP2 is consistent with previous findings observed in the vasopressin escape (Ecelbarger et al. 1998), suggesting that the lack of increase in AQP2 expression could be a result of a normal compensatory response related to the escape phenomenon. Although the explanation for the differences between cirrhosis induced by CBDL and CCl₄ administration remains to be determined, it is well known that the dysregulation of body water balance depends on the severity of cirrhosis (Gines et al. 1998; Kim et al. 2005; Wood et al. 1988). CBDL results in a compensated cirrhosis characterized by peripheral vasodilation and increased cardiac output, whereas cirrhosis induced by 12 weeks of CCl₄ administration may be associated with the late state of decompensated liver cirrhosis characterized by sodium retention, edema, and ascites (Gines et al. 1998; Kim et al. 2005; Levy and Wexler 1987). Thus, the downregulation of AQP2 observed in milder forms of cirrhosis (i.e., in a compensated stage without water retention) may represent a compensatory mechanism to prevent development of water retention. In contrast, the increased levels of vasopressin seen in severe *noncompensated* cirrhosis with ascites may induce an inappropriate upregulation of AQP2 that would in turn participate in the development of water retention.

5.3 *Experimental Nephrotic Syndrome*

The nephrotic syndrome is characterized by extracellular volume expansion with excessive renal salt and water reabsorption. The underlying mechanisms of salt and water retention are poorly understood; however, they can be expected to be associated with dysregulation of solute transporters and water channels (Apostol et al. 1997; Kim et al. 2004b). In contrast to congestive heart failure and liver cirrhosis, a marked downregulation of AQP2 and AQP3 expression was demonstrated in rats with PAN-induced and adriamycin-induced nephrotic syndrome (Apostol et al. 1997; Fernandez-Llama et al. 1998a, 1998b). The reduced expression of collecting duct water channels could represent a physiologically appropriate response to extracellular volume expansion. The signal transduction involved in this process is not clear, but circulating vasopressin levels are high in rats with PAN-induced nephrotic syndrome. Thus, the marked downregulation of AQP2 in experimental nephrotic syndrome may share similarities with the downregulation of AQP2 in water-loaded dDAVP-treated rats that escape from the action of vasopressin (Ecelbarger et al. 1997, 1998).

5.4 *SIADH and Vasopressin Escape*

Hyponatremia, defined as a serum sodium less than 135 mmol L⁻¹, is one of the most commonly encountered electrolyte disorders of clinical medicine (Flear et al.

1981). The predominant cause of hyponatremia is an inappropriate secretion of vasopressin relative to serum osmolality or the syndrome of inappropriate antidiuretic hormone secretion (SIADH) (Bartter and Schwartz 1967). SIADH occurs most frequently in association with vascular, infectious, or neoplastic abnormalities in the lung or central nervous system. In an experimental rat model of SIADH it was shown that AQP2 mRNA expression and AQP2 protein expression were increased in the collecting duct (Fujita et al. 1995). Thus, increased expression of AQP2 in the collecting duct accounts for the water retention and hyponatremia in SIADH.

The degree of the hyponatremia is limited by a process that counteracts the water retaining action of vasopressin, namely *vasopressin escape*. Vasopressin escape is characterized by a sudden increase in urine volume with a decrease in urine osmolality independent of high circulating vasopressin levels. The onset of escape coincided temporally with a marked decrease in renal AQP2 protein as measured by immunoblotting as well as decreased mRNA expression, as assessed by Northern blotting (Ecelbarger et al. 1998). In contrast to AQP2, there were no decreases in renal expression of AQP1, AQP3, and AQP4 (Ecelbarger et al. 1998). These results suggest that escape from vasopressin-induced antidiuresis is attributable, at least in part, to a selective vasopressin-independent decrease in AQP2 expression in the renal collecting duct.

Acknowledgments The Water and Salt Research Centre at the University of Aarhus is established and supported by the Danish National Research Foundation (Danmarks Grundforskningsfond). Support for this study was provided by The Karen Elise Jensen Foundation, The Commission of the European Union (QLRT-2000-00987 and QLRT-2000-00778), The Human Frontier Science Program, The WIRED program (Nordic Council and the Nordic Centre of Excellence Program in Molecular Medicine), The Danish Medical Research Council, The University of Aarhus, and The Korea Science and Engineering Foundation grant funded by the MOST (R01-2007-000-20441-0).

References

- Advani RJ, Bae HR, Bock JB et al (1998) Seven novel mammalian SNARE proteins localize to distinct membrane compartments. *J Biol Chem* 273:10317–10324
- Agre P, King LS, Yasui M et al (2002) Aquaporin water channels – from atomic structure to clinical medicine. *J Physiol* 542:3–16
- Agre P, Preston GM, Smith BL et al (1993) Aquaporin CHIP: the archetypal molecular water channel. *Am J Physiol* 265:F463–F476
- Anderson RJ, Gordon JA, Kim J et al (1982) Renal concentration defect following nonoliguric acute renal failure in the rat. *Kidney Int* 21:583–591
- Apostol E, Ecelbarger CA, Terris J et al (1997) Reduced renal medullary water channel expression in puromycin aminonucleoside-induced nephrotic syndrome. *J Am Soc Nephrol* 8:15–24
- Arthus MF, Lonergan M, Crumley MJ et al (2000) Report of 33 novel AVPR2 mutations and analysis of 117 families with X-linked nephrogenic diabetes insipidus. *J Am Soc Nephrol* 11:1044–1054
- Asahina Y, Izumi N, Enomoto N et al (1995) Increased gene expression of water channel in cirrhotic rat kidneys. *Hepatology* 21:169–173
- Bajjalieh SM, Scheller RH (1995) The biochemistry of neurotransmitter secretion. *J Biol Chem* 270:1971–1974

- Barile M, Pisitkun T, Yu MJ et al (2005) Large scale protein identification in intracellular aquaporin-2 vesicles from renal inner medullary collecting duct. *Mol Cell Proteomics* 4:1095–1106
- Bartter FC, Schwartz WB (1967) The syndrome of inappropriate secretion of antidiuretic hormone. *Am J Med* 42:790–806
- Bedford JJ, Leader JP, Jing R et al (2008) Amiloride restores renal medullary osmolytes in lithium-induced nephrogenic diabetes insipidus. *Am J Physiol Renal Physiol* 294:F812–F820
- Bichet DG (1996) Vasopressin receptors in health and disease. *Kidney Int* 49:1706–1711
- Bichet DG (2008) Vasopressin receptor mutations in nephrogenic diabetes insipidus. *Semin Nephrol* 28:245–251
- Birnbaumer M, Seibold A, Gilbert S et al (1992) Molecular cloning of the receptor for human antidiuretic hormone. *Nature* 357:333–335
- Bondy C, Chin E, Smith BL et al (1993) Developmental gene expression and tissue distribution of the CHIP28 water-channel protein. *Proc Natl Acad Sci USA* 90:4500–4504
- Boton R, Gaviria M, Battle DC (1987) Prevalence, pathogenesis, and treatment of renal dysfunction associated with chronic lithium therapy. *Am J Kidney Dis* 10:329–345
- Bouley R, Breton S, Sun T et al (2000) Nitric oxide and atrial natriuretic factor stimulate cGMP-dependent membrane insertion of aquaporin 2 in renal epithelial cells. *J Clin Invest* 106:1115–1126
- Bouley R, Hawthorn G, Russo LM et al (2006) Aquaporin 2 (AQP2) and vasopressin type 2 receptor (V2R) endocytosis in kidney epithelial cells: AQP2 is located in 'endocytosis-resistant' membrane domains after vasopressin treatment. *Biol Cell* 98:215–232
- Brown D, Verbavatz JM, Valenti G et al (1993a) Localization of the CHIP28 water channel in reabsorptive segments of the rat male reproductive tract. *Eur J Cell Biol* 61:264–273
- Brown EM, Gamba G, Riccardi D et al (1993b) Cloning and characterization of an extracellular Ca^{2+} -sensing receptor from bovine parathyroid. *Nature* 366:575–580
- Bustamante M, Hasler U, Leroy V et al (2008) Calcium-sensing receptor attenuates AVP-induced aquaporin-2 expression via a calmodulin-dependent mechanism. *J Am Soc Nephrol* 19:109–116
- Calakos N, Bennett MK, Peterson KE et al (1994) Protein–protein interactions contributing to the specificity of intracellular vesicular trafficking. *Science* 263:1146–1149
- Cheng X, Zhang H, Lee HL et al (2004) Cyclooxygenase-2 inhibitor preserves medullary aquaporin-2 expression and prevents polyuria after ureteral obstruction. *J Urol* 172:2387–2390
- Chou CL, Christensen BM, Frische S et al (2004) Non-muscle myosin II and myosin light chain kinase are downstream targets for vasopressin signaling in the renal collecting duct. *J Biol Chem* 279:49026–49035
- Chou CL, Ma T, Yang B et al (1998) Fourfold reduction of water permeability in inner medullary collecting duct of aquaporin-4 knockout mice. *Am J Physiol* 274:C549–C554
- Chou CL, Yip KP, Michea L et al (2000) Regulation of aquaporin-2 trafficking by vasopressin in the renal collecting duct. Roles of ryanodine-sensitive Ca^{2+} stores and calmodulin. *J Biol Chem* 275:36839–36846
- Christensen BM, Kim YH, Kwon TH et al (2006) Lithium treatment induces a marked proliferation of primarily principal cells in rat kidney inner medullary collecting duct. *Am J Physiol Renal Physiol* 291:F39–F48
- Christensen BM, Marples D, Kim YH et al (2004) Changes in cellular composition of kidney collecting duct cells in rats with lithium-induced NDI. *Am J Physiol Cell Physiol* 286:C952–C964
- Christensen BM, Wang W, Frokiaer J et al (2003) Axial heterogeneity in basolateral AQP2 localization in rat kidney: effect of vasopressin. *Am J Physiol Renal Physiol* 284:F701–F717
- Christensen BM, Zelenina M, Aperia A et al (2000) Localization and regulation of PKA-phosphorylated AQP2 in response to V(2)-receptor agonist/antagonist treatment. *Am J Physiol Renal Physiol* 278:F29–F42
- Christensen BM, Marples D, Jensen UB et al (1998) Acute effects of vasopressin V2-receptor antagonist on kidney AQP2 expression and subcellular distribution. *AJP - Renal Physiology* 275:F285–F297

- Christensen S, Kusano E, Yusufi AN et al (1985) Pathogenesis of nephrogenic diabetes insipidus due to chronic administration of lithium in rats. *J Clin Invest* 75:1869–1879
- Cogan E, Abramow M (1986) Inhibition by lithium of the hydroosmotic action of vasopressin in the isolated perfused cortical collecting tubule of the rabbit. *J Clin Invest* 77:1507–1514
- Cogan E, Svoboda M, Abramow M (1987) Mechanisms of lithium-vasopressin interaction in rabbit cortical collecting tubule. *Am J Physiol* 252:F1080–F1087
- Coleman RA, Wu DC, Liu J et al (2000) Expression of aquaporins in the renal connecting tubule. *Am J Physiol Renal Physiol* 279:F874–F883
- Crawford JD, Kennedy GC (1959) Chlorothiazid in diabetes insipidus. *Nature* 183:891–892
- de Mattia F, Savelkoul PJ, Bichet DG et al (2004) A novel mechanism in recessive nephrogenic diabetes insipidus: wild-type aquaporin-2 rescues the apical membrane expression of intracellularly retained AQP2-P262L. *Hum Mol Genet* 13:3045–3056
- de Seigneux S, Nielsen J, Olesen ET et al (2007) Long-term aldosterone treatment induces decreased apical but increased basolateral expression of AQP2 in CCD of rat kidney. *Am J Physiol Renal Physiol* 293:F87–F99
- de Sousa RC, Grosso A (1979) Vanadate blocks cyclic AMP-induced stimulation of sodium and water transport in amphibian epithelia. *Nature* 279:803–804
- Deen PM, van Aubel RA, van Lieburg AF et al (1996) Urinary content of aquaporin 1 and 2 in nephrogenic diabetes insipidus. *J Am Soc Nephrol* 7:836–841
- Deen PM, Verdijk MA, Knoers NV et al (1994a) Requirement of human renal water channel aquaporin-2 for vasopressin-dependent concentration of urine. *Science* 264:92–95
- Deen PM, Weghuis DO, Sinke RJ et al (1994b) Assignment of the human gene for the water channel of renal collecting duct Aquaporin 2 (AQP2) to chromosome 12 region q12→q13. *Cytogenet Cell Genet* 66:260–262
- DiBona DR (1983) Cytoplasmic involvement in ADH-mediated osmosis across toad urinary bladder. *Am J Physiol* 245:C297–C307
- DiGiovanni SR, Nielsen S, Christensen EI et al (1994) Regulation of collecting duct water channel expression by vasopressin in Brattleboro rat. *Proc Natl Acad Sci USA* 91:8984–8988
- Ding GH, Franki N, Condeelis J et al (1991) Vasopressin depolymerizes F-actin in toad bladder epithelial cells. *Am J Physiol* 260:C9–C16
- Ecelbarger CA, Chou CL, Lee AJ et al (1998) Escape from vasopressin-induced antidiuresis: role of vasopressin resistance of the collecting duct. *Am J Physiol* 274:F1161–F1166
- Ecelbarger CA, Nielsen S, Olson BR et al (1997) Role of renal aquaporins in escape from vasopressin-induced antidiuresis in rat. *J Clin Invest* 99:1852–1863
- Ecelbarger CA, Terris J, Frindt G et al (1995) Aquaporin-3 water channel localization and regulation in rat kidney. *Am J Physiol* 269:F663–F672
- Echevarria M, Windhager EE, Tate SS et al (1994) Cloning and expression of AQP3, a water channel from the medullary collecting duct of rat kidney. *Proc Natl Acad Sci USA* 91:10997–11001
- Elkjaer ML, Kwon TH, Wang W et al (2002) Altered expression of renal NHE3, TSC, BSC-1, and ENaC subunits in potassium-depleted rats. *Am J Physiol Renal Physiol* 283:F1376–F1388
- Elkjaer ML, Nejsum LN, Gresz V et al (2001) Immunolocalization of aquaporin-8 in rat kidney, gastrointestinal tract, testis, and airways. *Am J Physiol Renal Physiol* 281:F1047–F1057
- Fenton RA, Brond L, Nielsen S et al (2007) Cellular and subcellular distribution of the type-2 vasopressin receptor in the kidney. *Am J Physiol Renal Physiol* 293:F748–F760
- Fenton RA, Moeller HB (2008) Recent discoveries in vasopressin-regulated aquaporin-2 trafficking. *Prog Brain Res* 170:571–579
- Fenton RA, Moeller HB, Hoffer JD et al (2008) Acute regulation of aquaporin-2 phosphorylation at Ser-264 by vasopressin. *Proc Natl Acad Sci USA* 105:3134–3139
- Fernandez-Llama P, Andrews P, Ecelbarger CA et al (1998a) Concentrating defect in experimental nephrotic syndrome: altered expression of aquaporins and thick ascending limb Na⁺ transporters. *Kidney Int* 54:170–179
- Fernandez-Llama P, Andrews P, Nielsen S et al (1998b) Impaired aquaporin and urea transporter expression in rats with adriamycin-induced nephrotic syndrome. *Kidney Int* 53:1244–1253

- Fernandez-Llama P, Andrews P, Turner R et al (1999a) Decreased abundance of collecting duct aquaporins in post-ischemic renal failure in rats. *J Am Soc Nephrol* 10:1658–1668
- Fernandez-Llama P, Jimenez W, Bosch-Marce M et al (2000) Dysregulation of renal aquaporins and Na–Cl cotransporter in CCl₄-induced cirrhosis. *Kidney Int* 58:216–228
- Fernandez-Llama P, Turner R, Dibona G et al (1999b) Renal expression of aquaporins in liver cirrhosis induced by chronic common bile duct ligation in rats. *J Am Soc Nephrol* 10:1950–1957
- Flear CT, Gill GV, Burn J (1981) Hyponatraemia: mechanisms and management. *Lancet* 2:26–31
- Foster LJ, Yeung B, Mohtashami M et al (1998) Binary interactions of the SNARE proteins syntaxin-4, SNAP23, and VAMP-2 and their regulation by phosphorylation. *Biochemistry* 37:11089–11096
- Franki N, Macaluso F, Schubert W et al (1995) Water channel-carrying vesicles in the rat IMCD contain cellubrevin. *Am J Physiol* 269:C797–C801
- Frigeri A, Gropper MA, Turck CW et al (1995) Immunolocalization of the mercurial-insensitive water channel and glycerol intrinsic protein in epithelial cell plasma membranes. *Proc Natl Acad Sci USA* 92:4328–4331
- Frokiær J, Christensen BM, Marples D et al (1997) Downregulation of aquaporin-2 parallels changes in renal water excretion in unilateral ureteral obstruction. *Am J Physiol* 273:F213–F223
- Frokiær J, Marples D, Knepper MA et al (1996) Bilateral ureteral obstruction downregulates expression of vasopressin-sensitive AQP-2 water channel in rat kidney. *Am J Physiol* 270:F657–F668
- Frokiær J, Marples D, Valtin H et al (1999) Low aquaporin-2 levels in polyuric DI +/+ severe mice with constitutively high cAMP-phosphodiesterase activity. *Am J Physiol* 276:F179–F190
- Fujita N, Ishikawa SE, Sasaki S et al (1995) Role of water channel AQP-CD in water retention in SIADH and cirrhotic rats. *Am J Physiol* 269:F926–F931
- Fujiwara TM, Bichet DG (2005) Molecular biology of hereditary diabetes insipidus. *J Am Soc Nephrol* 16:2836–2846
- Fushimi K, Sasaki S, Marumo F (1997) Phosphorylation of serine 256 is required for cAMP-dependent regulatory exocytosis of the aquaporin-2 water channel. *J Biol Chem* 272:14800–14804
- Fushimi K, Uchida S, Hara Y et al (1993) Cloning and expression of apical membrane water channel of rat kidney collecting tubule. *Nature* 361:549–552
- Gheorghiadu M, Niazi I, Ouyang J et al (2003) Vasopressin V₂-receptor blockade with tolvaptan in patients with chronic heart failure: results from a double-blind, randomized trial. *Circulation* 107:2690–2696
- Gines P, Berl T, Bernardi M et al (1998) Hyponatremia in cirrhosis: from pathogenesis to treatment. *Hepatology* 28:851–864
- Gong H, Wang W, Kwon TH et al (2003) Reduced renal expression of AQP2, p-AQP2 and AQP3 in haemorrhagic shock-induced acute renal failure. *Nephrol Dial Transplant* 18:2551–2559
- Gong H, Wang W, Kwon TH et al (2004) EPO and alpha-MSH prevent ischemia/reperfusion-induced down-regulation of AQPs and sodium transporters in rat kidney. *Kidney Int* 66:683–695
- Gresz V, Kwon TH, Hurley PT et al (2001) Identification and localization of aquaporin water channels in human salivary glands. *Am J Physiol Gastrointest Liver Physiol* 281:G247–G254
- Hanley MJ (1980) Isolated nephron segments in a rabbit model of ischemic acute renal failure. *Am J Physiol* 239:F17–F23
- Harris HW, Jr., Zeidel ML, Jo I et al (1994) Characterization of purified endosomes containing the antidiuretic hormone-sensitive water channel from rat renal papilla. *J Biol Chem* 269:11993–12000
- Hasegawa H, Lian SC, Finkbeiner WE et al (1994a) Extrarenal tissue distribution of CHIP28 water channels by in situ hybridization and antibody staining. *Am J Physiol* 266:C893–C903
- Hasegawa H, Ma T, Skach W et al (1994b) Molecular cloning of a mercurial-insensitive water channel expressed in selected water-transporting tissues. *J Biol Chem* 269:5497–5500
- Hayashi M, Sasaki S, Tsuganezawa H et al (1994) Expression and distribution of aquaporin of collecting duct are regulated by vasopressin V₂ receptor in rat kidney. *J Clin Invest* 94:1778–1783

- Hazama A, Kozono D, Guggino WB et al (2002) Ion permeation of AQP6 water channel protein. Single channel recordings after Hg²⁺ activation. *J Biol Chem* 277:29224–29230
- Henderson IW, McKeever A, Kenyon CJ (1979) Captopril (SQ 14225) depresses drinking and aldosterone in rats lacking vasopressin. *Nature* 281:569–570
- Henn V, Edemir B, Stefan E et al (2004) Identification of a novel A-kinase anchoring protein 18 isoform and evidence for its role in the vasopressin-induced aquaporin-2 shuttle in renal principal cells. *J Biol Chem* 279:26654–26665
- Hober C, Vantghem MC, Racadot A et al (1992) Normal hemodynamic and coagulation responses to 1-deamino-8-D-arginine vasopressin in a case of lithium-induced nephrogenic diabetes insipidus. Results of treatment by a prostaglandin synthesis inhibitor (indomethacin). *Horm Res* 37:190–195
- Hoffert JD, Nielsen J, Yu MJ et al (2007) Dynamics of aquaporin-2 serine-261 phosphorylation in response to short-term vasopressin treatment in collecting duct. *Am J Physiol Renal Physiol* 292:F691–F700
- Hoffert JD, Pisitkun T, Wang G et al (2006) Quantitative phosphoproteomics of vasopressin-sensitive renal cells: regulation of aquaporin-2 phosphorylation at two sites. *Proc Natl Acad Sci USA* 103:7159–7164
- Hozawa S, Holtzman EJ, Ausiello DA (1996) cAMP motifs regulating transcription in the aquaporin 2 gene. *Am J Physiol* 270:C1695–C1702
- Ikeda M, Beitz E, Kozono D et al (2002) Characterization of aquaporin-6 as a nitrate channel in mammalian cells. Requirement of pore-lining residue threonine 63. *J Biol Chem* 277:39873–39879
- Inoue T, Nielsen S, Mandon B et al (1998) SNAP-23 in rat kidney: colocalization with aquaporin-2 in collecting duct vesicles. *Am J Physiol* 275:F752–F760
- Ishibashi K, Imai M, Sasaki S (2000) Cellular localization of aquaporin 7 in the rat kidney. *Exp Nephrol* 8:252–257
- Ishibashi K, Kuwahara M, Gu Y et al (1997a) Cloning and functional expression of a new water channel abundantly expressed in the testis permeable to water, glycerol, and urea. *J Biol Chem* 272:20782–20786
- Ishibashi K, Sasaki S, Fushimi K et al (1994) Molecular cloning and expression of a member of the aquaporin family with permeability to glycerol and urea in addition to water expressed at the basolateral membrane of kidney collecting duct cells. *Proc Natl Acad Sci USA* 91:6269–6273
- Ishibashi K, Sasaki S, Fushimi K et al (1997b) Immunolocalization and effect of dehydration on AQP3, a basolateral water channel of kidney collecting ducts. *Am J Physiol* 272:F235–F241
- Jensen AM, Li C, Praetorius HA et al (2006) Angiotensin II mediates downregulation of aquaporin water channels and key renal sodium transporters in response to urinary tract obstruction. *Am J Physiol Renal Physiol* 291:F1021–F1032
- Jonassen TE, Nielsen S, Christensen S et al (1998) Decreased vasopressin-mediated renal water reabsorption in rats with compensated liver cirrhosis. *Am J Physiol* 275:F216–F225
- Jonassen TE, Promeneur D, Christensen S et al (2000) Decreased vasopressin-mediated renal water reabsorption in rats with chronic aldosterone-receptor blockade. *Am J Physiol Renal Physiol* 278:F246–F256
- Kachadorian WA, Ellis SJ, Muller J (1979) Possible roles for microtubules and microfilaments in ADH action on toad urinary bladder. *Am J Physiol* 236:F14–F20
- Kachadorian WA, Levine SD, Wade JB et al (1977) Relationship of aggregated intramembranous particles to water permeability in vasopressin-treated toad urinary bladder. *J Clin Invest* 59:576–581
- Kachadorian WA, Wade JB, DiScala VA (1975) Vasopressin: induced structural change in toad bladder luminal membrane. *Science* 190:67–69
- Kamsteeg EJ, Bichet DG, Konings IB et al (2003) Reversed polarized delivery of an aquaporin-2 mutant causes dominant nephrogenic diabetes insipidus. *J Cell Biol* 163:1099–1109
- Kamsteeg EJ, Heijnen I, van Os CH et al (2000) The subcellular localization of an aquaporin-2 tetramer depends on the stoichiometry of phosphorylated and nonphosphorylated monomers. *J Cell Biol* 151:919–930

- Kamsteeg EJ, Hendriks G, Boone M et al (2006) Short-chain ubiquitination mediates the regulated endocytosis of the aquaporin-2 water channel. *Proc Natl Acad Sci USA* 103:18344–18349
- Kanno K, Sasaki S, Hirata Y et al (1995) Urinary excretion of aquaporin-2 in patients with diabetes insipidus. *N Engl J Med* 332:1540–1545
- Katsura T, Ausiello DA, Brown D (1996) Direct demonstration of aquaporin-2 water channel recycling in stably transfected LLC-PK1 epithelial cells. *Am J Physiol* 270:F548–F553
- Katsura T, Gustafson CE, Ausiello DA et al (1997) Protein kinase A phosphorylation is involved in regulated exocytosis of aquaporin-2 in transfected LLC-PK1 cells. *Am J Physiol* 272:F817–F822
- Kim GH, Ecelbarger CA, Mitchell C et al (1999) Vasopressin increases Na–K–2Cl cotransporter expression in thick ascending limb of Henle's loop. *Am J Physiol* 276:F96–F103
- Kim GH, Lee JW, Oh YK et al (2004a) Antidiuretic effect of hydrochlorothiazide in lithium-induced nephrogenic diabetes insipidus is associated with upregulation of aquaporin-2, Na–Cl co-transporter, and epithelial sodium channel. *J Am Soc Nephrol* 15:2836–2843
- Kim SW, Schou UK, Peters CD et al (2005) Increased apical targeting of renal epithelial sodium channel subunits and decreased expression of type 2 11beta-hydroxysteroid dehydrogenase in rats with CCl4-induced decompensated liver cirrhosis. *J Am Soc Nephrol* 16:3196–3210
- Kim SW, Wang W, Nielsen J et al (2004b) Increased expression and apical targeting of renal ENaC subunits in puromycin aminonucleoside-induced nephrotic syndrome in rats. *Am J Physiol Renal Physiol* 286:F922–F935
- Kim YH, Kwon TH, Christensen BM et al (2003) Altered expression of renal acid-base transporters in rats with lithium-induced NDI. *Am J Physiol Renal Physiol* 285:F1244–F1257
- Kishore BK, Wade JB, Schorr K et al (1998) Expression of synaptotagmin VIII in rat kidney. *Am J Physiol* 275:F131–F142
- Klein PS, Melton DA (1996) A molecular mechanism for the effect of lithium on development. *Proc Natl Acad Sci USA* 93:8455–8459
- Klussmann E, Maric K, Wiesner B et al (1999) Protein kinase A anchoring proteins are required for vasopressin-mediated translocation of aquaporin-2 into cell membranes of renal principal cells. *J Biol Chem* 274:4934–4938
- Knepper M, Burg M (1983) Organization of nephron function. *Am J Physiol* 244:F579–F589
- Knepper MA, Nielsen S, Chou CL et al (1994) Mechanism of vasopressin action in the renal collecting duct. *Semin Nephrol* 14:302–321
- Kotnik P, Nielsen J, Kwon TH et al (2005) Altered expression of COX-1, COX-2, and mPGES in rats with nephrogenic and central diabetes insipidus. *Am J Physiol Renal Physiol* 288:F1053–F1068
- Kuriyama H, Kawamoto S, Ishida N et al (1997) Molecular cloning and expression of a novel human aquaporin from adipose tissue with glycerol permeability. *Biochem Biophys Res Commun* 241:53–58
- Kuwahara M, Fushimi K, Terada Y et al (1995) cAMP-dependent phosphorylation stimulates water permeability of aquaporin-collecting duct water channel protein expressed in *Xenopus* oocytes. *J Biol Chem* 270:10384–10387
- Kuwahara M, Iwai K, Oeda T et al (2001) Three families with autosomal dominant nephrogenic diabetes insipidus caused by aquaporin-2 mutations in the C-terminus. *Am J Hum Genet* 69:738–748
- Kuwahara M, Verkman AS (1989) Pre-steady-state analysis of the turn-on and turn-off of water permeability in the kidney collecting tubule. *J Membr Biol* 110:57–65
- Kwon TH, Frokiaer J, Fernandez-Llama P et al (1999a) Reduced abundance of aquaporins in rats with bilateral ischemia-induced acute renal failure: prevention by alpha-MSH. *Am J Physiol* 277:F413–F427
- Kwon TH, Frokiaer J, Fernandez-Llama P et al (1999b) Altered expression of Na transporters NHE-3, NaPi-II, Na-K-ATPase, BSC-1, and TSC in CRF rat kidneys. *Am J Physiol* F257–F270
- Kwon TH, Frokiaer J, Knepper MA et al (1998) Reduced AQP1, -2, and -3 levels in kidneys of rats with CRF induced by surgical reduction in renal mass. *Am J Physiol* 275:F724–F741
- Kwon TH, Hager H, Nejsum LN et al (2001) Physiology and pathophysiology of renal aquaporins. *Semin Nephrol* 21:231–238

- Kwon TH, Laursen UH, Marples D et al (2000) Altered expression of renal AQP2 and Na⁺ transporters in rats with lithium-induced NDI. *Am J Physiol Renal Physiol* 279:F552–F564
- Kwon TH, Nielsen J, Knepper MA et al (2005) Angiotensin II AT1 receptor blockade decreases vasopressin-induced water reabsorption and AQP2 levels in NaCl-restricted rats. *Am J Physiol Renal Physiol* 288:F673–F684
- Kwon TH, Nielsen J, Masilamani S et al (2002) Regulation of collecting duct AQP3 expression: response to mineralocorticoid. *Am J Physiol Renal Physiol* 283:F1403–F1421
- Lai KN, Li FK, Lan HY et al (2001) Expression of aquaporin-1 in human peritoneal mesothelial cells and its upregulation by glucose in vitro. *J Am Soc Nephrol* 12:1036–1045
- Lande MB, Jo I, Zeidel ML et al (1996) Phosphorylation of aquaporin-2 does not alter the membrane water permeability of rat papillary water channel-containing vesicles. *J Biol Chem* 271:5552–5557
- Lankford SP, Chou CL, Terada Y et al (1991) Regulation of collecting duct water permeability independent of cAMP-mediated AVP response. *Am J Physiol* 261:F554–F566
- Laursen UH, Pihakaski-Maunsbach K, Kwon TH et al (2004) Changes of rat kidney AQP2 and Na,K-ATPase mRNA expression in lithium-induced nephrogenic diabetes insipidus. *Nephron Exp Nephrol* 97:e1–e16
- Lee YJ, Song IK, Jang KJ et al (2007) Increased AQP2 targeting in primary cultured IMCD cells in response to angiotensin II through AT1 receptor. *Am J Physiol Renal Physiol* 292:F340–F350
- Levy M, Wexler MJ (1987) Hepatic denervation alters first-phase urinary sodium excretion in dogs with cirrhosis. *Am J Physiol* 253:F664–F671
- Li C, Wang W, Kwon TH et al (2001) Downregulation of AQP1, -2, and -3 after ureteral obstruction is associated with a long-term urine-concentrating defect. *Am J Physiol Renal Physiol* 281:F163–F171
- Li C, Wang W, Kwon TH et al (2003) Altered expression of major renal Na transporters in rats with bilateral ureteral obstruction and release of obstruction. *Am J Physiol Renal Physiol* 285:F889–F901
- Li Y, Shaw S, Kamsteeg EJ et al (2006) Development of lithium-induced nephrogenic diabetes insipidus is dissociated from adenylyl cyclase activity. *J Am Soc Nephrol* 17:1063–1072
- Liebhoff U, Rosenthal W (1995) Identification of Rab3-, Rab5a- and synaptobrevin II-like proteins in a preparation of rat kidney vesicles containing the vasopressin-regulated water channel. *FEBS Lett* 365:209–213
- Liu K, Kozono D, Kato Y et al (2005) Conversion of aquaporin 6 from an anion channel to a water-selective channel by a single amino acid substitution. *Proc Natl Acad Sci USA* 102:2192–2197
- Loonen AJ, Knoers NV, van Os CH et al (2008) Aquaporin 2 mutations in nephrogenic diabetes insipidus. *Semin Nephrol* 28:252–265
- Lorenz D, Krylov A, Hahm D et al (2003) Cyclic AMP is sufficient for triggering the exocytic recruitment of aquaporin-2 in renal epithelial cells. *EMBO Rep* 4:88–93
- Lu H, Sun TX, Bouley R et al (2004) Inhibition of endocytosis causes phosphorylation (S256)-independent plasma membrane accumulation of AQP2. *Am J Physiol Renal Physiol* 286:F233–F243
- Lu HA, Sun TX, Matsuzaki T et al (2007) Heat shock protein 70 interacts with aquaporin-2 and regulates its trafficking. *J Biol Chem* 282:28721–28732
- Ma T, Frigeri A, Hasegawa H et al (1994) Cloning of a water channel homolog expressed in brain meningeal cells and kidney collecting duct that functions as a stilbene-sensitive glycerol transporter. *J Biol Chem* 269:21845–21849
- Ma T, Song Y, Yang B et al (2000) Nephrogenic diabetes insipidus in mice lacking aquaporin-3 water channels. *Proc Natl Acad Sci USA* 97:4386–4391
- Ma T, Yang B, Gillespie A et al (1997) Generation and phenotype of a transgenic knockout mouse lacking the mercurial-insensitive water channel aquaporin-4. *J Clin Invest* 100:957–962
- Ma T, Yang B, Gillespie A et al (1998) Severely impaired urinary concentrating ability in transgenic mice lacking aquaporin-1 water channels. *J Biol Chem* 273:4296–4299

- Mandon B, Chou CL, Nielsen S et al (1996) Syntaxin-4 is localized to the apical plasma membrane of rat renal collecting duct cells: possible role in aquaporin-2 trafficking. *J Clin Invest* 98:906–913
- Mandon B, Nielsen S, Kishore BK et al (1997) Expression of syntaxins in rat kidney. *Am J Physiol* 273:F718–F730
- Marples D, Barber B, Taylor A (1996a) Effect of a dynein inhibitor on vasopressin action in toad urinary bladder. *J Physiol* 490 (Part 3):767–774
- Marples D, Christensen S, Christensen EI et al (1995a) Lithium-induced downregulation of aquaporin-2 water channel expression in rat kidney medulla. *J Clin Invest* 95:1838–1845
- Marples D, Frokiaer J, Dorup J et al (1996b) Hypokalemia-induced downregulation of aquaporin-2 water channel expression in rat kidney medulla and cortex. *J Clin Invest* 97:1960–1968
- Marples D, Knepper MA, Christensen EI et al (1995b) Redistribution of aquaporin-2 water channels induced by vasopressin in rat kidney inner medullary collecting duct. *Am J Physiol* 269:C655–C664
- Marples D, Schroer TA, Ahrens N et al (1998) Dynein and dynactin colocalize with AQP2 water channels in intracellular vesicles from kidney collecting duct. *Am J Physiol* 274:F384–F394
- Marr N, Bichet DG, Lonergan M et al (2002) Heterooligomerization of an aquaporin-2 mutant with wild-type aquaporin-2 and their misrouting to late endosomes/lysosomes explains dominant nephrogenic diabetes insipidus. *Hum Mol Genet* 11:779–789
- Martin PY, Abraham WT, Lieming X et al (1999) Selective V2-receptor vasopressin antagonism decreases urinary aquaporin-2 excretion in patients with chronic heart failure. *J Am Soc Nephrol* 10:2165–2170
- Matsumura Y, Uchida S, Rai T et al (1997) Transcriptional regulation of aquaporin-2 water channel gene by cAMP. *J Am Soc Nephrol* 8:861–867
- McDill BW, Li SZ, Kovach PA et al (2006) Congenital progressive hydronephrosis (cph) is caused by an S256L mutation in aquaporin-2 that affects its phosphorylation and apical membrane accumulation. *Proc Natl Acad Sci USA* 103:6952–6957
- Morishita Y, Matsuzaki T, Hara-chikuma M et al (2005) Disruption of aquaporin-11 produces polycystic kidneys following vacuolization of the proximal tubule. *Mol Cell Biol* 25:7770–7779
- Mouillac B, Chini B, Balestre MN et al (1995) The binding site of neuropeptide vasopressin V1a receptor. Evidence for a major localization within transmembrane regions. *J Biol Chem* 270:25771–25777
- Mulders SM, Bichet DG, Rijss JP et al (1998) An aquaporin-2 water channel mutant which causes autosomal dominant nephrogenic diabetes insipidus is retained in the Golgi complex. *J Clin Invest* 102:57–66
- Muller J, Kachadorian WA (1984) Aggregate-carrying membranes during ADH stimulation and washout in toad bladder. *Am J Physiol* 247:C90–C98
- Murer L, Addabbo F, Carmosino M et al (2004) Selective decrease in urinary aquaporin 2 and increase in prostaglandin E2 excretion is associated with postobstructive polyuria in human congenital hydronephrosis. *J Am Soc Nephrol* 15:2705–2712
- Murillo-Carretero MI, Ilundain AA, Echevarria M (1999) Regulation of aquaporin mRNA expression in rat kidney by water intake. *J Am Soc Nephrol* 10:696–703
- Nejsum LN, Elkjaer M, Hager H et al (2000) Localization of aquaporin-7 in rat and mouse kidney using RT-PCR, immunoblotting, and immunocytochemistry. *Biochem Biophys Res Commun* 277:164–170
- Nejsum LN, Zelenina M, Aperia A et al (2005) Bidirectional regulation of AQP2 trafficking and recycling: involvement of AQP2-S256 phosphorylation. *Am J Physiol Renal Physiol* 288:F930–F938
- Nielsen J, Hoffert JD, Knepper MA et al (2008a) Proteomic analysis of lithium-induced nephrogenic diabetes insipidus: mechanisms for aquaporin 2 down-regulation and cellular proliferation. *Proc Natl Acad Sci USA* 105:3634–3639
- Nielsen J, Kwon TH, Christensen BM et al (2008b) Dysregulation of renal aquaporins and epithelial sodium channel in lithium-induced nephrogenic diabetes insipidus. *Semin Nephrol* 28:227–244

- Nielsen J, Kwon TH, Praetorius J et al (2006) Aldosterone increases urine production and decreases apical AQP2 expression in rats with diabetes insipidus. *Am J Physiol Renal Physiol* 290:F438–F449
- Nielsen J, Kwon TH, Praetorius J et al (2003) Segment-specific ENaC downregulation in kidney of rats with lithium-induced NDI. *Am J Physiol Renal Physiol* 285:F1198–F1209
- Nielsen S, Chou CL, Marples D et al (1995a) Vasopressin increases water permeability of kidney collecting duct by inducing translocation of aquaporin-CD water channels to plasma membrane. *Proc Natl Acad Sci USA* 92:1013–1017
- Nielsen S, DiGiovanni SR, Christensen EI et al (1993a) Cellular and subcellular immunolocalization of vasopressin-regulated water channel in rat kidney. *Proc Natl Acad Sci USA* 90:11663–11667
- Nielsen S, Frokiaer J, Marples D et al (2002) Aquaporins in the kidney: from molecules to medicine. *Physiol Rev* 82:205–244
- Nielsen S, Kwon TH, Christensen BM et al (1999) Physiology and pathophysiology of renal aquaporins. *J Am Soc Nephrol* 10:647–663
- Nielsen S, Kwon TH, Frokiaer J et al (2007) Regulation and dysregulation of aquaporins in water balance disorders. *J Intern Med* 261:53–64
- Nielsen S, Kwon TH, Dimke H et al (2008c) Aquaporin water channels in mammalian kidney. In: Alpern RJ, Hebert SC (ed) *The kidney*, 4th edn. Elsevier, San Diego
- Nielsen S, Kwon TH, Frokiaer J et al (2000) Key roles of renal aquaporins in water balance and water-balance disorders. *News Physiol Sci* 15:136–143
- Nielsen S, Marples D, Birn H et al (1995b) Expression of VAMP-2-like protein in kidney collecting duct intracellular vesicles. Colocalization with aquaporin-2 water channels. *J Clin Invest* 96:1834–1844
- Nielsen S, Pallone T, Smith BL et al (1995c) Aquaporin-1 water channels in short and long loop descending thin limbs and in descending vasa recta in rat kidney. *Am J Physiol* 268:F1023–F1037
- Nielsen S, Smith BL, Christensen EI et al (1993b) Distribution of the aquaporin CHIP in secretory and resorptive epithelia and capillary endothelia. *Proc Natl Acad Sci USA* 90:7275–7279
- Nielsen S, Smith BL, Christensen EI et al (1993c) CHIP28 water channels are localized in constitutively water-permeable segments of the nephron. *J Cell Biol* 120:371–383
- Nielsen S, Terris J, Andersen D et al (1997) Congestive heart failure in rats is associated with increased expression and targeting of aquaporin-2 water channel in collecting duct. *Proc Natl Acad Sci USA* 94:5450–5455
- Norregaard R, Jensen BL, Li C et al (2005) COX-2 inhibition prevents downregulation of key renal water and sodium transport proteins in response to bilateral ureteral obstruction. *Am J Physiol Renal Physiol* 289: F322–F333
- Norregaard R, Jensen BL, Topcu SO et al (2006) Cyclooxygenase type 2 is increased in obstructed rat and human ureter and contributes to pelvic pressure increase after obstruction. *Kidney Int* 70:872–881
- Novak A, Dedhar S (1999) Signaling through beta-catenin and Lef/Tcf. *Cell Mol Life Sci* 56:523–537
- Pallone TL, Turner MR, Edwards A et al (2003) Countercurrent exchange in the renal medulla. *Am J Physiol Regul Integr Comp Physiol* 284:R1153–R1175
- Pearl M, Taylor A (1983) Actin filaments and vasopressin-stimulated water flow in toad urinary bladder. *Am J Physiol* 245:C28–C39
- Pevsner J, Hsu SC, Braun JE et al (1994) Specificity and regulation of a synaptic vesicle docking complex. *Neuron* 13:353–361
- Phillips ME, Taylor A (1989) Effect of nocodazole on the water permeability response to vasopressin in rabbit collecting tubules perfused in vitro. *J Physiol* 411:529–544
- Phillips ME, Taylor A (1992) Effect of colcemid on the water permeability response to vasopressin in isolated perfused rabbit collecting tubules. *J Physiol* 456:591–608
- Pisitkun T, Shen RF, Knepper MA (2004) Identification and proteomic profiling of exosomes in human urine. *Proc Natl Acad Sci USA* 101:13368–13373

- Preston GM, Agre P (1991) Isolation of the cDNA for erythrocyte integral membrane protein of 28 kilodaltons: member of an ancient channel family. *Proc Natl Acad Sci USA* 88:11110–11114
- Preston GM, Carroll TP, Guggino WB et al (1992) Appearance of water channels in *Xenopus* oocytes expressing red cell CHIP28 protein. *Science* 256:385–387
- Procino G, Carmosino M, Marin O et al (2003) Ser-256 phosphorylation dynamics of aquaporin 2 during maturation from the ER to the vesicular compartment in renal cells. *FASEB J* 17:1886–1888
- Procino G, Carmosino M, Tamma G et al (2004) Extracellular calcium antagonizes forskolin-induced aquaporin 2 trafficking in collecting duct cells. *Kidney Int* 66:2245–2255
- Promeneur D, Kwon TH, Frokiaer J et al (2000) Vasopressin V(2)-receptor-dependent regulation of AQP2 expression in Brattleboro rats. *Am J Physiol Renal Physiol* 279:F370–F382
- Puliyanda DP, Ward DT, Baum MA et al (2003) Calpain-mediated AQP2 proteolysis in inner medullary collecting duct. *Biochem Biophys Res Commun* 303:52–58
- Radomski JL, Fuyathn, Nelson AA et al (1950) The toxic effects, excretion and distribution of lithium chloride. *J Pharmacol Exp Ther* 100:429–444
- Rao R, Zhang MZ, Zhao M et al (2005) Lithium treatment inhibits renal GSK-3 activity and promotes cyclooxygenase 2-dependent polyuria. *Am J Physiol Renal Physiol* 288:F642–F649
- Riccardi D, Hall AE, Chattopadhyay N et al (1998) Localization of the extracellular Ca²⁺/polyvalent cation-sensing protein in rat kidney. *Am J Physiol* 274:F611–F622
- Riccardi D, Lee WS, Lee K et al (1996) Localization of the extracellular Ca(2+)-sensing receptor and PTH/PTHrP receptor in rat kidney. *Am J Physiol* 271:F951–F956
- Risinger C, Bennett MK (1999) Differential phosphorylation of syntaxin and synaptosome-associated protein of 25 kDa (SNAP-25) isoforms. *J Neurochem* 72:614–624
- Rojek A, Fuchtbauer EM, Kwon TH et al (2006) Severe urinary concentrating defect in renal collecting duct-selective AQP2 conditional-knockout mice. *Proc Natl Acad Sci USA* 103:6037–6042
- Rojek A, Praetorius J, Frokiaer J et al (2008) A current view of the mammalian aquaglyceroporins. *Annu Rev Physiol* 70:301–327
- Russo LM, McKee M, Brown D (2006) Methyl-beta-cyclodextrin induces vasopressin-independent apical accumulation of aquaporin-2 in the isolated, perfused rat kidney. *Am J Physiol Renal Physiol* 291:F246–F253
- Sabolic I, Katsura T, Verbavatz JM et al (1995) The AQP2 water channel: effect of vasopressin treatment, microtubule disruption, and distribution in neonatal rats. *J Membr Biol* 143:165–175
- Sabolic I, Valenti G, Verbavatz JM et al (1992) Localization of the CHIP28 water channel in rat kidney. *Am J Physiol* 263:C1225–C1233
- Saito T, Ishikawa SE, Sasaki S et al (1997) Alteration in water channel AQP-2 by removal of AVP stimulation in collecting duct cells of dehydrated rats. *Am J Physiology* 272:F183–F191
- Sasaki S, Fushimi K, Saito H et al (1994) Cloning, characterization, and chromosomal mapping of human aquaporin of collecting duct. *J Clin Invest* 93:1250–1256
- Schermann J, Chou CL, Ma T et al (1998) Defective proximal tubular fluid reabsorption in transgenic aquaporin-1 null mice. *Proc Natl Acad Sci USA* 95:9660–9664
- Schrier RW (2008) Vasopressin and aquaporin 2 in clinical disorders of water homeostasis. *Semin Nephrol* 28:289–296
- Seibold A, Brabet P, Rosenthal W et al (1992) Structure and chromosomal localization of the human antidiuretic hormone receptor gene. *Am J Hum Genet* 51:1078–1083
- Sharples EJ, Patel N, Brown P et al (2004) Erythropoietin protects the kidney against the injury and dysfunction caused by ischemia-reperfusion. *J Am Soc Nephrol* 15:2115–2124
- Shaw S, Marples D (2005) N-ethylmaleimide causes aquaporin-2 trafficking in the renal inner medullary collecting duct by direct activation of protein kinase A. *Am J Physiol Renal Physiol* 288:F832–F839
- Shi Y, Li C, Thomsen K et al (2004a) Neonatal ureteral obstruction alters expression of renal sodium transporters and aquaporin water channels. *Kidney Int* 66:203–215
- Shi Y, Pedersen M, Li C et al (2004b) Early release of neonatal ureteral obstruction preserves renal function. *Am J Physiol Renal Physiol* 286:F1087–F1099

- Shimazaki Y, Nishiki T, Omori A et al (1996) Phosphorylation of 25-kDa synaptosome-associated protein. Possible involvement in protein kinase C-mediated regulation of neurotransmitter release. *J Biol Chem* 271:14548–14553
- Smith BL, Agre P (1991) Erythrocyte Mr 28,000 transmembrane protein exists as a multisubunit oligomer similar to channel proteins. *J Biol Chem* 266:6407–6415
- Sohara E, Rai T, Miyazaki J et al (2005) Defective water and glycerol transport in the proximal tubules of AQP7 knockout mice. *Am J Physiol Renal Physiol* 289:F1195–F1200
- Sollner T, Whiteheart SW, Brunner M et al (1993) SNAP receptors implicated in vesicle targeting and fusion. *Nature* 362:318–324
- Stambolic V, Ruel L, Woodgett JR (1996) Lithium inhibits glycogen synthase kinase-3 activity and mimics wingless signalling in intact cells. *Curr Biol* 6:1664–1668
- Stamer WD, Snyder RW, Smith BL et al (1994) Localization of aquaporin CHIP in the human eye: implications in the pathogenesis of glaucoma and other disorders of ocular fluid balance. *Invest Ophthalmol Vis Sci* 35:3867–3872
- Stamoutos BA, Carpenter RG, Grossman SP (1981) Role of angiotensin-II in the polydipsia of diabetes insipidus in the Brattleboro rat. *Physiol Behav* 26:691–693
- Star RA, Nonoguchi H, Balaban R et al (1988) Calcium and cyclic adenosine monophosphate as second messengers for vasopressin in the rat inner medullary collecting duct. *J Clin Invest* 81:1879–1888
- Stefan E, Wiesner B, Baillie GS et al (2007) Compartmentalization of cAMP-dependent signaling by phosphodiesterase-4D is involved in the regulation of vasopressin-mediated water reabsorption in renal principal cells. *J Am Soc Nephrol* 18:199–212
- Sudhof TC, De CP, Niemann H et al (1993) Membrane fusion machinery: insights from synaptic proteins. *Cell* 75:1–4
- Sugawara M, Hashimoto K, Ota Z (1988) Involvement of prostaglandinE2, cAMP, and vasopressin in lithium-induced polyuria. *Am J Physiol* 254:R863–R869
- Tajika Y, Matsuzaki T, Suzuki T et al (2004) Aquaporin-2 is retrieved to the apical storage compartment via early endosomes and phosphatidylinositol 3-kinase-dependent pathway. *Endocrinology* 145:4375–4383
- Tajika Y, Matsuzaki T, Suzuki T et al (2005) Differential regulation of AQP2 trafficking in endosomes by microtubules and actin filaments. *Histochem Cell Biol* 124:1–12
- Tamma G, Wiesner B, Furkert J et al (2003) The prostaglandin E2 analogue sulprostone antagonizes vasopressin-induced antidiuresis through activation of Rho. *J Cell Sci* 116:3285–3294
- Tannen RL, Regal EM, Dunn MJ et al (1969) Vasopressin-resistant hyposthenuria in advanced chronic renal disease. *N Engl J Med* 280:1135–1141
- Tanner GA, Sloan KL, Sophasan S (1973) Effects of renal artery occlusion on kidney function in the rat. *Kidney Int* 4:377–389
- Teitelbaum I, McGuinness S (1995) Vasopressin resistance in chronic renal failure. Evidence for the role of decreased V2 receptor mRNA. *J Clin Invest* 96:378–385
- Terris J, Ecelbarger CA, Marples D et al (1995) Distribution of aquaporin-4 water channel expression within rat kidney. *Am J Physiol* 269:F775–F785
- Terris J, Ecelbarger CA, Nielsen S et al (1996) Long-term regulation of four renal aquaporins in rats. *Am J Physiol* 271:F414–F422
- Timmer RT, Sands JM (1999) Lithium intoxication. *J Am Soc Nephrol* 10:666–674
- Topcu SO, Pedersen M, Norregaard R et al (2007) Candesartan prevents long-term impairment of renal function in response to neonatal partial unilateral ureteral obstruction. *Am J Physiol Renal Physiol* 292:F736–F748
- Umenishi F, Narikiyo T, Vandewalle A et al (2006) cAMP regulates vasopressin-induced AQP2 expression via protein kinase A-independent pathway. *Biochim Biophys Acta* 1758:1100–1105
- Valenti G, Laera A, Gouraud S et al (2002) Low-calcium diet in hypercalciuric enuretic children restores AQP2 excretion and improves clinical symptoms. *Am J Physiol Renal Physiol* 283:F895–F903
- Valenti G, Laera A, Pace G et al (2000) Urinary aquaporin 2 and calciuria correlate with the severity of enuresis in children. *J Am Soc Nephrol* 11:1873–1881

- Valtin H, Schroeder HA (1964) Familial hypothalamic diabetes insipidus in rats (Brattleboro strain). *Am J Physiol* 206:425–430
- van Balkom BW, Savelkoul PJ, Markovich D et al (2002) The role of putative phosphorylation sites in the targeting and shuttling of the aquaporin-2 water channel. *J Biol Chem* 277:41473–41479
- Van Hoek AN, Ma T, Yang B et al (2000) Aquaporin-4 is expressed in basolateral membranes of proximal tubule S3 segments in mouse kidney. *Am J Physiol Renal Physiol* 278:F310–F316
- Venkatachalam MA, Bernard DB, Donohoe JF et al (1978) Ischemic damage and repair in the rat proximal tubule: differences among the S1, S2, and S3 segments. *Kidney Int* 14:31–49
- Verkman AS (2008) Dissecting the roles of aquaporins in renal pathophysiology using transgenic mice. *Semin Nephrol* 28:217–226
- Wade JB, Kachadorian WA (1988) Cytochalasin B inhibition of toad bladder apical membrane responses to ADH. *Am J Physiol* 255:C526–C530
- Wade JB, Stetson DL, Lewis SA (1981) ADH action: evidence for a membrane shuttle mechanism. *Ann N Y Acad Sci* 372:106–117
- Wall SM, Han JS, Chou CL et al (1992) Kinetics of urea and water permeability activation by vasopressin in rat terminal IMCD. *Am J Physiol* 262:F989–F998
- Wang W, Kwon TH, Li C et al (2002a) Reduced expression of Na-K-2Cl cotransporter in medullary TAL in vitamin D-induced hypercalcemia in rats. *Am J Physiol Renal Physiol* 282:F34–F44
- Wang W, Li C, Kwon TH et al (2002b) AQP3, p-AQP2, and AQP2 expression is reduced in polyuric rats with hypercalcemia: prevention by cAMP-PDE inhibitors. *Am J Physiol Renal Physiol* 283:F1313–F1325
- Wen H, Frokiaer J, Kwon TH et al (1999) Urinary excretion of aquaporin-2 in rat is mediated by a vasopressin-dependent apical pathway. *J Am Soc Nephrol* 10:1416–1429
- Wood LJ, Massie D, McLean AJ et al (1988) Renal sodium retention in cirrhosis: tubular site and relation to hepatic dysfunction. *Hepatology* 8:831–836
- Xu DL, Martin PY, Ohara M et al (1997) Upregulation of aquaporin-2 water channel expression in chronic heart failure rat. *J Clin Invest* 99:1500–1505
- Yamamoto T, Sasaki S, Fushimi K et al (1995) Vasopressin increases AQP-CD water channel in apical membrane of collecting duct cells in Brattleboro rats. *Am J Physiol* 268:C1546–51
- Yasui M, Hazama A, Kwon TH et al (1999a) Rapid gating and anion permeability of an intracellular aquaporin. *Nature* 402:184–187
- Yasui M, Kwon TH, Knepper MA et al (1999b) Aquaporin-6: An intracellular vesicle water channel protein in renal epithelia. *Proc Natl Acad Sci USA* 96:5808–5813
- Yip KP (2002) Coupling of vasopressin-induced intracellular Ca²⁺ mobilization and apical exocytosis in perfused rat kidney collecting duct. *J Physiol* 538:891–899
- Zelenina M, Christensen BM, Palmer J et al (2000) Prostaglandin E(2) interaction with AVP: effects on AQP2 phosphorylation and distribution. *Am J Physiol Renal Physiol* 278:F388–F394
- Zelenina M, Zelenin S, Bondar AA et al (2002) Water permeability of aquaporin-4 is decreased by protein kinase C and dopamine. *Am J Physiol Renal Physiol* 283:F309–F318

Regulation of Aquaporin-2 Trafficking

Pavel I. Nedvetsky, Grazia Tamma, Sven Beulshausen, Giovanna Valenti,
Walter Rosenthal, and Enno Klussmann

Contents

1	Introduction	134
2	AQP2 Trafficking	137
2.1	Role of Phosphorylation in AQP2 Trafficking	137
2.2	Compartmentalization of cAMP Signaling in Renal Principal Cells: A Role for AKAPs and PDEs	139
2.3	The Involvement of Cytoskeletal Elements	141
2.4	Role of Calcium in AQP2 Trafficking	144
3	Regulation of Endocytosis	145
4	Phosphorylation-Independent Translocation of AQP2 to the Plasma Membrane	146
5	Dysfunction of AQP2 Trafficking Causes Nephrogenic Diabetes Insipidus (NDI)	146
6	Concluding Remarks	149
	References	150

Abstract Principal cells lining renal collecting ducts control the fine-tuning of body water homeostasis by regulating water reabsorption through the water channels aquaporin-2 (AQP2), aquaporin-3 (AQP3), and aquaporin-4 (AQP4). While the localization of AQP2 is subject to regulation by arginine-vasopressin (AVP), AQP3 and AQP4 are constitutively expressed in the basolateral plasma membrane. AVP adjusts the amount of AQP2 in the plasma membrane by triggering its redistribution from intracellular vesicles into the plasma membrane. This permits water entry into the cells and water exit through AQP3 and AQP4. The translocation of AQP2 is initiated by an increase in cAMP following V2R activation through AVP. The AVP-induced rise in cAMP activates protein kinase A (PKA), which in turn phosphorylates AQP2, and thereby triggers the redistribution of AQP2. Several proteins participating in the control of cAMP-dependent AQP2 trafficking have been identified; for example, A kinase anchoring proteins (AKAPs) tethering PKA

E. Klussmann (✉)

Leibniz-Institut für Molekulare Pharmakologie, Robert-Rössle-Street 10, Campus Berlin-Buch,
D-13125 Berlin, Germany
klussmann@fmp-berlin.de

to cellular compartments; phosphodiesterases (PDEs) regulating the local cAMP level; cytoskeletal components such as F-actin and microtubules; small GTPases of the Rho family controlling cytoskeletal dynamics; motor proteins transporting AQP2-bearing vesicles to and from the plasma membrane for exocytic insertion and endocytic retrieval; SNAREs inducing membrane fusions, hsc70, a chaperone, important for endocytic retrieval. In addition, cAMP-independent mechanisms of translocation mainly involving the F-actin cytoskeleton have been uncovered. Defects of AQP2 trafficking cause diseases such as nephrogenic diabetes insipidus (NDI), a disorder characterized by a massive loss of hypoosmotic urine.

This review summarizes recent data elucidating molecular mechanisms underlying the trafficking of AQP2. In particular, we focus on proteins involved in the regulation of trafficking, and physiological and pathophysiological stimuli determining the cellular localization of AQP2. The identification of proteins and protein-protein interactions may lead to the development of drugs targeting AQP2 trafficking. Such drugs may be suitable for the treatment of diseases associated with dysregulation of body water homeostasis, including NDI or cardiovascular diseases (e.g., chronic heart failure) where the AVP level is elevated, inducing excessive water retention.

Abbreviations

AKAPA	kinase anchoring protein
AngII	angiotensin II
AQP	aquaporin
AVP	arginine-vasopressin
CaR	calcium sensing receptor
Epac	exchange protein directly activated by cAMP
G-CK	golgi casein kinase
NDI	nephrogenic diabetes insipidus
PDE	phosphodiesterase
PKA	protein kinase A
PGE ₂	Prostaglandin E ₂
PP1 and 2A	protein phosphatases 1 and 2A, respectively

1 Introduction

Human kidneys produce approximately 180 L of primary urine per day by glomerular filtration. Water is reabsorbed as urine passes through the nephron. A rapid flow of water from the lumen of the nephron through the epithelial cells lining it is ensured by water channels called aquaporins (AQPs) (Agre et al. 2002; Agre 2006). At least eight different AQPs are expressed in the kidneys (Nielsen 2002). AQP1, expressed in the proximal tubule and descending thin limb, is responsible for constitutively high water permeability of these tubule segments and therefore for the reabsorption of about 90% of the water. The rest is reabsorbed by the collecting

duct principal cells. Principal cells express three different AQPs: AQP2, AQP3, and AQP4 (Nielsen 2002). The water permeability of the basolateral plasma membrane is constitutively high due to the presence of AQP3 and AQP4 in this membrane compartment. The cellular localization of AQP2, and thus water permeability of the collecting duct, is controlled by arginine vasopressin (AVP). In the absence of AVP, AQP2 resides in intracellular vesicles. Under this condition, the apical plasma membrane of principal cells facing the primary urine contains only low amounts of water channels and consequently possesses low water permeability. Binding of AVP to its cognate V2 receptor (V2R) in the basolateral plasma membrane initiates cAMP signaling, which leads to the translocation of AQP2 from intracellular vesicles into the plasma membrane, mainly the apical plasma membrane (Nielsen et al. 1995). This results in a strong increase of water permeability of this membrane compartment and accelerated reabsorption of water from primary urine. Water exits principal cells *via* AQP3 and AQP4 (Fig. 1).

One of the first models to study the AVP-dependent water transport was the toad urinary bladder, which corresponds functionally to the mammalian collecting duct (Leaf and Hays 1962). Stimulation of this epithelium with AVP increases the water permeability and results in the appearance of intracellular membrane particles on the apical cell surface (Kachadorian et al. 1975). Freeze-fracture electron microscopic studies, first in the amphibian urinary bladder and later in isolated renal collecting ducts, showed that these particles were localized in clathrin-coated pits and might contain AVP-regulated water channels (Kachadorian et al. 1975; Bourguet et al. 1976; Brown and Orci 1983). This hypothesis was confirmed in 1993, shortly after AQP2 was cloned. Fushimi et al. cloned a water channel that, in the kidney, is expressed exclusively in the collecting duct principal cells (Fushimi et al. 1993). Using antiserum raised against this protein, Nielsen and colleagues demonstrated increases of apical membrane labeling after water deprivation (Nielsen et al. 1993).

To investigate the expression and the intracellular trafficking of AQP2, several cell models have been generated, which can be classified into non-mammalian and mammalian systems. The first group includes the heterologous expression of mammalian AQP2 in *Xenopus laevis* oocytes and in yeasts. The second group comprises primary cultures of principal cells isolated from inner medullary collecting duct (IMCD) tubules (Maric et al. 1998), the immortalized mouse collecting duct cell line (mpkCCD) (Duong et al. 1998), and different cell lines stably transfected with cDNA encoding AQP2. The latter include the rabbit collecting duct cells line CD8 (Valenti et al. 1996), Madin–Darby canine kidney cells (MDCK cells) (Deen et al. 1997), a renal epithelial cell line derived from the proximal tubule of porcine kidney (LLC – PK₁) (Katsura et al. 1997), and the mouse collecting duct cell line (MCD4 cells) (Iolascon et al. 2007). While biophysical properties of water channels and their mutants were studied in non-mammalian systems, mammalian cells expressing AQP2 are utilized to investigate the intracellular signals regulating AQP2 trafficking (short-term regulation of AQP2), and its long-term regulation, i.e., its expression.

A fundamental problem handling primary cultured principal cells is the loss of AQP2 gene expression under culture conditions due to rapid repression (Furuno et al. 1996). The reason for that is the AVP-dependence of AQP2 expression.

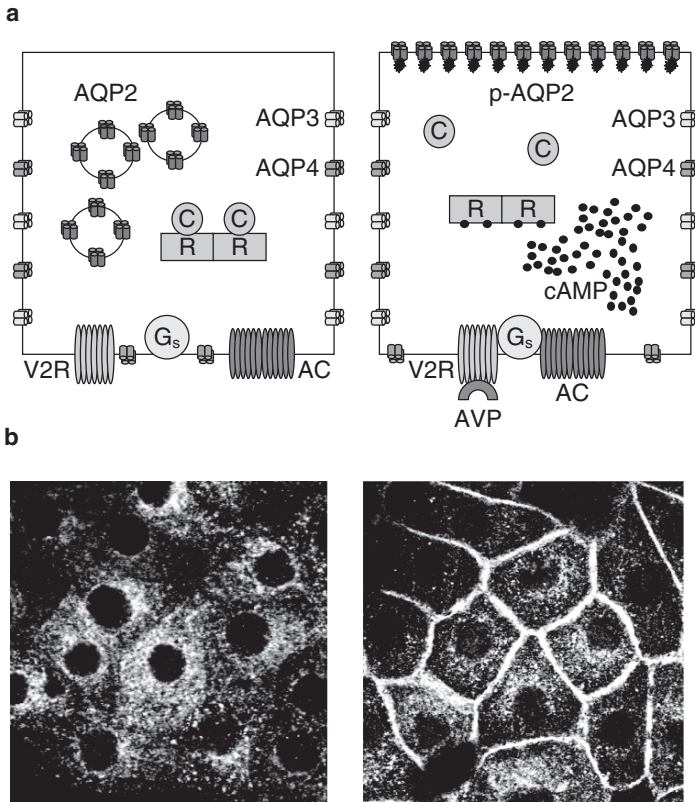


Fig. 1 Arginine vasopressin (AVP)-dependent water reabsorption requires the redistribution of aquaporin-2 (AQP2) from intracellular vesicles into the plasma membrane of renal principal cells. (a) Model of the exocytic insertion of AQP2 into the plasma membrane. Binding of AVP to the vasopressin V2 receptor (V2R) in the basolateral plasma membrane of renal principal cells activates the G_s/adenylyl system, inducing elevation of intracellular cAMP levels. Cyclic AMP, in turn, activates protein kinase A (PKA) by binding to the regulatory (R) subunits. The binding induces a conformational change releasing catalytic (C) subunits from the PKA holoenzyme. They phosphorylate AQP2, and thereby trigger AQP2 redistribution to the plasma membrane and thus allow water reabsorption from primary urine. At least three AQP2 molecules within a tetramer must be phosphorylated for the translocation to occur [147]. (b) Detection of AQP2 in control and AVP-treated primary cultured inner medullary collecting duct (IMCD) cells by immunofluorescence microscopy with a specific anti-AQP2 antiserum. In resting cells, AQP2 resides on intracellular vesicles. The incubation with AVP induces its redistribution to the plasma membrane (Maric et al. 1998; Nedvetsky et al. 2007)

To maintain the endogenous expression of AQP2, primary cultured principal cells from IMCD were constitutively exposed to a cAMP analog, dibutyryl-cAMP (db-cAMP) (Maric et al. 1998). Similarly, in an immortalized mouse collecting duct cell line, mpkCCD_{c14}, AQP2 protein levels and mRNA levels were low under basal conditions, but drastically increased upon prolonged treatment with AVP (Hasler et al. 2002).

2 AQP2 Trafficking

2.1 Role of Phosphorylation in AQP2 Trafficking

AQP2 was the first water channel found to change its subcellular localization in response to different stimuli (for review, see Brown 2003; Klussmann et al. 2000; King et al. 2004). The phosphorylation of AQP2 by cAMP-dependent protein kinase (PKA) on serine 256 (S256) plays a central role in this process (Katsura et al. 1997). The relevance of this phosphorylation site for the regulation of AQP2 trafficking has been demonstrated by mutational analysis. The AQP2–S256A mutant, which cannot be phosphorylated by PKA, does not translocate to the plasma membrane in response to cAMP-elevating agents (Katsura et al. 1997; van Balkom et al. 2002), while the AQP2–S256D mutant, mimicking phosphorylation, constitutively resides in the plasma membrane, independent of the cAMP level (van Balkom et al. 2002). The conclusion from these data is that phosphorylation at S256 is necessary and sufficient to induce trafficking of AQP2 to the plasma membrane (Katsura et al. 1997; van Balkom et al. 2002). However, recent studies indicate that, at least in some models, the phosphorylation of AQP2 is not sufficient to maintain the water channel at the plasma membrane. In MDCK cells expressing AQP2–S256D, its internalization could be induced by treatment of the cells with the PKA inhibitor, H89 (Nejsum et al. 2005). The effect of H89 was mimicked by treatment of the cells with dopamine or PGE₂, both causing internalization of AQP2–S256D (Nejsum et al. 2005). To explain these observations, the authors proposed that PKA-dependent phosphorylation of additional proteins, besides AQP2 itself, is involved in the regulation of AQP2 trafficking.

Valenti and colleagues have demonstrated that phosphorylation of AQP2 by Golgi casein kinase (G-CK) during its passage through the Golgi is necessary for its routing to the vesicular post-Golgi compartment (Procino et al. 2003). The mutants AQP2–E258K and AQP2–S256A are not substrates for G-CK and are directed to lysosomes. The E258K mutation causes a dominant form of nephrogenic diabetes insipidus (NDI) (Procino et al. 2003; Mulders et al. 1998). Thus, phosphorylation of AQP2 at S256 may be required for maturation of the protein and its trafficking from the endoplasmic reticulum (ER) to the Golgi apparatus, and further to the post-Golgi compartment.

Besides PKA and G-CK, several other kinases may phosphorylate AQP2 on S256. For example, cGMP-dependent protein kinase (PKG) phosphorylates AQP2 in vitro (Bouley et al. 2000). Stimuli activating cGMP-dependent protein kinase (PKG) such as nitric oxide donors, natriuretic peptide, or an inhibitor of cGMP-specific phosphodiesterase PDE5, sildenafil, cause a translocation of AQP2 to the plasma membrane in LLC – PK₁ cells (Bouley et al. 2000, 2005). Here, phosphorylation of S256 is the key event, as the AQP2–S256A mutant did not respond to elevation cGMP by redistribution to the plasma membrane (Bouley et al. 2000). It remains to be clarified whether PKG in cells phosphorylates AQP2 directly or whether its effect is mediated by cross-activation of PKA (Bouley et al. 2000).

In addition to the S256 phosphorylation site, human AQP2 contains one consensus site for PKC phosphorylation (S231) and three sites for phosphorylation by CKII (S148, S229, and T244) (van Balkom et al. 2002). Activation of PKC through receptor agonists such as endothelin, prostaglandin E₂, ATP, or muscarinergic agents inhibits AVP-induced increases of osmotic water permeability of collecting duct principal cells. van Balkom et al. (2002) suggested that the inhibitory effect of PKC activation on the AVP-induced increases of osmotic water permeability are mediated by PKC-triggered endocytosis of AQP2. According to the authors, PKC does not phosphorylate AQP2 (van Balkom et al. 2002). PKC may exert its inhibitory action by activation of CKII (van Balkom et al. 2002). However, elimination of any of the CKII consensus phosphorylation sites or mimicking phosphorylation by introducing aspartate (see above) did not influence the effects of PKA or PKC on the subcellular localization of AQP2. Only the mutant S148D (see above) was retained in the ER, probably as a consequence of misfolding (van Balkom et al. 2002).

Recently, phosphoproteomic analysis using a combination of phosphopeptide enrichment and mass spectrometry indicated that S256 is not the only phosphorylated site of AQP2 (Hoffert et al. 2006). Under basal conditions, pS261 is 24-fold more abundant than pS256. Stimulation of isolated IMCDs with AVP results in similar abundances of both pS256 and pS261, due to phosphorylation at S256 and, perhaps additionally, dephosphorylation at S261 (Hoffert et al. 2006, 2007). The physiological significance of this additional phosphorylation site is unclear.

Phosphorylation of AQP2 at S264 and T269 has also been observed (Hoffert et al. 2006; Fenton et al. 2008). Treatment of Brattleboro rats with dDAVP resulted in a fourfold increase of AQP2 phosphorylated at S264 (Fenton et al. 2008). The role of these two phosphorylation sites in the regulation of AQP2 is also unclear.

The phosphorylation status of AQP2, and hence its cellular localization, depends not only on protein kinases but also on protein phosphatases. So far, little is known about the involvement of protein phosphatases in the regulation of AQP2 trafficking. The inhibitor of serine/threonine phosphatases 1 and 2A (PP1 and PP2A), okadaic acid, increased phosphorylation of AQP2 and induced its translocation to the plasma membrane in CD8 cells (Valenti et al. 2000). The okadaic acid-induced increase in the phosphorylation of AQP2 could be blocked by low concentrations of the PKA inhibitor H89. Curiously, H89 was not able to prevent okadaic acid-induced translocation of AQP2 to the plasma membrane (Valenti et al. 2000). The authors proposed that the effect of okadaic acid may be indirect *via* reorganization of actin filaments, which occurs in okadaic acid-treated CD8 cells (Valenti et al. 2000). Protein phosphatase 2B (PP2B) has been shown to be present on AQP2-bearing vesicles within a complex consisting of regulatory RII-subunit of PKA, a 90-kDa AKAP, PP2B, and PKC ζ (Jo et al. 2001). PP2B is much less sensitive to okadaic acid (K_i about 5 μ M) than PP1 and PP2A and was presumably not inhibited by the drug at concentrations used by Valenti and colleagues (1 μ M) (Valenti et al. 2000). PP2B dephosphorylates AQP2 on isolated vesicles *in vitro* (Jo et al. 2001). However, its role *in vivo* remains elusive.

2.2 Compartmentalization of cAMP Signaling in Renal Principal Cells: A Role for AKAPs and PDEs

Signaling proteins do not usually move freely in cells, but are organized in complexes through protein–protein interactions at defined cellular sites. The basis of such multiprotein signaling complexes is found to be scaffold proteins, such as A kinase anchoring proteins (AKAPs). AKAPs interact with PKA and other signaling proteins and tether them to cellular compartments (Cooper 2005; Lynch et al. 2006; Szaszak et al. 2008; Tasken and Aandahl 2004; Wong and Scott 2004).

The role of AKAPs in cAMP-dependent AQP2 trafficking has been demonstrated by using peptides derived from the PKA-binding domains of AKAP-Lbc and AKAP18 δ disrupting interactions between PKA and AKAPs (Szaszak et al. 2008; Hundsrucker et al. 2006; Klussmann et al. 1999). Treatment of primary cultured IMCD cells with these peptides prevented the AVP-induced translocation of AQP2 to the plasma membrane (Szaszak et al. 2008; Klussmann et al. 1999). Thus, compartmentalization of PKA by AKAPs is a prerequisite for the AVP-induced AQP2 shuttle. This conclusion is supported by the observation that AVP induces a localized increase of PKA activity in the perinuclear space, where AQP2-bearing vesicles are mainly localized under resting conditions (Stefan et al. 2007). AKAP-dependent attachment of PKA to AQP2-bearing vesicles may be the reason for this localized PKA activation (Stefan et al. 2007) and would explain the effect of AKAP-Lbc- and AKAP18 δ -derived peptides (Szaszak et al. 2008; Klussmann et al. 1999). Presumably, the peptides prevent PKA-dependent phosphorylation of AQP2.

Several AKAPs were found to be present on AQP2-bearing vesicles (Jo et al. 2001; Klussmann et al. 1999; Henn et al. 2004). Harris and colleagues detected a 90-kDa AKAP on AQP2-bearing endosomes (Jo et al. 2001). Besides PKA, the 90-kDa AKAP binds PKC ζ , and PP2B (Jo et al. 2001). In our group, AKAP18 δ , was identified and found – among other locations – on AQP2-bearing vesicles (Henn et al. 2004). In addition to PKA, AKAP18 δ appears to attach PDE4D to AQP2-bearing vesicles (Stefan et al. 2007). The presence of different signaling molecules on AQP2-bearing vesicles may allow integration of several pathways regulating water reabsorption in the collecting duct. Thus, due to interaction with signaling molecules that are activated by different second messengers such as PKC (Ca²⁺) and PKA (cAMP), AKAPs integrate different signaling pathways rather than forming signal modules controlling cAMP signaling only. While the role of PKC and PP2B in these signaling modules remains elusive, PDE4D seems to regulate the cAMP level in close vicinity of AQP2 (Stefan et al. 2007). PDE4D may ensure low local PKA activity, thereby preventing plasma membrane insertion of AQP2 under resting conditions and thus inappropriate water reabsorption.

In LLC – PK₁ cells, ectopic expression of PDE4 blunted the AVP-induced cAMP elevation (Yamaki et al. 1993), indicating an important role of this PDE in regulation of the cAMP level in renal epithelial cells. In mice with hereditary NDI (DI +/+ mice), Dousa and colleagues found that the disease may be caused by elevated PDE activity, resulting in the inability of AVP to induce cAMP increases in

IMCD and cortical collecting duct cells (Homma et al. 1991). Treatment of IMCD cells with rolipram, a selective inhibitor of PDE4 (but not with cilostamide, an inhibitor of PDE3), restored the ability of AVP to increase cAMP levels (Homma et al. 1991). In mouse collecting ducts, a combination of rolipram and cilostamide

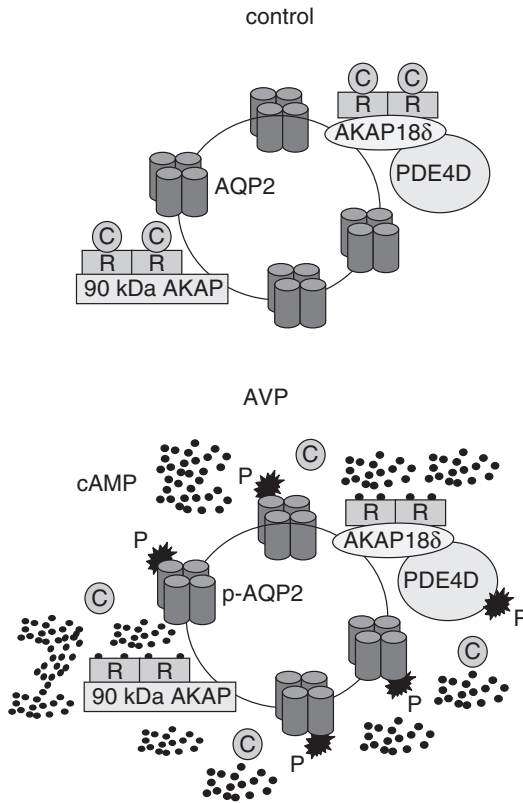


Fig. 2 Local cAMP signaling regulates the cellular localization of AQP2. PKA and cAMP-specific phosphodiesterase 4D (PDE4D) are located on AQP2-bearing vesicles. AKAP18 δ directly interacts with PKA and PDE4D. Of the nine splice variants of PDE4D, PDE4D3 and/or PDE4D9 are located on AQP2-bearing vesicles. The selective PDE4 inhibitor rolipram increases AKAP-tethered PKA activity on AQP2-bearing vesicles, enhances the AQP2 shuttle, and thereby enhances the osmotic water permeability. Thus, vesicular PDE4D appears to prevent activation of vesicular AKAP-tethered PKA in resting principal cells, and hence inappropriate translocation of AQP2 to the plasma membrane by local hydrolysis of cAMP. AVP increases the level of cAMP. Cyclic AMP binds to regulatory RII subunits of PKA, inducing a conformational change that causes dissociation of catalytic (C) subunits, which, in the free form, phosphorylate their substrates. The activities of all long isoforms of PDE4A–D are increased by PKA phosphorylation. For example, PDE4D3 is PKA-phosphorylated at serine 54. The phosphorylation accelerates hydrolysis of cAMP, thereby lowering PKA activity in close proximity to AQP2. This further limits AQP2 phosphorylation and translocation to the plasma membrane (Stefan et al. 2007). Additional AKAPs, including one with a molecular weight of 90 kDa, are located on AQP2-bearing vesicles (Jo et al. 2001; Henn et al. 2004)

restored the AVP-induced translocation of AQP2 to the plasma membrane, measured as appearance of intramembraneous particle clusters in the apical plasma membrane (Coffey et al. 1991). As only the combination of both PDE inhibitors was used in this study, it remains to be shown that inhibition of PDE4 alone restores AQP2 trafficking in this mouse model. Recently, Uchida and colleagues have developed a mouse knockin model of autosomal-dominant NDI, where a frame shift mutation (763–772 del) was introduced. In heterozygous knockin mice, rolipram (but not milrinone, which is an inhibitor of PDE3) improved urine concentrating ability by directing a fraction of wild-type AQP2 to the plasma membrane (Sohara et al. 2006). In a clinical study, however, Bichet and colleagues had not found any improvement of polyuria in two NDI patients treated with rolipram (Bichet et al. 1990), suggesting that inhibition of PDE4 is not an option for the treatment of all NDI patients.

A number of signaling proteins localized on AQP2-bearing vesicles were identified by a proteomics approach (Barile et al. 2005), suggesting that localization of signaling proteins on the surface of AQP2-bearing vesicles may be required for efficient regulation of AQP2 trafficking. However, the physiological relevance of most of these proteins for the control of AQP2 trafficking is still unknown.

2.3 The Involvement of Cytoskeletal Elements

An increasing body of evidence suggests that dynamic changes of the cytoskeleton play a key role in the redistribution of AQP2 in renal principal cells.

2.3.1 Microfilaments

A role of the cytoskeleton in the transport of the AVP-dependent water channel had been postulated before AQP2 was cloned (Fushimi et al. 1993; Pearl and Taylor 1983; Wade and Kachadorian 1988). The first data indicating a role of the cytoskeleton in the AVP-induced increase of water permeability were observations showing that the F-actin-depolymerizing drug, cytochalasin D, prevented an AVP-induced increase of water permeability in toad bladders (Pearl and Taylor 1983; Wade and Kachadorian 1988). Further studies indicated that treatment of toad bladder granular cells and primary cultured mammalian IMCD cells with AVP resulted in the reorganization of actin the cytoskeleton (Holmgren et al. 1992; Simon et al. 1993).

Knepper and colleagues have demonstrated the presence of myosin light chain kinase, the myosin regulatory light chain (MLC), and the IIA and IIB isoforms of the non-muscle myosin heavy chain in rat IMCD cells (Chou et al. 2004). Stimulation of V2R with a synthetic AVP analog desmopressin, 1-Desamino-8-D-Arginin-Vasopressin (dDAVP), induced phosphorylation of MLC, and an inhibitor of myosin light chain kinase, ML-7, blocked this phosphorylation. In addition, ML-7 substantially reduced the dDAVP-induced increase in water permeability (Chou et al. 2004).

On the basis of these data, a role of non-muscle myosin II in AQP2 trafficking has been postulated (Chou et al. 2004).

We recently identified myosin Vb as a motor protein involved in the transport of AQP2-bearing vesicles in renal principal cells (Nedvetsky et al. 2007). Myosin Vb is recruited to AQP2-bearing vesicles *via* its vesicular receptor Rab11 (marker protein of the recycling compartment) and an intermediate protein Rab11-FIP2 (Nedvetsky et al. 2007). Overexpression of dominant-negative forms of myosin Vb or Rab11-FIP2 prevented redistribution of AQP2 to the plasma membrane in response to AVP or forskolin in both IMCD and CD8 cells (Nedvetsky et al. 2007). Mammalian myosin Vb has several potential PKA-phosphorylation sites but, to our knowledge, no report about PKA-dependent phosphorylation of myosin Vb has been published. Therefore, it is not clear whether the function of myosin Vb is regulated by cAMP-dependent phosphorylation. The yeast homolog of myosin V, Myo2p, has been shown to be a subject for regulation by PKA (Legesse-Miller et al. 2006). Additionally, a role of cAMP in the regulation of apical trafficking has been described (Pimplikar and Simons 1993; Hansen and Casanova 1994), and cAMP-elevating agents induced the redistribution of Rab11 in cultured IMCD cells (Vossenkamper et al. 2007).

A C-terminal fragment of AQP2 comprising residues 231–271 directly interacts with actin (Noda et al. 2004). Another study by Noda et al. identified further proteins (e.g., SPA-1, myosin light chain isoforms 2-A and 2-B, non-muscle myosin heavy chain, annexins A2 and A6) interacting with AQP2 (Noda et al. 2005). At least one of these proteins, SPA-1, interacts directly with AQP2. Interference with Spa-1 function by overexpression of a dominant-negative mutant or knockdown by siRNA results in impairment of AQP2 trafficking (Noda et al. 2004). SPA-1 is a GTPase activating protein (GAP) of the Ras family GTPase, Rap1, and involved in the regulation of Ras/ERK signaling, morphogenesis, cell differentiation, and cytoskeletal organization (Kooistra et al. 2007; Stork and Dillon 2005; Caron 2003). Trafficking of AQP2 was impaired in MDCK cells expressing a SPA-1 mutant lacking GAP activity and in SPA-1 deficient mice (Noda et al. 2004).

F-actin may not only represent the tracks for trafficking of AQP2-bearing vesicles, but also serves as a barrier in their passage to the plasma membrane. This makes dynamic changes in cytoskeletal architecture an important determinant of AQP2 trafficking. In line with this, treatment of IMCD cells with cytochalasin D, which depolymerizes cortical F-actin, resulted in transient translocation of AQP2 to the plasma membrane (Klussmann et al. 2001; Tamma et al. 2001).

Small GTPases of the Rho family are important regulators of cytoskeletal dynamics (Etienne-Manneville and Hall 2002; Hall 1998). Activation of RhoA induces formation of so-called stress fibers, long F-actin-containing fibers running through the cell (Hall 1998). Treatment of CD8 cells with forskolin results in inhibition of RhoA through PKA-dependent phosphorylation of RhoA. Phosphorylated RhoA associates with Rho-GDI, which maintains RhoA in an inactive state (Tamma et al. 2003). Inhibition of RhoA with C3 toxin resulted in the translocation of AQP2 to the plasma membrane of primary cultured IMCD and CD8 cells (Klussmann et al. 2001; Tamma et al. 2001). Both AVP- or C3 toxin-mediated inhibition of RhoA is accompanied by partial depolymerization of F-actin, which therefore seems to be

necessary for the redistribution of AQP2 from intracellular vesicles to the plasma membrane.

Many different signaling pathways regulate actin dynamics and many of them may be also involved in the regulation of AQP2 trafficking. Indeed, several diuretic agents regulate AQP2 trafficking *via* modulation of F-actin. For example, stimulation of the prostaglandin EP₃-receptor in IMCD cells increased the F-actin content and inhibited the AVP-induced translocation of AQP2 to the plasma membrane (Tamma et al. 2003). In CD8 cells, a bradykinin-dependent decrease of AQP2 trafficking to the plasma membrane is accompanied by an activation of RhoA and an increase of F-actin (Tamma et al. 2005).

Ezrin-radixin-moesin (ERM) proteins play an important role in activation of Rho proteins (Bretscher 1999; Bretscher et al. 2002). In CD8 cells, a peptide corresponding to the C-terminal region of moesin inhibited phosphorylation (and consequent activation) of moesin, and induced depolymerization of F-actin and translocation of AQP2 to the plasma membrane in the absence of cAMP-elevating agents. The peptide treatment was thought to result in inactivation of moesin and release of RhoGDI, which in turn interacts and inhibits RhoA (Tamma et al. 2005; Ishikawa et al. 1988). Thus, the effect of the peptide on the localization of AQP2 is presumably mediated by RhoA inhibition.

RhoA is not the only small GTPase of the Rho family involved in the regulation of AQP2 trafficking. Recently, it was demonstrated that a hypotonicity-induced decrease of AQP2 at the plasma membrane of CD8 cells was associated with reorganization of F-actin, an effect blunted by overexpression of a dominant-negative version of the Rho family member Cdc42 (Tamma et al. 2007).

2.3.2 Microtubules

Several lines of evidence suggest an involvement of microtubules in AQP2 trafficking. In primary cultured IMCD cells, AVP-induced AQP2 translocation to the plasma membrane is accompanied by reorganization of microtubules (Vossenkamper et al. 2007). The microtubule-dependent motor protein, dynein, has been found on AQP2-bearing vesicles (Marples et al. 1998). The microtubule-disrupting agents, nocodazole or colcemide, prevented the AVP-induced increase of water permeability in rabbit collecting ducts (Phillips and Taylor 1989, 1992), and erythro-9-[3-(2-hydroxyonyl)]adenine (EHNA), an inhibitor of dynein, had the same effect in toad urinary bladders (Marples et al. 1996). Collectively, these data suggest a role of microtubule-dependent transport in AQP2 trafficking. Surprisingly, the AVP-dependent redistribution of AQP2 to the plasma membrane was not affected by the microtubule-disrupting agents nocodazole or colcemide in two different models: MDCK cells stably transfected with AQP2 (Tajika et al. 2005) and primary cultured rat IMCD cells (Vossenkamper et al. 2007). In both model systems, disruption of microtubules or inhibition of dynein resulted in the redistribution of AQP2 from the perinuclear region to cell periphery in the absence of AVP (Vossenkamper et al. 2007; Tajika et al. 2005). These data suggest that microtubule-dependent transport

is involved in positioning of AQP2-bearing vesicles in the perinuclear region, but is not essential for their transport to the cell periphery. Parallel changes in the distribution of AQP2 and Rab11 in IMCD cells treated with nocodazole indicate that microtubule disruption results in dispersion of the recycling compartment. It is not understood why an AVP-induced increase of osmotic water permeability in collecting ducts is prevented by nocodazole (Phillips and Taylor 1989; Dousa and Barnes 1974), while the agent has no effect on trafficking of AQP2 in cell models (Vossenkamper et al. 2007; Tajika et al. 2005). Since the amount of AQP2 in the apical plasma membrane is limiting for osmotic water permeability of collecting ducts, even modest decreases of AQP2 trafficking to the plasma membrane or partial misrouting to the basolateral membrane should result in a decrease of osmotic water permeability, but may not be detectable by immunostaining. Indeed, in IMCD cells we have not observed any effects of nocodazole on the AQP2 trafficking to the plasma membrane when analyzed by immunocytochemistry. However, a forskolin-induced increase of osmotic water permeability was slightly but significantly reduced by nocodazole (Vossenkamper et al. 2007).

2.4 Role of Calcium in AQP2 Trafficking

The role of intracellular Ca^{2+} in the AVP-induced redistribution of AQP2 is controversially discussed. In some model systems, stimulation of the V2R has been observed to induce increases in both cAMP and intracellular Ca^{2+} , e.g. in isolated IMCD (Ishikawa et al. 1988; Champigneulle et al. 1993; Ecelbarger et al. 1996; Maeda et al. 1993; Star et al. 1988; Yip 2002; Chou et al. 2000). AVP does not mediate activation of G_q , which is the classical G protein leading to Ca^{2+} mobilization, nor does it affect phosphoinositide hydrolysis in IMCD cell suspensions (Chou et al. 1998), arguing against the involvement of inositol 1,4,5-trisphosphate (IP_3)-sensitive Ca^{2+} stores in AVP-induced Ca^{2+} elevation. cAMP analogs induce Ca^{2+} oscillations in perfused collecting ducts (Yip 2006), indicating that Ca^{2+} mobilization through AVP may be a downstream effect following G_s -dependent activation of adenylyl cyclase. PKA seems not to be involved in this effect, since PKA inhibitors, H89 or KT5720, did not prevent AVP-induced Ca^{2+} -mobilization (Yip 2006). More likely, another cAMP-effector, exchange protein directly activated by cAMP (Epac), mediates Ca^{2+} -mobilization, as 8-pCPT-2'-O-Me-cAMP, a cAMP analog selectively activating Epac, induced Ca^{2+} oscillations in isolated IMCD. This effect was blocked by ryanodine, a ryanodine receptor antagonist, indicating the role of Ca^{2+} -induced Ca^{2+} release through ryanodine receptors in the ER (Yip 2006). In addition, 8-pCPT-2'-O-Me-cAMP induced the translocation of AQP2 to the apical plasma membrane in the presence of Rp-cAMP, an inhibitor of PKA (Yip 2006), indicating that, in those experiments, activation of Epac, but not of PKA, was required for the AQP2 translocation to the plasma membrane. The AVP-induced increase of osmotic water permeability in isolated IMCD was also consistently blocked by ryanodine (Chou et al. 2000).

Although these data suggest that Ca^{2+} mobilization is involved in AQP2 trafficking, the AQP2 redistribution to the plasma membrane proceeds in the absence of Ca^{2+} just as efficiently. For example, in primary cultured IMCD cells, AVP induced Ca^{2+} oscillations, but clamping of the intracellular Ca^{2+} concentration at the basal level (25 nM) did not prevent the AQP2 translocation (Lorenz et al. 2003). PKA inhibition with H89 prevents the AVP-induced AQP2 shuttle in IMCD and LLC-PK1 cells (Klussmann et al. 1999; Katsura et al. 1997), demonstrating PKA dependence of the AVP-induced AQP2 shuttle. The controversy regarding the role of intracellular Ca^{2+} in AQP2 trafficking is still not resolved and requires additional studies.

Hypercalcemia is associated with urine concentrating defects (Cohen et al. 1957; Gill and Bartter 1961), and hypercalcemic rats are not able to increase urine osmolarity in response to infused AVP (Levi et al. 1983). In isolated IMCD, luminal Ca^{2+} concentration of 5 mM reduced the AVP-induced increase of osmotic water permeability (Sands et al. 1997). This effect is most likely mediated by the apically expressed calcium-sensing receptor (CaR), since an agonist, neomycin, mimicked the effect of high Ca^{2+} (Sands et al. 1997). The signaling pathways mediating the effect of CaR activation on AQP2 trafficking were studied in CD8 cells. As in isolated IMCD, incubation of CD8 cells with 5 mM extracellular Ca^{2+} strongly inhibited the forskolin-induced translocation of AQP2 to the plasma membrane (Procino et al. 2004). Under these conditions, forskolin-induced cAMP production was decreased, PKC was activated, and the F-actin content was increased (Procino et al. 2004), all events reducing AQP2 translocation to the plasma membrane (see above).

3 Regulation of Endocytosis

Not only are exocytic steps of AQP2 trafficking regulated, but its endocytosis is also tightly regulated by several factors. Activation of PKC accelerates internalization of AQP2 (van Balkom et al. 2002) and directs internalized AQP2 to lysosomes (Kamsteeg et al. 2006). These effects are not accompanied by PKC-dependent phosphorylation of AQP2 and do not require dephosphorylation of AQP2 at S256 (van Balkom et al. 2002). Activation of PKC leads to short-chain ubiquitination of AQP2 at lysine 270, directing the protein to lysosomal degradation (Kamsteeg et al. 2006). PKC activity may be regulated *via* hormones whose receptors are coupled to the G-protein G_q . Surprisingly, activation of angiotensin AT_1 receptors on the surface of IMCD cells potentiated the effect of AVP on the translocation of AQP2 to the plasma membrane in a PKC-dependent manner (Katsura et al. 1996; Lee et al. 2007). Here, activation of PKC led to an increase of the cAMP level and stimulated the translocation of AQP2 to the plasma membrane, induced by low doses of AVP.

Another protein important for the internalization of AQP2 is the chaperon hsc70, which possesses ATPase activity (Lu et al. 2007). Hsc70 was coimmunoprecipitated with AQP2 from rat kidney and AQP2-expressing LLC – PK₁ cells. Treatment of AQP2-expressing LLC – PK₁ cells with AVP resulted in increased interaction be-

tween hsc70 and AQP2 (Lu et al. 2007). Overexpression of ATPase-deficient hsc70 resulted in accumulation of AQP2 at the plasma membrane of LLC – PK₁ cells, which was accompanied by decreased internalization of rhodamine-transferrin (Lu et al. 2007). Hsc70 plays an important role in the uncoating of clathrin-coated vesicles, providing clathrin for the next round of internalization (Chappell et al. 1986; Newmyer and Schmid 2001; Chang et al. 2002). It remains to be clarified whether interaction between AQP2 and hsc70 is necessary for the internalization of AQP2, or whether AQP2 depends on hsc70 because of its general role in the uncoating of clathrin-coated vesicles.

4 Phosphorylation-Independent Translocation of AQP2 to the Plasma Membrane

The cAMP-dependent PKA phosphorylation of AQP2 at S256 has been postulated to be required and to be sufficient to induce the AQP2 redistribution to the plasma membrane (see above) (van Balkom et al. 2002). However, AQP2 also redistributes to the plasma membrane in a cAMP-independent manner. For example, translocation of the AQP2 S256A mutant to the plasma membrane is inducible by inhibition of endocytosis (Lu et al. 2004); wild-type AQP2 accumulates in the plasma membrane upon disruption of F-actin by cytochalasin D or inhibition of RhoA, associated with disruption of F-actin (Klussmann et al. 2001; Tamma et al. 2001). Thus, it appears that multiple stimuli and events regulate the localization and trafficking of AQP2 partially or completely independent from each other, and phosphorylation of AQP2 by PKA is only one regulatory mechanism.

5 Dysfunction of AQP2 Trafficking Causes Nephrogenic Diabetes Insipidus (NDI)

Congenital NDI is a genetic disease characterized by the inability of the kidney to respond to AVP, which results in a massive loss of hypotonic urine and causes polydipsia. Congenital NDI can be classified into X-linked and autosomal NDI. The X-linked form is due to mutations in the AVPR2 gene encoding the V2R (Bichet 1996). More rarely (in 5–10% of patients), congenital NDI is an autosomal disease caused by mutations in the gene encoding AQP2 (AQP2 gene mutations are listed at <http://www.medicine.mcgill.ca/nephros/aqp2.html>) (Deen et al. 1996). So far, 39 mutations have been reported, of which 32 cause recessive NDI (Table 1). The recessive AQP2 mutants are retained in the ER due to misfolding, and are degraded. Often, patients have two identical mutations in both AQP2 alleles. The concentrating ability of the kidneys of these patients is strongly reduced (<100 mos ml per KgH₂O)(Fujiwara et al. 1995). Almost all autosomal recessive

Table 1 List of nephrogenic diabetes insipidus-causing mutations in AQP2

Mutation	Amino acid substitution		References
83T > C	L28P	r	Marr et al. (2002)
170A > C	Q57P	r	Lin et al. (2002)
190G > A	G64R	r	van Lieburg et al. (1994); Deen et al. (1995); Marr et al. (2001)
197–198 del CA	Frameshift	r	Tajima et al. (2003)
293A > G	N68S	r	Marr et al. (2001); Mulders et al. (1997)
211G > A	V71M	r	Marr et al. (2002)
253C > T	R85*	r	Vargas-Poussou et al. (1998)
298G > A	G100R	r	Carroll et al. (2006)
299C > T	G100* (stop codon)	r	Hochberg et al. (1997)
299G > T	G100V	r	Lin et al. (2002)
369delC	Frameshift	r	van Lieburg et al. (1994)
374C > T	T125M	r	Marr et al. (2002); Goji et al. (1998); Kuwahara (1998)
377C > T	T126M	r	Marr et al. (2001); Mulders et al. (1997); Goji et al. (1998)
439G > A	A147T	r	Marr et al. (2001); Mulders et al. (1997)
450T > A	D150E	r	Iolascon et al. (2007)
502G > A	V168M	r	Vargas-Poussou et al. (1998); Boccalandro et al. (2004)
523G > A	G175R	r	Marr et al. (2002); Goji et al. (1998); Kuwahara (1998)
537G > A	G180S	r	Carroll et al. (2006)
543C > G	C181W	r	Canfield et al. (1997); Tamarappoo and Verkman (1998); Moses et al. (1984)
553C > G	P185A	r	Marr et al. (2002)
559C > T	R187C	r	van Lieburg et al. (1994); Marr et al. (2001); Deen et al. (1994)
643G > T	G215C	r	Iolascon et al. (2007)
928G > A	A190T	r	Marr et al. (2001); Kuwahara (1998); de Mattia et al. (2004)
587G > A	G196D	r	Iolascon et al. (2007)
606G > T	W202C/splice	r	Oksche et al. (1996)
c606 + 1G > A	Splice	r	Marr et al. (2002)
646T > C	S216P	r	Marr et al. (2001); Deen et al. (1994); Deen et al. (1995)
652delC	Frameshift	r	Marr et al. (2002)
721delG	Frameshift	d	Kuwahara et al. (2001)
727delG	Frameshift	d	Marr et al. (2002)

(Continued)

mutations of AQP2 are localized in the segments involved in the formation of the water pore and therefore do not tolerate structural alterations.

Table 1 Continued

Mutation	Amino acid substitution	References
761G > T	R254L	d de Mattia et al. (2005); Marr et al. (2001)
763–772del	Frameshift	d Kuwahara et al. (2001)
772G > A	E258K	d Mulders et al. (1998)
779–780insA	Frameshift	d Kamsteeg et al. (2003)
785C > T	P262L	r Marr et al. (2001); Kuwahara (1998); de Mattia et al. (2004)
812–818del	Frameshift	d Kuwahara et al. (2001)
1502G > A	Transition splice site	r Tajima et al. (2003)

c606 + 1G > A describes a patient heterozygote for a mutation in the splice donor site of exon3/intron3 (c606 + 1G > A) in one allele, and a nucleotide substitution (c580G > A) combined with a nucleotide deletion (c652delC) in the other allele. *r* recessive; *d* dominant; *del* deletion; *ins* insertion

Autosomal dominant NDI, discovered in a few families, is caused by mutations that affect the intracellular trafficking of the protein. In autosomal dominant NDI, AQP2 is either retained in the Golgi, sorted to late endosomes, lysosomes, or to the basolateral plasma membrane. The mutants form heterotetramers with wild-type AQP2 and thereby prevent the wild-type protein from reaching the plasma membrane (Bichet 2006; Sohara et al. 2006). All dominant mutations identified so far are located within the C-terminus of AQP2, which is a region important for the regulation of intracellular trafficking (see above)(Bichet 2006). For example, AQP2-R254L, described in one family, is located within the PKA phosphorylation consensus site, RRR-X-S/T, and, ablates the PKA phosphorylation at S256. This mutant forms complexes with wild-type AQP2 and is retained in intracellular vesicles, mimicking the S256A phenotype (de Mattia et al. 2005).

So far, a causal therapy for NDI is not available. It is crucial for patients to compensate the water loss by appropriate supply of fluid, combined with a low salt diet, to reduce the obligate water excretion (Bichet 2006; Konoshita et al. 2004). The most commonly used treatments paradoxically include diuretics such as hydrochlorothiazide and amiloride. The thiazide diuretics inhibit the NaCl cotransporter in the distal convoluted tubule, decreasing sodium reabsorption. The consequent increase of sodium excretion leads to extracellular volume contraction, decreasing the glomerular filtration rate and increasing the sodium and water reabsorption in the proximal tubule (Earley and Orloff 1962; Kennedy and Crawford 1961). The combined treatment with thiazide and inhibitors of cyclooxygenases, such as indomethacin, decreases the urinary volume more effectively than thiazides alone. However, this treatment may cause severe side effects, including dysregulation of ion homeostasis and gastrointestinal disturbances (Konoshita et al. 2004).

6 Concluding Remarks

Our understanding of the AQP2 trafficking in health and disease has progressed since the cloning of AQP2. However, our knowledge is still fragmentary. For example, the functional consequences of AQP2 glycosylation for its maturation, trafficking, and function are not clear. The attempts to identify direct protein interaction partners regulating the trafficking have yielded initial results, but are still at the very early stages. The exocytic insertion of AQP2 into the plasma membrane is an excellent example of cAMP-triggered exocytic processes. A detailed mechanistic insight into its regulation will contribute to our understanding of vesicular trafficking of other aquaporins (AQPs1, 4, 5 and 8), the cellular localization of which is subject to control by various stimuli and, in addition, of other cAMP-dependent

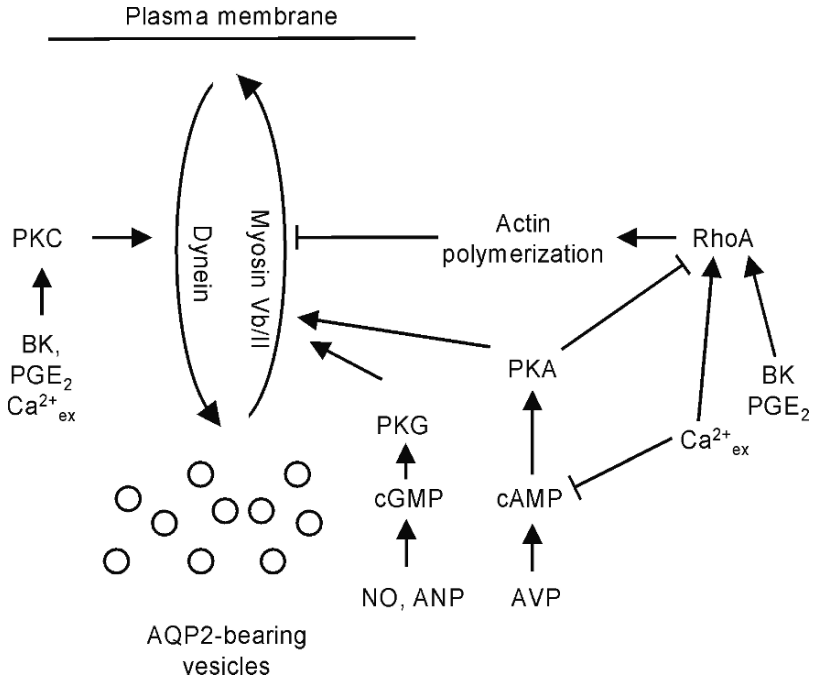


Fig. 3 Regulation of AQP2 trafficking. In renal principal cells, the redistribution of AQP2 from the intracellular vesicular pool to the plasma membrane is initiated by AVP-dependent elevation of cAMP, which activates PKA. PKA phosphorylates AQP2 and thereby triggers its redistribution to the plasma membrane. PKA also phosphorylates and thereby inhibits RhoA, decreasing the amount of F-actin. Bradykinin (BK), PGE₂, and extracellular Ca²⁺ counteract the effects of AVP by activating RhoA and/or lowering the cAMP level and activation of PKC. PKC accelerates internalization of AQP2 and its lysosomal degradation. AQP2 may also be phosphorylated by PKG, and therefore its redistribution to the plasma membrane can be induced by stimuli elevating cGMP (e.g., NO or ANP). Trafficking of AQP2 to the plasma membrane is mediated by the motor protein myosin Vb along F-actin, while the transport of AQP2 to the perinuclear region after internalization is mediated by dynein along microtubules. In addition, myosin II also appears to be involved in F-actin-dependent transport of AQP2 to the plasma membrane

exocytic processes such as renin secretion from renal juxtaglomerular cells, acid secretion from gastric parietal cells, and insulin secretion pancreatic β -cells (Szaszak et al. 2008; Woo et al. 2008; Carmosino et al. 2007; Tietz et al. 2006; Garcia et al. 2001).

While impaired AQP2 trafficking to the plasma membrane of renal principal cells causes NDI, i.e., the loss of water, increases in AQP2 abundance in the plasma membrane due to increased AVP levels in the blood in cardiovascular diseases (e.g., chronic heart failure, CHF), hyponatremia, or liver cirrhosis lead to inappropriate water retention (Xu et al. 1997; Schrier 2007). Thus, modulating AQP2 trafficking in such patients appears to be a suitable concept for treatment. The concept of pharmacological interference with renal principal cell function has been validated with the introduction of dDAVP, a V2R agonist for the treatment of central NDI, a form of NDI where AVP is lacking (Andersson and Arner 1972; Aronson et al. 1973; Edwards et al. 1973). Currently, the concept is being validated for the treatment of CHF with a new class of drugs, vaptans, which block the V2R and thereby reduce the afterload in the patients (Gheorghide et al. 2003; Ali et al. 2007; Lemmens-Gruber and Kamyar 2006).

In summary, a detailed understanding of the regulation of AQP2 trafficking will provide new insights into cAMP-dependent exocytic processes, and establish new drug targets as the basis for the development of novel pharmacological strategies to treat patients suffering of/from diseases associated with dysfunction of body water homeostasis (Figs. 2 and 3).

Acknowledgments This work was supported by grants from Deutsche Forschungsgemeinschaft (Forschergruppe 667, project KL 1415/3-1 and Forschergruppe 806, project KL1415/4-1), the European Union (project thera cAMP – proposal 037189), and the GoBio program of the German Ministry of Education and Science (BMBF, FKZ 0315097).

References

- Agre P (2006) The aquaporin water channels. *Proc Am Thorac Soc* 3:5–13
- Agre P, King LS, Yasui M, Guggino WB, Ottersen OP, Fujiyoshi Y, Engel A, Nielsen S (2002) Aquaporin water channels – from atomic structure to clinical medicine. *J Physiol* 542:3–16
- Ali F, Guglin M, Vaitkevicius P, Ghali JK (2007) Therapeutic potential of vasopressin receptor antagonists. *Drugs* 67:847–858
- Andersson KE, Arner B (1972) Effects of DDAVP, a synthetic analogue of vasopressin, in patients with cranial diabetes insipidus. *Acta Med Scand* 192:21–27
- Aronson AS, Andersson KE, Bergstrand CG, Mulder JL (1973) Treatment of diabetes insipidus in children with DDAVP, a synthetic analogue of vasopressin. *Acta Paediatr Scand* 62:133–140
- Barile M, Pisitkun T, Yu MJ, Chou CL, Verbalis MJ, Shen RF, Knepper MA (2005) Large scale protein identification in intracellular aquaporin-2 vesicles from renal inner medullary collecting duct. *Mol Cell Proteomics* 4:1095–1106
- Bichet DG (1996) Vasopressin receptors in health and disease. *Kidney Int* 49:1706–1711
- Bichet DG (2006) Nephrogenic diabetes insipidus. *Adv Chronic Kidney Dis* 13:96–104

- Bichet DG, Ruel N, Arthus MF, Lonergan M (1990) Rolipram, a phosphodiesterase inhibitor, in the treatment of two male patients with congenital nephrogenic diabetes insipidus. *Nephron* 56:449–450
- Boccalandro C, de Mattia F, Guo DC, Xue L, Orlander P, King TM, Gupta P, Deen PMT, Lavis VR, Milewicz DM (2004) Characterization of an aquaporin-2 water channel gene mutation causing partial nephrogenic diabetes insipidus in a Mexican family: evidence of increased frequency of the mutation in the town of origin. *J Am Soc Nephrol* 15:1223–1231
- Bouley R, Breton S, Sun TX, McLaughlin M, Nsumu NN, Lin HY, Ausiello DA, Brown D (2000) Nitric oxide and atrial natriuretic factor stimulate cGMP-dependent membrane insertion of aquaporin 2 in renal epithelial cells. *J Clin Invest* 106:1115–1126
- Bouley R, Pastor-Soler N, Cohen O, McLaughlin M, Breton S, Brown D (2005) Stimulation of AQP2 membrane insertion in renal epithelial cells in vitro and in vivo by the cGMP phosphodiesterase inhibitor sildenafil citrate (Viagra). *Am J Physiol Renal Physiol* 288:F1103–F1112
- Bourguet J, Chevalier J, Hugon JS (1976) Alterations in membrane-associated particle distribution during antidiuretic challenge in frog urinary bladder epithelium. *Biophys J* 16:627–639
- Bretscher A (1999) Regulation of cortical structure by the ezrin–radixin–moesin protein family. *Curr Opin Cell Biol* 11:109–116
- Bretscher A, Edwards K, Fehon RG (2002) ERM proteins and merlin: integrators at the cell cortex. *Nat Rev Mol Cell Biol* 3:586–599
- Brown D (2003) The ins and outs of aquaporin-2 trafficking. *Am J Physiol Renal Physiol* 284:F893–F901
- Brown D, Orci L (1983) Vasopressin stimulates formation of coated pits in rat kidney collecting ducts. *Nature* 302:253–255
- Canfield MC, Tamarappoo BK, Moses AM, Verkman AS, Holtzman EJ (1997) Identification and characterization of aquaporin-2 water channel mutations causing nephrogenic diabetes insipidus with partial vasopressin response. *Hum Mol Genet* 6:1865–1871
- Carmosino M, Procino G, Tamma G, Mannucci R, Svelto M, Valenti G (2007) Trafficking and phosphorylation dynamics of AQP4 in histamine-treated human gastric cells. *Biol Cell* 99:25–36
- Caron E (2003) Cellular functions of the Rap1 GTP-binding protein: a pattern emerges. *J Cell Sci* 116:435–440
- Carroll P, Al Mojalli H, Al Abbad A, Al Hassoun I, Al Hamed M, Al Amr R, Butt AI, Meyer BF (2006) Novel mutations underlying nephrogenic diabetes insipidus in Arab families. *Genet Med* 8:443–447
- Champigneulle A, Siga E, Vassent G, Imbert-Teboul M (1993) V2-like vasopressin receptor mobilizes intracellular Ca²⁺ in rat medullary collecting tubules. *Am J Physiol Renal Physiol* 265:F35–F45
- Chang HC, Newmyer SL, Hull MJ, Ebersold M, Schmid SL, Mellman I (2002) Hsc70 is required for endocytosis and clathrin function in *Drosophila*. *J Cell Biol* 159:477–487
- Chappell TG, Welch WJ, Schlossman DM, Palter KB, Schlesinger MJ, Rothman JE (1986) Uncoating ATPase is a member of the 70 kilodalton family of stress proteins. *Cell* 45:3–13
- Chou CL, Rapko SI, Knepper MA (1998) Phosphoinositide signaling in rat inner medullary collecting duct. *Am J Physiol Renal Physiol* 274:F564–F572
- Chou CL, Yip KP, Michea L, Kador K, Ferraris JD, Wade JB, Knepper MA (2000) Regulation of aquaporin-2 trafficking by vasopressin in the renal collecting duct. Roles of Ryanodine-Sensitive Ca²⁺ Stores and Calmodulin. *J Biol Chem* 275:36839–36846
- Chou CL, Christensen BM, Frische S, Vorum H, Desai RA, Hoffert JD, de Lanerolle P, Nielsen S, Knepper MA (2004) Non-muscle myosin II and myosin light chain kinase are downstream targets for vasopressin signaling in the renal collecting duct. *J Biol Chem* 279:49026–49035
- Coffey AK, O’Sullivan DJ, Homma S, Dousa TP, Valtin H (1991) Induction of intramembranous particle clusters in mice with nephrogenic diabetes insipidus. *Am J Physiol* 261:F640–F646
- Cohen SI, Fitzgerald MG, Fourman P, Griffiths WJ, De Wardener HE (1957) Polyuria in hyperparathyroidism. *Q J Med* 26:423–431

- Cooper DM (2005) Compartmentalization of adenylate cyclase and camp signaling. *Biochem Soc Trans* 33:1319–1322
- Deen PM, Verdijk MA, Knoers NV, Wieringa B, Monnens LA, van Os CH, Van Oost BA (1994) Requirement of human renal water channel aquaporin-2 for vasopressin-dependent concentration of urine. *Science* 264:92–95
- Deen PM, Croes H, van Aubel RA, Ginsel LA, van Os CH (1995) Water channels encoded by mutant aquaporin-2 genes in nephrogenic diabetes insipidus are impaired in their cellular routing. *J Clin Invest* 95:2291–2296
- Deen PM, van Aubel RA, van Lieburg AF, van Os CH (1996) Urinary content of aquaporin 1 and 2 in nephrogenic diabetes insipidus. *J Am Soc Nephrol* 7:836–841
- Deen PM, Rijss JP, Mulders SM, Errington RJ, van Baal J, van Os CH (1997) Aquaporin-2 transfection of Madin–Darby canine kidney cells reconstitutes vasopressin-regulated transcellular osmotic water transport. *J Am Soc Nephrol* 8:1493–1501
- de Mattia F, Savelkoul PJ, Bichet DG, Kamsteeg EJ, Konings IB, Marr N, Arthus MF, Lonergan M, van Os CH, van der SP, Robertson G, Deen PM (2004) A novel mechanism in recessive nephrogenic diabetes insipidus: wild-type aquaporin-2 rescues the apical membrane expression of intracellularly retained AQP2-P262L. *Hum Mol Genet* 13:3045–3056
- de Mattia F, Savelkoul PJ, Kamsteeg EJ, Konings IBM, van der Sluijs P, Mallmann R, Oksche A, Deen PM (2005) Lack of arginine vasopressin-induced phosphorylation of aquaporin-2 mutant AQP2-R254L explains dominant nephrogenic diabetes insipidus. *J Am Soc Nephrol* 16:2872–2880
- Dousa TP, Barnes LD (1974) Effects of colchicine and vinblastine on the cellular action of vasopressin in mammalian kidney. A possible role of microtubules. *J Clin Invest* 54:252–262
- Duong VH, Bens M, Vandewalle A (1998) Differential effects of aldosterone and vasopressin on chloride fluxes in transimmortalized mouse cortical collecting duct cells. *J Membr Biol* 164:79–90
- Earley LE, Orloff J (1962) The mechanism of antidiuresis associated with the administration of hydrochlorothiazide to patients with vasopressin-resistant diabetes insipidus. *J Clin Invest* 41:1988–1997
- Ecelbarger CA, Chou CL, Lolait SJ, Knepper MA, DiGiovanni SR (1996) Evidence for dual signaling pathways for V2 vasopressin receptor in rat inner medullary collecting duct. *Am J Physiol Renal Physiol* 270:F623–F633
- Edwards CR, Kitau MJ, Chard T, Besser GM (1973) Vasopressin analogue DDAVP in diabetes insipidus: clinical and laboratory studies. *Br Med J* 3:375–378
- Etienne-Manneville S, Hall A (2002) Rho GTPases in cell biology. *Nature* 420:629–635
- Fenton RA, Moeller HB, Hoffert JD, Yu MJ, Nielsen S, Knepper MA (2008) Acute regulation of aquaporin-2 phosphorylation at Ser-264 by vasopressin. *Proc Natl Acad Sci U S A* 105:3134–3139
- Fujiwara TM, Morgan K, Bichet DG (1995) Molecular biology of diabetes insipidus. *Annu Rev Med* 46:331–343
- Furuno M, Uchida S, Marumo F, Sasaki S (1996) Repressive regulation of the aquaporin-2 gene. *Am J Physiol Renal Physiol* 271:F854–F860
- Fushimi K, Uchida S, Hara Y, Hirata Y, Marumo F, Sasaki S (1993) Cloning and expression of apical membrane water channel of rat kidney collecting tubule. *Nature* 361:549–552
- Garcia F, Kierbel A, Larocca MC, Gradilone SA, Splinter P, Larusso NF, Marinelli RA (2001) The water channel aquaporin-8 is mainly intracellular in rat hepatocytes, and its plasma membrane insertion is stimulated by cyclic AMP. *J Biol Chem* 276:12147–12152
- Gheorghide M, Niazi I, Ouyang J, Czerwiec F, Kambayashi JJ, Zampino M, Orlandi C (2003) Vasopressin V2-receptor blockade with tolvaptan in patients with chronic heart failure: results from a double-blind, randomized trial. *Circulation* 107:2690–2696
- Gill JR Jr, Bartter FC (1961) On the impairment of renal concentrating ability in prolonged hypercalcemia and hypercalciuria in man. *J Clin Invest* 40:716–722

- Goji K, Kuwahara M, Gu Y, Matsuo M, Marumo F, Sasaki S (1998) Novel mutations in aquaporin-2 gene in female siblings with nephrogenic diabetes insipidus: evidence of disrupted water channel function. *J Clin Endocrinol Metab* 83:3205–3209
- Hall A (1998) Rho GTPases and the actin cytoskeleton. *Science* 279:509–514
- Hansen SH, Casanova JE (1994) Gs alpha stimulates transcytosis and apical secretion in MDCK cells through camp and protein kinase A. *J Cell Biol* 126:677–687
- Hasler U, Mordasini D, Bens M, Bianchi M, Cluzeaud F, Rousselot M, Vandewalle A, Feraille E, Martin PY (2002) Long term regulation of aquaporin-2 expression in vasopressin-responsive renal collecting duct principal cells. *J Biol Chem* 277:10379–10386
- Henn V, Edemir B, Stefan E, Wiesner B, Lorenz D, Theilig F, Schmitt R, Vossebein L, Tamma G, Beyermann M, Krause E, Herberg FW, Valenti G, Bachmann S, Rosenthal W, Klussmann E (2004) Identification of a novel A-kinase anchoring protein 18 isoform and evidence for its role in the vasopressin-induced aquaporin-2 shuttle in renal principal cells. *J Biol Chem* 279:26654–26665
- Hochberg Z, Van Lieburg A, Even L, Brenner B, Lanir N, Van Oost BA, Knoers NV (1997) Autosomal recessive nephrogenic diabetes insipidus caused by an aquaporin-2 mutation. *J Clin Endocrinol Metab* 82:686–689
- Hoffert JD, Pisitkun T, Wang G, Shen RF, Knepper MA (2006) Quantitative phosphoproteomics of vasopressin-sensitive renal cells: regulation of aquaporin-2 phosphorylation at two sites. *Proc Natl Acad Sci U S A* 103:7159–7164
- Hoffert JD, Nielsen J, Yu MJ, Pisitkun T, Schleicher SM, Nielsen S, Knepper MA (2007) Dynamics of aquaporin-2 serine-261 phosphorylation in response to short-term vasopressin treatment in collecting duct. *Am J Physiol Renal Physiol* 292:F691–F700
- Holmgren K, Magnusson KE, Franki N, Hays RM (1992) ADH-induced depolymerization of F-actin in the toad bladder granular cell: a confocal microscope study. *Am J Physiol* 262:C672–C677
- Homma S, Gapstur SM, Coffey A, Valtin H, Dousa TP (1991) Role of camp-phosphodiesterase isozymes in pathogenesis of murine nephrogenic diabetes insipidus. *Am J Physiol Renal Physiol* 261:F345–F353
- Hundsrucker C, Krause G, Beyermann M, Prinz A, Zimmermann B, Diekmann O, Lorenz D, Stefan E, Nedvetsky P, Dathe M, Christian F, McSorley T, Krause E, McConnachie G, Herberg FW, Scott JD, Rosenthal W, Klussmann E (2006) High-affinity AKAP7delta-protein kinase A interaction yields novel protein kinase A-anchoring disruptor peptides. *Biochem J* 396:297–306
- Iolascon A, Aglio V, Tamma G, D'Apolito M, Addabbo F, Procino G, Simonetti MC, Montini G, Gesualdo L, Debler EW, Svelto M, Valenti G (2007) Characterization of two novel missense mutations in the AQP2 gene causing nephrogenic diabetes insipidus. *Nephron Physiol* 105:33–41
- Ishikawa S, Okada K, Saito T (1988) Arginine vasopressin increases cellular free calcium concentration and adenosine 3',5'-monophosphate production in rat renal papillary collecting tubule cells in culture. *Endocrinology* 123:1376–1384
- Jo I, Ward DT, Baum MA, Scott JD, Coghlan VM, Hammond TG, Harris HW (2001) AQP2 is a substrate for endogenous PP2B activity within an inner medullary AKAP-signaling complex. *Am J Physiol Renal Physiol* 281:F958–F965
- Kachadorian WA, Wade JB, DiScala VA (1975) Vasopressin: induced structural change in toad bladder luminal membrane. *Science* 190:67–69
- Kamsteeg EJ, Bichet DG, Konings IBM, Nivet H, Lonergan M, Arthus MF, van Os CH, Deen PMT (2003) Reversed polarized delivery of an aquaporin-2 mutant causes dominant nephrogenic diabetes insipidus. *J Cell Biol* 163:1099–1109
- Kamsteeg EJ, Hendriks G, Boone M, Konings IB, Oorschot V, van der SP, Klumperman J, Deen PM (2006) Short-chain ubiquitination mediates the regulated endocytosis of the aquaporin-2 water channel. *Proc Natl Acad Sci U S A* 103:18344–18349
- Katsura T, Ausiello DA, Brown D (1996) Direct demonstration of aquaporin-2 water channel recycling in stably transfected LLC-PK1 epithelial cells. *Am J Physiol Renal Physiol* 270:F548–F553

- Katsura T, Gustafson CE, Ausiello DA, Brown D (1997) Protein kinase A phosphorylation is involved in regulated exocytosis of aquaporin-2 in transfected LLC-PK1 cells. *Am J Physiol* 272:F817–F822
- Kennedy GC, Crawford JD (1961) A comparison of the effects of adrenalectomy and of chlorothiazide in experimental diabetes insipidus. *J Endocrinol* 22:77–86
- King LS, Kozono D, Agre P (2004) From structure to disease: the evolving tale of aquaporin biology. *Nat Rev Mol Cell Biol* 5:687–698
- Klussmann E, Maric K, Wiesner B, Beyersmann M, Rosenthal W (1999) Protein kinase A anchoring proteins are required for vasopressin-mediated translocation of aquaporin-2 into cell membranes of renal principal cells. *J Biol Chem* 274:4934–4938
- Klussmann E, Maric K, Rosenthal W (2000) The mechanisms of aquaporin control in the renal collecting duct. *Rev Physiol Biochem Pharmacol* 141:33–95
- Klussmann E, Tamma G, Lorenz D, Wiesner B, Maric K, Hofmann F, Aktories K, Valenti G, Rosenthal W (2001) An inhibitory role of Rho in the vasopressin-mediated translocation of aquaporin-2 into cell membranes of renal principal cells. *J Biol Chem* 276:20451–20457
- Kooistra MR, Dube N, Bos JL (2007) Rap1: a key regulator in cell-cell junction formation. *J Cell Sci* 120:17–22
- Konoshita T, Kuroda M, Kawane T, Koni I, Miyamori I, Tofuku Y, Mabuchi H, Takeda R (2004) Treatment of congenital nephrogenic diabetes insipidus with hydrochlorothiazide and amiloride in an adult patient. *Horm Res* 61:63–67
- Kuwahara M (1998) Aquaporin-2, a vasopressin-sensitive water channel, and nephrogenic diabetes insipidus. *Intern Med* 37:215–217
- Kuwahara M, Iwai K, Oeoda T, Igarashi T, Ogawa E, Katsushima Y, Shinbo I, Uchida S, Terada Y, Arthus MF, Lonergan M, Fujiwara TM, Bichet DG, Marumo F, Sasaki S (2001) Three families with autosomal dominant nephrogenic diabetes insipidus caused by aquaporin-2 mutations in the C-terminus. *Am J Hum Genet* 69:738–748
- Leaf A, Hays RM (1962) Permeability of the isolated toad bladder to solutes and its modification by vasopressin. *J Gen Physiol* 45:921–932
- Lee YJ, Song IK, Jang KJ, Nielsen J, Frokiaer J, Nielsen S, Kwon TH (2007) Increased AQP2 targeting in primary cultured IMCD cells in response to angiotensin II through AT1 receptor. *Am J Physiol Renal Physiol* 292:F340–F350
- Legesse-Miller A, Zhang S, Santiago-Tirado FH, Van Pelt CK, Bretscher A (2006) Regulated phosphorylation of budding yeast's essential myosin V heavy chain, Myo2p. *Mol Biol Cell* 17:1812–1821
- Lemmens-Gruber R, Kamyar M (2006) Vasopressin antagonists. *Cell Mol Life Sci* 63:1766–1779
- Levi M, Peterson L, Berl T (1983) Mechanism of concentrating defect in hypercalcemia. Role of polydipsia and prostaglandins. *Kidney Int* 23:489–497
- Lin SH, Bichet DG, Sasaki S, Kuwahara M, Arthus MF, Lonergan M, Lin YF (2002) Two novel aquaporin-2 mutations responsible for congenital nephrogenic diabetes insipidus in Chinese families. *J Clin Endocrinol Metab* 87:2694–2700
- Lorenz D, Krylov A, Hahm D, Hagen V, Rosenthal W, Pohl P, Maric K (2003) Cyclic AMP is sufficient for triggering the exocytic recruitment of aquaporin-2 in renal epithelial cells. *EMBO Rep* 4:88–93
- Lu H, Sun TX, Bouley R, Blackburn K, McLaughlin M, Brown D (2004) Inhibition of endocytosis causes phosphorylation (S256)-independent plasma membrane accumulation of AQP2. *Am J Physiol Renal Physiol* 286:F233–F243
- Lu HAJ, Sun TX, Matsuzaki T, Yi XH, Eswara J, Bouley R, McKee M, Brown D (2007) Heat shock protein 70 interacts with aquaporin-2 and regulates its trafficking. *J Biol Chem* 282:28721–28732
- Lynch MJ, Hill EV, Houslay MD (2006) Intracellular targeting of phosphodiesterase-4 underpins compartmentalized camp signaling. *Curr Top Dev Biol* 75:225–259
- Maeda Y, Han JS, Gibson CC, Knepper MA (1993) Vasopressin and oxytocin receptors coupled to Ca²⁺ mobilization in rat inner medullary collecting duct. *Am J Physiol Renal Physiol* 265:F15–F25

- Maric K, Oksche A, Rosenthal W (1998) Aquaporin-2 expression in primary cultured rat inner medullary collecting duct cells. *Am J Physiol* 275:F796–F801
- Marples D, Barber B, Taylor A (1996) Effect of a dynein inhibitor on vasopressin action in toad urinary bladder. *J Physiol* 490:(Pt 3):767–774
- Marples D, Schroer TA, Ahrens N, Taylor A, Knepper MA, Nielsen S (1998) Dynein and dynactin colocalize with AQP2 water channels in intracellular vesicles from kidney collecting duct. *Am J Physiol* 274:F384–F394
- Marr N, Kamsteeg EJ, van Raak M, van Os CH, Deen PM (2001) Functionality of aquaporin-2 missense mutants in recessive nephrogenic diabetes insipidus. *Pflugers Arch* 442:73–77
- Marr N, Bichet DG, Hoefs S, Savelkoul PJM, Konings IBM, de Mattia F, Graat MPJ, Arthus MF, Lonergan M, Fujiwara TM, Knoers NVAM, Landau D, Balfe WJ, Oksche A, Rosenthal W, Muller D, van Os CH, Deen PMT (2002) Cell-biologic and functional analyses of five new aquaporin-2 missense mutations that cause recessive nephrogenic diabetes insipidus. *J Am Soc Nephrol* 13:2267–2277
- Moses AM, Scheinman SJ, Oppenheim A (1984) Marked hypotonic polyuria resulting from nephrogenic diabetes insipidus with partial sensitivity to vasopressin. *J Clin Endocrinol Metab* 59:1044–1049
- Mulders SM, Knoers NV, van Lieburg AF, Monnens LA, Leumann E, Wuhl E, Schober E, Rijss JP, van Os CH, Deen PM (1997) New mutations in the AQP2 gene in nephrogenic diabetes insipidus resulting in functional but misrouted water channels. *J Am Soc Nephrol* 8:242–248
- Mulders SM, Bichet DG, Rijss JPL, Kamsteeg EJ, Arthus MF, Lonergan M, Fujiwara M, Morgan K, Leijendekker R, van der Sluijs P, van Os CH, Deen PMT (1998) An aquaporin-2 water channel mutant which causes autosomal dominant nephrogenic diabetes insipidus is retained in the golgi complex. *J Clin Invest* 102:57–66
- Nedvetsky PI, Stefan E, Frische S, Santamaria K, Wiesner B, Valenti G, Hammer JA, III, Nielsen S, Goldenring JR, Rosenthal W, Klusmann E (2007) A role of myosin Vb and Rab11-FIP2 in the aquaporin-2 shuttle. *Traffic* 8:110–123
- Nejsum LN, Zelenina M, Aperia A, Frokiaer J, Nielsen S (2005) Bidirectional regulation of AQP2 trafficking and recycling: involvement of AQP2-S256 phosphorylation. *Am J Physiol Renal Physiol* 288:F930–F938
- Newmyer SL, Schmid SL (2001) Dominant-interfering Hsc70 mutants disrupt multiple stages of the clathrin-coated vesicle cycle in vivo. *J Cell Biol* 152:607–620
- Nielsen S (2002) Renal aquaporins: an overview. *BJU Int* 90:(Suppl 3):1–6
- Nielsen S, DiGiovanni SR, Christensen EI, Knepper MA, Harris HW (1993) Cellular and subcellular immunolocalization of vasopressin-regulated water channel in rat kidney. *Proc Natl Acad Sci U S A* 90:11663–11667
- Nielsen S, Chou C, Marples D, Christensen EI, Kishore BK, Knepper MA (1995) Vasopressin increases water permeability of kidney collecting duct by inducing translocation of aquaporin-CD water channels to plasma membrane. *Proc Natl Acad Sci U S A* 92:1013–1017
- Noda Y, Horikawa S, Katayama Y, Sasaki S (2004a) Water channel aquaporin-2 directly binds to actin. *Biochem Biophys Res Commun* 322:740–745
- Noda Y, Horikawa S, Furukawa T, Hirai K, Katayama Y, Asai T, Kuwahara M, Katagiri K, Kinashi T, Hattori M, Minato N, Sasaki S (2004b) Aquaporin-2 trafficking is regulated by PDZ-domain containing protein SPA-1. *FEBS Lett* 568:139–145
- Noda Y, Horikawa S, Katayama Y, Sasaki S (2005) Identification of a multiprotein “motor” complex binding to water channel aquaporin-2. *Biochem Biophys Res Commun* 330:1041–1047
- Oksche A, Moller A, Dickson J, Rosendahl W, Rascher W, Bichet DG, Rosenthal W (1996) Two novel mutations in the aquaporin-2 and the vasopressin V2 receptor genes in patients with congenital nephrogenic diabetes insipidus. *Hum Genet* 98:587–589
- Pearl M, Taylor A (1983) Actin filaments and vasopressin-stimulated water flow in toad urinary bladder. *Am J Physiol* 245:C28–C39
- Phillips ME, Taylor A (1989) Effect of nocodazole on the water permeability response to vasopressin in rabbit collecting tubules perfused in vitro. *J Physiol* 411:529–544

- Phillips ME, Taylor A (1992) Effect of colcemid on the water permeability response to vasopressin in isolated perfused rabbit collecting tubules. *J Physiol* 456:591–608
- Pimplikar SW, Simons K (1993) Regulation of apical transport in epithelial cells by a G_s class of heterotrimeric G protein. *Nature* 362:456–458
- Procino G, Carmosino M, Marin O, Brunanti AM, Contri A, Pinna LA, Mannucci R, Nielsen S, Tae H, Svelto M, Valenti G (2003) Ser-256 phosphorylation dynamics of aquaporin 2 during maturation from the endoplasmic reticulum to the vesicular compartment in renal cells. *FASEB J* 17:1886–1888
- Procino G, Carmosino M, Tamma G, Gouraud S, Laera A, Riccardi D, Svelto M, Valenti G (2004) Extracellular calcium antagonizes forskolin-induced aquaporin 2 trafficking in collecting duct cells. *Kidney Int* 66:2245–2255
- Sands JM, Naruse M, Baum M, Jo I, Hebert SC, Brown EM, Harris HW (1997) Apical extracellular calcium/polyvalent cation-sensing receptor regulates vasopressin-elicited water permeability in rat kidney inner medullary collecting duct. *J Clin Invest* 99:1399–1405
- Schrier RW (2007) Aquaporin-related disorders of water homeostasis. *Drug News Perspect* 20:447–453
- Simon H, Gao Y, Franki N, Hays RM (1993) Vasopressin depolymerizes apical F-actin in rat inner medullary collecting duct. *Am J Physiol* 265:C757–C762
- Sohara E, Rai T, Yang SS, Uchida K, Nitta K, Horita S, Ohno M, Harada A, Sasaki S, Uchida S (2006) Pathogenesis and treatment of autosomal-dominant nephrogenic diabetes insipidus caused by an aquaporin 2 mutation. *Proc Natl Acad Sci U S A* 103:14217–14222
- Star RA, Nonoguchi H, Balaban R, Knepper MA (1988) Calcium and cyclic adenosine monophosphate as second messengers for vasopressin in the rat inner medullary collecting duct. *J Clin Invest* 81:1879–1888
- Stefan E, Wiesner B, Baillie GS, Mollajew R, Henn V, Lorenz D, Furkert J, Santamaria K, Nedvetsky P, Hundsrucker C, Beyermann M, Krause E, Pohl P, Gall I, MacIntyre AN, Bachmann S, Houslay MD, Rosenthal W, Klussmann E (2007) Compartmentalization of camp-dependent signaling by phosphodiesterase-4D is involved in the regulation of vasopressin-mediated water reabsorption in renal principal cells. *J Am Soc Nephrol* 18:199–212
- Stork PJ, Dillon TJ (2005) Multiple roles of Rap1 in hematopoietic cells: complementary versus antagonistic functions. *Blood* 106:2952–2961
- Szaszak M, Christian F, Rosenthal W, Klussmann E (2008) Compartmentalized camp signaling in regulated exocytic processes in non-neuronal cells. *Cell Signal* 20:590–601
- Tajika Y, Matsuzaki T, Suzuki T, Ablimit A, Aoki T, Hagiwara H, Kuwahara M, Sasaki S, Takata K (2005) Differential regulation of AQP2 trafficking in endosomes by microtubules and actin filaments. *Histochem Cell Biol* 124:1–12
- Tajima T, Okuhara K, Satoh K, Nakae J, Fujieda K (2003) Two novel aquaporin-2 mutations in a sporadic Japanese patient with autosomal recessive nephrogenic diabetes insipidus. *Endocr J* 50:473–476
- Tamarappoo BK, Verkman AS (1998) Defective aquaporin-2 trafficking in nephrogenic diabetes insipidus and correction by chemical chaperones. *J Clin Invest* 101:2257–2267
- Tamma G, Klussmann E, Maric K, Aktories K, Svelto M, Rosenthal W, Valenti G (2001) Rho inhibits camp-induced translocation of aquaporin-2 into the apical membrane of renal cells. *Am J Physiol Renal Physiol* 281:F1092–F1101
- Tamma G, Klussmann E, Procino G, Svelto M, Rosenthal W, Valenti G (2003a) cAMP-induced AQP2 translocation is associated with RhoA inhibition through RhoA phosphorylation and interaction with RhoGDI. *J Cell Sci* 116:1519–1525
- Tamma G, Wiesner B, Furkert J, Hahn D, Oksche A, Schaefer M, Valenti G, Rosenthal W, Klussmann E (2003b) The prostaglandin E2 analogue sulprostone antagonizes vasopressin-induced antidiuresis through activation of Rho. *J Cell Sci* 116:3285–3294
- Tamma G, Carmosino M, Svelto M, Valenti G (2005a) Bradykinin signaling counteracts camp-elicited aquaporin 2 translocation in renal cells. *J Am Soc Nephrol* 16:2881–2889

- Tamma G, Klussmann E, Oehlke J, Krause E, Rosenthal W, Svelto M, Valenti G (2005b) Actin remodeling requires ERM function to facilitate AQP2 apical targeting. *J Cell Sci* 118:3623–3630
- Tamma G, Procino G, Strafino A, Bononi E, Meyer G, Paulmichl M, Formoso V, Svelto M, Valenti G (2007) Hypotonicity induces aquaporin-2 internalization and cytosol-to-membrane translocation of ICLn in renal cells. *Endocrinology* 148:1118–1130
- Tasken K, Aandahl EM (2004) Localized effects of camp mediated by distinct routes of protein kinase A. *Physiol Rev* 84:137–167
- Tietz PS, McNiven MA, Splinter PL, Huang BQ, Larusso NF (2006) Cytoskeletal and motor proteins facilitate trafficking of AQP1-containing vesicles in cholangiocytes. *Biol Cell* 98:43–52
- Valenti G, Frigeri A, Ronco PM, D'Ettorre C, Svelto M (1996) Expression and functional analysis of water channels in a stably AQP2-transfected human collecting duct cell line. *J Biol Chem* 271:24365–24370
- Valenti G, Procino G, Carosino M, Frigeri A, Mannucci R, Nicoletti I, Svelto M (2000) The phosphatase inhibitor okadaic acid induces AQP2 translocation independently from AQP2 phosphorylation in renal collecting duct cells. *J Cell Sci* 113:1985–1992
- van Balkom BW, Savelkoul PJ, Markovich D, Hofman E, Nielsen S, van der SP, Deen PM (2002) The role of putative phosphorylation sites in the targeting and shuttling of the aquaporin-2 water channel. *J Biol Chem* 277:41473–41479
- van Lieburg AF, Verdijk MA, Knoers VV, van Essen AJ, Proesmans W, Mallmann R, Monnens LA, Van Oost BA, van Os CH, Deen PM (1994) Patients with autosomal nephrogenic diabetes insipidus homozygous for mutations in the aquaporin 2 water-channel gene. *Am J Hum Genet* 55:648–652
- Vargas-Poussou R, Forestier L, Dautzenberg MD, Niaudet P, Dechaux M, Antignac C (1998) Mutations in the vasopressin V2 receptor and aquaporin-2 genes in twelve families with congenital nephrogenic diabetes insipidus. *Adv Exp Med Biol* 449:387–390
- Vossenkamper A, Nedvetsky PI, Wiesner B, Furkert J, Rosenthal W, Klussmann E (2007) Microtubules are needed for the perinuclear positioning of aquaporin-2 after its endocytic retrieval in renal principal cells. *Am J Physiol Cell Physiol* 293:C1129–C1138
- Wade JB, Kachadorian WA (1988) Cytochalasin B inhibition of toad bladder apical membrane responses to ADH. *Am J Physiol* 255:C526–C530
- Wong W, Scott JD (2004) AKAP signaling complexes: focal points in space and time. *Nat Rev Mol Cell Biol* 5:959–970
- Woo J, Chae YK, Jang SJ, Kim MS, Baek JH, Park JC, Trink B, Ratovitski E, Lee T, Park B, Park M, Kang JH, Soria JC, Lee J, Califano J, Sidransky D, Moon C (2008) Membrane trafficking of AQP5 and camp dependent phosphorylation in bronchial epithelium. *Biochem Biophys Res Commun* 366:321–327
- Xu DL, Martin PY, Ohara M, St John J, Pattison T, Meng X, Morris K, Kim JK, Schrier RW (1997) Upregulation of aquaporin-2 water channel expression in chronic heart failure rat. *J Clin Invest* 99:1500–1505
- Yip KP (2002) Coupling of vasopressin-induced intracellular Ca^{2+} mobilization and apical exocytosis in perfused rat kidney collecting duct. *J Physiol* 538:891–899
- Yip KP (2006) Epac-mediated Ca^{2+} mobilization and exocytosis in inner medullary collecting duct. *Am J Physiol Renal Physiol* 291:F882–F890
- Yamaki M, McIntyre S, Murphy JM, Swinnen JV, Conti M, Dousa TP (1993) ADH resistance of LLC-pk1 cells caused by overexpression of camp-phosphodiesterase type-IV. *Kidney Int* 43:1286–1297

Role of Aquaporin-4 in Cerebral Edema and Stroke

Zsolt Zador, Shirley Stiver, Vincent Wang, and Geoffrey T. Manley

Contents

1	Introduction	160
2	Aquaporins	161
2.1	Aquaporins in the Central Nervous System	162
3	Cerebral Edema in Stroke	163
3.1	Cerebral Edema in Hemorrhagic stroke	164
3.2	Cerebral Edema in Ischemic Stroke	165
4	AQP4 and Cerebral Edema	165
4.1	Mouse Models Lacking AQP4 Expression	166
4.2	Mouse Models Lacking Polarized AQP4 Expression	166
5	Aquaporin-4 as a Therapeutic Target in Stroke	167
	References	167

Abstract Cerebral edema plays a central role in the pathophysiology of many diseases of the central nervous system (CNS) including ischemia, trauma, tumors, inflammation, and metabolic disturbances. The formation of cerebral edema results in an increase in tissue water content and brain swelling which, if unchecked, can lead to elevated intracranial pressure (ICP), reduced cerebral blood flow, and ultimately cerebral herniation and death. Despite the clinical significance of cerebral edema, the mechanism of brain water transport and edema formation remain poorly understood. As a result, current therapeutic tools for managing cerebral edema have changed little in the past 90 years. “Malignant ischemic stroke” is characterized by high mortality (~80%) and represents a major clinical problem in cerebrovascular disease. Widespread ischemic injury in these patients causes progressive cerebral edema, increased ICP, and rapid clinical decline. In response to these observations, a series of recent studies have begun to target cerebral edema in the management of large ischemic strokes. During cerebral edema formation, the glial water channel aquaporin-4 (AQP4) has been shown to facilitate astrocyte swelling

G.T. Manley (✉)

Department of Neurosurgery, University of California, San Francisco, 1001 Potrero Avenue
Room 101, San Francisco, CA 94110, USA
manleyg@neurosurg.ucsf.edu

(“cytotoxic swelling”). AQP4 has also been seen to be responsible for the reabsorption of extracellular edema fluid (“vasogenic edema”). In the present review, the role of AQP4 in the development of cerebral edema is discussed with emphasis on its contribution to ischemic edema. We also examine the potential of AQP4 as a therapeutic target in edema associated with stroke.

1 Introduction

Cerebral edema is characterized by the pathological swelling of brain tissue due to progressive increase in brain water content. It is a frequent and feared clinical complication that develops in a broad range of cerebral insults such as ischemia (Ribeiro Mde et al. 2006), trauma (Zador et al. 2007), tumors (Saadoun et al. 2002) and inflammation (Papadopoulos and Verkman 2005). The rigid cranium opposes the progressive swelling of brain tissue, leading to elevated intracranial pressure, decreased cerebral blood flow, and ultimately cerebral herniation and death. Klatzo broadly categorized the mechanisms of brain tissue swelling as cytotoxic edema and vasogenic edema in 1967 (Klatzo 1967). The former process involves progressive cell swelling due to rapid water uptake, whereas in the case of vasogenic edema water leaks into the extracellular space due to defects in the blood–brain barrier. Although these two mechanisms coexist in most brain pathologies, instead of a pure cytotoxic edema or vasogenic edema, there is typically an appreciable dominance of one type over the other in each disease. For example, vasogenic edema seems to dominate in tumors and cerebral abscesses, while cytotoxic edema develops in ischemic stroke and brain trauma.

Cytotoxic edema is a significant clinical problem that can develop in response to a large (“malignant”) middle cerebral artery (MCA) occlusion (Hacke et al. 1996; Bardutzky and Schwab 2007) and has been associated with approximately 80% mortality rate. Cerebral vascular occlusion initiates a sequence of events involving cell swelling, followed by BBB leakage and hemorrhagic conversion of the tissue (Simard et al. 2007). The strategy for the treatment of cerebral edema associated with these large ischemic strokes is limited to the use of intravascular administration of hyperosmolar solutions to remove the excess water from the brain, or removal of a large bone flap to allow the brain to swell outside the rigid cranium (decompressive craniectomy). These methods have remained unchanged for the past 90 years. More recently, the discovery of aquaporin membrane water channels has provided new insights into the molecular mechanisms of edema formation and brain water transport.

The glial membrane water channel aquaporin-4 (AQP4) is largely expressed in astrocytic processes adjacent to cerebral capillaries and pial membranes lining the subarachnoid space (Fig. 1). Such strategic localization at these tissue-water interfaces, and the high water permeability of the channel, makes AQP4 an important route for transporting water to and from the brain. A large body of evidence from transgenic mice deficient in AQP4 has demonstrated the role of this water channel

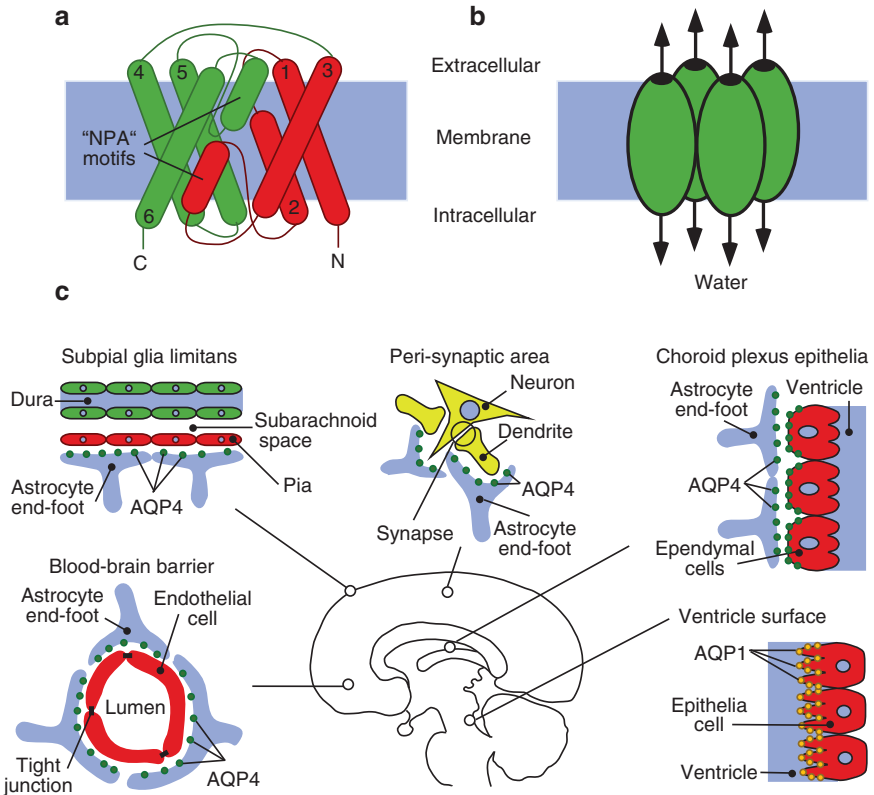


Fig. 1 (a, b) Diagram depicts the structure of an AQP monomer and its clustering into tetramers. (a) Schematic demonstration of the transmembrane α -helices of AQP4 numbered from 1–6, which surround the highly selective water pore. The highly conserved “NPA” motifs are indicated. (b) AQP organizes into tetramers in the cell membrane with each unit functioning as an independent pore. (c) The distribution of CNS AQPs. AQP4 is polarized at the glial end-feet facing CSF–brain, blood–brain barrier and peri-synaptic areas. Ependymal cells have basolateral expression of AQP4. The apical processes of the choroid plexus cells are rich in AQP1 expression (adapted from Zador and Manley 2008)

in cytotoxic and vasogenic edema. These findings suggest AQP4 is a potential therapeutic target in the treatment of cerebral edema developing in response to various CNS pathologies including stroke.

2 Aquaporins

Aquaporins are highly permeable water channels widely found in different tissues of the body (Verkman 2005). Structurally, a single AQP channel is formed by a six transmembrane helix protein that forms a water selective pore in the center of the molecule. The channel functions as tetramers in the cell membrane. The structural

significance of the AQP4 subtype is that its tetramers organize into large (~100 nm) clusters termed orthogonal array particles (OAPs), visible through freeze fracture electron microscopy of astrocyte processes (Rash et al. 1998).

The first aquaporin (AQP1) was discovered as the membrane water channel responsible for rapid red blood cell swelling in response to osmotic challenge. In addition to facilitating water flux through cell membranes, some family members such as AQP3, AQP7, and AQP9 also allow glycerol transport and may be involved in cell metabolism (Hara-Chikuma and Verkman 2006). Recent data has shown a number of unusual roles for AQPs in cellular functions such as tumor angiogenesis (Saadoun et al. 2005a), glial scar formation (Saadoun et al. 2005b), pain (Oshio et al. 2006) and neuroexcitation (Binder et al. 2006; Padmawar et al. 2005).

2.1 Aquaporins in the Central Nervous System

Aquaporins in the CNS are seen to facilitate water transport between the major compartments of the brain (Fig. 2): (1) the CSF space defined as the cerebral ventricles and subarachnoid space; (2) the brain parenchyma consisting of intracellular

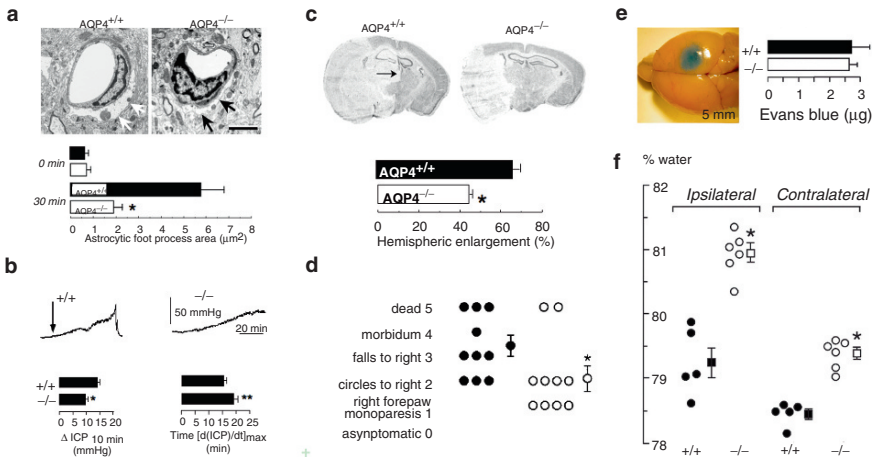


Fig. 2 The bimodal role of AQP4 in the pathomechanism of cerebral edema. **(a)** Electron micrographs demonstrating pronounced perivascular astrocyte foot process swelling (arrows) 30 min after acute water intoxication in wild-type mice, whereas AQP4^{-/-} mice lack cytototoxic cell swelling. (bar = 3 μm) **(b)** Wild-type mice show accelerated brain swelling and intracranial pressure increase (ICP) compared to AQP4^{-/-} mice following IP water intoxication. Increased brain water uptake in wild-type mice is demonstrated by higher relative ICP elevation at 10 min (Δ ICP_{10 min}) and significantly shorter time required to reach maximal ICP value (time to $[d(ICP)/dt]_{max}$). **(c)** Reduced hemispheric enlargement in AQP4^{-/-} mice compared to wild type controls 24 h following permanent MCA occlusion. Note the midline shift in the wild-type brain (arrow). **(d)** Improved functional outcome 24 h after MCA occlusion in AQP4^{-/-} mice. **(e)** Cortical freeze injury disrupts the blood-brain barrier as assessed by Evans Blue extravasation and causes vasogenic edema. **(f)** Brain water content increase in AQP4^{-/-} mice compared to wild-type controls in vasogenic edema

and extracellular space; and (3) the intravascular compartment (Zador et al. 2007). Two members of the aquaporin family, AQP1 and AQP4 largely manifest at the interfaces between these compartments where they participate in the maintenance of brain water homeostasis.

2.1.1 Aquaporin-4 in the Central Nervous System

In the CNS, AQP4 expression is restricted to astrocytes throughout the brain and spinal cord and the ependymal cells that line the cerebral ventricles (Nielsen et al. 1997). There is a characteristic subcellular distribution of AQP4 in astrocytes: it is highly concentrated at cell surfaces of the blood–brain and CSF–brain barriers such as the astrocytic end-feet and glia limitans. At these important water transport sites, AQP4 colocalizes with the inwardly rectifying potassium channel Kir4.1 where it is proposed to act as a water-potassium transport complex (Connors and Kofuji 2002; Nagelhus et al. 2004). The dystroglycan complex (DGC) provides the molecular scaffolding for the polarized colocalization of these two channels. Deletion of one of the DGC complex proteins, alpha-syntrophin, results in the failure of AQP4 to properly colocalize in the plasma membrane without altering overall AQP4 protein expression (Neely et al. 2001). The polarized expression of AQP4 is critical for its function in brain water homeostasis, as the deletion of alpha-syntrophin creates a phenotype similar to that of the AQP4-deficient mice.

2.1.2 Aquaporin-1 in the Central Nervous System

AQP1 is expressed in the apical membrane of the choroid plexus epithelia where it facilitates cerebrospinal fluid (CSF) production. The transcellular water flux through AQP1 contributes approximately 20–30% of CSF volume as demonstrated by AQP1-deficient mice (Oshio et al. 2005). In physiological circumstances, the remaining part of the brain is void of AQP1, in contrast to other organs of the body where it is abundantly expressed in capillary endothelium. However, in pathological states of the CNS such as tumors, there is an upregulation of AQP1 (Papadopoulos et al. 2002) in the endothelia of cerebral capillaries. Based on this finding, it seems that AQP1 is predominantly expressed in the choroid plexus and functions primarily to contribute to CSF production. However in the brain, some AQP1 pathologies are expressed *de novo* in cerebral endothelia, possibly to aid clearance of edema fluid from the brain.

3 Cerebral Edema in Stroke

Based on their pathomechanism, strokes can be categorized as hemorrhagic or ischemic, and account for 20% and 80% of the cases respectively. Pathways leading to edema formation in hemorrhagic stroke differ from those in ischemic stroke (Fig. 3).

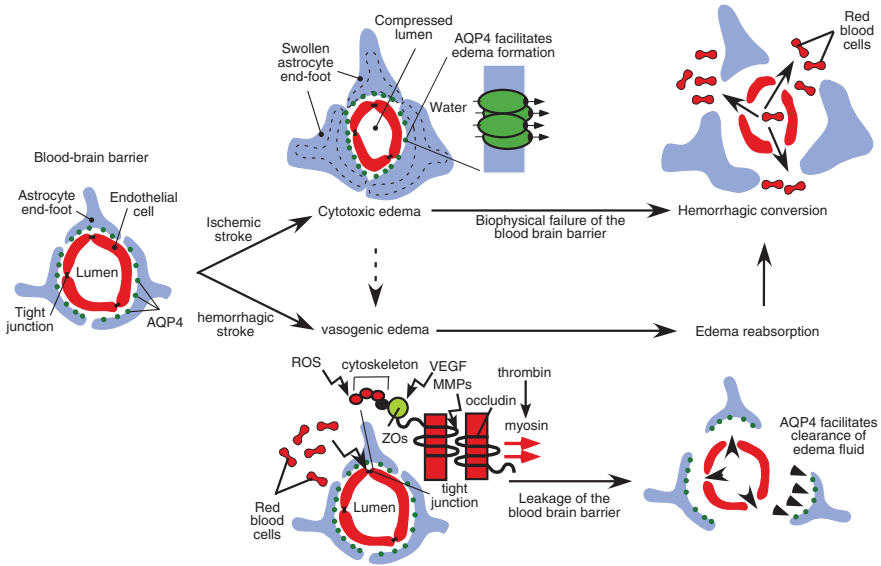


Fig. 3 Mechanism of edema formation in ischemic and hemorrhagic stroke (see text for details). In ischemic stroke (above) AQP4 facilitates water uptake of perivascular astrocyte end-feet resulting in subsequent compression of the adjacent capillary lumen. As cellular damage evolves, the mechanism shifts into vasogenic edema and later hemorrhagic conversion. During hemorrhagic stroke, factors derived from the clot act on different components of the endothelial tight junction, leading the disruption of the BBB seal. AQP4 facilitates the reabsorption of edema fluid from the extracellular space

3.1 Cerebral Edema in Hemorrhagic stroke

In hemorrhagic stroke, following the initial physical trauma from the hydrostatic effect of intracerebral hemorrhage, perifocal edema formation is initiated by clot derived proteins and vasoactive substances impairing BBB integrity through direct or indirect mechanisms (Xi et al. 2006). The intracerebral injection of blood substrates in animal models show thrombin, plasminogen activator and urokinase contribute to brain edema formation (Matsuoka and Hamada 2002; Lee et al. 1995; Figueroa et al. 1998). The activation of thrombin was shown to cause inflammatory-cell infiltration, and scar formation (Xi et al. 2006) as well as direct disruption of the BBB by inducing endothelial cell retraction (Satpathy et al. 2004). The presence of tissue plasminogen activator and urokinase has been found to enhance this effect, presumably by competing for thrombin inhibitors. The opening of the BBB seal leads to the formation of a proteinacious ultrafiltrate causing vasogenic edema peaking at 10–20 days in humans following ICH (Xi et al. 2006). The complement is introduced through the BBB defect, leading to formation of membrane attack complexes (MAC) and destruction of CNS cells and RBCs (Hua et al. 2000). A subsequent component of edema formation is the lysis of red blood cells followed by liberation of hemoglobin, which inflict cellular damage (hemoglobin toxicity) through

caspsases (Wang et al. 2002) and oxidative mechanisms (Goldstein et al. 2003). Cytotoxic edema ensues in concert with secondary cellular injury. In later phases of clot evolution and degradation, thrombin, hemoglobin degradation products, inflammatory mediators, interleukins, and metalloproteinases together facilitate both vasogenic and cytotoxic edema (Rincon and Mayer 2004). Vasogenic and cytotoxic edema together last 2–4 weeks. Empirically, intravenous hyperosmolar therapy with mannitol is used in ICH for indications of raised ICP or imaging with findings of significant cerebral edema. Randomized studies have not been conducted and no evidence based conclusions can be made regarding the use of hyperosmolar therapy for acute intracerebral hemorrhage (Bereczki et al. 2000). The role, if any, of AQP expression and function in intracerebral hemorrhage has not been explored.

3.2 Cerebral Edema in Ischemic Stroke

Ischemic stroke initiates a sequence of different edema mechanisms in a stepwise fashion (Simard et al. 2007). The formation of a thrombus occludes the cerebral artery and impairs cellular metabolism resulting in cellular swelling (cytotoxic edema), followed by leakage of the BBB (vasogenic edema) and finally the ischemic tissue undergoes hemorrhagic conversion. The disruption of cerebral blood flow in ischemia leads to the impairment of ATP synthesis, leading to insufficient Na^+/K^+ ATPase function. The sodium fluxes driven by the transmembrane electrochemical gradient remain unopposed, causing net accumulation of intracellular sodium. The anaerobic glycolysis initiated in response to ischemia cause accumulation of lactate, which acts together with sodium to draw water into the cell creating cytotoxic edema. Further cellular damage caused by ischemia results in BBB disruption through a number of proposed mechanisms such as reverse pinocytosis (Castejon 1984), disputed Ca^{2+} signaling (Brown and Davis 2002), and actions of other agents such as VEGF (Weis and Cheresch 2005), and MMPs (Asahi 2001). Depending on the depth of ischemia, the BBB may lose its entire physical integrity leading to hemorrhagic conversion: all components of the blood are extravasated into the brain parenchyma leading to catastrophic tissue destruction. The role of AQP4 has been explored in several models of ischemic stroke where it participates in the formation of cerebral edema.

4 AQP4 and Cerebral Edema

Multiple mouse models have been employed to explore the role of AQP4 in the pathogenesis cerebral edema. The main approaches have been either to knock-out AQP4 expression completely or to disrupt the polarized subcellular expression of AQP4.

4.1 Mouse Models Lacking AQP4 Expression

Phenotypic analysis of AQP4-deficient mice has provided new insights into the mechanisms of water transport during the development of cerebral edema (Manley et al. 2004). Because AQP4 allows bidirectional water flux through cell membranes, it is unsurprising that it facilitates water transport to and from the CNS. These experiments demonstrate the role of AQP4 in facilitating cellular water uptake as well as clearance of extracellular fluid from the brain.

The loss of AQP4 function has a significant impact on pathological response of the CNS. In disease models, such as acute cerebral ischemia (Manley et al. 2000), water intoxication (Manley et al. 2000; Yang et al. 2008) and traumatic brain injury, water moves into the cell resulting in cytotoxic brain edema. The deletion of AQP4 has shown to impair cell water uptake in all of these models tested to date (Fig. 2a–d), as demonstrated by reduced brain water content, infarct size, lesion volume, and lower ICP values. These favorable measures recorded from AQP4-deficient mice were mirrored by improved survival and better functional outcome compared to wild-type mice.

In another subset of CNS pathologies such as brain tumors, cold brain injury, and persistent ischemia, edema is created via leakage of iso-osmolar fluid through defective blood–brain barrier (BBB) into the brain extracellular space resulting in vasogenic edema. In these models, deletion of AQP4 resulted in worsening of cerebral edema assessed by brain wet to dry weight ratio and intracranial pressure (Papadopoulos et al. 2004). The detrimental effect of AQP4 deletion also translated to lower neurological score. Based on these findings it was concluded that AQP4 facilitates the clearance of vasogenic cerebral edema in pathologies where edema fluid accumulates in the extracellular space.

4.2 Mouse Models Lacking Polarized AQP4 Expression

As an alternative approach to testing AQP4 function, experiments were aimed at disrupting the polarized pattern of AQP4 distribution. The anchoring of AQP4 to the astrocytic foot processes is dependent on the dystrophin- α -syntrophin complex (Amiry-Moghaddam et al. 2003a, 2004a). Dystrophin is the protein mutated in Duchenne Muscular Dystrophy and is part of a large membrane assembly that link the cytoskeleton to the extracellular matrix (Worton 1995). Dystrophin binds to dystrobrevin, which provides a scaffold for syntrophins including α -syntrophin (Peters et al. 1997). The dystrophin complex is localized to many tissues that express AQP4, including perivascular astrocytic foot process, renal collecting duct and skeletal muscle (Neely et al. 2001). This prompted the investigation of expression level of AQP4 in mice deficient in various components of the dytroglycan complex (Neely et al. 2001; Vajda et al. 2002).

Co-immunoprecipitation studies show that AQP4 binds to the dystrophin complex through its interaction with α -syntrophin and Dp71 (Neely et al. 2001). Alpha

syntrophin deficient mice lack polarized expression of AQP4 in astrocytic end-feet: Immunogold labeling demonstrates an ~eightfold reduction of AQP4 reactivity at the perivascular astrocytic end-feet of α -syntrophin deficient mice compared to wild-type controls (Neely et al. 2001). Such mislocalization translates into a near equivalent phenotype of AQP4 knock out mice. Following repetitive orthodromic stimulation of hippocampal slides, recovery of extracellular potassium significantly slows in α -syntrophin deficient mice (Amiry-Moghaddam et al. 2003b). The development of cytotoxic edema also significantly retards in α -syntrophin deficient mice following acute hyponatremia (Amiry-Moghaddam et al. 2004b) and transient cerebral ischemia (Amiry-Moghaddam et al. 2003a). The complete deficiency of the dystroglycan complex in *dmx* mice has similar impact, resulting in delayed development of cytotoxic brain edema following acute hyponatremia (Vajda et al. 2002). Although both these mouse strains have similar AQP4 expression as the wild-type controls, the mere mislocalization of AQP4 is sufficient to impair channel function to a significant extent. Recent data has demonstrated marked reduction of AQP4 in glial cells of the retinal (Muller cells) isolated from Dp71- deficient mice (Fort et al. 2008). Electrophysiological studies have shown reduced potassium currents in relation to the reduced AQP4 expression further fortifying the concept of a Kir4.1-AQP4 potassium-water trafficking complex.

Further studies in models of cerebral edema using latter mouse strains could be of merit. The abolishment of AQP4 polarization by modulating the DCG components is a more attractive strategy than manipulating the AQP4 expression directly because it avoids changing AQP4 expression in other tissues.

5 Aquaporin-4 as a Therapeutic Target in Stroke

An important goal in the treatment of stroke is the control and reduction of cerebral edema. While formulating strategies targeting AQP4 in edema therapy the bimodal role of AQP4 in the development of vasogenic and cytotoxic edema has to be borne in mind. The reabsorption of vasogenic edema appearing in hemorrhagic stroke and late ischemic stroke could be facilitated by increased expression of functional AQP4, as the development of cytotoxic edema in early ischemia could be controlled by AQP4 inhibition. Thus, the type of stroke to be treated and the timing of AQP4 modulation will have to be carefully considered in the development of any targeted intervention.

Acknowledgement Supported by NIH NS050173 and the UCSF Brain and Spinal Injury Center.

References

- Amiry-Moghaddam M, Otsuka T, Hurn PD, et al. (2003a) An alpha-syntrophin-dependent pool of AQP4 in astroglial end-feet confers bidirectional water flow between blood and brain. *Proc Natl Acad Sci U S A* 100:2106–2111

- Amiry-Moghaddam M, Williamson A, Palomba M, et al. (2003b) Delayed K⁺ clearance associated with aquaporin-4 mislocalization: phenotypic defects in brains of alpha-syntrophin-null mice. *Proc Natl Acad Sci U S A* 100:13615–13620
- Amiry-Moghaddam M, Frydenlund DS, Ottersen OP (2004a) Anchoring of aquaporin-4 in brain: molecular mechanisms and implications for the physiology and pathophysiology of water transport. *Neuroscience* 129:999–1010
- Amiry-Moghaddam M, Xue R, Haug FM, et al. (2004b) Alpha-syntrophin deletion removes the perivascular but not endothelial pool of aquaporin-4 at the blood–brain barrier and delays the development of brain edema in an experimental model of acute hyponatremia. *FASEB J* 18:542–544
- Asahi M, Wang X, Mori T, Sumii T, Jung JC, Moskowitz MA, Fini ME, Lo EH. Effects of matrix metalloproteinase-9 gene knock-out on the proteolysis of blood-brain barrier and white matter components after cerebral ischemia. *J Neurosci*. 2001 Oct 1;21(19):7724–32
- Bardutzky J, Schwab S (2007) Antiedema therapy in ischemic stroke. *Stroke* 38:3084–3094
- Berezcki D, Liu M, Prado GF, Fekete I (2000) Cochrane report: a systematic review of mannitol therapy for acute ischemic stroke and cerebral parenchymal hemorrhage. *Stroke* 31:2719–2722
- Binder DK, Yao X, Zador Z, Sick TJ, Verkman AS, Manley GT (2006) Increased seizure duration and slowed potassium kinetics in mice lacking aquaporin-4 water channels. *Glia* 53:631–636
- Brown RC, Davis TP (2002) Calcium modulation of adherens and tight junction function: a potential mechanism for blood–brain barrier disruption after stroke. *Stroke* 33:1706–1711
- Castejon OJ (1984) Formation of transendothelial channels in traumatic human brain edema. *Pathol Res Pract* 179:7–12
- Connors NC, Kofuji P (2002) Dystrophin Dp71 is critical for the clustered localization of potassium channels in retinal glial cells. *J Neurosci* 22:4321–4327
- Figueroa BE, Keep RF, Betz AL, Hoff JT (1998) Plasminogen activators potentiate thrombin-induced brain injury. *Stroke* 29:1202–1207; discussion 1208
- Fort PE, Sene A, Pannicke T, et al. (2008) Kir4.1 and AQP4 associate with Dp71- and utrophin-DAPs complexes in specific and defined microdomains of Muller retinal glial cell membrane. *Glia* 56:597–610
- Goldstein L, Teng ZP, Zeserson E, Patel M, Regan RF (2003) Hemin induces an iron-dependent, oxidative injury to human neuron-like cells. *J Neurosci Res* 73:113–121
- Hacke W, Schwab S, Horn M, Spranger M, De Georgia M, von Kummer R (1996) ‘Malignant’ middle cerebral artery territory infarction: clinical course and prognostic signs. *Arch Neurol* 53:309–315
- Hara-Chikuma M, Verkman AS (2006) Physiological roles of glycerol-transporting aquaporins: the aqaglyceroporins. *Cell Mol Life Sci* 63:1386–1392
- Hua Y, Xi G, Keep RF, Hoff JT (2000) Complement activation in the brain after experimental intracerebral hemorrhage. *J Neurosurg* 92:1016–1022
- Klatzo I (1967) Presidential address. Neuropathological aspects of brain edema. *J Neuropathol Exp Neurol* 26:1–14
- Lee KR, Betz AL, Keep RF, Chenevert TL, Kim S, Hoff JT (1995) Intracerebral infusion of thrombin as a cause of brain edema. *J Neurosurg* 83:1045–1050
- Manley GT, Fujimura M, Ma T, et al. (2000) Aquaporin-4 deletion in mice reduces brain edema after acute water intoxication and ischemic stroke. *Nat Med* 6:159–163
- Manley GT, Binder DK, Papadopoulos MC, Verkman AS (2004) New insights into water transport and edema in the central nervous system from phenotype analysis of aquaporin-4 null mice. *Neuroscience* 129:983–991
- Matsuoka H, Hamada R (2002) Role of thrombin in CNS damage associated with intracerebral haemorrhage: opportunity for pharmacological intervention? *CNS Drugs* 16:509–516
- Nagelhus EA, Mathiisen TM, Ottersen OP (2004) Aquaporin-4 in the central nervous system: cellular and subcellular distribution and coexpression with KIR4.1. *Neuroscience* 129:905–913
- Neely JD, Amiry-Moghaddam M, Ottersen OP, Froehner SC, Agre P, Adams ME (2001) Syntrophin-dependent expression and localization of Aquaporin-4 water channel protein. *Proc Natl Acad Sci U S A* 98:14108–14113

- Nielsen S, Nagelhus EA, Amiry-Moghaddam M, Bourque C, Agre P, Ottersen OP (1997) Specialized membrane domains for water transport in glial cells: high-resolution immunogold cytochemistry of aquaporin-4 in rat brain. *J Neurosci* 17:171–180
- Oshio K, Watanabe H, Song Y, Verkman AS, Manley GT (2005) Reduced cerebrospinal fluid production and intracranial pressure in mice lacking choroid plexus water channel Aquaporin-1. *FASEB J* 19:76–78
- Oshio K, Watanabe H, Yan D, Verkman AS, Manley GT (2006) Impaired pain sensation in mice lacking aquaporin-1 water channels. *Biochem Biophys Res Commun* 341:1022–1028
- Padmawar P, Yao X, Bloch O, Manley GT, Verkman AS (2005) K⁺ waves in brain cortex visualized using a long-wavelength K⁺-sensing fluorescent indicator. *Nat Methods* 2:825–827
- Papadopoulos MC, Verkman AS (2005) Aquaporin-4 gene disruption in mice reduces brain swelling and mortality in pneumococcal meningitis. *J Biol Chem* 280:13906–13912
- Papadopoulos M, Saadoun S, Krishna S, Bell B, Davies D (2002) The aquaporin-1 water channel protein is abnormally expressed in oedematous human brain tumours. *J Anat* 200:531–532
- Papadopoulos MC, Manley GT, Krishna S, Verkman AS (2004) Aquaporin-4 facilitates reabsorption of excess fluid in vasogenic brain edema. *FASEB J* 18:1291–3
- Peters MF, O'Brien KF, Sadoulet-Puccio HM, Kunkel LM, Adams ME, Froehner SC (1997) beta-dystrobrevin, a new member of the dystrophin family. Identification, cloning, and protein associations. *J Biol Chem* 272:31561–31569
- Rash JE, Yasumura T, Hudson CS, Agre P, Nielsen S (1998) Direct immunogold labeling of aquaporin-4 in square arrays of astrocyte and ependymocyte plasma membranes in rat brain and spinal cord. *Proc Natl Acad Sci U S A* 95:11981–11986
- Ribeiro Mde C, Hirt L, Bogousslavsky J, Regli L, Badaut J (2006) Time course of aquaporin expression after transient focal cerebral ischemia in mice. *J Neurosci Res* 83:1231–1240
- Rincon F, Mayer SA (2004) Novel therapies for intracerebral hemorrhage. *Curr Opin Crit Care* 10:94–100
- Saadoun S, Papadopoulos MC, Davies DC, Krishna S, Bell BA (2002) Aquaporin-4 expression is increased in oedematous human brain tumours. *J Neurol Neurosurg Psychiatry* 72:262–265
- Saadoun S, Papadopoulos MC, Hara-Chikuma M, Verkman AS (2005a) Impairment of angiogenesis and cell migration by targeted aquaporin-1 gene disruption. *Nature* 434:786–792
- Saadoun S, Papadopoulos MC, Watanabe H, Yan D, Manley GT, Verkman AS (2005b) Involvement of aquaporin-4 in astroglial cell migration and glial scar formation. *J Cell Sci* 118:591–598
- Satpathy M, Gallagher P, Lizotte-Waniewski M, Srinivas SP (2004) Thrombin-induced phosphorylation of the regulatory light chain of myosin II in cultured bovine corneal endothelial cells. *Exp Eye Res* 79:477–486
- Simard JM, Kent TA, Chen M, Tarasov KV, Gerzanich V (2007) Brain oedema in focal ischaemia: molecular pathophysiology and theoretical implications. *Lancet Neurol* 6:258–268
- Vajda Z, Pedersen M, Fuchtbauer EM, et al. (2002) Delayed onset of brain edema and mislocalization of aquaporin-4 in dystrophin-null transgenic mice. *Proc Natl Acad Sci U S A* 99:13131–13136
- Verkman AS (2005) More than just water channels: unexpected cellular roles of aquaporins. *J Cell Sci* 118:3225–3232
- Wang X, Mori T, Sumii T, Lo EH (2002) Hemoglobin-induced cytotoxicity in rat cerebral cortical neurons: caspase activation and oxidative stress. *Stroke* 33:1882–1888
- Weis SM, Cheresh DA (2005) Pathophysiological consequences of VEGF-induced vascular permeability. *Nature* 437:497–504
- Worton R (1995) Muscular dystrophies: diseases of the dystrophin-glycoprotein complex. *Science* (New York, NY) 270:755–756
- Xi G, Keep RF, Hoff JT (2006) Mechanisms of brain injury after intracerebral haemorrhage. *Lancet Neurol* 5:53–63
- Yang B, Zador Z, Verkman AS (2008) Glial cell aquaporin-4 overexpression in transgenic mice accelerates cytotoxic brain swelling. *J Biol Chem* 283:15280–15286

- Zador Z, Bloch O, Yao X, Manley GT (2007) Aquaporins: role in cerebral edema and brain water balance. *Prog Brain Res* 161:185–194
- Zsolt Zador MD, Xiaoming Yao MD, Ph.D., and Geoffrey T Manley MD, Ph.D. Role of Aquaporins in Non-synaptic Mechanisms of Epilepsy *Encyclopedia of Basic Epilepsy Research* Ed. Schwartzkroin, P., Elsevier, Amsterdam (In Press)

Aquaporins as Potential Drug Targets for Meniere's Disease and its Related Diseases

Taizo Takeda and Daizo Taguchi

Contents

1	Introduction	172
2	Expression of Aquaporins (AQPs) in the Inner Ear	172
2.1	Distribution of AQPs in the Inner Ear	172
2.2	Detailed Localization of AQPs	172
3	Hormonal Regulation of AQPs Water Channels	178
3.1	Arginine Vasopressin-AQP2 (AVP-AQP2) System in the Inner Ear	178
3.2	Corticosteroids Mediated Regulation of AQPs Expression	180
4	Role of AVP-AQP2 System on Endolymphatic Hydrops and its Treatment	181
	References	182

Abstract The homeostasis of water in the inner ear is essential for maintaining function of hearing and equilibrium. Since the discovery of aquaporin water channels, it has become clear that these channels play a crucial role in inner ear fluid homeostasis. Indeed, proteins or mRNAs of AQP1, AQP2, AQP3, AQP4, AQP5, AQP6, AQP7 and AQP9 are expressed in the inner ear. Many of them are expressed mainly in the stria vascularis and the endolymphatic sac, which are the main sites of secretion and/or absorption of endolymph. Vasopressin type2 receptor is also expressed there. Water homeostasis of the inner ear is regulated in part via the arginine vasopressin-AQP2 system in the same fashion as in the kidney, and endolymphatic hydrops, a morphological characteristic of Meniere's disease, is thought to be caused by mal-regulation of this system. Therefore, aquaporins appear to be important for the development of novel drug therapies for Meniere's disease and related disorders.

T. Takeda (✉)

Department of Otolaryngology, Head and Neck Surgery, Kochi Medical School, Kohasu, Oko-cho, Nankoku, Kochi, 783-8505, Japan
takedat@kochi-u.ac.jp

1 Introduction

The inner ear is composed of membranous labyrinth and surrounding bony labyrinth. The sensory epithelium, which responds to auditory and vestibular stimuli, is involved in the membranous labyrinth. The membranous labyrinth separates two compartments which are filled with fluids of completely different composition. The lumen of the membranous labyrinth is filled with endolymph, K-rich, positively polarized fluid, whereas the surrounding spaces are filled with perilymph, with a composition similar to usual extracellular fluid. The inner ear fluids play a major role in the cochlear and vestibular physiology, through transmission of mechanical stimuli to the hair cells, on one hand, and transduction of this signal to a nerve potential, on the other. The homeostasis of the inner ear fluids is therefore essential for maintenance of audio-vestibular function.

Generally, homeostasis of fluids of living organisms is conducted in close and complex association with ions and water regulation. As regards ion regulation in the inner ear, the role of ion channels, ion pumps or cotransporters is fairly well studied. Water regulation has been less studied till recently. Since the discovery of aquaporin (AQP) water channels (Agre et al. 1993), however, it appears that these channels may play a crucial role in inner ear fluid homeostasis. The present paper is focused on a review of the contribution of AQP water channels to the regulation of the inner ear fluids, especially endolymph, and the role of AQP water channels in the formation of endolymphatic hydrops which is the most common histological feature of Meniere's disease.

2 Expression of Aquaporins (AQPs) in the Inner Ear

2.1 Distribution of AQPs in the Inner Ear

AQP water channels play an important role in water homeostasis in all living organisms. As the major component of the inner ear is water, various subtypes of aquaporins are expected to be expressed in the inner ear. Actually, PC-R and histochemistry studies have revealed that multiple types of AQPs are expressed in the cochlea, vestibule, and/or the endolymphatic sac. Table 1 shows the distribution of AQPs in the cochlea, vestibule and endolymphatic sac. Expressions of AQPs mRNA and/or protein are widely distributed in the inner ear. In particular, multiple isoforms of AQP are abundantly expressed in the endolymphatic sac, which is thought to be one of the main sites of secretion and/or absorption of endolymph (Sterkers et al. 1988).

2.2 Detailed Localization of AQPs

2.2.1 AQP1

In the cochlea, AQP1 immunoreactivity was seen in type III fibrocytes in the spiral ligament (Huang et al. 2002; Merves et al. 2003; Sawada et al. 2003; Stankovic et al.

Table 1 Distribution of AQPs in the Inner Ear

Isoform	Cochlea	Vestibulum	Endolymphatic sac	References
AQP1	+		+	Stankovic et al. (1995); Takumi et al. (1998); Beitz et al. (1999); Sawada et al. (2003); Kakigi et al. (2008); Nishimura et al. (2008)
AQP2	+		+	Kumagami et al. (1998); Beitz et al. (1999); Mhatre et al. (2002); Sawada et al. (2002); Couloigner et al. (2004); Fukushima et al. (2005); Taguchi et al. (2007); Nishimura et al. (2008)
AQP3	+	+	+	Beitz et al. (1999); Kakigi et al. (2008); Nishimura et al. (2008)
AQP4	+		+	Minami et al. (1998); Takumi et al. (1998); Li et al. (2001); Huang et al. (2002); Lopez et al. (2007); Kakigi et al. (2008); Nishimura et al. (2008)
AQP5	+			Mhatre et al. (1999); Löwenheim et al. (2004)
AQP6	+	+	+	Beitz et al. (1999); Fukushima et al. (2004); Taguchi et al. (2008)
AQP7	+	+	+	Huang et al. (2002); Nishimura et al. (2008)
AQP8	+	+	+	Han et al. (2005); Nishimura et al. (2008)
AQP9	+	+	+	Huang et al. (2002); Nishimura et al. (2008)

1995), and also observed in the stria vascularis (Sawada et al. 2003). Immunoelectron microscopic study revealed that AQP1 immunoreactivity localized to plasma membranes of the intermediate cells of the stria vascularis (Sawada et al. 2003). AQP1 was also present in perilymphatic bone lining cells and in the capillary wall under the spiral ligament (Huang et al. 2002; Merves et al. 2003; Stankovic et al. 1995). In the vestibular system, immunoreactivity of AQP1 was observed strongly in the endolymphatic side of the saccular membrane, but only weakly in the utricle membrane (Huang et al. 2002). Weak AQP1 immunoreactivity was also seen in some connective tissue fibrocytes near the bone of the ampullary crista and in the membrana limitans. However, its staining was clearly absent in the sensory epithelium. In the endolymphatic sac, strong AQP1 immunoreactivity was observed in fibrocytes of subepithelial connective tissue at the juncture between the rugose and smooth portions of mouse and rat endolymphatic sac (Huang et al. 2002; Merves et al. 2003; Sawada et al. 2003; Kakigi et al. 2008; Nishimura et al. 2008). In the human cochlea, AQP1 immunoreactivity was confirmed to be localized in the fibrocytes of the spiral ligament of the human cochlea (Lopez et al. 2007).

2.2.2 AQP2

There is some difference of opinion about AQP2 expression in the inner ear. Kumagami et al. (1998) and Beitz et al. (1999) reported AQP2 mRNA expression was not seen in any inner ear region other than the endolymphatic sac. Further, Huang et al. (2002) recorded AQP2 mRNA could not be detected in the whole inner ear tissues of mice, although the primer used was confirmed to amplify AQP2 mRNA from the kidney tissues. In contrast, Sawada et al. (2002) showed AQP2 mRNA was expressed in the cochlea and the endolymphatic sac, and the expression of AQP mRNA was up-regulated by an elevation in arginine vasopressin (AVP). Mhatre et al. (2002) also observed that AQP2 protein was expressed in structures bordering the endolymph, including Reissner's membrane, the organ of Corti, inner and outer sulcus cells, and the spiral limbus in the rat and mouse cochlea. However, Zhong et al. (Zhong and Liu 2003) noted AQP2 was labeled only in Reissner's membrane, and not the epithelial cell layer separating the cochlear duct from scala vestibuli, the organ of Corti and supporting cells, including cells of Claudius and Hensen, and those of the inner and outer sulcus. Both reports were in agreement with the observations that AQP2 was not expressed in the stria vascularis, which surrounds the scala media containing endolymph. According to studies of the developmental temporal and spatial expression pattern of AQP2 in the developing mouse inner ear (Marples et al. 1998), however, the endolymphatic sac and stria vascularis expression of AQP2 occur fairly late during development, but demonstrate a distinct pattern of immunolabeling. In our observation, AQP2 protein was clearly expressed not only in the stria vascularis but also in the endolymphatic sac of rats (Fukushima et al. 2005; Nishimura et al. 2008).

Regarding AQP2 expression in the endolymphatic sac, RT-PCR, autoradiography and immunohistochemistry studies supported that AQP2 was expressed in the epithelium of the endolymphatic sac (Beitz et al. 1999; Fukushima et al. 2005; Kumagami et al. 1998; Merves et al. 2000; Sawada et al. 2002). AQP2 expression was also confirmed in human endolymphatic sac tissues (Couloigner et al. 2004; Taguchi et al. 2007).

AQP2 is also known to be expressed in the vestibular organ fairly late during development of the inner ear (Marples et al. 1998). Although the sensory epithelium of the vestibule is one of main sites of secretion and/or resorption of endolymph, there is no report supporting AQP2 expression in the vestibular organ.

2.2.3 AQP3

Only one report exists concerning immunolocalization of AQP3 in the mouse inner ear. According to this report (Huang et al. 2002), in the cochlea, AQP3 is abundant in a portion of the spiral ligament near the area where the basilar membrane anchors, and in cells bordering the inner spiral tunnel. In the vestibular system, AQP3 is expressed in the fibrocytes in the subepithelial connective tissues of the saccule, but not of the utricle. In the endolymphatic sac, immunostaining of AQP3 is noticed at the rugose portion, but only weakly in the intradural portion. Our re-

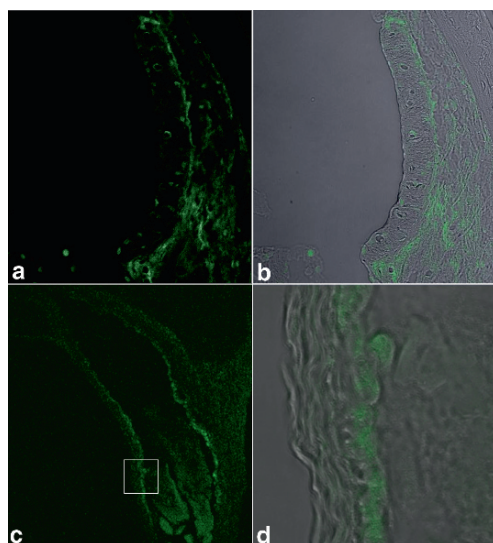


Fig. 1 Confocal images of AQP3 immunoreactivity. Distinct immunostaining of AQP3 is observed in the stria vascularis (a). Immunofluorescence images of AQP3 (green) are projected onto differential interference contrast microscopic images (b). The immunoreactivity is mainly localized on the basal cells of the stria vascularis. Moderate immunostaining of AQP3 is also observed in the endolymphatic sac (c). An enlarged view of the region as outlined by frame is given in (d). Immunofluorescence images of AQP3 (green) are superimposed on differential interference contrast microscopic images. Immunoreactivity of AQP3 is localized in intracellular pools of the epithelium of the endolymphatic sac

cent immunohistochemistry study revealed that AQP3 was expressed in the basal cells of the stria vascularis (Fig. 1a, b) and the epithelium of the endolymphatic sac (Fig. 1c, d). Since the stria vascularis, subepithelial fibrocytes in the saccule and the endolymphatic sac, where AQP3 is expressed, are the main sites of secretion and/or absorption of endolymph, AQP3 in the inner ear may be involved in the homeostasis of endolymph.

2.2.4 AQP4

According to Huang's report (Huang et al. 2002), AQP4 is largely expressed in the inner ear. In situ hybridization and immunofluorescence labeling reveals. AQP4 is expressed and localized at the basolateral plasma membrane of Hensen's cells, Claudius cells, and inner sulcus cells (Li and Verkman 2001; Minami et al. 1998; Takumi et al. 1998). AQP4 is also expressed in the supporting cells of the vestibular endorgans, and in the central portion of the cochlear and vestibular nerves of rats and mice (Mhatre et al. 2002; Takumi et al. 1998). An investigation using human tissues shows that AQP4 immunoreactivity is localized at the outer sulcus cells, Hensen's cells, Claudius' cells, and vestibular supporting cells (Lopez et al. 2007). In our recent histochemistry study, AQP4 is confirmed to be expressed in the epithelium of the human endolymphatic sac (Kakigi et al. 2008; Nishimura et al. 2008).

In mice lacking AQP4 expression there is a moderate impairment of hearing with normal neural conduction time (Li and Verkman 2001; Mhatre et al. 2002). Since there is no morphological abnormality in the inner ear, physiological dysfunction of the cochlea may be responsible for the hearing impairment in AQP4-null mice. It is likely that AQP4 in the supporting cells in the organ of Corti is involved in maintaining osmotic balance during K⁺ recycling. Deafness may be caused by altered basal ionic composition of the endolymph and/or outer hair cell volume (Li and Verkman 2001).

2.2.5 AQP5

AQP5 is localized in the external sulcus cells and the cells of the spiral prominence in the lateral wall of the rat cochlear duct (Löwenheim and Hirt 2004; Mhatre et al. 1999). The restricted expression of AQP5 in the apical turns of the cochlea suggests its potential role in low-frequency hearing (Mhatre et al. 1999). However, adult AQP5-null mice showed normal inner ear structure and hearing, suggesting that AQP5 plays a limited role in inner ear fluid homeostasis.

2.2.6 AQP6

Beitz et al. (2003) detailed unpublished results of AQP6 mRNA expression in the endolymphatic sac of the rat. Lopez et al. (2007) reported that AQP6 protein was expressed in the apical portion of interdental cells of the spiral limbus and in the apical portion of vestibular supporting cells. Recently, Taguchi et al. (2008) reported in more detail that not just AQP6 mRNA but also AQP6 protein is expressed in the cochlea, endolymphatic sac and vestibule. Immunoelectron microscopic studies revealed that immunolabeled gold was diffusely seen in the intracellular area of the stria vascularis, endolymphatic sac and vestibule, but never in the plasma membranes. Since AQP6 expression is localized in the main site of absorption and/or resorption of the endolymph, AQP6 might play some role in the homeostasis of endolymph in the inner ear. The lack of AQP6 expression on the plasma membrane indicates that it does not have a direct role in water flux via the plasma membrane.

2.2.7 AQP7

Huang et al. (2002) reported detailed localization of AQP7 in the inner ear. Cochlea, strong immunoreactivity of AQP7 was observed at the Reissner's membrane, and moderate staining was seen in the cochlear supporting cells (Deiter's cells, Hensen's cell and inner phalangeal cells and border cells), the basilar membrane and stria vascularis. The laminar surface of the stria marginal cells showed strong immunoreactivity to AQP7. The AQP7 expression in the stria marginal cells was confirmed by us (Fig. 2a). In the vestibular end organs, AQP7 immunostaining was observed in

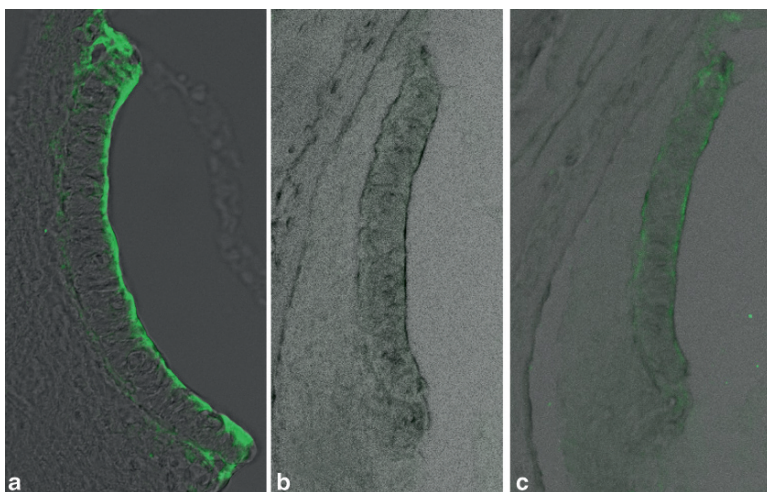


Fig. 2 Immunofluorescence microscopic images of AQP7, 8, 9 immunoreactivity in the stria vascularis. Fluorescent images are overlaid with polarized images. Strong immunostaining of AQP7 is observed on the luminal surface of the marginal cells (a). Immunoreactivity to AQP8 is weak or absent in the stria vascularis (b). Weak immunostaining of AQP9 is observed in the luminal surface of the stria vascularis (c)

supporting cells of both saccule and utricle, as well as in the saccular and utricular walls. Our recent study (unpublished) showed that AQP7 mRNA and protein were also expressed in the epithelium of the endolymphatic sac (Nishimura et al. 2008).

2.2.8 AQP8

Huang et al. (2002) noted the transcription levels of AQP8 in the inner ear were below the detection limit of the dot-blot assay. However, according to Han et al. (2005) AQP8 was broadly distributed in the epithelium surrounding the membranous labyrinth, including the organ of Corti, the inner and outer spiral sulcus, the stria vascularis, fibrocytes of the spiral ligament and the spiral limbus, saccular and utricular wall, and the endolymphatic sac. In our immunohistochemistry study, AQP8 expression was detected not in the stria vascularis (Fig. 2b), but in the endolymphatic sac (Nishimura et al. 2008). AQP8 may play some role in endolymph homeostasis, in the endolymphatic sac, which is thought to be one of the important sites of absorption and/or secretion of endolymph.

2.2.9 AQP9

In the cochlea, immunoreactivity to AQP9 was observed in the interdental cells, cells bordering the inner spiral tunnel and the Reissner's membrane. Strong immunostaining was seen in the vestibular system at the endolymphatic side (epithelial cell) of

the saccular wall and weakly at the surface of the sensory epithelium of the saccule (Huang et al. 2002). In our histochemistry study, AQP9 was confirmed to be expressed at the apical site of the marginal cells of the stria vascularis (Fig. 2c) and in the epithelium of the endolymphatic sac (Nishimura et al. 2008), where endolymph secretion and/or absorption were/was thought to be actively conducted.

2.2.10 AQP10, 11, 12

In mammalian cells, 13 isoforms of AQPs (AQP0–AQP12) have been identified so far. However, no information about expression of AQP10–12 (Gorelick et al. 2006; Itoh et al. 2005; Li et al. 2005) exists.

3 Hormonal Regulation of AQPs Water Channels

The driving force of AQPs water channels is a transepithelial hydrostatic pressure generated by a transepithelial osmotic gradient. Fundamentally, the amount of water moving per unit of time and surface is dependent on an osmotic or hydrostatic gradient and the AQPs concentration on the epithelium (Parisi et al. 1997).

Regarding the regulation of AQPs water channels, two types of regulation system are known; (1) Regulation by gating. Water channels can be open or closed according to the intracellular pH, but the detailed mechanism is still unknown. (2) Hormonal regulation. AQPs expression in the kidney is well known to be mediated by vasopressin and corticosteroids (Nielsen et al. 2002; Parisi et al. 1997). In the inner ear, there is evidence suggesting a similar hormonal regulation system.

3.1 Arginine Vasopressin-AQP2 (AVP-AQP2) System in the Inner Ear

Multiple isoforms of AQPs are expressed in the inner ear. It should be noted that expression of AQP2 mRNA and protein is detected in the stria vascularis and endolymphatic sac, which are thought to be the main sites of secretion and/or absorption of endolymph. In addition, vasopressin renal type (type 2) receptor (V2-R), through which AQP2 expression is mediated by AVP, is also expressed in the cochlea and endolymphatic sac (Fig. 3) (Gu et al. 2006; Kitano et al. 1997; Taguchi et al. 2007). These facts indicate that an AQP2 water regulation system mediated by AVP (AVP–AQP2 system) exists in the inner ear.

In collecting duct principal cells, the AVP–AQP2 system has been well researched. According to Nielsen et al. (1999), AVP acts on V2-R in the basolateral plasma membrane (Fig. 3). Through the GTP-binding protein Gs, adenylate cyclase is activated, thereby accelerating the production of cAMP from ATP. Then cAMP binds to the regulatory subunit of protein kinase A (PKA), activating the catalytic

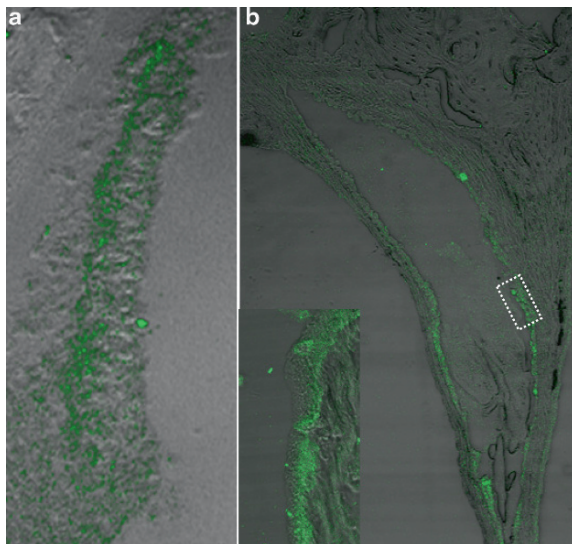


Fig. 3 Confocal images of immunoreactivity to V2-receptor. Fluorescent images are overlaid with differential interference contrast microscopic images. Distinct immunoreactivity is observed in the basal cells of the stria vascularis (**a**) and in the epithelium of the endolymphatic sac (**b**). The insert is an enlarged view as outlined in the dotted frame. The immunoreactivity to V2-receptor seems to be localized in the basolateral site of the endolymphatic sac epithelium

subunit of PKA. PKA phosphorylates AQP2 in intracellular vesicles and possibly other cytosolic or membrane proteins. Microtubule motor proteins (dynein/dynactin) and vesicle targeting receptors (VAMP-2, syntaxin-4, NSF) may participate in the specificity of AQP2 targeting the apical plasma membrane to increase water permeability. cAMP also participates in long-term regulation of AQP2 by increasing the levels of the catalytic subunit of PKA in the nuclei, which is thought to phosphorylate transcription factors such as CREB-P (cAMP responsive element binding protein) and c-Jun/c-Fos. Binding of these factors is thought to increase gene transcription of AQP2 resulting in synthesis of AQP2 protein, which in turn enters the regulated trafficking system. If the AVP–AQP2 system in the inner ear acts in the same fashion as in the kidney, the activation of this system might up-regulate the expression of AQP2 mRNA and protein, and the inhibition might down-regulate it. Actually, molecular biological studies revealed that the expression of AQP-2 mRNA in the cochlea and endolymphatic sac was up-regulated by the systemic application of AVP and down-regulated by systemic and local application of V2-antagonist (OPC-31260) (Gu et al. 2006; Sawada et al. 2002; Takeda et al. 2003). Lithium, which may affect adenylate cyclase activity, also suppresses the expression of AQP2 mRNA and protein in the cochlea and endolymphatic sac (Fukushima et al. 2005).

A rise in AQP2 abundance is known to increase water permeability in the collecting duct's principal cells; the reverse is also true (Nielsen et al. 1999; Fleeman et al. 2000). In the inner ear, a change in AQP2 abundance is also expected to similarly regulate water permeability. The direction of water flux via AQPs water channel

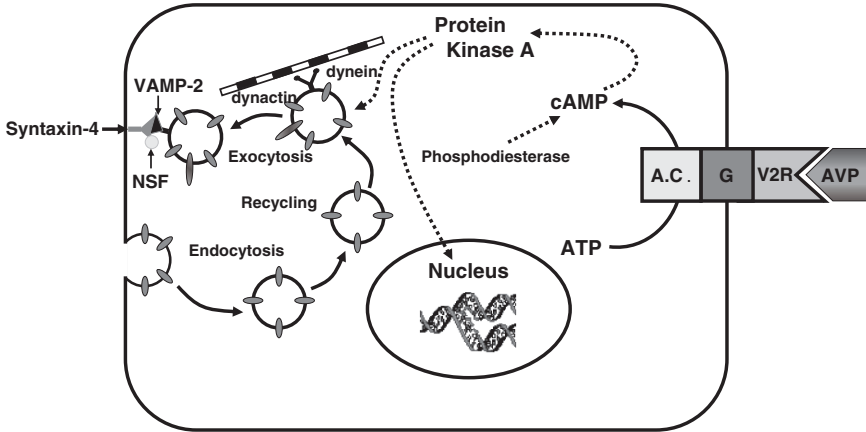


Fig. 4 Regulation of AQP2 trafficking and expression in collecting duct principal cells. AVP vasopressin; V2R vasopressin type 2 receptor; AC adenylate cyclase (modified from Nielsen's report Nielsen et al. 1999)

depends on the osmotic gradient. Since the osmolarity of endolymph is higher than that of perilymph or cerebrospinal fluid (Sterkers et al. 1984), an increase in AQP2 expression in the inner ear may promote water influx into the endolymph, and vice versa. Actually, chronic application of AVP produces an increase in the volume of endolymphatic compartment, so-called endolymphatic hydrops (Takeda et al. 2000). Conversely, the inhibitors of AVP–AQP2 system, V2-antagonist (OPC-31260) and lithium, contribute to a decrease in the volume of the endolymphatic compartment, and endolymphatic collapse (Fukushima et al. 2005; Takeda et al. 2003). Thus, the evidence is conclusive that water homeostasis of the inner ear is regulated in part via the AVP–AQP2 system, as in the kidney (Nielsen et al. 1999) (Fig. 4).

3.2 Corticosteroids Mediated Regulation of AQPs Expression

The adrenocortical hormones, glucocorticoid and mineralocorticoid, are involved in the normal modulation of renal water excretion and regulation of extracellular fluid volume. Collecting duct principal cells are known to be responsible for water and Na reabsorption under the control of adrenal corticosteroid hormones as well as AVP, regulation of which is described above (Kwon et al. 2002; Nielsen et al. 2002; Stoeniu et al. 2003). However, there are only a few reports on corticosteroids-mediated regulation. In these reports, mineralocorticoid regulate, at least in part, AQP3 expression in the collecting duct (Kwon et al. 2002). Meanwhile, glucocorticoid induces an increase in the expression of AQP1 (Stoeniu et al. 2003). In the inner ear, the intratympanic injection of dexamethasone up-regulates AQP1 mRNA of the rat cochlea (Fukushima et al. 2002), while intraperitoneal injection (Fukushima et al. 2004) and intra-endolymphatic sac instillation (Kitahara et al. 2003) of dexamethasone up-regulates AQP3 mRNA in the endolymphatic sac

and the cochlea, respectively. With regard to the discrepancy of up-regulated AQP among the routes of administration, the authors speculate that the intratympanic injection of dexamethasone directly penetrates into the inner ear fluid, affecting its homeostasis through glucocorticoid receptor, but systemic administration does not achieve sufficiently high local drug levels. However, no clear-cut explanation is given concerning the up-regulation of AQP3 by the intra-endolymphatic sac instillation of dexamethasone, which is another direct drug delivery into the inner ear. These results suggest that steroids may affect water homeostasis in the rat inner ear via AQPs.

4 Role of AVP-AQP2 System on Endolymphatic Hydrops and its Treatment

Meniere's disease is histologically characterized by endolymphatic hydrops in the inner ear (Hallpike and Cairns 1938; Yamakawa 1983). The mechanisms underlying overaccumulation of endolymph remain obscure. It is generally accepted that the formation of endolymphatic hydrops in Meniere's disease is retention hydrops, caused by mal-absorption of the endolymphatic sac. This assumption is based on the morphological findings that the endolymphatic sac and duct are poorly developed (Shambaugh et al. 1969; Takeda et al. 1997), or otherwise are fibrotic in cases of Meniere's disease (Lindsay 1942; Shambaugh et al. 1969; Yazawa and Kitahara 1981). However, fluctuating hearing loss and/or episodic vertiginous attacks can not be explained, based only on retention hydrops which is expected to develop slowly and gradually. In addition to the passive process of fluid retention, some active process that promotes the over-production of endolymph is required. The clinical observations of high plasma AVP (p-AVP) levels in Meniere's disease and its related diseases (Aoki et al. 2005; Takeda et al. 1995; Takeda et al. 2008) seem to provide a key to the solution of the mechanism underlying the overaccumulation of endolymph in Meniere's disease. Since an elevation in p-AVP was not observed in hydrops animals with surgical obliteration of the endolymphatic duct (Kitano et al. 1994), high p-AVP levels are thought to result not from the formation of the endolymphatic hydrops, but in the development of the endolymphatic hydrops.

As described above, AQP2 protein was confirmed to be expressed in the stria vascularis and endolymphatic sac, which are the main sites of the secretion and/or absorption of endolymph (Fukushima et al. 2005). Molecular biological studies reveal AQP2 mRNA expression in the cochlea as well as in the endolymphatic sac are up-regulated by systemic application of AVP (Sawada et al. 2002), and down-regulated by V2-antagonist (OPC-31260) application into the scala tympani (Takeda et al. 2003). Morphologically, the endolymphatic space is increased by systemic application of AVP (Takeda et al. 2000), and decreased by the application of OPC into the scala tympani (Takeda et al. 2003). These experimental results indicate water homeostasis of the inner ear fluid is regulated via the AVP-AQP2 system. i.e., the AVP-AQP2 system is thought to operate in such a way, that its activation results

in an influx of endolymph into the endolymphatic compartment, while its inhibition results in an efflux of endolymph from the endolymphatic compartment. Such clinical and basic lines of evidence strongly suggest over activity of the AVP–AQP2 system is one of the etiological factors in Meniere's disease.

Treatment of Meniere's and related diseases are principally aimed at reducing the excess water retention in the endolymphatic compartment. Osmotic diuretic is one of the options. Since the mal-regulation of the AVP–AQP2 system in the inner ear is assumed to play an important role in the pathogenesis of Meniere's disease, application of an inhibitor of the AVP–AQP system also appears to be a rational treatment strategy for Meniere's disease. V2-antagonist or lithium (an inhibitor of adenylate cyclase) is the second alternative. But there is the counter-argument that systemic application of osmotic diuretics, V2-antagonis, and lithium produces excessive urinary excretion, which causes dehydration and increase in plasma osmolarity, resulting in rise in the p-AVP level (Kakigi et al. 2006; Marples et al. 1998). This elevation of p-AVP levels counteracts the inhibitory action of these agents on AVP–AQP2 system in the inner ear. Therefore, these agents exert a dehydrating effect on the inner ear via the VP–AQP2 system in the inner ear, whereas high p-AVP exerts a hydrating effect on the inner ear. These two effects are suspected to work in the inner ear in a competitive manner, consequently decreasing the decompression effect. One of the solutions to this problem is adequate hydration to control p-AVP within the normal range. Another solution is local application to the inner ear via the round window. OPC (V2-antagonist) delivery via the round window is confirmed to exert a decompression effect on the endolymphatic compartment (Takeda et al. 2006).

Endolymphatic hydrops as well as stria atrophy or sensorineural degeneration is an important pathologic condition in the inner ear. Recently evidence is conclusive that mal-regulation of the AVP–AQP2 system in the inner ear is responsible for the formation and development of endolymphatic hydrops. Therefore, AQPs appears to be a promising target for the development of novel drug therapies for Meniere's and other related diseases.

References

- Agre P, Sasaki S, Chrispeels MJ (1993) Aquaporins: a family of water channel proteins. *Am J Physiol Renal Physiol* 265:F461
- Aoki M, Ando K, Kuze B et al. (2005) The association of antidiuretic hormone levels with an attack of Meniere's disease. *Clin Otolaryngol* 30:521–525
- Beitz E, Kumagami H, Krippeit-Drews P et al. (1999) Expression pattern of aquaporin water channels in the inner ear of the rat. The molecular basis for a water regulation system in the endolymphatic sac. *Hear Res* 132:76–84
- Beitz E, Zenner HP, Schultz JE (2003) Aquaporin-mediated fluid regulation in the inner ear. *Cell Mol Neurobiol* 23:315–329
- Couloigner V, Berrebi D, Teixeira M et al. (2004) Aquaporin-2 in the human endolymphatic sac. *Acta Otolaryngol* 124:449–453
- Fleeman LM, Irewin PJ, Phillips PA et al. (2000) Effects of an oral vasopressin receptor antagonist (OPC-31260) in a dog with syndrome of inappropriate secretion of antidiuretic hormone. *Aust Vet J* 78:825–830

- Fukushima M, Kitahara T, Uno Y et al. (2002) Effects of intratympanic injection of steroids on changes in rat inner ear aquaporin expression. *Acta Otolaryngol* 122:600–606
- Fukushima M, Kitahara T, Fuse Y et al. (2004) Changes in aquaporin expression in the inner ear of the rat after i.p. injection of steroids. *Acta Otolaryngol Suppl* 553:13–18
- Fukushima K, Takeda T, Kakigi A et al. (2005) Effects of lithium on endolymph homeostasis and experimentally induced endolymphatic hydrops. *ORL J Otorhinolaryngol Relat Spec* 67: 282–288
- Gorelick DA, Praetorius J, Tsunenari T (2006) Aquaporin-11: a channel protein lacking apparent transport function expressed in brain. *BMC Biochem* 7:14
- Gu FM, Han HL, Zhang LS (2006) Effects of vasopressin on gene expression in rat inner ear. *Hear Res* 222:70–78
- Hallpike CS, Cairns H (1938) Observation on the pathology of Meniere's syndrome. *J Laryngol* 53:625–655
- Han H, Zhang L, Gu F (2005) Expression and its significance of aquaporins in normal guinea pig inner ears. *Lin Chuang Er Bi Yan Hou Ke Za Zhi* 19:883–885 (Chinese)
- Huang D, Chen P, Chen S et al. (2002) Expression patterns of aquaporins in the inner ear: evidence for concerted actions of multiple types of aquaporins to facilitate water transport in the cochlea. *Hear Res* 165:85–95
- Itoh T, Rai T, Kuwahara M (2005) Identification of a novel aquaporin, AQP12, expressed in pancreatic acinar cells. *Biochem Biophys Res Commun* 330:832–838
- Kakigi A, Takeda T, Sawada S et al. (2006) Antidiuretic hormone and osmolality in isosorbide therapy and glycerol test. *ORL J Otorhinolaryngol Relat Spec* 68:217–220
- Kakigi A, Nishimura M, Takeda T, et al. (2008) Expression of aquaporin 1, 3, 4, NKCC1, and NKCC2 in the human endolymphatic sac. *Auris Nasu Larynx* [Epub ahead of print]
- Kitahara T, Fukushima M, Uno Y et al. (2003) Up-regulation of cochlear aquaporin-3 mRNA expression after intra-endolymphatic sac application of dexamethasone. *Neurol Res* 25:865–870
- Kitano H, Takeda T, Pulec JL et al. (1994) The relationship between vasopressin and endolymphatic hydrops in the guinea pig. *Ear Nose Throat J* 73(12):921–925
- Kitano H, Takeda T, Suzuki M et al. (1997) Vasopressin and oxytocin receptor mRNAs are expressed in the rat inner ear. *Neuroreport* 8:2289–2292
- Kumagami H, Loewenheim H, Beitz E et al. (1998) The effect of anti-diuretic hormone on the endolymphatic sac of the inner ear. *Pflugers Arch* 436:970–975
- Kwon TH, Nielsen J, Masilamani S et al. (2002) Regulation of collecting duct AQP3 expression: response to mineralocorticoid. *Am J Physiol Renal Physiol* 283:F1403–F1421
- Li J, Verkman AS (2001) Impaired hearing in mice lacking aquaporin-4 water channels. *J Biol Chem* 276:31233–31237
- Li H, Kamiie J, Morishita Y (2005) Expression and localization of two isoforms of AQP10 in human small intestine. *Biol Cell* 97:823–829
- Lindsay JR (1942) Labyrinthine hydrops and Meniere's disease. *Arch Otolaryngol* 35:853–867
- Lopez IA, Ishiyama G, Lee M et al. (2007) Immunohistochemical localization of aquaporins in the human inner ear. *Cell Tissue Res* 328:453–460
- Löwenheim H, Hirt B (2004). Aquaporine. Discovery, function, and significance for otorhinolaryngology. *HNO* 52(8):673–678
- Marples D, Christensen BM, Frokiaer J et al. (1998) Dehydration reverses vasopressin antagonist-induced diuresis and aquaporin-2 downregulation in rats. *Am J Physiol Renal Physiol* 275:F400–F409
- Merves M, Bobbitt B, Parker K et al. (2000) Developmental expression of aquaporin 2 in the mouse inner ear. *Laryngoscope* 10:1925–1930
- Merves M, Krane CM, Dou H et al. (2003) Expression of aquaporin 1 and 5 in the developing mouse inner ear and audiovestibular assessment of an Aqp5 null mutant. *J Assoc Res Otolaryngol* 4:264–275
- Mhatre AN, Steinbach S, Hribar K et al. (1999) Identification of aquaporin 5 (AQP5) within the cochlea: cDNA cloning and in situ localization. *Biochem Biophys Res Commun* 264:157–162

- Mhatre AN, Jero J, Chiappini I et al. (2002) Aquaporin-2 expression in the mammalian cochlea and investigation of its role in Meniere's disease. *Hear Res* 170:59–69
- Mhatre AN, Stern RE, Li J (2002) Aquaporin 4 expression in the mammalian inner ear and its role in hearing. *Biochem Biophys Res Commun* 297:987–996
- Minami Y, Shimada S, Miyahara H et al. (1998) Selective expression of mercurial-insensitive water channel (AQP-4) gene in Hensen and Claudius cells in the rat cochlea. *Acta Otolaryngol Suppl* 533:19–21
- Nielsen S, Knowlton T, Christensen BM et al. (1999) Physiology and pathophysiology of renal aquaporins. *J Am Soc Nephrol* 10:647–663
- Nielsen S, Frøkiaer J, Marples D et al. (2002) Aquaporins in the kidney: from molecules to medicine. *Physiol Rev* 82:205–244
- Nishimura M, Kakigi A, Takeda T, Takeda S, Doi K. (2008) Expression of aquaporins, vasopressin type 2 receptor and $\text{Na}^+ \text{K}^+ \text{Cl}^-$ cotransporters in the rat endolymphatic sac. *Acta Otolaryngol* [Epub ahead of print]
- Parisi M, Amodeo G, Capurro C et al. (1997) Biophysical properties of epithelial water channels. *Biophys Chem* 68:255–263
- Sawada S, Takeda T, Kitano H et al. (2002) Aquaporin-2 regulation by vasopressin in the rat inner ear. *Neuroreport* 13:1127–1129
- Sawada S, Takeda T, Kitano H et al. (2003) Aquaporin-1 (AQP1) is expressed in the stria vascularis of rat cochlea. *Hear Res* 181:15–19
- Shambaugh GE, Clemis JD, Arenberg IK (1969) Endolymphatic duct and sac in Meniere's disease. 1. Surgical and histopathologic observations. *Arch Otolaryngol* 89:816–825
- Stankovic KM, Adams JC, Brown D (1995) Immunolocalization of aquaporin CHIP in the 1995, guinea pig inner ear. *Am J Physiol* 269:C1450–C1456
- Sterkers O, Ferrary E, Amiel C (1984) Inter- and intracompartmental osmotic gradients within the rat cochlea. *Am J Physiol* 247:F602–F606
- Sterkers O, Ferrary E, Amiel C (1988) Production of inner ear fluids. *Physiol Rev* 68:1083–1128
- Stoenoiu MS, Ni J, Verkaeren C et al. (2003) Corticosteroids induce expression of aquaporin-1 and increase transcellular water transport in rat peritoneum. *J Am Soc Nephrol* 14:555–565
- Taguchi D, Takeda T, Kakigi A et al. (2007) Expression of aquaporin-2, vasopressin type 2 receptor, transient receptor potential channel vanilloid (TRPV)1, and TRPV4 in the human endolymphatic sac. *Laryngoscope* 117:695–698
- Taguchi D, Takeda T, Kakigi A et al. (2008) Expression and immunolocalization of Aquaporin-6 (Aqp6) in the rat inner ear. *Acta Otolaryngol* 128:832–840
- Takeda T, Kakigi A, Saito H et al. (1995) Antidiuretic hormone (ADH) and endolymphatic hydrops. *Acta Otolaryngol Suppl* 519:219–222
- Takeda T, Sawada S, Kakigi A et al. (1997) Computed radiographic measurement of the dimensions of the vestibular aqueduct in Meniere's disease. *Acta Otolaryngol Suppl* 528:80–84
- Takeda T, Takeda S, Kitano H et al. (2000) Endolymphatic hydrops induced by chronic administration of vasopressin. *Hear Res* 140:1–6
- Takeda T, Sawada S, Takeda S et al. (2003) The effects of V2-antagonist (OPC-31260) on endolymphatic hydrops. *Hear Res* 182:9–18
- Takeda T, Takeda S, Kakigi A et al. (2006) A comparison of dehydration effects of V2-antagonist (OPC-31260) on the inner ear between systemic and round window applications. *Hear Res* 218:89–97
- Takeda T, Kakigi A, Nishoka R et al. (2008) Plasma antidiuretic hormone in cases with the early onset of profound unilateral deafness. *Auris Nasus Larynx* [Epub ahead of print]
- Takumi Y, Nagelhus EA, Eidet J et al. (1998) Select types of supporting cell in the inner ear express aquaporin-4 water channel protein. *Eur J Neurosci* 10:3584–3595
- Yamakawa K (1983) Über die pathologische Veränderung bei einem Menière-Kranken. *J Otolaryngol Jpn* 44:2310–2312 (in Japanese)
- Yazawa Y, Kitahara M (1981) Electron microscopic studies of the endolymphatic sac in Meniere's disease. *ORL J Otorhinolaryngol Relat Spec* 43:121–130
- Zhong SX, Liu ZH (2003) Expression of aquaporins in the cochlea and endolymphatic sac of guinea pig. *ORL J Otorhinolaryngol Relat Spec* 65:284–289

Aquaporins in Secretory Glands and their Role in Sjögren's Syndrome

Christine Delporte

Contents

1	Introduction	186
2	Aquaporins	186
3	Morphology of Salivary and Lacrimal Glands, and Pancreas	187
4	AQP Expression and Localisation in Salivary and Lacrimal Glands and Pancreas	187
4.1	Salivary Glands	187
4.2	Lacrimal Glands	189
4.3	Pancreas	189
5	Secretion and Fluid Transport Mechanisms in Salivary Glands, Lacrimal Glands and Pancreas	190
5.1	Salivary Glands	190
5.2	Lacrimal Glands	192
5.3	Pancreas	193
6	Sjögren's Syndrome	194
6.1	Pathogenesis of Sjögren's Syndrome	194
6.2	AQPs and Sjögren's Syndrome	195
7	Conclusion	197
	References	197

Abstract Salivary, lacrimal and pancreatic secretions are known to account for multiple physiological functions. These exocrine secretions are watery fluids containing electrolytes, and a mixture of proteins, and can be stimulated by a number of agonists. Since water movement is involved in exocrine secretion, aquaporins (AQPs) have been hypothesised to contribute to fluid production in exocrine glands. This chapter will focus on the expression, localisation and function of AQPs in salivary and lacrimal glands and pancreas. The role of multiple water and ion transporters and channels in exocrine fluid secretion will also be reviewed. Finally, this chapter will address the potential role of AQPs in Sjögren's syndrome.

C. Delporte

Laboratory of Biological Chemistry and Nutrition, Université Libre de Bruxelles, Bat G/E CP611, 808 Route de Lennik, B-1070 Brussels, Belgium
cdelpor@ulb.ac.be

1 Introduction

Aquaporins (AQPs), a family of water-permeable channel proteins, have been shown to account for transcellular permeability in many organisms (Agre 2004; Verkman 2005). As the main function of secretory glands is fluid secretion, hypothesis was made that such glands could express AQPs. Numerous studies evaluated the expression of AQPs in secretory glands, such as salivary and lacrimal glands, and pancreas. Functional roles of AQPs in secretory glands have been investigated using physiological and biochemical approaches, and analyzing the phenotype of transgenic mice lacking an AQP.

In this chapter, an overview of the expression and role of aquaporins in secretory tissues (salivary and lacrimal glands, and pancreas) and the role of AQPs in Sjögren's syndrome will be discussed.

2 Aquaporins

Based on membrane permeability measurements performed in epithelia and various cell types, the existence of a protein channel allowing passage of water was hypothesised for many years. The first water-specific channel, named CHIP28 (channel-forming integral protein of 28 kDa) and renamed aquaporin-1 (AQP1), was isolated from red blood cells as a 28-kDa protein, prior to it being cloned and biophysically characterised (Smith and Agre 1991; Preston and Agre 1991; Preston et al. 1992). AQP1 presents high amino acid homology with major intrinsic protein (MIP) of the lens, indicating AQP1 is a member of the MIP family of membrane proteins (Preston and Agre 1991). Since the discovery of AQP1, several other aquaporins have been cloned from a wide range of organisms including mammals (Agre 2004; Verkman 2005), anurans (Suzuki et al. 2007), yeast (Pettersson et al. 2005), bacteria (Tanghe et al. 2006), parasites (Beitz 2006) and plants (Maurel 2007). In mammals, aquaporin family has 13 members: AQP0 to AQP12.

AQPs are small hydrophobic integral membrane proteins of approximately 270 amino acids. They exist as monomers of 28–30-kDa that can associate in tetramers (Verbavatz et al. 1993). AQPs present six transmembrane domains in each monomer, as well as three extracellular and two intracellular loops (Preston and Agre 2001). Two repeating Asn-Pro-Ala (NPA) sequences, present in the first intracellular and third extracellular loop, represent the amino acid signature sequence motifs of the AQPs (Agre 2004). On the basis of their permeability characteristics and their amino acid sequences, members of the AQPs family can be divided in three groups: aquaporins, aquaglyceroporins, and aquaporins containing unusual NPA motifs. Aquaporins (AQP0, AQP1, AQP2, AQP4, AQP5, AQP6, AQP8) are primarily permeable to water, whereas aquaglyceroporins (AQP3, AQP7, AQP9, AQP10) also transport glycerol and small solutes (Agre 2004; King et al. 2004; Takata et al. 2004; Krane and Goldstein 2007). Aquaporins containing unusual NPA motifs appear to be more distantly related to other mammalian aquaporins and aquaglyceroporins (Agre 2004; Ishibashi 2006).

3 Morphology of Salivary and Lacrimal Glands, and Pancreas

Typical exocrine secretory glands include salivary glands, lacrimal glands and pancreas. Exocrine secretory glands are multilobular tissues mainly composed of acinar, ductal and myoepithelial cells. Acinar cells are the sites of synthesis, storage and secretion of proteins. Acinar cells are either serous, mucous, or seromucous. The terms serous and mucous derive from classical histological terminology defining the physical consistency of secretions of acinar cells as being either viscous or watery, respectively (Denny et al. 1997). Mucous acinar cells secrete mucins-large glycoproteins negatively charged, contributing to the viscosity of mucous secretions. Serous acinar cells secrete a variety of proteins and lack mucins. Seromucous acinar cells are more closely related to mucous than serous cells due to their functional and biochemical properties, and their substantial secretion of mucins. Acinar cells drain into the intercalated ducts, and groups of intercalated ducts converge into larger intralobular ducts. These in turn drain into extralobular ducts and finally to the main collecting duct (pancreas) or excretory ducts (salivary and lacrimal glands). The primary function of ductal cells is to modify the primary fluid secreted by acinar cells. The multiple processes of myoepithelial cells surround the basal area of acinar and ductal cells. Myoepithelial cells, containing α -smooth muscle actin, are thought to contract and force fluid out of the ducts.

Salivary glands in mammals are composed of three major pairs of parotid, submandibular and sublingual glands, as well as numerous minor salivary glands scattered throughout the oral cavity. Parotid glands of most species, including rodents and human, are entirely composed of serous acinar cells, whereas submandibular and sublingual glands contain both serous and mucous acinar cells. In human submandibular glands, serous acinar cells outnumber mucous acinar cells, whereas the opposite is true for the human sublingual glands. Seromucous cells, featuring secretory granules rich in sialomucin, are present in both submandibular and sublingual glands. Lacrimal glands possess an acinous structure similar to salivary glands and are made of serous acinar cells; the exocrine pancreas is also composed of serous acinar cells. Contrary to salivary and lacrimal glands, the terminal portion of the pancreatic duct system extends into the acini, so that flattened duct cells (known as centroacinar cells) are interposed between some of the acinar cells and the lumen. Salivary and lacrimal glands, and pancreas, possess intercalated ducts.

4 AQP Expression and Localisation in Salivary and Lacrimal Glands and Pancreas

4.1 Salivary Glands

Parotid glands, both AQP1 mRNA and protein were detected in rats (Li et al. 1994) (Table 1). Immunolocalisation studies revealed the presence of AQP1 on both apical and basolateral membranes from non-fenestrated endothelial cells of capillaries and

Table 1 AQPs expressed in salivary and lacrimal glands, and pancreas

Secretory gland	AQP	Cell type	Subcellular localization		Remarks
			Rat	Human	
Salivary gland	AQP1	Endothelial myoepithelial	A + B	A + B	
	AQP3	Acinar		B	Controversy
	AQP4	Ductal	B		Controversy
	AQP5	Acinar	A + B SG	A + B	B: controversy Not confirmed
	AQP8	Ductal Myoepithelial	A		Controversy
Lacrimal gland	AQP5	Acinar	A		
	AQP4	Acinar	B		
Pancreas	AQP1	Acinar	SG		Not confirmed
		Endothelial	A + B	A + B	
		Ductal	A + B	A + B	
	AQP5	Ductal	A	A	
AQP8	Acinar	A	A		

A apical; *B* basolateral; *SG* secretory granules (see text for detail and references)

venules, while no labelling of the glandular tissue was detected (Li et al. 1994; Nielsen et al. 1993; He et al. 1997; Delporte et al. 1997). In rat submandibular glands, AQP1 is constitutively expressed in the microvasculature (King et al. 1997; Akamatsu et al. 2003). In human parotid, submandibular and labial glands, AQP1 mRNA was seen (Gresz et al. 1999; Gresz et al. 2001; Wang et al. 2003) and AQP1 protein was located in myoepithelial and endothelial cells, rather than in glandular tissues (Gresz et al. 1999; Gresz et al. 2001; Mobasher and Marples 2004).

AQP5 was detected in rat and mouse parotid, submandibular and sublingual glands (King et al. 1997; Raina et al. 1995; Krane et al. 1999). In rat submandibular glands, AQP5 expression was noted in the apical membrane of serous acinar cells (He et al. 1997; Nielsen et al. 1997; Funaki et al. 1998). It was shown from Sprague–Dawley rats that AQP5 expression level could be high or low in rat submandibular glands (Murdiastuti et al. 2002). In animals expressing high levels of AQP5, the AQP5 protein was identified at the apical, basal and lateral membranes of acinar cells, while in animals expressing low levels of AQP5, the AQP5 protein was located at the apical and/or lateral membranes of acinar cells (Murdiastuti et al. 2002). AQP5 was also detected in rat parotid acinar secretory granules, with amino and carboxyl domain of the protein being localized at the luminal side (Matsuki et al. 2005). While most studies could not detect AQP5 labelling in rat submandibular ductal cells (He et al. 1997; Funaki et al. 1998; Murdiastuti et al. 2002), few studies reported AQP5 expression at the apical membranes of intercalated ducts in submandibular glands (Nielsen et al. 1997; Matsuzaki et al. 1999) and intracellular in interlobular ducts in parotid glands (Ishikawa et al. 2005). In rat minor salivary glands of the tongue, AQP5 was mainly located at the apical membranes of the acinar cells (Matsuzaki et al. 2003). In human parotid, submandibular and labial glands, AQP5 labelling was

confined to the apical membrane of acinar cells, but absent in ductal cells (Wang et al. 2003; Steinfeld et al. 2001).

Though originally AQP8 was reported as being expressed in rat salivary gland acinar cells (Koyama et al. 1997; Wellner et al. 2000), it is now believed to be located in myoepithelial cells (Elkjaer et al. 2001; Wellner et al. 2006). The expression of AQP3 and AQP4 in salivary gland remains controversial. In rat submandibular glands, AQP3 mRNA was noted (Akamatsu et al. 2003), but the expression of the AQP3 protein was not observed (Nielsen et al. 1993; King et al. 1997). Although not confirmed by others, AQP3 mRNA was detected in human parotid, submandibular, sublingual and labial glands, (Gresz et al. 2001; Wang et al. 2003) and AQP3 protein was localized at basal and lateral membranes of both serous and mucous acinar cells (Gresz et al. 2001; Beroukas et al. 2002). In rat and human salivary glands, AQP4 mRNA (Gresz et al. 2001; Wang et al. 2003; Akamatsu et al. 2003; Hasegawa et al. 1994; Delporte and Steinfeld 2006), as well as AQP4 protein detection (Gresz et al. 2001; King et al. 1997; Frigeri et al. 1995; Nielsen et al. 1997) was not consistent. The detection of AQP6 and AQP7 mRNA in human parotid glands (Wang et al. 2003) has not been confirmed by other studies.

4.2 Lacrimal Glands

In mouse extraorbital and intraorbital lacrimal glands, AQP4 labelling was located at the basolateral membrane of acinar cells, while AQP5 was situated at the apical membrane of acinar and ductal cells (Ishida et al. 1997; Hamann et al. 1998). In response to pilocarpine-induced lacrimal secretion, the AQP5 protein expression was increased at the apical membrane of acinar cells (Ishida et al. 1997). In rat extraorbital and intraorbital lacrimal glands, AQP5 mRNA was by Northern blot analysis (Raina et al. 1995) and AQP5 protein was exclusively located at the apical membrane of acinar cells (Matsuzaki et al. 1999; Hamann et al. 1998; Funaki et al. 1998) (Table 1).

4.3 Pancreas

In rat exocrine pancreas, while AQP1, AQP4, AQP5 and AQP8 mRNA was detected, only the expression of the AQP1, AQP5 and AQP8 proteins was observed (Hurley et al. 2001; Burghardt et al. 2003) (Table 1). AQP1 expression was seen in rat intralobular and interlobular ducts (Furuya et al. 2002) and microvasculature (Hurley et al. 2001), but not in acinar cells, centroacinar cells, and intercalated ducts (Furuya et al. 2002; Ko et al. 2002). In intralobular and interlobular ductal cells, AQP1 was located at the apical and basolateral membranes, as well as in caveolae and vesicle-like structures (Furuya et al. 2002; Ko et al. 2002). AQP1 was also found in pancreatic acinar zymogen granules (Cho et al. 2002). AQP5

was located at the apical membrane of centroacinar and intercalated ductal cells (Burghardt et al. 2006). AQP8 expression was confined to the apical membrane of acinar cells (Hurley et al. 2001).

In human pancreas, while AQP1, AQP3, AQP4, AQP5 and AQP8 mRNA are noted, only the expression of AQP1, AQP5 and AQP8 protein was observed (Burghardt et al. 2003). AQP1 was located in capillaries, centroacinar cells, and in both apical and basolateral membranes of intercalated ductal cells (Burghardt et al. 2003). AQP5 was observed at the apical membrane of intercalated ductal cells, while AQP8 was confined to the apical membrane of acinar cells (Burghardt et al. 2003).

AQP12 protein was noticed intracellularly in mouse pancreatic acinar cells (Itoh et al. 2005).

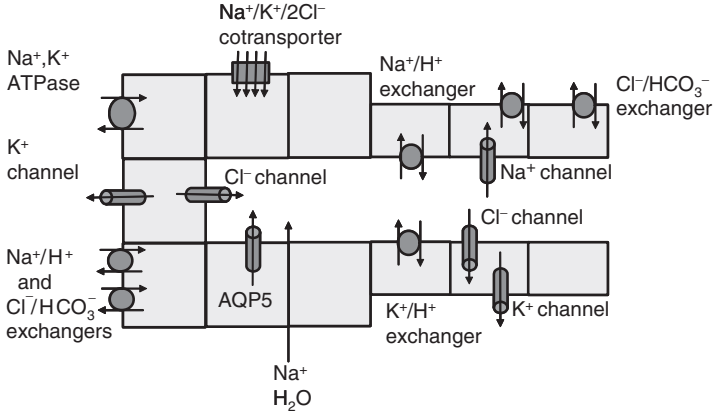
5 Secretion and Fluid Transport Mechanisms in Salivary Glands, Lacrimal Glands and Pancreas

5.1 Salivary Glands

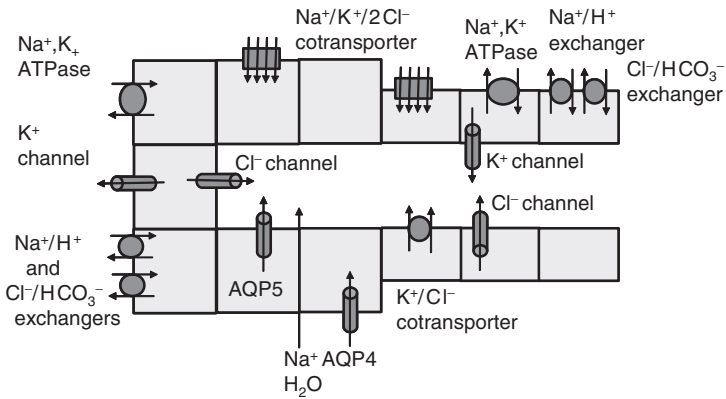
The average daily output of saliva in man is about 750–1,000 ml. The functions of saliva include protection and hydration of mucosal structures within the oral cavity, oropharynx and oesophagus. Saliva also contributes to initiation of digestion, and contains many antimicrobial agents. Salivary dysfunction clinically manifests as dysphagia, oral pain, dental caries, and infections from opportunistic microorganisms (Ship et al. 2002).

Secretion of primary isotonic fluid by acinar cells into the lumen of the acini requires coordinated regulation of many water and ion transporters and channels (Fig. 1a) (Melvin et al. 2005; Turner and Sugiyama 2002; McManaman et al. 2006). The Na^+/K^+ ATPase, located at the basolateral membrane of acinar cells, leads to an inwardly-directed Na^+ chemical gradient. The intracellular Cl^- concentration is increased beyond its electrochemical gradient by the $\text{Na}^+/\text{K}^+/2\text{Cl}^-$ co-transporter using the Na^+ gradient, located at the basolateral membrane, as well as by the paired basolateral $\text{Cl}^-/\text{HCO}_3^-$ and Na^+/H^+ exchangers. The opening of K^+ and Cl^- channels, located respectively at both the basolateral and apical membranes, is triggered by agonist-stimulation and subsequent intracellular Ca^{2+} mobilization, leading to negative electrical potential difference allowing passive movements of cations across acinar cell tight junctions. HCO_3^- is secreted across the apical membrane via an ion channel, possibly through the same Cl^- channel involved in Cl^- secretion. Accumulation of ions into the lumen generates a transepithelial osmotic gradient driving water movement through the apical AQP5 channels and paracellular pathways. While the primary isotonic fluid secretion passes through ducts, NaCl is reabsorbed through Na^+ channels, Cl^- channels and Na^+/H^+ exchangers, while K^+ and HCO_3^- are secreted via $\text{Cl}^-/\text{HCO}_3^-$ and K^+/H^+ exchangers. The final hypotonic secreted saliva results from relative water impermeability of the ducts

a Salivary glands



b Lacrimal glands



c Pancreas

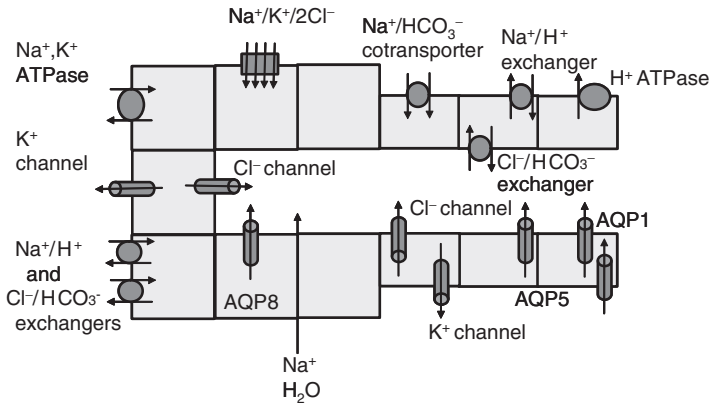


Fig. 1 Salivary, lacrimal and pancreatic secretions. Acinar cells (*grey squares*) secrete a primary fluid which is modified by ductal cells (*grey rectangles*). Water and ion transporters and channels expressed in acinar and ductal cells are indicated in figure (see text for details)

(Mangos and McSherry 1970; Mangos et al. 1973; Baum 1993; Cook et al. 1994; Turner and Sugiya 2002). The composition of saliva depends on both the origin of the stimulation (sympathic or parasympathic) and the type of salivary gland stimulated (Proctor and Carpenter 2007).

In rat parotid acinar secretory granules, inhibition of AQP5 induces secretory granules swelling and lysis (Matsuki et al. 2005). Due to the involvement of AQP5 in the osmoregulation of rat parotid secretory granules and the hypothesis that AQPs can function as osmosensors, rather than water channels (Shachar-Hill and Hill 2002; Hill et al. 2004), AQP5 is suggested to act as an osmosensor in these secretory granules (Sugiya and Matsuki 2006). AQP5 is also suggested to play the role of an osmosensor controlling the paracellular flow in rat salivary glands (Murakami et al. 2006; Hill and Shachar-Hill 2006).

Intracellular AQP5 labelling has been found in rat parotid acinar cells (Matsuzaki et al. 1999) and AQP5 is reported to translocate from intracellular vesicles to plasma membrane *in vitro* in response to stimulation of muscarinic receptors (Ishikawa et al. 1998), although such translocation has not been detected *in vivo* (Gresz et al. 2004).

Transgenic mice lacking AQP are helpful in understanding the role of AQP in saliva secretion. Transgenic mice lacking AQP1 (Ma et al. 1999; Verkman et al. 2000) or AQP8 (Yang et al. 2005) revealed no defect in pilocarpine-induced saliva secretion (not in volume or in composition), suggesting that neither AQP1, nor AQP8 plays a major role in the salivation process. However, transgenic mice lacking AQP5 displayed reduced pilocarpine-stimulated saliva secretion ($\pm 60\%$), hypertonic (420 mosm) and more viscous saliva, while amylase and protein secretion were not modified (Ma et al. 1999). Other studies showed that hyposalivation was due to a dramatic reduction in water membrane permeability of acinar cells, rather than changes in whole body fluid homeostasis (Krane et al. 2001). Latter data suggests that AQP5 plays a key role in saliva secretion. No data is currently available to assess a possible role of other AQPs in the salivary secretion process. While contradictory data exists concerning localisation of AQP5 in ductal cells (see above), further studies will be needed to investigate the functional role of AQP5 in the absorption and/or secretion of small solutes in ductal cells.

5.2 Lacrimal Glands

The average daily output of lacrimal secretion in man is about 5 ml. Lacrimal secretion contributes to the aqueous layer of the precorneal tear film. The rate of lacrimal secretion is controlled by parasympathetic and sympathetic innervations. Since the acinar cells secrete an isotonic fluid, and the final lacrimal secretion is hypertonic, it is suggested that ductal cells secreted additional K^+ and Cl^- (Mircheff 1989; Matsuzaki et al. 1999; Hamann et al. 1998; Funaki et al. 1998; Mircheff et al. 1994).

In acinar cells, the underlying mechanisms responsible for lacrimal secretion are quite similar to those occurring during salivary and pancreatic secretion (Fig. 1b). The presence of AQP4 and AQP5, at the basolateral and the apical membrane of

acinar cells respectively, suggested the involvement of those AQPs in the lacrimal secretory process (Ishida et al. 1997; Hamann et al. 1998). However, knockout mice lacking AQP1, AQP3, AQP4 or AQP5 displayed no modification in basal and pilocarpine-stimulated lacrimal secretion (not in volume or in composition). This strongly suggests that these AQPs do not play a major role in tear formation. The role of ductal cells in the K^+ and Cl^- secretion has recently been elucidated (Toth-Molnar et al. 2007). Following parasympathetic stimulation, Na^+ and Cl^- enter ductal cells in response to the activation of Na^+/H^+ and Cl^-/HCO_3^- exchangers at the basolateral membrane (Fig. 1b). Additionally, Na^+ was also shown to enter the cells via the $Na^+/K^+/2Cl^-$ cotransporters (Walcott et al. 2005). Intracellular available H^+ and HCO_3^- , necessary for Na^+ and Cl^- influx, are generated by the dehydration of carbonic acid by carbonic anhydrase. The elevated intracellular Na^+ can be exchanged for K^+ through the basolateral Na^+/K^+ ATPase and consequently induces an intracellular increase in the K^+ concentration. Both intracellular Cl^- and K^+ are finally secreted into the ductal lumen through Cl^- (CFTR) and K^+ channels, and/or K^+/Cl^- cotransporters (Toth-Molnar et al. 2007).

5.3 Pancreas

In humans, approximately 1,500 ml of pancreatic fluid is secreted per day. The functions of the pancreatic fluid include neutralization of fluid arriving from the stomach, hydrolysis of starch, proteins, lipids and nucleic acids. Contrary to salivary and lacrimal glands, most fluid secretion generated by the pancreas derives from ductal rather than acinar cells.

The ionic mechanisms responsible for pancreatic secretion by acinar cells are quite similar to those described for salivary glands (McManaman et al. 2006) and lead to production of a NaCl-rich isotonic fluid (Fig. 1c). Water moves to the acinar lumen through tight junctions and possibly via AQP8 located at the apical membrane (Hurley et al. 2001; Burghardt et al. 2003). The contribution of AQP8 to the water membrane permeability of rat pancreatic acinar cells, evaluated using video microscopy to measure the cell swelling in response to hypotonic stress following or not the exposure to $HgCl_2$ (an AQP blocker), was estimated at 90% (Hurley et al. 2001). However, probably due to small amount of fluid generated by acinar cells, knockout mice lacking AQP8 seemed to display normal pancreatic function since there was no obvious defect in the processing of dietary fat (Yang et al. 2005). On the other hand, in rat pancreatic acinar zymogen granules, AQP1 was shown to participate in basal as well as GTP-mediated vesicle water entry and swelling (Cho et al. 2002; Abu-Hamdah et al. 2004). Pancreatic ductal cells secrete most of the fluid rich in HCO_3^- to alkalinize and hydrate the primary fluid secreted by the acinar cells (Fig. 1c).

At the basolateral membrane of ductal cells, HCO_3^- uptake is achieved by $Na^+-HCO_3^-$ cotransporters and also by H^+ ATPase and Na^+/H^+ exchangers acting together with carbonic anhydrase. At the apical membrane, HCO_3^- secretion is

explained by the combined activity of $\text{Cl}^-/\text{HCO}_3^-$ exchangers and Cl^- conductance; also either the CFTR or a Ca^{2+} -activated Cl^- channel (Steward et al. 2005; McManaman et al. 2006). In rat interlobular ducts, shown to express AQP1, fluid secretion evoked by secretin was almost completely abolished by HgCl_2 (80–90% decrease), suggesting that AQP1 represented the main water pathway (Ko et al. 2002). In rodents, knockout mice lacking either AQP1 or AQP5 have not yet shown any abnormality in pancreatic secretion. Several explanations might account for this data: the weak expression of AQP1 and AQP5 or the redundancy of having them expressed in the intercalated ducts thought to be the main site of fluid secretion (Burghardt et al. 2003), or the possible existence of a slow secretory rate. Analysis of double AQP1 and AQP5 knockout mice would be valuable in determining the joint contribution of these AQPs to pancreatic fluid secretion.

6 Sjögren's Syndrome

6.1 Pathogenesis of Sjögren's Syndrome

Sjögren's syndrome is an autoimmune lacrimal and salivary gland disease characterised by lymphocyte infiltrates of the exocrine glands and/or the production of auto-antibodies. Clinically, patients suffering from Sjögren's syndrome present keratoconjunctivitis sicca and xerostomia. A subset of patients may develop systemic nonglandular manifestations (Thanou-Stavraki and James 2007; Garcia-Carrasco et al. 2006). Patients may have either primary or secondary (including another autoimmune disease, e.g., rheumatoid arthritis, systemic lupus erythematosus, ankylosing spondylitis ...) Sjögren's syndrome (Fox 2005; Konttinen et al. 2006). Primary Sjögren's syndrome has a prevalence of 0.5% and a female predominance ratio of 9:1 compared with men. The American-European criteria for diagnosis of Sjögren's syndrome published in 2002 (Vitali et al. 2002) includes inflammatory infiltrates in lip biopsy, auto-antibodies and clinical features. Despite extensive molecular, histological and clinical studies, the underlying cause of Sjögren's syndrome remains unknown. Pathogenesis seems to be multifactorial, where several steps are necessary to establish the disease. The initial step in the establishment of the disease probably involves glandular epithelial cells, vascular endothelial cells, stromal and dendritic cells (Fox 2005). Further steps include environmental triggers (such as viral infection of the glands or intercurrent infection stimulating dendritic or glandular epithelial cells), participation of genetic factors, migration of lymphocytes to the gland in response to cytokines and chemokines, co-stimulation of innate and acquired immune systems, glandular destruction, apoptosis, activation of T- and B-lymphocytes within the glands, production of auto-antibodies (for example against the muscarinic M3 type receptor for acetylcholine, the nuclear proteins Ro/SSA and La/SSB, α -fodrin...), and development of eye and mouth dryness (Fox 2005; Ramos-Casals and Font 2005; Garcia-Carrasco et al. 2006).

Salivary and lacrimal glands of patients with Sjögren's syndrome display infiltrating lymphocytes and local glandular destruction (Fox 2005). The degree of glandular destruction does not necessarily correlate with secretory dysfunction (Humphreys-Beher et al. 1999). There is evidence that subclinical exocrine pancreatic disease may also be present in some patients with Sjögren's syndrome. Auto-antibodies against pancreatic duct cells (also cross-reacting with parotid, sub-mandibular and lacrimal ductal cells (Ludwig et al. 1977)), and increased serum antibodies against CA 19-9, a marker of pancreatic tumour that can also be elevated with pancreatitis, have been reported in some patients suffering from Sjögren's syndrome (Safadi et al. 1998). Functional pancreatic impairment, such as elevated immunoreactive trypsin, amylase and pancreatic isoamylase, appear to be more severe in patients with longer disease duration, and related to the degree of alteration of salivary flow rather than the degree of histological salivary gland changes or the type of Sjögren's syndrome (primary or secondary) (Coll et al. 1989; Ostuni et al. 1996; Pal et al. 1987).

Ethical issues and delay in the appearance of symptoms, makes it difficult to study the wide array of factors intervening in the pathogenesis of Sjögren's syndrome in human patients. To circumvent this problem, several animal models have been developed for studying different aspects of the physiopathology of the disease. Most of the animal models for Sjögren's syndrome present a loss of secretory lacrimal and salivary functions (van Blokland and Versnel 2002; Soyfoo et al. 2007a).

6.2 AQPs and Sjögren's Syndrome

In labial salivary gland biopsies of Sjögren's syndrome patients, AQP1 distribution in myoepithelial cells decreased by 38%, while no changes were observed in endothelial cells of non-fenestrated capillaries (Beroukas et al. 2002). This decreased AQP1 expression in myoepithelial cells led to the hypothesis that myoepithelial cell dysfunction plays a role in its pathogenesis (Beroukas et al. 2002). The treatment of a patient suffering from Sjögren's syndrome with rituximab revealed great improvement of xerostomia, a marked increase in AQP1 expression in myoepithelial cells (Ring et al. 2006). Type 3 muscarinic receptor activation by acetylcholine induced the contraction of myoepithelial cells (Beroukas et al. 2002) and cell volume modification mediated by AQP1 could participate to vascular smooth muscle cell contraction (Shanahan et al. 1999). A hypothesis has been proposed that if AQP1 translocates, similar to AQP5 (Ishikawa et al. 1998), in response to acetylcholine stimulation, AQP1 might participate in rapid myoepithelial cell volume modifications and contraction (Shanahan et al. 1999). The contraction of myoepithelial cells, embracing the acini, will constrict the acini lumen and facilitate saliva flow. However, this hypothesis is not supported by data obtained with transgenic mice lacking AQP1 (Ma et al. 1999; Verkman et al. 2000).

Dacryoadenitis mice models such as MRL/lpr (24-week-old), NOD/Shi Jci (10-week-old), NFS/s-TX (10-week-old), or lipopolysaccharide-injected mice (Hirai

et al. 2000) exhibited higher AQP5 protein concentration in tears, suggesting that AQP5 leaks into tears, when acinar cells of lacrimal glands are damaged by lymphocyte infiltration. Similar results were further obtained with patients suffering from Sjögren's syndrome and presenting a dry eye syndrome (Ohashi et al. 2003).

Immunohistochemical distribution of AQP5 in normal human labial salivary (Steinfeld et al. 2001; Beroukas et al. 2001) and lacrimal glands (Tsubota et al. 2001) revealed that AQP5 was expressed at the apical membrane of acinar cells, similar to its localisation in human parotid glands (Gresz et al. 2001). In contrast to its normal apical localization in acinar cells, AQP5 was abnormally contained at either the basal membrane or the cytoplasm of acinar cells from respective minor salivary (Steinfeld et al. 2001) or lacrimal glands (Tsubota et al. 2001) for patients suffering from Sjögren's syndrome. Contradictory data documenting normal AQP5 distribution in minor salivary gland biopsies from patients suffering from Sjögren's syndrome (Beroukas et al. 2001) could be explained by the use of distinct antibodies, or differences existing between the investigated populations. More recently, in non-obese diabetic (NOD) mice, generally considered to be a good animal model for Sjögren's syndrome (Humphreys-Beyer et al. 1994; Cha et al. 2002; Soyfoo et al. 2007a), abnormal AQP5 distribution was also observed in salivary glands (Konttinen et al. 2005; Soyfoo et al. 2007b). Indeed, in NOD mice, two independent studies reported that AQP5 distribution was not restricted to apical membrane of acinar cells as in control mice, but rather, present at both apical and basolateral membranes (Konttinen et al. 2005; Soyfoo et al. 2007b). This data further supports observations that implied a loss of ordered and polarised expression of AQP5 in human minor salivary and lacrimal glands of patients suffering from Sjögren's syndrome. Reduced AQP1 expression in myoepithelial cells of salivary glands (Beroukas et al. 2002) and abnormal AQP5 expression in acinar cells of both salivary and lacrimal glands (Steinfeld et al. 2001; Tsubota et al. 2001; Konttinen et al. 2005; Soyfoo et al. 2007b) suggested that both AQP1 and AQP5 could participate in the pathogenesis of Sjögren's syndrome, although they could not directly account for salivary and lacrimal secretory defects.

B-cell-depleting therapies, such as rituximab (anti-CD20), appear promising for the treatment of Sjögren's syndrome (Thanou-Stavraki and James 2007; Ramos-Casals and Brito-Zeron 2007). Several studies using rituximab have shown improvement of sicca features and glandular manifestations, as well as complete remission of lymphoma in some cases (Ramos-Casals and Brito-Zeron 2007). Interestingly, rituximab was reported to improve xerostomia and increase the AQP5 expression at the apical membrane of acinar cells in patients with Sjögren's syndrome (Ring et al. 2006). It has also been suggested that treatment of ductal cells (which preferentially survive in secretory glands of patients with Sjögren's syndrome) with 5-aza-2'-deoxycytidine (a DNA demethylation agent) could result in increased expression of AQP5 (Motegi et al. 2005).

Further studies in Sjögren's syndrome patients are required to elucidate if changes of AQP5 expression and/or localisation are directly linked to the inflammatory mechanisms or are secondary effects caused by prolonged hyposalivation.

7 Conclusion

Several AQPs have been shown to be expressed in salivary and lacrimal glands and pancreas. Though, water movement contributes to exocrine secretions, a direct participation of AQPs has not been demonstrated in all secretory glands. Indeed, while certain data supports the involvement of AQP5 in the salivary secretion, a major role of AQPs in lacrimal and pancreatic secretion has not yet been clearly demonstrated. In Sjögren's syndrome patients, modification of AQP1 and AQP5 expression and abnormal AQP5 distribution might be either linked to the inflammatory mechanisms or are secondary effects caused by prolonged hyposalivation; they are however unlikely to directly account for salivary and lacrimal secretory defects.

Acknowledgments We acknowledge the contributions of Dr Bruce Baum and Dr Martin Steward in helpful comments and discussion. This work was supported by grant 3.4604.05 from the Fund for Medical Scientific Research (FRSM, Belgium).

References

- Abu-Hamdah R, Cho WJ, Cho SJ et al. (2004) Regulation of the water channel aquaporin-1: isolation and reconstitution of the regulatory complex. *Cell Biol Int* 28:7–17
- Agre P (2004) Aquaporin water channels (Nobel Lecture). *Angew Chem Int Ed Engl* 43:4278–4290
- Akamatsu T, Parvin MN, Murdiastuti K et al. (2003) Expression and localization of aquaporins, members of the water channel family, during development of the rat submandibular gland. *Pflugers Arch* 446:641–651
- Baum BJ (1993) Principles of saliva secretion. *Ann N Y Acad Sci* 694:17–23
- Beitz E (2006) Aquaporin water and solute channels from malaria parasites and other pathogenic protozoa. *Chem Med Chem* 1:587–592
- Beroukas D, Hiscock J, Jonsson R et al. (2001) Subcellular distribution of aquaporin 5 in salivary glands in primary Sjögren's syndrome. *Lancet* 358:1875–1876
- Beroukas D, Hiscock J, Gannon BJ et al. (2002) Selective down-regulation of aquaporin-1 in salivary glands in primary Sjögren's syndrome. *Lab Invest* 82:1547–1552
- Beroukas D, Goodfellow R, Hiscock J et al. (2002) Up-regulation of M₃-muscarinic receptors in labial salivary gland acini in primary Sjögren's syndrome. *Lab Invest* 82:203–210
- Burghardt B, Elkaer ML, Kwon TH et al. (2003) Distribution of aquaporin water channels AQP1 and AQP5 in the ductal system of the human pancreas. *Gut* 52:1008–1016
- Burghardt B, Nielsen S, Steward MC (2006) The role of aquaporin water channels in fluid secretion by the exocrine pancreas. *J Membr Biol* 210:143–153
- Cha S, Peck AB, Humphreys-Beher MG (2002) Progress in understanding autoimmune exocrinopathy using the non-obese diabetic mouse: an update. *Crit Rev Oral Biol Med* 13:5–16
- Cho SJ, Sattar AK, Jeong EH et al. (2002) Aquaporin 1 regulates GTP-induced rapid gating of water in secretory vesicles. *Proc Natl Acad Sci U S A* 99:4720–4724
- Coll J, Navarro S, Tomas R et al. (1989) Exocrine pancreatic function in Sjögren's syndrome. *Arch Intern Med* 149:848–852
- Cook DI, Van Lennep EW, Roberts ML et al. (1994) Secretion by the major salivary glands. In: Johnson LR, Christensen J, Jackson M, Jacobson E, Walsh J (eds.) *Physiology of the gastrointestinal tract*, 3rd edn. Raven Press, New York, pp. 1061–1117

- Delporte C, Steinfeld S (2006) Distribution and roles of aquaporins in salivary glands. *Biochim Biophys Acta* 1758:1061–1070
- Delporte C, O'Connell BC, He X et al. (1997) Increased fluid secretion after adenoviral-mediated transfer of the aquaporin-1 cDNA to irradiated rat salivary glands. *Proc Natl Acad Sci U S A* 94:3268–3273
- Denny PC, Ball WD, Redman RS (1997) Salivary glands: a paradigm for diversity of gland development. *Crit Rev Oral Biol Med* 8:51–75
- Elkjaer ML, Nejsum LN, Gresz V et al. (2001) Immunolocalization of aquaporin-8 in rat kidney, gastrointestinal tract, testis, and airways. *Am J Physiol Renal Physiol* 281:F1047–F1057
- Fox RI (2005) Sjogren's syndrome. *Lancet* 366:321–331
- Frigeri A, Gropper MA, Umenishi F et al. (1995) Localization of MIWC and GLIP water channel homologs in neuromuscular, epithelial and glandular tissues. *J Cell Sci* 108:2993–3002
- Funaki H, Yamamoto T, Koyama Y et al. (1998) Localization and expression of AQP5 in cornea, serous salivary glands, and pulmonary epithelial cells. *Am J Physiol* 275:C1151–C1157
- Furuya S, Naruse S, Ko SB et al. (2002) Distribution of aquaporin 1 in the rat pancreatic duct system examined with light- and electron-microscopic immunohistochemistry. *Cell Tissue Res* 308:75–86
- Garcia-Carrasco M, Fuentes-Alexandro S, Escarcega RO et al. (2006) Pathophysiology of Sjogren's syndrome. *Arch Med Res* 37:921–932
- Gresz V, Burghardt B, Ferguson CJ et al. (1999) Expression of aquaporin 1 (AQP1) water channels in human labial salivary glands. *Arch Oral Biol* 44:S53–S57
- Gresz V, Kwon TH, Hurley PT et al. (2001) Identification and localization of aquaporin water channels in human salivary glands. *Am J Physiol Gastrointest Liver Physiol* 281:G247–G254
- Gresz V, Kwon TH, Gong H et al. (2004) Immunolocalization of AQP-5 in rat parotid and submandibular salivary glands after stimulation or inhibition of secretion in vivo. *Am J Physiol Gastrointest Liver Physiol* 287:G151–G161
- Hamann S, Zeuthen T, La Cour M et al. (1998) Aquaporins in complex tissues: distribution of aquaporins 1–5 in human and rat eye. *Am J Physiol* 274:C1332–C1345
- Hasegawa H, Ma T, Skach W et al. (1994) Molecular cloning of a mercurial-insensitive water channel expressed in selected water-transporting tissues. *J Biol Chem* 269:5497–5500
- He X, Tse CM, Donowitz M et al. (1997) Polarized distribution of key membrane transport proteins in the rat submandibular gland. *Pflugers Arch* 433:260–268
- Hill AE, Shachar-Hill B, Shachar-Hill Y (2004) What are aquaporins for? *J Membr Biol* 197:1–32
- Hill AE, Shachar-Hill B (2006) A new approach to epithelial isotonic fluid transport: an osmosensor feedback model. *J Membr Biol* 210:77–90
- Hirai S, Ishida N, Watanabe K et al. (2000) Leakage of aquaporin 5 in the tear of dacryoadenitis mice. *Invest Ophthalmol Vis Sci* 41:2432–2437
- Humphreys-Beher MG, Peck AB, Dang H et al. (1999) The role of apoptosis in the initiation of the autoimmune response in Sjogren's syndrome. *Clin Exp Immunol* 116:383–387
- Humphreys-Beher MG, Hu Y, Nakagawa Y et al. (1994) Utilization of the non-obese diabetic (NOD) mouse as an animal model for the study of secondary Sjogren's syndrome. *Adv Exp Med Biol* 350:631–636
- Hurley PT, Ferguson CJ, Kwon TH et al. (2001) Expression and immunolocalization of aquaporin water channels in rat exocrine pancreas. *Am J Physiol Gastrointest Liver Physiol* 280:G701–G709
- Ishibashi K (2006) Aquaporin subfamily with unusual NPA boxes. *Biochim Biophys Acta* 1758:989–993
- Ishida N, Hirai SI, Mita S (1997) Immunolocalization of aquaporin homologs in mouse lacrimal glands. *Biochem Biophys Res Commun* 238:891–895
- Ishikawa Y, Eguchi T, Skowronski MT et al. (1998) Acetylcholine acts on M₃ muscarinic receptors and induces the translocation of aquaporin5 water channel via cytosolic Ca²⁺ elevation in rat parotid glands. *Biochem Biophys Res Commun* 245:835–840

- Ishikawa F, Suga S, Uemura T et al. (2005) Identification of AQP5 in lipid rafts and its translocation to apical membranes by activation of M3 mAChRs in interlobular ducts of parotid gland. *Am J Physiol Cell Physiol* 289:C1303–C1311
- Itoh T, Rai T, Kuwahara M et al. (2005) Identification of a novel aquaporin, AQP12, expressed in pancreatic acinar cells. *Biochem Biophys Res Commun* 330:832–828
- King LS, Nielsen S, Agre P (1997) Aquaporins in complex tissues. I. Developmental patterns in respiratory and glandular tissues of rat. *Am J Physiol* 273:C1541–C1548
- King LS, Kozono D, Agre P (2004) From structure to disease: the evolving tale of aquaporin biology. *Nat Rev Mol Cell Biol* 5:687–698
- Ko SB, Naruse S, Kitagawa M et al. (2002) Aquaporins in rat pancreatic interlobular ducts. *Am J Physiol Gastrointest Liver Physiol* 282:G324–G331
- Konttinen YT, Tensing EK, Laine M et al. (2005) Abnormal distribution of aquaporin-5 in salivary glands in the NOD mouse model for Sjögren's syndrome. *J Rheumatol* 32:1071–1075
- Konttinen YT, Porola P, Konttinen L et al. (2006) Immunohistopathology of Sjögren's syndrome. *Autoimmun Rev* 6:16–20
- Koyama Y, Yamamoto T, Kondo D et al. (1997) Molecular cloning of a new aquaporin from rat pancreas and liver. *J Biol Chem* 272:30329–30333
- Krane CM, Towne JE, Menon AG (1999) Cloning and characterization of murine Aqp5: evidence for a conserved aquaporin gene cluster. *Mamm Genome* 10:498–505
- Krane CM, Melvin JE, Nguyen HV et al. (2001) Salivary acinar cells from aquaporin 5-deficient mice have decreased membrane water permeability and altered cell volume regulation. *J Biol Chem* 276:23413–23420
- Krane CM, Goldstein DL (2007) Comparative functional analysis of aquaporins/glyceroporins in mammals and anurans. *Mamm Genome* 18:452–462
- Li J, Nielsen S, Dai Y et al. (1994) Examination of rat salivary glands for the presence of the aquaporin CHIP. *Pflugers Arch* 428:455–460
- Ludwig H, Scherthaner G, Scherak O et al. (1977) Antibodies to pancreatic duct cells in Sjögren's syndrome and rheumatoid arthritis. *Gut* 18:311–315
- Nielsen S, Smith BL, Christensen EI et al. (1993) Distribution of the aquaporin CHIP in secretory and absorptive epithelia and capillary endothelia. *Proc Natl Acad Sci U S A* 90:7275–7279
- Ma T, Song Y, Gillespie A et al. (1999) Defective secretion of saliva in transgenic mice lacking aquaporin-5 water channels. *J Biol Chem* 274:20071–20074
- Mangos JA, McSherry NR (1970) Micropuncture study of urea excretion in parotid saliva of the rat. *Am J Physiol* 218:1329–1332
- Mangos JA, Maragos N, McSherry NR (1973) Micropuncture and microperfusion study of glucose excretion in rat parotid saliva. *Am J Physiol* 224:1260–1264
- Matsuki M, Hashimoto S, Shimono M et al. (2005) Involvement of aquaporin-5 water channel in osmoregulation in parotid secretory granules. *J Membr Biol* 203:119–126
- Matsuzaki T, Suzuki T, Koyama H et al. (1999) Aquaporin-5 (AQP5), a water channel protein, in the rat salivary and lacrimal glands: immunolocalization and effect of secretory stimulation. *Cell Tissue Res* 295:513–521
- Matsuzaki T, Tajika Y, Suzuki T et al. (2003) Immunolocalization of the water channel, aquaporin-5 (AQP5), in the rat digestive system. *Arch Histol Cytol* 66:307–315
- Maurel C (2007) Plant aquaporins: novel functions and regulation properties. *FEBS Lett* 581:2227–2236
- McManaman JL, Reyland ME, Throther EC (2006) Secretion and fluid transport mechanisms in the mammary gland: comparisons with the exocrine pancreas and the salivary gland. *J Mammary Gland Biol Neoplasia* 11:249–268
- Melvin JE, Yule D, Shuttleworth T et al. (2005) Regulation of fluid and electrolyte secretion in salivary gland acinar cells. *Annu Rev Physiol* 67:445–469
- Mirchekff AK (1989) Lacrimal fluid and electrolyte secretion: a review. *Curr Eye Res* 8:607–617
- Mirchekff AK, Lambert RW, Lambert RW et al. (1994) Subcellular organization of ion transporters in lacrimal acinar cells: secretagogue-induced dynamics. *Adv Exp Med Biol* 350:79–86

- Mobasher A, Marples D (2004) Expression of the AQP-1 water channel in normal human tissues: a semi-quantitative study using tissue microarray technology. *Am J Physiol Cell Physiol* 286:C529–C537
- Motegi K, Azuma M, Tamatani T et al. (2005) Expression of aquaporin-5 in and fluid secretion from immortalized human salivary gland ductal cells by treatment with 5-aza-2'-deoxycytidine: a possibility for improvement of xerostomia in patients with Sjögren's syndrome. *Lab Invest* 85:342–353
- Murakami M, Murdiastuti K, Hosoi K et al. (2006) AQP and the control of fluid transport in a salivary gland. *J Membr Biol* 210:91–103
- Murdiastuti K, Miki O, Yao C et al. (2002) Divergent expression and localization of aquaporin 5, an exocrine-type water channel, in the submandibular gland of Sprague-Dawley rats. *Pflugers Arch* 445:405–412
- Nielsen S, King LS, Christensen BM et al. (1997) Aquaporins in complex tissues. II. Subcellular distribution in respiratory and glandular tissues of rat. *Am J Physiol* 273:C1549–C1561
- Ohashi Y, Ishida R, Kojima T et al. (2003) Abnormal protein profiles in tears with dry eye syndrome. *Am J Ophthalmol* 136:291–299
- Ostuni PA, Gazzetto G, Chieco-Bianchi F et al. (1996) Pancreatic exocrine involvement in primary Sjögren's syndrome. *Scand J Rheumatol* 25:47–51
- Pal B, Griffiths ID, Katrak A et al. (1987) Salivary amylase and pancreatic enzymes in Sjögren's syndrome. *Clin Chem* 33:305–307
- Pettersson N, Filipsson C, Becit E et al. (2005) Aquaporins in yeasts and filamentous fungi. *Biol Cell* 97:487–500
- Preston GM, Agre P (1991) Isolation of the cDNA for erythrocyte integral membrane protein of 28 kilodaltons: member of an ancient channel family. *Proc Natl Acad Sci U S A* 88:11110–11114
- Preston GM, Carroll TP, Guggino WB et al. (1992) Appearance of water channels in *Xenopus* oocytes expressing red cell CHIP28 protein. *Science* 256:385–387
- Proctor GB, Carpenter GH (2007) Regulation of salivary gland function by autonomic nerves. *Auton Neurosci* 133:3–18
- Raina S, Preston GM, Guggino WB et al. (1995) Molecular cloning and characterization of an aquaporin cDNA from salivary, lacrimal, and respiratory tissues. *J Biol Chem* 270:1908–1912
- Ramos-Casals M, Font J (2005) Primary Sjögren's syndrome: current and emergent aetiopathogenic concepts. *Rheumatology (Oxford)* 44:1354–1367
- Ramos-Casals M, Brito-Zeron P (2007) Emerging biological therapies in primary Sjögren's syndrome. *Rheumatology (Oxford)* 46:1389–1396
- Ring T, Kallenbach M, Praetorius J et al. (2006) Successful treatment of a patient with primary Sjögren's syndrome with Rituximab. *Clin Rheumatol* 25:891–894
- Safadi R, Ligumsky M, Goldin E et al. (1998) Increased serum CA 19–9 antibodies in Sjögren's syndrome. *Postgrad Med J* 74:543–544
- Shachar-Hill B, Hill AE (2002) Paracellular fluid transport by epithelia. *Int Rev Cytol* 215:319–350
- Shanahan CM, Connolly DL, Tyson KL et al. (1999) Aquaporin-1 is expressed by vascular smooth muscle cells and mediates rapid water transport across vascular cell membranes. *J Vasc Res* 36:353–362
- Ship JA, Pillemer SR, Baum BJ (2002) Xerostomia and the geriatric patient. *J Am Geriatr Soc* 50:535–543
- Smith BL, Agre P (1991) Erythrocyte Mr 28,000 transmembrane protein exists as a multisubunit oligomer similar to channel proteins. *J Biol Chem* 266:6407–6415
- Soyfoo MS, Steinfeld S, Delporte C (2007a) Usefulness of mouse models to study the pathogenesis of Sjögren's syndrome. *Oral Dis* 13:366–375
- Soyfoo MS, De Vriese C, Debaix H et al. (2007b) Modified aquaporin 5 expression and distribution in submandibular glands from NOD mice displaying autoimmune exocrinopathy. *Arthritis Rheum* 56:2566–2574
- Steinfeld S, Cogan E, King LS et al. (2001) Abnormal distribution of aquaporin-5 water channel protein in salivary glands from Sjögren's syndrome patients. *Lab Invest* 81:143–148

- Steward MC, Ishiguro H, Case RM (2005) Mechanisms of bicarbonate secretion in the pancreatic duct. *Annu Rev Physiol* 67:377–409
- Sugiya H, Matsuki M (2006) AQP8 and control of vesicle volume in secretory cells. *J Membr Biol* 210:155–159
- Suzuki M, Hasegawa T, Ogushi Y et al. (2007) Amphibian aquaporins and adaptation to terrestrial environments: a review. *Comp Biochem Physiol A Mol Integr Physiol* 148:72–81
- Takata K, Matsuzaki T, Tajika Y (2004) Aquaporins: water channel proteins of the cell membrane. *Prog Histochem Cytochem* 39:1–83
- Tanghe A, Van Dijck P, Thevelein JM (2006) Why do microorganisms have aquaporins?. *Trends Microbiol* 14:78–85
- Thanou-Stavraki A, James JA (2007) Primary Sjögren's syndrome: current and prospective therapies. *Semin Arthritis Rheum* 37:273–292
- Turner RJ, Sugiya H (2002) Understanding salivary fluid and protein secretion. *Oral Dis* 8:3–11
- Toth-Molnar E, Venglovecz V, Ozsvari B et al. (2007) New experimental method to study acid/base transporters and their regulation in lacrimal gland ductal epithelia. *Invest Ophthalmol Vis Sci* 48:3746–3755
- Tsubota K, Hirai S, King LS et al. (2001) Defective cellular trafficking of lacrimal gland aquaporin-5 in Sjögren's syndrome. *Lancet* 357:688–689
- van Blokland SC, Versnel MA (2002) Pathogenesis of Sjögren's syndrome: characteristics of different mouse models for autoimmune exocrinopathy. *Clin Immunol* 103:111–124
- Verbavatz JM, Brown D, Sabolic I et al. (1993) Tetrameric assembly of CHIP28 water channels in liposomes and cell membranes: a freeze-fracture study. *J Cell Biol* 123:605–618
- Verkman AS, Yang B, Song Y et al. (2000) Role of water channels in fluid transport studied by phenotype analysis of aquaporin knockout mice. *Exp Physiol* 85:233S–241S
- Verkman AS (2005) Novel roles of aquaporins revealed by phenotype analysis of knockout mice. *Rev Physiol Biochem Pharmacol* 155:31–55
- Vitali C, Bombardieri S, Jonsson R et al. (2002) Classification criteria for Sjögren's syndrome: a revised version of the European criteria proposed by the American-European Consensus Group. *Ann Rheum Dis* 61:554–558
- Walcott B, Birzgalis A, Moore LC et al. (2005) Fluid secretion and the Na⁺-K⁺-2Cl⁻ cotransporter in mouse exorbital lacrimal gland. *Am J Physiol Cell Physiol* 289:C860–C867
- Wang W, Hart PS, Piesco NP et al. (2003) Aquaporin expression in developing human teeth and selected orofacial tissues. *Calcif Tissue Int* 72:222–227
- Wellner RB, Hoque AT, Goldsmith CM et al. (2000) Evidence that aquaporin-8 is located in the basolateral membrane of rat submandibular gland acinar cells. *Pflugers Arch* 441:49–56
- Wellner RB, Redman RS, Swain WD et al. (2006) Further evidence for AQP8 expression in the myoepithelium of rat submandibular and parotid glands. *Pflugers Arch* 451:642–645
- Yang B, Song Y, Zhao D et al. (2005) Phenotype analysis of aquaporin-8 null mice. *Am J Physiol Cell Physiol* 288:C1161–C1170

Part III
Aquaporin Glycerol Permeability
in Mammalian Physiology

Skin Aquaporins: Function in Hydration, Wound Healing, and Skin Epidermis Homeostasis

Mathieu Boury-Jamot, Jean Daraspe, Frédéric Bonté, Eric Perrier, Sylvianne Schnebert, Marc Dumas, and Jean-Marc Verbavatz

Contents

1	Introduction	206
2	Skin Epidermis	206
3	AQP3 in Skin	207
3.1	Role and Regulation of AQP3 in Skin Hydration	208
3.2	Role of AQP3 in Skin Glycerol Metabolism	211
3.3	Role of AQP3 in Cell Proliferation, Migration, and Wound Healing in Skin Epidermis	212
3.4	New Aquaporins in Skin Epidermis	213
4	Conclusions	215
	References	215

Abstract Several aquaporins (AQPs) are expressed in mammalian skin. Some are directly involved in water transport, such as AQP5, which is involved in sweat secretion. In contrast, the physiological role of skin aquaglyceroporins, which permeate both water and glycerol, appears more and more complex. AQP3 is the most abundant skin aquaglyceroporin. Both water and glycerol transport by AQP3 appear to play an important role in hydration of mammalian skin epidermis. In addition, recent data suggest that glycerol transport by AQP3 is involved in the metabolism of lipids in skin as well as in the regulation of proliferation and differentiation of keratinocytes. Finally, AQP3 is also believed to be important in wound healing, as a water channel by facilitating cell migration, and as a glycerol transporter by enhancing keratinocyte proliferation and differentiation.

J.-M. Verbavatz (✉)

IBITEC-S and CNRS URA 2096, CEA-Saclay F-91191 Gif-sur-Yvette and LRA17V,
University of Paris-Sud 11, F-91400 Orsay, France
jean-marc.verbavatz@cea.fr

1 Introduction

In mammals, the aquaporin (AQP) family of channels comprises 13 homologous proteins. They can be divided functionally into three distinct groups: AQP0, 1, 2, 4, 5, and 8 are water channels, while AQP3, 7, 9, and 10, called aquaglyceroporins, also transport glycerol and other small solutes. Finally, AQP6, 11, and 12, sometimes referred to as unorthodox aquaporins, have specific or as yet unelucidated properties (Rojek et al. 2008). A large spectrum of aquaporins, including strict water channels and aquaglyceroporins, is found in mammalian skin. The aquaporin-1 (AQP1) water channel is expressed in vascular endothelial cells throughout the body, including the skin, where it facilitates water exchange between blood and skin dermis. Also, as in other tissues, aquaporin-7, an aquaglyceroporin, is found in adipocytes of skin dermis/hypodermis, where it is believed to be involved in glycerol transport (Hibuse et al. 2005; Hara-Chikuma et al. 2005). These two aquaporins and their functions as described above are not restricted to mammalian skin. In fact, neither water channels nor glycerol transporters were expected to exist in mammalian skin, except in sweat glands. A specific role for the aquaporin-5 (AQP5) water channel in sweat secretion has been demonstrated (Nejsum et al. 2002). This is consistent with the role of AQP5 in other exocrine glands, such as salivary glands (Delporte and Steinfeld 2006).

2 Skin Epidermis

The epidermis of the skin is an effective barrier against water evaporation. Skin epidermis is a multi-layered epithelium, which is primarily composed of keratinocytes (Fig. 1). Undifferentiated keratinocytes proliferate at the basal layer of

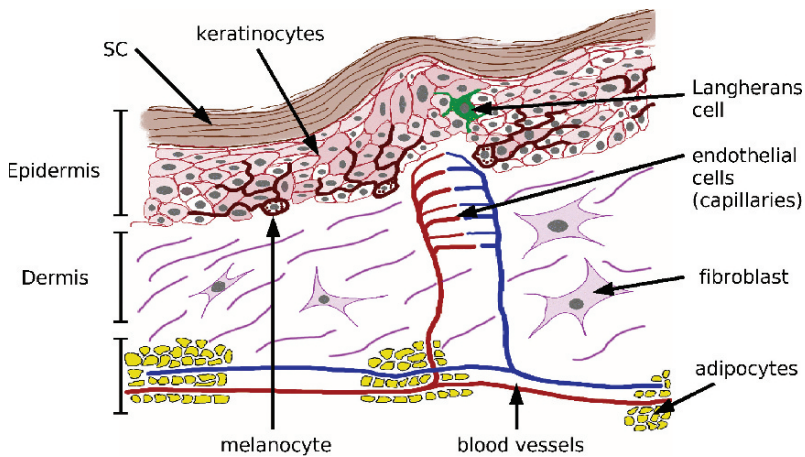


Fig. 1 Schematic structure of human skin. The epidermis is primarily composed of keratinocytes, which proliferate in the basal layer, differentiate, migrate towards the skin surface, and terminally differentiate into corneocytes in the *stratum corneum*. Melanocytes are also found in skin epidermis. From Boury-Jamot et al. (2006)

the epidermis, the *stratum basale*. Keratinocytes gradually differentiate as they migrate toward the skin surface through the *stratum spinosum* and the *stratum granulosum*. They undergo corneification at the *stratum corneum* (SC), which is the actual barrier against water loss by evaporation. The water content in the epidermis is high (~75%), and constant across the deepest layers of the epidermis. Skin water content drops sharply in the SC (~35%). Nevertheless, hydration of the SC is an important determinant of its barrier function. SC hydration relies on many factors, such as water-retaining agents (natural moisturizing factors), intercellular lipids arranged to form a barrier against water evaporation, and the presence of tight junctions with the *stratum granulosum* (Verdier-Sévrain and Bonté 2007). Interestingly, several members of the aquaporin family are expressed in skin epidermis. The purpose of this paper is to review their potential functions in this tissue.

3 AQP3 in Skin

AQP3 was initially cloned from the kidney (Ma et al. 1994; Ishibashi et al. 1994; Echevarria et al. 1994), where it is involved in water reabsorption across the basolateral membrane of collecting duct epithelial cells. Indeed, transgenic mice deficient in AQP3 are markedly polyuric (Ma et al. 2000, 2002). AQP3 was then identified in a large number of rat tissues, like the eye conjunctiva, the GI tract, and the skin (Frigeri et al. 1995; Matsuzaki et al. 1999). Because neither water movement nor glycerol transport were thought to be significant features in skin epidermis, and the expression of skin AQPs in general and the function of skin AQP3 in particular was not investigated until recently. In our first study (Sougrat et al. 2002), we demonstrated that AQP3 is abundant in human skin epidermis and that it is located in keratinocyte plasma membranes in the *stratum basale* and the *stratum spinosum* (Fig. 2a). Interestingly, AQP3 was not detected in the *stratum granulosum* and the *stratum corneum*, which are the most superficial layers of the epidermis. We also demonstrated that AQP3 is a functional pH-sensitive water channel, consistent with

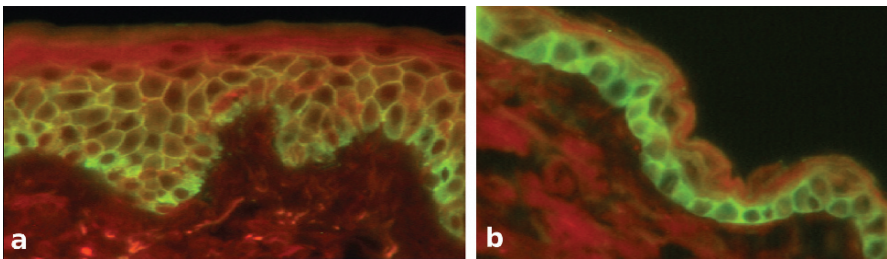


Fig. 2 Immunolocalization of AQP3 by indirect immunofluorescence (green) in human (a) and mouse (b) epidermis. In human epidermis, AQP3 is found in the *stratum basale* and *stratum spinosum*. In mouse epidermis, AQP3 is only detected in the *stratum basale*. Little or no staining of the *stratum granulosum* or *stratum corneum* is detected in either species. Adapted from Boury-Jamot et al. (2006)

its function in *in vitro* swelling assays and with its physiological role in the kidney (Zeuthen and Klaerke 1999).

3.1 Role and Regulation of AQP3 in Skin Hydration

Phenotypic studies in transgenic mice lacking AQP3 confirmed the physiological importance of AQP3 in skin hydration. In contrast to human or rat skin, AQP3 in mouse epidermis is localized only to the *stratum basale* (Ma et al. 2002) (Fig. 2b), consistent with the absence of a visible *stratum spinosum* in mouse epidermis. Mice lacking AQP3 had no defect in skin morphology, but they exhibited dry skin (reduced water content in the *stratum corneum*) and reduced water and glycerol permeability (Ma et al. 2002). AQP3 deletion in mice was also associated with reduced skin elasticity, delayed barrier recovery and wound healing, and reduced glycerol contents (Hara et al. 2002). As an aquaglyceroporin, AQP3 can transport both water and glycerol, and therefore the functional relevance of either water or glycerol transport by AQP3 in skin epidermis and the consequences of this on skin hydration, wound healing, and keratinocyte proliferation and differentiation have been the object of several studies.

AQP3 and water loss: As AQP3 is clearly involved in water transport in the kidney (Ma et al. 2000), the first assumption was that AQP3 was also a water channel in skin (Sougrat et al. 2002). The expression of a water channel in a water-impermeable tissue like skin seemed to be a paradox. It was tempting to assume that the role of AQP3 was replacement of water loss by evaporation. In the absence of AQP3, it was thus expected that skin water content would be more sensitive to water loss. This was not the case; on the contrary, the hydration of skin changed upon exposure to dry air or after occlusion in AQP3-expressing epidermis, but not in AQP3-deleted skin (Ma et al. 2002), and wild-type mice had dry skin after exposure to low, 10% humidity, as present in AQP3-deleted animals. The next hypothesis was that AQP3 was involved in increasing epidermal water loss and therefore in possible skin dehydration during development (Agren et al. 2003), or in disease when AQP3 is overexpressed (Olsson et al. 2006). In fact, AQP3 deletion did not result in a significant decrease in transepidermal water loss by evaporation (TEWL) (Hara et al. 2002), demonstrating that AQP3 is not specifically involved in increasing TEWL. Finally, it was shown that increased AQP3 expression is simultaneously associated with increased skin hydration and increased TEWL in DHCR24-deficient mice (Mirza et al. 2008). TEWL is a measure of the permeability barrier of skin epidermis. The barrier function relies on several features, and SC structure is believed to be the most important determinant of the permeability barrier (Imakado et al. 1995; Proksch et al. 2006; Verdier-Sévrain and Bonté 2007; Cao et al. 2008). However, impaired AQP3 did not result in an apparent change in SC structure (Ma et al. 2002; Hara et al. 2002). Consequently, there does not appear to be a link between AQP3 expression and transepidermal water loss by evaporation.

AQP3 and dry skin: In a number of studies, AQP3 alterations have been associated with dry skin either in mice (Ma et al. 2002; Hara et al. 2002; Hara and Verkman 2003; Boury-Jamot et al. 2006) or in humans (Boury-Jamot et al. 2006; Olsson et al. 2006; Cao et al. 2008). However, authors disagree on the mechanism involving AQP3 in skin hydration. According to Olsson et al. (2006), increased expression of AQP3 and altered distribution may contribute to water loss and dry skin in atopic eczema in humans, through increased transepidermal water evaporation. In contrast, Boury-Jamot et al. (2006) have shown decreased AQP3 in eczematous skin epidermis and conclude that decreased water transport by AQP3 in the epidermis is the cause of dry skin in the disease, and is possibly the cause of increased water loss due to barrier disruption. In agreement with the latter, Cao et al. (2008) and observations by our group (unpublished) have shown a UV-radiation-induced downregulation of AQP3 associated with skin dehydration.

In fact, it has been established that changes in AQP3 regulation can be either the cause or the consequence of skin dehydration; AQP3 deletion in mice resulted in dry skin (Ma et al. 2002; Hara et al. 2002). Conversely, Sugiyama et al. (2001) reported that osmotic stress upregulates AQP3 gene expression in cultured human keratinocytes. We have also shown that the AQP3 protein itself is upregulated in keratinocyte cell cultures in response to hyperosmolality (Sougrat et al. 2000; Dumas et al. 2007). This is also consistent with the early observation that AQP3 is expressed in tissues exposed to water loss (Matsuzaki et al. 1999).

AQP3 and glycerol transport: The discovery that epidermal glycerol content, and not just epidermal water content, was altered in AQP3-deleted mice (Hara et al. 2002) opened new perspectives on the functional role of aquaglyceroporins in skin and other mammalian tissues. This study was rapidly followed by a comprehensive study of glycerol in AQP3-null mouse epidermis, based on glycerol replacement (Hara and Verkman 2003). The conclusion was that glycerol replacement corrected skin hydration and mechanical defects observed in AQP3-deficient mice.

However, the results of the second study could have been interpreted quite differently. Figure 3 is adapted from a Hara and Verkman (2003) study. Figure 3a shows the glycerol contents of the epidermis and SC before and after intraperitoneal

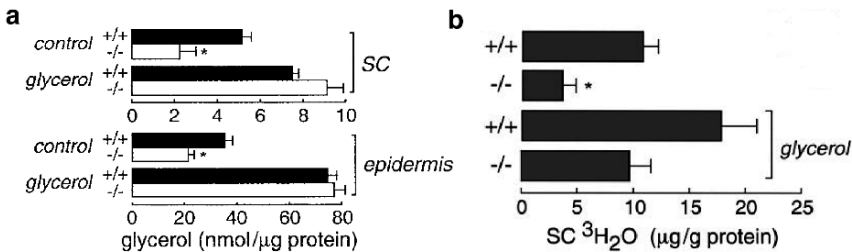


Fig. 3 Glycerol and water content in wild-type (+/+) and AQP3-null (-/-) mice. (a) Glycerol content in SC and epidermis before (control) and after (glycerol) intraperitoneal glycerol administration. (b) Water content (measured from ³H₂O radioactivity) in the SC of control (top) or after glycerol administration for 24 h (glycerol). (n = 5 mean + SE). Adapted from Hara and Verkman (2003)

glycerol administration. As claimed by the authors, glycerol administration does increase epidermis and SC glycerol contents in AQP3-null mice. In fact, glycerol concentrations increase well above the control values of wild-type mice. After exogenous administration, glycerol also increases above normal values in wild-type mice. Thus, the conclusion from this experiment is that glycerol is transported through the epidermis to the SC, whether or not AQP3 is expressed. This clearly speaks against any significant role of AQP3 in transepidermal glycerol transport. Similarly, glycerol administration resulted in increased epidermis water content in both AQP3-null and wild-type animals (Fig. 3b), which does not suggest any specific role of AQP3-mediated glycerol transport in skin hydration. These results collectively confirm the ability of glycerol to improve skin epidermis hydration, whether or not AQP3 is present. This property of glycerol has been known for centuries, which is why it is one of the key components of all manufactured hydrating products. Therefore, the mechanism involving AQP3 in mouse skin hydration remains unresolved to date, and the question still is: which of the three – water transport, glycerol transport, or both water and glycerol transport by AQP3 – is most relevant for skin hydration?

AQP3 in human epidermis: Our group has been most interested in human skin. As shown above, human epidermis (Fig. 2a) is markedly thicker than mouse epi-

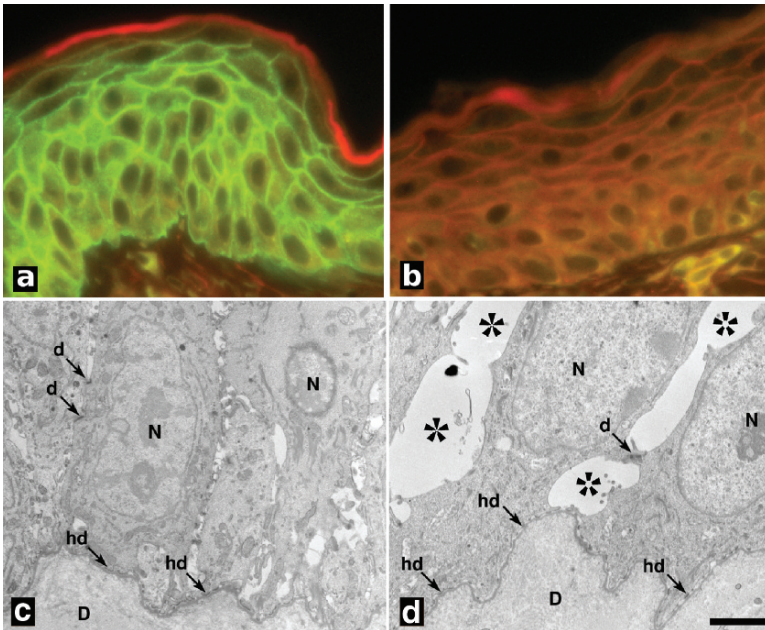


Fig. 4 Immunolocalization of AQP3 in the epidermis of wild-type (a) and AQP3-deleted (b) mice after tape-stripping-induced hyperplasia. AQP3 is detected only in AQP3-expressing mice, but tape stripping induces keratinocyte proliferation and hyperplasia in both genotypes. In thick epidermis, AQP3 deletion results in intercellular edema (d,*), but not in AQP3-positive epidermis (c), suggesting a role of AQP3 in transcellular water transport. *N* nuclei, *D* dermis, *d* desmosomes. Adapted from Boury-Jamot et al. (2006)

dermis (Fig. 2b), where no *stratum spinosum* is visible. Because AQP3 deletion useful for phenotypic analyses is only available in mice, we examined the distribution of AQP3 and the ultrastructure of skin epidermis in mice in which the epidermis had been artificially thickened by repeated tape-stripping (Boury-Jamot et al. 2006). Following induction of hyperplasia, AQP3 was no longer restricted to the basal layer of the epidermis in the mice (Fig. 4a). In treated mice expressing AQP3, epidermis thickness and AQP3 distribution became comparable to human epidermis (Fig. 4a vs. Fig. 2a). As expected, AQP3 remained absent from the epidermis in treated AQP3-null mice (Fig. 4b) but, over 8 days, AQP3-deletion did not significantly prevent the keratinocyte proliferation leading to epidermal hyperplasia. Although no ultrastructural consequence of AQP3-deletion in mouse skin had been detected in previous studies (Ma et al. 2002; Hara et al. 2002), AQP3-deletion in a multi-layered epidermis specifically resulted in dilated keratinocyte intercellular spaces (Fig. 4d vs. Fig. 4c). This phenotype, also seen in association with human AQP3 downregulation in skin spongiosis (Boury-Jamot et al. 2006), strongly suggests a defect in water transport in AQP3-deficient epidermis. Indeed, because the permeability of cell membranes becomes limited, water transport through the extracellular compartment is increased, to guarantee an osmotic equilibrium across several epithelial layers of the epithelium. This transport is not necessary in normal mouse epidermis, where only one layer, the *stratum basale*, needs to be highly hydrated. Thus, water transport by AQP3 in keratinocyte plasma membranes is possibly a central feature of skin hydration in humans, if not in mice.

3.2 Role of AQP3 in Skin Glycerol Metabolism

Nevertheless, SC glycerol is an important determinant of skin hydration. Endogenous SC glycerol appears to be generated, at least in part, from triglyceride hydrolysis in sebaceous glands (Choi et al. 2005). Indeed, in asebia mice that display profound sebaceous gland hypoplasia, Fluhr et al. (2003) have shown that sebaceous gland-derived glycerol is an important contributor to *stratum corneum* hydration. Though lipase activity can be detected both in the SC and in sebaceous glands, triglycerides in the epidermis are utilized as an energy source. Thus, they are only available in sebaceous glands, where they can be hydrolyzed into glycerol and transported to the SC. Therefore, the absence of AQP3 in sebaceous glands of AQP3-null mice could account for lower SC glycerol. The correlation between sebaceous gland-derived glycerol and skin hydration was later confirmed (Choi et al. 2005).

Glycerol is an important intermediate of energy metabolism and a substrate for the biosynthesis of various lipids (Brisson et al. 2001). In the presence of glycerol, phospholipase D can metabolize phosphatidylcholine into phosphatidylglycerol (Zheng et al. 2003). Coprecipitation studies have suggested that AQP3 and phospholipase-D2 are colocalized in keratinocytes (Zheng and Bollag 2003). Thus, glycerol transport by AQP3 may also facilitate phosphatidylglycerol synthesis. Phosphatidylglycerol is an activator of PKC and acts as a lipid second messenger to

modulate keratinocyte function (Denning 2004). Recently, Bollag et al. (2007) further demonstrated that glycerol transport by AQP3 triggers keratinocyte differentiation: following AQP3 overexpression, keratinocyte proliferation was decreased, but DNA synthesis in differentiating keratinocytes and the synthesis of differentiation markers such as involucrin were increased. Altogether, these results suggest that glycerol transport by AQP3 may play a complex but important role in the regulation of keratinocyte proliferation and differentiation.

3.3 Role of AQP3 in Cell Proliferation, Migration, and Wound Healing in Skin Epidermis

Wound healing is an extremely important feature of skin epidermis. More generally, the efficiency of the barrier function of the epidermis is provided for by the SC and derived from the continuous and regulated proliferation of keratinocytes, their migration towards skin surface, and differentiation into corneocytes (Houben et al. 2007). Wound healing particularly involves both increased cell proliferation and cell migration. Interestingly, new roles for aquaporins in cell migration and cell proliferation have been recently postulated. These functions of aquaporins may thus be particularly relevant to skin epidermis.

The role of AQP1 in cell migration was first postulated by Saadoun et al. (2005a). Since then, other AQPs have been demonstrated to facilitate cell migration in various tissues (reviewed in Papadopoulos et al., 2008), including AQP3 (Cao et al. 2006; Levin and Verkman 2006; Hara-Chikuma and Verkman 2008a) and AQP4 (Saadoun et al. 2005b). As cell migration is accompanied by changes in cellular shape and water movement, the role of aquaporins in cell migration has been attributed to their water transport properties. Accordingly, cell migration is facilitated either by aquaglyceroporins like AQP3, or aquaporins specific for water permeation, like AQP1 and AQP4. In an elegant study on mouse and human cells, Hara-Chikuma and Verkman (2008a) demonstrated that: (a) keratinocyte migration and wound healing was slower in cells lacking AQP3 expression, and (b) keratinocyte migration was restored by infecting AQP3-deficient cells either with the aquaglyceroporin AQP3 or the water channel AQP1. Therefore, this study satisfactorily demonstrates the key physiological role of AQP3 as a water channel in mammalian skin epidermis cell migration.

A recent study revealed defective proliferation of cornea cells in AQP3 knockout mice (Levin and Verkman 2006). The role of AQP3 in keratinocyte proliferation was investigated by the same group (Hara-Chikuma and Verkman 2008a, b). In the first study, they found impaired epidermal cell proliferation in AQP3-negative epidermis (Hara-Chikuma and Verkman 2008b). This decrease was associated with decreased metabolism: lower glycerol, glucose, and ATP contents, and reduced CO₂ production. Glycerol is an important intermediate of metabolism (Brisson et al. 2001). In particular, it is largely metabolized to glycerol-3-phosphate, a key intermediate for the production of ATP. Therefore, these results support glycerol transport by AQP3 for cell metabolism during keratinocyte proliferation. Consequently,

glycerol replacement largely abolished the proliferation defect in AQP3-deficient keratinocytes (Hara-Chikuma and Verkman 2008a). However, as discussed above for skin hydration, this cannot be taken as direct evidence that defective glycerol transport by AQP3-deficient cells is responsible for decreased cell proliferation. Figure 5 is adapted from a Hara-Chikuma and Verkman (2008a) study. In human keratinocytes cultures *in vitro*, the glycerol replacement strategy significantly increased proliferation in both AQP3-positive cells and AQP3-deficient-cells (Fig. 5a), suggesting that the proliferative effect of glycerol may be partially independent of AQP3. *In vivo*, however, the glycerol replacement strategy effectively restored keratinocyte proliferation in mouse epidermis and also ablated differences between AQP3-positive and AQP3-negative tissues (Fig. 5b), which confirms that facilitated transport of glycerol by AQP3 is an important feature of cell proliferation in epidermis regeneration after injury. Together with the role of AQP3 in water transport for keratinocyte migration, these findings could account for impaired wound healing observed in the epidermis of AQP3-deleted mice (Hara et al. 2002). Further analysis of the regulation of cell proliferation also demonstrated the absence of skin tumors in mice lacking AQP3 (Hara-Chikuma and Verkman 2008b). Conversely, carcinoma of the skin (Nakakoshi et al. 2006) and of the kidney (Kafé et al. 2004) were shown to express AQP3. In skin tumors, glycerol replacement corrected the proliferative defect (Hara-Chikuma and Verkman 2008b), which suggests that glycerol transport in the epidermis is an important determinant of tumorigenesis (Verkman et al. 2008). This is an interesting hypothesis, because glycerol has been a major component of cosmetics for years. However, the presence of AQP3 in kidney collecting duct and keratinocyte carcinoma is not a major surprise, because this protein is natively expressed in these cell types. In fact, this is why AQP3 expression in carcinoma has been proposed as a marker of collecting duct carcinoma (Kafé et al. 2004). Similarly, not just aquaglyceroporins, but also strict aquaporins, which do not transport glycerol, were shown to facilitate tumor formation (reviewed in Verkman et al. 2008). Finally, while AQP3 repression was shown to decrease cell proliferation (Hara-Chikuma and Verkman 2008a, b), upregulation of AQP3 was also shown to decrease cell proliferation and to promote keratinocyte differentiation in a phosphatidylglycerol-dependent manner, as discussed above (Bollag et al. 2007).

Overall, the proliferative role of glycerol in cell metabolism and the potential role of phosphatidylglycerol in the regulation of keratinocyte differentiation suggest that AQP3-mediated glycerol transport in skin is involved in complex regulation of cell proliferation and differentiation, which are central features of epidermal homeostasis and regeneration.

3.4 New Aquaporins in Skin Epidermis

AQP3 was the first AQP detected in skin epidermis. It is the most abundant and has been the best studied so far, as discussed above. Nevertheless, other aquaporins have also been found in skin epidermis recently: in human skin, AQP10 has been

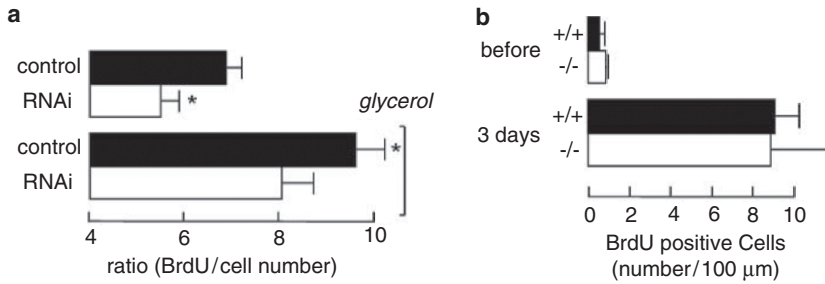


Fig. 5 Effect of glycerol on cell proliferation. **(a)** in human keratinocytes, 10 mM glycerol (*bottom*) markedly enhances cell proliferation in control and AQP3 RNAi knockdown keratinocytes with respect to controls (*top*). Proliferation is significantly higher in control cells. **(b)** in mouse skin epidermis, glycerol (3 days) increases cell proliferation in skin epidermis of wild-type (+/+) and AQP3-deleted mice (-/-) during wound healing. Differences between genotypes are not significant. Adapted from Hara-Chikuma and Verkman (2008a)

detected by RT-PCR in undifferentiated keratinocytes (Boury-Jamot et al. 2006), whereas AQP9 was found in differentiated keratinocytes (not shown). In mouse skin the AQP9 protein was localized to the plasma membrane of keratinocytes in the *stratum granulosum*, where AQP3 is absent (Rojek et al. 2007). Like AQP3, AQP9 is an aquaglyceroporin. Studies on AQP9-deficient mice suggest that AQP9 plays a central role in glycerol metabolism (Rojek et al. 2007), but its function in skin has not yet been studied extensively. Because of their comparable and potentially redundant transport properties in skin, it would be interesting to examine the skin phenotype of AQP3/AQP9 double mutant mice. For example, AQP9, like AQP3, was also shown to play a role in cell motility (Loitto et al. 2007) and could therefore be an additional player in wound healing.

Though keratinocytes are the major epidermis cell type, melanocytes are extremely important cells of skin epidermis. Melanocytes are dendritic cells, responsible for the synthesis and accumulation of melanin. Melanin is responsible for skin pigmentation and provides protection against radiation. Melanocytes accumulate melanin in melanosomes. Following the transport of melanosomes along melanocyte dendrites, melanin is then transferred from melanocytes to keratinocytes. The later steps of melanin transfer from melanocytes to keratinocytes are not fully understood (Van Den Bossche et al. 2006). Although the protein expression has not been shown, Boury-Jamot et al. (2006) reported the expression of AQP1 mRNA in human melanocytes. Since melanocytes represent only a small fraction of epidermal cells (Fig. 1), water transport by AQP1 in melanocytes is not expected to play a significant role in skin hydration. However, if AQP1 expression is confirmed, recent discoveries on the role of AQPs in cell shape and migration suggest that AQP1 expression in melanocytes could be involved in the growth of melanocyte dendrites and possibly in melanosome transfer to keratinocytes.

4 Conclusions

AQP3 expression in mammalian skin epidermis was once regarded as physiologically irrelevant. Recent studies now suggest that AQP3 is involved in water and glycerol transport for skin hydration, in water transport for cell migration, in glycerol transport for the metabolism of lipids and ATP, which are important for cell proliferation, cell differentiation, and wound healing. Some of the functional consequences of AQP expression in skin need to be confirmed and further investigated, particularly with respect to some of the most recent properties of aquaglyceroporins for cell migration and proliferation and with respect to the recent demonstration that additional AQPs, such as AQP9, are also expressed in skin. It has become clear, however, that AQPs play a significant role in the homeostasis of skin epidermis.

References

- Agren J, Zelenin S, Håkansson M, Eklöf AC, Aperia A, Nejsum LN, Nielsen S, Sedin G (2003) Transepidermal water loss in developing rats: role of aquaporins in the immature skin. *Pediatr Res* 53(4):558–565
- Bollag WB, Xie D, Zheng X, Zhong X (2007) A potential role for the phospholipase D2-aquaporin-3 signaling module in early keratinocyte differentiation: production of a phosphatidylglycerol signaling lipid. *J Invest Dermatol* 127(12):2823–2831
- Boury-Jamot M, Sougrat R, Tailhardat M, Le Varlet B, Bonté F, Dumas M, Verbavatz JM (2006) Expression and function of aquaporins in human skin: Is aquaporin-3 just a glycerol transporter? *Biochim Biophys Acta* 1758(8):1034–1042
- Brisson D, Vohl MC, St-Pierre J, Hudson TJ, Gaudet D (2001) Glycerol: a neglected variable in metabolic processes? *Bioessays* 23(6):534–542
- Cao C, Sun Y, Healey S, Bi Z, Hu G, Wan S, Kouttab N, Chu W, Wan Y (2006) EGFR-mediated expression of aquaporin-3 is involved in human skin fibroblast migration. *Biochem J* 400(2):225–234
- Cao C, Wan S, Jiang Q, Amaral A, Lu S, Hu G, Bi Z, Kouttab N, Chu W, Wan Y (2008) All-trans retinoic acid attenuates ultraviolet radiation-induced down-regulation of aquaporin-3 and water permeability in human keratinocytes. *J Cell Physiol* 215(2):506–516
- Choi EH, Man MQ, Wang F, Zhang X, Brown BE, Feingold KR, Elias PM (2005) Is endogenous glycerol a determinant of stratum corneum hydration in humans? *J Invest Dermatol* 125(2):288–293
- Delporte C, Steinfeld S (2006) Distribution and roles of aquaporins in salivary glands. *Biochim Biophys Acta* 1758(8):1061–1070
- Denning MF (2004) Epidermal keratinocytes: regulation of multiple cell phenotypes by multiple protein kinase C isoforms. *Int J Biochem Cell Biol* 36(7):1141–1146
- Dumas M, Sadick NS, Noblesse E, Juan M, Lachmann-Weber N, Boury-Jamot M, Sougrat R, Verbavatz JM, Schnebert S, Bonté F (2007) Hydrating skin by stimulating biosynthesis of aquaporins. *J Drugs Dermatol* 6(Suppl):s20–s24
- Echevarria M, Windhager EE, Tate SS, Frindt G (1994) Cloning and expression of AQP3, a water channel from the medullary collecting duct of rat kidney. *Proc Natl Acad Sci U S A* 91(23):10997–11001
- Fluhr JW, Mao-Qiang M, Brown BE, Wertz PW, Crumrine D, Sundberg JP, Feingold KR, Elias PM (2003) Glycerol regulates stratum corneum hydration in sebaceous gland deficient (asebia) mice. *J Invest Dermatol* 120(5):728–737

- Frigeri A, Gropper MA, Umenishi F, Kawashima M, Brown D, Verkman AS (1995) Localization of MIWC and GLIP water channel homologs in neuromuscular, epithelial and glandular tissues. *J Cell Sci* 108:(Pt 9):2993–3002
- Hara M, Verkman AS (2003) Glycerol replacement corrects defective skin hydration, elasticity, and barrier function in aquaporin-3-deficient mice. *Proc Natl Acad Sci U S A* 100(12):7360–7365
- Hara M, Ma T, Verkman AS (2002) Selectively reduced glycerol in skin of aquaporin-3-deficient mice may account for impaired skin hydration, elasticity, and barrier recovery. *J Biol Chem* 277(48):46616–46621
- Hara-Chikuma M, Verkman AS (2006) Physiological roles of glycerol-transporting aquaporins: the aquaglyceroporins. *Cell Mol Life Sci* 63(12):1386–1392
- Hara-Chikuma M, Verkman AS (2008a) Aquaporin-3 facilitates epidermal cell migration and proliferation during wound healing. *J Mol Med* 86(2):221–231
- Hara-Chikuma M, Verkman AS (2008b) Prevention of skin tumorigenesis and impairment of epidermal cell proliferation by targeted aquaporin-3 gene disruption. *Mol Cell Biol* 28(1):326–332
- Hara-Chikuma M, Sohara E, Rai T, Ikawa M, Okabe M, Sasaki S, Uchida S, Verkman AS (2005) Progressive adipocyte hypertrophy in aquaporin-7-deficient mice: adipocyte glycerol permeability as a novel regulator of fat accumulation. *J Biol Chem* 280(16):15493–15496
- Hibuse T, Maeda N, Funahashi T, Yamamoto K, Nagasawa A, Mizunoya W, Kishida K, Inoue K, Kuriyama H, Nakamura T, Fushiki T, Kihara S, Shimomura I (2005) Aquaporin 7 deficiency is associated with development of obesity through activation of adipose glycerol kinase. *Proc Natl Acad Sci U S A* 102(31):10993–10998
- Houben E, De Paepe K, Rogiers V (2007) A keratinocyte's course of life. *Skin Pharmacol Physiol* 20(3):122–132
- Imakado S, Bickenbach JR, Bundman DS, Rothnagel JA, Attar PS, Wang XJ, Walczak VR, Wisniewski S, Pote J, Gordon JS, et al. (1995) Targeting expression of a dominant-negative retinoic acid receptor mutant in the epidermis of transgenic mice results in loss of barrier function. *Genes Dev* 9(3):317–329
- Ishibashi K, Sasaki S, Fushimi K, Uchida S, Kuwahara M, Saito H, Furukawa T, Nakajima K, Yamaguchi Y, Gojibori T, et al. (1994) Molecular cloning and expression of a member of the aquaporin family with permeability to glycerol and urea in addition to water expressed at the basolateral membrane of kidney collecting duct cells. *Proc Natl Acad Sci U S A* 91(14):6269–6273
- Kafé H, Verbavatz JM, Cochand-Priollet B, Castagnet P, Vieillefond A (2004) Collecting duct carcinoma: an entity to be redefined? *Virchows Arch* 445(6):637–640
- Levin MH, Verkman AS (2006) Aquaporin-3-dependent cell migration and proliferation during corneal re-epithelialization. *Invest Ophthalmol Vis Sci* 47(10):4365–4372
- Loitto VM, Huang C, Sigal YJ, Jacobson K (2007) Filopodia are induced by aquaporin-9 expression. *Exp Cell Res* 313(7):1295–1306
- Ma T, Frigeri A, Hasegawa H, Verkman AS (1994) Cloning of a water channel homolog expressed in brain meningeal cells and kidney collecting duct that functions as a stilbene-sensitive glycerol transporter. *J Biol Chem* 269(34):21845–21849
- Ma T, Song Y, Yang B, Gillespie A, Carlson EJ, Epstein CJ, Verkman AS (2000) Nephrogenic diabetes insipidus in mice lacking aquaporin-3 water channels. *Proc Natl Acad Sci U S A* 97(8):4386–4391
- Ma T, Hara M, Sougrat R, Verbavatz JM, Verkman AS (2002) Impaired stratum corneum hydration in mice lacking epidermal water channel aquaporin-3. *J Biol Chem* 277(19):17147–17153
- Matsuzaki T, Suzuki T, Koyama H, Tanaka S, Takata K (1999) Water channel protein AQP3 is present in epithelia exposed to the environment of possible water loss. *J Histochem Cytochem* 47(10):1275–1286
- Mirza R, Hayasaka S, Kambe F, Maki K, Kaji T, Murata Y, Seo H (2008) Increased expression of aquaporin-3 in the epidermis of DHCR24 knockout mice. *Br J Dermatol* 158(4):697–684
- Nakakoshi M, Morishita Y, Usui K, Ohtsuki M, Ishibashi K (2006) Identification of a keratinocarcinoma cell line expressing AQP3. *Biol Cell* 98(2):95–100

- Nejsum LN, Kwon TH, Jensen UB, Fumagalli O, Frøkiaer J, Krane CM, Menon AG, King LS, Agre PC, Nielsen S (2002) Functional requirement of aquaporin-5 in plasma membranes of sweat glands. *Proc Natl Acad Sci U S A* 99(1):511–516
- Olsson M, Broberg A, Jernås M, Carlsson L, Rudemo M, Suurkula M, Svensson PA, Benson M (2006) Increased expression of aquaporin 3 in atopic eczema. *Allergy* 61(9):1132–1137
- Papadopoulos MC, Saadoun S, Verkman AS (2008) Aquaporins and cell migration. *Pflugers Arch* 456(4):693–700
- Proksch E, Fölster-Holst R, Jensen JM (2006) Skin barrier function, epidermal proliferation and differentiation in eczema. *J Dermatol Sci* 43(3):159–169
- Rojek AM, Skowronski MT, Füchtbauer EM, Füchtbauer AC, Fenton RA, Agre P, Frøkiaer J, Nielsen S (2007) Defective glycerol metabolism in aquaporin 9 (AQP9) knockout mice. *Proc Natl Acad Sci U S A* 104(9):3609–3614
- Rojek A, Praetorius J, Frøkjær J, Nielsen S, Fenton RA (2008) A current view of the mammalian aquaglyceroporins. *Annu Rev Physiol* 70:301–327
- Saadoun S, Papadopoulos MC, Hara-Chikuma M, Verkman AS (2005a) Impairment of angiogenesis and cell migration by targeted aquaporin-1 gene disruption. *Nature* 434(7034):786–792
- Saadoun S, Papadopoulos MC, Watanabe H, Yan D, Manley GT, Verkman AS (2005b) Involvement of aquaporin-4 in astroglial cell migration and glial scar formation. *J Cell Sci* 118(Pt 24):5691–5698
- Sougrat R, Morand M, Gondran C, Bonté F, Dumas M, Verbavatz JM (2000) Functional expression of AQP3 in human skin epidermis and keratinocyte cell cultures. In: Hohmann S, Nielsen S (eds.) *Molecular biology and physiology of water and solute transport*. Kluwer Academic/Plenum Publishers, New York, pp. 179–183
- Sougrat R, Morand M, Gondran C, Barré P, Gobin R, Bonté F, Dumas M, Verbavatz JM (2002) Functional expression of AQP3 in human skin epidermis and reconstructed epidermis. *J Invest Dermatol* 118(4):678–685
- Sugiyama Y, Ota Y, Hara M, Inoue S (2001) Osmotic stress up-regulates aquaporin-3 gene expression in cultured human keratinocytes. *Biochim Biophys Acta* 1522(2):82–88
- Van Den Bossche K, Naeyaert JM, Lambert J (2006) The quest for the mechanism of melanin transfer. *Traffic* 7(7):769–778
- Verdier-Sévrain S, Bonté F (2007) Skin hydration: a review on its molecular mechanisms. *J Cosmet Dermatol* 6(2):75–82
- Verkman AS, Hara-Chikuma M, Papadopoulos MC (2008) Aquaporins—new players in cancer biology. *J Mol Med* 86(5):523–529.
- Zeuthen T, Klaerke DA (1999) Transport of water and glycerol in aquaporin 3 is gated by H(+). *J Biol Chem* 274(31):21631–21636
- Zheng X, Bollag WB (2003) Aquaporin 3 colocalizes with phospholipase d2 in caveolin-rich membrane microdomains and is downregulated upon keratinocyte differentiation. *J Invest Dermatol* 121(6):1487–1495
- Zheng X, Ray S, Bollag WB (2003) Modulation of phospholipase D-mediated phosphatidylglycerol formation by differentiating agents in primary mouse epidermal keratinocytes. *Biochim Biophys Acta* 1643(1–3):25–36

Function of Aquaporin-7 in the Kidney and the Male Reproductive System

Eisei Sohara, Shinichi Uchida, and Sei Sasaki

Contents

1	Basic Features of the AQP7 Gene and the Encoded Protein	220
1.1	Basic Transport by AQP7	220
1.2	AQP7 Distribution in Mammalian Tissue	220
1.3	AQP7 in Different Species	221
2	AQP7 in the Kidney	221
2.1	AQP7 Localization in the Kidney	221
2.2	Glycerol Transport by AQP7 in the Kidney	222
2.3	Water Transport by AQP7 in the Kidney	224
2.4	Urea Transport by AQP7 in the Kidney	225
2.5	Regulation of AQP7 Expression in the Kidney	226
3	AQP7 in the Male Reproductive System	226
3.1	AQP7 Localization and Expression in the Male Reproductive System	227
3.2	AQP7 in Human Infertility	227
3.3	Reproductive Function of AQP7 in Knockout Mice	228
	References	229

Abstract The aquaporin-7 (AQP7) water channel is known to be a member of the aquaglyceroporins, which allow the rapid transport of glycerol and water. In this chapter, we review the physiological functions of AQP7 in the kidney and the male reproductive system.

In the kidney, AQP7 is abundantly present at the apical membrane of the proximal straight tubules. Although the contribution of AQP7 to the water permeability of proximal straight tubules was found to be minimal compared with that of AQP1, we identified a novel glycerol reabsorption pathway that may be important for preventing glycerol from being excreted into urine.

In the male reproductive system, AQP7 is present particularly in the spermatids, as well as in the testicular and epididymal spermatozoa, suggesting that AQP7 has

S. Sasaki (✉)

Department of Nephrology, Graduate School of Medicine, Tokyo Medical and Dental University, 1-5-45 Yushima Bunkyo Tokyo, 113-8519, Tokyo, Japan
ssasaki.kid@tmd.ac.jp

some role in late spermatogenesis. However, male AQP7 knockout mice were not sterile, and their sperm did not show any morphological or functional abnormalities.

1 Basic Features of the AQP7 Gene and the Encoded Protein

1.1 Basic Transport by AQP7

Aquaporins (AQPs) are membrane proteins that facilitate water transportation across the cell membrane (King and Agre 1996; Verkman 2002). To date, at least 13 AQPs have been identified in mammals (Morishita et al. 2004). Among them, AQP3, AQP7, and AQP9 have been reported as aquaglyceroporins, which are unique in terms of function and structure. They transport glycerol as well as water when they are expressed in *Xenopus* oocytes, while the other aquaporins transport only water.

Ishibashi et al. (1997) cloned AQP7 and showed that the expression of AQP7 in oocytes increased their osmotic water permeability tenfold. AQP7 also increased glycerol and urea transport five- and ninefold, respectively. Interestingly, this increased water permeability was not inhibited by 0.3 mM mercury chloride, as it is in the other AQPs.

Structurally, aquaglyceroporins are similar to the bacterial glycerol facilitator (GlpF), whereas the other aquaporins are more similar to the bacterial water channel (Zardoya 2005). In most AQPs, the most conserved motifs are two NPA boxes, which enable the pore to transport solute. However, the alanine in the second NPA motif in AQP7 is replaced by serine in all species, resulting in an NPS motif (Ishibashi et al. 1997).

In this chapter, we review AQP7 in the kidney and the male reproductive system.

1.2 AQP7 Distribution in Mammalian Tissue

AQP7 was cloned for the first time from rat testis, where it is abundantly expressed (Ishibashi et al. 1997). In rats, AQP7 is found in testis, kidney, brown adipose tissue (BAT), white adipose tissue (WAT), skeletal muscle, heart, brain, and intestine by Northern blotting (Ishibashi et al. 1998). Similar distribution was observed in mice, using AQP7 knockout mice as negative controls (Hara-Chikuma et al. 2005; Maeda et al. 2004; Skowronski et al. 2007; Sohara et al. 2005, 2007). Matsumura et al. (2007) also showed AQP7 expression in pancreatic beta cells. Shin et al. (2006) reported that AQP7 was largely found in the choroid plexus of the brain. AQP7 immunoreactivity in ependyma, pia, and blood vessels was increased during perinatal and postnatal development.

Capillary endothelium of BAT and WAT displayed prominent staining, whereas AQP7 labeling in adipocyte membranes was undetectable. Similarly, distinct immunolabeling of the capillary endothelium was also observed in both skeletal and

heart muscle, with no apparent staining of skeletal or cardiac myocytes (Skowronski et al. 2007). Further investigation will determine whether AQP7 actually localizes to membranes of adipocytes and myocytes.

In humans, AQP7 in adipose tissue was first reported by Kuriyama et al. (1997) from human adipocytes, and named aquaporin adipose. However, aquaporin adipose is identical to AQP7. In humans, AQP7 was detected in adipocytes, kidneys, testes, and the heart by RT-PCR (Kondo et al. 2002).

Precise localization of AQP7 in the kidney and the male reproductive system will be discussed later.

1.3 AQP7 in Different Species

Although human, rat, and mouse AQP7s have similar function and distribution, it is interesting that the primary structure of AQP7 is not well conserved among these species. The deduced amino acid sequences of human and mouse AQP7 were 68% and 79% identical to those of rat AQP7, respectively. The mouse AQP7 is 67% identical to the human AQP7 (Ishibashi et al. 1998). This low conservation of AQP7 among species is unusual in the aquaporin family. For example, 91% identity is found in rat and human AQP5 (Lee et al. 1996) and AQP3 (Ishibashi et al. 1995). Thus, function and distribution of AQP7 may differ slightly among species.

2 AQP7 in the Kidney

2.1 AQP7 Localization in the Kidney

AQP7 is abundantly expressed in the kidney in mammals (Ishibashi et al. 1997; Kishida et al. 2000). Immunoblotting with antibodies to either rat or mouse AQP7 revealed a 28-kDa band in the kidney and testes from rat and mouse, respectively (Ishibashi et al. 2000). RT-PCR of rat and mouse kidney zones revealed AQP7 mRNA in the cortex and outer stripe of the outer medulla, whereas no signal was observed in the inner medulla or inner stripe of the outer medulla (Nejsum et al. 2000). RT-PCR on microdissected nephron segments revealed AQP7 mRNA in proximal convoluted and straight tubules. However, immunocytochemistry revealed strong AQP7 labeling of proximal straight tubules (S3 segment) in both rat and mouse kidneys (Ishibashi et al. 2000; Nejsum et al. 2000). The labeling was almost exclusively confined to the brush border, with no basolateral labeling. This localization of AQP7 on the apical membrane of proximal straight tubules was also confirmed with an AQP7 knockout mouse as the negative control (Skowronski et al. 2007; Sahara et al. 2005).

2.2 Glycerol Transport by AQP7 in the Kidney

2.2.1 Glycerol Reabsorption in the Kidney by AQP7

According to the review by Lin (1977), plasma glycerol can be filtered by the glomerulus; urine glycerol in the glomerular filtrate of mammals is known to be completely reabsorbed in the tubules, but the reabsorption pathway(s) of glycerol in tubules had not been identified. Sohara et al. (2005) reported that AQP7 knockout mice showed marked glyceroluria, which was later confirmed by another group (Skowronski et al. 2007), indicating that glycerol can be reabsorbed through AQP7 in the proximal straight tubule segment S3, and that there might be no other glycerol reabsorbing system to compensate for this defect in the more distal nephron segment (Fig. 1a). Plasma glycerol level abnormality cannot explain this glyceroluria, because three independent groups have confirmed that the serum glycerol level was not significantly different between wild-type and AQP7 knockout mice (Matsumura

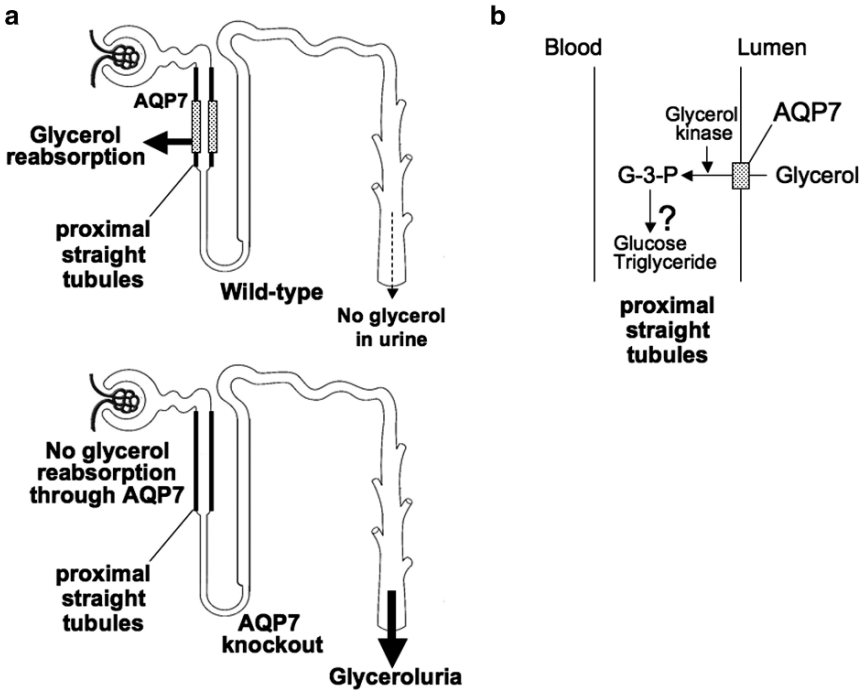


Fig. 1 Schema of glycerol reabsorption in the proximal straight tubules mediated by AQP7. (a) Although wild-type mice did not have glycerol in their urine, AQP7 knockout mice did have glyceroluria, indicating that glycerol is reabsorbed mainly in the proximal straight tubules through AQP7. (b) After glycerol is reabsorbed through AQP7 from urine, the first enzymic step in glycerol metabolism is only phosphorylation by glycerol kinase, which forms L-glycerol 3-phosphate (G-3-P). However, the main metabolic product of glycerol (e.g., glucose, triglyceride) in the kidney is still unknown

et al. 2007; Skowronski et al. 2007; Sohara et al. 2005), although Maeda et al. (2004) reported that AQP7 knockout mice had significantly lower plasma glycerol levels than wild-type mice. However, even when AQP7 knockout mice had lower plasma glycerol levels than wild-type mice, glyceroluria in AQP7 knockout mice was not due to an increase in plasma glycerol levels, but to the reduction or elimination of the glycerol reabsorption pathway in the kidney.

Although AQP7 was found as the pathway for glycerol reabsorption in tubules, the function of glycerol reabsorption at proximal tubules is still unknown. Besides the liver and BAT, the kidney is the only organ that plays a major role in mammalian glycerol metabolism, accounting for up to 20% of the whole-body glycerol turnover (Huq et al. 1997; Lin 1977).

Glycerol kinase exhibits highest activities in the liver and kidney (Vernon and Walker 1970; Wieland and Suyter 1957), parallel with the distribution of glycerol metabolism. Glycerol kinase activity in BAT was also reported to be comparable to, though lower than, that in the kidney (Huq et al. 1997). Other organs or tissues, including WAT, may utilize glycerol, but at insignificant rates (Wirthensohn et al. 1981).

In vivo, the glycerol uptake by the kidney is proportional to its plasma concentration (Himms-Hagen 1968). Similarly, Robinson and Newsholme (1969) demonstrated that rat cortical slices take up glycerol in proportion to the glycerol concentration in the medium. On the other hand, glycerol was shown to be one of the precursors for renal gluconeogenesis (Krebs et al. 1963). Since gluconeogenesis is located in the proximal tubule of the kidney (Burch et al. 1978; Guder and Schmidt 1974; Vandewalle et al. 1981), it could be assumed that glycerol metabolism is also located in this nephron segment. Wirthensohn et al. (1981) reported that glycerol kinase in rabbits is located exclusively in proximal convoluted and straight tubules, but negligible in the other nephron segments. This finding clearly pointed to the proximal tubules as the site of renal glycerol metabolism, because the first enzymic step in glycerol metabolism is only phosphorylation by glycerol kinase, which forms L-glycerol 3-phosphate (Wirthensohn et al. 1981) (Fig. 1b). Proximal tubules, where AQP7 is expressed, should contribute to reabsorption of glycerol in nephrons. In addition, AQP7 itself should be important for the glycerol reabsorption mechanism in the kidney.

We cannot exclude the possibility that some unknown mechanism exists in addition to proximal straight tubules, especially in proximal convoluted tubules, where glycerol kinase activity is high in rabbit kidneys. Interestingly, in rats, AQP7 mRNA was detected in proximal convoluted tubules by RT-PCR and subtle staining of AQP7 using immunohistochemistry (Nejsum et al. 2000), although Ishibashi et al. (2000) reported AQP7 in rat kidneys only at proximal straight tubules. In mouse kidneys, immunohistochemistry has shown AQP7 protein in proximal straight tubules, but not in proximal convoluted tubules (Skowronski et al. 2007; Sohara et al. 2005). This mouse AQP7 localization must be more reliable, because AQP7 knockout mice were used as the negative control in these studies. However, we cannot exclude the possibility of some difference of AQP7 localization between species.

Although AQP7 was found to constitute the glycerol pathway in the kidney, some questions about renal AQP7 remain to be investigated. First, it is not clear whether AQP7 is the only glycerol reabsorption pathway in tubules, as another aquaglyceroporin, i.e., AQP3, is localized in the collecting ducts; yet, there is no evidence that AQP3 is involved in glycerol reabsorption in the kidney. Second, the physiological significance of glycerol reabsorption in proximal tubules is not well understood. Apart from the possible role of glycerol as a metabolic fuel, pyruvate, glucose, and acylglycerol (e.g., triglyceride) are the major metabolic products of renal glycerol metabolism. Several possibilities may be suggested for the role of renal glycerol reabsorption in this segment: to maintain plasma levels of metabolic products of glycerol (e.g., glucose, triglyceride), to maintain proximal straight tubule cells where high renal oxygen consumption and metabolic rates have been found, and/or other functions. Further investigation is needed to determine the function of AQP7 and glycerol metabolism in the kidney.

Nevertheless, the fact remains that AQP7 prevents glycerol from being excreted into urine, and that the other glycerol reabsorbing pathway(s), if any, cannot completely compensate for the deletion of AQP7.

2.2.2 Glyceroluria as a Possible Biomarker of Proximal Straight Tubule Injury

The finding that renal AQP7 constitutes a glycerol reabsorbing pathway, which is restricted to the proximal straight tubules, suggested the hypothesis that glyceroluria is a new biomarker for injury to proximal straight tubular segment S3. To investigate whether proximal tubule injury can cause glycerol to leak into urine, Sohara et al. (2005) measured urine glycerol levels in two mouse models of proximal straight tubular injury: the cisplatin-induced acute renal failure (ARF) model and the ischemic-reperfusion ARF model.

In both these S3 injury models, mice showed higher urine glycerol concentrations than did untreated or fasting control mice. Plasma glycerol levels could not explain these changes, indicating that the urine leakage of glycerol was due to failure of glycerol reabsorption. Therefore, the measurement of urine glycerol levels could be used as a new and more sensitive method for detecting proximal straight tubule injury than conventional markers. Further clinical investigation is needed to use glyceroluria as a segment S3 injury marker in humans.

2.3 Water Transport by AQP7 in the Kidney

AQP7 is expressed on the apical membrane of the proximal straight tubule S3 segment (Ishibashi et al. 1997), where AQP1 is also present. Studies of AQP1 knockout mice have demonstrated that AQP1 plays a major role in proximal tubular water transport (Ma et al. 1998; Schnermann et al. 1998). In fact, AQP1 knockout mice show polyuria due to both defective water reabsorption in the proximal tubules and a dysfunctional countercurrent mechanism in the inner medulla (Verkman 1999).

In humans, AQP1 mutation causes a urine concentrating defect, although it is milder than that in AQP1 knockout mice (King et al. 2001). Other renal AQPs, such as AQP2, AQP3, and AQP4, are expressed in the collecting ducts and are directly involved in water reabsorption to generate the final concentrated urine (Fushimi et al. 1993; Ma et al. 2000, 1997). In particular, an AQP2 mutation causes nephrogenic diabetes insipidus in humans, and pathogenesis of disease-causing AQP2 mutations were investigated using cells and knockin mice (Sohara et al. 2006b; Yang et al. 2001). Considering the other AQPs that localize to the apical membrane in renal tubules, AQP7 was expected to play some role in water reabsorption in the kidney (Ishibashi et al. 2000; Nejsum et al. 2000).

To investigate whether AQP7 contributes to the water permeability of the brush border membranes in proximal straight tubules, Sohara et al. (2005) measured water permeability of the brush border membrane vesicles obtained from the outer medulla of the kidney by the stopped-flow method. In AQP7 knockout mice ($18.0 \times 10^{-3} \text{ cm s}^{-1}$), water permeability of these vesicles was slightly but significantly lower than that in wild-type mice ($20.0 \times 10^{-3} \text{ cm s}^{-1}$), indicating that AQP7 makes a small contribution to the water permeability of the proximal straight tubules.

To compare the contribution of AQP7 with that of AQP1, they also measured the water permeability of the brush border membrane vesicles from AQP1/AQP7 double knockout mice, which was found to be decreased more in the AQP1/AQP7 knockout mice than in the AQP1 knockout mice ($\text{AQP1}, 3.3 \times 10^{-3} \text{ cm s}^{-1}$ vs. $\text{AQP1/AQP7}, 2.4 \times 10^{-3} \text{ cm s}^{-1}$). Based on these results and previously published data (Ma et al. 1998), the estimated contribution of AQP7 to the water permeability in the proximal straight tubules is one-eighth that of AQP1.

As expected from the small decrease in water permeability of the AQP7 solo knockout mice, AQP7 knockout mice did not show a urine concentrating defect (Sohara et al. 2005), which was observed in AQP1 knockout mice (Ma et al. 1998).

Thus, Sohara et al. (2005) compared the urine concentrating ability of AQP1/AQP7 double knockout mice with that of AQP1 knockout mice, to investigate whether the additional decrease in water permeability of the brush border membranes caused by AQP7 deletion resulted in any additional functional consequences. AQP1/AQP7 double knockout mice showed a more severe urine concentrating defect than AQP1 knockout mice, even under normal conditions.

These results clearly showed that AQP7 made a small contribution to water permeability of brush border membranes in the proximal straight tubule segment S3. However, as anticipated from the restricted distribution of AQP7 compared with AQP1, the role of AQP7 in water reabsorption in the proximal tubules is minor.

2.4 Urea Transport by AQP7 in the Kidney

Several animal and human studies suggest that urea secretion takes place in the mammalian kidney through the proximal straight tubule S3 segment (Beyer and Gelarden 1988). Actually, Kawamura and Kokko (1976) reported a modest but significant secretion of urea in the S3 segment of rabbit proximal straight tubules. Urea secreted in the proximal straight tubule S3 segment could have contributed to

urea recycling (Yang and Bankir 2005). Thus, AQP7 was suggested as a component of the pathway for urea in the proximal straight tubules (Ishibashi et al. 2000; Knepper and Gamba 2003), to complete urea recycling.

However, plasma and urine urea levels in AQP7 knockout mice did not differ from those in wild-type mice (Sohara et al. 2005, 2006a). There was also no difference between AQP7 knockout and wild-type mice in the urea content of the papilla. Even with a low-protein diet, which limits the urea supply to the kidney, the same experiments showed no difference between AQP7 knockout mice and wild-type mice, nor was there a urine concentrating defect with a low-protein diet and dehydration.

Therefore, to date, there is no evidence that AQP7 plays a role in urea recycling in the kidney *in vivo*.

2.5 Regulation of AQP7 Expression in the Kidney

In mouse adipocyte tissue, fasting increased and re-feeding suppressed AQP7 mRNA and protein levels in proportion to plasma glycerol levels and conversely to plasma insulin levels (Kishida et al. 2001; Skowronski et al. 2007). A search of the promoter region of the AQP7 gene for consensus sequences showed several putative binding sites for transcription factors. Several binding sites for CCAAT enhancer binding protein (C/EBP) and cAMP-regulatory element binding protein (CRE-BP) were found in the promoter. In addition, a putative insulin response element (IRE) was found in the promoter (Kondo et al. 2002). mRNA expression and promoter activities of the mouse AQP7 gene were shown to be negatively regulated by insulin through the IRE, indicating that the expression of AQP7 in adipose tissue is involved in glucose metabolism and insulin resistance status.

It is interesting that regulation of AQP7 expression in the kidney is different from that in adipose tissue, in spite of the same promoter. Skowronski et al. (2007) reported that renal AQP7 expression did not increase in either 72-h starvation or streptozotocin-induced diabetes mellitus models, although AQP7 in adipose tissue increased noticeably in the same mice.

AQP7 mRNA and protein did not increase after dehydration. Similarly, there was no compensatory increase in AQP1 and AQP7 expression in AQP7 and AQP1 knockout mice respectively, indicating that AQP7 expression is not regulated by water balance (Sohara et al. 2005).

Thus, in the kidney, AQP7 expression is not regulated by either glucose metabolism or water balance. This finding is very interesting, and implies that AQP7 has some other function (or functions) specific for the kidney.

3 AQP7 in the Male Reproductive System

Cell volume reduction is one of the most distinct morphological changes that occur during spermatogenesis. It has been proposed that the cells' marked water efflux explains this cytoplasm condensation (Russell 1979; Sprando and Russell 1987).

Several AQPs (AQP1, AQP7, AQP8, and AQP9) are expressed in the testis, and it was considered that they played a role in water movement across the testicular cell membranes (Badran and Hermo 2002; Calamita et al. 2001; Elkjaer et al. 2000). In fact, a recent report found that the testes of AQP8 knockout mice were heavier than those of wild-type mice (Yang et al. 2005). It was thought that AQP7 might be important in terms of glycerol transport, too. As mentioned above, AQP7 is expressed abundantly in testes. Therefore, investigators focused on the function of AQP7, especially in male infertility.

3.1 AQP7 Localization and Expression in the Male Reproductive System

In the male reproductive system, AQP7 was found in the cells of late stages of spermatogenesis; late to maturing spermatids were selectively stained in the first report of AQP7 (Ishibashi et al. 1997).

Precise experiments on mouse and rat AQP7 localization in the male reproductive system have been performed by several groups. AQP7 was first observed, using immunohistochemistry, at postnatal day 45 (P45) in the luminal aspect of the seminiferous epithelium of some tubules. It increased until P75, and all seminiferous tubules stained. AQP7 was restricted to the plasma membrane and cytoplasmic mass of elongated spermatids, testicular spermatozoa, and residual bodies in the seminiferous epithelium. With higher magnification, strong labeling was seen over a Golgi-like apparatus in the cytoplasmic mass of elongated spermatids. (Calamita et al. 2001; Kageyama et al. 2001; Suzuki-Toyota et al. 1999) In the epididymis, AQP7 was also localized to the tail of spermatozoa (Skowronski et al. 2007).

Suzuki-Toyota et al. (1999) also reported that, after spermiation, the immunoreactivity of AQP7 remained at the middle piece and in the cytoplasmic droplet in the testicular spermatozoon. These observations suggested that AQP7 contributes to the volume reduction of spermatids, as AQP7 is localized on the plasma membrane covering the condensing cytoplasmic mass of the elongated spermatid, and as the seminiferous tubule fluid is hypertonic.

In humans, AQP7 was expressed at the tail of spermatids and spermatozoa in the testis, as in the mouse and rat. AQP7 protein was also detected at the middle piece and the anterior tale portion of ejaculated sperm (Saito et al. 2004).

Developmental expression of AQP7 in rat testis was also examined (Calamita et al. 2001; Kageyama et al. 2001). Using semiquantitative RT-PCR and Western blotting, the AQP7 mRNA was detected beginning from P45, while the signal reached the maximal intensity at P90 and thereafter.

3.2 AQP7 in Human Infertility

Saito et al. (2004) investigated AQP7 expression in the human testis and ejaculated sperm from fertile men and from infertile patients. As mentioned above, AQP7 was

expressed at the tail of spermatids and spermatozoa in the human testis. AQP7 protein was also detected at the middle piece and the anterior tale portion of ejaculated sperm. Interestingly, they found that some infertile patients lacked AQP7 expression in ejaculated sperm, although all fertile men expressed AQP7 protein. The motility rate of AQP7-negative sperm was significantly lower than that of AQP7-positive sperm, suggesting that AQP7 is involved in the maintenance of sperm motility and a lack of AQP7 expression in sperm may be an underlying cause of male infertility.

However, a male human subject with a point mutation in AQP7 was reported not to be infertile, although he had defective glycerol metabolism (Kondo et al. 2002). Therefore, the involvement of human AQP7 in male infertility is still controversial.

3.3 Reproductive Function of AQP7 in Knockout Mice

To date, four groups have generated and independently reported on AQP7 knockout mice (Maeda et al. 2004; Matsumura et al. 2007; Skowronski et al. 2007; Sohara et al. 2005). All reported that AQP7 knockout mice did not show male infertility. In addition, two groups also mentioned that histology and testis weight from an AQP7 knockout mouse was not different from that from a wild-type mouse (Skowronski et al. 2007; Sohara et al. 2007). Sperm from AQP7 knockout mice did not show any morphological difference from wild-type mice either (Sohara et al. 2007). The number of offspring from wild-type female mice mated with wild-type male mice was not different from that of AQP7 knockout female mice mated with AQP7 knockout male mice, indicating that AQP7 absence had no effect on the number of offspring (Sohara et al. 2007).

AQP7 is considered to have several roles in testicular germ cells. AQP7 may be involved in the rapid reduction of spermatid volume during spermiogenesis. However, the daily production of sperm did not decrease in the absence of AQP7 (Sohara et al. 2007), suggesting that AQP7 is not involved in spermiogenesis, or that other compensatory mechanisms exist.

It has also been proposed that AQP7 regulates sperm-egg fusion because AQP7 is structurally similar to the bacterial glycerol facilitator GlpF (Ishibashi et al. 1997), which is involved in cell fusion (Philips and Herskowitz 1997). Therefore, to determine whether AQP7 has a role in sperm-egg fusion, an *in vitro* fertilization experiment was performed (Sohara et al. 2007). However, the fertilization rate of spermatozoa from AQP7 knockout mice was not different from that of wild-type mice, indicating that AQP7 may not have a major role in the sperm-egg fusion process.

As mentioned above, Saito et al. (2004) reported that ejaculated sperm of some infertile human patients lacked AQP7 protein expression, and that all fertile men expressed AQP7 protein. Furthermore, they found that the motility rate of AQP7-negative sperm was significantly lower than that of AQP7-positive sperm. However, the motility of sperm from AQP7 knockout mice was not significantly different from that of wild-type mice (Sohara et al. 2007). This difference in findings may reflect species differences, although further investigations are required.

In summary, the role of AQP7 in the testis and sperm of AQP7 knockout mice is not clear as yet, although AQP7 is expressed abundantly in the testis and sperm. However, the lack of phenotype in the absence of AQP7 in spermatids and spermatozoa of mice does not exclude a potential role for AQP in concentrating sperm and in promoting sperm maturation, as the defect may have been compensated for by other mechanisms.

References

- Badran HH, Hermo LS (2002) Expression and regulation of aquaporins 1, 8, and 9 in the testis, efferent ducts, and epididymis of adult rats and during postnatal development. *J Androl* 23:358–373
- Beyer KH Jr, Gelarden RT (1988) Active transport of urea by mammalian kidney. *Proc Natl Acad Sci U S A* 85:4030–4031
- Burch HB, Narins RG, Chu C, Fagioli S, Choi S, McCarthy W, Lowry OH (1978) Distribution along the rat nephron of three enzymes of gluconeogenesis in acidosis and starvation. *Am J Physiol* 235:F246–F253
- Calamita G, Mazzone A, Bizzoca A, Svelto M (2001) Possible involvement of aquaporin-7 and -8 in rat testis development and spermatogenesis. *Biochem Biophys Res Commun* 288:619–625
- Elkjaer M, Vajda Z, Nejsum LN, Kwon T, Jensen UB, Amiry-Moghaddam M, Frokiaer J, Nielsen S (2000) Immunolocalization of AQP9 in liver, epididymis, testis, spleen, and brain. *Biochem Biophys Res Commun* 276:1118–1128
- Fushimi K, Uchida S, Hara Y, Hirata Y, Marumo F, Sasaki S (1993) Cloning and expression of apical membrane water channel of rat kidney collecting tubule. *Nature* 361:549–552
- Guder WG, Schmidt U (1974) The localization of gluconeogenesis in rat nephron. Determination of phosphoenolpyruvate carboxykinase in microdissected tubules. *Hoppe Seylers Z Physiol Chem* 355:273–278
- Hara-Chikuma M, Sohara E, Rai T, Ikawa M, Okabe M, Sasaki S, Uchida S, Verkman AS (2005) Progressive adipocyte hypertrophy in aquaporin-7-deficient mice: adipocyte glycerol permeability as a novel regulator of fat accumulation. *J Biol Chem* 280:15493–15496
- Himms-Hagen J (1968) Glycerol metabolism in rabbits. *Can J Biochem* 46:1107–1114
- Huq AH, Lovell RS, Ou CN, Beaudet AL, Craigen WJ (1997) X-linked glycerol kinase deficiency in the mouse leads to growth retardation, altered fat metabolism, autonomous glucocorticoid secretion and neonatal death. *Hum Mol Genet* 6:1803–1809
- Ishibashi K, Sasaki S, Saito F, Ikeuchi T, Marumo F (1995) Structure and chromosomal localization of a human water channel (AQP3) gene. *Genomics* 27:352–354
- Ishibashi K, Kuwahara M, Gu Y, Kageyama Y, Tohsaka A, Suzuki F, Marumo F, Sasaki S (1997) Cloning and functional expression of a new water channel abundantly expressed in the testis permeable to water, glycerol, and urea. *J Biol Chem* 272:20782–20786
- Ishibashi K, Yamauchi K, Kageyama Y, Saito-Ohara F, Ikeuchi T, Marumo F, Sasaki S (1998) Molecular characterization of human aquaporin-7 gene and its chromosomal mapping. *Biochim Biophys Acta* 1399:62–66
- Ishibashi K, Imai M, Sasaki S (2000) Cellular localization of aquaporin 7 in the rat kidney. *Exp Nephrol* 8:252–257
- Kageyama Y, Ishibashi K, Hayashi T, Xia G, Sasaki S, Kihara K (2001) Expression of aquaporins 7 and 8 in the developing rat testis. *Andrologia* 33:165–169
- Kawamura S, Kokko JP (1976) Urea secretion by the straight segment of the proximal tubule. *J Clin Invest* 58:604–612
- King LS, Agre P (1996) Pathophysiology of the aquaporin water channels. *Annu Rev Physiol* 58:619–648

- King LS, Choi M, Fernandez PC, Cartron JP, Agre P (2001) Defective urinary-concentrating ability due to a complete deficiency of aquaporin-1. *N Engl J Med* 345:175–179
- Kishida K, Kuriyama H, Funahashi T, Shimomura I, Kihara S, Ouchi N, Nishida M, Nishizawa H, Matsuda M, Takahashi M, Hotta K, Nakamura T, Yamashita S, Tochino Y, Matsuzawa Y (2000) Aquaporin adipose, a putative glycerol channel in adipocytes. *J Biol Chem* 275:20896–20902
- Kishida K, Shimomura I, Kondo H, Kuriyama H, Makino Y, Nishizawa H, Maeda N, Matsuda M, Ouchi N, Kihara S, Kurachi Y, Funahashi T, Matsuzawa Y (2001) Genomic structure and insulin-mediated repression of the aquaporin adipose (AQPap), adipose-specific glycerol channel. *J Biol Chem* 276:36251–36260
- Knepper MA, Gamba G (2003) Urine concentration and dilution. In: Brenner MD, Livine SA (eds.) *The kidney*. Philadelphia, W.B. Saunders
- Kondo H, Shimomura I, Kishida K, Kuriyama H, Makino Y, Nishizawa H, Matsuda M, Maeda N, Nagaretani H, Kihara S, Kurachi Y, Nakamura T, Funahashi T, Matsuzawa Y (2002) Human aquaporin adipose (AQPap) gene. Genomic structure, promoter analysis and functional mutation. *Eur J Biochem* 269:1814–1826
- Krebs HA, Bennett DA, De Gasquet P, Gasquet P, Gascoyne T, Yoshida T (1963) Renal gluconeogenesis. The effect of diet on the gluconeogenic capacity of rat-kidney-cortex slices. *Biochem J* 86:22–27
- Kuriyama H, Kawamoto S, Ishida N, Ohno I, Mita S, Matsuzawa Y, Matsubara K, Okubo K (1997) Molecular cloning and expression of a novel human aquaporin from adipose tissue with glycerol permeability. *Biochem Biophys Res Commun* 241:53–58
- Lee MD, Bhakta KY, Raina S, Yonescu R, Griffin CA, Copeland NG, Gilbert DJ, Jenkins NA, Preston GM, Agre P (1996) The human aquaporin-5 gene. Molecular characterization and chromosomal localization. *J Biol Chem* 271:8599–8604
- Lin EC (1977) Glycerol utilization and its regulation in mammals. *Annu Rev Biochem* 46:765–795
- Ma T, Yang B, Gillespie A, Carlson EJ, Epstein CJ, Verkman AS (1997) Generation and phenotype of a transgenic knockout mouse lacking the mercurial-insensitive water channel aquaporin-4. *J Clin Invest* 100:957–962
- Ma T, Yang B, Gillespie A, Carlson EJ, Epstein CJ, Verkman AS (1998) Severely impaired urinary concentrating ability in transgenic mice lacking aquaporin-1 water channels. *J Biol Chem* 273:4296–4299
- Ma T, Song Y, Yang B, Gillespie A, Carlson EJ, Epstein CJ, Verkman AS (2000) Nephrogenic diabetes insipidus in mice lacking aquaporin-3 water channels. *Proc Natl Acad Sci USA* 97:4386–4391
- Maeda N, Funahashi T, Hibuse T, Nagasawa A, Kishida K, Kuriyama H, Nakamura T, Kihara S, Shimomura I, Matsuzawa Y (2004) Adaptation to fasting by glycerol transport through aquaporin 7 in adipose tissue. *Proc Natl Acad Sci U S A* 101:17801–17806
- Matsumura K, Chang BH, Fujimiya M, Chen W, Kulkarni RN, Eguchi Y, Kimura H, Kojima H, Chan L (2007) Aquaporin 7 is a beta-cell protein and regulator of intracellular glycerol content and glycerol kinase activity, beta-cell mass, and insulin production and secretion. *Mol Cell Biol* 27:6026–6037
- Morishita Y, Sakube Y, Sasaki S, Ishibashi K (2004) Molecular mechanisms and drug development in aquaporin water channel diseases: aquaporin superfamily (superaquaporins): expansion of aquaporins restricted to multicellular organisms. *J Pharmacol Sci* 96:276–279
- Nejsum LN, Elkjaer M, Hager H, Frokiaer J, Kwon TH, Nielsen S (2000) Localization of aquaporin-7 in rat and mouse kidney using RT-PCR, immunoblotting, and immunocytochemistry. *Biochem Biophys Res Commun* 277:164–170
- Philips J, Herskowitz I (1997) Osmotic balance regulates cell fusion during mating in *Saccharomyces cerevisiae*. *J Cell Biol* 138:961–974
- Robinson J, Newsholme EA (1969) The effects of dietary conditions and glycerol concentration on glycerol uptake by rat liver and kidney-cortex slices. *Biochem J* 112:449–453
- Russell LD (1979) Spermatid-Sertoli tubulobulbar complexes as devices for elimination of cytoplasm from the head region of late spermatids of the rat. *Anat Rec* 194:233–246

- Saito K, Kageyama Y, Okada Y, Kawakami S, Kihara K, Ishibashi K, Sasaki S (2004) Localization of aquaporin-7 in human testis and ejaculated sperm: possible involvement in maintenance of sperm quality. *J Urol* 172:2073–2076
- Schnermann J, Chou CL, Ma T, Traynor T, Knepper MA, Verkman AS (1998) Defective proximal tubular fluid reabsorption in transgenic aquaporin-1 null mice. *Proc Natl Acad Sci U S A* 95:9660–9664
- Shin I, Kim HJ, Lee JE, Gye MC (2006) Aquaporin7 expression during perinatal development of mouse brain. *Neurosci Lett* 409:106–111
- Skowronski MT, Lebeck J, Rojek A, Praetorius J, Fuchtbauer EM, Frokiaer J, Nielsen S (2007) AQP7 is localized in capillaries of adipose tissue, cardiac and striated muscle: implications in glycerol metabolism. *Am J Physiol Renal Physiol* 292:F956–965
- Sohara E, Rai T, Miyazaki J, Verkman AS, Sasaki S, Uchida S (2005) Defective water and glycerol transport in the proximal tubules of AQP7 knockout mice. *Am J Physiol Renal Physiol* 289:F1195–1200
- Sohara E, Rai T, Sasaki S, Uchida S (2006a) Physiological roles of AQP7 in the kidney: Lessons from AQP7 knockout mice. *Biochim Biophys Acta* 1758:1106–1110
- Sohara E, Rai T, Yang SS, Uchida K, Nitta K, Horita S, Ohno M, Harada A, Sasaki S, Uchida S (2006b) Pathogenesis and treatment of autosomal-dominant nephrogenic diabetes insipidus caused by an aquaporin 2 mutation. *Proc Natl Acad Sci U S A* 103:14217–14222
- Sohara E, Ueda O, Tachibe T, Hani T, Jishage K, Rai T, Sasaki S, Uchida S (2007) Morphologic and functional analysis of sperm and testes in aquaporin 7 knockout mice. *Fertil Steril* 87:671–676
- Sprando RL, Russell LD (1987) Comparative study of cytoplasmic elimination in spermatids of selected mammalian species. *Am J Anat* 178:72–80
- Suzuki-Toyota F, Ishibashi K, Yuasa S (1999) Immunohistochemical localization of a water channel, aquaporin 7 (AQP7), in the rat testis. *Cell Tissue Res* 295:279–285
- Vandewalle A, Wirthensohn G, Heidrich HG, Guder WG (1981) Distribution of hexokinase and phosphoenolpyruvate carboxykinase along the rabbit nephron. *Am J Physiol* 240:F492–F500
- Verkman AS (1999) Lessons on renal physiology from transgenic mice lacking aquaporin water channels. *J Am Soc Nephrol* 10:1126–1135
- Verkman AS (2002) Aquaporin water channels and endothelial cell function. *J Anat* 200:617–627
- Vernon RG, Walker DG (1970) Glycerol metabolism in the neonatal rat. *Biochem J* 118:531–536
- Wieland O, Suyter M (1957) Glycerokinase; isolation and properties of the enzyme. *Biochem Z* 329:320–331
- Wirthensohn G, Vandewalle A, Guder WG (1981) Renal glycerol metabolism and the distribution of glycerol kinase in rabbit nephron. *Biochem J* 198:543–549
- Yang B, Bankir L (2005) Urea and urine concentrating ability: new insights from studies in mice. *Am J Physiol Renal Physiol* 288:F881–F896
- Yang B, Gillespie A, Carlson EJ, Epstein CJ, Verkman AS (2001) Neonatal mortality in an aquaporin-2 knock-in mouse model of recessive nephrogenic diabetes insipidus. *J Biol Chem* 276:2775–2779
- Yang B, Song Y, Zhao D, Verkman AS (2005) Phenotype analysis of aquaporin-8 null mice. *Am J Physiol Cell Physiol* 288:C1161–C1170
- Zardoya R (2005) Phylogeny and evolution of the major intrinsic protein family. *Biol Cell* 97:397–414

Role of Aquaporin-7 and Aquaporin-9 in Glycerol Metabolism; Involvement in Obesity

Norikazu Maeda, Toshiyuki Hibuse, and Tohru Funahashi

Contents

1	Introduction	234
2	Characteristics of Adipocytes	235
3	AQP7	236
3.1	Molecular Cloning, Tissue Distribution, and Functional Analysis of AQP7	236
3.2	Regulation of AQP7 in Adipocytes	237
3.3	Role of AQP7 in other Organs	239
4	AQP9	239
4.1	Molecular Cloning and Tissue Distribution of AQP9	239
4.2	Functional Analysis and Regulation of AQP9 in Liver	240
4.3	Coordination of Adipose and Liver Glycerol Channels	241
4.4	Role of AQP9 in other Organ	242
5	Analysis of AQP7-Deficient Mice	242
5.1	Adipose-Derived Glycerol and Gluconeogenesis through AQP7	242
5.2	Adipocytes Dysfunction in AQP7-Deficient Cells	243
6	Analysis of AQP9-Deficient Mice	244
7	Role of AQP7 and AQP9 in Human	244
8	Conclusions and Outlook	245
	References	246

Abstract The discovery of aquaporin (AQP) has had a great impact on life sciences. So far, 13 AQPs have been identified in human. AQP3, 7, 9, and 10 are subcategorized as aquaglyceroporins which permeabilize glycerol as well as water. Many investigators have demonstrated that AQPs play a crucial role in maintaining water homeostasis, but the physiological significance of some AQPs as a glycerol channel has not been fully understood. Adipocyte is considered to be a major source of

N. Maeda (✉)

Department of Metabolic Medicine, Graduate School of Medicine, Osaka University,
2-2-B5 Yamada-oka, Suita, Osaka 565-0871, Japan
nmaeda@imed2.med.osaka-u.ac.jp

E. Beitz (ed.), *Aquaporins*, Handbook of Experimental Pharmacology 190,
© Springer-Verlag Berlin Heidelberg 2009

233

glycerol which is one of substrates for hepatic gluconeogenesis. This review focuses on recent studies of glycerol metabolism through AQP7 and AQP9, and discusses the importance of glycerol channel in adipose tissues and liver.

Abbreviations

AQP	aquaporin
FFA	free fatty acid
GLUT4	glucose transporter 4
HSL	hormone sensitive lipase
TG	triglyceride
WAT	white adipose tissue

1 Introduction

In adipocytes, lipogenesis and lipolysis are observed in response to whole body energy balance. Adipocytes store triglyceride (TG) in case of excess of nutrition, while adipocytes release free fatty acid (FFA) and glycerol into the blood stream by hydrolyzing TG under starvation and/or sympathetic nerve-activation state and these substrates were taken into the energy expenditure organs (Ramsay 1996). Historically human starvation has been a matter of life or death. Adipocytes play a crucial role in energy supply under starvation to maintain energy homeostasis, and contribute to the survival of human beings during long starvation periods. However, today, over-nutrition and lack of exercise cause over-accumulation of fat, especially in industrial countries (Kahn and Flier 2000; Spiegelman and Flier 2001; Friedman 2004). This socio-environmental change leads to and increases life-style related diseases, such as diabetes, dyslipidemia, hypertension, and atherosclerosis commonly recognized as metabolic syndrome (Zimmet et al. 2001). Fat accumulation, especially intra-abdominal fat deposits, is located in the pathological upstream of metabolic syndrome (Fujioka et al. 1987; Kanai et al. 1990; Nakamura et al. 1994; Yamashita et al. 1996). Consistent with the concept of metabolic syndrome, many investigators have tried to clarify the underlying molecular mechanism of obesity-based pathophysiology. To find a novel therapy for metabolic syndrome, there is a need to focus on the biology and science of adipocyte, which the authors term "Adiposcience". Recent progress in this field shows that the pathogenesis of metabolic syndrome is associated with adipocyte dysfunction (Funahashi et al. 1999).

Adipocytes hydrolyze TG and rapidly liberate FFA and glycerol into the circulation. It is presumed that glycerol channel in adipocytes prevent acute rise in intracellular osmotic pressure when glycerol production is rapidly increased during lipolysis. However, the underlying mechanism responsible for glycerol release from adipocytes remains elusive. The authors identified aquaporin (AQP) 7 from the human adipose tissue cDNA library in 1997 (Kuriyama et al. 1997).

In this review, the authors focused on AQP7 and AQP9 involving glycerol metabolism and metabolic disorders.

2 Characteristics of Adipocytes

Adipocytes have a unique feature; lipid droplets occupy a large part of the intracellular region, while the nucleus and cytosome are located in the periphery. In comparison, the nucleus is located in the center of cell in other tissue cells. Thus, adipocytes are morphologically characterized by TG accumulation. Adipocytes serve as an energy storage organ to maintain systemic energy balance (Fig. 1). Pancreatic β -cells release insulin in response to an increase of plasma glucose level during feeding state. Insulin acts on adipose tissues as well as skeletal muscles, transfers glucose transporter 4 (GLUT4) to plasma membrane, and takes glucose into adipocytes (Shepherd and Kahn 1999). Insulin also activates lipoprotein lipase (LPL) located on the cell surface of the vascular endothelium. LPL removes fatty acids from

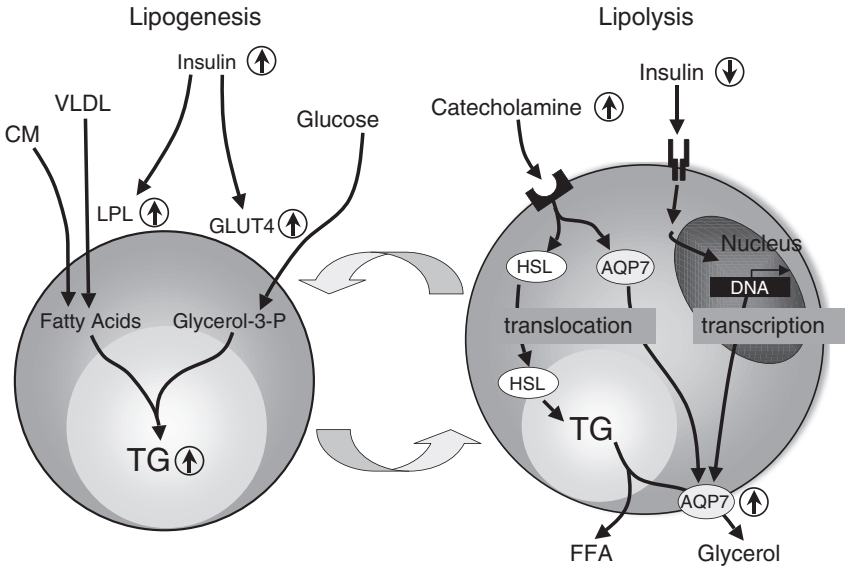


Fig. 1 A model illustrating lipogenesis and lipolysis in adipocytes. Under lipogenic conditions, insulin binds to the insulin receptor located on the surface of adipocytes and transfers glucose transporter 4 (GLUT4) to the plasma membrane, and takes glucose into the cell. Intracellular glucose is converted to glycerol-3-phosphate (Glycerol-3-P). Insulin also activates lipoprotein lipase (LPL) located on the cell surface of the vascular endothelium. Activated-LPL removes fatty acids from intestine-derived chylomicron (CM) and liver-derived very low density lipoprotein (VLDL), and then fatty acids are taken into adipocytes. Fatty acids and glycerol-3-P are esterified into triglyceride (TG). Under lipolytic conditions, sympathetic nerves are activated and catecholamines are increased. Catecholamines stimulate adrenergic receptors located on the surface of adipocytes. Activation of adrenergic receptors translocates hormone sensitive lipase (HSL), which is a key enzyme hydrolyzing TG to FFA and glycerol, to the lipid droplets, while related stimuli moves AQP7 to the plasma membrane. FFA and glycerol are released into the bloodstream and utilized for thermogenesis and gluconeogenesis, respectively. Moreover, AQP7 mRNA levels are elevated by the decrease of insulin signaling cascade. Thus, long-term regulation of AQP7 is under the control of insulin while short-term regulation is under catecholamines. These two different regulatory pathways of AQP7 assure the efficient release of glycerol from adipocytes under fasting conditions

intestine-derived chylomicron (CM) and liver-derived very low density lipoprotein (VLDL), and then fatty acids are taken into adipocytes (Mead et al. 2002). In lipogenic condition, glycerol-3-phosphate (glycerol-3-P) converted from glucose and fatty acids are esterified into TG in adipocytes. Fatty acid binding protein (FABP) (Stremmel et al. 1985), fatty acid translocase (FAT) (Ibrahimi et al. 1996; Motojima et al. 1998), and fatty acid transporter protein (FATP) (Motojima et al. 1998; Schaffer and Lodish 1994) are recognized as fatty acid transporters in adipocytes.

In contrast to the feeding state, exercise and/or fasting condition induces lipolysis in adipocytes (Londos et al. 1999). Fasting stimulates sympathetic nerves and elevates catecholamines, such as adrenaline and noradrenalin, which in turn stimulate adrenergic receptor located on cell surface of adipocytes. Activation of adrenergic receptor results in converting adenosine 5'-triphosphate (ATP) to cyclic adenosine monophosphate (cAMP). Elevation of intracellular cAMP activates hormone-sensitive lipase (HSL) by phosphorylation. Phosphorylated-HSL hydrolyzes TG to FFA and glycerol, and both are released into the bloodstream. FFA and glycerol are utilized for thermogenesis and gluconeogenesis, respectively. Thus, lipogenesis and lipolysis in adipocytes contribute to maintain energy balance in the whole body.

3 AQP7

3.1 Molecular Cloning, Tissue Distribution, and Functional Analysis of AQP7

The authors analyzed the gene expression profile of human visceral and subcutaneous fat to clarify and understand the molecular mechanism of obesity-related diseases (Maeda et al. 1997). In this process, they identified a novel complementary DNA (cDNA) belonging to the AQP family, and named it aquaporin adipose (AQPap) because its mRNA is expressed abundantly in adipose tissues and adipocytes (Kuriyama et al. 1997). AQPap is a human counterpart of AQP7 that was independently cloned from rat testis by another group at the same time (Ishibashi et al. 1997). In mouse, AQP7 is highly expressed in white adipose tissue (WAT), brown adipose tissue (BAT), and testis. Furthermore, a weak expression of AQP7 is also observed in heart, skeletal muscle, and kidney. The transcript of testis AQP7 forms short length in comparison with the other organ AQP7, which is accounted for the different lengths of the untranslated region of cDNA locating at 3'-end (Kishida et al. 2001).

AQP7-expressing *Xenopus* oocytes gain water and glycerol permeability (Kishida et al. 2000). This gain of function is inhibited by HgCl₂ and its inhibition is recovered by 2-mercaptoethanol, similar to the other AQPs. This result indicates that AQP7 can be subcategorized as an aquaglyceroporin, which enhance permeation of glycerol, in addition to water. In mammals, AQP3, 7, 9, and 10 are believed to

belong to aquaglyceroporin family at present. Interestingly, *Escherichia coli* has one aquaporin (AqpZ) and one aquaglyceroporin (GlpF) (Agre et al. 2002). These findings indicate that glycerol channel is required even in *E. coli* and that glycerol is an essential substance for living.

3.2 Regulation of AQP7 in Adipocytes

AQP7 mRNA expression increases in parallel with adipocytes differentiation of 3T3-L1 cells. Glycerol release into the media also increases in parallel with AQP7 mRNA levels in differentiating 3T3-L1 adipocytes (Kishida et al. 2000). Peroxisome proliferator activated receptor γ (PPAR γ) is a master regulator of adipocytes differentiation and regulates several adipose-specific genes at the transcriptional level. PPAR γ forms a hetero-dimer with retinoic acid X receptor α (RXR α), and binds to peroxisome proliferator response element (PPRE) site. The PPRE site is identified in the promoter region of AQP7 gene based on analysis of the mouse AQP7 gene (Fig. 2). Heterodimers of PPAR γ and RXR α bind to the PPRE site of AQP7 promoter and up-regulates AQP7 mRNA expression in adipocytes (Kishida et al. 2001b). Furthermore, the administration of thiazolidinediones (TZDs), which are insulin-sensitizing agents and exogenous PPAR γ ligands, increase AQP7 mRNA levels in 3T3-L1 adipocytes and in adipose tissues of mice. The precise mechanism

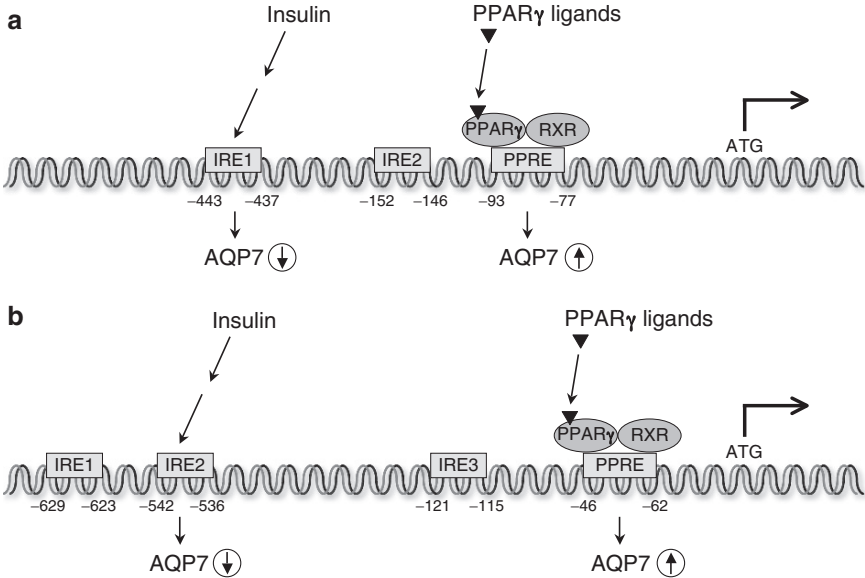


Fig. 2 Transcriptional regulation of AQP7 gene. A model illustrating AQP7 promoter gene in mouse (a) and human (b). IRE, insulin negative response element; PPAR, peroxisome proliferator activated receptor; RXR, retinoic acid X receptor; PPRE, peroxisome proliferator response element

of TZD in ameliorating insulin resistance is not fully understood. To clarify whether the TZD-induced adipose AQP7 is related to insulin sensitivity, further studies are required.

AQP7 mRNA levels are reduced by feeding and increased by fasting in parallel with plasma glycerol levels (Kishida et al. 2000). These nutrition-related changes in AQP7 and plasma glycerol are the opposites of plasma insulin levels. In fact, in 3T3-L1 adipocytes, insulin suppresses AQP7 mRNA levels in dose- and time-dependent ways. The insulin negative response element (IRE) is identified in the promoter region of AQP7 gene (Fig. 2). In mouse AQP7 gene, two IREs were identified and IRE1 (−443 to −437) was shown to be functional (Kishida et al. 2001a). In human AQP7 gene, IRE2 (−542 to −536) responded to insulin among three IREs (Kondo et al. 2002). This result indicates that AQP7 mRNA expression is closely regulated by insulin at the transcriptional level. Furthermore, glucose-6-phosphatase (G6Pase) and phosphoenolpyruvate carboxykinase (PEPCK), which are key enzymes of gluconeogenesis, also contain IRE in their promoter regions. Insulin also suppresses the mRNA levels of G6Pase and PEPCK. Taken together, plasma glycerol levels are partly determined by insulin through adipose AQP7, suggesting that adipose AQP7 may be associated with glucose metabolism.

In 3T3-L1 adipocytes, AQP7 is localized at the periphery of the nucleus in steady state. However, AQP7 translocates to the plasma membrane following adrenaline stimulation, which induces lipolysis (Kishida et al. 2000). Adrenaline does not affect AQP7 gene expression. Adrenaline elevates intracellular cAMP levels through adrenergic receptor and then activates protein kinase A (PKA). Interestingly, similar results are observed in AQP2, which is a key water channel of the kidney. AQP2 exists in the principal cells of the renal collecting duct. Immunogold electron microscopy studies showed that very little of AQP2 protein is found in the apical membrane of collecting duct principal cells, but most of AQP2 protein exists in the membranes of intracellular vesicles. However, AQP2 protein relocates to the apical plasma membrane when collecting duct cells are stimulated by vasopressin, an anti-diuretic hormone released from the brain (Nielsen et al. 1995). Vasopressin binds to V2 receptor at the basolateral membrane of the renal collecting duct causing activation of a G-coupled adenylylcyclase cascade resulting in phosphorylation of AQP2 by PKA (Kuwahara et al. 1995). The phosphorylation site of AQP2 is located at residue 256 on the C-terminus of its protein. Phosphorylated-AQP2 moves to the apical plasma membrane. These results suggest that AQP7, as well as AQP2, may be phosphorylated by PKA under the activation of adrenergic receptor. Database analysis indicates the six prospective sites of PKA phosphorylation in both human and mouse AQP7. It is therefore necessary to determine the phosphorylation site of AQP7.

Figure 1 right panel shows a model illustrating the regulation of AQP7 at fasting state. Collectively, catecholamine stimuli translocate HSL to the lipid droplets and moves AQP7 to the plasma membrane. Phosphorylated-HSL hydrolyzes TG to fatty acids and glycerol in cooperation with perilipin, which is another key molecule in lipolysis. Reduced insulin signal also results in up-regulation of AQP7 mRNA levels. Finally, glycerol produced by hydrolysis in adipocytes is released into the bloodstream through AQP7.

3.3 Role of AQP7 in other Organs

The authors' group discovered AQP7 during genomic analysis of human adipose tissue; at the same time another group identified AQP7 from the rat testis (Ishibashi et al. 1997). AQP7 is also expressed in human sperms. Lack of AQP7 expression in sperms is observed in several male infertile subjects. Other studies demonstrated that sperm AQP7 is associated with the capacity of sperm movement (Saito et al. 2004). Immunohistochemical analysis shows that AQP7 is also expressed in the proximal tubules of the kidney. AQP7-deficient mice exhibit hyperglycerourea, suggesting that AQP7 is involved in glycerol re-absorption in the kidney (Sohara et al. 2005).

Skeletal muscles express small amounts of AQP7 (Hibuse et al. 2006). Recent immunohistochemical studies using anti-AQP7 antibody demonstrated immunoreactivity at the myofiber surface of type 1 and type 2 fibers in human muscles and of type 2 fibers in mouse muscles (Wakayama et al. 2004). The role of AQP4 has been extensively investigated in skeletal muscles (Frigeri et al. 1998; Frigeri et al. 2001). AQP4 is reduced in the skeletal muscle of patients with Duchenne dystrophy (Frigeri et al. 2002; Wakayama et al. 2002), of mdx mice (Liu et al. 1999; Crosbie et al. 2002), and of patients with amyotrophic lateral sclerosis (Jimi et al. 2004). The nerve activity is thought to control the expression of AQP4 in skeletal muscles. While the function of AQP4 has been clarified in skeletal muscles, the physiological role of AQP7 in skeletal muscles has remained unclear. Heart tissue expresses small amounts of AQP7 (Hibuse et al. 2006). Fatty acids and/or glucose are widely recognized as energy source in the heart. Why does AQP7 exist as a glycerol channel in the heart? What is the role of glycerol in the heart? Currently no published studies on the functional role of AQP7 in the heart exist. Further investigations of skeletal muscle and/or heart AQP7 would need to be performed.

4 AQP9

4.1 Molecular Cloning and Tissue Distribution of AQP9

AQP9 was independently identified in human leukocytes (Ishibashi et al. 1998) and rat liver (Tsukaguchi et al. 1998; Ko et al. 1999). Northern blotting analysis identified human AQP9 expression in liver, leukocyte, lung, and spleen (Ishibashi et al. 1998). In rat, AQP9 mRNA is found in liver, testis, brain (Tsukaguchi et al. 1998), and lung (Ko et al. 1999). AQP9 is also highly expressed in mouse liver and testis. In hepatocytes, immunohistochemistry showed that AQP9 is localized at the sinusoidal plasma membrane (Elkjaer et al. 2000).

4.2 Functional Analysis and Regulation of AQP9 in Liver

Rat AQP9-expressing *Xenopus* oocytes exhibit water and glycerol permeability (Ishibashi et al. 1998). A series of studies on *Xenopus* oocytes also demonstrated that rat AQP9 permeates urea, mannitol, sorbitol, and uracil. Consistent with this finding, another group found that rat AQP9 is permeable to water, glycerol and urea (Ko et al. 1999). These results indicate a broad selectivity of rat AQP9. However, another group found the AQP9-induced permeability to be restricted to water and urea in humans (Ishibashi et al. 1998). Thus, there are conflicting results regarding AQP9-induced permeability between the rat and the human being. Future studies could provide more information, based on the physiological function of AQP9 and can be designed to analyze AQP9 knockout mice, and/or analyze human genetic mutation in AQP9 gene.

Arsenic trioxide uptake was examined with yeast expressing mammalian AQP7 or AQP9 as well as in oocytes expressing these proteins (Liu et al. 2002). The results of these studies showed that AQP7 and AQP9 might be the major routes of arsenite uptake into mammalian cells. Arsenic trioxide is uncharged at neutral pH values and is very toxic. Clinical features of greatest concern in arsenic poisoning include hepatocellular damage and hepatocellular carcinoma.

Intra-abdominal visceral fat accumulates mainly in the mesentery. The anatomical distribution of intra-abdominal visceral fat indicates that substances released from the visceral fat directly flow into the liver through the portal vein. FFA derived from visceral fat during lipolysis elevates liver acyl-coenzyme A synthetase (ACS) and microsomal triglyceride transfer protein (MTP) mRNA levels, and reduces degradation of apolipoprotein B (ApoB). These changes induce the release of ApoB from the liver and increase plasma triglyceride concentrations. Hypertriglyceridemia, which is often observed in subjects with visceral fat accumulation, partly account for the increase in FFA derived from adipose tissues (Kuriyama et al. 1998). Glycerol, which is another product from adipose TG during lipolysis, directly flows into the liver via portal vein and become substrate for gluconeogenesis. AQP9 is considered the sole glycerol channel in liver and is localized at the sinusoidal plasma membrane facing the portal vein (Elkjaer et al. 2000). Taken together, AQP9 may act as a channel for glycerol uptake in the liver (Fig. 3). AQP9 mRNA level is increased by fasting and is decreased by feeding (Kuriyama et al. 2002). These changes of AQP9 mRNA are similar to those of glycerol kinase, a key enzyme involved in the conversion of glycerol to glycerol-3-phosphate, and PEPCK, which is a key enzyme for gluconeogenesis. Insulin suppresses AQP9 mRNA levels in time- and dose-dependent manners in H4IIE hepatocytes. Promoter analysis demonstrates that insulin reduces AQP9 mRNA level via IRE locating at $-496/-502$ promoter region. Administration of streptozotocin (STZ) results in increased AQP9 mRNA (Kuriyama et al. 2002) and protein (Carbrey et al. 2003) levels in insulin-deficient mice.

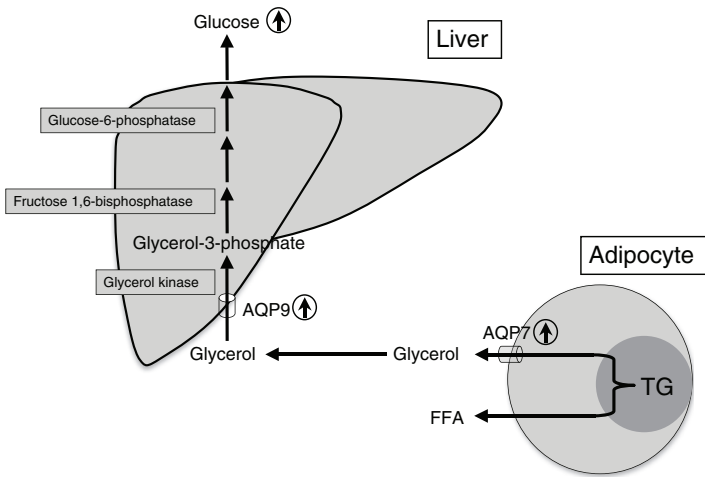


Fig. 3 Coordinated regulation of adipose AQP7 and liver AQP9 during fasting states. Fasting induces lipolysis in adipocytes and gluconeogenesis in liver. AQP7 mRNA levels are elevated, AQP7 protein translocates to the plasma membrane, and AQP7 serves as an efficient release of glycerol in adipocytes under fasting conditions. Fasting also increases AQP9 mRNA levels in liver; the increased portal glycerol directly flows into the liver, and AQP9 may contribute to the entry of glycerol into hepatocytes. In the liver, glycerol is one of substrates for gluconeogenesis. The glycerol cascade from adipose tissue to liver is maintained by the coordinated regulation of AQP7 and AQP9 under fasting state

4.3 Coordination of Adipose and Liver Glycerol Channels

In fasting condition, adipose AQP7 transfers to the plasma membrane and is enhanced at mRNA expression level thereby augmenting glycerol release from adipocytes. Liver AQP9 mRNA level is enhanced in parallel with adipose AQP7 elevation, suggesting that glycerol is taken into hepatocytes and is used for gluconeogenesis (Fig. 3). In feeding state, a rise in plasma insulin concentration results in the suppression of lipolysis and the reduction of adipose AQP7 mRNA level, and thus decreases glycerol release from adipocytes. Feeding also reduces liver AQP9 mRNA level and suppresses glycerol-based gluconeogenesis. However, high adipose AQP7 and liver AQP9 mRNA levels are observed in obese and insulin-resistant animals in spite of hyperinsulinemia. These animals show the increased glycerol release from adipose tissues in parallel with increase of AQP7 mRNA level, and also exhibit the increased glycerol levels in the portal vein. Finally, the high glycerol levels in the portal vein causes gluconeogenesis and results in hyperglycemia through the pathological induction of liver AQP9 (Kuriyama et al. 2002). Considered collectively, physiological and pathological coordinated regulation of organ-specific glycerol channels, adipose AQP7 and liver AQP9, may contribute to glycerol and glucose metabolism in vivo.

4.4 Role of AQP9 in other Organ

The role of AQP9, other than the liver, has been investigated. AQP9 is expressed in brain, especially in glial cells, in particular tanycytes and astrocytes, in endothelial cells, and in neurons (Badaut et al. 2001; Nicchia et al. 2001; Badaut et al. 2004). Interestingly, neurons expressing AQP9 are catecholaminergic and glucose sensitive. Similar to liver AQP9, AQP9 expression level in neurons was shown to be regulated by insulin, suggesting that brain AQP9 is involved in glucose metabolism and energy balance (Badaut and Regli 2004). Recently, AQP9 has been shown to play a crucial role as a glycerol channel in mouse erythrocytes (Liu et al. 2007). AQP3 is the major glycerol channel in human and rat erythrocytes, but AQP3 has not been detected in mouse erythrocytes. Glycerol permeability of erythrocytes derived from AQP9-null mice was deteriorated and AQP9-null mice were more resistant to malarial virulence compared to wild mice, suggesting that AQP9 serves as a glycerol channel in mouse erythrocytes. AQP9 also expresses in lung, but the significance of lung AQP9 remains uncertain.

5 Analysis of AQP7-Deficient Mice

5.1 Adipose-Derived Glycerol and Gluconeogenesis through AQP7

The authors generated and analyzed AQP7 knockout (AQP7-KO) mice (Maeda et al. 2004). AQP7-KO mice exhibit lower plasma and portal glycerol concentrations under fasting state than wild-type (WT) mice under the same condition. Administration of β 3-adrenergic agonist, which specifically effects on adipocytes and enhances lipolysis, results in impaired plasma glycerol elevation in AQP7-KO mice but does not modulate the normal increase of plasma FFA in both WT and AQP7-KO mice. Similar results are obtained in *in vitro* 3T3-L1 adipocytes introduced by RNAi. In short, adrenaline-mediated glycerol release is significantly disturbed in AQP7-knockdown 3T3-L1 adipocytes, while adrenaline-mediated FFA release from AQP7-knockdown adipocytes is similar to that of 3T3-L1 adipocytes transfected with control-RNAi. Longer starvation test demonstrated that AQP7-KO mice exhibit impaired plasma glycerol elevation associated with severe hypoglycemia in comparison with WT mice. The results of a series of studies indicate that AQP7 acts as an adipose glycerol channel *in vivo* and that adipose-derived glycerol is a significant substrate for gluconeogenesis (Fig. 4a).

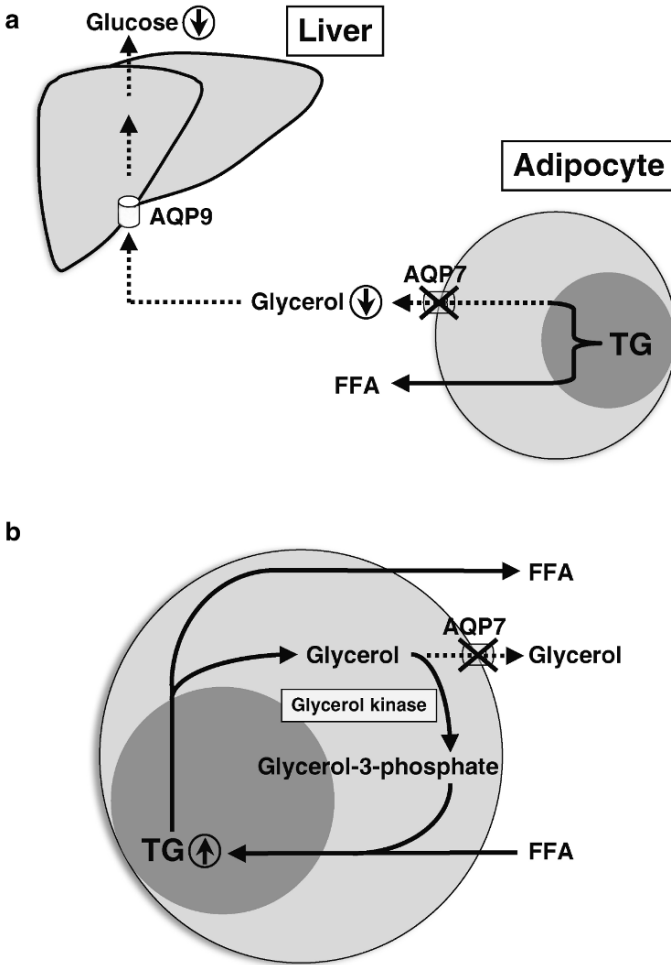


Fig. 4 Schematic presentation of the role of AQP7 based on the analysis of AQP7 knockout mice. (a) The summary of younger mice. Under starvation, AQP7 knockout (AQP7-KO) mice exhibit impairment of plasma glycerol elevation and result in severe hypoglycemia in comparison with wild-type (WT) mice. AQP7 acts as an adipose glycerol channel *in vivo* and that adipose-derived glycerol is a significant substrate for gluconeogenesis. (b) The summary of adipocyte hypertrophy in AQP7 deficiency. AQP7-KO mice develop obesity accompanied by adipocyte hypertrophy after 12 weeks of age. Knockdown of AQP7 increases the intracellular glycerol contents and induces the enzymatic activity of glycerol kinase in adipocytes. Glycerol kinase promotes re-esterification of glycerol and accelerates triglyceride (TG) accumulation in adipocytes

5.2 Adipocytes Dysfunction in AQP7-Deficient Cells

There is no difference in body weight of WT and AQP7-KO mice at young age; however AQP7-KO mice become obese beyond the age of 12 weeks (Hibuse et al. 2005). Adipose tissue of AQP7-KO mice are significantly heavier than WT mice at

20 weeks of age. Histological analysis shows an increase in hypertrophic adipocytes in epididymal WAT of AQP7-KO mice. Moreover, AQP7-KO mice exhibit whole body insulin resistance associated with obesity. Hara-Chikuma et al. (2005) also reported increased number of hypertrophic adipocytes in AQP7-KO mice, although the body weights of their AQP7-KO mice were similar to those of WT mice. The difference of phenotypes may be accounted for by the genetic background of mice.

Food intake, rectal temperature, and oxygen consumption of AQP7-KO mice are similar to WT mice at young age. At young age, there are no apparent differences in adipose mRNA levels, which are related to adipogenesis, lipogenesis, lipolysis, and thermogenesis, between AQP7-KO and WT mice. However, intracellular glycerol contents of AQP7-KO mice are significantly higher than those of WT mice at young age. A recent study reported that glycerol induces conformational changes and enzymatic activity of glycerol kinase, which is a key enzyme in the conversion of glycerol to glycerol-3-phosphate (Yeh et al. 2004). Actually, the activity of adipose glycerol kinase of AQP7-KO mice is elevated prior to development of obesity. Previous study indicated that over-expression of glycerol kinase promotes re-esterification of glycerol and accelerates TG accumulation in adipocytes (Guan et al. 2002). Knockdown of AQP7 in 3T3-L1 adipocytes increases intracellular glycerol contents, elevates glycerol kinase activities, enhances oleic acid uptake, and finally results in TG accumulation (Hibuse et al. 2005) (Fig. 4b).

In summary, deficiency of adipose AQP7 impacts on not only glycerol metabolism but also glucose metabolism in vivo.

6 Analysis of AQP9-Deficient Mice

Recently, AQP9-deficient mice were generated and analyzed (Rojek et al. 2007). AQP9^{-/-} mice exhibited a significant increase in plasma glycerol and triglyceride levels compared to AQP9^{+/-} mice. AQP9^{-/-} mice were also crossed with *Lepr^{db}/Lepr^{db}* mice those are obese and type 2 diabetes model mice. The blood glucose levels of *Lepr^{db}/Lepr^{db}* AQP9^{-/-} mice were lower than *Lepr^{db}/Lepr^{db}* AQP9^{+/-} mice under 3 h-fasting condition, indicating that AQP9 plays an important role in hepatic glycerol and glucose metabolism.

7 Role of AQP7 and AQP9 in Human

Human AQP7 gene mutation was investigated in 160 Japanese subjects (Kondo et al. 2002). In this population, three types of missense mutation were identified; R12C (a C → T substitution at nucleotide 206 in exon 3 led to substitution of arginine with cysteine at position 12, which resides in the N-terminal cytoplasmic domain); 1 subject, V59L (a G → C substitution at nucleotide 347 in exon 4 caused substitution of valine with leucine at position 59, residing in the first bilayer-spanning

domain): 13 subjects, G264V (a G → T substitution at nucleotide 963 in exon 8 led to substitution of glycine with valine at position 264, which resides in the 6th bilayer-spanning domain): six subjects. Functional analysis using *Xenopus* oocytes shows that the permeability of water and glycerol is disturbed in oocytes expressing G264V mutant protein while those expressing R12C or V59L mutant proteins retain water and glycerol permeability. G264V mutation is located in sixth bilayer-spanning domain. Structural analysis of AQP1 shows that the conserved GxxxGxxxG motif in the third and sixth bilayer-spanning domain is important for functional conformation of AQP family protein; glycine can be sometimes replaced by alanine in the motif (Murata et al. 2000; Heymann and Engel 2000). In the 6th bilayer-spanning domain of human AQP7, A260, G264, and G268 form this motif. Functional defect in the G264V mutant may be caused by disturbance of this motif. The subjects with homozygous mutation of G264V showed a similar exercise-induced rise in plasma noradrenalin compared to healthy volunteers whereas the increase in plasma glycerol was apparently disturbed during exercise (Kondo et al. 2002). This result indicates that AQP7 may be a crucial molecule for maintaining plasma glycerol levels in human. However, obesity and diabetes were not observed in subjects with homozygous mutation of G264V in Japanese population.

Recently, Ceperuelo-Mallafre et al. (2007) showed the association of AQP7 gene expression and obesity in Caucasian subjects. They demonstrated that adipose tissue AQP7 expression levels were significantly reduced and plasma glycerol concentrations were lower in severely obese women. Additionally, a subject with homozygous mutation of G264V had type 2 diabetes and was overweight (BMI = 28). Prudente et al. (2007) reported single nucleotide polymorphisms (SNPs) in AQP7 gene for the first time. They identified several SNPs in AQP7 gene, and showed that A-953G in the AQP7 promoter was associated with type 2 diabetes in 977 Caucasians. BMI was significantly higher in XG (AG + GG) than AA females. They also confirmed similar results in the independent case-control study. Interestingly, AQP7 mRNA levels were decreased according to the number of -953G alleles.

The authors could not find out reports demonstrating the association of human AQP9 gene and metabolic disorders at present. Further analysis of human AQP9 gene and/or frequency of AQP9 mutation in subjects with the metabolic syndrome should be performed.

8 Conclusions and Outlook

The discovery of AQP has significantly impacted on life sciences. Structural and functional analyses of AQPs indicate that AQPs do not only permeate water. Novel metabolic mechanisms have been clarified by the demonstration that some AQPs act as glycerol channels. Investigation of AQPs-dependent glycerol metabolism should help the design of novel therapeutic strategies for metabolic syndrome. Further studies may refine our understanding of the association between glycerol metabolism and AQPs.

References

- Agre P, King LS, Yasui M, Guggino WB, Ottersen OP, Fujiyoshi Y, Engel A, Nielsen S (2002) Aquaporin water channels – from atomic structure to clinical medicine. *J Physiol (London)* 542:3–16
- Badaut J, Regli L (2004) Distribution and possible roles of aquaporin 9 in the brain. *Neuroscience* 129:971–981
- Badaut J, Hirt L, Granziera C, Bogousslavsky J, Magistretti PJ, Regli L (2001) Astrocyte-specific expression of aquaporin-9 in mouse brain is increased after transient focal cerebral ischemia. *J Cereb Blood Flow Metab* 21:477–482
- Badaut J, Petit JM, Brunet JF, Magistretti PJ, Charriaud-Marlangue C, Regli L (2004) Distribution of Aquaporin 9 in the adult rat brain: preferential expression in catecholaminergic neurons and in glial cells. *Neuroscience* 128:27–38
- Carbrey JM, Gorelick-Feldman DA, Kozono D, Praetorius J, Nielsen S, Agre P (2003) Aquaglyceroporin AQP9: solute permeation and metabolic control of expression in liver. *Proc Natl Acad Sci U S A* 100:2945–2950
- Ceperuelo-Mallafre V, Miranda M, Chacón MR, Vilarrasa N, Megia A, Gutiérrez C, Fernández-Real JM, Gómez JM, Caubet E, Frühbeck G, Vendrell J (2007) Adipose tissue expression of the glycerol channel aquaporin-7 gene is altered in severe obesity but not in type 2 diabetes. *J Clin Endocrinol Metab* 92:3640–3645
- Crosbie RH, Dovico SA, Flanagan JD, Chamberlain JS, Ownby CL, Campbell KP (2002) Characterization of aquaporin-4 in muscle and muscular dystrophy. *FASEB J* 16:943–949
- Elkjaer M, Vajda Z, Nejsum LN, Kwon T, Jensen UB, Amiry-Moghaddam M, Frokiaer J, Nielsen S (2000) Immunolocalization of AQP9 in liver, epididymis, testis, spleen, and brain. *Biochem Biophys Res Commun* 276:1118–1128
- Executive Summary of The Third Report of The National Cholesterol Education Program (NCEP) (2001) Expert Panel on Detection, Evaluation, and Treatment of High Blood Cholesterol In Adults (Adult Treatment Panel III). *JAMA* 285:2486–2497
- Friedman JM (2004) Modern science versus the stigma of obesity. *Nat Med* 10:563–569
- Frigeri A, Nicchia GP, Verbavatz JM, Valenti G, Svelto M (1998) Expression of aquaporin-4 in fast-twitch fibers of mammalian skeletal muscle. *J Clin Invest* 102:695–703
- Frigeri A, Nicchia GP, Nico B, Quondamatteo F, Herken R, Roncali L, Svelto M (2001) Aquaporin-4 deficiency in skeletal muscle and brain of dystrophic mdx mice. *FASEB J* 15:90–98
- Frigeri A, Nicchia GP, Repetto S, Bado M, Minetti C, Svelto M (2002) Altered aquaporin-4 expression in human muscular dystrophies: a common feature?. *FASEB J* 16:1120–1122
- Fujioka S, Matsuzawa Y, Tokunaga K, Tarui S (1987) Contribution of intra-abdominal fat accumulation to the impairment of glucose and lipid metabolism in human obesity. *Metabolism* 36:54–59
- Funahashi T, Nakamura T, Shimomura I, Maeda K, Kuriyama H, Takahashi M, Arita Y, Kihara S, Matsuzawa Y (1999) Role of adipocytokines on the pathogenesis of atherosclerosis in visceral obesity. *Intern Med* 38:202–206
- Guan HP, Li Y, Jensen MV, Newgard CB, Stepan CM, Lazar MA (2002) A futile metabolic cycle activated in adipocytes by antidiabetic agents. *Nat Med* 8:1122–1128
- Hara-Chikuma M, Sohara E, Rai T, Ikawa M, Okabe M, Sasaki S, Uchida S, Verkman AS (2005) Progressive adipocyte hypertrophy in aquaporin-7-deficient mice: adipocyte glycerol permeability as a novel regulator of fat accumulation. *J Biol Chem* 280:15493–15496
- Heymann JB, Engel A (2000) Structural clues in the sequences of the aquaporins. *J Mol Biol* 295:1039–1053
- Hibuse T, Maeda N, Funahashi T, Yamamoto K, Nagasawa A, Mizunoya W, Kishida K, Inoue K, Kuriyama H, Nakamura T, Fushiki T, Kihara S, Shimomura I (2005) Aquaporin 7 deficiency is associated with development of obesity through activation of adipose glycerol kinase. *Proc Natl Acad Sci U S A* 102:10993–10998

- Hibuse T, Maeda N, Nagasawa A, Funahashi T (2006) Aquaporins and glycerol metabolism. *Biochim Biophys Acta* 1758:1004–1011
- Ibrahimi A, Sfeir Z, Magharaie H, Amri EZ, Grimaldi P, Abumrad NA (1996) Expression of the CD36 homolog (FAT) in fibroblast cells: effects on fatty acid transport. *Proc Natl Acad Sci U S A* 93:2646–2651
- Ishibashi K, Kuwahara M, Gu Y, Kageyama Y, Tohsaka A, Suzuki F, Marumo F, Sasaki S (1997) Cloning and functional expression of a new water channel abundantly expressed in the testis permeable to water, glycerol, and urea. *J Biol Chem* 272:20782–20786
- Ishibashi K, Kuwahara M, Gu Y, Tanaka Y, Marumo F, Sasaki S (1998) Cloning and functional expression of a new aquaporin (AQP9) abundantly expressed in the peripheral leukocytes permeable to water and urea, but not to glycerol. *Biochem Biophys Res Commun* 244:268–274
- Jimi T, Wakayama Y, Matsuzaki Y, Hara H, Inoue M, Shibuya S (2004) Reduced expression of aquaporin 4 in human muscles with amyotrophic lateral sclerosis and other neurogenic atrophies. *Pathol Res Pract* 200:203–209
- Kahn BB, Flier JS (2000) Obesity and insulin resistance. *J Clin Invest* 106:473–481
- Kanai H, Matsuzawa Y, Kotani K, Keno Y, Kobatake T, Nagai Y, Fujioka S, Tokunaga K, Tarui S (1990) Close correlation of intra-abdominal fat accumulation to hypertension in obese women. *Hypertension* 16:484–490
- Kishida K, Kuriyama H, Funahashi T, Shimomura I, Kihara S, Ouchi N, Nishida M, Nishizawa H, Matsuda M, Takahashi M, Hotta K, Nakamura T, Yamashita S, Tochino Y, Matsuzawa Y (2000) Aquaporin adipose, a putative glycerol channel in adipocytes. *J Biol Chem* 275:20896–20902
- Kishida K, Shimomura I, Kondo H, Kuriyama H, Makino Y, Nishizawa H, Maeda N, Matsuda M, Ouchi N, Kihara S, Kurachi Y, Funahashi T, Matsuzawa Y (2001a) Genomic structure and insulin-mediated repression of the aquaporin adipose (AQPap), adipose-specific glycerol channel. *J Biol Chem* 276:36251–36260
- Kishida K, Shimomura I, Nishizawa H, Maeda N, Kuriyama H, Kondo H, Matsuda M, Nagaretani H, Ouchi N, Hotta K, Kihara S, Kadowaki T, Funahashi T, Matsuzawa Y (2001b) Enhancement of the aquaporin adipose gene expression by a peroxisome proliferator-activated receptor gamma. *J Biol Chem* 276:48572–48579
- Kondo H, Shimomura I, Kishida K, Kuriyama H, Makino Y, Nishizawa H, Matsuda M, Maeda N, Nagaretani H, Kihara S, Kurachi Y, Nakamura T, Funahashi T, Matsuzawa Y (2002) Human aquaporin adipose (AQPap) gene. Genomic structure, promoter analysis and functional mutation. *Eur J Biochem* 269:1814–1826
- Ko SB, Uchida S, Naruse S, Kuwahara M, Ishibashi K, Marumo F, Hayakawa T, Sasaki S (1999) Cloning and functional expression of rAQP9L a new member of aquaporin family from rat liver. *Biochem Mol Biol Int* 47:309–318
- Kuriyama H, Kawamoto S, Ishida N, Ohno I, Mita S, Matsuzawa Y, Matsubara K, Okubo K (1997) Molecular cloning and expression of a novel human aquaporin from adipose tissue with glycerol permeability. *Biochem Biophys Res Commun* 241:53–58
- Kuriyama H, Yamashita S, Shimomura I, Funahashi T, Ishigami M, Aragane K, Miyaoka K, Nakamura T, Takemura K, Man Z, Toide K, Nakayama N, Fukuda Y, Lin MC, Wetterau JR, Matsuzawa Y (1998) Enhanced expression of hepatic acyl-coenzyme A synthetase and microsomal triglyceride transfer protein messenger RNAs in the obese and hypertriglyceridemic rat with visceral fat accumulation. *Hepatology* 27:557–562
- Kuriyama H, Shimomura I, Kishida K, Kondo H, Furuyama N, Nishizawa H, Maeda N, Matsuda M, Nagaretani H, Kihara S, Nakamura T, Tochino Y, Funahashi T, Matsuzawa Y (2002) Co-ordinated regulation of fat-specific and liver-specific glycerol channels, aquaporin adipose and aquaporin 9. *Diabetes* 51:2915–2921
- Kuwahara M, Fushimi K, Terada Y, Bai L, Marumo F, Sasaki S (1995) cAMP-dependent phosphorylation stimulates water permeability of aquaporin-collecting duct water channel protein expressed in *Xenopus* oocytes. *J Biol Chem* 270:10384–10387
- Liu JW, Wakayama Y, Inoue M, Shibuya S, Kojima H, Jimi T, Oniki H (1999) Immunocytochemical studies of aquaporin 4 in the skeletal muscle of mdx mouse. *J Neurol Sci* 164:24–28

- Liu Z, Shen J, Carbrey JM, Mukhopadhyay R, Agre P, Rosen BP (2002) Arsenite transport by mammalian aquaglyceroporins AQP7 and AQP9. *Proc Natl Acad Sci U S A* 99:6053–6058
- Liu Y, Promeneur D, Rojek A, Kumar N, Frøkiaer J, Nielsen S, King LS, Agre P, Carbrey JM (2007) Aquaporin 9 is the major pathway for glycerol uptake by mouse erythrocytes, with implications for malarial virulence. *Proc Natl Acad Sci U S A* 104:12560–12564
- Londos C, Brasaemle DL, Schultz CJ, Adler-Wailes DC, Levin DM, Kimmel AR, Rondinone CM (1999) On the control of lipolysis in adipocytes. *Ann N Y Acad Sci* 892:155–168
- Maeda K, Okubo K, Shimomura I, Mizuno K, Matsuzawa Y, Matsubara K (1997) Analysis of an expression profile of genes in the human adipose tissue. *Gene* 190:227–235
- Maeda N, Funahashi T, Hibuse T, Nagasawa A, Kishida K, Kuriyama H, Nakamura T, Kihara S, Shimomura I, Matsuzawa Y (2004) Adaptation to fasting by glycerol transport through aquaporin 7 in adipose tissue. *Proc Natl Acad Sci U S A* 101:17801–17806
- Mead JR, Irvine SA, Ramji DP (2002) Lipoprotein lipase: structure, function, regulation, and role in disease. *J Mol Med* 80:753–769
- Motojima K, Passilly P, Peters JM, Gonzalez FJ, Latruffe N (1998) Expression of putative fatty acid transporter genes are regulated by peroxisome proliferator-activated receptor alpha and gamma activators in a tissue- and inducer-specific manner. *J Biol Chem* 273:16710–16714
- Murata K, Mitsuoka K, Hirai T, Walz T, Agre P, Heymann JB, Engel A, Fujiyoshi Y (2000) Structural determinants of water permeation through aquaporin-1. *Nature* 407:599–605
- Nakamura T, Tokunaga K, Shimomura I, Nishida M, Yoshida S, Kotani K, Islam AH, Keno Y, Kobatake T, Nagai Y et al. (1994) Contribution of visceral fat accumulation to the development of coronary artery disease in non-obese men. *Atherosclerosis* 107:239–246
- Nicchia GP, Frigeri A, Nico B, Ribatti D, Svelto M (2001) Tissue distribution and membrane localization of aquaporin-9 water channel: evidence for sex-linked differences in liver. *J Histochem Cytochem* 49:1547–1556
- Nielsen S, Chou CL, Marples D, Christensen EI, Kishore BK, Knepper MA (1995) Vasopressin increases water permeability of kidney collecting duct by inducing translocation of aquaporin-CD water channels to plasma membrane. *Proc Natl Acad Sci U S A* 92:1013–1017
- Prudente S, Flex E, Morini E, Turchi F, Capponi D, De Cosmo S, Tassi V, Guida V, Avogaro A, Folli F, Maiani F, Frittitta L, Dallapiccola B, Trischitta V (2007) A functional variant of the adipocyte glycerol channel aquaporin 7 gene is associated with obesity and related metabolic abnormalities. *Diabetes* 56:1468–1474
- Ramsay TG (1996) Fat cells. *Endocrinol Metab Clin North Am* 25:847–870
- Rojek AM, Skowronski MT, Füchtbauer EM, Füchtbauer AC, Fenton RA, Agre P, Frøkiaer J, Nielsen S (2007) Defective glycerol metabolism in aquaporin 9 (AQP9) knockout mice. *Proc Natl Acad Sci U S A* 104:3609–3614
- Saito K, Kageyama Y, Okada Y, Kawakami S, Kihara K, Ishibashi K, Sasaki S (2004) Localization of aquaporin-7 in human testis and ejaculated sperm: possible involvement in maintenance of sperm quality. *J Urol* 172:2073–2076
- Schaffer JE, Lodish HF (1994) Expression cloning and characterization of a novel adipocyte long chain fatty acid transport protein. *Cell* 79:427–436
- Shepherd PR, Kahn BB (1999) Glucose transporters and insulin action-implications for insulin resistance and diabetes mellitus. *N Engl J Med* 341:248–257
- Sohara E, Rai T, Miyazaki JI, Verkman AS, Sasaki S, Uchida S (2005) Defective water and glycerol transport in the proximal tubules of AQP7 knockout mice. *Am J Physiol Renal Physiol* 289:F1195–F1200
- Spiegelman BM, Flier JS (2001) Obesity and the regulation of energy balance. *Cell*. 104:531–543
- Stremmel W, Strohmeyer G, Borchard F, Kochwa S, Berk PD (1985) Isolation and partial characterization of a fatty acid binding protein in rat liver plasma membranes. *Proc Natl Acad Sci U S A* 82:4–8
- Tsukaguchi H, Shayakul C, Berger UV, Mackenzie B, Devidas S, Guggino WB, van Hoek AN, Hediger MA (1998) Molecular characterization of a broad selectivity neutral solute channel. *J Biol Chem* 273:24737–24743

- Wakayama Y, Jimi T, Inoue M, Kojima H, Murahashi M, Kumagai T, Yamashita S, Hara H, Shibuya S (2002) Reduced aquaporin 4 expression in the muscle plasma membrane of patients with Duchenne muscular dystrophy. *Arch Neurol* 59:431–437
- Wakayama Y, Inoue M, Kojima H, Jimi T, Shibuya S, Hara H, Oniki H (2004) Expression and localization of aquaporin 7 in normal skeletal myofiber. *Cell Tissue Res* 316:123–129
- Yamashita S, Nakamura T, Shimomura I, Nishida M, Yoshida S, Kotani K, Kameda-Takemura K, Tokunaga K, Matsuzawa Y (1996) Insulin resistance and body fat distribution. *Diabetes Care* 19:287–291
- Yeh JI, Charrier V, Paulo J, Hou L, Darbon E, Claiborne A, Hol WG, Deutscher J (2004) Structures of enterococcal glycerol kinase in the absence and presence of glycerol: correlation of conformation to substrate binding and a mechanism of activation by phosphorylation. *Biochemistry* 43:362–373
- Zimmet P, Alberti KG, Shaw J (2001) Global and societal implications of the diabetes epidemic. *Nature* 414:782–787

New Members of Mammalian Aquaporins: AQP10–AQP12

Kenichi Ishibashi

Contents

1	Introduction	251
2	AQP10: An Aquaglyceroporin of the Gastrointestinal Tract	253
3	AQP11: A Superaquaporin for the Kidney Development	256
4	AQP12: A Superaquaporin of Pancreas	259
5	Conclusion	260
	References	260

Abstract Thirteen members of mammalian aquaporins have been identified. Initial ten members (AQP–AQP9) are relatively well detailed and their roles are clarified. However, the last three members, AQP10–AQP12, are poorly characterized and little is known about their roles though they were cloned 6 years ago. In this review, we focus on these three AQPs. AQP10 is an aquaglyceroporin while AQP11 and AQP12 belong to a new subfamily, superaquaporins. Knockout mice for these aquaporins are now available. The AQP11 null mouse has a remarkable phenotype, polycystic kidneys, which is neonatally fatal. On the other hand, the absence of the other two affected little. In some animals, AQP10 is even a pseudogene. This review summarizes the current knowledge on these AQPs and will hopefully stimulate future research on the subject.

1 Introduction

Currently, 13 aquaporins (AQPs) have been identified in mammals. Splice variants have also been found with AQP4 and AQP6 suggesting more complex nature of each AQP (Silberstein et al. 2004; Nagase et al. 2007). Furthermore, pseudogenes

K. Ishibashi

Department of Medical Physiology, Meiji Pharmaceutical University, 2-522-1 Noshio, Kiyose,
Tokyo 204-8588, Japan
kishiba@my-pharm.ac.jp

E. Beitz (ed.), *Aquaporins*, Handbook of Experimental Pharmacology 190,
© Springer-Verlag Berlin Heidelberg 2009

251

for AQP7 were identified (Kondo et al. 2002). Species-specific duplication of AQP7 was also reported (Dumas et al. 2007). Therefore, the scope of AQPs in mammals may be much wider than the current 13 members. Genome-wide searches for additional AQPs and splice-variants of current AQPs will be warranted, now that several genome projects have been completed.

The initial ten members of mammalian AQPs- AQP0-AQP9 -are relatively well characterized and their roles are clear with the identification of human diseases and the development of gene-disrupted mice. We were lucky to identify continuous members of aquaporins from AQP7 to AQP12 (Ishibashi et al. 1997a, b, 1998, 2000, 2002). Many investigators have examined their expressions, regulations and physiological functions. However, three most recently identified members, AQP10–AQP12, have failed to attract much research attention. Though they were identified by 2001 (Ishibashi et al. 2000; Hatakeyama et al. 2001), few papers have been published on them. This may be because their functions have not been clearly shown. They seem to be localized inside the cell. Their localizations, however, are controversial due to poor qualities of antibodies. No human diseases related to these AQPs have yet been identified.

In this review, we focus on the last three AQPs- AQP10–AQP12. AQP10 is a member of the aquaglycoporin subfamily and transports water and glycerol similar to other aquaglycoporins. On the other hand, AQP11 and AQP12 are members of a new subfamily. AQP11 and AQP12 were originally named AQPX1 and AQPX2 because their sequences were so deviated from conventional AQPs that it was difficult to include them in the AQP family (Ishibashi et al. 2000). As these were discovered before AQP10, they could have been named AQP10 and AQP11. But this was not done because it was expected that the number of AQPX members would increase. However, no further AQPX members were found in mammals. Since AQPX members were limited, we decided to rename them following the discovery of AQP10. This was the case with glucose facilitators (SLC2) which was originally named GlutX1 but later changed to Glut8.

As sequence data accumulated primarily through genome projects, a new subfamily with low homologies to other AQPs has emerged (Fig. 1; Ishibashi 2006a, b; Nozaki et al. 2007). The outstanding feature of conventional AQPs is the tandem repeats of highly conserved pore-forming amino acid residues named NPA boxes, signature sequences for AQPs. The NPA boxes of the new subfamily, however, are highly deviated with overall homology less than 20%, which indicates that they belong to a superfamily of AQPs. Based on the primary structure, we named it ‘superaquaporin subfamily’, in which ‘super’ represents ‘superfamily’ (Morishita et al. 2004). Although they are grouped in a single subfamily, there are small homologies among superaquaporins. Further, little is known about their functions, though some work as a water channel (Ishikawa et al. 2005). Each may have a unique function. Superaquaporins, therefore, will be further subclassified in the near future. Interestingly, no superaquaporins have yet been identified in unicellular organisms: bacteria and protozoa.

Knockout mice for these three aquaporins are now available and one of them has a remarkable phenotype. AQP11 null mice die from a polycystic kidney disease

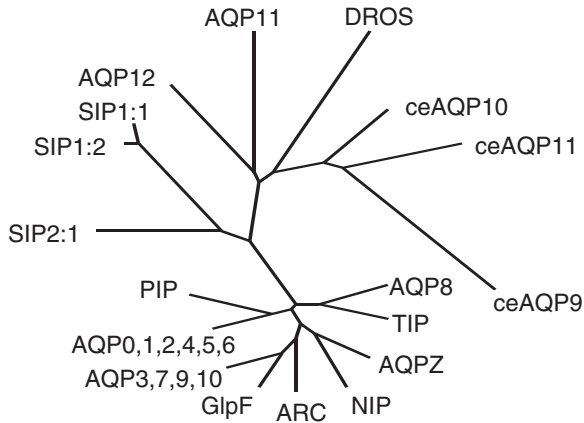


Fig. 1 Phylogenetic tree of aquaporin family. The phylogenetic tree was constructed by neighbor-joining methods as earlier (Ishibashi et al. 1994). AQP Z and GlpF are AQPs from *E. coli*, a bacteria. ARC is an aquaporin from *Archaeoglobus fulgidus*, an archae. SIP, TIP, NIP and PIP are AQPs from *Arabidopsis*, a plant. DROS is a superaquaporin of *Drosophila*, an insect. ceAQP9 ~ 11 are superaquaporins of *C. elegans*, a nematode. AQP0 ~ 12 are AQPs from humans

within 2 months. Their importance in health and disease has not yet been well appreciated. We hope this review will stimulate the research on these three AQPs and expand the scope of AQP research.

2 AQP10: An Aquaglyceroporin of the Gastrointestinal Tract

AQP10 was reported by two groups (Hatakeyama et al. 2001; Ishibashi et al. 2002). The first report by Hatakeyama et al., however, was complicated by a partially-spliced form of human AQP10 with poor function. This unspliced form of AQP10 has no sixth transmembrane domain after the second NPA box and a different carboxy terminal. The loss of a transmembrane will seriously affect the 3-D structure formation. Furthermore, the changed carboxy terminal will affect function and trafficking as the carboxy termini of AQPs are hydrophilic and present at the cytosol. Accordingly, the unspliced form may not function well. In fact they reported a limited stimulation of water permeability by 2.7-folds, which were stimulated by alkali pH. Independently, we cloned a fully-spliced form of human AQP10 with aquaglyceroporin function (Ishibashi et al. 2002). The oocytes expressing this authentic AQP10 revealed the stimulation of mercury-sensitive water permeability (by sixfolds) and glycerol permeability (by threefolds). Unlike AQP9, another aquaglyceroporin, AQP10 did not stimulate adenine permeability. Therefore, the pore of AQP10 seems to be smaller, similar to AQP3. AQP10 was expressed selectively in the duodenum and jejunum and not in other segments of the gastrointestinal tract or other human organs (Hatakeyama et al. 2001). We also reported similar results. We further examined the expression of the unspliced form by RNA protection assay

which is more sensitive than Northern blot. We failed to identify the expression of the unspliced AQP10 mRNA in a commercially available human small intestine (Ishibashi et al. 2002). However, another RNA protection assay revealed the expression of both forms of human AQP10 mRNA in the duodenum and jejunum (Li et al. 2007). The reason for this discrepancy is not clear but may be related to physiological states of the intestine. The presence of the unspliced form is intriguing. As this has not been reported in other AQPs. It may prolong the stability of the authentic AQP10 mRNA by serving as a decoy for RNA degradation. In this case, the unspliced form will enhance the function of AQP10. Alternatively, if the unspliced form is translated, the protein may modulate the function of AQP10 protein by forming heterotetramers.

In situ hybridization revealed AQP10 mRNA is expressed at the mucosa of the duodenum (Hatakeyama et al. 2001). The results of immunohistochemical studies, however, are controversial. One study using a commercially available antibody against specific amino acids for the unspliced AQP10 showed that the unspliced AQP10 is expressed at the apical membrane of epithelial cells in the small intestine (Mobasher et al. 2004). Another study using a similar antibody, however, showed that the unspliced AQP10 is expressed at endothelial cells of submucosal capillaries in the duodenum (Li et al. 2005). There is only one report on the localization of the authentic AQP10 using an antibody against specific amino acids for the fully-spliced AQP10. The result showed the authentic AQP10 was localized at the granular vesicles of enterochromaffin cells in the duodenum (Li et al. 2005). Since the unspliced and authentic forms of AQP10 are not expressed at the same cells, the above speculation of the heterotetramer formation will not be valid.

Although AQP10 may function as an aquaglyceroporin, its role in enterochromaffin cells is not clear. Enterochromaffin cells secrete hormones to the basal side, which are important for gastrointestinal function. AQP10 may function as a channel for intracellular vesicles, transporting water and unknown small substrates to the granular vesicles. Interestingly, in cholera patients, AQP10 mRNA was reported to be downregulated (Flach et al. 2007). Since serotonin is secreted in cholera, AQP10 may play some role in enterochromaffin cells to modulate its secretion. However, a direct stimulation by cholera toxin in CaCo-2 cells (cultured intestinal epithelial cells) did not change AQP10 mRNA expression (Flach et al. 2007).

AQP10 is not the first AQP to be found expressed at the secretory vesicular granules. Previous reports indicated that some AQPs are expressed at intracellular secretory granules. AQP1 has been shown to be expressed at pancreatic secretory granules (zymogen granules) and AQP6 at synaptic vesicles (Cho et al. 2002; Jeremic et al. 2005). Another report indicated the AQP5 expression at the granules of Brunner glands in the duodenum (Parvin et al. 2005). However, these studies are not confirmed by others probably due to different characters of antibodies. A previous report, for example, failed to detect AQP1 in pancreatic acinar cells (Hurley et al. 2001). These studies are mainly morphological and await further mechanistic studies.

The primary sequence of AQP10 indicates that it belongs to the aquaglyceroporin subfamily which has four members in mammals, AQP3, AQP7, AQP9 and AQP10.

Phylogenetic tree analysis revealed that AQP10 is closer to AQP7 (Zardoya 2005). Functionally, however, AQP10 is much closer to AQP3 as both AQP3 and AQP10 failed to transport arsenite (As(III)) while AQP7 and AQP9 did so (Liu et al. 2004). AQP3 has been shown to be expressed at the basolateral membrane of intestinal epithelial cells (Mobasher et al. 2004). As AQP3 and AQP10 appear to be localized at different cells, AQP3 will not compensate for the loss of AQP10.

Surprisingly, AQP10 was not expressed in the mouse jejunum even in dehydrated states as revealed by Northern blot (Morinaga et al. 2002). We searched a mouse genome for AQP10 and found that the mouse AQP10 gene had inserts and deletions preventing a proper transcription and translation (Morinaga et al. 2002). As a genomic Southern blot revealed, that mouse AQP10 was a single copy gene, we concluded that mouse AQP10 is a pseudogene without any authentic clones. Pseudogenes are usually produced by gene duplications where the duplicated gene turns to a pseudogene so that the authentic gene is available to preserve the original function. A pseudogene will modulate the mRNA stability of the authentic gene if it is transcribed. In the case of human AQP7, for example, there are three pseudogenes besides the authentic AQP7 (Kondo et al. 2002). Therefore, the absence of authentic AQP10 in the mouse genome suggests that AQP10 is not essential for mice, specifically for the enterochromaffin cell function, although it is possible that another AQP compensates for the loss of AQP10 in mice.

Like mice other animals could also have lost functional AQP10. We have extensively searched for the presence of AQP10 in mammalian genomes and Northern blot using human AQP10 as a probe. Rabbits, dogs, Macaca monkeys, chimpanzees, pigs, guinea pigs and horses have an authentic AQP10 in their genomes or clear bands in Northern blot. Even rats have an authentic AQP10 in their genome although its expression was not confirmed by Northern blot in multiple tissues (Ishibashi, unpublished observation). On the other hand, cow's AQP10 seems to be a pseudogene with inserts and deletions in the open reading frame and no AQP10 mRNA detected (Ishibashi, unpublished observation). Therefore, mice and cows are natural AQP10 null animals. The rat AQP10 may also be a pseudogene with possible mutations at the promoter sequence failing to be transcribed. They are not phylogenetically related and there seems to be no common characteristics for food preferences and gastrointestinal functions. As the phenotypes of most aquaporin null mice are generally mild, it is not surprising that some AQPs have lost their roles through the evolution and turn to pseudogenes. Even some humans may have defective mutations in their AQP10 in apparently healthy conditions. Human AQP10 is located at chromosome 1q21.3 with six exons. Since an AQP7 null human was accidentally found in a random search (Kondo et al. 2002), SNP analysis for AQP10 may identify AQP10 null humans.

Though we could not find AQP10 expression in any tissues other than the small intestine, some reported much wider distribution of AQP10 in humans. AQP10 was expressed at fetal teeth, masseter muscles and gums as revealed by RT-PCR (Wang et al. 2003). Their physiological significance is not clear. Obviously, the results need to be confirmed by protein detection. Interestingly, some animals have wider distribution of AQP10. In dog, AQP10 was also expressed in the colon (Fig. 2: Ishibashi,

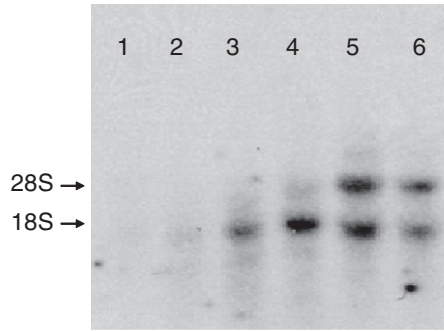


Fig. 2 Northern blot analysis of dog GI tracts for AQP10 expression. The full length of human AQP10 cDNA was used as a probe (Ishibashi et al. 2002). The 20 μ g of total RNA from a dog was loaded in each lane. **1** stomach, **2** duodenum, **3** jejunum, **4** ileum, **5** cecum, **6** colon. Ribosomal bands are indicated on the left side

unpublished observation). It will be necessary to examine further tissue distributions and species differences of AQP10 as well as regulation of its expression by various physiological and pathological conditions. Current array techniques could accidentally identify the expressions and modifications of AQP10 to reveal its unexpected roles (Flach et al. 2007).

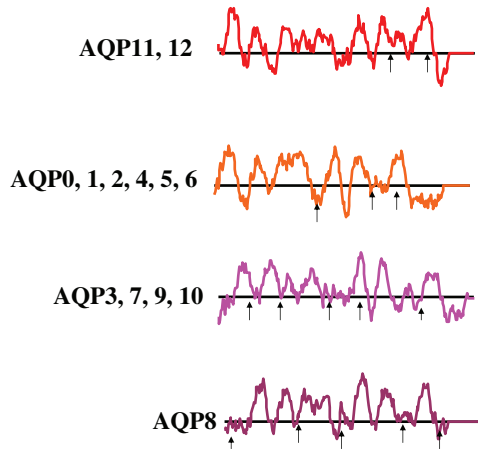
3 AQP11: A Superaquaporin for the Kidney Development

Contrary to most other AQPs, importance of AQP11 was clearly shown by the phenotype of AQP11 null mice (*vide infra*). However, the phenotype may not be easily explained by water channel activity and gene targeting may induce unexpected complications. We are now confident that the phenotype produced by AQP11 defect by targeted disruption is real for the following reasons. The gene targeting was performed in two separate ES cell lines and ENU-induced point mutation of AQP11 also produced similar phenotype (Tchekneva et al. 2006). Further, a similar phenotype was also observed in Zebrafish by AQP11 knockout and rescued by human AQP11 (Morricall et al. 2006).

Human AQP11 is localized at chromosome 11q13.5, where there are only three exons for AQP11. AQP11 and AQP12 have the simplest gene structure among human AQPs. Other AQP genes have four or six exons (Fig. 3). Such distinct genome structures of AQP11 and AQP12 support the claim that together they belong to a unique subfamily of AQPs.

Northern blot analyses showed that the AQP11 expression was highest in the testis, and moderate in the kidney and liver (Ishibashi et al. 2000; Morishita et al. 2005; Gorelick et al. 2006). Low amounts of AQP11 expression are observed in virtually every tissue when examined by RT-PCR, which may be due to its expression in vascular smooth muscles and leukocytes (Ishibashi, unpublished observation).

Fig. 3 The exon–intron boundaries of subfamilies of human AQPs. The exon–intron boundaries are indicated by arrows in hydrophathy-profiles. They are divided into four groups



Immunohistochemical studies revealed that AQP11 was expressed in kidney proximal tubules. Interestingly, it was expressed inside the cell most likely at the endoplasmic reticulum (ER) (Morishita et al. 2005). Intracellular localization was also reported in neurons (Gorelick et al. 2006). However, they failed to detect AQP11 expression in the kidney attributable to the possible maskings at amino- and carboxy-ends of AQP11 in the kidney, but not in the neuron. Histological confirmations of AQP11 expression await further studies.

Functional studies of AQP11 are also controversial. Using a *Xenopus* oocyte expression system one study showed the absence of water channel activity (Gorelick et al. 2006). AQP11 expression at the plasma membrane was confirmed in that study. In contrast, AQP11 reconstituted into liposomes was reported to have efficient water channel activity comparable to AQP1 (Yakata et al. 2007). Currently, the reason for this discrepancy is unclear. It will be more direct and physiological to measure osmotic water permeabilities of AQP11-expressing intracellular organelles in situ. Such studies will be technically demanding but necessary to explore the roles of AQP11 inside the cell. In fact, in cultured cells, AQP11 was expressed inside the cell (Gorelick et al. 2006)- most likely at the ER (Morishita et al. 2005).

In contrast to the absence of significant abnormalities due to the disruption of most AQPs, AQP11 knockout mice were fatal with polycystic kidneys (Morishita et al. 2005). Although AQP11 is expressed widely as stated above, only the kidney was affected by AQP11 disruption. AQP11 null mice were born normally but grew poorly. They died progressively with renal failure within 10 days after birth to 2 months. The renal cysts originated from the proximal tubule where AQP11 is specifically expressed. Interestingly, proximal tubular cells were swollen at 1 week after birth before the cyst formation. Electron microscopy revealed that the vacuoles continued to the nuclear membrane with attached ribosomes. The result indicated that the vacuoles originated from the ER. The brush border membrane and the mitochondria appeared normal, suggesting minimum cell damages. Similar vacuoles were also observed in other organs outside the kidney: hepatocytes around the portal

area and intestinal epithelial cells at the tip of villi. These cells also absorb water and solute abundantly like proximal tubular cells. However, they did not develop cysts or other abnormalities.

If AQP11 is a water channel, it may have some role in intracellular water transport, which will explain the limited abnormalities of AQP11 null mice in water transporting cells. Kidney proximal tubules absorb a huge amount of water. Transtubular water absorption is divided into two pathways: transcellular and paracellular. The transcellular pathway is conducted by AQP1 expressed at both the brush border and basolateral membranes, while the paracellular pathway is conducted by the tight junction between cells. In AQP1 null mice, the amount of water transport in the proximal tubule is reduced to one-tenth suggesting that 90% of transtubular transport is transcellular and 10% paracellular (Schnermann et al. 1998). We thus produced AQP1 and AQP11 double KO mice to examine the effect of restricting water influx into proximal tubular cells. Such reduction of water entry may ameliorate the damage produced by water entry at the proximal tubule of AQP11 null mice. However, vacuoles developed similarly with eventual polycysts even in double KO mice with limited water entry into proximal tubular cells (Fig. 4: Ishibashi, unpublished observation). Therefore, a massive water entry does not seem to be essential for vacuole development in AQP11 null mice.

Similar vacuoles are also observed in osmotic nephropathy. Hypertonic sucrose injection produces vacuoles mostly in the proximal tubule which was initially ascribed to the osmotic damage to the kidney. However, it is currently believed that accumulated non-metabolizable sucrose in the endosomes attracts water to produce vacuoles. Hence the proximal tubule is not severely damaged and the disease is reversible with cessation of sucrose (Schwartz et al. 1971). Similarly, the cause for vacuole development in AQP11 null mice, could be accumulated putative substances inside the ER, whose transport will be regulated by AQP11. The identification of such substances in vacuoles could help in the understanding of the function

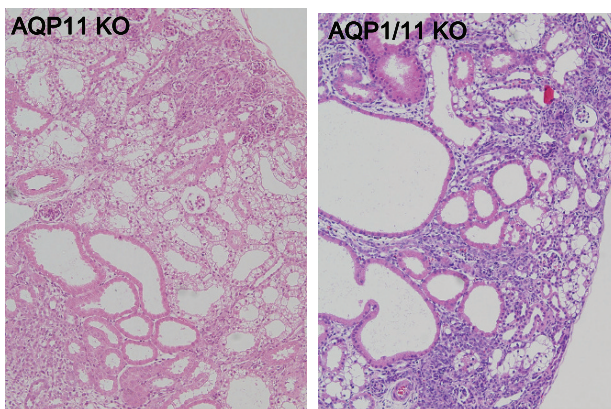


Fig. 4 Histological comparison of the kidneys between AQP11 KO mice (*left*) and AQP1/11 double KO mice (*right*) at 15 days after birth. Both have vacuolated tubular epithelial cells in the cortex

of AQP11. However, no substances have been found so far to be higher in the kidney of AQP11 null mice than the control (Ishibashi, unpublished observation).

Vacuoles in AQP11 null mice may indicate a nonspecific response to cell damages. Cyclosporin nephropathy has typical vacuoles in the proximal tubule due to cell damage by the drug. Another kidney model for vacuole formation is tunicamycin toxicity. Normal ER function is required for correct foldings and post-translational modifications of proteins, such as glycosylation and disulfide bond formation. ER stress is induced by disturbance of ER environment. Tunicamycin suppresses glycosylation leading to protein misfoldings. The eventual accumulated misfolded/unfolded proteins in the ER will induce ER stress responses. Such stressed cells appear like AQP11 null cells with vacuoles (Zinszner et al. 1998). Tunicamycin also induces ER stress-mediated apoptosis in renal proximal tubules in mice (Zinszner et al. 1998). If AQP11 is important for ER homeostasis, its disruption may lead to ER stress. Obviously, more studies are required to clarify the mechanism for vacuole formation and the eventual cyst development in AQP11 null mice.

4 AQP12: A Superaquaporin of Pancreas

AQP12 was seen to be using AQP11 as a query sequence by BLAST search (Ishibashi et al. 2000). AQP12 also belongs to supraaquaporin subfamily. It has the highest identity with AQP11 at 32% but low identities with other AQPs at less than 15%. With such a low homology, it is difficult to simulate three dimensional structures using AQP1 or GlpF as a guide. Although possible pore-forming NPA box-like sequences are present in tandem, it is difficult to assign amino acid residues to specific functions such as water and/or glycerol transports using molecular dynamics simulations. So far no functional studies on AQP12 have been reported. Our attempts to express AQP12 in *Xenopus* oocytes were unsuccessful due to failure to reach the plasma membrane. This result and expression studies in cultured cells (COS-7 and HEK293 cells) suggest that AQP12 is also localized inside the cell (Itoh et al. 2005). Poor quality of our AQP12 polyclonal antibodies precluded the subcellular localization studies of AQP12.

AQP12 is selectively expressed in the pancreas, specifically, at acinar cells, which was confirmed by RT-PCR of microdissected pancreas and *in situ* hybridization (Itoh et al. 2005). AQP12 was not expressed at the islet of Langerhans. Since pancreatic acinar cells express AQP1 and AQP8, a redundant expression of AQP12 in these cells is intriguing (Hurley et al. 2001; Cho et al. 2002). In fact, a preliminary study of AQP12 null mice indicated very limited abnormalities (Rai et al. 2005). Other AQPs may compensate for the defect of AQP12 as AQP1 or AQP8 null mice also showed no abnormalities in the pancreatic function. Further studies on double or even triple knockout mice for these AQPs will be necessary to reveal the roles of these AQPs in the pancreas. The AQP12 gene expression will also be regulated by physiological and pathological conditions, which will shed lights on their roles in the pancreatic function. These have not been examined yet.

The human genome analysis revealed that AQP12 is located at chromosome 2q37.2, where two AQP12 genes are present in the opposite directions. Accordingly, the authentic one is named AQP12A (NM_198998; [http://www.ncbi.nlm.nih.gov/mapview/maps.cgi?TAXID=9606&CHR=2&MAPS=ugHs,genes,rnaHs\[241259642.00%3A241275862.00\]-r&QSTR=aquaporin%2012b&QUERY=uid\(736940\)&CMD=DN](http://www.ncbi.nlm.nih.gov/mapview/maps.cgi?TAXID=9606&CHR=2&MAPS=ugHs,genes,rnaHs[241259642.00%3A241275862.00]-r&QSTR=aquaporin%2012b&QUERY=uid(736940)&CMD=DN)) and the other one is named AQP12B (BC041460; [http://www.ncbi.nlm.nih.gov/mapview/maps.cgi?TAXID=9606&CHR=2&MAPS=ugHs,genes,rnaHs\[241271807.00%3A241288027.00\]-r&QSTR=aquaporin%2012b&QUERY=uid\(736940\)&CMD=UP](http://www.ncbi.nlm.nih.gov/mapview/maps.cgi?TAXID=9606&CHR=2&MAPS=ugHs,genes,rnaHs[241271807.00%3A241288027.00]-r&QSTR=aquaporin%2012b&QUERY=uid(736940)&CMD=UP)). AQP12B is a partial gene and may be a pseudogene. Since AQP12B gene is highly homologous to AQP12A, it may modulate the stability of AQP12A mRNA or even the function of AQP12 if it is properly translated. Such local gene duplication is absent in the mouse genome. AQP12 gene is also composed of three exons. SNP (single nucleotide polymorphism) analysis will be complicated by this duplication.

Interestingly, the carboxy-termini of AQP12 are highly divergent among species. Although most AQPs are highly homologous in amino acid sequences among species, some AQPs have species-specific carboxy-termini such as AQP6, AQP7, and AQP12. Unidentified splice variants may explain some of these differences. Alternatively, local gene duplications may have occurred in some species and the homologous gene has been lost. Human AQP7 and AQP12 are also unique in AQPs for the presence of local gene duplications (Dumas et al. 2007).

5 Conclusion

Though more than 6 years have passed since the discovery of the latest AQPs, AQP10–AQP12, little progress has been made regarding clarification of their functions, regulations, and roles in normal and pathological conditions. Current on-going genome projects of various species and array techniques will be helpful to advance our knowledge on these AQPs. Still we need tedious old-fashioned style research to examine their localizations and functions. We hope this review has elucidated greater information on these AQPs, to stimulate research on these AQPs, especially, supraaquaporins which are widely distributed in multicellular organisms. In fact no reviews on AQPs will be complete without mentioning superaquaporins. Their clarification will exert important influences on our understandings of water and small solute metabolisms, where more surprises will be expected.

References

- Cho SJ, Sattar AK, Jeong EH, Satchi M, Cho JA, Dash S, Mayes MS, Stromer MH, Jena BP (2002) Aquaporin 1 regulates GTP-induced rapid gating of water in secretory vesicles. *Proc Natl Acad Sci U S A* 99:4720–4724

- Dumas L, Kim YH, Karimpour-Fard A, Cox M, Hopkins J, Pollack JR, Sikela JM (2007) Gene copy number variation spanning 60 million years of human and primate evolution. *Genome Res* 17:1266–1277
- Flach CF, Qadri F, Bhuiyan TR, Alam NH, Jennische E, Holmgren J, Lönnroth I (2007) Differential expression of intestinal membrane transporters in cholera patients. *FEBS Lett* 581:3183–3188
- Gorelick DA, Praetorius J, Tsunenari T, Nielsen S, Agre P (2006) Aquaporin-11: a channel protein lacking apparent transport function expressed in brain. *BMC Biochem* 7:1–14
- Hatakeyama S, Yoshida Y, Tani T, Koyama Y, Nihei K, Ohshiro K, Kamiie JI, Yaoita E, Suda T, Hatakeyama K, Yamamoto T (2001) Cloning of a new aquaporin (AQP10) abundantly expressed in duodenum and jejunum. *Biochem Biophys Res Commun* 287:814–819
- Hurley PT, Ferguson CJ, Kwon TH, Andersen ML, Norman AG, Steward MC, Nielsen S, Case RM (2001) Expression and immunolocalization of aquaporin water channels in rat exocrine pancreas. *Am J Physiol Gastrointest Liver Physiol* 280:G701–G709
- Ishibashi K (2006a) Aquaporin subfamily with unusual NPA boxes. *Biochim Biophys Acta* 1758:989–993
- Ishibashi K (2006b) Aquaporin superfamily with unusual npa boxes: S-aquaporins (superfamily, sip-like and subcellular-aquaporins). *Cell Mol Biol (Noisy-le-grand)* 52(7):20–27
- Ishibashi K, Sasaki S, Fushimi K, Uchida S, Kuwahara M, Saito H, Furukawa T, Nakajima K, Yamaguchi Y, Gojobori T, Marumo F (1994) Molecular cloning and expression of a member of the aquaporin family with permeability to glycerol and urea in addition to water expressed at the basolateral membrane of kidney collecting duct cells. *Proc Natl Acad Sci U S A* 91:6269–6273
- Ishibashi K, Kuwahara M, Gu Y, Kageyama Y, Tohsaka A, Suzuki F, Marumo F, Sasaki S (1997a) Cloning and functional expression of a new water channel abundantly expressed in the testis permeable to water, glycerol, and urea. *J Biol Chem* 272:20782–20786
- Ishibashi K, Kuwahara M, Kageyama Y, Tohsaka A, Marumo F, Sasaki S (1997b) Cloning and functional expression of a second new aquaporin abundantly expressed in testis. *Biochem Biophys Res Commun* 237:714–718
- Ishibashi K, Kuwahara M, Gu Y, Tanaka Y, Marumo F, Sasaki S (1998) Cloning and functional expression of a new aquaporin (AQP9) abundantly expressed in the peripheral leukocytes permeable to water and urea, but not to glycerol. *Biochem Biophys Res Commun* 244:268–274
- Ishibashi K, Kuwahara M, Kageyama Y, Sasaki S, Suzuki M, Imai M (2000) Molecular cloning of a new aquaporin superfamily in mammals: AQPX1 and AQPX2. Hohmann S, Nielsen S (eds.) *Molecular biology and physiology of water and solute transport*. Kluwer Academic/Plenum Publishers, New York, pp. 123–126
- Ishibashi K, Morinaga T, Kuwahara M, Sasaki S, Imai M (2002) Cloning and identification of a new member of water channel (AQP10) as an aquaglyceroporin. *Biochim Biophys Acta* 1576:335–340
- Ishikawa F, Suga S, Uemura T, Sato MH, Maeshima M (2005) Novel type aquaporin SIPs are mainly localized to the ER membrane and show cell-specific expression in *Arabidopsis thaliana*. *FEBS Lett* 579:5814–5820
- Itoh T, Rai T, Kawahara M, Ko SBH, Uchida S, Sasaki S, Ishibashi K (2005) Identification of a novel aquaporin, AQP12, expressed in pancreatic acinar cells. *Biochem Biophys Res Commun* 330:832–838
- Jeremic A, Cho WJ, Jena BP (2005) Involvement of water channels in synaptic vesicle swelling. *Exp Biol Med (Maywood)* 230:674–680
- Kondo H, Shimomura I, Kishida K, Kuriyama H, Makino Y, Nishizawa H, Matsuda M, Maeda N, Nagaretani H, Kihara S, Kurachi Y, Nakamura T, Funahashi T, Matsuzawa Y (2002) Human aquaporin adipose (AQPap) gene. Genomic structure, promoter analysis and functional mutation. *Eur J Biochem* 269:1814–1826
- Li H, Kamiie J, Morishita Y, Yoshida Y, Yaoita E, Ishibashi K, Yamamoto T (2005) Expression and localization of two isoforms of AQP10 in human small intestine. *Biol Cell* 97:823–829
- Liu Z, Carbrey JM, Agre P, Rosen BP (2004) Arsenic trioxide uptake by human and rat aquaglyceroporins. *Biochem Biophys Res Commun* 316:1178–1185

- Mobasher A, Shakibaei M, Marples D (2004) Immunohistochemical localization of aquaporin 10 in the apical membranes of the human ileum: a potential pathway for luminal water and small solute absorption. *Histochem Cell Biol* 121:463–471
- Morrill SO, Kane ME, DeChant BT, Ishibashi K, Obara T (2006) Aquaporin-11 (AQP11) knock-out revealed conserved function in fish and mammals. Abstract, Renal Week 2006
- Morinaga T, Nakakoshi M, Hirao A, Imai M, Ishibashi K (2002) Mouse aquaporin 10 gene (AQP10) is a pseudogene. *Biochem Biophys Res Commun* 294:630–634
- Morishita Y, Sakube Y, Sasaki S, Ishibashi K (2004) Molecular mechanisms and drug development in aquaporin water channel diseases: aquaporin superfamily (superaquaporins): expansion of aquaporins restricted to multicellular organisms. *J Pharmacol Sci* 96:276–279
- Morishita Y, Matsuzaki T, Hara-chikuma M, Andoo A, Shimono M, Matsuki A, Kobayashi K, Ikeda M, Yamamoto T, Verkman A, Kusano E, Ookawara S, Takata K, Sasaki S, Ishibashi K (2005) Disruption of aquaporin-11 produces polycystic kidneys following vacuolization of the proximal tubule. *Mol Cell Biol* 25:7770–7779
- Nagase H, Agren J, Saito A, Liu K, Agre P, Hazama A, Yasui M (2007) Molecular cloning and characterization of mouse aquaporin 6. *Biochem Biophys Res Commun* 352:12–16
- Nozaki K, Ishii D, Ishibashi K (2007) Intracellular aquaporins: clues for intracellular water transport? *Pflugers Arch* 456:701–707
- Parvin MN, Kurabuchi S, Murdiastuti K, Yao C, Kosugi-Tanaka C, Akamatsu T, Kanamori N, Hosoi K (2005) Subcellular redistribution of AQP5 by vasoactive intestinal polypeptide in the Brunner's gland of the rat duodenum. *Am J Physiol Gastrointest Liver Physiol* 288:G1283–G1291
- Rai T, Suda S, Itoh T, Sasaki S, Uchida S (2005) Generation and analysis of transgenic mice lacking aquaporin-12. In Abstract, Renal Week 2005
- Schnermann J, Chou CL, Ma T, Traynor T, Knepper MA, Verkman AS (1998) Defective proximal tubular fluid reabsorption in transgenic aquaporin-1 null mice. *Proc Natl Acad Sci U S A* 95:9660–9666
- Schwartz SL, Johnson CB (1971) Pinocytosis as the cause of sucrose nephrosis. *Nephron* 8:246–254
- Silberstein C, Bouley R, Huang Y, Fang P, Pastor-Soler N, Brown D, Van Hoek AN (2004) Membrane organization and function of M1 and M23 isoforms of aquaporin-4 in epithelial cells. *Am J Physiol Renal Physiol* 287:F501–F511
- Tchekneva EE, Rinchik EM, Dikov MM, Godfrey V, Klebig M, Kadkina V, Mohamed Y, Ishibashi K, Breyer MD (2006) Genetic complementation of sudden juvenile death syndrome (slds), a recessive ENU-induced mutation on ch7 is revealed by the compound heterozygous AQP11-/slds genotype. Abstract, Renal Week 2006
- Wang W, Hart PS, Piesco NP, Lu X, Gorry MC, Hart TC (2003) Aquaporin expression in developing human teeth and selected orofacial tissues. *Calcif Tissue Int* 72:222–227
- Yakata K, Hiroaki Y, Ishibashi K, Sohara E, Sasaki S, Mitsuoka K, Fujiyoshi Y (2007) Aquaporin-11 containing a divergent NPA motif has normal water channel activity. *Biochim Biophys Acta* 1768:688–693
- Zardoya R (2005) Phylogeny and evolution of the major intrinsic protein family. *Biol Cell* 97:397–414
- Zinszner H, Kuroda M, Wang XZ, Batchvarova N, Lightfoot RT, Remotti H, Stevens JL, Ron D (1998) CHOP is implicated in programmed cell death in response to impaired function of the endoplasmic reticulum. *Gene Dev* 12:982–995

Part IV
**Aquaporin Functions Apart from Water
and Glycerol Transport**

Structural Function of MIP/Aquaporin 0 in the Eye Lens; Genetic Defects Lead to Congenital Inherited Cataracts

Ana B. Chepelinsky

Contents

1	Introduction	266
1.1	How Major Intrinsic Protein of the Lens MIP became Aquaporin 0	266
2	Ocular Lens Structure and Development	268
2.1	Differentiation of Lens Epithelia into Lens Fibers	268
2.2	Primary Fibers and Secondary Fibers	269
2.3	Lens Sutures Formation	270
2.4	Differential Gene Expression during Lens Epithelia Differentiation into Fibers	270
2.5	Cataractogenesis	272
3	MIP/AQP0 Gene Expression in Lens Fibers	272
3.1	MIP/AQP0 Gene Expression During Lens Differentiation	272
3.2	MIP/AQP0 Post-translational Modifications	272
4	Multiple Functions of MIP/AQP0	273
4.1	MIP/AQP0 Functions as a Water Channel in the Lens Fibers	273
4.2	MIP/AQP0 Functions as an Interfiber Adhesion Molecule	279
4.3	MIP/AQP0 Intracellular Interaction with Lens Fiber Proteins	280
5	MIP/AQP0 Molecular Genetics	282
5.1	Mutations in the MIP/AQP0 Gene Result in Genetic Cataracts	282
5.2	Deficiency in MIP/AQP0 Gene Expression affects Lens Focusing	285
6	Summary and Conclusions	287
	References	287

Abstract Aquaporin 0 (AQP0) was originally characterized as a membrane intrinsic protein, specifically expressed in the lens fibers of the ocular lens and designated MIP, for major intrinsic protein of the lens. Once the gene was cloned, an internal repeat was identified, encoding for the amino acids Asp-Pro-Ala, the NPA repeat. Shortly, the MIP gene family was emerging, with members being characterized in mammals, insects, and plants. Once Peter Agre's laboratory developed a functional assay for water channels, the MIP family became the aquaporin family and MIP

A.B. Chepelinsky
National Institutes of Health, National Eye Institute, Bldg. 31, Room 6A-32, Bethesda,
MD 20892-2510, USA
abc@helix.nih.gov

became known as aquaporin 0. Besides functioning as a water channel, aquaporin 0 also plays a structural role, being required for maintaining the transparency and optical accommodation of the ocular lens. Mutations in the AQP0 gene in human and mice result in genetic cataracts; deletion of the MIP/AQP0 gene in mice results in lack of suture formation required for maintenance of the lens fiber architecture, resulting in perturbed accommodation and focus properties of the ocular lens. Crystallography studies support the notion of the double function of aquaporin 0 as a water channel (open configuration) or adhesion molecule (closed configuration) in the ocular lens fibers. The functions of MIP/AQP0, both as a water channel and an adhesive molecule in the lens fibers, contribute to the narrow intercellular space of the lens fibers that is required for lens transparency and accommodation.

Abbreviations

aa	amino acid
bp	base pair
kD	kilodaltons
AQP0	aquaporin 0
AQP1	aquaporin 1
MIP	major intrinsic protein of the lens
MP26	membrane protein 26
NPA	asparagine-proline-alanine

1 Introduction

In the period spanning approximately the last 30 years, MIP, a protein highly expressed in the ocular lens fiber membrane, puzzled investigators because various approaches suggested possible functions without conclusive results. However, contributions from various scientific disciplines have now unraveled the structure and function/s of MIP, now also known as aquaporin 0.

1.1 How Major Intrinsic Protein of the Lens MIP became Aquaporin 0

MIP, MP26, MIP26, and aquaporin 0 are the various names given to the same protein since its discovery as a lens membrane protein up until its characterization as a water channel. MIP (major intrinsic protein of the lens), was first identified biochemically as the most abundant intrinsic membrane protein of the ocular lens fibers (Bloemendal 1982; Bloemendal et al. 1977; Broekhuysse et al. 1976, 1979; Vermorken et al. 1977). It was also called MIP26 or MP26 because of its mobility as a 26-kD polypeptide in electrophoretic studies. However, another band with

22-kD mobility was also identified, later shown to be a proteolytic product of full-length MIP. MIP is specifically expressed in the lens fiber cells; no expression is detected in the lens epithelia (Fitzgerald et al. 1983; Yancey et al. 1988). As ultrastructural studies showed MIP immunolocalized to gap junctions, it was considered a gap junction protein (Bok et al. 1982; Fitzgerald et al. 1983, 1985; Paul and Goodenough 1983a, b). However, MIP was also shown to be present in thin junctions in the lens fibers and to form square arrays (Costello et al. 1989; Paul and Goodenough 1983b; Zampighi et al. 1989). Purified MIP formed channels when incorporated into liposomes (Girsch and Peracchia 1985a, b; Gooden et al. 1985a, b; Scaglione and Rintoul 1989; Swamy and Abraham 1992), and formed voltage-dependent channels when incorporated into planar lipid bilayers (Ehring et al. 1990, 1992; Modesto et al. 1996; Shen et al. 1991) and in transfected mammalian and insect cells (Drake et al. 2002). However, MIP expressed in *Xenopus* oocyte pairs did not induce cell-cell couplings as observed with other expressed connexins (Swenson et al. 1989), and MIP formed voltage-dependent symmetrical channels in contrast to the asymmetrical ones formed by connexins (Donaldson and Kistler 1992; Ehring et al. 1990). When the MIP cDNA was first cloned (Gorin et al. 1984), it became clear that it did not belong to the gap-junction-forming connexin family (Ebihara 1994; Peracchia et al. 1994). Additionally, MIP and lens fiber MP70 (later characterized as connexin 50) immunolocalize to different types of lens fiber membrane junctions: MIP to thin junctions and MP70 to thick junctions (Gruijters et al. 1987; Zampighi et al. 1989). However, other studies suggested that MIP localization to gap junctions may be due to a possible role in gap junction formation (Dunia et al. 1998; Gruijters 1989; Yu and Jiang 2004; Zampighi et al. 2002). Other studies suggested MIP may function as an adhesion molecule (Fotiadis et al. 2000; Gonen et al. 2004a, b, 2005; Michea et al. 1994, 1995).

1.1.1 MIP, the Founder of the MIP Family

The cloning of the MIP gene revealed an intramolecular repeat, one encoded in the first exon and the other distributed through three exons, suggesting that the MIP gene originated by gene duplication (Pisano and Chepelinsky 1991; Wistow et al. 1991). Sequence analysis of multiple cDNAs encoding membrane proteins from mammals, plants, and invertebrates, isolated in the 1990s, indicated the emergence of an ancient family of membrane proteins. They all shared an intramolecular repeat of three amino acids, asparagine (N), proline (P), and alanine (A), which became known as the NPA box. The family was named the MIP family, as MIP was the first member of the family to be isolated (Agre et al. 1993b; Chepelinsky 1994; Gorin et al. 1984; Jung et al. 1994; Pao et al. 1991; Park and Saier 1996; Reizer et al. 1993; Wistow et al. 1991).

1.1.2 The Aquaporin Family

Peter Agre's laboratory developed the *Xenopus* oocyte functional assay to demonstrate that CHIP28 functioned as water channel (Preston et al. 1992). At this point,

CHIP28 became aquaporin 1, the first aquaporin to be characterized as such, and the MIP family became the aquaporin family (Agre et al. 1993a, b). As MIP functioned as a water channel when assayed in the *Xenopus* oocyte swelling assay, it was designated as aquaporin 0 (Chandy et al. 1997; Mulders et al. 1995; Varadaraj et al. 1999). From then on, MIP was mainly known by that name; however, in some lens literature it still appears designated with both names.

The “hourglass model” predicted each of the two NPA repeats to be part of the hemipore forming the water channel pore of AQP1 (Agre et al. 1993a; Jung et al. 1994). Crystallographic studies later demonstrated that the NPA repeat indeed forms the water channel of all aquaporins (Agre et al. 1993a, 2002; Engel et al. 2000, 2008; Gonen and Walz 2006; Mitsuoka et al. 1999; Murata et al. 2000; Scheuring et al. 2000; Walz et al. 1997). However, two-dimensional crystals demonstrated that MIP can exist either as an open channel or as a closed channel. In the open configuration, MIP could function as a water channel and in the closed configuration as an adhesion molecule (Engel et al. 2008; Gonen et al. 2004a, b, 2005; Gonen and Walz 2006; Harries et al. 2004).

The following sections describe the sophisticated architecture of the lens and the tight spatial and temporal regulation of lens gene expression required for lens function, and the molecular genetics studies of MIP/AQP0 mutations leading to cataractogenesis. They provide the pieces of the puzzle that are required for understanding the key role that MIP/AQP0 plays in physiological functioning of the lens.

2 Ocular Lens Structure and Development

2.1 Differentiation of Lens Epithelia into Lens Fibers

The function of the ocular lens is to focus the light that enters the eye onto the retina. To accomplish this physiological function, the lens needs to be transparent and of the appropriate refractive index to focus the light onto the retina. This is attained by tightly-regulated gene expression that is temporally and spatially regulated to accomplish a sophisticated and ordered architecture. The whole lens is enclosed in the lens capsule. The anterior part of the lens faces the aqueous humor that separates it from the cornea, and the posterior part of the lens faces the vitreous humor that separates the lens from the retina. Figure 1 shows a schematic representation of the differentiation of the lens during embryonic development. Briefly, the lens arises from the surface ectoderm, first giving rise to the lens placode during early embryonic development; it later forms the lens pit that will, in turn, become the lens vesicle, composed of a monolayer of epithelial cells. The posterior cells in the lens vesicle start elongating, forming the primary fibers (see Fig. 1; panels *E11.25*, *E12.5*), until they completely fill the lens vesicle (*E17.5*). The anterior monolayer of epithelial cells becomes the anterior epithelia throughout the life of the adult lens (Fig. 1, label *AE*), and only the epithelial cells at the equatorial region (Fig. 1, label

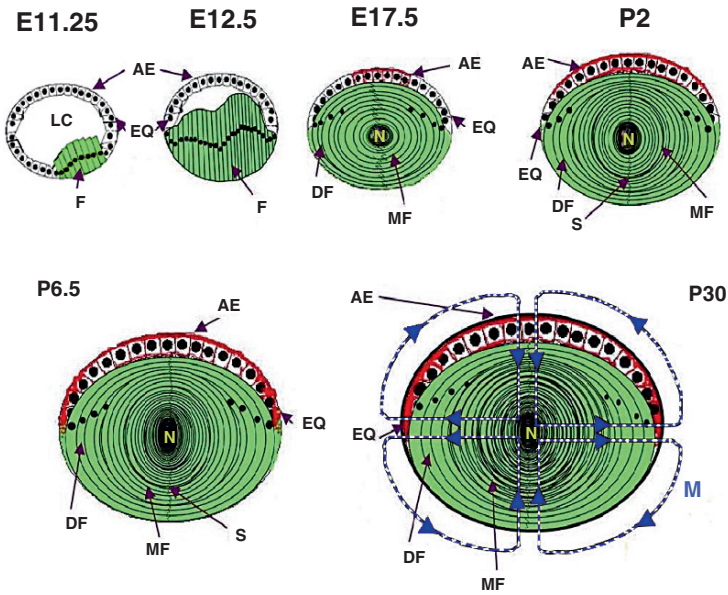


Fig. 1 Schematic representation of mouse lens development indicating MIP/AQP0 and AQP1 expression. *AE* anterior epithelia; *EQ* equatorial epithelia; *F* primary fibers; *DF* differentiating fibers; *MF* mature fibers; *S* sutures; *N* nuclear fibers. E11.25, embryonic day 11.25; E12.5, embryonic day 12.5; E17.5, embryonic day 17.5; P2, postnatal day 2; P6.5; postnatal day 6.5; P30; postnatal day 30. At E11.25, epithelial cells in the posterior part of the lens vesicle begin to elongate toward the center of the vesicle. At E12.5, the primary fibers continue to fill the lens vesicle; at E17.5, secondary fibers and nuclear fibers are already observed. Secondary fibers detach from the lens capsule in the posterior region of the lens and from the lens epithelia in the anterior region and fuse with other fibers, forming the lens sutures (*S*). Note that at E11.25 MIP/AQP0 is already expressed as soon as the first elongating cells start filling the lens vesicle to form the primary fibers, and continues to be expressed in the secondary fibers and nuclear fibers. Anterior epithelia cells start expressing AQP1 at a later stage, at E17.5. The four circuits indicated with arrow heads and broken lines in P30 indicate microcirculation (*M*). Adapted from Varadaraj et al., Fig. 6 (Varadaraj et al. 2007). Copyright 2007 Wiley-Liss Inc. Reprinted with permission of Wiley-Liss Inc, a subsidiary of John Wiley & Sons, Inc

EQ) are able to differentiate into secondary fibers (Fig. 1, label *DF*) (Cvekl and Piatigorsky 1996; Lovicu and McAvoy 2005; McAvoy 1980, 1981; McAvoy et al. 1999; Piatigorsky 1981).

2.2 Primary Fibers and Secondary Fibers

Primary fibers detach at the anterior end from the anterior epithelia and at the posterior end from the lens capsule. Continuous formation of secondary lens fiber cells results in growth shells added onto the primary fiber cell mass that will eventually

form the lens nucleus (Fig. 1, label *N*). Maturation of secondary fibers is complete when they detach at the anterior end from the anterior epithelia and at the posterior end from the lens capsule, to subsequently overlap with the end of other newly mature fibers to form the anterior and posterior lens sutures, respectively (Fig. 1, label *S*) (Kuszak et al. 2006b). The reader is referred to the animated Fig. 6 in the electronic version of the reference Kuszak et al (2006b) for illustration of rotation, migration, and elongation during maturation of secondary fibers in the adult lens (available at <http://www.molvis.org/molvis/v12/a28/>). The formation of mature fibers is also accompanied by loss of cell organelles and acquisition of new fiber properties (Bassnett 1997, 2002, 2005; Bassnett et al. 1994; Bassnett and Mataic 1997; Beebe et al. 2001; Donaldson et al. 2004; Grey et al. 2003; Rong et al. 2002; Shestopalov and Bassnett 2003; Webb and Donaldson 2008; Xia et al. 2006b).

2.3 Lens Sutures Formation

Sutures are formed when lens fibers, which are ribbon-like cells, detach at their posterior and anterior ends from the lens capsule and the anterior epithelia, respectively, and overlap with the ends of other fibers (see Fig. 1, label *S* and Fig. 2, panels *a* and *b*), (Kuszak 1995a; Kuszak et al. 2004b). The suture patterns are not conserved during evolution. Avian, reptilian, some amphibian, and teleost lenses form “umbilical” sutures. Frog and rabbit lenses form “line” sutures. Mouse, rat, guinea pig, hamster, sheep, bovine, pig, dog, and cat lenses feature “Y” sutures. Monkeys and humans form the most complex sutures; during embryonic development, they form “Y” sutures that later become “star” sutures through additional branching during postnatal development. During the formation of the different types of sutures, the elongating fiber ends could either taper or flare, during a process that may involve transient cell-to-cell fusion of adjacent fibers to assure proper suture formation (Kuszak 1995a; Kuszak et al. 2004b). The different types of sutures result in differences in the ability of the lens for focusing and accommodation in each species (Al-Ghoul et al. 2003b; Kuszak 1995b; Kuszak and Al-Ghoul 2002; Kuszak et al. 1991, 1994, 1996, 2004a, b, 2006a, b; Sivak et al. 1994).

2.4 Differential Gene Expression during Lens Epithelia Differentiation into Fibers

Morphological changes during the embryonic development of the lens are the result of signaling mechanisms that trigger expression of growth factors and transcription factors in the eye that subsequently turn on expression of a pattern of genes in the lens epithelia, whereas other genes remain turned off and are turned on only as the lens epithelia differentiate into fibers. This coordinated pattern of expression includes genes encoding structural proteins that are either soluble (i.e., crystallins) or

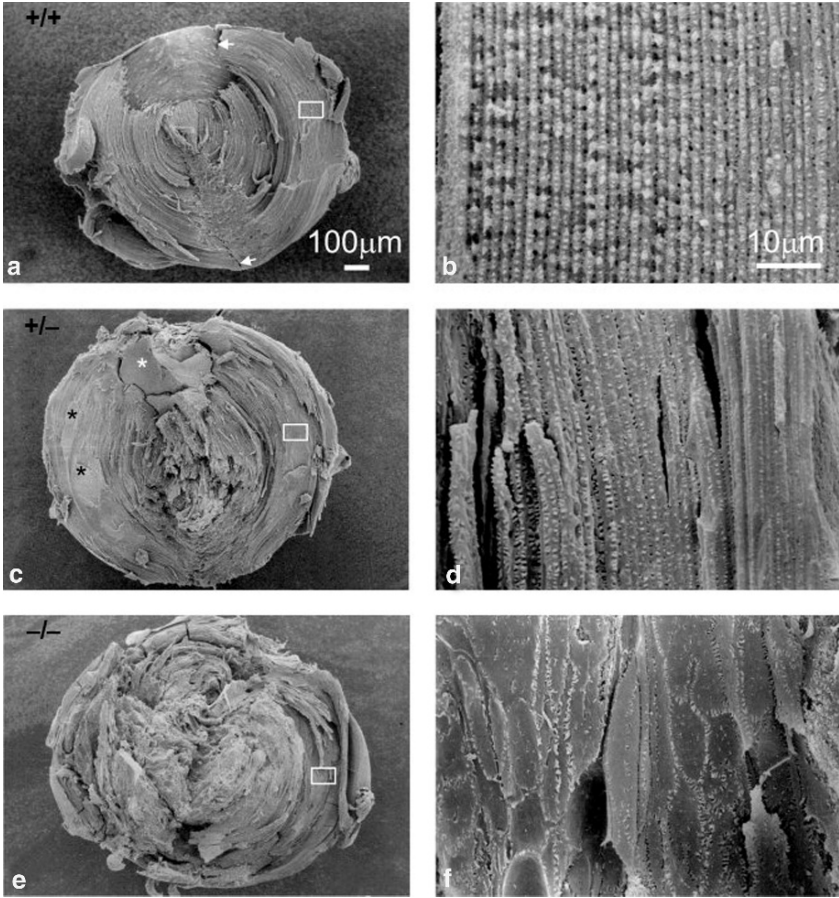


Fig. 2 Scanning electron micrographs (SEM) of wild-type and AQP0-deficient mouse lens split along the polar axis. (a) and (b) wild-type (+/+) lenses have transparent fibers of uniform shape and size arranged in ordered radial cell columns (RCC) and growth shells (GS); normal anterior and posterior suture planes are present (indicated by white arrows). (c) and (d) hemizygous (+/-) lenses have translucent fibers disoriented due to abnormally large fibers (indicated with black asterisks, *); regions of apparent fiber breakdown are indicated with white asterisks. (e) and (f) null (-/-) lenses have opaque fibers displaying a complete lack of uniformity with respect to size, shape, and arrangement. These fibers were not arranged in any discernible radial cell columns or growth shells and have not formed any sutures. Panels (b), (d), and (f) show, at higher magnification, the regions indicated with a white rectangle in panels (a), (c), and (e), respectively. Reprinted from Fig. 4 (Al-Ghoul et al. 2003a). Copyright 2003 Wiley-Liss Inc. Reprinted with permission of Wiley-Liss Inc, a subsidiary of John Wiley & Sons, Inc

membrane proteins (i.e., water channels, connexins) in both cellular compartments. Crystallins, due to their high concentration and short-range interaction, contribute to the transparency and appropriate refractive index of the lens. Beaded filaments and membrane proteins also contribute to lens transparency by maintaining the organized architecture required for lens function. Activation or repression of gene expression assures the precise temporal and spatial regulation of protein expression

in the lens that is required for physiological functioning of the lens (Blankenship et al. 2001; Cvekl and Piatigorsky 1996; de Jongh et al. 2001; Graw 2003; Grey et al. 2003; Kondoh 1999; Lovicu and McAvoy 2005; McAvoy and Chamberlain 1990; Perng et al. 2007; Piatigorsky 1981; Reza and Yasuda 2004a, b; Robinson 2006).

2.5 Cataractogenesis

Lens cataracts are characterized by loss of lens transparency and the appearance of opacities in the lens, resulting in light scattering and perturbation of normal visual function. The appearance of different types of opacity in the lens results from either posttranslational modification of lens proteins during aging, or from mutation/s in genes required for maintaining lens transparency and normal lens function or normal lens development. Mutations in multiple genes encoding crystallins (the major soluble proteins of the lens), cytoskeleton proteins, and membrane proteins have been identified as responsible for genetic cataract phenotypes (Al-Ghoul and Kuszak 1999; Al-Ghoul et al. 1998; Bettelheim et al. 1981, 1995, 1997; Bloemendal et al. 2004; Boyle et al. 1997; Boyle and Takemoto 1997; Francis et al. 1999; Gong et al. 2007; Graw 2004; Graw and Loster 2003; Hejtmancik 2008; Hejtmancik and Kantorow 2004; Sandilands et al. 2002; Shiels and Hejtmancik 2007).

3 MIP/AQP0 Gene Expression in Lens Fibers

3.1 MIP/AQP0 Gene Expression During Lens Differentiation

The MIP gene starts being expressed as soon as the first primary fibers begin filling the lens vesicle, and continues being expressed as the secondary fibers differentiate from the equatorial epithelial cells, as shown in Fig. 1 (Varadaraj et al. 2007; Yancey et al. 1988). Induction of differentiation of explanted lens epithelia into fibers by FGFs allows studying the activation of expression of the MIP gene during the differentiation of lens epithelia into fibers at the molecular level. Activation of the ERK and JNK signaling pathways are required for activation of the MIP gene promoter to be able to initiate MIP transcription as the lens epithelia differentiate into fibers (Golestaneh et al. 2004; Lovicu and McAvoy 2001, 2005; McAvoy and Chamberlain 1990; McAvoy et al. 1999). Premature differentiation of lens epithelia induced by ectopic expression of FGF3 in lens epithelia results in activation of the MIP gene (Robinson 2006; Robinson et al. 1998).

3.2 MIP/AQP0 Post-translational Modifications

MIP, a membrane intrinsic protein expressed as a 263 amino acids peptide, is inserted in the plasma membrane with six transmembrane bilayer-spanning domains

(*H1, H2, H3, H4, H5, H6*, as shown in Fig. 3), resulting in three extracellular loops (*A, C, and E*), two intracellular loops (*B and D*, as shown in Fig. 3), and the N- and C-terminal intracellular domains. The NPA box domains form two hemipores (*HB and HE*) embedded in the membrane, by folding back into the membrane of the first intracellular loop (*B*) and the last extracellular loop (*E*), where each of them is respectively located. Both hemipores come together to form the water pore channel spanning the lipid bilayer, in accordance with the predicted “hourglass model” (Agre et al. 1993a, 2002) that was later confirmed by crystallography studies. MIP is inserted in the plasma membrane as a tetramer (Aerts et al. 1990; Gonen et al. 2004a, b). MIP undergoes posttranslational modifications during differentiation and aging. MIP undergoes proteolysis at the N- and C-terminal ends, in the nuclear fibers of the normal lens, and also during cataractogenesis (Ball et al. 2004; Boyle and Takemoto 1997, 1999; David et al. 1988; Gooden et al. 1985b; Granstrom et al. 1989; Hoenders and Bloemendal 1983; Schey et al. 1999, 2000; Takemoto et al. 1986a, b, 1987a, b, 1988, 1991; Takemoto and Takehana 1986a, b). MIP is phosphorylated in several serines at the C-terminal end. MIP serine 235, evolutionarily conserved in mammals and amphibians (see Fig. 3), is the major phosphorylation site in humans, bovines, and rats (Ball et al. 2003, 2004; Schey et al. 1997, 1999, 2000). MIP phosphorylation is spatially regulated, being more abundant in the cortical fibers than in the nuclear fibers of the human lens (Ball et al. 2004). Serine 235 also plays a role in correct trafficking of MIP from the trans-Golgi network to the plasma membrane (Golestaneh et al. 2008). MIP has also been found to undergo glycation (Swamy-Mruthinti 2001; Swamy-Mruthinti and Schey 1997). Phosphorylation and glycation events at the MIP C-terminal domain regulate its binding to calmodulin (Rose et al. 2008; Swamy-Mruthinti 2001).

4 Multiple Functions of MIP/AQP0

4.1 MIP/AQP0 Functions as a Water Channel in the Lens Fibers

MIP/AQP0 has been shown to function as a water channel in two types of functional assays; one is the classical *Xenopus* oocyte assay for aquaporins developed in Peter Agre’s laboratory, with exogenous MIP/AQP0 being expressed in *Xenopus* oocytes (Chandy et al. 1997; Kushmerick et al. 1995; Mulders et al. 1995; Varadaraj et al. 1999). In the other functional assay, membrane vesicles formed from freshly isolated groups of lens fiber cells developed in Rick Mathias’ laboratory have been used to study the function of the endogenous MIP/AQP0 expressed in the lens fibers of mouse, frog, and rabbit (Varadaraj et al. 1999, 2005, 2007). As MIP/AQP0 is expressed only in the lens fibers whereas AQP1 is expressed in the lens epithelia (Hamann et al. 1998; Stamer et al. 1994; Varadaraj et al. 2005, 2007), as shown in Fig. 1, comparative water permeability assays in fiber membrane vesicles and lens epithelial cells can be used to compare the water channel

properties of both aquaporins in their respective physiological cellular environment, as shown in Fig. 4a (Varadaraj et al. 2005, 2007). MIP/AQP0 water channels show different properties from those formed by AQP1 in either endogenous or exogenous functional assays. MIP/AQP0 water channels, besides functioning with lower efficiency than those formed by AQP1, are Hg^{2+} -insensitive and pH-dependent, whereas AQP1 channels are inhibited by Hg^{2+} and are pH-independent (Mulders et al. 1995; Nemeth-Cahalan and Hall 2000; Varadaraj et al. 1999, 2005, 2007).

The water permeability of anterior lens epithelial cells isolated from mice between 2 and 30 days of age increases gradually. However, the equatorial lens epithelial cells show a significant increase in water permeability later, between 6 and 30 days of age (Varadaraj et al. 2007), as shown in Fig. 4a. Water permeability in both anterior and equatorial epithelia throughout this age period is inhibited by Hg^{2+} , confirming that AQP1 is responsible for the observed water permeability (Varadaraj et al. 2007). These results are consistent with the expression pattern of AQP1 in the developing lens that begins in the central epithelia late in embryonic development and continues increasing gradually towards the equatorial epithelia until postnatal day 30, as shown in Fig. 1 (Varadaraj et al. 2007). However, the lower water permeability of the endogenous MIP/AQP0 in the lens fibers vesicles, as shown by its insensitivity to Hg^{2+} , remains approximately constant during the 6- to 30-day age period, as shown in Fig. 4A (Varadaraj et al. 2007).

The mouse lens shows changes in transparency during postnatal development (see Fig. 4b). The lens becomes totally transparent at 30 days of age, coinciding with the time that the water permeability of the equatorial and anterior epithelial cells (AQP1, Hg^{2+} -sensitive) reaches its peak. All these observations fit very nicely with the lens microcirculation model, indicated with arrow heads and broken lines in Fig. 1, panel P30 (Donaldson et al. 2001; Mathias et al. 1997, 2007; Mathias

Fig. 3 Evolutionary conservation of MIP/AQP0 amino acid sequence. Alignment of MIP/AQP0 amino acid sequence from (1) human (Pisano and Chepelinsky 1991); (2) chimpanzee (accession # XP_001168857); (3) Rhesus monkey (accession # XP_001115118); (4) horse (accession # XP_001504894); (5) bovine (Gorin et al. 1984); (6) sheep (Gonen et al. 2004a); (7) dog (accession # ABM67547); (8) rabbit (accession # ABO41863); (9) guinea pig (Han et al. 2004); (10) rat (Kent and Shiels 1990); (11) mouse (Shiels and Bassnett 1996); (12) *Rana pipiens* (Austin et al. 1993); (13) *Xenopus tropicalis* (accession # NP-001090816); (14) killifish (*Fundulus heteroclitus*) (Virkki et al. 2001); (15) zebrafish MIP1 (*Danio rerio*) (Vihtelic et al. 2005); (16) zebrafish MIP2 (*Danio rerio*) (Vihtelic et al. 2005); (17) chicken (Yu and Jiang 2004); and (18) platypus (accession # XP_001507447). Indicated accession # corresponds to that listed in GenPept at Genbank, NCBI, NIH. Conserved amino acid residues are indicated as (—). The NPA repeat is indicated as a shaded box. The location of the six transmembrane domains (**H1**, **H2**, **H3**, **H4**, **H5**, **H6**) is indicated with solid lines. The location of the hemichannels **HB** and **HE** are indicated with broken lines. The location of extracellular loops (**A**, **C**, **E**) and intracellular loops (**B**, **D**) is indicated between the corresponding transmembrane domains. Underlined amino acids 224–238 indicate calmodulin-binding domain (Girsch and Peracchia 1991; Rose et al. 2008). Histidine 40 (in extracellular loop **A**) is conserved in all the mammals' MIP amino acid sequences presently available. Histidine 40 is substituted by asparagine in fish (zebrafish1, killifish), amphibia (*Rana pipiens*, *Xenopus tropicalis*), and platypus; by glycine in chicken. (*) Chicken is 262 amino acids long; (**) platypus is 264 amino acids long

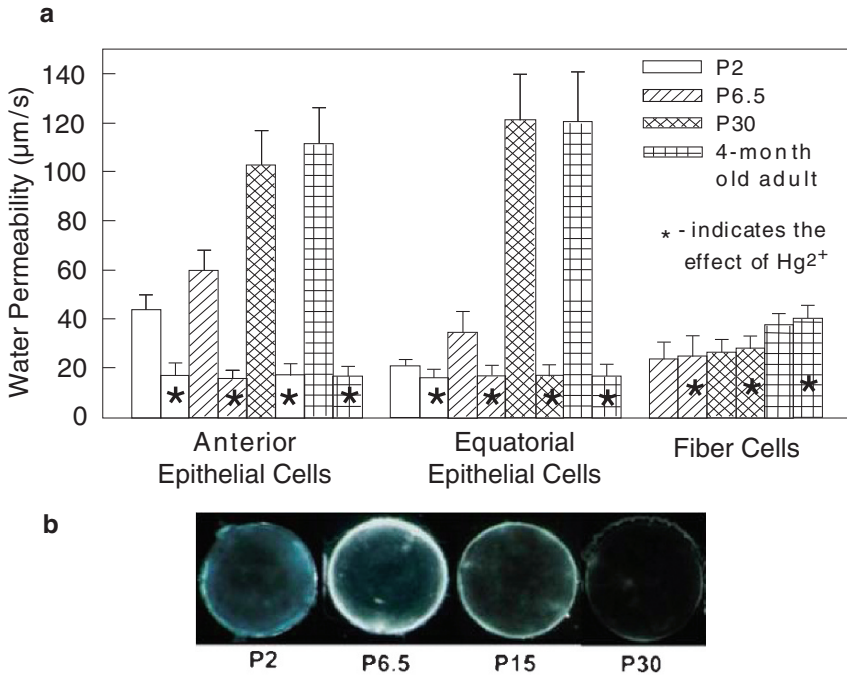


Fig. 4 (a) Water permeability of mouse lens anterior epithelial, equatorial epithelial, and fiber cells membrane vesicles at postnatal days 2 (P2), 6.5 (P6.5), 15 (P15), 30 (P30) and at 4-months. Histogram blocks labeled with (*) indicate water permeability in the presence of Hg^{2+} . Note that lens epithelial cells water permeability is inhibited by Hg^{2+} (due to the presence of AQP1), but is insensitive to Hg^{2+} in fiber cells due to the presence of AQP0. (b) Comparison of mouse lens transparency at P2, P6.5, P15, and P30. Note that lenses at P2 to P15 are not totally transparent; they become completely transparent at day 30; this coincides with the time at which water permeability in anterior and equatorial epithelial cells reaches its maximum. Figure adapted from Varadaraj et al., Fig. 5 (Varadaraj et al. 2007). Copyright 2007 Wiley-Liss Inc. Reprinted with permission of Wiley-Liss Inc, a subsidiary of John Wiley & Sons, Inc

and Rae 2004; Varadaraj et al. 2007), – which would require both MIP/AQP0 in the fibers and AQP1 in the anterior and equatorial epithelia to be functional water channels, to assure normal homeostasis and physiological function of the lens.

4.1.1 MIP/AQP0 Water Channel is pH-Dependent

Both bovine and mouse MIP/AQP0 water permeability increases as external pH decreases from 7.5 to 6.5, when each one is assayed in *Xenopus* oocytes (Nemeth-Cahalan and Hall 2000; Varadaraj et al. 2005). Similar pH dependency of water permeability has been observed with endogenous rabbit or mouse MIP/AQP0 in lens fiber vesicles from either rabbit or mouse lenses (Varadaraj et al. 2005). Histidine at position 40, conserved in bovine, mouse, and rabbit MIP (see Fig. 3), has been

demonstrated to be responsible for the higher water channel activity of MIP/AQP0 at pH 6.5 than at pH 7.5. Killifish MIP/AQP0, with histidine at position 39 but not at position 40, showed a different pH dependency, and increased water permeability at alkaline pH (pH 8.5) rather than acid pH (pH 6.5) when assayed in *Xenopus* oocytes (Nemeth-Cahalan et al. 2004; Virkki et al. 2001). Mutation of killifish MIP/AQP0 amino acid 40 to histidine changes the pH sensitivity to the acid range, and mutation of bovine MIP/AQP0 histidine 40 to cysteine changes its pH sensitivity to the alkaline range (Nemeth-Cahalan and Hall 2000; Nemeth-Cahalan et al. 2004, 2007). Frog MIP/AQP0, with histidine at position 40 replaced by a different amino acid (see Fig. 3), forms water channels that are not pH-dependent when assayed in lens fiber cell vesicles from frog lenses at neutral and acid pHs (Varadaraj et al. 1999, 2005). Lens AQP1, which lacks histidine 40, lacks pH sensitivity as well, when assayed either as the endogenous AQP1 in rabbit lens epithelia (Varadaraj et al. 2005, 2007) or as exogenous human AQP1 in *Xenopus* oocytes (Nemeth-Cahalan and Hall 2000).

Interestingly, the pH in the lens decreases from the cortical to the nuclear fibers in the same pH range (Bassnett and Duncan 1985; Mathias et al. 1991; Varadaraj et al. 2007), suggesting that MIP/AQP0 is required to function with a higher efficiency in the mature fibers than in the cortical fibers of the lens to maintain the necessary microcirculation to assure lens transparency (Donaldson et al. 2001; Mathias et al. 1991, 1997, 2007; Mathias and Rae 2004; Varadaraj et al. 2007).

Histidine 40 (in extracellular loop A) is conserved in all the mammals' MIP amino acid sequences available so far (mouse, rat, guinea pig, rabbit, dog, sheep, horse, bovine, monkey, and human). However, histidine 40 is substituted by asparagine in fish (zebrafish, killifish), amphibia (*Rana pipiens*, *Xenopus tropicalis*), and the monotreme platypus (see Fig. 3). The differences in MIP/AQP0 water channel regulation by pH from mammals to fish and amphibians suggest possible differences in lens physiology that may in some way be related to different lens-focusing properties in air versus water environments. Chicken MIP does not have histidine 40, predicting that MIP water channels in birds may not be pH-regulated in the acid range either.

It is interesting to note that two MIP cDNAs have been identified in zebra fish: one of them with histidine at position 40, the other with a different amino acid at this position, both listed in Fig. 3 (Vihtelic et al. 2005). The first one would show higher water channel activity in the acid range and the other one in the basic range, suggesting the ability of MIP water channel activity in zebra fish to be regulated at a broader pH range. The presence of two MIP genes in the zebra fish genome opens the possibility of independent activation of expression of each gene in different regions of the lens fibers and/or the ability to respond to different physiological environments.

4.1.2 MIP/AQP0 Water Channel is Ca²⁺/Calmodulin-Dependent

Endogenous mouse, rabbit, and frog MIP/AQP0 water channel permeability increases when increasing Ca²⁺ concentrations in lens fiber vesicles from either

mouse, rabbit, or frog lenses, respectively (Varadaraj et al. 2005). However, the opposite effect is observed when either exogenous mouse or bovine MIP/AQP0 is assayed in *Xenopus* oocytes (Nemeth-Cahalan and Hall 2000; Nemeth-Cahalan et al. 2004; Varadaraj et al. 2005). Histidine 40 is involved in the water channel activity inhibition by Ca^{2+} in the oocytes (Nemeth-Cahalan and Hall 2000); however, the water channel permeability increase by Ca^{2+} observed in frog lens fiber vesicles indicates a different mechanism, as histidine 40 is replaced by another amino acid at position 40 (Varadaraj et al. 2005). The differences in Ca^{2+} sensitivity between both assay systems may be due to the particular properties of the lens fiber membrane that may differ from those of the oocyte membrane. In fact, Ca^{2+} concentrations increase from the cortical to the nuclear fibers, being consistent with a requirement for higher water permeability in the nuclear fibers than in the cortical fibers (Varadaraj et al. 2007). Calmodulin interacts with the MIP C-terminal domain, and this binding is Ca^{2+} -dependent (Girsch and Peracchia 1991; Louis et al. 1990; Rose et al. 2008). The Ca^{2+} effect on MIP/AQP0 water channel activity in either the endogenous lens or exogenous oocyte assay is dependent on calmodulin, most likely through Ca^{2+} -calmodulin binding to the proximal domain of the C-terminus (Kalman et al. 2006; Varadaraj et al. 2005; Nemeth-Cahalan and Hall 2000). MIP/AQP0 phosphorylation modulates the calmodulin-mediated Ca^{2+} response and water permeability in *Xenopus* oocytes (Kalman et al. 2008). Lens AQP1, which does not have a similar domain at the C-terminal, does not show calcium sensitivity when assayed either as the endogenous AQP1 in rabbit lens epithelia (Varadaraj et al. 2005, 2007) or exogenous human AQP1 in *Xenopus* oocytes (Nemeth-Cahalan and Hall 2000).

4.1.3 MIP/AQP0 Water Channel is Zn^{2+} -Dependent

Zinc increases water permeability of bovine MIP/AQP0 expressed in *Xenopus* oocytes and prevents any additional increase induced by acid pH. Both His40 (in loop A) and His122 (in loop C) are necessary for zinc modulation of MIP/AQP0 water permeability, implying structural constraints for zinc binding and functional modulation. Neither killifish MIP/AQP0 nor human AQP1, which lack His40, are sensitive to zinc. These results, suggesting that positive cooperativity among subunits of the MIP/AQP0 tetramer is required for zinc modulation, imply the tetramer to be the functional unit (Nemeth-Cahalan et al. 2007). Even though each monomer contains the pore for a functional water channel, the tetrameric structure would stabilize the water pore structure of each of the four tetrameric components. MIP/AQP0 forms tetramers endogenously in lens fiber membranes (Zampighi et al. 1982, 1989) and expressed exogenously in *Xenopus* oocytes (Chandy et al. 1997).

Histidines 40 and 122 are both required for the Zn^{2+} effect on water channel activity. All mammal MIPs sequenced so far have both histidines. However, chicken, frogs, and fish probably do not undergo this type of regulation, as either one or the other histidine is not conserved (see Fig. 3). Water channel activity of killifish MIP, lacking histidine either at position 40 or position 122 is not activated by Zn^{2+} . However, it is important to point out that the increased level of water channel activity

of bovine MIP that has histidines at both positions, when activated by Zn^{2+} , is still lower than that of killifish. These results indicate that fish MIP/AQP0 water channel activity, which is as efficient as that of AQP1, functions at its maximum efficiency without Zn^{2+} .

4.2 MIP/AQP0 Functions as an Interfiber Adhesion Molecule

Three different types of observations provided clues for solving this part of the puzzle:

- MIP is present in thin junctions of the lens fibers, and also forms square arrays that are more abundant in the nuclear fibers than in the cortex (Costello et al. 1989; Paul and Goodenough 1983b; Zampighi et al. 1989).
- MIP undergoes C-terminal proteolysis in the lens nuclear fibers (Ball et al. 2004; Schey et al. 1997, 2000; Takemoto and Takehana 1986b).
- MIP two-dimensional crystallography studies, with MIP isolated from either lens cortical or nuclear fibers, show different structures (Fotiadis et al. 2000; Gonen et al. 2004a, b, 2005).

MIP/AQP0 is expressed as a full-length protein in cortical fibers, but becomes increasingly cleaved in the lens core region (Ball et al. 2004; Schey et al. 1997, 2000; Takemoto and Takehana 1986a, b). Reconstitution of MIP/AQP0 isolated from the core of sheep lenses containing a proportion of truncated MIP, produced double-layered two-dimensional crystals that displayed the same dimensions as the thin 11 nm lens fiber junctions, which are prominent in the lens core, recapitulating the *in vivo* junctions (Costello et al. 1989; Fotiadis et al. 2000; Gonen et al. 2004a; Hasler et al. 1998; Paul and Goodenough 1983b; Zampighi et al. 1989). In contrast, reconstitution of full-length MIP/AQP0 isolated from the lens cortex resulted in single-layered two-dimensional crystals. The cleavage of the intracellular C-terminus enhances the adhesive properties of the extracellular surface of MIP/AQP0, indicating a conformational change in the molecule. As a result of this conformational change, MIP/AQP0 changes its function from water channel in the cortex to adhesion molecule in the nuclear region of the lens (Gonen et al. 2004a, b; Gonen and Walz 2006).

The sheep MIP/AQP0 membrane junction as determined by electron crystallography is formed by localized interactions between MIP/AQP0 tetramers of two adjoining membranes, mainly mediated by prolines in extracellular loops A and C, evolutionarily conserved in MIP/AQP0 but not present in most aquaporins. Prolines 38 in loop A of the eight subunits come together at the center of two interacting tetramers, forming a rosette-like-structure. The C loops connect each AQP0 molecule to two molecules in the opposite membrane through prolines 109 and 110. The water pore is closed in MIP/AQP0 junctions. The water pathway in MIP/AQP0 also contains an additional pore constriction not seen in other aquaporin structures, which may be responsible for pore gating (Gonen et al. 2004b, 2005; Gonen and Walz 2006). Crystallographic studies with recombinant bovine MIP/AQP0 3D

crystals also indicate its ability to form octamers by interactions between tetramers, with loops *A* interacting at the center of the octamers; a somewhat different amino acid interaction of loops *A* and *C* appear to be involved (Palanivelu et al. 2006).

4.3 MIP/AQP0 Intracellular Interaction with Lens Fiber Proteins

Besides making intermolecular contacts with other MIP/AQP0 monomers to form tetramers in the same cell membrane or octamers resulting from tetramer interactions between two adjunct fiber membranes, MIP/AQP0 also interacts intracellularly with other lens fiber proteins. The MIP/AQP0 C-terminal domain, located intracellularly, is involved in interactions with other proteins also expressed in the lens fibers – such as connexins, beaded filament proteins, and crystallins – thereby fulfilling another structural function in the lens fibers.

4.3.1 Connexins

Gap junctions, formed by connexins, are channels connecting neighboring cells to allow passage of small molecules between the cytoplasm of two adjacent cells. The hemichannel of each of the adjacent cells, the connexon, is formed by connexin hexamers, with the channel at its center. Connexins 46 (alpha 3, *Gja3*) and 50 (alpha 8, *Gja8*), specifically expressed in the lens fiber cells, are the components of the gap junctions involved in cell-cell communication and transport of small solutes in the lens fibers (Gong et al. 2007; Jacobs et al. 2004; Lin et al. 1998; Paul et al. 1991; Shearer et al. 2008; White 2002; White et al. 1992; Xia et al. 2006b). Mutations in or deletion of either of these genes result in cataracts (Arora et al. 2008; DeRosa et al. 2006, 2007; Gao et al. 2004; Gong et al. 2007; Graw 2004; Martinez-Wittinghan et al. 2003; Pal et al. 1999; Shiels and Hejtmancik 2007; Xia et al. 2006a, b). Several studies suggest that interactions between MIP and gap junctions may play a role in gap junction formation in the lens fibers (Dunia et al. 1998, 2006; Gruijters 1989; Yu and Jiang 2004; Zampighi et al. 2002). It has recently been demonstrated that MIP/AQP0 and connexins do interact at the molecular level. Studies by surface plasmon resonance indicated that the C-terminal domain of the chicken ortholog of MIP interacts specifically at two binding sites within the intracellular loop of connexin 45.6 (the chicken ortholog of connexin 50). Chicken MIP/AQP0 does not interact with connexin 56 (the chicken ortholog of connexin 46) (Yu et al. 2005). As the intracellular loop of connexin 45.6 is cleaved during chicken lens fiber differentiation, MIP/AQP0 may play a role in the formation of connexons in the cortical fibers during this developmental stage (Yu et al. 2005; Yu and Jiang 2004). In fact, one of the microdomains of MIP/AQP0 characterized in rat lens equatorial fibers was composed by MIP/AQP0 channels within gap junctions (Zampighi et al. 2002). Recent atomic force microscopy studies showing the supramolecular organization

in sheep lens core fiber membranes indicated that MIP/AQP0 and connexons organize in junctional microdomains within large planar lipid bilayers. Thus, thin junctions formed by MIP/AQP0 in these junctional microdomains minimize the inter-fiber space to assure the efficient exchange of small molecules through the gap junctions of the nuclear fibers for the lens microcirculation required to maintain lens transparency (Buzhynskyy et al. 2007; Scheuring et al. 2007).

4.3.2 Beaded Filaments Proteins

Filensin (BFSP1) and phakinin (CP49, BSP2) are specifically expressed in the lens fibers and together form the beaded filaments, a specialized cytoskeletal structure unique to lens fibers (Perng and Quinlan 2005; Perng et al. 2007).

The interaction of either human filensin or phakinin with human MIP/AQP0 was characterized by affinity purification of human lens cytosolic proteins with a peptide corresponding to human MIP C-terminal amino acids 240–263 and pull-down assays using proteomic approaches. Immunofluorescence microscopy and immunoelectron microscopy confirmed the colocalization of MIP/AQP0 with either filensin or phakinin in the cortical lens fibers (Lindsey Rose et al. 2006).

Beaded filaments assemble during the differentiation of the cortical fibers. Phakinin and filensin are present in the cytoplasm during the initial stages of fiber formation, switch to a predominantly plasma membrane localization in the cortical fibers, and are later absent in the nuclear fiber cells (Blankenship et al. 2001). Mutations in or deletion of the filensin and phakinin genes result in light scattering, with perturbations in lens transparency and focusing ability (Alizadeh et al. 2002, 2003; Oka et al. 2008; Perng and Quinlan 2005; Quinlan et al. 1999; Sandilands et al. 2003; Shiels and Hejtmancik 2007). Thus, the interaction of MIP/AQP0 with beaded filaments also plays a structural role in maintaining the architecture of cortical fibers.

4.3.3 Crystallins

Crystallins are soluble proteins expressed in the lens, some expressed in both lens epithelia and fibers, others specifically expressed in the lens fibers. They contribute to the refractive index of the lens due to their high concentration and short-range interactions. Multiple mutations in the various members of the crystallin families are linked to genetic autosomal dominant cataracts (Graw 2004; Sandilands et al. 2002; Shiels and Hejtmancik 2007). Biochemical studies in the 1980s suggested association of crystallins with MIP in the lens fiber membrane fraction (Mulders et al. 1985; Ramaekers et al. 1980). However, only recently have the interactions between MIP/AQP0 and some members of the crystallin families been characterized at the molecular level.

The interaction of the mouse MIP/AQP0 C-terminal domain with two members of the gamma crystallin family, gamma E-crystallin and gamma F-crystallin, was identified by using the two-yeast hybrid system and screening an embryonic

rat lens cDNA expression library with a bait encoding MIP amino acids 190–263. Furthermore, this specific interaction results in the recruitment of gamma E- and gamma F-crystallin to the plasma membrane of mammalian cells coexpressing MIP. MIP does not interact with the *Elo* mutant of γ E-crystallin, which has been linked to a dominant cataract phenotype in mice (Fan et al. 2004, 2005). These findings provide evidence for a functional link between MIP and gamma-crystallins, and suggest that MIP/AQP0 may play a role as a scaffold to organize gamma-crystallins in the lens and/or it may play a role in protecting gamma-crystallins from degradation. Human MIP/AQP0 coexpressed in human epithelial cells with either alpha A-, alpha B-, beta B2-, or gamma C-crystallin, interacts with each of them when their interaction was studied in living cells by FRET (Liu and Liang 2008). These experiments provide evidence of MIP/AQP0 interaction with soluble lens proteins at the molecular level, suggesting a structural role for MIP/AQP0 in the organization of crystallins in lens fibers.

5 MIP/AQP0 Molecular Genetics

5.1 Mutations in the MIP/AQP0 Gene Result in Genetic Cataracts

Mutations in the MIP/AQP0 gene, located on mouse chromosome 10 and human chromosome 12, respectively, have been linked to mouse and human genetic cataracts, suggesting an important role for MIP/AQP0 in maintaining lens transparency. Table 1 lists the locations of natural mutations identified in the MIP/AQP0 gene in each species. All the characterized MIP/AQP0 mutations present bilateral cataracts as the autosomal dominant phenotype, indicating that MIP plays a structural role in the lens.

5.1.1 MIP/AQP0 Gene Mutations in Mice

Mutations in different domains of the MIP/AQP0 gene have been characterized in four mouse mutant strains. The *Lop* (Lens opacity) cataract results from a point mutation at amino acid 51 (A51P) (Shiels and Bassnett 1996), located in the transmembrane domain *H2* (see Fig. 3). In the *Cat^{Fr}* (Fraser) cataract, a transposon insertion in the MIP/AQP0 gene at the junction of intron 3/exon 4 results in the replacement of the last 61 amino acids at the MIP C-terminus by a transposon sequence (Shiels and Bassnett 1996), encompassing amino acids 203–263 (transmembrane *H6* and cytoplasmic C-terminal domains, as shown in Fig. 3). In the *Hfi* (Hydropic lens) cataract, splicing signals required for correctly splicing of exon 2 are deleted due to a 76-base pair deletion in the MIP/AQP0 gene at the junction of exon 2/intron 2 and, as a result, the 165-base pairs corresponding to exon 2 are deleted in the final MIP transcript; thus, amino acids 128–175 (encompassing transmembrane *H4* and

Table 1 Mutations in the MIP/AQP0 gene result in autosomal dominant cataracts

Species	Cataract	Mutation MIP gene	Mutation MIP protein	MIP protein domain location ^a
<i>Mouse</i>	<i>Cat^{Fr}</i> (<i>Fraser</i>) (Shiels and Bassnett 1996)	Insertion transposon in intron 3/exon 4 junction	Replacement aa #203 to #263 at C-terminal by transposon sequence (MIP 261 aa)	Transmembrane <i>H6</i> and cytoplasmic C-terminal
<i>Mouse</i>	<i>Lop</i> (<i>Lens opacity</i>) (Shiels and Bassnett 1996)	Point mutation G to C transversion (exon 1)	Point mutation A51 to P (MIP 263 aa)	Transmembrane <i>H2</i>
<i>Mouse</i>	<i>Hfi</i> (<i>Hydropic lens</i>) (Sidjanin et al. 2001)	Deletion 76 bp junction exon 2/intron 2 Deletion exon 2 in MIP transcript	Deletion 55 aa #121 to #175 (MIP 208 aa)	Transmembrane <i>H4</i> and <i>H5</i> extracellular loop <i>C</i> and intracellular loop <i>D</i>
<i>Mouse</i>	<i>Cat^{Tohm}</i> (<i>Tohoku</i>) (Okamura et al. 2003)	Deletion 12 bp (exon 1)	Deletion aa #46 to #49 (MIP 259 aa)	Transmembrane <i>H2</i>
<i>Human</i>	<i>Family A</i> (Berry et al. 2000)	Point mutation C to G transversion (exon 2)	Point mutation T138 to R (MIP 263 aa)	Transmembrane <i>H4</i>
<i>Human</i>	<i>Family B</i> (Berry et al. 2000)	Point mutation A to G transition (exon 2)	Point mutation E134 to G (MIP 263 aa)	Transmembrane <i>H4</i>
<i>Human</i>	<i>Family ADC2</i> (Geyer et al. 2006)	One bp deletion (exon 4)	Frameshift codon 213 Mutation aa #213 to #257 at C-terminal (MIP 257 aa)	Transmembrane <i>H6</i> and cytoplasmic C-terminal
<i>Human</i>	<i>Chinese Family 1</i> (Gu et al. 2007)	Point mutation C to T transition (exon 1)	Point mutation R33 to C (MIP 263 aa)	Extracellular loop <i>A</i>
<i>Human</i>	<i>Chinese Family 2</i> (Lin et al. 2007)	Point mutation G to A transition (exon 4)	Point mutation R233 to K (MIP 263 aa)	cytoplasmic C-terminal

^aMIP protein domains correspond to the ones indicated in Fig. 3

H5 domains and loop *D*, shown in Fig. 3) are deleted in the translated MIP product (Sidjanin et al. 2001). The *Cat^{Tohm}* (*Tohoku*) cataract, caused by a 12-base pair deletion in MIP/AQP0 exon 1 without changing the reading frame, results in deletion of four amino acids (amino acids 46–49 in transmembrane domain *H2*, shown in Fig. 3) in the translated MIP product (Okamura et al. 2003). The MIP/AQP0 gene mutations involving deletions are reflected in the size of the MIP/AQP0 transcript without affecting the efficiency of transcription (Shiels and Griffin 1993; Sidjanin et al. 2001). However, the main effect of the four MIP/AQP0 gene mutations is on the fate of the translated product at the endoplasmic reticulum. In the four mouse MIP mutants indicated in Table 1, the translated product of the mutant MIP gene is retained in the endoplasmic reticulum, thereby preventing the insertion of the defective protein in the plasma membrane (Okamura et al. 2003; Shiels and Bassnett 1996; Shiels et al.

2000; Sidjanin et al. 2001). Membrane proteins forming multimers oligomerize at the endoplasmic reticulum. The mutations in one or more transmembrane domains of the MIP peptide perturb MIP tertiary structure formation, thereby preventing its oligomerization; this protein misfolding event prevents its ability to pass the endoplasmic reticulum quality control required for trafficking to the plasma membrane and is instead targeted for degradation (Hebert and Molinari 2007; Nakatsukasa and Brodsky 2008; Sanders and Myers 2004).

The lens cataract in mouse mutants can be observed as early as embryonic day 13, coinciding with the time MIP/AQP0 starts being expressed in embryonic development, confirming that MIP/AQP0 is required for lens transparency as soon as it begins being expressed in the primary fibers (Hamai and Kuwabara 1975; Muggleton-Harris et al. 1987; Shiels and Bassnett 1996; Shiels et al. 1991; Zwaan and Williams 1968). Differentiation of lens fibers is disrupted and swollen fibers and large vacuoles are observed in these MIP/AQP0 mouse mutants, supporting the role of MIP/AQP0 in maintaining osmotic balance and a narrow interfiber space.

Lens fiber swelling and vacuole formation followed by cell necrosis was observed as early as embryonic day 13–14 in the *Cat^{Fr}* (Fraser) mouse (Hamai and Kuwabara 1975; Zwaan and Williams 1968). At 21 days postnatally, the water channel activity of lens fiber vesicles from the *Mip/Aqp0 Cat^{Fr}* (Fraser) mice is already affected in the heterozygous (+/*Cat^{Fr}*) and drastically decreased in the homozygous (*Cat^{Fr}/Cat^{Fr}*) mice (Varadaraj et al. 1999). In the heterozygous (+/*Cat^{Fr}*) mouse, the cortical lens fibers already show an irregular swollen shape and abnormal end curvatures that failed to form sutures; the mature lens fibers are unable to stratify into concentric growth shells, resulting in disorganization of the entire optical axis (Shiels et al. 2000).

5.1.2 MIP/AQP0 Gene Mutations in Humans

Mutations in the human orthologous MIP/AQP0 gene resulting in autosomal dominant cataracts have been characterized in five families, as listed in Table 1 (Berry et al. 2000; Francis et al. 2000a, b; Geyer et al. 2006; Gu et al. 2007; Lin et al. 2007). Three of these MIP mutations have been reconstructed and expressed in heterologous systems, providing insights into the molecular mechanism responsible for the dominant effect of these mutations. The MIP/AQP0 point mutations characterized in families 1 and 2, T138R, and E134G, respectively, localize in each case to transmembrane *H4* domain, as shown in Fig. 3 (Berry et al. 2000; Francis et al. 2000a). When the mutated human MIP cDNAs are engineered by recombinant DNA techniques and their mRNAs individually injected and expressed in *Xenopus* oocytes, the mutated protein being expressed in each case is retained in the cytoplasm, not capable of being inserted in the oocyte plasma membrane to function as a water channel (Francis et al. 2000b). The genetic dominant cataract characterized in family *ADC2* is due to a 1-base pair deletion in the MIP/AQP0 gene that changes the reading frame starting at amino acid 213, localized in transmembrane domain *H6*, as shown in Fig. 3 (Geyer et al. 2006). When this mutated human MIP cDNA is engineered by recombinant DNA techniques, transfected, and transiently

expressed in mammalian cells, the translated product does not incorporate in the plasma membrane and is retained in the endoplasmic reticulum (Varadaraj et al. 2008). FRET analysis of ADC2 mutant and wild-type MIP/AQP0 coexpressed in mammalian cells demonstrated that this dominant mutation is the result of the hetero-oligomerization of the wild-type and mutant MIP molecules resulting in the trapping of the wild-type MIP in the endoplasmic reticulum (Varadaraj et al. 2008). Furthermore, the end point of the cytotoxicity resulting from this protein misassembly event is cell death by necrosis (Varadaraj et al. 2008).

5.2 Deficiency in MIP/AQP0 Gene Expression affects Lens Focusing

As described in the previous section, natural mutations in the mouse and the human MIP/AQP0 gene resulting in a gain of function mutation with a cataract phenotype are the result of their cytotoxic effect in the endoplasmic reticulum. Therefore, it became important to elucidate how the deletion of the MIP gene (which would result in decreasing to half the amount of expressed MIP protein inserted in the plasma membrane in the hemizygous mouse, or completely abolishing it in the null mouse) would affect normal physiological functioning of the lens without being deleterious to the translation and assembly machinery of the endoplasmic reticulum. The deletion of the mouse MIP/AQP0 gene resulted in dominant cataracts (Shiels et al. 2001). The water channel activity of lens fiber vesicles from the MIP/AQP0-deficient mice decreased approximately 50% in the hemizygous (+/-) and approximately 20% remains in the homozygous (-/-) null mice, as shown in Fig. 5 (Shiels et al. 2001), simultaneously losing the ability to be regulated by

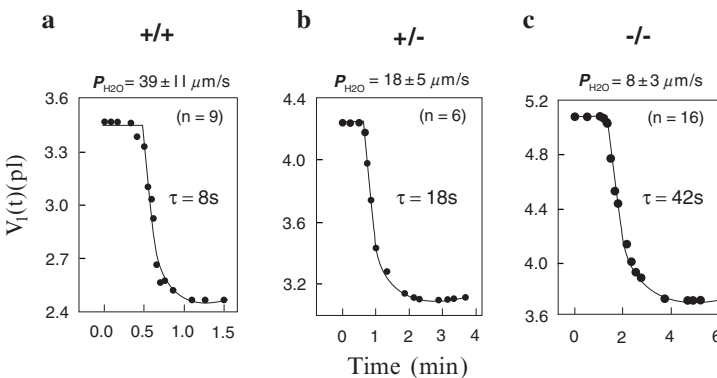


Fig. 5 Osmotic water permeability (P_{H_2O}) of lens fiber cell membrane vesicles from AQP0-deficient mice at postnatal days 21–28. (a) wild-type (+/+) vesicles. (b) hemizygous (+/-) vesicles. (c) null (-/-) vesicles. Reprinted from Fig. 5 (Shiels et al. 2001). Copyright 2001 The American Physiological Society. Reprinted with permission of The American Physiological Society

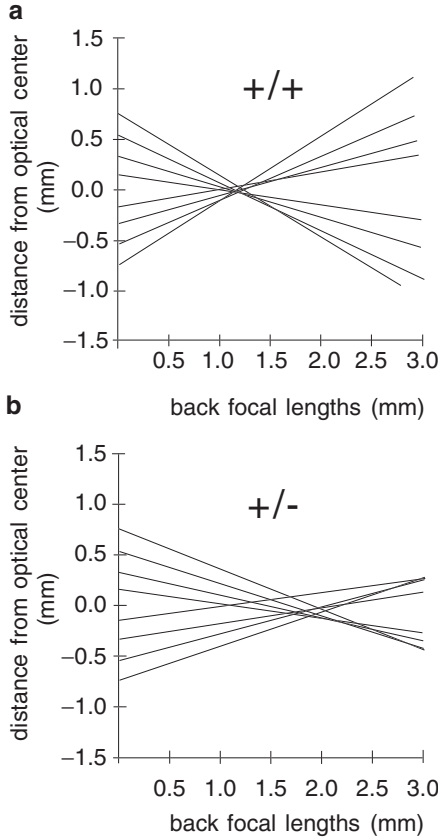


Fig. 6 Representative laser-scan profiles of lenses from age matched (5–6 months old) wild-type (+/+) and AQP0 (+/-) mice. Horizontal axis indicates back focal length; vertical axis indicates the distance from the optical center (0.0) of the lens of the series of incident laser beams passed through the lens. (a) in the wild-type (+/+) lens, all laser beams intersect at a fairly sharp focal point. (b) in the hemizygous (+/-) lens, laser beams fail to intersect at a consistent focal point. Reprinted from Fig. 6 (Shiels et al. 2001). Copyright 2001 The American Physiological Society. Reprinted with permission of The American Physiological Society

pH and Ca^{2+} (Varadaraj et al. 2005). The disruption of lens suture formation was already evident in the hemizygous (+/-) lens, as shown in Fig. 2 (Al-Ghoul et al. 2003a), resulting in the inability of the lens to focus, as shown in Fig. 6 (Shiels et al. 2001). These experiments clearly demonstrate the requirement for MIP/AQP0 as an essential component of the lens fiber membrane for maintaining osmotic balance, tight fiber-to-fiber contact with minimal interfiber space and normal suture formation. Furthermore, a critical concentration of MIP/AQP0 tetramers at the fiber membrane needs to be maintained for the transparency and focusing properties of the normal lens.

6 Summary and Conclusions

MIP/AQP0 functions as a structural protein and water channel in the ocular lens, and these functions are modulated in concert with changes also undergone by other molecules according to their spatial localization in the lens fibers. It is important to view the physiological functions of MIP/AQP0 in the lens in the context of the tight spatial and temporal regulation of gene expression and posttranslational modification of lens fiber proteins that modulate membrane protein functions during the maturation process of the lens fibers. The interaction of the MIP C-terminal domain with other lens proteins has major consequences for lens organization and physiology. This domain is cleaved in cataractogenesis and aging. The nuclear fibers, which are the oldest fibers in the lens, the primary ones formed during embryonic development, have lost their nuclei and cytoplasmic organelles and are tightly packed. It is in this environment that MIP loses its C-terminal domain, which previously interacted with other proteins such as connexins, filensin, phakinin, and crystallins in the cortical fibers. After C-terminal cleavage, MIP/AQP0 tetramers undergo conformational changes, MIP/AQP0 water channels pores close, and MIP function switches from water channel to adhesion molecule by interaction of MIP/AQP0 tetramers in adjacent fibers through their extracellular loops to form octamers in the arrangements of tight junctions to maintain a minimal interfiber space. MIP/AQP0 functions as an osmometer to allow the microcirculation within the lens and to prevent swelling of lens fibers, and also as an interfiber adhesion molecule to maintain a narrow interfiber space, as tightly packed fibers are required for lens transparency.

Mutations in any of the molecules interacting with MIP/AQP0 also result in cataract formation, thereby demonstrating the intricate coordination required for the contribution of each protein to the transparency, appropriate refractive index, accommodation, and focusing ability of the lens to accomplish the lens's function to focus light onto the retina. Thus, there is a functional link between each of these proteins and MIP/AQP0 in the maintenance of lens transparency.

Acknowledgments Thanks to all the research groups that contributed during the past 30 years or so to understanding the important role MIP plays in the lens, to allow us a wonderful vision of the world.

References

- Aerts T, Xia JZ, Slegers H, de Block J, Clauwaert J (1990) Hydrodynamic characterization of the major intrinsic protein from the bovine lens fiber membranes. Extraction in n-octyl-beta-D-glucopyranoside and evidence for a tetrameric structure. *J Biol Chem* 265:8675–8680
- Agre P, Preston GM, Smith BL, Jung JS, Raina S, Moon C, Guggino WB, Nielsen S (1993a) Aquaporin CHIP: the archetypal molecular water channel. *Am J Physiol* 265:F463–F476
- Agre P, Sasaki S, Chrispeels MJ (1993b) Aquaporins: a family of water channel proteins. *Am J Physiol* 265:F461
- Agre P, King LS, Yasui M, Guggino WB, Ottersen OP, Fujiyoshi Y, Engel A, Nielsen S (2002) Aquaporin water channels—from atomic structure to clinical medicine. *J Physiol* 542:3–16

- Al-Ghoul KJ, Kuszak JR (1999) Anterior polar cataracts in CS rats: a predictor of mature cataract formation. *Invest Ophthalmol Vis Sci* 40:668–679
- Al-Ghoul KJ, Novak LA, Kuszak JR (1998) The structure of posterior subcapsular cataracts in the Royal College of Surgeons (RCS) rats. *Exp Eye Res* 67:163–177
- Al-Ghoul KJ, Kirk T, Kuszak AJ, Zoltoski RK, Shiels A, Kuszak JR (2003a) Lens structure in MIP-deficient mice. *Anat Rec* 273:714–730
- Al-Ghoul KJ, Kuszak JR, Lu JY, Owens MJ (2003b) Morphology and organization of posterior fiber ends during migration. *Mol Vis* 9:119–128
- Alizadeh A, Clark JI, Seeberger T, Hess J, Blankenship T, Spicer A, FitzGerald PG (2002) Targeted genomic deletion of the lens-specific intermediate filament protein CP49. *Invest Ophthalmol Vis Sci* 43:3722–3727
- Alizadeh A, Clark J, Seeberger T, Hess J, Blankenship T, FitzGerald PG (2003) Targeted deletion of the lens fiber cell-specific intermediate filament protein filensin. *Invest Ophthalmol Vis Sci* 44:5252–5258
- Arora A, Minogue PJ, Liu X, Addison PK, Russel-Eggitt I, Webster AR, Hunt DM, Ebihara L, Beyer EC, Berthoud VM, Moore AT (2008) A novel connexin50 mutation associated with congenital nuclear pulverulent cataracts. *J Med Genet* 45:155–160
- Austin LR, Rice SJ, Baldo GJ, Lange AJ, Haspel HC, Mathias RT (1993) The cDNA sequence encoding the major intrinsic protein of frog lens. *Gene* 124:303–304
- Ball LE, Little M, Nowak MW, Garland DL, Crouch RK, Schey KL (2003) Water permeability of C-terminally truncated aquaporin 0 (AQP0 1–243) observed in the aging human lens. *Invest Ophthalmol Vis Sci* 44:4820–4828
- Ball LE, Garland DL, Crouch RK, Schey KL (2004) Post-translational modifications of aquaporin 0 (AQP0) in the normal human lens: spatial and temporal occurrence. *Biochemistry* 43:9856–9865
- Bassnett S (1997) Fiber cell denucleation in the primate lens. *Invest Ophthalmol Vis Sci* 38:1678–1687
- Bassnett S (2002) Lens organelle degradation. *Exp Eye Res* 74:1–6
- Bassnett S (2005) Three-dimensional reconstruction of cells in the living lens: the relationship between cell length and volume. *Exp Eye Res* 81:716–723
- Bassnett S, Duncan G (1985) Direct measurement of pH in the rat lens by ion-sensitive microelectrodes. *Exp Eye Res* 40:585–590
- Bassnett S, Mataic D (1997) Chromatin degradation in differentiating fiber cells of the eye lens. *J Cell Biol* 137:37–49
- Bassnett S, Kuszak JR, Reinisch L, Brown HG, Beebe DC (1994) Intercellular communication between epithelial and fiber cells of the eye lens. *J Cell Sci* 107:(Pt 4):799–811
- Beebe DC, Vasiliev O, Guo J, Shui YB, Bassnett S (2001) Changes in adhesion complexes define stages in the differentiation of lens fiber cells. *Invest Ophthalmol Vis Sci* 42:727–734
- Berry V, Francis P, Kaushal S, Moore A, Bhattacharya S (2000) Missense mutations in MIP underlie autosomal dominant ‘polymorphic’ and lamellar cataracts linked to 12q. *Nat Genet* 25:15–17
- Bettelheim FA, Siew EL, Chylack LT Jr (1981) Studies on human cataracts. III. Structural elements in nuclear cataracts and their contribution to the turbidity. *Invest Ophthalmol Vis Sci* 20:348–354
- Bettelheim FA, Qin C, Zigler JS Jr (1995) Calcium cataract: a model for optical anisotropy fluctuations. *Exp Eye Res* 60:153–157
- Bettelheim FA, Churchill AC, Zigler JS Jr (1997) On the nature of hereditary cataract in strain 13/N guinea pigs. *Curr Eye Res* 16:917–924
- Blankenship TN, Hess JF, FitzGerald PG (2001) Development- and differentiation-dependent reorganization of intermediate filaments in fiber cells. *Invest Ophthalmol Vis Sci* 42:735–742
- Bloemendal H (1982) Lens proteins. *CRC Crit Rev Biochem* 12:1–38
- Bloemendal H, Vermorken AJ, Kibbelaar M, Dunia I, Benedetti EL (1977) Nomenclature for the polypeptide chains of lens plasma membranes. *Exp Eye Res* 24:413–415

- Bloemendal H, de Jong W, Jaenicke R, Lubsen NH, Slingsby C, Tardieu A (2004) Ageing and vision: structure, stability and function of lens crystallins. *Prog Biophys Mol Biol* 86:407–485
- Bok D, Dockstader J, Horwitz J (1982) Immunocytochemical localization of the lens main intrinsic polypeptide (MIP26) in communicating junctions. *J Cell Biol* 92:213–220
- Boyle DL, Takemoto LJ (1997) Confocal microscopy of human lens membranes in aged normal and nuclear cataracts. *Invest Ophthalmol Vis Sci* 38:2826–2832
- Boyle DL, Takemoto LJ (1999) Localization of MIP 26 in nuclear fiber cells from aged normal and age-related nuclear cataractous human lenses. *Exp Eye Res* 68:41–49
- Boyle DL, Blunt DS, Takemoto LJ (1997) Confocal microscopy of cataracts from animal model systems: relevance to human nuclear cataract. *Exp Eye Res* 64:565–572
- Broekhuysen RM, Kuhlmann ED, Stols AL (1976) Lens membranes II. Isolation and characterization of the main intrinsic polypeptide (MIP) of bovine lens fiber membranes. *Exp Eye Res* 23:365–371
- Broekhuysen RM, Kuhlmann ED, Winkens HJ (1979) Lens membranes VII. MIP is an immunologically specific component of lens fiber membranes and is identical with 26K band protein. *Exp Eye Res* 29:303–313
- Buzhynskyy N, Hite RK, Walz T, Scheuring S (2007) The supramolecular architecture of junctional microdomains in native lens membranes. *EMBO Reports* 8:51–55
- Chandy G, Zampighi GA, Kremann M, Hall JE (1997) Comparison of the water transporting properties of MIP and AQP1. *J Membr Biol* 159:29–39
- Chepelinsky AB (1994) The MIP transmembrane channel gene family. In: Peracchia C (ed.) *Handbook of membrane channels, molecular and cellular physiology*. Academic Press, San Diego, CA, pp. 413–432
- Costello MJ, McIntosh TJ, Robertson JD (1989) Distribution of gap junctions and square array junctions in the mammalian lens. *Invest Ophthalmol Vis Sci* 30:975–989
- Cvekl A, Piatigorsky J (1996) Lens development and crystallin gene expression: many roles for Pax-6. *Bioessays* 18:621–630
- David LL, Takemoto LJ, Anderson RS, Shearer TR (1988) Proteolytic changes in main intrinsic polypeptide (MIP26) from membranes in selenite cataract. *Curr Eye Res* 7:411–417
- de Jongh RU, Lovicu FJ, Overbeek PA, Schneider MD, Joya J, Hardeman ED, McAvoy JW (2001) Requirement for TGFbeta receptor signaling during terminal lens fiber differentiation. *Development* (Cambridge, England) 128:3995–4010
- DeRosa AM, Mui R, Srinivas M, White TW (2006) Functional characterization of a naturally occurring Cx50 truncation. *Invest Ophthalmol Vis Sci* 47:4474–4481
- DeRosa AM, Xia CH, Gong X, White TW (2007) The cataract-inducing S50P mutation in Cx50 dominantly alters the channel gating of wild-type lens connexins. *J Cell Sci* 120:4107–4116
- Donaldson P, Kistler J (1992) Reconstitution of channels from preparations enriched in lens gap junction protein MP70. *J Membr Biol* 129:155–165
- Donaldson P, Kistler J, Mathias RT (2001) Molecular solutions to mammalian lens transparency. *News Physiol Sci* 16:118–123
- Donaldson PJ, Grey AC, Merriman-Smith BR, Sisley AM, Soeller C, Cannell MB, Jacobs MD (2004) Functional imaging: new views on lens structure and function. *Clin Exp Pharmacol Physiol* 31:890–895
- Drake KD, Schuette D, Chepelinsky AB, Jacob TJ, Crabbe MJ (2002) pH-Dependent channel activity of heterologously-expressed main intrinsic protein (MIP) from rat lens. *FEBS Lett* 512:199–204
- Dunia I, Recouvreur M, Nicolas P, Kumar N, Bloemendal H, Benedetti EL (1998) Assembly of connexins and MP26 in lens fiber plasma membranes studied by SDS-fracture immunolabeling. *J Cell Sci* 111:(Pt 15):2109–2120
- Dunia I, Cibert C, Gong X, Xia CH, Recouvreur M, Levy E, Kumar N, Bloemendal H, Benedetti EL (2006) Structural and immunocytochemical alterations in eye lens fiber cells from Cx46 and Cx50 knockout mice. *Eur J Cell Biol* 85:729–752
- Ebihara L (1994) Gap junction proteins in the lens. In: Peracchia C (ed.) *Handbook of membrane channels, molecular and cellular physiology* Academic Press, San Diego, CA, pp. 403–410

- Ehring GR, Zampighi G, Horwitz J, Bok D, Hall JE (1990) Properties of channels reconstituted from the major intrinsic protein of lens fiber membranes. *J Gen Physiol* 96:631–664
- Ehring GR, Lagos N, Zampighi GA, Hall JE (1992) Phosphorylation modulates the voltage dependence of channels reconstituted from the major intrinsic protein of lens fiber membranes. *J Membr Biol* 126:75–88
- Engel A, Fujiyoshi Y, Agre P (2000) The importance of aquaporin water channel protein structures. *EMBO J* 19:800–806
- Engel A, Fujiyoshi Y, Gonen T, Walz T (2008) Junction-forming aquaporins. *Curr Opin Struct Biol* 18:229–235
- Fan J, Donovan AK, Ledee DR, Zelenka PS, Fariss RN, Chepelinsky AB (2004) gammaE-crystallin recruitment to the plasma membrane by specific interaction between lens MIP/aquaporin-0 and gammaE-crystallin. *Invest Ophthalmol Vis Sci* 45:863–871
- Fan J, Fariss RN, Purkiss AG, Slingsby C, Sandilands A, Quinlan R, Wistow G, Chepelinsky AB (2005) Specific interaction between lens MIP/Aquaporin-0 and two members of the gamma-crystallin family. *Mol Vis* 11:76–87
- Fitzgerald PG, Bok D, Horwitz J (1983) Immunocytochemical localization of the main intrinsic polypeptide (MIP) in ultrathin frozen sections of rat lens. *J Cell Biol* 97:1491–1499
- FitzGerald PG, Bok D, Horwitz J (1985) The distribution of the main intrinsic membrane polypeptide in ocular lens. *Curr Eye Res* 4:1203–1218
- Fotiadis D, Hasler L, Muller DJ, Stahlberg H, Kistler J, Engel A (2000) Surface tongue-and-groove contours on lens MIP facilitate cell-to-cell adherence. *J Mol Biol* 300:779–789
- Francis PJ, Berry V, Moore AT, Bhattacharya S (1999) Lens biology: development and human cataractogenesis. *Trends Genet* 15:191–196
- Francis P, Berry V, Bhattacharya S, Moore A (2000a) Congenital progressive polymorphic cataract caused by a mutation in the major intrinsic protein of the lens, MIP (AQP0). *Br J Ophthalmol* 84:1376–1379
- Francis P, Chung JJ, Yasui M, Berry V, Moore A, Wyatt MK, Wistow G, Bhattacharya SS, Agre P (2000b) Functional impairment of lens aquaporin in two families with dominantly inherited cataracts. *Hum Mol Genet* 9:2329–2334
- Gao J, Sun X, Martinez-Wittinghan FJ, Gong X, White TW, Mathias RT (2004) Connections between connexins, calcium, and cataracts in the lens. *J Gen Physiol* 124:289–300
- Geyer DD, Spence MA, Johannes M, Flodman P, Clancy KP, Berry R, Sparkes RS, Jonsen MD, Isenberg SJ, Bateman JB (2006) Novel single-base deletion mutation in major intrinsic protein (MIP) in autosomal dominant cataract. *Am J Ophthalmol* 141:761–763
- Girsch SJ, Peracchia C (1985a) Lens cell-to-cell channel protein: I. Self-assembly into liposomes and permeability regulation by calmodulin. *J Membr Biol* 83:217–225
- Girsch SJ, Peracchia C (1985b) Lens cell-to-cell channel protein: II. Conformational change in the presence of calmodulin. *J Membr Biol* 83:227–233
- Girsch SJ, Peracchia C (1991) Calmodulin interacts with a C-terminus peptide from the lens membrane protein MIP26. *Curr Eye Res* 10:839–849
- Golestaneh N, Fan J, Fariss RN, Lo WK, Zelenka PS, Chepelinsky AB (2004) Lens major intrinsic protein (MIP)/aquaporin 0 expression in rat lens epithelia explants requires fibroblast growth factor-induced ERK and JNK signaling. *J Biol Chem* 279:31813–31822
- Golestaneh N, Fan J, Zelenka P, Chepelinsky AB (2008) PKC putative phosphorylation site Ser235 is required for MIP/AQP0 translocation to the plasma membrane. *Mol Vis* 14:1006–1014
- Gonen T, Walz T (2006) The structure of aquaporins. *Q Rev Biophys* 39:361–396
- Gonen T, Cheng Y, Kistler J, Walz T (2004a) Aquaporin-0 membrane junctions form upon proteolytic cleavage. *J Mol Biol* 342:1337–1345
- Gonen T, Sliz P, Kistler J, Cheng Y, Walz T (2004b) Aquaporin-0 membrane junctions reveal the structure of a closed water pore. *Nature* 429:193–197
- Gonen T, Cheng Y, Sliz P, Hiroaki Y, Fujiyoshi Y, Harrison SC, Walz T (2005) Lipid-protein interactions in double-layered two-dimensional AQP0 crystals. *Nature* 438:633–638
- Gong X, Cheng C, Xia CH (2007) Connexins in lens development and cataractogenesis. *J Membr Biol* 218:9–12

- Gooden M, Rintoul D, Takehana M, Takemoto L (1985a) Major intrinsic polypeptide (MIP26K) from lens membrane: reconstitution into vesicles and inhibition of channel forming activity by peptide antiserum. *Biochem Biophys Res Commun* 128:993–999
- Gooden MM, Takemoto LJ, Rintoul DA (1985b) Reconstitution of MIP26 from single human lenses into artificial membranes. I. Differences in pH sensitivity of cataractous vs. normal human lens fiber cell proteins. *Curr Eye Res* 4:1107–1115
- Gorin MB, Yancey SB, Cline J, Revel JP, Horwitz J (1984) The major intrinsic protein (MIP) of the bovine lens fiber membrane: characterization and structure based on cDNA cloning. *Cell* 39:49–59
- Granstrom D, Swamy M, Abraham E, Takemoto L (1989) Covalent change in the major intrinsic polypeptide (MIP26K) during cataract development in the streptozotocin-induced diabetic rat. *Curr Eye Res* 8:589–593
- Graw J (2003) The genetic and molecular basis of congenital eye defects. *Nat Rev* 4:876–888
- Graw J (2004) Congenital hereditary cataracts. *Int J Dev Biol* 48:1031–1044
- Graw J, Loster J (2003) Developmental genetics in ophthalmology. *Ophthalmic Genet* 24:1–33
- Grey AC, Jacobs MD, Gonen T, Kistler J, Donaldson PJ (2003) Insertion of MP20 into lens fiber cell plasma membranes correlates with the formation of an extracellular diffusion barrier. *Exp Eye Res* 77:567–574
- Grujters WT (1989) A non-connexon protein (MIP) is involved in eye lens gap-junction formation. *J Cell Sci* 93:(Pt 3):509–513
- Grujters WT, Kistler J, Bullivant S, Goodenough DA (1987) Immunolocalization of MP70 in lens fiber 16–17-nm intercellular junctions. *J Cell Biol* 104:565–572
- Gu F, Zhai H, Li D, Zhao L, Li C, Huang S, Ma X (2007) A novel mutation in major intrinsic protein of the lens gene (MIP) underlies autosomal dominant cataract in a Chinese family. *Mol Vis* 13:1651–1656
- Hamai Y, Kuwabara T (1975) Early cytologic changes of Fraser cataract. An electron microscopic study. *Invest Ophthalmol* 14:517–527
- Hamann S, Zeuthen T, La Cour M, Nagelhus EA, Ottersen OP, Agre P, Nielsen S (1998) Aquaporins in complex tissues: distribution of aquaporins 1–5 in human and rat eye. *Am J Physiol* 274:C1332–C1345
- Han J, Little M, David LL, Giblin FJ, Schey KL (2004) Sequence and peptide map of guinea pig aquaporin 0. *Mol Vis* 10:215–222
- Harries WE, Akhavan D, Miercke LJ, Khademi S, Stroud RM (2004) The channel architecture of aquaporin 0 at a 2.2-Å resolution. *Proc Natl Acad Sci U S A* 101:14045–14050
- Hasler L, Walz T, Tittmann P, Gross H, Kistler J, Engel A (1998) Purified lens major intrinsic protein (MIP) forms highly ordered tetragonal two-dimensional arrays by reconstitution. *J Mol Biol* 279:855–864
- Hebert DN, Molinari M (2007) In and out of the ER: protein folding, quality control, degradation, and related human diseases. *Physiol Rev* 87:1377–1408
- Hejtmancik JF (2008) Congenital cataracts and their molecular genetics. *Semin Cell Dev Biol* 19:134–149
- Hejtmancik JF, Kantorow M (2004) Molecular genetics of age-related cataract. *Exp Eye Res* 79:3–9
- Hoenders HJ, Bloemendal H (1983) Lens proteins and aging. *J Gerontol* 38:278–286
- Jacobs MD, Soeller C, Sisley AM, Cannell MB, Donaldson PJ (2004) Gap junction processing and redistribution revealed by quantitative optical measurements of connexin46 epitopes in the lens. *Invest Ophthalmol Vis Sci* 45:191–199
- Jung JS, Preston GM, Smith BL, Guggino WB, Agre P (1994) Molecular structure of the water channel through aquaporin CHIP. The hourglass model. *J Biol Chem* 269:14648–14654
- Kalman K, Nemeth-Cahalan KL, Froger A, Hall JE (2006) AQP0-LTR of the Cat Fr mouse alters water permeability and calcium regulation of wild type AQP0. *Biochim Biophys Acta* 1758:1094–1099

- Kalman K, Nemeth-Cahalan KL, Froger A, Hall JE (2008) Phosphorylation determines the calmodulin-mediated CA2+response and water permeability of AQP0. *J Biol Chem* 283:21278–21283
- Kent NA, Shiels A (1990) Nucleotide and derived amino-acid sequence of the major intrinsic protein of rat eye-lens. *Nucleic Acids Res* 18:4256
- Kondoh H (1999) Transcription factors for lens development assessed in vivo. *Curr Opin Genet Dev* 9:301–308
- Kushmerick C, Rice SJ, Baldo GJ, Haspel HC, Mathias RT (1995) Ion, water and neutral solute transport in *Xenopus* oocytes expressing frog lens MIP. *Exp Eye Res* 61:351–362
- Kuszak JR (1995a) The development of lens sutures. *Prog Retin Eye Res* 14:567–591
- Kuszak JR (1995b) The ultrastructure of epithelial and fiber cells in the crystalline lens. *Int Rev Cytol* 163:305–350
- Kuszak JR, Al-Ghoul KJ (2002) A quantitative analysis of sutural contributions to variability in back vertex distance and transmittance in rabbit lenses as a function of development, growth, and age. *Optom Vis Sci* 79:193–204
- Kuszak JR, Sivak JG, Weerheim JA (1991) Lens optical quality is a direct function of lens sutural architecture. *Invest Ophthalmol Vis Sci* 32:2119–2129
- Kuszak JR, Peterson KL, Sivak JG, Herbert KL (1994) The interrelationship of lens anatomy and optical quality. II. Primate lenses. *Exp Eye Res* 59:521–535
- Kuszak JR, Peterson KL, Brown HG (1996) Electron microscopic observations of the crystalline lens. *Microsc Res Tech* 33:441–479
- Kuszak JR, Zoltoski RK, Sivertson C (2004a) Fiber cell organization in crystalline lenses. *Exp Eye Res* 78:673–687
- Kuszak JR, Zoltoski RK, Tiedemann CE (2004b) Development of lens sutures. *Int J Dev Biol* 48:889–902
- Kuszak JR, Mazurkiewicz M, Jison L, Madurski A, Ngando A, Zoltoski RK (2006a) Quantitative analysis of animal model lens anatomy: accommodative range is related to fiber structure and organization. *Vet Ophthalmol* 9:266–280
- Kuszak JR, Mazurkiewicz M, Zoltoski R (2006b) Computer modeling of secondary fiber development and growth: I. Nonprimate lenses. *Mol Vis* 12:251–270
- Lin JS, Eckert R, Kistler J, Donaldson P (1998) Spatial differences in gap junction gating in the lens are a consequence of connexin cleavage. *Eur J Cell Biol* 76:246–250
- Lin H, Hejtmancik JF, Qi Y (2007) A substitution of arginine to lysine at the COOH-terminus of MIP caused a different binocular phenotype in a congenital cataract family. *Mol Vis* 13:1822–1827
- Lindsey Rose KM, Gourdie RG, Prescott AR, Quinlan RA, Crouch RK, Schey KL (2006) The C terminus of lens aquaporin 0 interacts with the cytoskeletal proteins filensin and CP49. *Invest Ophthalmol Vis Sci* 47:1562–1570
- Liu BF, Liang JJ (2008) Confocal fluorescence microscopy study of interaction between lens MIP26/AQP0 and crystallins in living cells. *J Cell Biochem* 104:51–58
- Louis CF, Hogan P, Visco L, Strasburg G (1990) Identity of the calmodulin-binding proteins in bovine lens plasma membranes. *Exp Eye Res* 50:495–503
- Lovicu FJ, McAvoy JW (2001) FGF-induced lens cell proliferation and differentiation is dependent on MAPK (ERK1/2) signaling. *Development (Cambridge, England)* 128:5075–5084
- Lovicu FJ, McAvoy JW (2005) Growth factor regulation of lens development. *Dev Biol* 280:1–14
- Martinez-Wittingham FJ, Sellitto C, Li L, Gong X, Brink PR, Mathias RT, White TW (2003) Dominant cataracts result from incongruous mixing of wild-type lens connexins. *J Cell Biol* 161:969–978
- Mathias RT, Rae JL (2004) The lens: local transport and global transparency. *Exp Eye Res* 78:689–698
- Mathias RT, Riquelme G, Rae JL (1991) Cell to cell communication and pH in the frog lens. *J Gen Physiol* 98:1085–1103
- Mathias RT, Rae JL, Baldo GJ (1997) Physiological properties of the normal lens. *Physiol Rev* 77:21–50

- Mathias RT, Kistler J, Donaldson P (2007) The lens circulation. *J Membr Biol* 216:1–16
- McAvoy JW (1980) Induction of the eye lens. *Differentiation* 17:137–149
- McAvoy JW (1981) The spatial relationship between presumptive lens and optic vesicle/cup during early eye morphogenesis in the rat. *Exp Eye Res* 33:447–458
- McAvoy JW, Chamberlain CG (1990) Growth factors in the eye. *Prog Growth Factor Res* 2:29–43
- McAvoy JW, Chamberlain CG, de Iongh RU, Hales AM, Lovicu FJ (1999) Lens development. *Eye* (London, England) 13:(Pt 3b):425–437
- Michea LF, de la Fuente M, Lagos N (1994) Lens major intrinsic protein (MIP) promotes adhesion when reconstituted into large unilamellar liposomes. *Biochemistry* 33:7663–7669
- Michea LF, Andrinolo D, Ceppi H, Lagos N (1995) Biochemical evidence for adhesion-promoting role of major intrinsic protein isolated from both normal and cataractous human lenses. *Exp Eye Res* 61:293–301
- Mitsuoka K, Murata K, Walz T, Hirai T, Agre P, Heymann JB, Engel A, Fujiyoshi Y (1999) The structure of aquaporin-1 at 4.5-Å resolution reveals short alpha-helices in the center of the monomer. *J Struct Biol* 128:34–43
- Modesto E, Lampe PD, Ribeiro MC, Spray DC, Campos de Carvalho AC (1996) Properties of chicken lens MIP channels reconstituted into planar lipid bilayers. *J Membr Biol* 154:239–249
- Muggleton-Harris AL, Festing MF, Hall M (1987) A gene location for the inheritance of the cataract Fraser (CatFr) mouse congenital cataract. *Genet Res* 49:235–238
- Mulders JW, Stokkermans J, Leunissen JA, Benedetti EL, Bloemendal H, de Jong WW (1985) Interaction of alpha-crystallin with lens plasma membranes. Affinity for MP26. *Eur J Biochem/FEBS* 152:721–728
- Mulders SM, Preston GM, Deen PM, Guggino WB, van Os CH, Agre P (1995) Water channel properties of major intrinsic protein of lens. *J Biol Chem* 270:9010–9016
- Murata K, Mitsuoka K, Hirai T, Walz T, Agre P, Heymann JB, Engel A, Fujiyoshi Y (2000) Structural determinants of water permeation through aquaporin-1. *Nature* 407:599–605
- Nakatsukasa K, Brodsky JL (2008) The recognition and retrotranslocation of misfolded proteins from the endoplasmic reticulum. *Traffic* (Copenhagen, Denmark) 9:861–870
- Nemeth-Cahalan KL, Hall JE (2000) pH and calcium regulate the water permeability of aquaporin 0. *J Biol Chem* 275:6777–6782
- Nemeth-Cahalan KL, Kalman K, Hall JE (2004) Molecular basis of pH and Ca²⁺ regulation of aquaporin water permeability. *J Gen Physiol* 123:573–580
- Nemeth-Cahalan KL, Kalman K, Froger A, Hall JE (2007) Zinc modulation of water permeability reveals that aquaporin 0 functions as a cooperative tetramer. *J Gen Physiol* 130:457–464
- Oka M, Kudo H, Sugama N, Asami Y, Takehana M (2008) The function of filensin and phakinin in lens transparency. *Mol Vis* 14:815–822
- Okamura T, Miyoshi I, Takahashi K, Mototani Y, Ishigaki S, Kon Y, Kasai N (2003) Bilateral congenital cataracts result from a gain-of-function mutation in the gene for aquaporin-0 in mice. *Genomics* 81:361–368
- Pal JD, Berthoud VM, Beyer EC, Mackay D, Shiels A, Ebihara L (1999) Molecular mechanism underlying a Cx50-linked congenital cataract. *Am J Physiol (Cell Physiol)* 45) 276:C1443–C1446
- Palanivelu DV, Kozono DE, Engel A, Suda K, Lustig A, Agre P, Schirmer T (2006) Co-axial association of recombinant eye lens aquaporin-0 observed in loosely packed 3D crystals. *J Mol Biol* 355:605–611
- Pao GM, Wu LF, Johnson KD, Hofte H, Chrispeels MJ, Sweet G, Sandal NN, Saier MH Jr. (1991) Evolution of the MIP family of integral membrane transport proteins. *Mol Microbiol* 5:33–37
- Park JH, Saier MH Jr (1996) Phylogenetic characterization of the MIP family of transmembrane channel proteins. *J Membr Biology* 153:171–180
- Paul DL, Goodenough DA (1983a) In vitro synthesis and membrane insertion of bovine MP26, an integral protein from lens fiber plasma membrane. *J Cell Biol* 96:633–638
- Paul DL, Goodenough DA (1983b) Preparation, characterization, and localization of antisera against bovine MP26, an integral protein from lens fiber plasma membrane. *J Cell Biol* 96: 625–632

- Paul DL, Ebihara L, Takemoto LJ, Swenson KI, Goodenough DA (1991) Connexin46, a novel lens gap junction protein, induces voltage-gated currents in nonjunctional plasma membrane of *Xenopus* oocytes. *J Cell Biol* 115:1077–1089
- Peracchia C, Lazrak A, Peracchia LL (1994) Molecular models of channel interaction and gating in gap junctions. In: Peracchia C (ed.) *Handbook of membrane channels, molecular and cellular physiology* Academic Press, San Diego, CA, pp. 361–377
- Perng MD, Quinlan RA (2005) Seeing is believing! The optical properties of the eye lens are dependent upon a functional intermediate filament cytoskeleton. *Exp Cell Res* 305:1–9
- Perng MD, Zhang Q, Quinlan RA (2007) Insights into the beaded filament of the eye lens. *Exp Cell Res* 313:2180–2188
- Piatigorsky J (1981) Lens differentiation in vertebrates. A review of cellular and molecular features. *Differentiation* 19:134–153
- Pisano MM, Chepelinsky AB (1991) Genomic cloning, complete nucleotide sequence, and structure of the human gene encoding the major intrinsic protein (MIP) of the lens. *Genomics* 11:981–990
- Preston GM, Carroll TP, Guggino WB, Agre P (1992) Appearance of water channels in *Xenopus* oocytes expressing red cell CHIP28 protein. *Science (New York, NY)* 256:385–387
- Quinlan RA, Sandilands A, Procter JE, Prescott AR, Hutcheson AM, Dahm R, Gribbon C, Wallace P, Carter JM (1999) The eye lens cytoskeleton. *Eye (London, England)* 13:(Pt 3b):409–416
- Ramaekers FC, Seltén-Versteegen AM, Bloemendal H (1980) Interaction of newly synthesized alpha-crystallin with isolated lens plasma membranes. *Biochim Biophys Acta* 596:57–63
- Reizer J, Reizer A, Saier MH Jr (1993) The MIP family of integral membrane channel proteins: sequence comparisons, evolutionary relationships, reconstructed pathway of evolution, and proposed functional differentiation of the two repeated halves of the proteins. *Crit Rev Biochem Mol Biol* 28:235–257
- Reza HM, Yasuda K (2004a) Lens differentiation and crystallin regulation: a chick model. *Int J Dev Biol* 48:805–817
- Reza HM, Yasuda K (2004b) Roles of Maf family proteins in lens development. *Dev Dyn* 229:440–448
- Robinson ML (2006) An essential role for FGF receptor signaling in lens development. *Semin Cell Dev Biol* 17:726–740
- Robinson ML, Ohtaka-Maruyama C, Chan CC, Jamieson S, Dickson C, Overbeek PA, Chepelinsky AB (1998) Disregulation of ocular morphogenesis by lens-specific expression of FGF-3/int-2 in transgenic mice. *Dev Biol* 198:13–31
- Rong P, Wang X, Niesman I, Wu Y, Benedetti LE, Dunia I, Levy E, Gong X (2002) Disruption of Gja8 (alpha8 connexin) in mice leads to microphthalmia associated with retardation of lens growth and lens fiber maturation. *Development (Cambridge, England)* 129:167–174
- Rose KM, Wang Z, Magrath GN, Hazard ES, Hildebrandt JD, Schey KL (2008) Aquaporin 0-calmodulin interaction and the effect of aquaporin 0 phosphorylation. *Biochemistry* 47:339–347
- Sanders CR, Myers JK (2004) Disease-related misassembly of membrane proteins. *Annu Rev Biophys Biomol Struct* 33:25–51
- Sandilands A, Hutcheson AM, Long HA, Prescott AR, Vrensen G, Loster J, Klopp N, Lutz RB, Graw J, Masaki S, Dobson CM, MacPhee CE, Quinlan RA (2002) Altered aggregation properties of mutant gamma-crystallins cause inherited cataract. *EMBO J* 21:6005–6014
- Sandilands A, Prescott AR, Wegener A, Zoltoski RK, Hutcheson AM, Masaki S, Kuszak JR, Quinlan RA (2003) Knockout of the intermediate filament protein CP49 destabilizes the lens fiber cell cytoskeleton and decreases lens optical quality, but does not induce cataract. *Exp Eye Res* 76:385–391
- Scaglione BA, Rintoul DA (1989) A fluorescence-quenching assay for measuring permeability of reconstituted lens MIP26. *Invest Ophthalmol Vis Sci* 30:961–966

- Scheuring S, Buzhynskyy N, Jaroslowski S, Goncalves RP, Hite RK, Walz T (2007) Structural models of the supramolecular organization of AQP0 and connexons in junctional microdomains. *J Struct Biol* 160:385–394
- Scheuring S, Tittmann P, Stahlberg H, Ringler P, Borgnia M, Agre P, Gross H, Engel A (2000) The aquaporin sidedness revisited. *J Mol Biol* 299:1271–1278
- Schey KL, Fowler JG, Schwartz JC, Busman M, Dillon J, Crouch RK (1997) Complete map and identification of the phosphorylation site of bovine lens major intrinsic protein. *Invest Ophthalmol Vis Sci* 38:2508–2515
- Schey KL, Fowler JG, Shearer TR, David L (1999) Modifications to rat lens major intrinsic protein in selenite-induced cataract. *Invest Ophthalmol Vis Sci* 40:657–667
- Schey KL, Little M, Fowler JG, Crouch RK (2000) Characterization of human lens major intrinsic protein structure. *Invest Ophthalmol Vis Sci* 41:175–182
- Shearer D, Ens W, Standing K, Valdimarsson G (2008) Posttranslational modifications in lens fiber connexins identified by off-line-HPLC MALDI-quadrupole time-of-flight mass spectroscopy. *Invest Ophthalmol Vis Sci* 49:1553–1562
- Shen L, Shrager P, Girsch SJ, Donaldson PJ, Peracchia C (1991) Channel reconstitution in liposomes and planar bilayers with HPLC-purified MIP26 of bovine lens. *J Membr Biol* 124:21–32
- Shestopalov VI, Bassnett S (2003) Development of a macromolecular diffusion pathway in the lens. *J Cell Sci* 116:4191–4199
- Shiels A, Bassnett S (1996) Mutations in the founder of the MIP gene family underlie cataract development in the mouse. *Nat Genet* 12:212–215
- Shiels A, Griffin CS (1993) Aberrant expression of the gene for lens major intrinsic protein in the CAT mouse. *Curr Eye Res* 12:913–921
- Shiels A, Hejtmancik JF (2007) Genetic origins of cataract. *Arch Ophthalmol* 125:165–173
- Shiels A, Griffin CS, Muggleton-Harris AL (1991) Immunochemical comparison of the major intrinsic protein of eye-lens fiber cell membranes in mice with hereditary cataracts. *Biochim Biophys Acta* 1097:318–324
- Shiels A, Mackay D, Bassnett S, Al-Ghoul K, Kuszak J (2000) Disruption of lens fiber cell architecture in mice expressing a chimeric AQP0-LTR protein. *FASEB J* 14:2207–2212
- Shiels A, Bassnett S, Varadaraj K, Mathias R, Al-Ghoul K, Kuszak J, Donoviel D, Lilleberg S, Friedrich G, Zambrowicz B (2001) Optical dysfunction of the crystalline lens in aquaporin-0-deficient mice. *Physiol Genom* 7:179–186
- Sidjanin DJ, Parker-Wilson DM, Neuhauser-Klaus A, Pretsch W, Favor J, Deen PM, Ohtaka-Maruyama C, Lu Y, Bragin A, Skach WR, Chepelinsky AB, Grimes PA, Stambolian DE (2001) A 76-bp deletion in the Mip gene causes autosomal dominant cataract in Hfi mice. *Genomics* 74:313–319
- Sivak JG, Herbert KL, Peterson KL, Kuszak JR (1994) The interrelationship of lens anatomy and optical quality. I. Non-primate lenses. *Exp Eye Res* 59:505–520
- Stamer WD, Snyder RW, Smith BL, Agre P, Regan JW (1994) Localization of aquaporin CHIP in the human eye: implications in the pathogenesis of glaucoma and other disorders of ocular fluid balance. *Invest Ophthalmol Vis Sci* 35:3867–3872
- Swamy MS, Abraham EC (1992) Glycation of lens MIP26 affects the permeability in reconstituted liposomes. *Biochem Biophys Res Commun* 186:632–638
- Swamy-Mruthinti S (2001) Glycation decreases calmodulin binding to lens transmembrane protein, MIP. *Biochim Biophys Acta* 1536:64–72
- Swamy-Mruthinti S, Schey KL (1997) Mass spectroscopic identification of in vitro glycosylated sites of MIP. *Curr Eye Res* 16:936–941
- Swenson KI, Jordan JR, Beyer EC, Paul DL (1989) Formation of gap junctions by expression of connexins in *Xenopus* oocyte pairs. *Cell* 57:145–155
- Takemoto L, Takehana M (1986a) Covalent change of major intrinsic polypeptide (MIP26K) of lens membrane during human senile cataractogenesis. *Biochem Biophys Res Commun* 135:965–971

- Takemoto L, Takehana M (1986b) Major intrinsic polypeptide (MIP26K) from human lens membrane: characterization of low-molecular-weight forms in the aging human lens. *Exp Eye Res* 43:661–667
- Takemoto L, Takehana M, Horwitz J (1986a) Antisera to synthetic peptides of MIP26K as probes of membrane changes during human cataractogenesis. *Exp Eye Res* 42:497–501
- Takemoto L, Takehana M, Horwitz J (1986b) Covalent changes in MIP26K during aging of the human lens membrane. *Invest Ophthalmol Vis Sci* 27:443–446
- Takemoto L, Kodama T, Takemoto D (1987a) Antisera to synthetic peptides of MIP26K as probes of changes in opaque vs. transparent regions within the same human cataractous lens. *Exp Eye Res* 45:179–183
- Takemoto L, Smith J, Kodama T (1987b) Major intrinsic polypeptide (MIP26K) of the lens membrane: covalent change in an internal sequence during human senile cataractogenesis. *Biochem Biophys Res Commun* 142:761–766
- Takemoto L, Kuck J, Kuck K (1988) Changes in the major intrinsic polypeptide (MIP26K) during opacification of the Emory mouse lens. *Exp Eye Res* 47:329–336
- Takemoto LJ, Gorthy WC, Morin CL, Steward DE (1991) Changes in lens membrane major intrinsic polypeptide during cataractogenesis in aged Hannover Wistar rats. *Invest Ophthalmol Vis Sci* 32:556–561
- Varadaraj K, Kushmerick C, Baldo GJ, Bassnett S, Shiels A, Mathias RT (1999) The role of MIP in lens fiber cell membrane transport. *J Membr Biol* 170:191–203
- Varadaraj K, Kumari S, Shiels A, Mathias RT (2005) Regulation of aquaporin water permeability in the lens. *Invest Ophthalmol Vis Sci* 46:1393–1402
- Varadaraj K, Kumari SS, Mathias RT (2007) Functional expression of aquaporins in embryonic, postnatal, and adult mouse lenses. *Dev Dyn* 236:1319–1328
- Varadaraj K, Kumari SS, Patil R, Wax MB, Mathias RT (2008) Functional characterization of a human aquaporin 0 mutation that leads to a congenital dominant lens cataract. *Exp Eye Res* 87:9–21
- Vermorken AJ, Hilderink JM, Dunia I, Benedetti EL, Bloemendal H (1977) Changes in membrane protein pattern in relation to lens cell differentiation. *FEBS Lett* 83:301–306
- Vihelic TS, Fadoo JM, Gao J, Thornton KA, Hyde DR, Wistow G (2005) Expressed sequence tag analysis of zebrafish eye tissues for NEIBank. *Mol Vis* 11:1083–1100
- Virkki LV, Cooper GJ, Boron WF (2001) Cloning and functional expression of an MIP (AQP0) homolog from killifish (*Fundulus heteroclitus*) lens. *Am J Physiol Regul Integr Comp Physiol* 281:R1994–R2003
- Walz T, Hirai T, Murata K, Heymann JB, Mitsuoka K, Fujiyoshi Y, Smith BL, Agre P, Engel A (1997) The three-dimensional structure of aquaporin-1. *Nature* 387:624–627
- Webb KF, Donaldson PJ (2008) Differentiation-dependent changes in the membrane properties of fiber cells isolated from the rat lens. *Am J Physiol* 294:C1133–C1145
- White TW (2002) Unique and redundant connexin contributions to lens development. *Science (New York, NY)* 295:319–320
- White TW, Bruzzone R, Goodenough DA, Paul DL (1992) Mouse Cx50, a functional member of the connexin family of gap junction proteins, is the lens fiber protein MP70. *Mol Biol Cell* 3:711–720
- Wistow GJ, Pisano MM, Chepelinsky AB (1991) Tandem sequence repeats in transmembrane channel proteins. *Trends Biochem Sci* 16:170–171
- Xia CH, Cheng C, Huang Q, Cheung D, Li L, Dunia I, Benedetti LE, Horwitz J, Gong X (2006a) Absence of alpha3 (Cx46) and alpha8 (Cx50) connexins leads to cataracts by affecting lens inner fiber cells. *Exp Eye Res* 83:688–696
- Xia CH, Liu H, Cheung D, Cheng C, Wang E, Du X, Beutler B, Lo WK, Gong X (2006b) Diverse gap junctions modulate distinct mechanisms for fiber cell formation during lens development and cataractogenesis. *Development (Cambridge, England)* 133:2033–2040
- Yancey SB, Koh K, Chung J, Revel JP (1988) Expression of the gene for main intrinsic polypeptide (MIP): separate spatial distributions of MIP and beta-crystallin gene transcripts in rat lens development. *J Cell Biol* 106:705–714

- Yu XS, Jiang JX (2004) Interaction of major intrinsic protein (aquaporin-0) with fiber connexins in lens development. *J Cell Sci* 117:871–880
- Yu XS, Yin X, Lafer EM, Jiang JX (2005) Developmental regulation of the direct interaction between the intracellular loop of connexin 45.6 and the C terminus of major intrinsic protein (aquaporin-0). *J Cell Biol* 280:22081–22090
- Zampighi G, Simon SA, Robertson JD, McIntosh TJ, Costello MJ (1982) On the structural organization of isolated bovine lens fiber junctions. *J Cell Biol* 93:175–189
- Zampighi GA, Hall JE, Ehring GR, Simon SA (1989) The structural organization and protein composition of lens fiber junctions. *J Cell Biol* 108:2255–2275
- Zampighi GA, Eskandari S, Hall JE, Zampighi L, Kreman M (2002) Micro-domains of AQP0 in lens equatorial fibers. *Exp Eye Res* 75:505–519
- Zwaan J, Williams RM (1968) Morphogenesis of the eye lens in a mouse strain with hereditary cataracts. *J Exp Zool* 169:407–421

pH Regulated Anion Permeability of Aquaporin-6

Masato Yasui

Contents

1	Expression and Distribution of AQP6 in Rat Kidney	300
2	Functions of AQP6	301
2.1	Activation by Mercurials	301
2.2	Ion Permeability	302
3	Structure and Function Relationship	303
4	Extrarenal Expression of AQP6	306
5	Summary	306
	References	307

Abstract The kidney is a model organ for transport physiology (Nielsen 1996). AQPs are well-characterized in mammalian kidneys, where they facilitate transepithelial water reabsorption. Most renal AQPs are expressed either in proximal tubule cells or in collecting duct principal cells, which are known as sites for water reabsorption. AQP1 is present in both apical and basolateral membranes of proximal tubules, and in descending limbs of Henle's loop where 70% of filtrated water is isoosmotically reabsorbed (King and Agre 1996). AQP2 is expressed in principal cells of the collecting duct; in response to vasopressin, AQP2 translocates from intracellular vesicles to the apical plasma membranes, thereby increasing water permeability to concentrate urine (Nielsen et al. 1993, 1995; Knepper 1997; Schrier 2006). AQP3 and AQP4 reside in the basolateral membranes of collecting duct principal cells, where they may provide the exit pathways for urine. AQP7, AQP8, and AQP11 are also present in the proximal tubules (Nielsen et al. 1998).

A rat cDNA clone encoding AQP6 was isolated by PCR-based homologous cloning from a rat kidney cDNA library (Ma et al. 1993; Yasui et al. 1999). AQP6 has high sequence homology to AQP0, AQP2, and AQP5. A human AQP6 was also cloned (Ma et al. 1996). Interestingly, the genes encoding AQP2, AQP5, and AQP6 are mapped to chromosome band 12q13 as a family gene cluster at this locus

M. Yasui

Department of Pharmacology, Keio University School of Medicine, Tokyo, Japan
myasui@sc.itc.keio.ac.jp

(Ma et al. 1997). Nevertheless, AQP6 is distinct from AQP0, AQP2, and AQP5 in terms of function. Among the renal aquaporins mentioned above, AQP6 has a unique distribution and a distinct function.

1 Expression and Distribution of AQP6 in Rat Kidney

The distribution of AQP6 in rat kidney was examined with rabbit polyclonal antibodies against the C-terminus of rat AQP6 (Yasui et al. 1999b). Anti-AQP6 antibodies recognize a major 30-kDa band and a 28-kDa band on immunoblots of membranes from oocytes expressing rat AQP6, rat renal cortex, outer medulla, and inner medulla. A 30-kDa band was completely digested by peptide/*N*-glycosidase F or by endoglycosidase Hf, suggesting that AQP6 is a *N*-glycosidated protein. Immunohistochemistry revealed that AQP6 is abundant in intercalated cells of connecting tubules, cortical collecting ducts, the outer medullary collecting ducts, and the inner medullary collecting ducts in the proximal 25% of inner medulla. The labeling pattern strongly suggests labeling of type A intercalated cells, which was confirmed by immunocytochemistry using anti-AQP2 to label adjacent principal cells in parallel semithin cryosections and by immuno electron microscopy (immuno EM) (Yasui et al. 1999b; Ohshiro et al. 2001). Immuno EM of type-A intercalated cells revealed that AQP6 is localized in intracellular vesicles and tubulocisternal profiles, both in the subapical domains and in basolateral domains (Fig. 1). Note that no labeling of the apical or basolateral plasma membranes was observed. Double labeling

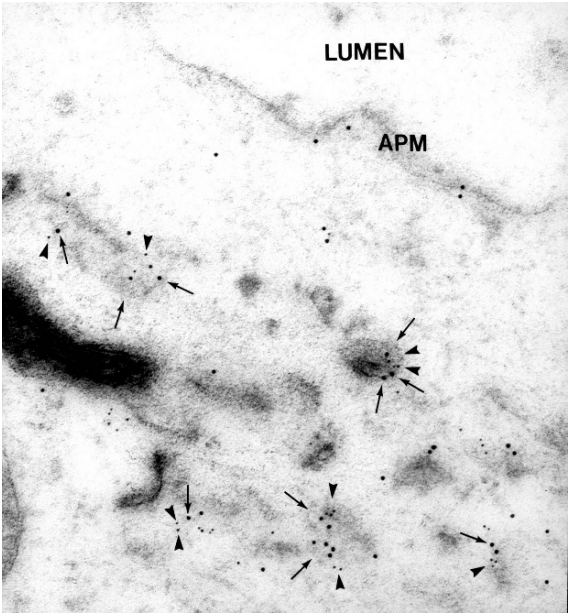


Fig. 1 Immunogold electron microscopic colocalization of AQP6 (5 nm particles, *arrowheads*) and H⁺-ATPase (10 nm particles) in intracellular vesicles of type-A intercalated cells of rat renal collecting duct (×57,000). Reprinted from (Yasui et al. 1999)

indicated that AQP6 is colocalized alongside H^+ -ATPase in intracellular vesicles, but not in the plasma membranes where H^+ -ATPase is also expressed. These observations strongly suggest that AQP6 is an intracellular vesicle water channel; therefore, AQP6 may play a role in acid–base regulation, but not in water reabsorption.

The physiological relevance of AQP6 was examined using *in vivo* rat models (Promeneur et al. 2000). AQP6 abundance and mRNA expression in rat kidney were significantly regulated in response to chronically altered acid/alkali load, as well as to changes in water balance. A marked increase in AQP6 abundance is observed in water loading of rats or rats with lithium-induced NDI, a condition where AQP2 abundance in the kidney is significantly reduced (Marples et al. 1995). This indicates that AQP6 is not important for urinary concentration. AQP6 expression was also significantly upregulated in chronic alkali-loaded ($NaHCO_3$ -loaded) rats. In contrast, NH_4Cl loading in rats (with clamped daily water and food intake) did not show changes in AQP6 expression. Note that there was no evidence of trafficking and redistribution of AQP6 from intracellular vesicles to plasma membranes, despite an altered AQP6 expression. Chloride-depleted metabolic alkalosis was associated with withdrawal of H^+ -ATPase from the apical plasma membrane to subapical cytoplasmic tubulovesicles in type-A intercalated cells, where AQP6 is exclusively localized, with an increased number of numerous subapical tubulovesicles. The up-regulation of AQP6 expression in response to alkali loading may be important for the endocytic processes. Additional studies will be needed to identify the mechanisms of the increase in AQP6 expression in response to alkalosis.

2 Functions of AQP6

2.1 Activation by Mercurials

AQP6 resides in intracellular compartments in *in vivo* kidney tissue. In contrast, when expressed in *Xenopus laevis* oocytes, AQP6 is localized in the oocyte plasma membrane. The plasma membrane expression of AQP6 in oocytes allowed us to examine the functions of AQP6. The osmotic water permeability of AQP6 was limited under basal condition (Ma et al. 1993; Yasui et al. 1999a). It is well known that mercuric ions inhibit the water permeability of most aquaporins. Very surprisingly, we found that low concentrations (0.1 mM) of mercuric chloride significantly increased the water permeability of AQP6 oocytes and induced accompanying membrane currents (Yasui et al. 1999a). To our knowledge, AQP6 is the only aquaporin that is activated by mercuric chloride. Urea and glycerol permeability of AQP6 is also induced by mercuric chloride (Holm et al. 2004).

Mercurials inhibit the water permeability of most aquaporins, including AQP1, for which Cys-189 was identified as the single site of mercurial inhibition (Agre et al. 2002). Three cysteines are present in rat AQP6: Cys-6, Cys-155, and Cys-190. Site-directed mutagenesis identified Cys-155 and Cys-190 residues as the sites of

Hg²⁺ activation of AQP6 (Hazama et al. 2002). It is intriguing that the binding of Hg²⁺ to the corresponding sites (Cys-189 for AQP1 and Cys-190 for AQP6) leads to inhibition of AQP1 but activation of AQP6. We could not distinguish whether the binding of Hg²⁺ to AQP1 simply occludes the pore or whether it decreases the open probability of channel gating. In case of AQP6, pore occlusion is not the reason, as AQP6 is not inhibited but activated by Hg²⁺. The corresponding residue for Cys-155 is Cys-152 for AQP1; however, Hg²⁺ has no effect on Cys-152 in AQP1. This also suggests that the mechanisms of Hg²⁺ effects on AQP6 are different from those on AQP1.

2.2 Ion Permeability

Aquaporins are freely permeated by water, but generally not permeated by ions or charged solutes. However, electrophysiological assessments using a two-electrode voltage clamp revealed that a large increase in membrane currents of AQP6 oocytes was induced by application of HgCl₂ in a dose-dependent manner (Yasui et al. 1999a; Hazama et al. 2002). In contrast, water-injected oocytes and AQP0, AQP1, and AQP2 oocytes failed to exhibit inducible currents. Ion permeability of AQP6 was further characterized by a single channel recording (Hazama et al. 2002). Cell-attached patch recordings of AQP6 expressed in oocytes indicated that AQP6 is a gated channel with intermediate conductance (49 picosiemens in 100 mM NaCl) induced by 10 μM HgCl₂. Hg²⁺-induced AQP6 conductance is voltage-independent (Hazama et al. 2002; Pohl 2004). The excised outside-out patch recordings revealed rapid activation of AQP6 by HgCl₂, which was reversed by the application of β-mercaptoethanol. AQP6 activation is achieved by Hg²⁺ binding to Cys-155 or Cys-190 residue in each monomer for both water and ion permeability, as site-directed mutagenesis revealed that changes in water permeability resulted in equivalent changes in ion conductance. These findings suggest that each monomer forms a pore region for water and ions, rather than ionic permeation through the center of homotetramer.

AQP6 is colocalized with H⁺-ATPase in intracellular vesicles of acid-secreting intercalated cells in renal collecting ducts. This localization suggests that AQP6 might be regulated by low pH. Indeed, a membrane current rapidly appeared in AQP6 oocytes at pH 4.0, with slightly outward rectifying, which was immediately reversed after return to pH 7.5 (Yasui et al. 1999a; Ikeda et al. 2002). The low pH induced current is much more selective to Cl⁻ ions than to Na⁺ ions ($P_{Na}/P_{Cl} = 0.28$). The anion selectivity was changed in K72E mutant AQP6 (Yasui et al. 1999a). As Lys-72 residue is positioned at the cytoplasmic mouth of the aqueous pore, the membrane currents in AQP6 oocytes are inherent channel permeation properties of AQP6, rather than endogenous channels.

Ion permeation by AQP6 was assessed not only in oocytes but also in mammalian cells (Ikeda et al. 2002). AQP6 is not expressed at the plasma membranes in transiently transfected mammalian cell lines like in vivo rat kidney tissues. However, the

addition of a green fluorescence protein (GFP) tag to the N-terminus of rat AQP6 (GFP-AQP6) redirects the protein to the plasma membranes of transfected HEK 293 cells. At pH 4.0, currents are rapidly and reversibly activated in HEK 293 cells expressing GFP-AQP6 (Fig. 2). The features of acid-induced currents in cells expressing GFP-AQP6 are similar to measurements of AQP6 overexpressed in oocytes. A series of ion replacement experiments gave the following halide permeability sequence: $\text{NO}_3^- > \text{I}^- \gg \text{Br}^- > \text{Cl}^- \gg \text{F}^-$ ($P_{\text{NO}_3}/P_{\text{Cl}} > 9.8$). In cells expressing GFP-AQP6, outward-rectifying currents were observed at pH 7.4, with a notable negative shift in the solution containing NaCl with NaNO_3 , suggesting some basal channel activity of AQP6 at pH 7.4. At pH 4.0, the amplitudes of the outward currents were enhanced in a solution with NaNO_3 . The calculated $P_{\text{NO}_3}/P_{\text{Cl}}$ at pH 4.0 is 14.7, which is 9.8 at pH 7.4. Taken together, AQP6 is a pH-regulated anion channel with high permeability for nitrate. Site-directed mutagenesis revealed that the pore-lining threonine residue (Thr-63) at the midpoint of the channel is important for $\text{NO}_3^-/\text{Cl}^-$ selectivity, further supporting the theory that nitrate ions permeate through the aqueous pore of AQP6.

3 Structure and Function Relationship

The atomic structure of AQP1 protein provides marked insight into the mechanisms of how water is selectively permeated through the aqueous pore while blocking ions, including hydronium (Engel et al. 2000; Kozono et al. 2002). The amino acid sequence of AQP6 reveals that AQP6 potentially meets the mechanisms for permeation of water and for repulsing ions, based on the atomic structure model of AQP1. Nevertheless, AQP6 is exceptionally permeated by anions, suggesting that subtle differences in the sequence of AQP6 may lead to major differences in biophysical function.

On the basis of insight provided by structural models, careful analysis of aquaporin sequence alignments led us to identify a critical amino acid residue for anion permeability by AQP6 (Fig. 3). A series of site-directed mutageneses revealed that Asn-60 (in rat AQP6) is critical for ion permeation via AQP6 (Liu et al. 2005). Asn-60 in rat AQP6 corresponds to Gly-57 in human AQP1. The glycine residue at this position is conserved among all other mammalian aquaporins. The atomic model of AQP1 revealed that Gly-57 is located in the middle of TM2 and interacts with Gly-174, which is also conserved among all mammalian aquaporins in the middle of TM5. The fitting of ridges into grooves in TM2 and TM5 locks the two AQP1 helical bundles together near the fourfold axis of the tetramer. This implies that the structure of AQP1 is relatively rigid, and that having asparagine residue at this position allows AQP6 channel gating with anion permeability. A single amino acid substitution at Asn-60 for Gly-60 (N60G mutant) totally eliminates the anion permeability of AQP6 when expressed in *Xenopus* oocytes (Liu et al. 2005). Lack of inducible currents in N60G mutant oocytes is not due to impaired membrane trafficking of the mutant protein, because the plasma membrane

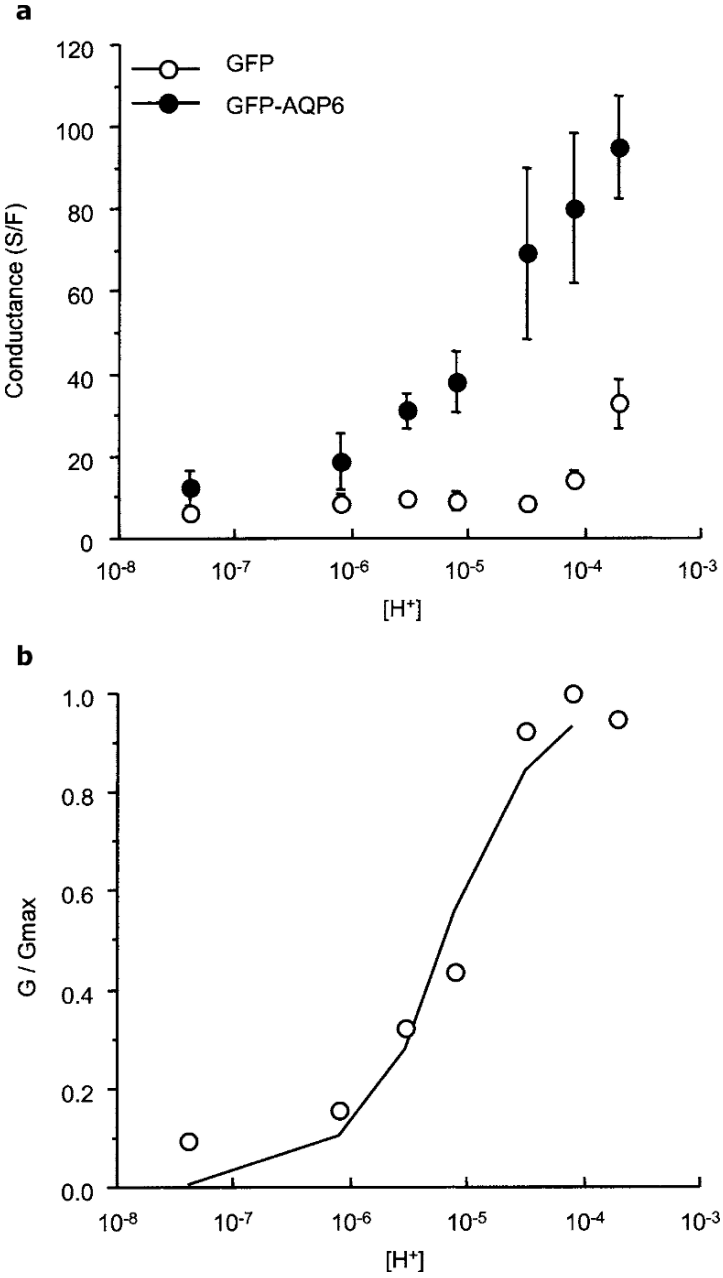


Fig. 2 Relationship between AQP6 ion conductance and extracellular proton concentration. Ion conductance (a) of cells transected with GFP (open circles) or GFP-AQP6 (solid circles) was measured in solutions with various pH levels. Normalized conductances (b) were calculated as the ratio of the corrected conductance and the maximum conductance (pH 4.1), plotted against the logarithmic scale of external proton concentration, and fitted to the Hill equation. Reprinted from (Ikeda et al. 2002)

a

	TM2													
AQP0	HVLQVALAF	GLA	L	L	A	T	L	V	Q	T	V	G	H	I
AQP1	DNVKVSLAF	G	L	S	I	A	T	L	A	Q	S	V	G	H
AQP2	SVLQIAVAF	G	L	G	I	G	I	L	V	Q	A	L	G	H
AQP4	DMVLISLCF	G	L	S	I	A	T	M	V	Q	C	F	G	H
AQP5	TILQISIAF	G	L	A	I	G	T	L	A	Q	A	L	G	P
AQP6	SVLQVAITF	N	L	A	T	A	T	A	V	Q	I	S	W	K
		60		63								71-2		

	TM5													
AQP0	RMGSVALAV	G	F	S	L	T	L	G	H	L	F	G	M	Y
AQP1	LGGSAPLAI	G	L	S	V	A	L	G	H	L	L	A	I	D
AQP2	NLGSPALSI	G	F	S	V	T	L	G	H	L	L	G	I	Y
AQP4	VTGSVALAI	G	F	S	V	A	I	G	H	L	F	A	I	N
AQP5	PVGSPALSI	G	L	S	V	T	L	G	H	L	V	G	I	Y
AQP6	TLGSPAAMI	G	T	S	V	A	L	G	H	L	I	G	I	Y
														174

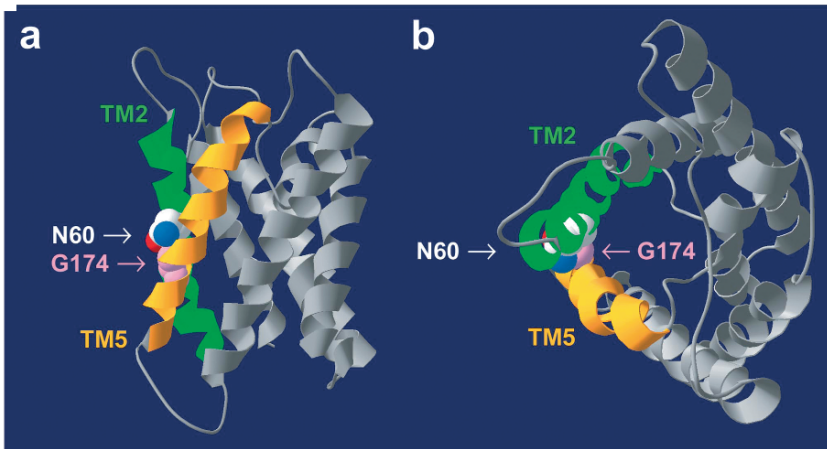
b

Fig. 3 Unique residues in AQP6 structure. **(a)** Sequence alignment of TM2 and TM5 of rat aquaporins (AQP0–AQP6). **(b)** Structural model of AQP6 based on threading through the atomic structure of AQP0. Reprinted from (Liu et al. 2005)

localization of N60G was confirmed by immunofluorescence, using confocal microscopy. Moreover, N60G mutant oocytes had significantly increased water permeability, which is not inhibited by HgCl_2 . Taken together, a single amino acid substitution at Asn-60 for Gly-60 (N60G mutant) switches the function of AQP6 from that of an anion channel to that of a water-selective channel. N60G/G174N double mutant and reciprocal glycine to asparagine mutations in AQP0, AQP1, and AQP2 all failed to traffic to the plasma membrane, suggesting that the interaction of TM2 and TM5 is precisely defined, and that subtle differences here lead to significant conformational changes (Warshel 2005). It may be necessary, but not sufficient,

to have an asparagine residue at its key position for anion permeability and channel gating. Neither wild-type AQP6 nor N60G mutant crystal structure has been determined. The structural comparison of these mutants will give us a better understanding of how AQP6 is permeated by anions and why other aquaporins are not permeated by any ions, including protonated water.

4 Extrarenal Expression of AQP6

Although AQP6 was initially cloned from the kidney and is most abundant in the kidney, among the tissues examined, the evidence shows extra-renal distribution of AQP6. AQP6 mRNA has been detected in mouse cerebellum by using reverse transcription/polymerase chain reaction (Nagase et al. 2007). However, expression of AQP6 protein has not been confirmed yet. Alternative splicing mRNA was found in neonatal cerebellum and kidney. However, in terms of mercurial activation and ion permeation, the protein translated from the alternative AQP6 mRNA does not function in the same way as does rat AQP6. Further investigation is needed to understand the roles of the alternatively spliced product.

Both AQP6 mRNA and protein are expressed in rat parotid glands (Matsuki-Fukushima et al. 2008). Immuno EM showed the presence of AQP6 labeling in the parotid secretory granule membrane and also in the plasma membrane near the tight junction area at the luminal side. Salivary gland acinar cells secrete large amounts of water and electrolytes, suggesting roles of aquaporins in this process. Indeed, AQP5-null mice reveal more than a 60% reduction in pilocarpine-stimulated saliva production (Song and Verkman 2001; Sasaki et al. 2007). The presence and localization of AQP6 in rat acinar cells suggest that AQP6 play a role in saliva production. As AQP6 is permeated by anions, it may contribute to anion secretion in saliva.

5 Summary

The localization of AQP6 in intracellular vesicles with H⁺-ATPase in renal collecting ducts suggests that AQP6 may be involved in the secretion of acid. Unique anion permeability by AQP6, which is activated at low pH, supports the possible role in acid secretion. Studies of rats exposed to chronic acidosis did not reveal changes in AQP6 expression, but chronic alkalosis and water loading resulted in a significant increase in AQP6 expression. AQP6 is well permeated by nitrate ions. The biological significance of nitrate permeation needs to be elucidated. These studies are being further delineated by analysis of mice bearing targeted disruption of the gene encoding AQP6 (M. Yasui, unpublished observations). At present, it is considered that AQP6 may be linked to some forms of acid–base disturbances.

References

- Agre P, King LS, Yasui M et al. (2002) Aquaporin water channels – from atomic structure to clinical medicine. *J Physiol* 542:3–16
- Engel A, Fujiyoshi Y, Agre P (2000) The importance of aquaporin water channel protein structures. *EMBO J* 19:800–806
- Hazama A, Kozono D, Guggino WB et al. (2002) Ion permeation of AQP6 water channel protein. Single channel recordings after Hg²⁺ activation. *J Biol Chem* 277:29224–29230
- Holm LM, Klaerke DA, Zeuthen T (2004) Aquaporin 6 is permeable to glycerol and urea. *Pflügers Arch* 448:181–186
- Ikeda M, Beitz E, Kozono D et al. (2002) Characterization of aquaporin-6 as a nitrate channel in mammalian cells. Requirement of pore-lining residue threonine 63. *J Biol Chem* 277:39873–39879
- King L S, Agre P (1996) Pathophysiology of the aquaporin water channels. *Annu Rev Physiol* 58:619–648
- Knepper M A (1997) Molecular physiology of urinary concentrating mechanism: regulation of aquaporin water channels by vasopressin. *Am J Physiol* 272:F3–F12
- Kozono D, Yasui M, King L S et al. (2002) Aquaporin water channels: atomic structure molecular dynamics meet clinical medicine. *J Clin Invest* 109:1395–1399
- Liu K, Kozono D, Kato Y et al. (2005) Conversion of aquaporin 6 from an anion channel to a water-selective channel by a single amino acid substitution. *Proc Natl Acad Sci U S A* 102:2192–2197
- Ma T, Frigeri A, Skach W et al. (1993) Cloning of a novel rat kidney cDNA homologous to CHIP28 and WCH-CD water channels. *Biochem Biophys Res Commun* 197:654–659
- Ma T, Yang B, Kuo W L et al. (1996) cDNA cloning and gene structure of a novel water channel expressed exclusively in human kidney: evidence for a gene cluster of aquaporins at chromosome locus 12q13. *Genomics* 35:543–550
- Ma T, Yang B, Umenishi F et al. (1997) Closely spaced tandem arrangement of AQP2, AQP5, and AQP6 genes in a 27-kilobase segment at chromosome locus 12q13. *Genomics* 43:387–389
- Marples D, Christensen S, Christensen E I et al. (1995) Lithium-induced downregulation of aquaporin-2 water channel expression in rat kidney medulla. *J Clin Invest* 95:1838–1845
- Matsuki-Fukushima M, Hashimoto S, Shimono M et al. (2008) Presence and localization of aquaporin-6 in rat parotid acinar cells. *Cell Tissue Res* 332:73–80
- Nagase H, Agren J, Saito A et al. (2007) Molecular cloning and characterization of mouse aquaporin 6. *Biochem Biophys Res Commun* 352:12–16
- Nielsen S (1996) Aquaporin water channels in the kidney: localization and regulation. *Perit Dial Int* 16(Suppl. 1):S25–S27
- Nielsen S, Chou C L, Marples D et al. (1995) Vasopressin increases water permeability of kidney collecting duct by inducing translocation of aquaporin-CD water channels to plasma membrane. *Proc Natl Acad Sci U S A* 92:1013–1017
- Nielsen S, DiGiovanni S R, Christensen E I et al. (1993) Cellular and subcellular immunolocalization of vasopressin-regulated water channel in rat kidney. *Proc Natl Acad Sci U S A* 90:11663–11667
- Nielsen S, Fror J, Knepper M A (1998) Renal aquaporins: key roles in water balance and water balance disorders. *Curr Opin Nephrol Hypertens* 7:509–516
- Ohshiro K, Yaoita E, Yoshida Y et al. (2001) Expression and immunolocalization of AQP6 in intercalated cells of the rat kidney collecting duct. *Arch Histol Cytol* 64:329–338
- Pohl P (2004) Combined transport of water and ions through membrane channels. *Biol Chem* 385:921–926
- Promeneur D, Kwon T H, Yasui M et al. (2000) Regulation of AQP6 mRNA and protein expression in rats in response to altered acid-base or water balance. *Am J Physiol Renal Physiol* 279:F1014–F1026
- Sasaki Y, Tsubota K, Kawedia J D et al. (2007) The difference of aquaporin 5 distribution in acinar and ductal cells in lacrimal and parotid glands. *Curr Eye Res* 32:923–929

- Schrier R W (2006) Body water homeostasis: clinical disorders of urinary dilution and concentration. *J Am Soc Nephrol* 17:1820–1832
- Song Y, Verkman A S (2001) Aquaporin-5 dependent fluid secretion in airway submucosal glands. *J Biol Chem* 276:41288–41292
- Warshel A (2005) Inverting the selectivity of aquaporin 6: gating versus direct electrostatic interaction. *Proc Natl Acad Sci U S A* 102:1813–1814
- Yasui M, Hazama A, Kwon T H et al. (1999a) Rapid gating and anion permeability of an intracellular aquaporin. *Nature* 402:184–187
- Yasui M, Kwon T H, Knepper M A et al. (1999b) Aquaporin-6: an intracellular vesicle water channel protein in renal epithelia. *Proc Natl Acad Sci U S A* 96:5808–5813

Aquaglyceroporins and Metalloid Transport: Implications in Human Diseases

Hiranmoy Bhattacharjee, Barry P. Rosen, and Rita Mukhopadhyay

Contents

1	Introduction	310
2	Aquaglyceroporins as Metalloid Transporters	311
2.1	Metalloid Transport in Prokaryotes	311
2.2	Metalloid Transport in Eukaryotes	313
3	Aquaglyceroporins in Human Health	316
3.1	Metalloid Transport and Cancer Chemotherapy	316
3.2	Metalloid Transport and Antiprotozoal Activity	318
4	Concluding Remarks	321
	References	322

Abstract Aquaglyceroporin (AQP) channels facilitate the diffusion of a wide range of neutral solutes, including water, glycerol, and other small uncharged solutes. More recently, AQPs have been shown to allow the passage of trivalent arsenic and antimony compounds. Arsenic and antimony are metalloid elements. At physiological pH, the trivalent metalloids behave as molecular mimics of glycerol, and are conducted through AQP channels. Arsenicals and antimonials are extremely toxic to cells. Despite their toxicity, both metalloids are used as chemotherapeutic agents for the treatment of cancer and protozoan parasitic diseases. The metalloid homeostasis property of AQPs can be a mixed blessing. In some cases, AQPs form part of the detoxification pathway, and extrude metalloids from cells. In other instances, AQPs allow the transport of metalloids into cells, thereby conferring sensitivity. Understanding the factors that modulate AQP expression will aid in a better understanding of metalloid toxicity and also provide newer approaches to metalloid based chemotherapy.

R. Mukhopadhyay (✉)

Department of Biochemistry and Molecular Biology, Wayne State University, School of Medicine, Detroit, MI 48201, USA
rmukhopa@med.wayne.edu

Abbreviations

APL	acute promyelocytic leukemia
AQP	aquaglyceroporin
As ₂ O ₃	arsenic trioxide
EXAFS	extended X-ray absorption fine structure
GSH	glutathione
HAT	human African trypanosomiasis
MAPK	mitogen-activated protein kinase
MIP	major intrinsic protein
SAM	S-adenosylmethionine
XAS	X-ray absorption spectroscopy

1 Introduction

Arsenic (As) and antimony (Sb) are metalloids that display some of the qualities of both metals and nonmetals. Arsenic is widely distributed in the Earth's crust and occurs primarily in four oxidation states: +5, +3, 0, and -3. Chronic exposure to arsenic causes cancer, cardiovascular disease, peripheral neuropathies, and diabetes mellitus (Abernathy et al. 2003), and arsenic has consistently ranked first on the U.S. Department of Health and Human Services' Superfund Priority List of Hazardous Substances <<http://www.atsdr.cdc.gov/cercla/05list.html>>. Humans are exposed to arsenic from mining, copper smelting, coal burning, other combustion processes, and also from volcanic eruptions that release arsenic into the environment. Anthropogenic sources of arsenic include its use in various commonly used herbicides, insecticides, rodenticides, wood-preservatives, animal feeds, paints, dyes, and semiconductors. In addition, arsenic enters the food chain from drinking water that has flowed through arsenic-rich soil.

Although antimony is less abundant than arsenic, their chemical properties are very similar. Antimony compounds are used in the semiconductor industry, ceramics and plastics, flame-retardant applications, and are often alloyed with other metals to increase their strength and hardness. Exposure to antimony can occur from natural sources and also from industrial activities. The primary effects from chronic exposure to antimony in humans are respiratory problems, lung damage, cardiovascular effects, gastrointestinal disorders, and adverse reproductive outcome. Antimony has not as yet been classified as a human carcinogen by either the Department of Health and Human Services or the Environmental Protection Agency.

Despite their toxicity, arsenic and antimony compounds have been used as chemotherapeutic agents for over 2,000 years (Klaassen 1996). In the eighteenth century, Thomas Fowler developed a bicarbonate-based arsenic trioxide (As₂O₃) solution (Fowler's solution), which was used empirically to treat a variety of diseases over the next two centuries (Kwong and Todd 1997). The use of arsenical pastes for skin and breast cancer, and arsenous acid for hypertension, bleeding

gastric ulcers, heartburn, and chronic rheumatism, have been described in the pharmacological texts of the 1880s (Aronson 1994). In 1910, Noble laureate Paul Ehrlich developed Salvarsan (dihydroxydiaminoarsenobenzenedihydrochloride), an organic arsenical for the treatment of syphilis and sleeping sickness. Even today, the arsenic-containing drug Melarsoprol is the first line of treatment against late stage sleeping sickness (Staff 1999). “Ailing-1”, a solution of crude As_2O_3 and herbal extracts from China, formed the basis for the treatment of acute promyelocytic leukemia (APL) (Klaassen 1996). A controlled clinical trial with As_2O_3 showed complete remission of APL (Soignet et al. 1998). Antimonials also have been used as medicine since biblical times. For example, tartar emetic, an antimonial preparation, was used earlier as an anthelmintic treatment for schistosomal infection (Cioli et al. 1995). The pentavalent antimony-containing drugs Pentostam and Glucantime are still the first line of treatment for leishmaniasis.

For the metalloids to work either as a drug or poison, they must be accumulated in cells. In this chapter we will discuss the role of aqua-glyceroporins in metalloid transport and the functional consequences in various human diseases.

2 Aqua-glyceroporins as Metalloid Transporters

2.1 Metalloid Transport in Prokaryotes

The two biologically important oxidation states of arsenic are the pentavalent arsenate ($As(V)$) and trivalent arsenite ($As(III)$) forms. In solution, the pentavalent form, H_3AsO_4 , exists as the oxyanion $As(V)$, which is a substrate analogue of phosphate and hence a competitive inhibitor for many enzymes. The toxicity of arsenate stems from its ability to enter cells via the phosphate transport system and interfere with normal phosphorylation processes. In *Escherichia coli*, there are two phosphate transporters, Pit and Pst (Rosenberg et al. 1977), both of which catalyze arsenate uptake (Willsky and Malamy 1980a, b). In the yeast *Saccharomyces cerevisiae*, arsenate is also taken up by phosphate transporters (Bun-ya et al. 1996). It is likely that arsenate is similarly taken up by phosphate transporters in most organisms, including humans. Normally the intracellular levels of phosphate are sufficiently high that arsenate does not directly cause arsenic toxicity.

Trivalent arsenite is much more toxic than pentavalent arsenate, and is primarily responsible for the biological effects of this metalloid. Arsenite is toxic because of its propensity to form strong, nearly covalent bonds with the thiolates of closely spaced cysteine residues, thereby inhibiting the function of many proteins. As a solid, the unhydrated trivalent form of arsenic is arsenic trioxide (As_2O_3). Reflecting a pK_a of 9.2, in solution arsenic trioxide is the undissociated acid $As(OH)_3$ (Ramirez-Solis et al. 2004). Even though it is not an oxyanion in solution, $As(OH)_3$ is frequently called arsenite or $As(III)$, and so $As(III)$ will be used interchangeably with arsenic trioxide in this chapter.

How does As(III), the most toxic inorganic form of arsenic, get into cells? In a search for genes responsible for the accumulation of metalloids in *Escherichia coli*, Sanders et al. (1997) used *TnphoA* to create a pool of random insertional mutants. An advantage of this strategy is that insertions into the genes of membrane proteins can generate blue colonies when the gene for alkaline phosphatase (*phoA*) is exposed to the periplasmic space, enriching for insertions in the genes for transporters. They selected on media containing either As(III) or antimonite (Sb(III)) and isolated a single mutant, OSBR1, which was resistant to Sb(III) (Sanders et al. 1997) and exhibited a 90% reduction in the rate of As(III) uptake (Meng et al. 2004). Sequence analysis showed that the *TnphoA* insertion was located in the *glpF* gene, coding for the glycerol facilitator GlpF (Sweet et al. 1990). The mutant was shown to be defective in polyol transport by GlpF. These results suggested that, in solution, either As(III) or Sb(III) is recognized as a polyol by the glycerol facilitator (Fig. 1).

Uptake of glycerol in *E. coli* was first described by Edmund Chi Chien Lin (1928–2006) in 1968 (Sanno et al. 1968). In 1972, he showed that the *glpF* gene encodes a transporter that catalyzes facilitated diffusion of glycerol (Richey and Lin 1972). In a series of papers, he and his collaborator at Harvard Medical School, Thomas H. Wilson, characterized GlpF as a glycerol channel. In 1989, the sequence of the *glpF* gene was reported (Muramatsu and Mizuno 1989) and, in 1990, E.C.C. Lin cloned the *glpF* gene in collaboration with W. Boos (Sweet et al. 1990). GlpF is a member of the major intrinsic protein (MIP) superfamily that allows the transport of water and small solutes such as glycerol and urea by an energy-independent

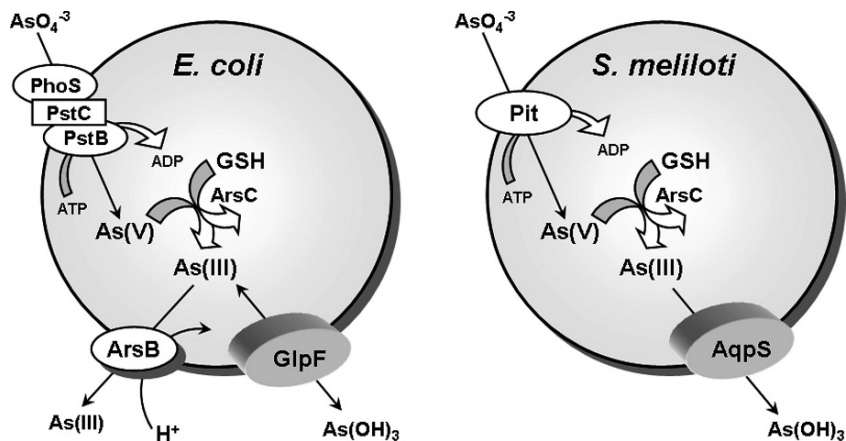


Fig. 1 Metalloid transport in bacteria. In both *E. coli* and *S. meliloti*, arsenate is brought into cells by the phosphate transporters. The first step of detoxification involves reduction of arsenate to arsenite by either *E. coli* or *S. meliloti* ArsC (Bhattacharjee and Rosen 2007). Subsequent detoxification steps in *E. coli* involves removal of the trivalent form of the metalloid from the cytosol by active extrusion through the $\text{As(OH)}_3/\text{H}^+$ antiporter ArsB (Meng et al. 2004), while in *S. meliloti* the AqpS channel facilitates downhill transport of As(III) (Yang et al. 2005). Since arsenite can be taken up directly by cells, using either GlpF in *E. coli* or AqpS in *S. meliloti*, the detoxification mechanism functions when *S. meliloti* cells are exposed to arsenate

mechanism. Members of the MIP superfamily fall into two main evolutionary groups: aquaporins or water specific channels, and aquaglyceroporins, which allow the transport of water, glycerol, and other small uncharged solutes (King et al. 2004; Zardoya 2005). Both groups are expressed widely in all living organisms.

How can trivalent inorganic arsenic, which is often considered to be the anion arsenite in solution, be taken up by GlpF, a channel for neutral species? The pK_a of arsenite is 9.2, and is therefore expected to be protonated at physiological pH. To examine this question, X-ray absorption spectroscopy (XAS) was used to determine the nearest neighbor coordination environment of As(III) under a variety of solution conditions (Ramirez-Solis et al. 2004). Extended X-ray Absorption Fine Structure (EXAFS) analysis demonstrated three oxygen ligands at 1.78 Å from the arsenic atom, showing that the major species in solution is $As(OH)_3$, an inorganic molecular mimic of glycerol. Additionally, structural, thermodynamic, and electrostatic comparison of As(III) and Sb(III) at physiological pH showed that both compounds exhibit similar conformation and charge distribution and a slightly smaller volume than glycerol, which may aid in their passage through the narrowest region of the GlpF channel (Porquet and Filella 2007).

While the aquaglyceroporin GlpF has been shown to facilitate the adventitious uptake of As(III) and Sb(III), the legume symbiont *Sinorhizobium meliloti* employs aquaglyceroporin as a novel route for arsenic detoxification (Fig. 1). When *S. meliloti* is exposed to environmental As(V), As(V) enters the cell through the phosphate transport system and is reduced to As(III) by the arsenate reductase, ArsC. Internally generated As(III) is extruded out of the cell by downhill movement through AqpS, an aquaglyceroporin homologue that shows sequence homology with GlpF (Yang et al. 2005). Therefore, AqpS and ArsC together form a novel pathway of As(V) detoxification in *S. meliloti*. This is the only example of an aquaglyceroporin with a physiological role in arsenic resistance. This pathway may be widespread in organisms that are exposed primarily to As(V). The above examples show that, depending upon the concentration gradient, aquaglyceroporins can facilitate movement of arsenite either into or out of cells.

2.2 Metalloid Transport in Eukaryotes

Jacques Monod (1910–1976; Nobel Prize in Physiology or Medicine in 1965) said, regarding the value of model systems for understanding human biology and disease, “what is true for *E. coli* is true for the elephant, except more so.” Identification of the pathway of As(III) uptake in *E. coli* led first to an understanding of its chemical nature in solution and then to its pathway of uptake in humans. It was a logical extension of the previous studies to determine whether aquaglyceroporins (AQPs) in other species could conduct $As(OH)_3$. In the yeast *Saccharomyces cerevisiae*, the GlpF homologue Fps1p is a glycerol channel involved in osmoregulation. In 2001, Markus Tamás and his group showed that disruption of Fps1p led to resistance to both As(III) and Sb(III) (Wysocki et al. 2001), a conclusion reached independently

by Liu et al. (2002). Fps1p mediates the influx of both metalloids in yeast. Cells expressing a constitutively open form of the Fps1p channel are highly sensitive to both arsenite and antimonite. Under high osmolarity conditions, when the Fps1p channel is closed, wild-type cells show the same degree of As(III) and Sb(III) tolerance as the *fps1*Δ mutant. Direct uptake assays also indicated that arsenite uptake is mediated by Fps1p. The Fps1p-mediated pathway is therefore involved in metalloid uptake in yeast and plays a role in metalloid tolerance (Fig. 2). Phosphorylation of Fps1p at the N-terminus by the mitogen-activated protein kinase (MAPK) homologue Hog1p regulates influx of As(OH)₃ in *S. cerevisiae* (Thorsen et al. 2006).

In mammals, 13 AQPs (0–12) have been identified so far. Among them, four are classical aquaglyceroporins: AQP3, 7, 9, and 10 (Hara-Chikuma and Verkman 2006). For heterologous expression of mammalian AQPs, a yeast strain lacking Fps1p was used to functionally express rat AQP9 (Liu et al. 2002). Cells lacking

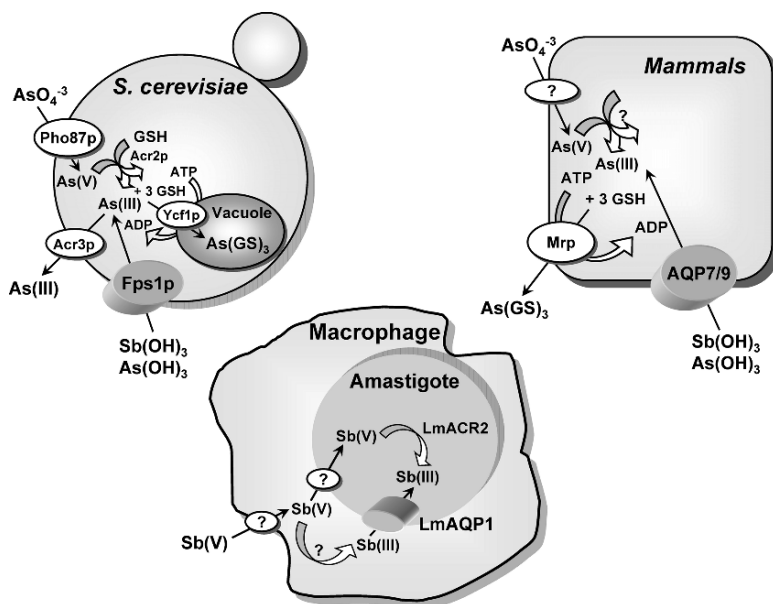


Fig. 2 Metalloid transport in eukaryotes. Arsenate (As(V)) is taken up by phosphate transporters (Bun-ya et al. 1996), and As(III) is taken up by aquaglyceroporins – Fps1p in yeast (Wysocki et al. 2001), and Aqp7 and Aqp9 in mammals (Liu et al. 2002). In yeast, arsenate is reduced to arsenite by Acr2p (Mukhopadhyay et al. 2000). Glutathione and glutaredoxin serve as the source of reducing potential (Mukhopadhyay et al. 2000). The proteins responsible for arsenate uptake and reduction in mammals have not yet been identified. In yeast, Acr3p is a plasma membrane arsenite efflux protein (Bobrowicz et al. 1997; Wysocki et al. 1997), and Ycf1p, which is a member of the MRP family of the ABC superfamily of drug-resistance pumps, transports As(GS)₃ into the vacuole (Ghosh et al. 1999). In mammals, Mrp isoforms pump As(GS)₃ out of cells (Cole et al. 1994; Zaman et al. 1995). In leishmania, Sb(V) is taken up by macrophages, and a portion is reduced to Sb(III), which is then transported into the amastigote by the leishmania aquaglyceroporin LmAQP1 (Gourbal et al. 2004). The other portion of Sb(V) is taken into the amastigote and reduced to Sb(III) by LmACR2 (Zhou et al. 2004) and perhaps other enzymes such as TDR1 (Denton et al. 2004)

Fps1p were resistant to $\text{As}(\text{OH})_3$ and $\text{Sb}(\text{OH})_3$ and had very low rates of uptake of the two metalloids. Cells expressing the yeast *fps1* gene on a plasmid regained both sensitivity and uptake. However, when rat AQP9 gene was expressed, even higher rates of uptake and even greater sensitivity was observed, suggesting that AQP9 is a better channel for $\text{As}(\text{OH})_3$ than Fps1p. *Xenopus laevis* oocytes microinjected with either AQP7 or AQP9 cRNA showed that AQP9 and, to a lesser degree, AQP7, conduct As(III) (Liu et al. 2002).

The ability of the four known human members of the aquaglyceroporin family, hAQP3, hAQP7, hAQP9, and hAQP10, to facilitate $\text{As}(\text{OH})_3$ movement in *Xenopus* oocytes was also examined (Liu et al. 2004). Human AQP9 was found to be a more effective As(III) transporter than hAQP7, with little or no transport by hAQP3 or hAQP10. To explore whether the two polyhydroxylated substrate glycerol and $\text{As}(\text{OH})_3$ share a common channel, the requirement for specific residues in AQP9 for $\text{As}(\text{OH})_3$ conduction was examined by site-directed mutagenesis (Liu et al. 2004). From the crystal structure of two homologues, bovine AQP1 (Sui et al. 2001) and *Escherichia coli* GlpF (Fu et al. 2000), AQP9 residues Phe64 and Arg219 were predicted to serve as part of the selectivity filter. The conduction of $\text{As}(\text{OH})_3$ and glycerol in oocytes expressing rat AQP9 mutants R219A, R219K, F64A, F64T, and F64W was analyzed. A lysine, but not an alanine residue, could substitute for the highly conserved Arg219, indicating that a positive charge, but not an arginine, is required at the entry to the channel. In contrast, the phenylalanine residue, which is believed to position substrates near the conserved arginine, was not required for either arsenic trioxide or glycerol uptake. From these results, it appears that $\text{As}(\text{OH})_3$ and glycerol use the same translocation pathway in AQP9.

AQP9 is the primary liver isoform, and the liver is the organ of arsenic detoxification. In the liver, $\text{As}(\text{OH})_3$ is methylated by the enzyme As(III)-S-adenosylmethionine (SAM) methyltransferase (AS3MT) (Thomas et al. 2004). The final fate of the methylated species is excretion, both in urine and in feces. How these compounds find their way from liver to other tissues such as blood, kidney, or cecum is not certain, and the routes of efflux of methylated arsenical from hepatocytes and uptake into other cell types are unknown. The ability of rat AQP9 to facilitate movement of methylated arsenicals was examined. Rat AQP9 transported methylarsonous acid ($\text{CH}_3\text{As}(\text{OH})_2$ or $\text{MAs}(\text{III})$) at a higher rate than inorganic $\text{As}(\text{OH})_3$ (Liu et al. 2006). Once inside human cells, As(III) is methylated to a variety of species, of which the monomethylated form, $\text{MAs}(\text{III})$, represents a significant fraction of total arsenic found in most tissues (Hughes et al. 2003; Kenyon et al. 2005). The primary site of methylation is the liver, but other organs such as the kidney or testes may also methylate As(III) (Healy et al. 1998). In solution at physiological pH, inorganic trivalent arsenic is $\text{As}(\text{OH})_3$ (Ramirez-Solis et al. 2004). The monomethylated species, $\text{CH}_3\text{As}(\text{OH})_2$, would be molecularly similar to, but less polar than, $\text{As}(\text{OH})_3$. AQP9 is highly expressed in the liver (Abedin et al. 2002), where it plays an essential role in glycerol and urea transport (Carbrey et al. 2003). Because the liver is a key site for the metabolism of arsenic, we propose a model in which AQP9 catalyzes a key step in uptake of $\text{As}(\text{OH})_3$ and efflux of $\text{CH}_3\text{As}(\text{OH})_2$ (Fig. 3). $\text{As}(\text{OH})_3$ is taken up from the bloodstream by hepatocytes via AQP9. Inside the hepatocyte, it is

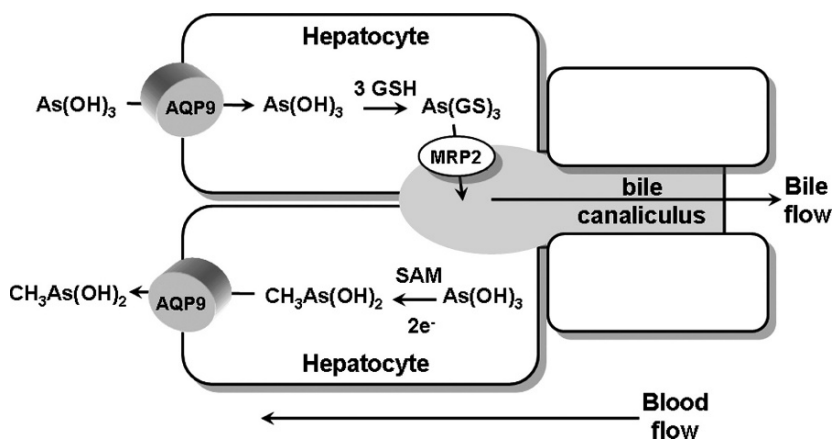


Fig. 3 Proposed pathways of metalloid transport in liver. Arsenite in the form of $\text{As}(\text{OH})_3$ flows down a concentration gradient from blood into hepatocytes through AQP9, which is the major aquaglyceroporin in the liver (Carbrey et al. 2003). In the cytosol of the hepatocyte, $\text{As}(\text{OH})_3$ can be either glutathionylated to $\text{As}(\text{GS})_3$ or methylated to $\text{MAs}(\text{V})$, which is reduced to $\text{MAs}(\text{III})$. $\text{As}(\text{GS})_3$ is pumped into bile by MRP2 (Liu et al. 2001), and perhaps by other members of the ABC superfamily of ATPases. Alternatively, $\text{As}(\text{OH})_3$ can be methylated and reduced to $\text{CH}_3\text{As}(\text{OH})_2$, which then flows down its concentration gradient via AQP9 into blood

methylated and reduced to $\text{MAs}(\text{III})$, which has a number of possible fates. It can be further methylated or glutathionylated. In mammals, both $\text{As}(\text{GS})_3$ and methylarsine diglutathione ($\text{MAs}(\text{GS})_2$) are pumped into bile by multidrug resistance-associated protein 2 (MRP2) or homologues (Kala et al. 2000). Internally generated $\text{MAs}(\text{III})$ can also flow out of the cell, down its concentration into the bloodstream. AQP9 expression in rat liver was induced up to 20-fold by fasting (Carbrey et al. 2003), suggesting that uptake of $\text{As}(\text{III})$ and redistribution of $\text{MAs}(\text{III})$ may be nutritionally responsive. Once in the bloodstream, $\text{MAs}(\text{III})$ can be redistributed into other tissues, including blood cells and kidney, where it is excreted.

3 Aquaglyceroporins in Human Health

3.1 Metalloid Transport and Cancer Chemotherapy

Paracelsus (1493–1541), sometimes called the father of toxicology, wrote “All things are poison and nothing is without poison, only the dose permits something not to be poisonous.” Although arsenic has been classified as a potent human carcinogen and co-carcinogen, it is also used as a drug. Arsenic trioxide (As_2O_3) is now being used as a treatment for acute promyelocytic leukemia (APL). APL is characterized by the $t(15;17)(q22;q21)$ chromosome translocation that fuses the promyelocytic leukemia gene (*PML*) with the retinoic acid receptor α gene (*RAR\alpha*) (Brown

et al. 1997). The resulting fusion gene, *PML-RAR α* , encodes a chimeric protein that causes an arrest of maturation at the promyelocyte stage of myeloid-cell development (Soignet et al. 1998). Although the precise mechanism of action of arsenic trioxide in APL chemotherapy is not clear, it is suggested that As_2O_3 at low concentrations (0.1–0.5 μM) induces differentiation of malignant promyelocytes through inactivation of the *PML-RAR α* fusion protein, while at high concentrations (0.5–2.0 μM) As_2O_3 triggers apoptosis of the promyelocytes and other cancer cells through several different mechanisms (Dilda and Hogg 2007). The metalloid also induces proliferation arrest in a number of cancer cells, and is currently being tested for the treatment of hematological malignancies and solid tumors, which are mostly refractory to current therapies (Dilda and Hogg 2007; Verstovsek et al. 2006). To appreciate the action of arsenical-containing drugs, it is important to elucidate the pathways of drug uptake, factors that modulate the uptake, as well as regulation of drug uptake pathways.

Overexpression of AQP3, in addition to AQP7 and AQP9, has been shown to render human leukemia cells hypersensitive to the metalloids as a result of higher steady state levels of accumulation (Mukhopadhyay et al., unpublished data and Bhattacharjee et al. 2004). Sensitivity to As_2O_3 has been found to be directly proportional to AQP9 expression in leukemia cells of different lineages (Leung et al. 2007). The APL cell line NB4 showed the highest expression level of AQP9 and is most sensitive to As_2O_3 . In contrast, the chronic myeloid leukemia cell line K562 showed very low endogenous AQP9 expression and is insensitive to As_2O_3 . When human AQP9 was overexpressed either in K562 or the promyelocytic leukemia cell line HL60, both became hypersensitive to As(III) and Sb(III), due to higher accumulation of the metalloids (Bhattacharjee et al. 2004; Leung et al. 2007).

Pretreatment of HL60 cells with vitamin D showed higher expression of AQP9 and hypersensitivity to both As(III) and Sb(III). This sensitivity was due to higher rates of uptake of the trivalent metalloids due to increased expression of AQP9 drug uptake system (Bhattacharjee et al. 2004). Also, pretreatment of HL60 cells with all-trans retinoic acid (ATRA) upregulated AQP9 expression, leading to a significantly increased arsenic uptake (Leung et al. 2007). This may explain the improved response from APL patients when treated concomitantly with ATRA and As_2O_3 (Aribi et al. 2007; Zhou et al. 2007). Drug hypersensitivity can therefore be correlated with increased expression of the drug uptake system. The possibility of using pharmacological agents to increase AQP9 expression delivers the promise of new therapies for the treatment of leukemia.

Is it possible for cancer cells to become arsenic resistant by downregulating aquaglyceroporin expression? Lee et al. (2006) examined the expression of AQPs in an arsenic-resistant cell line (R15) derived from a human lung adenocarcinoma cell line (CL3). R15 cells were tenfold more resistant to $As(OH)_3$ than the parental CL3 cells. R15 cells accumulated less $As(OH)_3$ and expressed little AQP7 or AQP9, but AQP3 mRNA levels were twofold lower than in CL3 cells. When AQP3 expression in CL3 cells was knocked down by RNA interference, the cells exhibited a reduction in $As(OH)_3$ uptake and an increase in resistance. Moreover, overexpression of AQP3 in the human embryonic kidney 293T cells resulted in an increase

in both accumulation of and sensitivity to $\text{As}(\text{OH})_3$. Therefore downregulation of aquaglyceroporin expression may lead to metalloid resistance phenotype.

Little is known about how signaling proteins and transcriptional regulators sense the presence of metalloids and activate aquaglyceroporin channels in eukaryotes. It has been shown that hyperosmotic stress induced by mannitol increased the expression of AQP4 and AQP9 in cultured rat astrocytes, while a p38 mitogen-activated protein kinase (MAPK) inhibitor suppressed their expression (Arima et al. 2003). This suggested that modulation of MAPK activity would affect the expression of AQPs. Verma et al. (2002) have shown that As_2O_3 induces activation of the p38 MAPK in leukemia cell lines. Pharmacological inhibition of p38 MAPK potentiated arsenic-dependent apoptosis and suppression of growth of leukemia cell lines, suggesting that this signaling cascade negatively regulates induction of anti-leukemic responses by As_2O_3 . A direct link has been established between the regulation of aquaglyceroporins by MAPK and metalloid transport in *S. cerevisiae* (Thorsen et al. 2006). *S. cerevisiae* Hog1p is a homologue of p38 MAPK. Cells impaired in Hog1p function are metalloid hypersensitive, whereas cells with elevated Hog1p activity displayed improved tolerance. Hog1p is phosphorylated in response to $\text{As}(\text{III})$, which remains primarily cytoplasmic and does not mediate a major transcriptional response. Instead, *hog1Δ* strains show elevated cellular arsenic levels due to increased $\text{As}(\text{III})$ influx, which is mediated by the aquaglyceroporin, Fps1p. Moreover, Hog1p was also shown to affect Fps1p phosphorylation, and this phosphorylation led to reduced uptake of $\text{As}(\text{III})$ and $\text{Sb}(\text{III})$. This suggests that downregulation of MAPK activity may be an effective way to sensitize cells by increasing metalloid influx, thereby inhibiting malignant cell growth.

3.2 Metalloid Transport and Antiprotozoal Activity

Leishmaniasis is a parasitic protozoan disease of the genus *Leishmania* that is transmitted to humans via the bite of sandflies. The disease is endemic in parts of 88 countries across five continents, and the majority of the affected countries are in the tropics and subtropics. Approximately 12 million people worldwide are affected by leishmaniasis, while a total of 350 million people are at a risk of contracting the disease (<http://www.who.int/tdr/diseases/leish/>). The *Leishmania* parasite exists in two forms: the promastigote form resides within the insect vector, while the amastigote form resides in macrophages and other mononuclear phagocytes in the mammalian host. The 20 or so infective species and subspecies of the parasite cause a range of symptoms from simple self-healing skin ulcers, to severe life-threatening symptoms. Furthermore, *Leishmania*/HIV co-infection is currently emerging as an extremely serious new disease among persons who are immunosuppressed, particularly in patients infected with human immunodeficiency virus (Choi and Lerner 2002; Silva et al. 2002). Treatment of leishmaniasis often requires a long course of pentavalent antimonials such as sodium stibogluconate (Pentostam) or meglumine antimonate (Glucantime). Clinical resistance to this treatment is becoming prevalent

(Faraut-Gambarelli et al. 1997; Jackson et al. 1990). In fact, more than 50% of visceral leishmaniasis cases in Northeast India are resistant to Pentostam (Sundar et al. 2000).

Despite being used for several decades, the mode of action of pentavalent antimonials is poorly understood. The possibility of in vivo metabolic conversion of pentavalent [Sb(V)] to trivalent [Sb(III)] antimonials was suggested more than 50 years ago (Goodwin 1995). Several investigators have shown that Sb(III) is more toxic than Sb(V) to either the promastigote or amastigote forms of different *Leishmania* species (Mottram and Coombs 1985; Roberts et al. 1995; Sereno and Lemesre 1997). It has been suggested that a putative metalloid reductase residing within the macrophage catalyzes the conversion of Sb(V) to Sb(III) (Sereno et al. 1998). To exert its antiparasitic action, the internally generated antimonite enters the parasite through an aquaglyceroporin (Gourbal et al. 2004).

The *Leishmania major* genome encodes for five AQPs: LmAQP1, LmAQP α , LmAQP β , LmAQP γ , and LmAQP δ . LmAQP1 shows strong similarity to bacterial AQPs, while the other *L. major* aquaporins (LmAQP $\alpha - \delta$) are closer to plant AQPs. This is a peculiarity of LmAQPs, because other parasitic AQPs known, to date, are either bacteria- or plant-like, and not a mixed population (Beitz 2005). However, this should not be surprising, as trypanosomatids such as *Leishmania*, which are in the phylum Euglenozoa, have a number of plant-like genes and probably had plastids that were lost when they diverged from true plants (Hannaert et al. 2003). Only LmAQP1 has been studied in some detail, while the roles of the other LmAQPs are yet to be established. LmAQP1 belongs to the intermediate class of water channels; its water conduction capacity is 65% that of AQP1, which is a classical water channel. Interestingly, in contrast to *Plasmodium* and *Trypanosome* AQPs that are inhibited by mercurials, LmAQP1 water movement is not inhibited by HgCl₂, thereby classifying LmAQP1 as a mercurial independent water channel. LmAQP1 also conducts glycerol, glyceraldehyde, and dihydroxyacetone. In contrast, there is negligible urea conduction by LmAQP1, and this property probably helps the parasite to survive the hostile environment of liver cells (Figarella et al. 2007). LmAQP1 is localized exclusively to the flagellum of promastigotes, while in amastigotes it is found in the flagellar pocket, rudimentary flagellum, and contractile vacuoles. LmAQP1 plays an important physiological role in water and solute transport, volume regulation, and osmotaxis. These properties help the parasite to face the osmotic challenges during a swim towards the proboscis of the sandfly and transmission to the vertebrate host (Figarella et al. 2007).

LmAQP1 was also shown to be a metalloid transporter. Transfection of LmAQP1 into three different species of *Leishmania* (*Leishmania tarentolae*, *Leishmania infantum*, and *Leishmania major*) produced hypersensitivity to both As(III) and Sb(III) in all three strains (Gourbal et al. 2004). LmAQP1 expression in a variety of drug resistant parasites also restored metalloid sensitivity in every strain, independent of the mechanism of resistance. Transport experiments indicated that this hypersensitivity was caused by an increased rate of uptake of Sb(III) or As(III) in the promastigotes, consistent with increased amounts of the LmAQP1 channel. Upon disruption of one of the two *LmAQP1* alleles in *L. major*, the disrupted strain

showed a tenfold increase in resistance to trivalent antimony, compared to the wild-type. Also, overexpression of LmAQP1 in either the promastigote or amastigote forms of drug-resistant field isolates of *L. donovani* from India results in marked hypersensitivity to Pentostam (Mukhopadhyay et al. unpublished data). These results indicate that a major route of entry of trivalent antimony, the activated form of Pentostam or Glucantime, into *Leishmania* is catalyzed by LmAQP1 (Fig. 2). Significantly, the results also demonstrate that loss of LmAQP1 can produce resistance and that increased expression of LmAQP1 in drug-resistant parasites can reverse resistance (Gourbal et al. 2004). Downregulation of LmAQP1 leads to drug resistance. LmAQP1 mRNA was shown to be significantly decreased in either the Sb(III)- or As(III)- resistant *L. major* and *L. tarentolae* cells (Marquis et al. 2005). Similarly, Pentostam-resistant field isolates of *L. donovani* from Nepal showed downregulation of AQP1, leading to reduced uptake of antimonite (Decuyperre et al. 2005). It is therefore clearly evident that aquaglyceroporins play a major role in *Leishmania* cellular physiology and drug resistance. Therefore, modulation of expression of *Leishmania* aquaglyceroporin channels by pharmacological agents may be an effective way of combating the drug-resistant form of the parasite.

Human African trypanosomiasis (HAT), or sleeping sickness, is a parasitic disease caused by protozoa of the genus *Trypanosoma* and transmitted by the tsetse fly. This disease constitutes a serious public health threat in Africa, particularly in central Africa, where approximately 60 million persons are at risk of contracting the disease. The disease has reached epidemic proportions in Sudan, Uganda, the Democratic Republic of Congo, and Angola, with a prevalence of over 20% in some areas. HAT develops in two stages, the first involving the hemolymphatic system, and the second, the neurological system. Left untreated, HAT is invariably fatal. Stage 1 of the disease is usually treated with intravenous Pentamidine or Suramin, but the later stage (stage 2) can only be treated with Melarsoprol, a trivalent organoarsenical (Bouteille et al. 2003). Although Melarsoprol has been used against HAT for many years, its mode of action is still largely unknown, and is proposed to be a non-specific inhibitor of many different enzymes (Wang 1995). Resistance to Melarsoprol therapy have been reported and linked to diminished drug uptake (de Koning 2001).

The role of aquaglyceroporins in metalloloid transport in trypanosomes is currently being investigated. *Trypanosoma brucei*, causative for HAT, contains three aquaglyceroporins, TbAQP1–3, which show a 40–45% identity to the mammalian AQP3 and 9. For functional characterization, all three proteins were heterologously expressed in yeast and *Xenopus* oocytes. When expressed in the yeast *fps1*Δ mutant, each of the TbAQPs suppressed hypoosmosensitivity and rendered cells to a hyperosmosensitive phenotype, as expected for unregulated glycerol channels. Under iso- and hyperosmotic conditions, these cells constitutively released glycerol, consistent with a glycerol efflux function of TbAQP proteins. TbAQP expression in *Xenopus* oocytes increased permeability for water, glycerol, and dihydroxyacetone. Except for urea, TbAQPs were virtually impermeable to other polyols; only TbAQP3 transported erythritol and ribitol (Uzcategui et al. 2004). The expression profile of *TbAQP* transcripts suggests a distinct importance of the respective

proteins throughout the life cycle. TbAQP3 is the major AQP in the logarithmically growing slender blood stream form, whereas, *TbAQP1* is heavily expressed in the stationary phase stumpy bloodstream form. *TbAQP2* is scarcely expressed in all three life stages examined, and may be a candidate for organelle localization. Each of the TbAQPs is able to transport either As(III) or Sb(III) (Mukhopadhyay and Duszenko, unpublished data). However, their roles in Melarsoprol transport, and whether downregulation of TbAQPs leads to drug-resistant parasites, remain open questions.

4 Concluding Remarks

Human exposure to inorganic arsenic occurs mainly through ingestion of drinking water contaminated with naturally occurring arsenic. Chronic arsenic poisoning is becoming an emerging epidemic in Asia, where over 100 million people are exposed to underground water with high concentrations of arsenic (Wang et al. 2007). Epidemiological studies have shown that chronic arsenic poisoning through ingestion of arsenic-contaminated water is associated with such effects as gastroenteritis, neurological manifestations, cardiovascular diseases, diabetes, and cancers (Abernathy et al. 2003; Wang et al. 2007). These effects increase in severity based on the concentration and duration of arsenic exposure. The interaction between genetic, environmental, and nutritional factors may play an important role in arsenic-induced diseases in the human population.

Factors that modulate aquaglyceroporin expression in different tissues may play a role in arsenic toxicity. For example, expression of AQP9 is increased several-fold in the liver by starvation and in uncontrolled diabetes mellitus. AQP9 expression fluctuates depending on the nutritional status of the subject and the circulating insulin levels (Carbrey et al. 2003). Thus, people suffering from malnutrition and also exposed to arsenic from drinking water are more at risk of hepatic arsenic toxicity (Agre and Kozono 2003). Butler et al. (2006) have shown that AQP3, 7, and 9 are expressed in human cardiac cells. Therefore, factors that influence increased AQP expression will lead to increased influx of arsenite into cardiac cells, leading to serious cardiac problems. Several studies have indicated that AQP9 is under the control of steroid hormones in rat epididymal cells (Pastor-Soler et al. 2002), cAMP in cultured rat astrocytes (Yamamoto et al. 2002), and glucagon in porcine hepatic tissue (Caperna et al. 2007). Factors that modulate the hormone status of individuals can therefore affect aquaglyceroporin expression, and consequently influence arsenic transport and accompanying toxicity in different organs and tissues. The relationship between aquaglyceroporin expression, arsenic transport, and consequent pharmacological response is much in its infancy, and more research is needed before we begin to fully appreciate their roles in human health and diseases.

Acknowledgments This work was supported by National Institutes of Health Grants AI58170, GM52216, and GM55425.

References

- Abedin MJ, Cresser MS, Meharg AA, Feldmann J, Cotter-Howells J (2002) Arsenic accumulation and metabolism in rice (*Oryza sativa* L.). *Environ Sci Technol* 36:962–968
- Abernathy CO, Thomas DJ, Calderon RL (2003) Health effects and risk assessment of arsenic. *J Nutr* 133:1536S–1538S
- Agre P, Kozono D (2003) Aquaporin water channels: molecular mechanisms for human diseases. *FEBS Lett* 555:72–78
- Aribi A, Kantarjian HM, Estey EH, Koller CA, Thomas DA, Kornblau SM, Faderl SH, Laddie NM, Garcia-Manero G, Cortes JE (2007) Combination therapy with arsenic trioxide, all-trans retinoic acid, and gemtuzumab ozogamicin in recurrent acute promyelocytic leukemia. *Cancer* 109:1355–1359
- Arima H, Yamamoto N, Sobue K, Umenishi F, Tada T, Katsuya H, Asai K (2003) Hyperosmolar mannitol simulates expression of aquaporins 4 and 9 through a p38 mitogen-activated protein kinase-dependent pathway in rat astrocytes. *J Biol Chem* 278:44525–44534
- Aronson SM (1994) Arsenic and old myths. *R I Med* 77:233–234
- Beitz E (2005) Aquaporins from pathogenic protozoan parasites: structure, function and potential for chemotherapy. *Biol Cell* 97:373–383
- Bhattacharjee H, Rosen BP (2007) Arsenic metabolism in prokaryotic and eukaryotic microbes. In: Nies DH, Silver S (eds.) *Molecular microbiology of heavy metals*. Springer, Berlin/Heidelberg, pp. 371–406
- Bhattacharjee H, Carbrey J, Rosen BP, Mukhopadhyay R (2004) Drug uptake and pharmacological modulation of drug sensitivity in leukemia by AQP9. *Biochem Biophys Res Commun* 322:836–841
- Bobrowicz P, Wysocki R, Owsianik G, Goffeau A, Ulaszewski S (1997) Isolation of three contiguous genes, *ACRI*, *ACR2* and *ACR3*, involved in resistance to arsenic compounds in the yeast *Saccharomyces cerevisiae*. *Yeast* 13:819–828
- Bouteille B, Oukem O, Bisser S, Dumas M (2003) Treatment perspectives for human African trypanosomiasis. *Fundam Clin Pharmacol* 17:171–181
- Brown D, Kogan S, Lagasse E, Weissman I, Alcalay M, Pelicci PG, Atwater S, Bishop JM (1997) A *PMLRARA* transgene initiates murine acute promyelocytic leukemia. *Proc Natl Acad Sci U S A* 94:2551–2556
- Bun-ya M, Shikata K, Nakade S, Yompakdee C, Harashima S, Oshima Y (1996) Two new genes, *PHO86* and *PHO87*, involved in inorganic phosphate uptake in *Saccharomyces cerevisiae*. *Curr Genet* 29:344–351
- Butler TL, Au CG, Yang B, Egan JR, Tan YM, Hardeman EC, North KN, Verkman AS, Winlaw DS (2006) Cardiac aquaporin expression in humans, rats, and mice. *Am J Physiol Heart Circ Physiol* 291:H705–H713
- Caperna TJ, Shannon AE, Richards MP, Garrett WM, Talbot NC (2007) Identification and characterization of aquaporin-9 (AQP9) in porcine hepatic tissue and hepatocytes in monolayer culture. *Domest Anim Endocrinol* 32:273–286
- Carbrey JM, Gorelick-Feldman DA, Kozono D, Praetorius J, Nielsen S, Agre P (2003) Aquaglyceroporin AQP9: solute permeation and metabolic control of expression in liver. *Proc Natl Acad Sci U S A* 100:2945–2950
- Choi CM, Lerner EA (2002) Leishmaniasis: recognition and management with a focus on the immunocompromised patient. *Am J Clin Dermatol* 3:91–105
- Cioli D, Pica-Mattoccia L, Archer S (1995) Antischistosomal drugs: past, present... and future?. *Pharmacol Ther* 68:35–85
- Cole SP, Sparks KE, Fraser K, Loe DW, Grant CE, Wilson GM, Deeley RG (1994) Pharmacological characterization of multidrug resistant MRP-transfected human tumor cells. *Cancer Res* 54:5902–5910
- de Koning HP (2001) Transporters in African trypanosomes: role in drug action and resistance. *Int J Parasitol* 31:512–522

- Decuyper S, Rijal S, Yardley V, De Doncker S, Laurent T, Khanal B, Chappuis F, Dujardin JC (2005) Gene expression analysis of the mechanism of natural Sb(V) resistance in *Leishmania donovani* isolates from Nepal. *Antimicrob Agents Chemother* 49:4616–4621
- Denton H, McGregor JC, Coombs GH (2004) Reduction of anti-leishmanial pentavalent antimonial drugs by a parasite-specific thiol-dependent reductase, TDR1. *Biochem J* 381:405–412
- Dilda PJ, Hogg PJ (2007) Arsenical-based cancer drugs. *Cancer Treat Rev* 33:542–564
- Faraut-Gambarelli F, Piarroux R, Deniau M, Giusiano B, Marty P, Michel G, Faugere B, Dumon H (1997) In vitro and in vivo resistance of *Leishmania infantum* to meglumine antimoniate: a study of 37 strains collected from patients with visceral leishmaniasis. *Antimicrob Agents Chemother* 41:827–830
- Figarella K, Uzcategui NL, Zhou Y, Lefurgey A, Ouellette M, Bhattacharjee H, Mukhopadhyay R (2007) Biochemical characterization of *Leishmania major* aquaglyceroporin LmAQP1: possible role in volume regulation and osmotaxis. *Mol Microbiol* 65:1006–1017
- Fu D, Libson A, Miercke LJ, Weitzman C, Nollert P, Krucinski J, Stroud RM (2000) Structure of a glycerol-conducting channel and the basis for its selectivity. *Science* 290:481–486
- Ghosh M, Shen J, Rosen BP (1999) Pathways of As(III) detoxification in *Saccharomyces cerevisiae*. *Proc Natl Acad Sci U S A* 96:5001–5006
- Goodwin LG (1995) Pentostam (sodium stibogluconate); a 50-year personal reminiscence. *Trans R Soc Trop Med Hyg* 89:339–341
- Gourbal B, Sonuc N, Bhattacharjee H, Legare D, Sundar S, Ouellette M, Rosen BP, Mukhopadhyay R (2004) Drug uptake and modulation of drug resistance in *Leishmania* by an aquaglyceroporin. *J Biol Chem* 279:31010–31017
- Hannaert V, Saavedra E, Duffieux F, Szikora JP, Rigden DJ, Michels PA, Opperdoes FR (2003) Plant-like traits associated with metabolism of *Trypanosoma* parasites. *Proc Natl Acad Sci U S A* 100:1067–1071
- Hara-Chikuma M, Verkman AS (2006) Physiological roles of glycerol-transporting aquaporins: the aquaglyceroporins. *Cell Mol Life Sci* 63:1386–1392
- Healy SM, Casarez EA, Ayala-Fierro F, Aposhian H (1998) Enzymatic methylation of arsenic compounds. V. Arsenite methyltransferase activity in tissues of mice. *Toxicol Appl Pharmacol* 148:65–70
- Hughes MF, Kenyon EM, Edwards BC, Mitchell CT, Razo LM, Thomas DJ (2003) Accumulation and metabolism of arsenic in mice after repeated oral administration of arsenate. *Toxicol Appl Pharmacol* 191:202–210
- Jackson JE, Tally JD, Ellis WY, Mebrahtu YB, Lawyer PG, Were JB, Reed SG, Panisko DM, Limmer BL (1990) Quantitative in vitro drug potency and drug susceptibility evaluation of *Leishmania* ssp. from patients unresponsive to pentavalent antimony therapy. *Am J Trop Med Hyg* 43:464–480
- Kala SV, Neely MW, Kala G, Prater CI, Atwood DW, Rice JS, Lieberman MW (2000) The MRP2/cMOAT transporter and arsenic-glutathione complex formation are required for biliary excretion of arsenic. *J Biol Chem* 275:33404–33408
- Kenyon EM, Del Razo LM, Hughes MF (2005) Tissue distribution and urinary excretion of inorganic arsenic and its methylated metabolites in mice following acute oral administration of arsenate. *Toxicol Sci* 85:468–475
- King LS, Kozono D, Agre P (2004) From structure to disease: the evolving tale of aquaporin biology. *Nat Rev Mol Cell Biol* 5:687–698
- Klaassen CD (1996) Heavy metals and heavy metal antagonists. McGraw-Hill, New York
- Kwong YL, Todd D (1997) Delicious poison: arsenic trioxide for the treatment of leukemia. *Blood* 89:3487–3488
- Lee TC, Ho IC, Lu WJ, Huang JD (2006) Enhanced expression of multidrug resistance-associated protein 2 and reduced expression of aquaglyceroporin 3 in an arsenic-resistant human cell line. *J Biol Chem* 281:18401–18407
- Leung J, Pang A, Yuen WH, Kwong YL, Tse EW (2007) Relationship of expression of aquaglyceroporin 9 with arsenic uptake and sensitivity in leukemia cells. *Blood* 109:740–746

- Liu J, Chen H, Miller DS, Saavedra JE, Keefer LK, Johnson DR, Klaassen CD, Waalkes MP (2001) Overexpression of glutathione S-transferase II and multidrug resistance transport proteins is associated with acquired tolerance to inorganic arsenic. *Mol Pharmacol* 60:302–309
- Liu Z, Shen J, Carbrey JM, Mukhopadhyay R, Agre P, Rosen BP (2002) Arsenite transport by mammalian aquaglyceroporins AQP7 and AQP9. *Proc Natl Acad Sci U S A* 99:6053–6058
- Liu Z, Carbrey JM, Agre P, Rosen BP (2004) Arsenic trioxide uptake by human and rat aquaglyceroporins. *Biochem Biophys Res Commun* 316:1178–1185
- Liu Z, Styblo M, Rosen BP (2006) Methylarsonous acid transport by aquaglyceroporins. *Environ Health Perspect* 114:527–531
- Marquis N, Gourbal B, Rosen BP, Mukhopadhyay R, Ouellette M (2005) Modulation in aquaglyceroporin *AQP1* gene transcript levels in drug-resistant *Leishmania*. *Mol Microbiol* 57:1690–1699
- Meng YL, Liu Z, Rosen BP (2004) As(III) and Sb(III) uptake by GlpF and efflux by ArsB in *Escherichia coli*. *J Biol Chem* 279:18334–18341
- Mottram JC, Coombs GH (1985) *Leishmania mexicana*: enzyme activities of amastigotes and promastigotes and their inhibition by antimonials and arsenicals. *Exp Parasitol* 59:151–160
- Mukhopadhyay R, Shi J, Rosen BP (2000) Purification and characterization of Acr2p, the *Saccharomyces cerevisiae* arsenate reductase. *J Biol Chem* 275:21149–21157
- Muramatsu S, Mizuno T (1989) Nucleotide sequence of the region encompassing the *glpKF* operon and its upstream region containing a bent DNA sequence of *Escherichia coli*. *Nucleic Acids Res* 17:4378
- Pastor-Soler N, Isnard-Bagnis C, Herak-Kramberger C, Sabolic I, Van Hoek A, Brown D, Breton S (2002) Expression of aquaporin 9 in the adult rat epididymal epithelium is modulated by androgens. *Biol Reprod* 66:1716–1722
- Porquet A, Filella M (2007) Structural evidence of the similarity of Sb(OH)₃ and As(OH)₃ with glycerol: implications for their uptake. *Chem Res Toxicol* 20:1269–1276
- Ramirez-Solis A, Mukopadhyay R, Rosen BP, Stemmler TL (2004) Experimental and theoretical characterization of arsenite in water: insights into the coordination environment of As-O. *Inorg Chem* 43:2954–2959
- Richey DP, Lin EC (1972) Importance of facilitated diffusion for effective utilization of glycerol by *Escherichia coli*. *J Bacteriol* 112:784–790
- Roberts WL, Berman JD, Rainey PM (1995) In vitro antileishmanial properties of tri- and pentavalent antimonial preparations. *Antimicrob Agents Chemother* 39:1234–1239
- Rosenberg H, Gerdes RG, Chegwiddden K (1977) Two systems for the uptake of phosphate in *Escherichia coli*. *J Bacteriol* 131:505–511
- Sanders OI, Rensing C, Kuroda M, Mitra B, Rosen BP (1997) Antimonite is accumulated by the glycerol facilitator GlpF in *Escherichia coli*. *J Bacteriol* 179:3365–3367
- Sanno Y, Wilson TH, Lin EC (1968) Control of permeation to glycerol in cells of *Escherichia coli*. *Biochem Biophys Res Commun* 32:344–349
- Sereno D, Lemesre JL (1997) Axenically cultured amastigote forms as an in vitro model for investigation of antileishmanial agents. *Antimicrob Agents Chemother* 41:972–976
- Sereno D, Cavaleyra M, Zemzoumi K, Maquaire S, Ouaisi A, Lemesre JL (1998) Axenically grown amastigotes of *Leishmania infantum* used as an in vitro model to investigate the pentavalent antimony mode of action. *Antimicrob Agents Chemother* 42:3097–3102
- Silva ES, Pacheco RS, Gontijo CM, Carvalho IR, Brazil RP (2002) Visceral leishmaniasis caused by *Leishmania (Viannia) braziliensis* in a patient infected with human immunodeficiency virus. *Rev Inst Med Trop Sao Paulo* 44:145–149
- Soignet SL, Maslak P, Wang ZG, Jhanwar S, Calleja E, Dardashti LJ, Corso D, DeBlasio A, Gabrilove J, Scheinberg DA, Pandolfi PP, Warrell RPJ Jr (1998) Complete remission after treatment of acute promyelocytic leukemia with arsenic trioxide. *N Engl J Med* 339:1341–1348
- Staff NRC (1999) Arsenic in drinking water. National Academy Press, Washington, DC
- Sui H, Han BG, Lee JK, Walian P, Jap BK (2001) Structural basis of water-specific transport through the AQP1 water channel. *Nature* 414:872–878

- Sundar S, More DK, Singh MK, Singh VP, Sharma S, Makharia A, Kumar PC, Murray HW (2000) Failure of pentavalent antimony in visceral leishmaniasis in India: report from the center of the Indian epidemic. *Clin Infect Dis* 31:1104–1107
- Sweet G, Gandor C, Voegelé R, Wittekindt N, Beuerle J, Truniger V, Lin EC, Boos W (1990) Glycerol facilitator of *Escherichia coli*: cloning of *glpF* and identification of the *glpF* product. *J Bacteriol* 172:424–430
- Thomas DJ, Waters SB, Styblo M (2004) Elucidating the pathway for arsenic methylation. *Toxicol Appl Pharmacol* 198:319–326
- Thorsen M, Di Y, Tangemo C, Morillas M, Ahmadvour D, Van der Does C, Wagner A, Johansson E, Boman J, Posas F, Wysocki R, Tamas MJ (2006) The MAPK Hog1p modulates Fps1p-dependent arsenite uptake and tolerance in yeast. *Mol Biol Cell* 17:4400–4410
- Uzcategui NL, Szallies A, Pavlovic-Djuranovic S, Palmada M, Figarella K, Boehmer C, Lang F, Beitz E, Duszenko M (2004) Cloning, heterologous expression, and characterization of three aquaglyceroporins from *Trypanosoma brucei*. *J Biol Chem* 279:42669–42676
- Verma A, Mohindru M, Deb DK, Sassano A, Kambhampati S, Ravandi F, Minucci S, Kalvakolanu DV, Platanias LC (2002) Activation of Rac1 and the p38 mitogen-activated protein kinase pathway in response to arsenic trioxide. *J Biol Chem* 277:44988–44995
- Verstovsek S, Giles F, Quintas-Cardama A, Perez N, Ravandi-Kashani F, Beran M, Freireich E, Kantarjian H (2006) Arsenic derivatives in hematologic malignancies: a role beyond acute promyelocytic leukemia? *Hematol Oncol* 24:181–188
- Wang CC (1995) Molecular mechanisms and therapeutic approaches to the treatment of African trypanosomiasis. *Annu Rev Pharmacol Toxicol* 35:93–127
- Wang CH, Hsiao CK, Chen CL, Hsu LI, Chiou HY, Chen SY, Hsueh YM, Wu MM, Chen CJ (2007) A review of the epidemiologic literature on the role of environmental arsenic exposure and cardiovascular diseases. *Toxicol Appl Pharmacol* 222:315–326
- Willsky GR, Malamy MH (1980a) Characterization of two genetically separable inorganic phosphate transport systems in *Escherichia coli*. *J Bacteriol* 144:356–365
- Willsky GR, Malamy MH (1980b) Effect of arsenate on inorganic phosphate transport in *Escherichia coli*. *J Bacteriol* 144:366–374
- Wysocki R, Bobrowicz P, Ulaszewski S (1997) The *Saccharomyces cerevisiae* *ACR3* gene encodes a putative membrane protein involved in arsenite transport. *J Biol Chem* 272:30061–30066
- Wysocki R, Chery CC, Wawrzycka D, Van Hulle M, Cornelis R, Thevelein JM, Tamas MJ (2001) The glycerol channel Fps1p mediates the uptake of arsenite and antimonite in *Saccharomyces cerevisiae*. *Mol Microbiol* 40:1391–1401
- Yamamoto N, Sobue K, Fujita M, Katsuya H, Asai K (2002) Differential regulation of aquaporin-5 and -9 expression in astrocytes by protein kinase A. *Brain Res Mol Brain Res* 104:96–102
- Yang HC, Cheng J, Finan TM, Rosen BP, Bhattacharjee H (2005) Novel pathway for arsenic detoxification in the legume symbiont *Sinorhizobium meliloti*. *J Bacteriol* 187:6991–6997
- Zaman GJ, Lankelma J, van Tellingen O, Beijnen J, Dekker H, Paulusma C, Oude Elferink RP, Baas F, Borst P (1995) Role of glutathione in the export of compounds from cells by the multidrug-resistance-associated protein. *Proc Natl Acad Sci USA* 92:7690–7694
- Zardoya R (2005) Phylogeny and evolution of the major intrinsic protein family. *Biol Cell* 97:397–414
- Zhou Y, Messier N, Ouellette M, Rosen BP, Mukhopadhyay R (2004) *Leishmania major* LmACR2 is a pentavalent antimony reductase that confers sensitivity to the drug pentostam. *J Biol Chem* 279:37445–37451
- Zhou GB, Zhang J, Wang ZY, Chen SJ, Chen Z (2007) Treatment of acute promyelocytic leukaemia with all-trans retinoic acid and arsenic trioxide: a paradigm of synergistic molecular targeting therapy. *Philos Trans R Soc Lond B Biol Sci* 362:959–971

Ammonia and Urea Permeability of Mammalian Aquaporins

Thomas Litman, Rikke Sogaard, and Thomas Zeuthen

Contents

1	Introduction	328
2	Electrochemical Models of Ammonia Transport	332
2.1	Transport Equations	332
2.2	How to Distinguish between Transport Modes	334
3	Experimental Evidence for Ammonia Transport	338
3.1	Permeability of NH_3 , Quantitative Measurements	338
3.2	Permeability of NH_3 , Qualitative Estimates from Reflection Coefficients	339
3.3	In which Form does Ammonia Permeate? Evidence from Electrophysiology	341
4	Molecular Structure and Ammonia Permeability	343
4.1	The Molecular Signature of Ammonia-Permeable Aquaporins	347
4.2	Single Mutations can Abolish or Induce Ammonia Permeability in Aquaporins	348
5	Physiological Relevance of Ammonia Permeability in Aquaporins	349
5.1	Lessons from Simpler Organisms	350
5.2	Tissue Distribution of Ammonia Permeable Aquaporins in Mammals	350
5.3	Colocalization of Aquaporins, Rh Proteins, and Urea Transporters	352
6	General Summary	353
	References	354

Abstract The human aquaporins, AQP3, AQP7, AQP8, AQP9, and possibly AQP10, are permeable to ammonia, and AQP7, AQP9, and possibly AQP3, are permeable to urea. In humans, these aquaporins supplement the ammonia transport of the Rhesus (Rh) proteins and the urea transporters (UTs). The mechanism by which ammonium is transported by aquaporins is not fully resolved. A comparison of transport equations, models, and experimental data shows that ammonia is transported in its neutral form, NH_3 . In the presence of NH_3 , the aquaporin stimulates H^+ transport. Consequently, this transport of H^+ is only significant at alkaline pH. It is debated whether the

T. Zeuthen (✉)

Nordic Center for Water Imbalance Related Disorders. Institute of Cellular and Molecular Medicine, The Panum Institute, Blegdamsvej 3C, University of Copenhagen, DK-2200N, Denmark
tzeuthen@mfi.ku.dk

E. Beitz (ed.), *Aquaporins*, Handbook of Experimental Pharmacology 190,
© Springer-Verlag Berlin Heidelberg 2009

327

H^+ ion passes via the aquaporin or by some external route; the investigation of this problem requires the aquaporin-expressing cell to be voltage-clamped. The ammonia-permeable aquaporins differ from other aquaporins by having a less restrictive aromatic/arginine region, and an exclusively water-permeable aquaporin can be transformed into an ammonia-permeable aquaporin by single point mutations in this region. The ammonia-permeable aquaporins fall into two groups: those that are permeable (AQP3, 7, 9, 10) and those that are impermeable (AQP8) to glycerol. The two groups differ in the amino acid composition of their aromatic/arginine regions. The location of the ammonia-permeable aquaporins in the body parallels that of the Rh proteins. This applies to erythrocytes and to cells associated with nitrogen homeostasis and high rates of anabolism. In the liver, AQPs 8 and 9 are found together with Rh proteins in cells exposed to portal blood coming from the intestine. In the kidney, AQP3 might participate in the excretion of NH_4^+ in the collecting duct. The interplay between the ammonia-permeable aquaporins and the other types of ammonia- and urea-permeable proteins is not well understood.

1 Introduction

Nitrogen, as a component of amino acids, is vital for all organisms. Most prokaryotes can take up nitrogen as ammonia (NH_3) or ammonium ions (NH_4^+); some can even take up N_2 from the atmosphere, i.e. nitrogen fixation by diazotroph bacteria. (In this review, NH_3 and NH_4^+ are referred to collectively as ammonia; if a distinction is required, the chemical symbols have been used). For higher organisms such as mammals, ammonia is obtained by import and digestion of amino acids in the intestine and the liver. Up to 1 mole of amino groups is metabolized each day by the liver, and the nitrogen is eliminated via the urine in the form of urea, $(NH_2)_2CO$, or NH_4^+ . Ammonia is toxic, and cellular levels have to be precisely regulated. In hepatic failure, blood levels of ammonia increase and fatal brain edema may ensue. The main mechanisms for removal of ammonia are the urea cycle and the conversion of ammonia and glutamate into glutamine, a process catalyzed by glutamine synthase. Thus, in order to sustain various catabolic and anabolic processes and for the body to be under homeostatic control, nitrogen must be transported across membranes, not only as amino acid compounds, but also in the form of NH_3 or NH_4^+ .

The discovery of specific ammonium transporters is relatively new. In mammals, the membrane proteins of the Rhesus-type (Rh) were found to function as ammonia transporters as well as giving rise to the antigens of the red blood cells (Huang and Liu 2001; Liu et al. 2001, 2000; Marini et al. 2000; Westhoff et al. 2002). There are several isoforms of the Rh protein. RhAG is located to the erythrocytes, while other homologues, such as RhBG and RhCG, are found in the liver, kidney, ovary, testes, CNS, or skin. The protein belongs to the ammonium transporter/methylamine permease/Rhesus (Amt/MEP/Rh) protein family. (For reviews, see Huang and Liu 2001; Khademi and Stroud 2006; Winkler 2006.) Amt are found in bacteria, plants, and invertebrates, while MEPs are associated with yeast.

Membrane proteins designed for other purposes such as K^+ channels and NKCC1 ($Na^+/K^+/Cl^-$ cotransporter) have been reported to transport ammonia (Knepper et al. 1989). Gaseous diffusion of NH_3 across the lipid bilayers is also an option.

It was recently discovered that members of an entirely different group of membrane proteins, the aquaporins (AQPs), were able to transport ammonia (Beitz et al. 2006; Holm et al. 2005; Jahn et al. 2004; Loque et al. 2005; Yang et al. 2006a; Zeuthen et al. 2006b). Aquaporins are relatively small (about 26 kDa) pore-forming membrane proteins. As their name implies, they transport water passively in response to osmotic driving forces. Indeed, some of them are exclusively permeable to water, but a large fraction is also permeable to larger substrates such as glycerol, urea and, as will be reviewed here, ammonia. Aquaporins belong to the large major intrinsic protein (MIP) family, which has members in all living organisms (Zardoya 2005). In the present review, we restrict ourselves mainly to the mammalian aquaporins AQP1 to 10; they have physiological significance and their transport properties are well established. AQPs 11 and 12 have been described, but their function and transport properties are unclear at present (Rojek et al. 2008a). For comparison, we include an aquaporin from a plant (TaTIP2;1 from wheat, *Tritium aestivum*), from an eukaryotic microorganism (PfAQP from malaria, *Plasmodium falciparum*), from a bacterium (AQPZ, *Escherichia coli*), and from an archeal microorganism (AQPM, *Methanothermobacter marburgensis*). We also compare to the glycerol transporter GlpF (from *Escherichia coli*), which belongs to the MIP family, but is largely water impermeable (Table 1).

The mammalian aquaporins fall into three functional groups (Fig. 1). The first group comprises the true aquaporins, which are only permeable to water: AQPs 1, 2, 4, 5. AQP6 is a special case; its water permeability is stimulated at low pH and by mercury ions, Hg^{++} (Yasui et al. 1999). When stimulated by Hg^{++} , AQP6 also becomes permeable to glycerol, urea, and anions (Holm et al. 2004; Yasui et al. 1999). Members of the second group (AQPs 3, 7, 9, and possibly 10) are permeable to ammonia, glycerol, and urea, although the ability of AQP3 to transport urea is debated (Meinild et al. 1998; Rojek et al. 2008a). The third group is only permeable to water and ammonia, and has only one member among the mammalian aquaporins (AQP8). This pattern of permeability is not unique, however; aquaporins with the same property are found in plants such as TaTIP2;1 (Jahn et al. 2004). Thus, glycerol permeability implies ammonium permeability and possibly urea permeability but, importantly, the opposite is not the case; ammonium-permeable aquaporins need not be glycerol-permeable. Of the aquaporins AQP10, AQPZ, AQPM, and GlpF, none has been tested directly for ammonia permeability, but when their structures and amino acid sequences are compared to the other aquaporins, it is predicted that AQP10, AQPM and GlpF are permeable to ammonia, while AQPZ is not (see Sect. 4.1).

With the discovery of the ammonia-permeable aquaporins, any formal grouping becomes complicated. There are now three groups: the aquaporins, the aquaglyceroporins, and the aquaammoniaporins (Jahn et al. 2004). This division upon functional lines may be premature, as the precise physiological function of some of these aquaporins is not resolved as yet. For example, AQP8 was recently found to be permeable

Table 1 Permeability and tissue distribution of aquaporins AQP

	H ₂ O	Ammonia	Urea	Glycerol	Tissue or cells
AQP0	(+)	ND	–	–	Eye lens fibers
AQP1	+	–	–	–	Erythrocyte, endothelia, choroid plexus, epithelium, corpus ciliare, kidney proximal tubules, etc
AQP2	+	–	–	–	Kidney collecting duct
AQP3	+	+	(+)	+	Colon, epidermis, airway epithelium, kidney collecting duct, eye
AQP4	+	–	–	–	Astroglial in spinal cord and brain, skeletal muscle
AQP5	+	–	–	–	Alveolar epithelium, glandular epithelia, corneal epithelium
AQP6	(+)	ND	(+)	(+)	Intercalated cells in kidney, organelles
AQP7	+	+	+	+	Adipose tissue, kidney proximal tubule, testis
AQP8	+	+	–	–	Liver, testis, kidney, pancreas
AQP9	(+)	+	+	+	Liver, testis, brain, leucocytes
AQP10	(+)	ND	+	+	Small intestine (intracellular)
AQPZ	+	ND	–	–	Bacteria, <i>Escherichia coli</i>
AQPM	+	ND	–	+	<i>Methanothermobacter marburgensis</i>
PfAQP	+	+	+	+	Malaria, <i>plasmodium falciparum</i>
TaTIP2;1	+	+	–	–	Wheat, <i>Tritium aestivum</i>
GlpF	–	ND	–	+	Bacteria, <i>Escherichia coli</i>

ND not determined. Parenthesis refers to comparatively low permeability. (Permeability data from Beitz et al. 2003; Borgnia et al. 1999; Calamita et al. 1995; Holm et al. 2004; Holm et al. 2005; Holm and Zeuthen 2007; Ishibashi et al. 1997; Ishibashi et al. 2002; Jahn et al. 2004; Kozono et al. 2003; Maurel et al. 1994; Meinild et al. 1998; Yasui et al. 1999; Zeuthen et al. 2006b) For more specific data on tissue distributions, see recent reviews: (Beitz 2006; Calamita 2000; Gonen and Walz 2006; King et al. 2004; Kruse et al. 2008; Rojek et al. 2008a; Verkman 2005)

to hydrogen peroxide, the significance of which is not fully understood (Bienert et al. 2006, 2007). (Also see review by Wu and Beitz 2007.)

The location of the ammonia-permeable aquaporins parallels that of the Rh group of proteins; this applies to the erythrocytes and to the cells associated with either nitrogen homeostasis or high rates of anabolism, as shown in Table 1. In analogy to this, the transport of urea is also taken care of by two distinct groups of proteins: the urea transporters (UTs) (You et al. 1993) and the aquaporins. The UTs are found in a variety of tissues, predominantly in the inner medulla collecting duct of the kidney, but also in the colon, brain, and erythrocytes (Bagnasco 2006). Interestingly, UTs have also been found to be efficient water channels (Ogami et al. 2006; Yang and Verkman 1998). The functional interplay between the aquaporins and the Rh proteins or the UTs has not been investigated.

In this review, we first give a brief description of the chemical properties and electrical manifestations of ammonia transport. This will be essential to define the concentrations and driving forces for the transport across a given cell membrane.

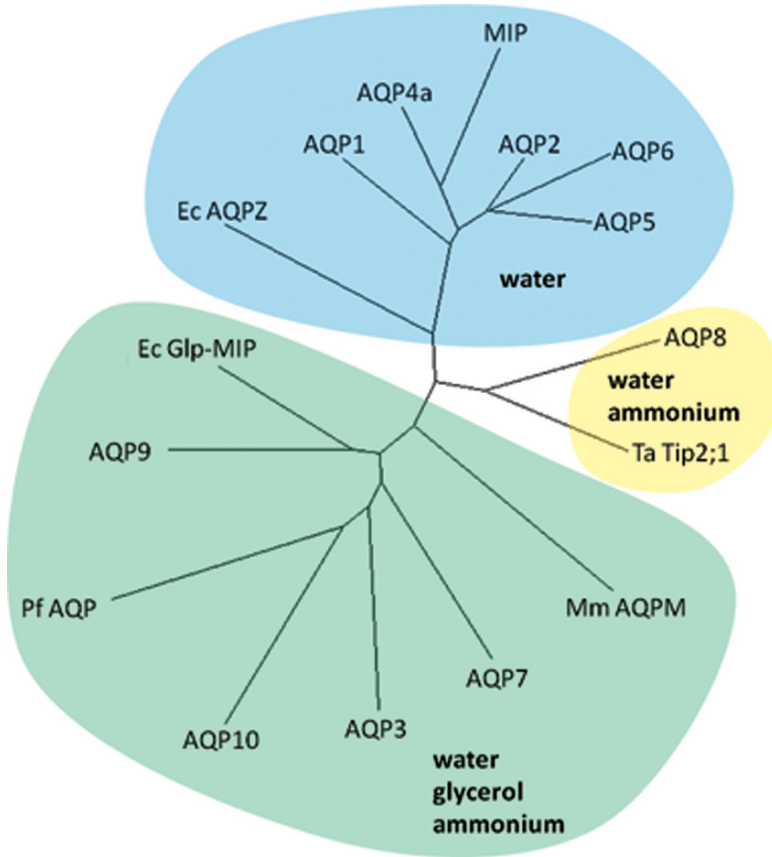


Fig. 1 Phylogenetic tree of aquaporins. The 11 human aquaporins, AQP0 to 10, can be divided into three functional groups: 1. The true aquaporins, which are predominantly permeable to water, comprising AQP0 (also called MIP), AQP1, 2, 4, 5, and 6 (blue background). The bacterial AQPZ (*Escherichia coli*) also belongs to this group. 2. The aquaporins permeable to ammonia and water, which comprises AQP8 (yellow background). The wheat aquaporin, TaTIP2;1 (*Triticum aestivum*) also belongs in this group. 3. The aquaporins permeable to ammonia and glycerol and other small hydrophilic molecules form a group that includes AQP3, 7, 9, and 10 (green background). These are conventionally named aquaglyceroporins. The malaria aquaporin PfAQP (*Plasmodium falciparum*), the glycerol facilitator GlpF-MIP (*Escherichia coli*), and the Achaean AQPM (*Methanothermobacter marburgensis*) also belong to this group. The evolutionary distance between two aquaporins is roughly proportional to the length of the path between them. The radial tree was made in TreeView 1.6.6 (Copyright Roderic DM Page 2001) based on a multiple sequence alignment in ClustalX 2.0

In addition, this will pinpoint the requirements for transport capacity and affinity of various transport mechanisms. Second, we review the evidence for ammonia permeability of aquaporins and discuss in which form ammonia is being transported. Third, we review the molecular structure of aquaporins and the basis for their selectivity. This division of aquaporins is confirmed by the fact that a water-selective

aquaporin can be transformed into an ammonia-permeable aquaporin, and vice-versa, by site-directed mutagenesis. Finally, we review the physiological requirements for ammonia transport and the localization of the ammonia/urea-permeable aquaporins and of the Rh proteins and the urea transporters.

2 Electrochemical Models of Ammonia Transport

Four possible mechanisms for ammonia transport in aquaporins will be considered, as shown in Fig. 2: (a) Ammonia is transported in the neutral form, NH₃. (b) This transport of base leads to the build-up of a transmembrane pH gradient that causes a parallel flux of H⁺ via the lipid cell membrane or some endogenous protein; (c) alternatively, the H⁺ may pass via the aquaporin itself; (d) The aquaporins transport the ion NH₄⁺. The two modes (c) and (d) will be referred to collectively as NH₃ + H⁺ transport. Each of the four modes of transport has specific electrical characteristics, which are recapitulated in the following.

2.1 Transport Equations

In aqueous solutions at physiological pH, the concentration of NH₄⁺ is always far higher than that of the conjugated base NH₃, which is always higher than that of the hydrogen ion H⁺. This can be quantified from equations of mass balance. Under equilibrium conditions:

$$pH = pK + \log\left[\frac{[NH_3]}{[NH_4^+]}\right] \tag{1}$$

where square brackets indicate concentrations. With a pK of 9.25, it is seen that, at physiological pH 7.4, the ammonium ion concentration [NH₄⁺] is about two orders of magnitude higher than that of the ammonia [NH₃]:

$$[NH_3] = [NH_4^+] 10^{pH-pK} \tag{2}$$

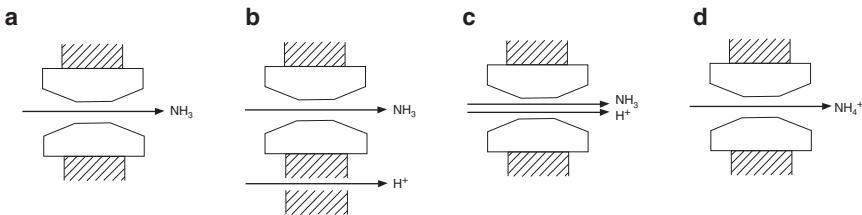


Fig. 2 Four hypotheses for ammonia transport in aquaporins. (a) Ammonia permeates the aqueous pore as NH₃. (b) The entry of NH₃ gives rise to H⁺ conduction by a separate pathway, i.e. the surrounding lipid membrane or an endogenous protein. (c) NH₃ and H⁺ both permeate the aquaporin. (d) Ammonia crosses the aquaporin in its ionic form, NH₄⁺

Thus, with a $[\text{NH}_4^+]$ of 1 mM at pH 7.4, $[\text{NH}_3]$ is 0.014 mM and $[\text{H}^+]$ is 0.00004 mM.

In case of NH_3 transport, the influx $J(\text{NH}_3)$ across a membrane of permeability P_{NH_3} is described by:

$$J(\text{NH}_3) = P_{\text{NH}_3}([\text{NH}_3]_o - [\text{NH}_3]_i) \quad (3)$$

The direction of transport is positive when going from the outside (o) to the inside compartment (i). As discussed above, the concentrations of NH_3 will be small under physiological conditions and very sensitive to the local pH (2). If, for example, the transport takes place into a cell, the influx of NH_3 will increase pH at the inside of the membrane, determined by the local buffer system. These changes in pH_i may be slow (see Sect. 2.2.2) and will affect the value of $[\text{NH}_3]_i$ and thus the driving force for the NH_3 flux. Finally, since the transport is based on substrates at low external concentrations, the transport mechanism should have a relatively high affinity for NH_3 .

In order to study the H^+ flux under well-defined conditions, the electrical potential across the membrane has to be clamped to a fixed value (see Sect. 2.2). The expression for the H^+ flux $J(\text{H}^+)$, (4), will be more complicated than (3), as it depends on the electrical potential difference across the membrane (ΔE). Under simplifying assumptions (see, for example, Hille 1992), the Goldman-Hodgkin-Katz flux equation applies:

$$J(\text{H}^+) = -P_{\text{H}^+} \cdot \frac{\Delta E F}{RT} \cdot \frac{[\text{H}^+]_o - [\text{H}^+]_i \exp(\Delta E \cdot F / RT)}{1 - \exp(\Delta E \cdot F / RT)} \quad (4)$$

where P_{H^+} is the permeability to H^+ , ΔE is the inside electrical potential minus the outside electrical potential, $E_i - E_o$. F is the Faraday constant, R the gas constant, and T the absolute temperature. At room temperature, RT/F amounts to 26 mV. The flux of H^+ is taken as positive when going into the cell. It will be zero when the electrical potential difference across the membrane equals the equilibrium potential E_{eq} for H^+ :

$$\Delta E = -E_i - E_o = E_{\text{eq}} = RT/F \ln[\text{H}^+]_o / [\text{H}^+]_i \quad (5)$$

In electrophysiological experiments, where the outside pH is held at values similar to the intracellular pH, typically between (6) and (7) (i.e. $[\text{H}^+]_i \approx [\text{H}^+]_o$), the equilibrium potential for H^+ will be close to zero.

If the ammonia transport takes place as NH_4^+ transport, the flux $J(\text{NH}_4^+)$, can be described in analogy to (4):

$$J(\text{NH}_4^+) = -P_{\text{NH}_4^+} \frac{\Delta E F}{RT} \frac{[\text{NH}_4^+]_o - [\text{NH}_4^+]_i \exp(\Delta E F / RT)}{1 - \exp(\Delta E F / RT)} \quad (6)$$

where $P_{\text{NH}_4^+}$ is the ammonium ion permeability. The flux of NH_4^+ will be zero when the actual electrical potential difference across the membrane equals the equilibrium potential E_{eq} for NH_4^+ :

$$\Delta E = E_i - E_o = E_{\text{eq}} = RT/F \ln[\text{NH}_4^+]_o / [\text{NH}_4^+]_i \quad (7)$$

In experiments in which the cell is exposed to short-term increases in NH_4^+ concentrations ($[\text{NH}_4^+]_o$ high), the intracellular concentration ($[\text{NH}_4^+]_i$) will remain small, and E_{eq} for NH_4^+ will reach large positive values.

2.2 How to Distinguish between Transport Modes

The discrete mechanisms of ammonia transport: NH_3 transport, $\text{NH}_3 + \text{H}^+$ transport, and NH_4^+ transport (Fig. 2) will manifest themselves differently in terms of electrogenicity, response times, reversal potentials, and affinities, as shown in Table 2.

2.2.1 Electrogenic or Neutral Transport

The question of whether a given transport is electrogenic or neutral has to be resolved in a system in which the voltage across the membrane is clamped. Any current that enters via the protein under investigation has to be compensated by a current of equal magnitude flowing out of the cell. For transporters expressed in larger cells such as *Xenopus* oocytes, voltage clamping is accomplished by inserting two microelectrodes in the cell; one measures the electrical potential and the other supplies the current required to fix the potential at the required value, as shown in Fig. 3a. Take, for example, the entry of NH_4^+ or H^+ via an ammonia transporting protein that has been expressed in a *Xenopus* oocyte. Without voltage clamping, the entry of only a few NH_4^+ or H^+ ions would cause the membrane potential to attain positive values and prevent further entry of NH_4^+ or H^+ . In that case, only entry of neutral forms (e.g. NH_3) would be recorded. An example of the rapid depolarizing

Table 2 How to distinguish between various modes of ammonia transport by electrophysiological measurements

Substrate ^a	Electrogenicity of flux	Changes in flux in response to changes in outside concentrations ^b	Equilibrium potential (mV)	Relative affinity
NH_3	Neutral	Slow	Not defined	Medium
$\text{NH}_3 + \text{H}^+$	Electrogenic	Slow	Around zero for external pHs of 6–7	Very high for H^+
NH_4^+	Electrogenic	Fast	Large, positive	Low

^a It should be emphasized that the case $\text{NH}_3 + \text{H}^+$ does not distinguish between whether H^+ permeates through the aquaporin itself or by some different pathway as, for example, via the surrounding lipid

^b A comparison between the slow response time of the $\text{NH}_3 + \text{H}^+$ transport mediated by AQP8 and the fast response time of the NH_4^+ transport induced by the plant transporter TaAmt1;1 (Jahn et al. 2004) are given in Fig. 5

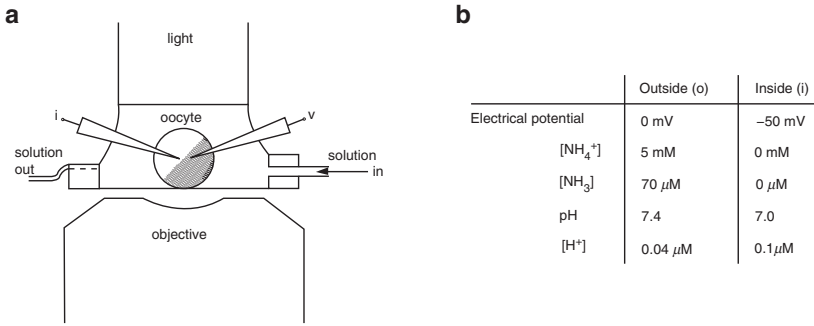


Fig. 3 Oocyte chamber for recording of solute and water transport rates and volume changes. (a) The aquaporin-expressing oocyte is placed on a thin cover glass and light supplied via a Perspex rod that also serves as the upper limitation of the bath. To estimate the rate of influx of osmotically active particles, the oocyte volume is monitored digitally via an inverted microscope. The rate of charge transport is monitored by two-electrode voltage clamp; the intracellular electrical potential is measured by the voltage electrode (*v*), while the current electrode (*i*) records the clamp current at the chosen membrane potential (-50mV). The external solution is exchanged in less than 5 s, and concurrent changes in transport rates, given by the clamp current and by the volume changes, can be monitored at high resolution (Zeuthen et al. 2006a). See also (2)–(7). (b) The table shows values of membrane potential, pH and ammonia concentrations in a typical experimental situation. The external solution contains 5 mM of NH₄⁺, for example in the form of NH₄Cl. At an external pH of 7.4, NH₄⁺ will be in equilibrium with about 70 μM of its conjugated base NH₃ (1). The internal solution is clamped to an electrical potential of -50mV relative to the outside. The intracellular pH is typically between 6 and 7

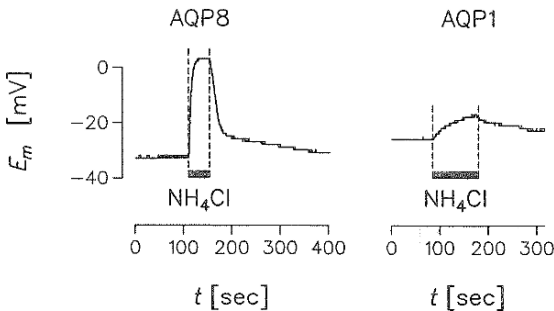


Fig. 4 The effects of NH₄⁺ on the membrane potential *E_m* of unclamped AQP8- and AQP1-expressing oocytes. The effects of the isosmotic addition of 20mmol L⁻¹ of NH₄Cl (replacing NaCl) at pH of 7.4 were investigated. This induced a rapid and large depolarization in the membrane potential *E_m* of AQP8-expressing oocytes, but only slow and small depolarizations in AQP1-expressing oocytes. The measurements show that AQP8 induces a large conductance of some charged form of ammonia in the oocytes, while AQP1 does not (adapted from Holm et al. 2005)

effect of NH₄Cl on unclamped AQP8-expressing oocytes is shown in Fig. 4. If the oocyte had been clamped to a negative potential, however, the entry of NH₄⁺ or H⁺ could have been recorded as a current leaving the cell via the voltage clamp microelectrode. Electrogenic transports induced by NH₄Cl in AQP8 and TaAmt1;1 expressed in *Xenopus* oocytes are shown in Fig. 5.

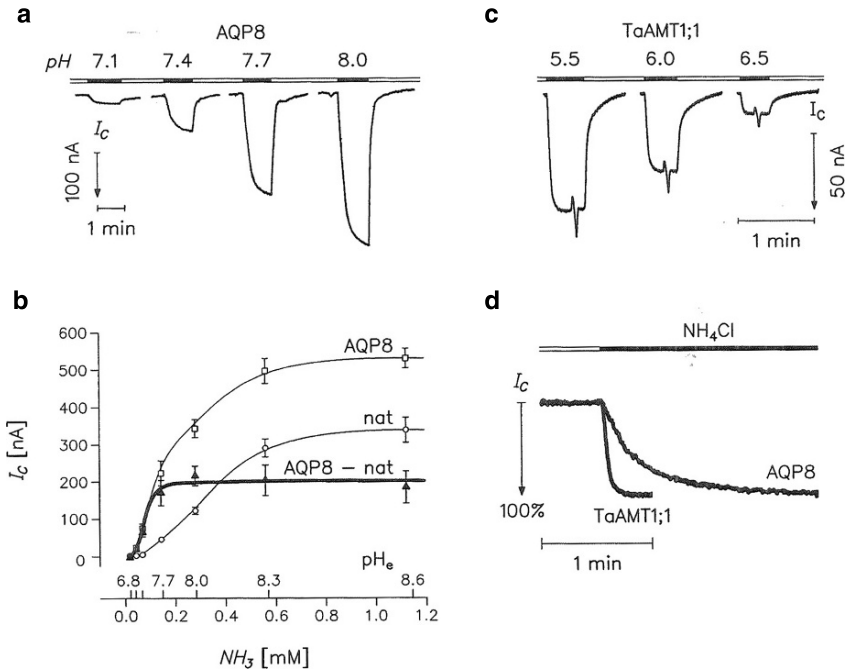


Fig. 5 Clamp currents induced by NH_4^+ in voltage-clamped oocytes expressing AQP8 or TaTIP1;1. (a) An AQP8-expressing oocyte was clamped to -50 mV, and 5 mmol L^{-1} of NH_4^+ was added to the bathing solution. Extracellular pH values of 7.1, 7.4, 7.7, and 8.0 were tested, and the test periods were 60 s. The resulting clamp currents (I_c) increased with increasing pH and NH_3 concentration. (b) A comparison between the clamp currents I_c from AQP8-expressing oocytes (open squares) and native oocytes (nat, open circles). The test solutions contained 5 mmol L^{-1} NH_4^+ at pH_e values of 6.8, 7.1, 7.4, 7.7, 8.0, 8.3, or 8.6; the corresponding NH_3 concentrations are given at the abscissa (2). Data obtained by subtracting I_c in the native oocytes from the I_c in AQP8-expressing oocytes (filled triangles, thick line) were fitted to a sigmoidal function that saturated around pH 7.7. Adapted from (Holm et al. 2005). (c) An experiment recording currents in oocytes expressing TaTIP1;1, performed with same the protocol as in (a). In this case, the NH_4^+ induced currents *decreased* with increasing external pH, in contrast to the AQP8 data. (d) The NH_4^+ induced current had a much faster rise time for TaTIP1;1 than for AQP8

For smaller cells or liposomes, voltage clamping may be more complicated. One possibility is to insert a highly conductive K^+ permeable ionophore (valinomycin) into the cell membrane. If the K^+ concentration gradient across the membrane is maintained, the electrical potential gradient will be fixed close to the K^+ equilibrium potential.

2.2.2 Response Time

Transport rates for NH_3 are expected to change relatively slowly in response to changes in external concentrations of NH_4Cl , as compared to a NH_4^+ current. The

rate of transport of NH_3 will be limited by the buffer capacity at the inside of the membrane, i.e. on how fast these buffers can be replenished. Protonated buffers will diffuse toward the inside of the membrane and buffers depleted of H^+ will diffuse away. As a result, any change in the transmembrane rate of NH_3 transport induced by changes in the external NH_3 concentrations will be relatively slow. If, on the other hand, the current is carried by the ion NH_4^+ , the current will change rapidly in response to changes in external concentrations. Ammonia currents induced in AQP8-expressing oocytes change relative slowly compared to the current induced in TaAmt1;1. This comparison suggests that the AQP8 mediates NH_3 transport, which, in turn, induces H^+ transport. The rapid response of the TaAmt1;1 strongly suggests NH_4^+ transport in this protein, as shown in Fig. 5a, c, d.

2.2.3 Reversal Potentials

The use of the equations for the equilibrium potentials (5 and 7) are best illustrated when applied to a specific example. Consider the case where an AQP8-expressing *Xenopus* oocyte is clamped to -50mV and the outside is bathed in 5mM NH_4^+ at pH 7.4 (Fig. 3b); this will result in an inward current of around 200nA (Holm et al. 2005). Is the current carried by NH_4^+ or by H^+ ? If the current were carried predominantly by NH_4^+ , (7) would predict a large positive reversal potential close to the equilibrium potential for NH_4^+ . In other words, only a large positive intracellular electrical potential could prevent NH_4^+ from entering the oocyte. If, on the other hand, the current were carried by predominantly by H^+ , the reversal potential should be small and negative, close to the equilibrium potential for H^+ , ideally around -20mV (5). Inspection of Fig. 5 in Holm et al. (2005) shows that transport of NH_4^+ is unlikely; rather, the data suggest H^+ transport.

2.2.4 Affinities and Permeabilities

It follows from the relative concentrations (1) and (2) that a transport mechanism based upon H^+ requires a high affinity, a mechanism based upon NH_3 a medium affinity, and a mechanism for NH_4^+ the lowest affinity. Equations (4) and (6) can be employed to estimate the absolute permeability of the given substrate. With the numerical example given above, (6) predicts a $P_{\text{NH}_4^+}$ of $4 \times 10^{-7}\text{cm s}^{-1}$. If it is assumed that the current is carried by H^+ , (4) predicts that P_{H^+} should be $2 \times 10^{-2}\text{cm s}^{-1}$, which is five orders of magnitude larger than the hypothetical $P_{\text{NH}_4^+}$. These numbers can be compared to the permeability for NH_3 (P_{NH_3}), which was measured directly in the experiment cited above, to about $2 \times 10^{-4}\text{cm s}^{-1}$, which is somewhere in between the two other estimates. Some of the electrophysiological characteristics of the various modes of ammonia transport are summarized in Table 2.

3 Experimental Evidence for Ammonia Transport

The first evidence for ammonia transport in aquaporins was obtained for human AQP8 and a plant aquaporin, TaTIP2;1, expressed in yeast or *Xenopus* oocytes (Jahn et al. 2004). In a mutant yeast deficient in ammonia transport, heterologous expression of AQP8 or TaTIP2;1 restored the ability for cell growth when NH_4^+ was present in the external medium. In oocytes, the aquaporins supported transport of ammonia and various ammonia analogues. Two important controls were performed: both AQP1 and aquaporins in which ammonia permeability had been abolished by mutations were unable to restore the growth of yeast or to sustain transport in oocytes (see Sect. 4.2).

Evidence for ammonia permeability in aquaporins has now been obtained in several different experimental systems, and a variety of methods have been employed, such as electrophysiology, uptake of radio-labeled ammonia analogues, insertion of purified proteins into artificial lipid bilayers, functional characterization of aquaporins altered by site-directed mutagenesis, and gene knockout experiments (Bertl and Kaldenhoff 2007; Holm et al. 2005; Jahn et al. 2004; Liu et al. 2006; Loque et al. 2005; Saparov et al. 2007; Yang et al. 2006a). In the following sections, we first review the evidence for uptake of ammonia in its neutral form, NH_3 . Next, we review the evidence that transport of NH_3 activates a parallel transport of H^+ , and discuss the possible routes for H^+ . In Sect. 4.2, we discuss the evidence suggesting that the locations and nature of critical amino acid residues in the arginine restriction region are responsible for whether an aquaporin is permeable to ammonia, or not. In other words, when amino acid residues in this region are mutated, the ammonia-impermeable aquaporins become ammonia-permeable, and vice-versa.

3.1 Permeability of NH_3 , Quantitative Measurements

The *Xenopus* oocyte expression system allows a detailed and quantitative investigation of the nature of the transport mechanisms. Uptake of NH_3 can be measured directly by bathing oocytes in an $\text{NH}_3/\text{NH}_4^+$ -containing solution of low buffer capacity. As NH_3 enters the oocytes, the rate of acidification of the bathing solution defines the permeability, as shown in Fig. 1 in Holm et al. (2005). For AQP7, AQP8, AQP9, and TIP2;1, P_{NH_3} was about $2 \times 10^{-4} \text{ cm s}^{-1}$. This permeability is about 10 times lower than the water permeability L_p , which is about $3.5 \times 10^{-3} \text{ cm s}^{-1}$ for AQP8 and TIP2;1-expressing oocytes. It is also possible to give a rough estimate of the ammonia permeability per aquaporin protein. If we assume that the unit water permeability of AQP8 is similar to that of other aquaporins, about $3 \times 10^{-14} \text{ cm s}^{-1}$ (Engel and Stahlberg 2002), there will be 10^{11} copies per cm^2 of oocyte membrane. Thus, P_{NH_3} per aquaporin is $2 \times 10^{-15} \text{ cm}^3 \text{ s}^{-1}$. This estimate of P_{NH_3} per molecule is ten times smaller than that obtained by Saparov et al. (2007) for AQP8 reconstituted into lipid bilayers. The discrepancy is acceptable, considering the methodological differences of the two investigations. First, the lipid bilayer method requires

that the measurements be performed at acid pH (pH 6). The estimate of P_{NH_3} in the *Xenopus* oocytes was performed at alkaline pHs of 7.4–8.4. Second, in the lipid bilayer assay, both sides of the membranes were bathed in well-defined aqueous solutions; for the *Xenopus* oocytes the inside of the membrane is exposed to cytoplasm, for which the buffers are not well defined. The ammonia permeabilities of AQP7, AQP8, AQP9, and TIP2;1 were similar, whereas AQP3 had values of approximately half of this (Holm et al. 2005; Holm and Zeuthen 2007).

The ammonia-permeable aquaporins were also permeable to the ammonia analogues, formamide $\text{NH}_2(\text{CHO})$ and methylammonium $\text{NH}_2(\text{CH}_3)$. This was ascertained by radiolabeled uptakes into *Xenopus* oocytes expressing AQP3, AQP7, AQP8, AQP9, or TIP2;1 (Holm et al. 2005; Holm and Zeuthen 2007; Jahn et al. 2004; Liu et al. 2006) and by light scattering studies of purified AQP8 inserted in liposomes (Liu et al. 2006). The formamide permeability was generally about 20–50 times smaller than that of ammonia, while the methylammonia permeability was about 100 times smaller (Holm et al. 2005). The rate of uptake of methylammonia was affected by ammoniumchloride, NH_4Cl . This was quantified for AQP8 where 5 mM of NH_4Cl completely inhibited methylammonium transport (Liu et al. 2006). This is good evidence that formamide and NH_4Cl follow the same pathway through the protein.

3.2 Permeability of NH_3 , Qualitative Estimates from Reflection Coefficients

Evidence for permeability can also be obtained from measurements of reflection coefficients (σ). In simple terms, the idea is as follows: In osmotic experiments, an impermeable osmolyte will give rise to larger water fluxes than a permeable osmolyte. One may imagine that in the latter case some of the molecules of the permeable solute cross the aqueous pore without contributing to the osmotic driving force. Thus, the difference in osmotic water flow provides qualitative evidence for permeation of a given substrate, as well as an idea of whether the substrate interacts with the water in the aqueous pore.

When cell shrinkage is induced by exposure to an increased external concentration of an impermeable solute, the osmotic water permeability L_p is obtained from:

$$J_v = (-dV/Vdt)V_o = L_p A \Delta\pi \quad (8)$$

where J_v is the volume flow out of the oocyte, $-dV/Vdt$ is the initial relative rate of shrinkage (usually measured within 10 s), V_o is the initial oocyte volume, A is the true oocyte surface area, and $\Delta\pi$ is the osmotic gradient of the impermeable solutes, usually mannitol or sucrose. If, however, the solute is permeable and follows the same pathway as the water, the rate of shrinkage is reduced by a factor, the reflection coefficient σ_s

$$L_{p,s} = \sigma_s L_p \quad (9)$$

Table 3 Reflection coefficient (σ) for osmolytes in aquaporin expressing *Xenopus* oocytes

	Mannitol	Urea	Glycerol	Acetamide	Formamide
AQP1	1	0.98	0.81	0.94	1.02
AQP3	1	1.00	0.24	0.72	0.38
AQP7	1	0.92	0.1	0.75	0.15
AQP8	1	1.01	0.97	0.97	0.20
AQP9	1 ^a	0.44	0.44	0.34	0.30
TIP2;1	1	1.20	1.06	1.07	0.09

Data from Holm et al. (2005); Holm and Zeuthen (2007); Meinild et al. (1998); Zeuthen and Klaerke (1999)

σ for the native oocyte membrane was 1 for mannitol, urea, acetamide, and formamide; for glycerol it was between 1 and 0.9

^a σ for mannitol in AQP9 is set to 1 as the osmotic effects of mannitol and sucrose were not significantly different. Values significant smaller than 1 are in bold

where $L_{p,s}$ is the apparent water permeability obtained with s as the osmolyte, and L_p is the true osmotic water permeability obtained with the impermeable osmolyte. Some relevant data for small hydrophilic substrates such as urea, glycerol, acetamide, and formamide obtained for aquaporins expressed in *Xenopus* oocytes are given in Table 3.

Several interesting facts can be deduced from Table 3. First, AQP1 has σ s equal to 1 for all solutes. This parallels the findings from AQP2, 4, 5, and 6, and shows that neither urea, glycerol, acetamide, or formamide are permeable in these aquaporins (Holm et al. 2004; Meinild et al. 1998). Second, all the ammonia-permeable aquaporins (AQP3, AQP7, AQP8, AQP9, TIP2;1) are also permeable to formamide. Third, the ammonia-permeable aquaporins separate into two groups: AQP3, 7, and 9 have low σ s for glycerol and acetamide and are therefore permeable to these substrates. This pattern applies also to PfAQP (Zeuthen et al. 2006b). For AQP8 and TIP2;1, however, σ for glycerol equals 1, and we conclude that these aquaporins are impermeable to glycerol. It should be emphasized that the measurement of reflection coefficients is a cruder way of assessing permeability than the use of radiotracers. A small permeability discovered by radiotracers may not be reflected in a reflection coefficient smaller than 1. On the other hand, a solute with a reflection coefficient smaller than 1 will give rise to an influx seen by radiotracers. AQP3 and AQP7 illustrate this situation. We find σ for urea around 1 for these aquaporins (Holm et al. 2005; Meinild et al. 1998). Yet, radiotracer measurements show some permeability (Echevarría et al. 1996; Ishibashi et al. 1994).

A reflection coefficient lower than 1 is a good indication that solute and water share the aqueous pathway in the aquaporin. A complete thermodynamic proof, however, requires that an osmotically-driven water flux is able to induce a flux of the solute by so-called solvent drag (Kedem and Katchalsky 1961). Unfortunately, it is rarely possible to perform such experiments in living cells. The osmotic water fluxes required to induce a measurable flux of the solute are usually prohibitively large. This stems from the fact that the average concentration of the solute in the aqueous pore is usually very low (Zeuthen and Klaerke 1999).

3.3 In which Form does Ammonia Permeate? Evidence from Electrophysiology

As outlined in Sect. 2, there are, in principle, four distinct ways aquaporins might facilitate the transport of ammonia (see Fig. 2). The equations that describe the various forms for transports were outlined in Sect. 2.1; in the following sections, we compare these transport modes to available experimental evidence.

3.3.1 Measurements in Unclamped Cells

In unclamped oocytes expressing ammonia-permeable aquaporins, external application of NH_4Cl results in a large and rapid depolarization of the membrane potential. In oocytes expressing aquaporins permeable only to water (i.e. AQP1), the depolarization is relatively small and slow (Fig. 4). This shows that ammonia-permeable aquaporins induce an efficient conductive pathway. To study this pathway further, the cell must be voltage clamped, otherwise the build-up of an intracellular positive potential will prevent flow of current (see Sect. 3.3.2).

In a recent study of the plant aquaporin TaTIP2;2, the authors dismissed the possibility of electrogenic transport of ammonia (Bertl and Kaldenhoff 2007). The aquaporin was expressed in yeast, and yeast protoplasts were investigated by measurements of intracellular pH and volume during challenges by osmotic gradients and ammonia gradients. The study clearly demonstrated osmotic water permeability and permeability to NH_3 , but went on to conclude that the ammonia transport was entirely electroneutral. However, the experimental setup does not allow this conclusion. The intracellular electrical potential was not clamped, and consequently any electrogenic transport will be prohibited for reasons of intracellular electroneutrality (see above). In the study, it was suggested that NH_3 and water do not share the same pathway in the aquaporin.

3.3.2 Measurements of Currents and Volume Changes in Voltage-Clamped Cells

The nature of the conductive pathway induced in aquaporins can be analyzed in voltage clamped cells. The intracellular electrical potential is clamped to a given potential and the current required to maintain this potential (the clamp current) is recorded. If the volume of the oocyte can be measured simultaneously, the direction of the ion flux that supports the current can be estimated directly (Fig. 3). Most of the data referred to in the following have been performed on AQP8 expressed in *Xenopus* oocytes, but similar results have been obtained for the other ammonia-permeable aquaporins (Holm et al. 2005; Zeuthen et al. 2006b).

Application of ammonia in the form of NH_4Cl gives rise to an inward current in AQP8-expressing oocytes (Fig. 5). The current depends of external pH and is vanishingly small at acid pHs below 6.8, but increases in a sigmoid fashion from zero

in a narrow pH range of 6.8–7.7. The AQP8-mediated current does not increase further with higher pH. The inward current is carried by positive ions entering the oocyte and not by negative ions, such as Cl^- , leaving the cell. This was ascertained by simultaneously monitoring the current and the volume of the oocyte at a high resolution; the number of osmotically active particles that would have entered if the current were carried by a positive current closely matched the swelling of the oocyte. Replacing Na^+ and K^+ in the bath by inert cations had no effect. Furthermore, recent observations show that the currents are not affected by removal of Cl^- from the bathing solutions (T. Zeuthen, unpublished). This shows that the inward current at basic pH is carried by ammonia, most likely in the form of $\text{NH}_3 + \text{H}^+$. The possibility of the current being carried by NH_4^+ can be ruled out on three accounts: (a) The current is present at alkaline pH only; below pH 7.0 it is absent (Fig. 5a, b). This shows that AQP8 does not function as a simple channel for NH_4^+ . (b) The currents observed at alkaline pH do not respond to the electrochemical gradients as would be expected from imposed gradients of NH_4^+ ; the reversal potential is numerically small, and positive (Holm et al. (2005) Fig. 5). With high extracellular concentrations of NH_4^+ and no NH_4^+ inside the oocyte, the reversal potential should be large and positive if the current were carried by NH_4^+ (see Table 2). In other words, inward currents should be present even at high positive intracellular electrical potentials. (c) The rise time of the ammonia-induced current is much slower than the NH_4^+ current observed for the ammonia transporter TaAMT1;1, which would imply that the rate-limiting step involves diffusion of NH_3 (see Table 2 and Fig. 5d).

3.3.3 Evidence from Aquaporins Reconstituted into Lipid Bilayers

So far, all studies confirm that AQP8 is permeable to NH_3 (Holm et al. 2005; Jahn et al. 2004; Liu et al. 2006; Saparov et al. 2007). The question is, how could the transport of NH_3 through the aquaporin lead to a flow of current? A recent study claims that transport is exclusively neutral, maintained by NH_3 permeation (Saparov et al. 2007). AQP8 was purified and reconstituted into artificial lipid bilayers and a NH_4Cl concentration difference was imposed across the bilayers, and the rates of transport of water and of NH_3 and NH_4^+ were derived from the concentration profiles arising in the adjacent unstirred layers. The gradients were measured by means of microelectrodes, the tips of which were moved perpendicular to the bilayers. Na^+ -sensitive electrodes were used to derive the rate of water transport from the profiles of dilution; H^+ -sensitive electrodes were used to monitor the pH gradient from which the transport of H^+ and NH_3 could be determined. Unfortunately, the measurements were restricted to an acidic pH of 6.0, because the concentration of NH_4^+ can only be assumed to be constant throughout the solutions at acid pH. As underscored by the authors, the method is not very accurate at alkaline pH (Antonenko et al. 1997). In sum, the paper by Saparov et al. (2007) supports the finding by Holm et al. (2005) that the transport is entirely electroneutral at acid pH, where only NH_3 is transported. Unfortunately, the study by Saparov et al. does not address transport at pH values higher than 7.0. Yet, this is the range in which we find electrogenic transport (Holm et al. 2005).

3.3.4 What is the Route of the H^+ that Accompanies NH_3 ?

At this point, it seems fair to conclude that NH_3 can cross aquaporins and that this process can lead to a parallel transport of H^+ . But which route is taken by the H^+ ? Does it go through the aquaporin or through the surrounding membrane (Fig. 2b, c)? The question is important from a physiological point of view. If the aquaporin itself mediates the transport of H^+ , the problem of cellular pH homeostasis associated with the influx of NH_3 will be solved directly. It will not be required to activate other H^+ transporters of the cell.

At present, there is not sufficient data to pinpoint the exact mechanism. Yet, the available data support the view that in the presence of NH_3 , H^+ can move through the aquaporin. Although the aqueous pore is fairly impermeable to ions, it has been suggested (Holm et al. 2005) that NH_3 , while residing in the pore, might act as a site for H^+ (Fig. 6). There are three indications: First, inflow of NH_3 in the absence of ammonia-permeable aquaporin does not give rise to any immediate influx of H^+ , as inferred from the shrinkage induced in AQP1-expressing oocytes (Fig. 7); rather, a small Cl^- conductance was activated. Second, AQP1 isoforms in which the composition of the aromatic/arginine restriction region has been modified in order to resemble that of the ammonia-permeable aquaporins become permeable to NH_3 as well as to H^+ (Beitz et al. 2006), as described in Sect. 4.2. Thirdly, the magnitude of the H^+ flux that can be achieved is in the same range as the simultaneous flux of NH_3 through the aquaporin.

4 Molecular Structure and Ammonia Permeability

The resolution of the tertiary structure of AQP1 to an accuracy of 2.2 Å (Murata et al. 2000) has revealed two highly conserved constriction regions residing at the inside of the water permeable pore: the double NPA (asparagine-proline-alanine)

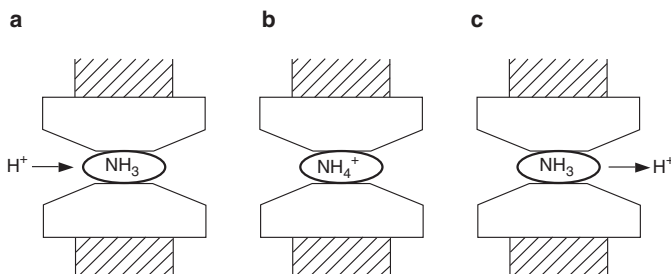


Fig. 6 A hypothesis of how NH_3 may induce conduction of H^+ in the aqueous pore of ammonia-permeable aquaporins. It is well established that ammonia can permeate aquaporins as NH_3 . The presence of NH_3 in the pore is assumed to facilitate the conduction of H^+ , probably by altering the free energy barrier for H^+ . The incoming H^+ is captured by the NH_3 , thus transiently forming NH_4^+ , and, in turn, (another) H^+ is released in the compartment with the most negative electrical potential, i.e. the intracellular compartment (adapted from Holm et al. 2005)

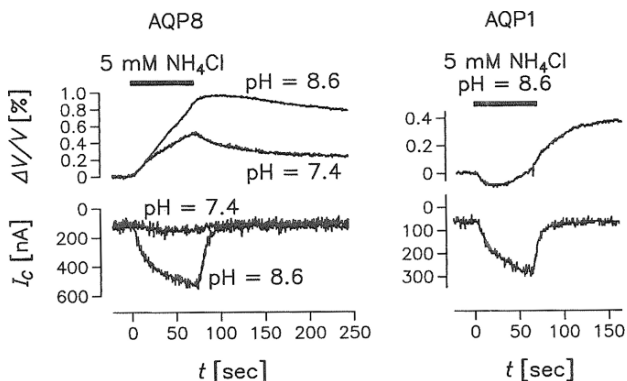


Fig. 7 Volume changes during NH_4^+ -induced clamp currents. The first panel shows the relative volume changes ($\Delta V/V$) of an AQP8-expressing oocyte when 5 mM of NH_4Cl is applied (isosmotic) to the external solution at pH 7.4 and pH 8.6. At pH 7.4, the clamp current I_C was small (about 50 nA), and the rate of volume increase declined with time. At pH 8.6, the clamp current was larger and associated with a linear increase in volume. The larger clamp currents were associated with an influx of osmolytes. Control experiments were performed with AQP1-expressing oocytes. In these oocytes, the clamp currents and volume changes were smaller (note the different scales in the two panels). Importantly, the AQP1-expressing oocyte shrank initially when exposed to NH_4Cl , most likely due to Cl^- ions leaving the cell. The AQP8- and AQP1-expressing oocytes had similar expression levels as estimated from their water permeability (adapted from Holm et al. 2005)

motif, and the aromatic/arginine (ar/R) motif (see Fig. 9). (For a recent review, see de Groot et al. 2003; de Groot and Grubmüller 2005.)

The defining feature of aquaporins is the two NPA motifs abutting each other in the center of the protein. The asparagine (N) is canonical, whereas the proline (P) and the alanine (A) are to some extent exchangeable. It is generally believed that the double NPA structure is important, in order to prevent H^+ ions from permeating the pore by breaking the continuity of hydrogen bonds between the water molecules stretching through the aqueous pore. This would prevent H^+ from moving along by a Grothuss mechanism.

The ar/R motif is localized about 7 Å toward the extracellular side from the NPA region. It is defined by the four locations, 56, 180, 189, and 195 (Fig. 8). In the following, we will follow the numbering of rat AQP1, where the N of the second NPA motif has number 192. In the predominantly water-permeable aquaporins (AQP1, 2, 4, 5, 6, AQPZ), the ar/R region is characterized by a phenylalanine at position 56, a histidine at position 180, a cysteine at position 189, and the arginine at position 195, which gives the region its name. This quartet is highly conserved and the ar/R motif constitutes the narrowest part of the pore (Fig. 9). Its restrictive function stems from two mechanisms: size selection and electrical repulsion. A water molecule accurately fits the diameter of the constriction region and the arginine ensures repulsion of positive charge. To a large extent, the nature of the amino acid residues occupying the ar/R restriction region determines the selectivity of a given aquaporin (Lee et al. 2005; Wu and Beitz 2007).



Fig. 8 Logoplots of the amino acid residues around the aromatic/arginine restriction regions. Logoplots for AQP1 and the ammonia-permeable aquaporins AQP3, 7, 8, 9, and 10, with emphasis on the sections that define the aromatic arginine region (ar/R): position 56, 180, 189, and the defining arginine in position 195 (all shaded grey). The latter section includes the second NPA motif (192–194). Numbers according to the rat sequence; see Fig. 9. The various groups of aquaporins are clearly distinguishable (see text). For example, there is always a histidine (H) in position 180 for the predominantly water-permeable aquaporins. For the ammonia- and glycerol-permeable aquaporins, this is usually replaced by a glycine (G) or, in the case of the ammonia- and water-permeable AQP8, an isoleucine (I). The differences between the groups extend beyond the ar/R region (marked by *arrows*). For example, there is always an isoleucine (I) in position 184 for the predominantly water-permeable aquaporins. This is replaced by a glycine (G) for the ammonia-permeable aquaporins. In position 190, there is a glycine (G) in the predominantly water-permeable aquaporins, while there is typically an alanine (A) or cysteine (C) in the ammonia-permeable aquaporins. The amino acid residues in locations 180 and 190 face the pore lumen. The logo plots were made in WebLogo3 (<http://weblogo.berkeley.edu/>), based on a multiple sequence alignment in ClustalX 2.0 (Thompson et al. 1997). Colors: red, acidic; blue, basic; green, neutral and hydrophilic; black, non-polar and hydrophobic

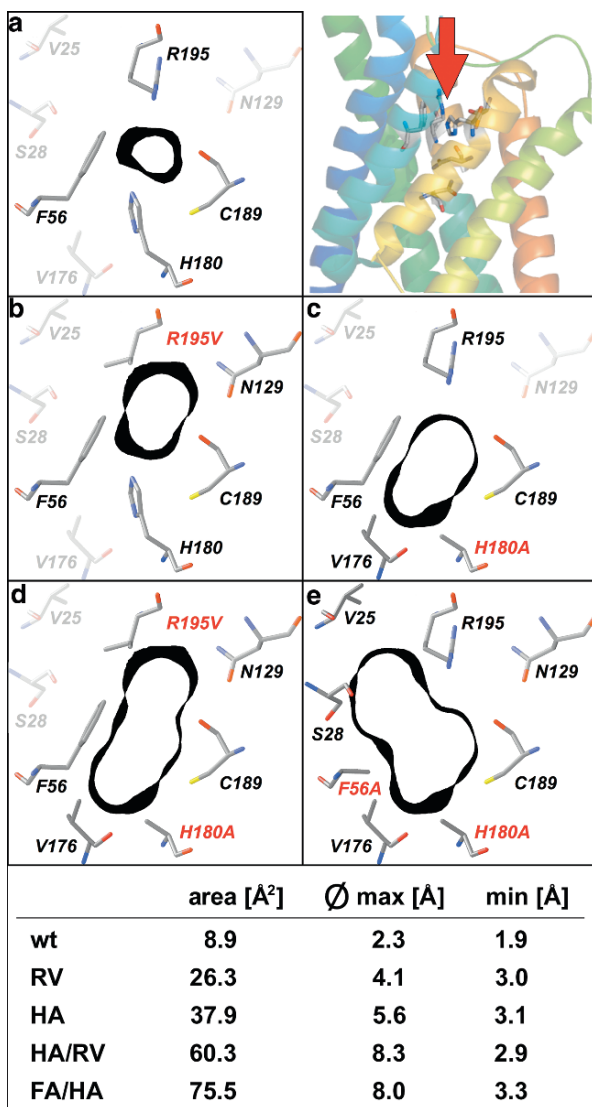


Fig. 9 Shape of the aromatic/arginine constriction region in AQP1 and some mutants. The top right shows a side view of the crystal structure of AQP1 with F56, H180, C189, and R195 as sticks (numbering according to the rat sequence). The red line defines the plane of the cross sections shown in (a)–(e), i.e. the ar/R constriction regions viewed head on from the outside solution. (a). The constriction region in the wild type AQP1 is shown; only residues contributing directly to the constriction are drawn in color. The black band denotes sections of 1 \AA thickness of the Connolly surface in this plane. (b)–(e) show the outlines of the mutated residues defined by the individual mutations printed in red. The table gives the cross section of the restriction region and the maximal and minimum diameter (from Beitz et al. 2006, with permission)

4.1 The Molecular Signature of Ammonia-Permeable Aquaporins

The ammonia-permeable aquaporins AQP3, AQP7, AQP8, AQP9, and AQP10 can be recognized by the amino acid residues that occupy the (ar/R) region (Fig. 8). At position 56, most aquaporins have residues with large aromatic side groups. In analogy with the predominantly water-permeable aquaporins, AQP3, AQP7, and AQP9 have a phenylalanine, but AQP8 has a histidine and GlpF a tryptophan. AQP10 is an exception, with a glycine in position 56. The amino acid residues found at position 180 are more useful for defining the properties of a given aquaporin. For the predominantly water-permeable aquaporins (AQP1, 2, 4, 5, 6), this position is always occupied by a histidine (large, basic, and hydrophilic), while in the aquaporins permeable to water, glycerol, and ammonia (AQP3, 7, 9, 10), we find the small glycine or, more rarely, an almost as small alanine. If an AQP1 mutant is generated, in which the histidine is replaced by an alanine, the aquaporin becomes ammonia-permeable (Sect. 4.2). In the aquaporins permeable to water and ammonia (AQP8), position 180 is occupied by an isoleucine. Residue 189 is also important in defining aquaporin properties. In aquaporins permeable to water (AQP1, 2, 5, 6) this position is occupied by a cysteine, which makes these aquaporins sensitive to mercury compounds; in the mercury-insensitive AQP4, position 189 is an alanine. In most of the aquaporins permeable to water, ammonia, and glycerol (AQP3, AQP7, PfAQP, GlpF), this position is occupied by amino acids with aromatic side-groups, such as proline, phenylalanine, or tyrosine. In AQP9, however, smaller residues are found in this position, which may account for the large variety of substrates that this aquaporin is permeable to; human AQP9 has a cysteine, while the rat and mouse homolog have a glycine in position 189. Finally, the aquaporins permeable to ammonia and water (AQP8 and TaTIP2;1) are characterized by a glycine or an alanine in position 189 (the two smallest amino acids). For all aquaporins, there is an arginine located in position 195, which is the one that gives the restriction its name. This arginine is well conserved among all aquaporins; mutations directed toward this site make aquaporins permeable to substrates larger than water (Beitz et al. 2006) (see Sect. 4.2).

Other characteristic variations are found at positions located to the inside of the aqueous pore, but outside the ar/R region (Murata et al. 2000; Wu and Beitz 2007). In the predominantly water-permeable aquaporins, position 184 is occupied by an isoleucine (large, nonpolar, and hydrophobic), while in all the ammonia- and glycerol-permeable aquaporins this position is always occupied by a smaller glycine residue (small, neutral, and hydrophilic), Fig. 8. This also applies to the malaria and plant aquaporins (PfAQP and TaTip2;1) and the glycerol facilitators (GlpF). In position 190, there is no overlap between the amino acid residues found in the exclusively water-permeable aquaporins and the ammonia-permeable ones. In the former there is a serine or glycine, while in the latter group we find alanine or cysteine. For most of the ammonia-permeable aquaporins there is a methionine (which contains a sulfur atom) in location 191, while the glycerol and ammonia-permeable aquaporins have an isoleucine or a valine. Finally, in position 179, which is not located precisely inside the aqueous pore, there is a glycine in the water-permeable aquaporins, an

isoleucine in the glycerol- and ammonia-permeable aquaporins, and an asparagine or an aspartic acid in the ammonia-permeable aquaporins. So far, no functional roles of the residues 179, 184, 190, and 191 have been determined experimentally.

In summary, the various mammalian aquaporins are recognized by clear molecular fingerprints. The predominantly water-permeable aquaporins (AQP1, 2, 4, 5, and 6) have a histidine in position 180 and an isoleucine in position 184. The water-, glycerol-, and ammonia-permeable aquaporins (AQP3, 7, 9, and 10) have a glycine in both positions 180 and 184. The water- and ammonia-permeable aquaporin (AQP8) has an isoleucine in position 180 and a glycine in position 184.

4.2 Single Mutations can Abolish or Induce Ammonia Permeability in Aquaporins

Mutations in the aromatic arginine (ar/R) region can transform an aquaporin that is ammonium- and water-permeable into a strictly water-permeable one. The reverse is also possible; a strictly water-permeable aquaporin can be transformed into an ammonium- and water-permeable protein.

The plant aquaporin TaTIP2;1 is permeable to water and ammonium (Holm et al. 2005; Jahn et al. 2004). If the isoleucine in position 180 is replaced by a histidine and the glycine at position 189 is replaced by a cysteine, the ammonia permeability is abolished, while, importantly, the water permeability appears to be unaffected, as shown in Fig. 8. The same idea has been applied to the mammalian aquaporins, in which case the reverse transformation was achieved: the entirely water-permeable AQP1 was transformed into an ammonia-permeable channel (Beitz et al. 2006). This was achieved by changing the histidine in position 180 to an alanine, the reverse of what was done in the plant aquaporin described above. This effect was enhanced by changing the arginine in position 195 to a valine. Such experiments serve as powerful control experiments for the concept of ammonia-permeable aquaporins.

Mutations in the ar/R region provide important insight into the relation between structure and function. When the available cross section of the ar/R region is increased by site-directed mutagenesis, aquaporins become permeable to ammonia, but also to urea, glycerol, or even H^+ ions (Beitz et al. 2006). Apparently, the NPA region is not an absolute barrier to these substrates, only a relative one. This is confirmed in molecular dynamics simulations (Chen et al. 2006). If the electrostatic interaction between the water molecules and the arginine in position 195 and the dehydration effect of the histidine in position 180 are removed, the bipolar field of the NPA-region is not sufficient to keep H^+ ions from permeating the aqueous pore (Fig. 10). It remains an interesting hypothesis that the presence of an NH_3 in the pore likewise would lower the overall free energy barrier for H^+ (Holm et al. 2005). This would explain the conductive transport induced in the ammonia-permeable aquaporins as an NH_3 -facilitated H^+ transport in the aqueous pore (Fig. 6).

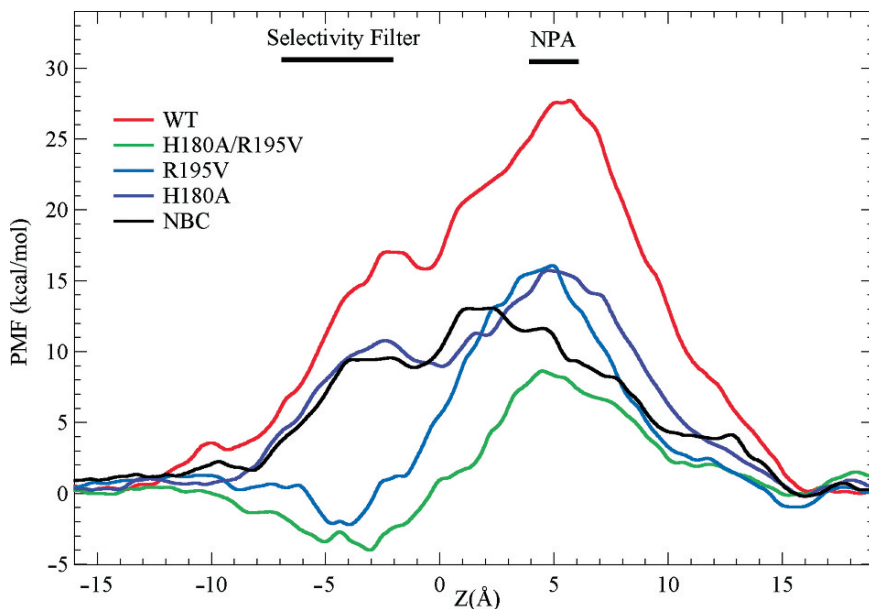


Fig. 10 The free-energy profile (the potential of mean force, PMF) for an excess proton passing through the aqu channel of the wild type AQP1 and the H180A/R195V, R195V, and H180A mutants. Also shown are the results of similar calculations performed on a hypothetical mutant (NBC, no backbone charges) in which the partial charges are set to zero on the half-membrane-spanning α -helices that form the NPA motifs (from Chen et al. 2006, with permission)

5 Physiological Relevance of Ammonia Permeability in Aquaporins

Ammonia is toxic and cellular levels have to be regulated precisely. The detrimental effects are seen in disorders such as hepatic failure, in which blood levels of ammonia increase and fatal brain edema follows, due to swelling of the astrocytes and permeability changes in their mitochondria (Norenberg et al. 2005). Accordingly, transport of ammonia is vital, as reflected in the variety of modes and routes of transport. To a lesser extent, ammonia may be transported by diffusion across the lipid membrane, although in certain locations, particularly in the gastric mucosa and the kidney, the lipid bilayer is relatively impermeable (Waisbren et al. 1994). In contrast, protein-mediated transport has the advantage of being localized and it can be adjusted to the requirements of the cell or organelle in question. The Rh proteins transport ammonia in the form of NH_3 (Mayer et al. 2006), in analogy to the mechanism suggested for the AmtB proteins (Khademi and Stroud 2006), although the possibility of transport of some charged form of ammonia cannot be excluded (Bakouh et al. 2004; Nakhoul et al. 2005, 2006; Westhoff et al. 2002). Interestingly, some types of Rh-like proteins in plants transport the charged form of ammonia, NH_4^+ , as shown for the tomato homolog LeAmt2;1 (Mayer et al.

2006) and for the wheat homolog TaAmt1;1, as shown in Fig. 5c, d (R. Sogaard and T. Zeuthen, unpublished). The aquaporins have been shown to transport NH_3 and possibly $\text{NH}_3 + \text{H}^+$ (Holm et al. 2005), as explained in Sect. 3. The possibility of cotransport of H^+ would alleviate the alkaline load associated with simple NH_3 transport, and thereby the requirement for activation of other H^+ transporters.

5.1 Lessons from Simpler Organisms

The strategies for ammonia transport adopted by simpler organisms show that each of the possible transport mechanisms suffices to sustain life. In some organisms, such as malaria parasites, the ammonia and water transport is taken care of by a single aquaporin. In certain bacteria, the ammonia and water transport functions are divided between an AmtB-like protein and an aquaporin. The malaria parasite *Plasmodium falciparum* has no way of converting ammonia into urea, and is therefore an ammonia-releasing organism. Furthermore, there are no AmtB or Rhesus-like proteins in its genome (Zeuthen et al. 2006b). The implication is that ammonia transport is taken care of by its ammonia-permeable aquaporin, PfAQP. In the blood of the host, the parasite releases ammonia, and plasma levels increase up to sixfold. The importance of the *Plasmodium* aquaporin is supported by the fact that parasites in which the aquaporin has been knocked out are not as virulent as wild type parasites (Promeneur et al. 2007). The initial survival of mice infected with *Plasmodium berghei*, the rodent orthologue to *Plasmodium falciparum*, was improved by about 50% if the gene for the corresponding aquaporin (PbAQP) had been knocked out. In the bacterium *Escherichia coli*, the mode of ammonia transport is different. At high levels of external ammonia, the component entering via the lipid bilayer is sufficient but as the external ammonia levels become growth limiting, an AmtB system is turned on (Khademi and Stroud 2006). Interestingly, *E. coli* does have an aquaporin denoted AQPZ (Calamita 2000; Calamita et al. 1995), but AQPZ is neither permeable to ammonia nor glycerol, as suggested by its amino acid sequence (Sect. 4.1).

5.2 Tissue Distribution of Ammonia Permeable Aquaporins in Mammals

The distribution and function of the ammonia-permeable aquaporins AQP3, AQP7, AQP8, AQP9, and AQP10 differ among the various organs of the body. (For recent reviews, see Hara-Chikuma and Verkman 2006; Hibuse et al. 2006; King et al. 2004; Rojek et al. 2008a; Verkman 2005.)

AQP3 has a wide tissue distribution. In the kidney, AQP3 has been found in the basolateral membrane of principal cells in cortical and outer medullary collecting ducts (Fenton and Knepper 2007; Nielsen et al. 2002). Hence, AQP3 could play a

direct role in the final steps of acid secretion via NH_4^+ , which takes place across the collecting duct epithelium (Knepper et al. 1989). AQP3 knockout mice have a marked urinary concentration defect, with severe polyuria (Ma et al. 2000). It is to be expected that these mice have tubular acidosis, and therefore reduced capacity for concentrating the final urine. The glycerol transport by AQP3 has been shown to be important for skin hydration (Hara-Chikuma and Verkman (2006).

AQP7 is present in late spermatids, proximal-tubule epithelium, skeletal myofibers, and adipocytes. (For recent reviews, see Fenton and Knepper 2007; Hara-Chikuma and Verkman 2006; Hibuse et al. 2006; Rojek et al. 2008a.) Its permeability to glycerol and ammonia clearly suggests a role in carbohydrate and amino acid metabolism. The ontogeny and distribution of AQP7 (and AQP8) in developing spermatocytes suggest a role in male fertility. Interestingly, AQP7 has been found to be permeable to arsenite-compounds and plays a key role in the toxicology of this metal (Liu et al. 2002). In analogy to AQP0 and AQP4, AQP7 is insensitive to mercurials.

AQP8 is expressed in a wide range of tissues. For most cells, it is predominantly located intracellularly in organelles (Calamita et al. 2001; Elkjær et al. 2001; Ferri et al. 2003; Garcia et al. 2001; Huebert et al. 2002; Portincasa et al. 2003), which would suggest a role in the metabolism of amino acids. In the liver, for example, AQP8 can be found in mitochondria of hepatocytes (Calamita et al. 2007), which suggests a direct role for the uptake of NH_4^+ to supply the urea cycle. Mitochondria have large negative membrane potentials of about -150 mV , which would facilitate inward transport of the accompanying H^+ ion. AQP8 also plays a role in hepatocytic bile formation by participating in the canalicular secretion of water (Carreras et al. (2007). Interestingly, AQP8 has recently been shown to be permeable to H_2O_2 , which suggests a role for transport of oxidants and signaling molecules. (For a review, see Bienert et al. 2006; Wu and Beitz 2007.)

AQP9 is found in a variety of tissues, such as liver, the male reproductive tract, brain, and skin. In the liver, AQP9 is found in the hepatocyte plasma membrane facing the sinusoids (Carbrey et al. 2003; Huebert et al. 2002; Portincasa et al. 2003; Rojek et al. 2008b). In humans, the portal venous blood (with a flow rate of about 20 mL s^{-1}) contains $0.2\text{--}0.5\text{ mmol L}^{-1}$ of NH_4^+ ions originating from the intestine. This adds to the ammonium produced inside the hepatocytes (Häussinger 1996a, b). This suggests that NH_4^+ is taken up from the blood into the periportal hepatocytes via AQP9, from where it may enter the (electro-negative) mitochondrion. During starvation, AQP9 expression increases in accordance with this hypothesis (Carbrey et al. 2003). Urea produced in the urea cycle may leave the cell again via AQP9 (Carbrey et al. 2003; Tsukaguchi et al. 1999). In rat brain, AQP9 is expressed preferentially in catecholaminergic neurons and glial cells (Badaut and Regli 2004). This suggests a role for AQP9 in transport of metabolites. For further discussion of the localization of AQP9 in the brain, see Rojek et al. (2008a).

AQP10 is less extensively studied; so far, it is only found in the small intestine (Hatakeyama et al. 2001; Ishibashi et al. 2002). It exists in two forms. The shorter form consists of 264 amino acid residues and has low water permeability and no permeability to urea or glycerol, while the longer form (301 amino acid residues) transports water, as well as urea and glycerol.

5.3 Colocalization of Aquaporins, Rh Proteins, and Urea Transporters

It is conceivable that the importance of ammonia transport has led to the parallel evolution of several kinds of ammonia transporters in mammals. Consequently, the ammonia-permeable aquaporins and the Rh proteins RhAG, RhBG, and RhCG would be found colocalized in tissues involved in ammonia transport. In the liver, RhBG is localized to the basolateral membrane of the perivenous hepatocyte (Weiner and Verlander 2003) together with AQP9 (Carbrey et al. 2003; Huebert et al. 2002). RhCG is found in the bile duct epithelium (Weiner and Verlander 2003), functionally close to the AQP8 in the liver canaliculi (Carreras et al. 2007). In the kidney, RhBG and RhCG are found in the connecting segment, the initial collecting tubule, and throughout the collecting duct (Mak et al. 2006; Quintin et al. 2003; Weiner and Verlander 2003). In general, RhBG is localized basolaterally, while RhCG is expressed apically. This overlaps to some degree with AQP3, which is localized basolaterally in the collecting duct epithelium, while AQP8 is found intracellularly. In the seminiferous tubule, AQP7 colocalizes with RhCG and, in skin, AQP3 colocalizes with RhBG, which suggests roles in anabolism (Rojek et al. 2008a; Verkman 2005). In erythrocytes, RhAG is present together with AQP3 and AQP9 (Ripoche et al. 2004) and, in the brain, RhCG is found together with AQP9 (Badaut and Regli 2004; Huang and Liu 2001). The respective roles of the various types of ammonium transporters are as yet unclear.

In contrast to the findings for the ammonia transporters, the urea transporters (UT) and the urea-permeable aquaporins are not colocalized to the same extent. The urea transporters UT1, UT2 and UT3 are not present in the liver, leaving AQP9 as the only candidate for the export of urea to the blood (Tsukaguchi et al. 1999). There is no functional overlap in the kidney, either. The urea transporters UTA1 and UTA3 colocalize with AQP3 in the collecting duct (Fenton and Knepper 2007), but AQP3 may be rather impermeable to urea (Table 1). The erythrocyte expresses the urea transporter UT-B (Bagnasco 2006), as well as the urea-permeable AQP9. The ability for urea transport would mitigate osmotic shrinkage of erythrocytes while passing through the kidney. The interdependence of the two modes of transport has not been investigated.

The duplication of ammonia transport mechanisms complicates the interpretation of experiments in which a given aquaporin is knocked out, i.e. the specific gene is targeted and the corresponding aquaporin removed from the phenotype. There may be two reasons for this. First, the remaining mechanism may be upregulated to compensate for the loss. Second, the mechanism that has been knocked out may only be responsible for a minor part of the total transport under normal conditions. It should be emphasized that any transport mechanism will be incorporated into the genome, even if it provides only a minor increase in the rate of reproduction. In crude terms, if the mechanism increases the reproduction rate by 2%, it will be incorporated in the genome within about 50 generations. Thus, the effect on viability of knocking out a useful transporter may be small. In experiments where

the ammonium-permeable AQP8 has been knocked out, there is only a weak change in the phenotype (Yang et al. 2005, b). The reason could be redundancy as outlined above; the ammonia transport is taken over by Rh proteins, the transport rate of which might be upregulated. An alternative explanation is that the main function of AQP8 is not ammonia transport but transport of H_2O_2 (Bienert et al. 2007), a substrate for which the AQP8 knockout phenotype has not been tested.

6 General Summary

Aquaporins constitute a group of membrane proteins that facilitate passive diffusion of small, usually electroneutral, hydrophilic substrates. Some aquaporins are strictly water-permeable, but the majority have an additional permeability for a variety of other substrates, such as ammonia, hydrogen peroxide, urea, glycerol, and even ions such as arsenite and nitrates (Wu and Beitz 2007). It seems that the predominantly water-permeable aquaporins only represent a refinement of a very versatile channel-forming protein.

The human aquaporins AQP3, 7, 8, 9, and possibly AQP10, are permeable to ammonia, a property they share with the Rhesus-like group of proteins. Likewise, the urea permeability of AQP7, AQP9, and possibly AQP3, is also shared by another group of proteins, the urea transporters, UTs. The exact mechanism by which ammonia is transported is not yet clear. A comparison of transport equations, models, and experimental data points to some general features. The aquaporins transport ammonia as the neutral form, NH_3 . The transport of NH_3 induces a parallel transport of H^+ , which can be observed at alkaline pH when the concentration of NH_3 is high. It is unclear whether the transport of H^+ takes place via the aquaporin or via a pathway endogenous to the expression system. Investigation of this electrogenic transport of NH_3 together with H^+ requires the aquaporin-expressing cell to be voltage-clamped.

The ammonia-permeable aquaporins have distinct molecular fingerprints as compared to the aquaporins permeable to water. The major difference can be localized to the aromatic/arginine region, which is the major size-limiting filter. In the ammonia-permeable aquaporins, the amino acid residues of this filter allow larger substrates to pass. In fact, an exclusively water-permeable aquaporin can be transformed into an ammonia-permeable aquaporin by one or two point mutations in the aromatic/arginine region, and vice versa. The ammonia-permeable aquaporins can be divided into two groups, one permeable to glycerol (AQP3, 7, 9, and possibly AQP10) and one impermeable to glycerol (AQP8). The two groups have different compositions of their aromatic/arginine regions.

The localization of the ammonia-permeable aquaporins parallels that of the Rh proteins. This applies to the erythrocytes and to the cells associated with either homeostasis or high rates of anabolism. In the liver, AQP8 and 9 are located together with Rh proteins in the cells exposed to portal blood, which arrives from the intestine and contains ammonia in high concentrations. In the kidney, AQP3 might

participate in the excretion of NH_4^+ in the collecting duct. Generally, the interplay between the ammonia-permeable aquaporins and the other types of ammonia- and urea-permeable proteins is not well understood.

Finally, it should be emphasized that the full spectrum of permeability for a given aquaporin is not known with certainty. The permeability of a yet unidentified substrate may turn out to be the most important function of the aquaporin. For example, AQP8 is permeable to ammonia and hydrogen peroxide; the relative importance of these two functions remains to be established.

Acknowledgments We are grateful for the technical assistance of S. Christoffersen, and T. Soland. We thank Dr. Nanna MacAulay and M. Alsterfjord for critical reading. The study was supported by the Nordic Center of Excellence Program in Molecular Medicine, the Danish Research Council, the Lundbeck Foundation, and the NovoNordisk Foundation.

References

- Antonenko YN, Pohl P, Denisov GA (1997) Permeation of ammonia across bilayer lipid membranes studied by ammonium ion selective microelectrodes. *Biophys J* 72:2187–2195
- Badaut J, Regli L (2004) Distribution and possible roles of aquaporin 9 in the brain. *Neuroscience* 129:971–981
- Bagnasco SM (2006) The erythrocyte urea transporter UT-B. *J Membr Biol* 212:133–138
- Bakouh N, Benjelloun F, Hulin P, Brouillard F, Edelman A, Chérif-Zahar B, Planelles G (2004) NH_3 is involved in the NH_4^+ transport induced by the functional expression of the human Rh C glycoprotein. *J Biol Biochem* 279:15975–15983
- Beitz E (2006) Aquaporin water and solute channels from malaria parasites and other pathogenic protozoa. *Chem Med Chem* 1:587–592
- Beitz E, Pavlovic-Djuranovic S, Yasui M, Agre P, Schultz JE (2003) Molecular dissection of water and glycerol permeability of the aquaporin from *Plasmodium falciparum* by mutational analysis. *Proc Natl Acad Sci U S A* 101:1153–1158
- Beitz E, Wu B, Holm LM, Schultz JE, Zeuthen T (2006) Point mutations in the aromatic/arginine region in aquaporin 1 allow passage of urea, glycerol, ammonia, and protons. *Proc Natl Acad Sci U S A* 103:269–274
- Bertl B, Kaldenhoff R (2007) Function of a separate NH_3 -pore in aquaporin TIP2;2 from wheat. *FEBS Lett* 581:5413–5417
- Bienert GP, Schjoerring JK, Jahn TP (2006) Membrane transport of hydrogen peroxide. *Biochim Biophys Acta* 1758:994–1003
- Bienert GP, Møller ALB, Kristiansen KA, Schulz A, Møller IM, Schjoerring JK, Jahn TP (2007) Specific aquaporins facilitate the diffusion of hydrogen peroxide across membranes. *J Biol Chem* 282:1183–1192
- Borgnia MJ, Kozono D, Calamita G, Maloney PC, Agre P (1999) Functional reconstitution and characterization of AqpZ, the *E. coli* water channel protein. *J Mol Biol* 291:1169–1179
- Calamita G (2000) The *Escherichia coli* aquaporin-Z water channel. *Mol Microbiol* 37:254–262
- Calamita G, Bishai WR, Preston GM, Guggino WB, Agre P (1995) Molecular cloning and characterization of AqpZ, a water channel from *Escherichia coli*. *Proc Natl Acad Sci U S A* 270:29063–29066
- Calamita G, Mazzone A, Bizzoca A, Cavalier A, Cassano G, Thomas D, Svelto M (2001) Expression and immunolocalization of the aquaporin-8 water channel in rat gastrointestinal tract. *Eur J Cell Biol* 80:711–719

- Calamita G, Moreno M, Ferri D, Silvestri E, Roberti P, Schiavo L, Gena P, Svelto M, Goglia F (2007) Triiodothyronine modulates the expression of aquaporin-8 in rat liver mitochondria. *J Endocrinol* 192:111–120
- Carbrey JM, Gorelick-Feldman DA, Kozono D, Praetorius J, Nielsen S, Agre P (2003) Aquaglyceroporin AQP9: solute permeation and metabolic control of expression in liver. *Proc Natl Acad Sci U S A* 100:2945–2950
- Carreras F, Lehmann GL, Ferri D, Tioni MF, Calamita G, Marinelli RA (2007) Defective hepatocyte aquaporin-8 expression and reduced canalicular membrane water permeability in estrogen-induced cholestasis. *Am J Physiol* 292:G905–G912
- Chen H, Wu Y, Voth GA (2006) Origins of proton transport behavior from selectivity domain mutations of the aquaporin-1 channel. *Biophys J: Biophys Lett* 70:L73–L75
- de Groot BL, Grubmüller H (2005) The dynamics and energetics of water permeation and proton exclusion in aquaporins. *Curr Opin Struct Biol* 15:176–183
- de Groot BL, Frigato T, Helms V, Grubmüller H (2003) The mechanism of proton exclusion in the aquaporin-1 water channel. *J Mol Biol* 333:279–293
- Echevarría M, Windhager EE, Frindt G (1996) Selectivity of the renal collecting duct water channel aquaporin-3. *J Biol Chem* 271:25079–25082
- Elkjær M-L, Nejsum LN, Gresz V, Kwon T-H, Jensen UB, Frøkiær J, Nielsen S (2001) Immunolocalization of aquaporin-8 in rat kidney, gastrointestinal tract, testis, and airways. *Am J Physiol* 281:F1047–F1057
- Engel A, Stahlberg H (2002) Aquaglyceroporins: channel proteins with a conserved core, multiple functions, and variable surfaces. *Int Rev Cytol* 215:75–104
- Fenton RA, Knepper MA (2007) Mouse models and the urinary concentrating mechanism in the new millennium. *Physiol Rev* 87:1083–1112
- Ferri D, Mazzone A, Liquori GE, Cassano G, Svelto M, Calamita G (2003) Ontogeny, distribution, and possible functional implications of an unusual aquaporin, AQP8, in mouse liver. *Hepatology* 38:947–957
- García F, Kierbel A, Larocca MC, Gradilone SA, Splinter P, LaRusso NF, Marinelli RA (2001) The water channel aquaporin-8 is mainly intracellular in rat hepatocytes, and its plasma membrane insertion is stimulated by cyclic AMP. *J Biol Chem* 276:12147–12152
- Gonen T, Walz T (2006) The structure of aquaporins. *Q Rev Biophys* 39:361–396
- Hara-Chikuma M, Verkman AS (2006) Physiological roles of glycerol-transporting aquaporins: the aquaglyceroporins. *Cell Mol Life Sci* 63:1386–1392
- Hatakeyama S, Yoshida Y, Tani T, Koyama Y, Nihei K, Ohshiro K, Kamiie JI, Yaoita E, Suda T, Hatakeyama K, Yamamoto T (2001) Cloning of a new aquaporin (AQP10) abundantly expressed in duodenum and jejunum. *Biochem Biophys Res Commun* 287:814–819
- Häussinger (1996a) Physiological functions of the liver. In: Greger R, Windhorst U (eds.) *Comprehensive human physiology*, vol. 2. Springer-Verlag, Berlin, Heidelberg, pp. 1369–1391
- Häussinger (1996b) Zonal metabolism in the liver. In: Greger R, Windhorst U (eds.) *Comprehensive human physiology*, vol. 2. Springer-Verlag, Berlin, Heidelberg, pp. 1393–1402
- Hibuse T, Maeda N, Nagasawa A, Funahashi T (2006) Aquaporins and glycerol metabolism. *Biochim Biophys Acta* 1758:1004–1011
- Hille B (1992) *Ionic channels of excitable membranes*, 2 edn. Sinauer Associates Inc., Sunderland, MA
- Holm, Zeuthen T (2007) Ammonia transport in aquaporins: molecular mechanisms and clinical relevance. In: Häussinger D, Kircheis G, Schliess F (eds.) *Hepatic encephalopathy and nitrogen metabolism*. Springer, Düsseldorf, pp. 387–393
- Holm LM, Klaerke DA, Zeuthen T (2004) Aquaporin 6 is permeable to glycerol and urea. *Pflügers Arch* 448:181–186
- Holm LM, Jahn TP, Møller ALB, Schjoerring JK, Ferri D, Klærke DA, Zeuthen T (2005) NH₃ and NH₄⁺ permeability in aquaporin-expressing *Xenopus* oocytes. *Pflügers Arch* 450:415–428
- Huang C-H, Liu PZ (2001) New insights into the Rh superfamily of genes and proteins in erythroid cells and nonerythroid tissues. *Blood Cells Mol Dis* 27:90–101

- Huebert RC, Splinter PL, Garcia F, Marinelli RA, LaRusso F (2002) Expression and localization of aquaporin water channels in rat hepatocytes. *J Biol Biochem* 277:22710–22717
- Ishibashi K, Kuwahara M, Gu Y, Kageyama Y, Tohsaka A, Suzuki F, Marumo F, Sasaki S (1997) Cloning and functional expression of a new water channel abundantly expressed in the testis permeable to water, glycerol, and urea. *J Biol Chem* 272:20782–20786
- Ishibashi K, Sasaki S, Fushimi K, Uchida S, Kuwahara M, Saito H, Furukawa T, Nakajima K, Yamaguchi M, Gojobori T, Marumo F (1994) Molecular cloning and expression of a member of the aquaporin family with permeability to glycerol and urea in addition to water expressed at the basolateral membrane of kidney collecting duct cells. *Proc Natl Acad Sci U S A* 91:6369–6273
- Ishibashi K, Morinaga T, Kuwahara M, Sasaki S, Imai M (2002) Cloning and identification of a new member of water channel (AQP10) as an aquaglyceroporin. *Biochim Biophys Acta* 1576:335–340
- Jahn TP, Møller ALB, Zeuthen T, Holm LM, Klaerke DA, Mohsin B, Kühlbrandt W, Schoerring JK (2004) Aquaporin homologues in plants and mammals transport ammonia. *FEBS Lett* 574: 31–36
- Kedem O, Katchalsky A (1961) A physical interpretation of the phenomenological coefficients of membrane permeability. *J Gen Physiol* 45:143–179
- Khademi S, Stroud RM (2006) The Amt/MEP/Rh family: structure of AmtB and the mechanism of ammonia gas conduction. *Physiology* 21:419–429
- King LS, Kozono D, Agre P (2004) From structure to disease: the evolving tale of aquaporin biology. *Nat Rev Mol Cell Biol* 5:687–698
- Knepper MA, Packer R, Good DW (1989) Ammonium transport in the kidney. *Physiol Rev* 69:179–249
- Kozono D, Ding X, Iwasaki I, Meng X, Kamagata Y, Agre P, Kitagawa Y (2003) Functional expression and characterization of an archaeal aquaporin. *J Biol Chem* 278:10649–10656
- Kruse E, Uehlein N, Kaldenhoff R (2008) The aquaporins. *Genome Biol* 7:206.1–206.6
- Lee JK, Kozono D, Remis J, Kitagawa Y, Agre P, Stroud RM (2005) Structural basis for conductance by the archaeal aquaporin AqpM at 1.68 Å. *Proc Natl Acad Sci U S A* 102:18932–18937
- Liu Z, Chen Y, Mo R, Hui C, Cheng J-F, Mohandas N, Huang C-H (2000) Characterization of human RhCG and mouse Rhcg as novel nonerythroid Rh glycoprotein homologues predominantly expressed in kidney and testis. *J Biol Chem* 275:25641–25651
- Liu Z, Peng J, Mo R, Hui C-C, Huang C-H (2001) Rh type B glycoprotein is a new member of the Rh superfamily and a putative ammonia transporter in mammals. *J Biol Chem* 276:1424–1433
- Liu Z, Shen J, Carbrey JM, Mukhopadhyay R, Agre P, Rosen BP (2002) Arsenite transport by mammalian aquaporins AQP7 and AQP9. *Proc Natl Acad Sci U S A* 99:6053–6058
- Liu K, Nagase H, Huang CG, Calamita G, Agre P (2006) Purification and functional characterization of aquaporin-8. *Biol Cell* 98:153–161
- Loque D, Ludewig U, Yuan L, von Wiren N (2005) Tonoplast intrinsic proteins AtTIP2;1 and AtTIP2;3 facilitate NH₃ transport into the vacuole. *Plant Physiol* 137:671–680
- Ma T, Song Y, Yang B, Gillespie A, Carlson EJ, Epstein CJ, Verkman AS (2000) Nephrogenic diabetes insipidus in mice lacking aquaporin-3 water channels. *Proc Natl Acad Sci U S A* 97:4386–4391
- Mak D-OM, Dang B, Weiner ID, Foskett JK, Westhoff CM (2006) Characterization of ammonia transport by the kidney Rh glycoproteins RhBG and RhCG. *Am J Physiol* 290:F297–F305
- Marini A-M, Matassi G, Raynal V, André B, Cartron J-P, Chérif-Zahar B (2000) The human rhesus-associated RhAG protein and a kidney homologue promote ammonium transport in yeast. *Nat Genet* 26:341–344
- Maurel C, Reizer J, Schroeder JJ, Chrispeels MJ, Saier Jr MH (1994) Functional characterization of the *Escherichia coli* glycerol facilitator, GlpF, in *Xenopus* Oocytes. *J Biol Chem* 269:11869–11872
- Mayer M, Schaaf G, Mouro I, Lopez C, Colin Y, Neumann P, Cartron J-P, Ludewig U (2006) Different transport mechanisms in plant and human AMT/Rh-type ammonium transporters. *J Gen Physiol* 127:133–144

- Meinild A-K, Klaerke DA, Zeuthen T (1998) Bidirectional water fluxes and specificity for small hydrophilic molecules in aquaporins 0 to 5. *J Biol Chem* 273:32446–32451
- Murata K, Mitsouka K, Hirai T, Walz T, Agre P, Heymann JB, Engel A, Fujiyoshi Y (2000) Structural determinants of water permeation through aquaporin-1. *Nature* 407:599–605
- Nakhoul NL, DeJong H, Abdunour-Nakhoul SM, Boulpaep EL, Hering-Smith K, Hamm LL (2005) Characteristics of renal Rhbg as an NH_4^+ transporter. *Am J Physiol* 288:F170–F181
- Nakhoul NL, Schmidt E, Abdunour-Nakhoul S-M, Hamm LL (2006) Electrogenic ammonium transport by renal Rhbg. *Transfus Clin Biol* 13:147–153
- Nielsen S, Frøtkier J, Marples D, Kwon T-H, Agre P, Knepper MA (2002) Aquaporins in the kidney: from molecules to medicine. *Physiol Rev* 82:205–244
- Norenberg MD, Rao KVR, Jayakumar AR (2005) Mechanisms of ammonia-induced astrocyte swelling. *Metab Brain Dis* 20:303–318
- Ogami A, Miyazaki H, Niisato N, Sugimoto T, Marunaka Y (2006) UT-B1 urea transporter plays a noble role as active water transporter in C6 glial cells. *Biochem Biophys Res Commun* 351:619–624
- Portincasa P, Moschetta A, Mazzone A, Palasciano G, Svelto M, Calamita G (2003) Water handling and aquaporins in bile formation: recent advances and research trends. *J Hepatol* 39:864–874
- Promeneur D, Lui Y, Maciel J, Agre P, King LS, Kumar N (2007) Aquaglyceroporin PbAQP during intraerythrocytic development of the malaria parasite *Plasmodium berghei*. *Proc Natl Acad Sci U S A* 104:2211–2216
- Quintin F, Eladari D, Cheval L, Lopez C, Goossens D, Colin Y, Cartron J-P, Paillard M, Chambrey R (2003) RhBG and RhCG, the putative ammonia transporters, are expressed in the same cells in the distal nephron. *J Am Soc Nephrol* 14:545–554
- Ripoche P, Bertrand O, Gane P, Birkenmeier C, Colin Y, Cartron J-P (2004) Human rhesus-associated glycoprotein mediates facilitated transport of NH_3 into red blood cells. *Proc Natl Acad Sci U S A* 101:17222–17227
- Rojek A, Praetorius J, Frøtkjaer J, Nielsen S, Fenton RA (2008a) A current view of the mammalian aquaglyceroporins. *Annu Rev Physiol* 70:12.1–12.27
- Rojek A, Skowronski MT, Füchtbauer E-M, Füchtbauer AC, Fenton RA, Agre P, Frøtkier J, Nielsen S (2008b) Defective glycerol metabolism in aquaporin 9 (AQP9) knockout mice. *Proc Natl Acad Sci U S A* 104:3609–3614
- Saparov MS, Liu K, Agre P, Pohl P (2007) Fast and selective ammonia transport by aquaporin-8. *J Biol Chem* 282:5296–5301
- Thompson JD, Gibson TJ, Plewniak F, Jeanmougin F, Higgins DG (1997) The CLUSTAL_X windows interface: flexible strategies for multiple sequence alignments aided by quality analysis tools. *Nucleic Acids Res* 25:4876–4882
- Tsukaguchi H, Weremowicz S, Morton CC, Hediger MA (1999) Functional and molecular characterization of the human neutral solute channel aquaporin-9. *Am J Physiol* 277:F685–F696
- Verkman AS (2005) More than just water channels: unexpected cellular roles of aquaporins. *J Cell Sci* 118:3225–3232
- Waisbren SJ, Geibel JP, Modlin IM, Boron WF (1994) Unusual permeability properties of gastric gland cells. *Nature* 368:332–335
- Weiner D, Verlander JW (2003) Renal and hepatic expression of the ammonium transporter proteins, Rh B glycoprotein and Rh C glycoprotein. *Acta Physiol Scand* 179:331–338
- Westhoff CM, Ferreri-Jacobia M, Mak DD, Foskett JK (2002) Identification of the erythrocyte Rh blood group glycoprotein as a mammalian ammonium transporter. *J Biol Chem* 277:12499–12502
- Winkler FK (2006) Amt/MEP/Rh proteins conduct ammonia. *Pflügers Arch* 451:701–707
- Wu B, Beitz E (2007) Aquaporins with selectivity for unconventional permeants. *Cell Mol Life Sci* 64:2413–2421
- Yang B, Verkman AS (1998) Urea transporter UT3 functions as an efficient water channel. *J Biol Chem* 273:9369–9372
- Yang B, Song Y, Zhao D, Verkman AS (2005) Phenotype analysis of aquaporin-8 null mice. *Am J Physiol* 288:C1161–C1170

- Yang B, Zhao D, Solenov E, Verkman AS (2006a) Evidence from knockout mice against physiologically significant aquaporin 8-facilitated ammonia transport. *Am J Physiol* 291:C417–C423
- Yang B, Zhao D, Verkman AS (2006b) Evidence against functionally significant aquaporin expression in mitochondria. *J Biol Chem* 281:16202–16206
- Yasui M, Hazama AEA, Kwon T-H, Nielsen S, Guggino WB, Agre P (1999) Rapid gating and anion permeability of an intracellular aquaporin. *Nature* 402:184–187
- You G, Smith CG, Kanai Y, Lee W-S, Steitzer M, Hediger MA (1993) Cloning and characterization of the vasopressin-regulated urea transporter. *Nature* 365:844–847
- Zardoya R (2005) Phylogeny and evolution of the major intrinsic protein family. *Biol Cell* 97:397–414
- Zeuthen T, Klaerke DA (1999) Transport of water and glycerol in aquaporin 3 is gated by H⁺. *J Biol Chem* 274:21631–21636
- Zeuthen T, Belhage B, Zeuthen E (2006a) Water transport by Na⁺-coupled cotransporters of glucose (SGLT1) and of iodide (NIS). The dependence of substrate size studied at high resolution. *J Physiol* 570.3:485–499
- Zeuthen T, Wu B, Pavlovic-Djuranovic S, Holm LM, Uzcategui NL, Duszenko M, Kun JFJ, Schultz JE, Beitz E (2006b) Ammonia permeability of the aquaglyceroporins from *Plasmodium falciparum*, *Toxoplasma gondii* and *Trypanosoma brucei*. *Mol Microbiol* 61:1598–1608

Knock-Out Models Reveal New Aquaporin Functions

Alan S. Verkman

Contents

1	Introduction	360
2	AQPs and the Urinary Concentrating Mechanism	360
3	AQPs in Active, Near-Isosmolar Fluid Secretion	362
4	AQP4 in Brain Swelling and Neural Signal Transduction	363
5	AQPs and Eye Physiology	367
6	AQPs in Angiogenesis and Cell Migration	369
7	Physiological Roles for Glycerol Transport by Aquaglyceroporins	371
7.1	AQP3 and Skin Function	372
7.2	AQP3 and Cell Proliferation	373
7.3	AQP7 and Fat Metabolism	375
8	Summary and Perspective	376
	References	377

Abstract Knockout mice have been informative in the discovery of unexpected biological functions of aquaporins. Knockout mice have confirmed the predicted roles of aquaporins in transepithelial fluid transport, as in the urinary concentrating mechanism and glandular fluid secretion. A less obvious, though predictable role of aquaporins is in tissue swelling under stress, as in the brain in stroke, tumor and infection. Phenotype analysis of aquaporin knockout mice has revealed several unexpected cellular roles of aquaporins whose mechanisms are being elucidated. Aquaporins facilitate cell migration, as seen in aquaporin-dependent tumor angiogenesis and tumor metastasis, by a mechanism that may involve facilitated water transport in lamellipodia of migrating cells. The ‘aquaglyceroporins’, aquaporins that transport both glycerol and water, regulate glycerol content in epidermis, fat and other tissues, and lead to a multiplicity of interesting consequences of gene disruption including dry skin, resistance to skin carcinogenesis, impaired cell

A.S. Verkman

Departments of Medicine and Physiology, Cardiovascular Research Institute,
University of California, San Francisco, CA, 94143-0521, USA
verkman@itsa.ucsf.edu

proliferation and altered fat metabolism. An even more surprising role of a mammalian aquaporin is in neural signal transduction in the central nervous system. The many roles of aquaporins might be exploited for clinical benefit by modulation of aquaporin expression/function – as diuretics, and in the treatment of brain swelling, glaucoma, epilepsy, obesity and cancer.

1 Introduction

The mammalian aquaporins (AQPs) are a family of at least 12 related proteins expressed in epithelial, endothelial and other tissues, many of which are involved in fluid transport such as kidney tubules, while others are not such as skin and fat cells. Functional measurements indicate that AQPs 1, 2, 4, 5 and 8 are primarily water-selective, whereas aquaporins 3, 7 and 9 (the ‘aquaglyceroporins’) also transport glycerol and perhaps other small solutes. Tissue distribution and regulation studies have provided indirect evidence for roles of AQPs in a variety of physiological processes. In the case of AQP2, nephrogenic diabetes insipidus in subjects with AQP2 mutation provides direct evidence for AQP2 involvement in the urinary concentrating mechanism (Deen et al. 1994). However, the unavailability to date of aquaporin inhibitors suitable for use *in vivo* has precluded direct investigation of their function.

This review will focus on physiologically important functions of the mammalian AQPs discovered from phenotype analysis of AQP knockout mice and follow-up cell/tissue studies. One of the paradigms that has emerged from phenotype studies of knockout mice is that tissue-specific AQP expression does not mandate AQP involvement in a physiologically important process, as in the case of lung AQPs (reviewed in Verkman 2007), AQPs in the intestine (reviewed in Verkman and Thiagarajah 2006), AQP4 in skeletal muscle (Yang et al. 2000), AQP5 in sweat gland (Song et al. 2002), and AQP8 in multiple tissues (Yang et al. 2005). However, data from knockout mice implicate important roles of AQPs in kidney, brain, eye, skin, fat and exocrine glands, suggesting their involvement in major organ functions and disease processes including urinary concentrating, brain swelling, epilepsy, glaucoma, cancer and obesity.

2 AQPs and the Urinary Concentrating Mechanism

A major and anticipated role of AQPs in kidney is in water transport across kidney tubules and vasa recta for the formation of concentrated urine. Figure 1a shows the distribution of the major renal AQPs. Deletion of AQP1 and/or AQP3 in mice results in marked polyuria, as seen in 24 h urine collections (Fig. 1B) (Ma et al. 1998, 2000b). A qualitatively similar urinary concentrating defect was found in rare humans with defective AQP1 (King et al. 2001). Figure 1c summarizes urine

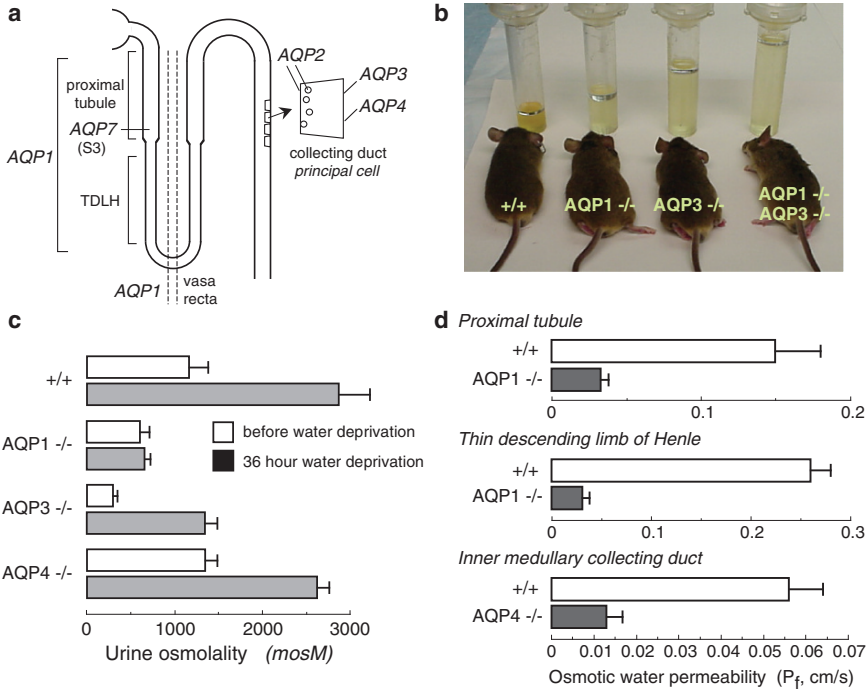


Fig. 1 Impaired urinary concentrating ability in AQP null mice. (a) Sites of AQP expression in kidney. (b) Twenty-four hour urine collections showing polyuria in mice lacking AQP1 and AQP3, individually and together. (c) Urine osmolalities before and after 36 h water deprivation (S.E.). (d) Transepithelial osmotic water permeability (P_f) in microperfused proximal tubule, thin descending limb of Henle and inner medullary collecting from mice of indicated genotype (S.E.). Data summarized from Ma et al. (1997, 1998, 2000b) and Schnermann et al. (1998)

osmolalities in mice before and after 36 h water deprivation. Urinary osmolality in AQP1 null mice is low and does not increase with water deprivation, resulting in severe dehydration. AQP3 null mice are able to generate partially concentrated urine in response to water deprivation, whereas AQP4 null mice manifest only a mild defect in maximum urinary concentrating ability.

AQP1 deletion produces polyuria and unresponsiveness to vasopressin or water deprivation by two distinct mechanisms – impaired near-isosmolar water reabsorption in proximal tubule and reduced medullary hypertonicity resulting from impaired countercurrent multiple and exchange. Transepithelial osmotic water permeability (P_f) in the isolated microperfused S2 segment of proximal tubule was reduced by ~fivefold in AQP1 knockout mice (Fig. 1d) (Schnermann et al. 1998), indicating that most water transport in proximal tubule is transcellular and AQP1-dependent. Free-flow micropuncture with end-proximal tubule fluid sampling showed ~50% reduced fluid absorption, with little effect on single nephron glomerular filtration rate (Schnermann et al. 1998), supporting a three-compartment model in which mild luminal hypotonicity drives osmotic water movement through highly water permeable cell membranes. AQP1 also provides the major route for transepithelial

water permeability in thin descending limb of Henle (TDLH) and outer medullary descending vasa recta (OMDVR) (Chou et al. 1999; Pallone et al. 2000). These results support the conclusions that AQP1 is the principal water channel in TDLH and OMDVR and causes osmotic equilibration in these segments, and plays a key role in the renal countercurrent concentrating mechanism. AQP1 deletion thus impairs urinary concentrating ability by impairing near-isosmolar fluid absorption by proximal tubule and by interfering with the normally hypertonic medullary interstitium generated by countercurrent multiplication and exchange. The precise degree of impairment in urinary concentrating ability is also influenced by secondary renal mechanisms, such as tubuloglomerular feedback, as well as altered expression of other genes in AQP1 null mice. AQP7 is expressed in a small distal segment (S3 segment) of the proximal tubule, though its deletion in mice is not associated with significant impairment in urinary concentrating ability, but rather with an impairment of glycerol clearance, whose significance remains unclear (Sohara et al. 2005).

AQP3 and AQP4 are expressed at the basolateral membrane of collecting duct epithelium, with relatively greater expression of AQP3 in cortical and outer medullary collecting duct and AQP4 in inner medullary collecting duct. In contrast to AQP1 null mice, countercurrent multiplication and exchange mechanisms in AQP3/AQP4 null mice are basically intact. The polyuria in AQP3 null mice results in large part from the more than threefold reduction in P_f of cortical collecting duct basolateral membrane (Ma et al. 2000b). In addition, AQP2 expression is reduced in AQP3 null mice, which appears to be a maladaptive renal response seen in various forms of acquired polyuria. AQP4 null mice manifest only a mild impairment in maximal urinary concentrating ability (Ma et al. 1997), despite fourfold reduced water permeability in microperfused inner medullary collecting duct (Fig. 1d) (Chou et al. 1998). Several mouse models of AQP2 gene deletion and mutation (reviewed in Verkman 2008) support the conclusion that AQP2 is the major vasopressin-regulated water channel whose apical membrane targeting in collecting duct during antidiuresis is crucial for the formation of concentrated urine.

3 AQPs in Active, Near-Isosmolar Fluid Secretion

As mentioned above, impaired fluid absorption in kidney proximal tubule in AQP1 deficiency indicates the need for high cell membrane water permeability for rapid, near-isosmolar fluid transport. The involvement of AQPs in fluid absorption or secretion in various exocrine glands (salivary, submucosal, sweat, lacrimal), absorptive epithelia (lung, airways), and secretory epithelia (choroid plexus and ciliary body) has been investigated using knockout mouse models. The general conclusion is that AQPs facilitate active, transepithelial secretion when sufficiently rapid, such that AQP deletion causes reduced secreted fluid volume and increased ion/solute content of secreted fluid. Because active, near-isosmolar fluid transport involves transepithelial water transport driven by relatively small osmotic gradients produced by salt pumping, AQP deficiency reduces transepithelial water flow. This paradigm

has been confirmed from defective fluid secretion in AQP5 knockout mice in salivary gland (Ma et al. 1999; Krane et al. 2001) and airway submucosal gland (Song and Verkman 2001). Defective fluid secretion has also been found in AQP1 knockout mice in ciliary epithelium (Zhang et al. 2002), which produces aqueous fluid in the eye and in choroid plexus (Oshio et al. 2005), which produces cerebrospinal fluid. However, AQPs appear not to be needed when fluid absorption or secretion rate (per unit epithelial surface area) is low, as in lung (Bai et al. 1999; Ma et al. 2000a; Song et al. 2000a), airways (Song and Verkman 2001), lacrimal gland (Moore et al. 2000) and sweat gland (Song et al. 2002), where AQP-independent water permeability is high enough to support slow fluid transport. In the case of the peritoneal and pleural cavities, though AQP1 facilitates osmotically driven water transport, AQP1 deficiency in mice does not impair the relatively slow absorption of excess fluid in these cavities (Yang et al. 1999; Song et al. 2000b). Together, these results support the anticipated role of AQPs in active fluid absorption and secretion, but indicate that the requirement for AQP-facilitated water transport depends on the rate of water transport.

4 AQP4 in Brain Swelling and Neural Signal Transduction

AQP4 is expressed in the brain and spinal cord at sites of fluid transport at blood–brain and brain–cerebrospinal fluid (CSF) interfaces. AQP4 expression is polarized to astrocytic foot processes in contact with blood vessels and in the dense astrocyte cell processes that form the glia limitans, which lines the CSF-bathed pial and ependymal surfaces in the subarachnoid space and the ventricles (Nielsen et al. 1997). Evidence that AQP4 provides the major route for water transport across astrocyte cell membranes came from osmotic water permeability measurements showing sevenfold reduced water transport in astrocytes cultured from AQP4 null mice (Solenov et al. 2004). Also, accumulation of brain water was found to be greatly slowed in AQP4 null mice in response to serum hypoosmolality, as monitored continuously *in vivo* by a non-invasive near-infrared optical method (Thiagarajah et al. 2005), or by brain wet-to-dry weight ratio measurements done at different times after water intoxication (Papadopoulos and Verkman 2005). Interestingly, AQP4 has been identified as a structural component of membrane ‘orthogonal arrays of proteins’ (OAPs), which are cobblestone-appearing structures, seen by freeze-fracture electron microscopy. OAPs were found in stably transfected CHO cells expressing functional AQP4 (Yang et al. 1996) and were absent in brain, kidney and skeletal muscle in AQP4 null mice (Verbavatz et al. 1997). Subsequently freeze-label electron microscopy studies confirmed the presence of AQP4 in OAPs (Rash et al. 1998). However, the functional significance of AQP4 assembly in OAPs is not known.

Evidence for involvement of AQP4 in brain water balance came from experiments showing reduced brain swelling and improved survival in AQP4 null vs. wildtype mice after water intoxication (Fig. 2a), reduced hemispheric swelling after

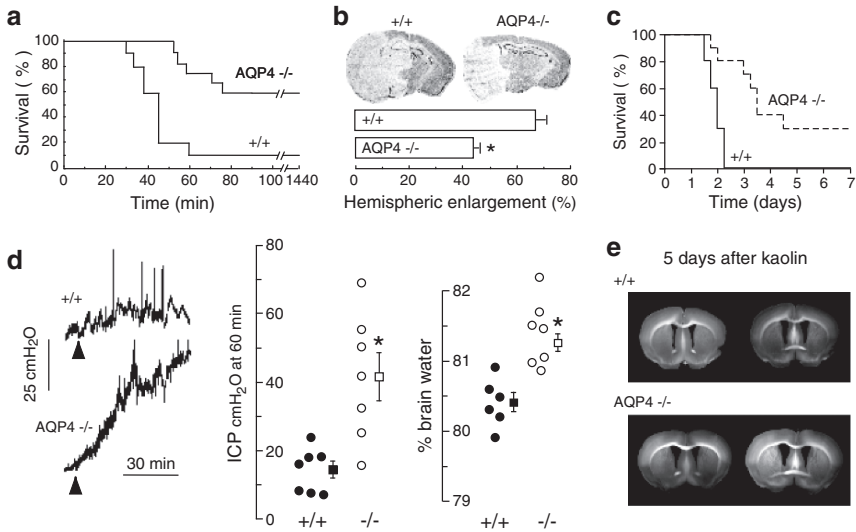


Fig. 2 AQP4 deletion reduces brain water accumulation in cytotoxic edema, but slows removal of excess brain water in vasogenic edema and hydrocephalus. **(a)** Water intoxication model of cytotoxic edema. Mouse survival after acute water intoxication produced by intraperitoneal water injection. **(b)** (*top*) Ischemic stroke model of cytotoxic edema. Brain sections of mice at 24 h after ischemic stroke produced by permanent middle cerebral artery occlusion. (*bottom*) Average hemispheric enlargement expressed as a percentage determined by image analysis of brain sections (S.E., * $P < 0.01$). **(c)** Mouse survival in a bacterial model of meningitis produced by cisternal injection of *S. pneumoniae*. **(d)** Reduced elevation in intracranial pressure (ICP, S.E., * $P < 0.01$) and brain water content (S.E., * $P < 0.001$) following continuous intraparenchymal infusion of artificial cerebrospinal fluid at $0.5 \mu\text{L min}^{-1}$. **(e)** Accelerated progression of hydrocephalus in AQP4 null mice. Coronal sections wildtype and AQP4 null mouse brain at 5 days after kaolin injection. Data from Manley et al. (2000), Papadopoulos et al. (2004), and Bloch et al. (2006)

focal cerebral ischemia (Fig. 2b) and improved survival after bacterial meningitis (Fig. 2c) (Manley et al. 2000; Papadopoulos and Verkman 2005). Reduced brain swelling was also reported in alpha-syntrophin null mice, which secondarily manifested disrupted brain AQP4 expression (Amiry-Moghaddam et al. 2003a). According to the Klatzo classification of brain edema, these are primarily models of cytotoxic (cell swelling) edema in which excess water moves from the vasculature into the brain parenchyma through an intact blood–brain barrier. The forces driving water flow to form cytotoxic edema are osmotic, generated in water intoxication by reduced plasma osmolality and in ischemia by impaired Na^+/K^+ ATPase pump function with consequent Na^+ and water flow from the intravascular and extracellular compartments into the intracellular compartment. AQP4 also plays a key role in elimination of excess brain water. When the blood–brain barrier becomes disrupted (brain tumor, brain abscess, focal freeze injury), water moves from the vasculature into the extracellular space of the brain in an AQP4-independent manner down a hydrostatic gradient to form, what was termed by Klatzo vasogenic edema. Excess water is eliminated primarily through the glia limiting membrane into the cere-

brospinal fluid. We found greater brain water accumulation and intracranial pressure in AQP4 null vs. wildtype mice with brain tumor, brain abscess, focal cortical freeze injury and after infusion of normal saline directly into the brain extracellular space (Fig. 2d) (Papadopoulos et al. 2004; Bloch et al. 2005), supporting the conclusion that in vasogenic edema fluid is eliminated by an AQP4-dependent route. In a kaolin model of hydrocephalus AQP4 null mice develop marked hydrocephalus, probably due to reduced transependymal water clearance (Fig. 2e) (Bloch et al. 2006). AQP4 thus is a major determinant in fluid movement into and out of the brain.

AQP4 also appears to play an unexpected role in neural signal transduction. AQP4 is expressed in supportive cells adjacent to electrically excitable cells, as in glia vs. neurons in brain and spinal cord, Müller vs. bipolar cells in retina, and hair vs. supportive cells in the inner ear. We found evidence for impaired auditory and visual signal transduction in AQP4 null mice, seen as increased auditory brainstem response thresholds (Li and Verkman 2001; Mhatre et al. 2002) and reduced electroretinographic potentials (Li et al. 2002). In brain, seizure susceptibility in response to the convulsant (GABA antagonist) pentylenetetrazol was remarkably increased in AQP4 null mice (Binder et al. 2004a); at 40 mg kg⁻¹ pentylenetetrazol, all wildtype mice exhibited seizure activity, whereas six out of seven AQP4 null mice did not exhibit seizure activity. In freely moving mice (Fig. 3a, *top*), electrically-induced seizures following hippocampal stimulation showed greater threshold and remarkably longer seizure duration in AQP4 null mice compared to wildtype mice (Fig. 3a, *bottom*) (Binder et al. 2006). In support of these findings, using a hyperthermia model of seizure induction, alpha-syntrophin deficient mice developed more severe seizures than wildtype mice (Amiry-Moghaddam et al. 2003b).

The mechanisms for altered neuroexcitation in AQP4 deficiency remain unknown. Delayed K⁺ uptake from brain extracellular space (ECS) in AQP4 deficiency has been suggested, which may account for the prolonged seizure phenotype. Direct measurements of [K⁺] in brain cortex in living mice using K⁺-sensitive microelectrodes showed significant slowing of K⁺ clearance following electrical stimulation (Fig. 3b). Using a K⁺-sensitive fluorescent dye, altered K⁺ wave dynamics was found in a cortical spreading depression model of neuroexcitation, again with delayed K⁺ clearance (Fig. 3c). It was proposed from immunocolocalization and immunoprecipitation studies that AQP4 is closely associated with the inwardly rectifying K⁺ channel Kir4.1 in astroglia and Müller cells, suggesting that reduced K⁺ channel function in AQP4 deficiency might account for the delay in K⁺ clearance. However, recent patch-clamp studies in astroglia (Zhang and Verkman 2008) and Müller cells (Ruiz-Ederra et al. 2007) provide evidence against this hypothesis. Another possible explanation involves ECS expansion in AQP4 deficiency, which may account in part for reduced seizure susceptibility and prolonged seizure duration in AQP4 deficiency. An expanded ECS would provide a larger aqueous volume to dilute K⁺ released into the ECS during neuroexcitation, thereby slowing changes in ECS K⁺ concentration. Evidence for an expanded ECS in AQP4 deficiency came from cortical surface photobleaching measurements of the diffusion of fluorescently-labeled macromolecules (Binder et al. 2004b). The ECS in

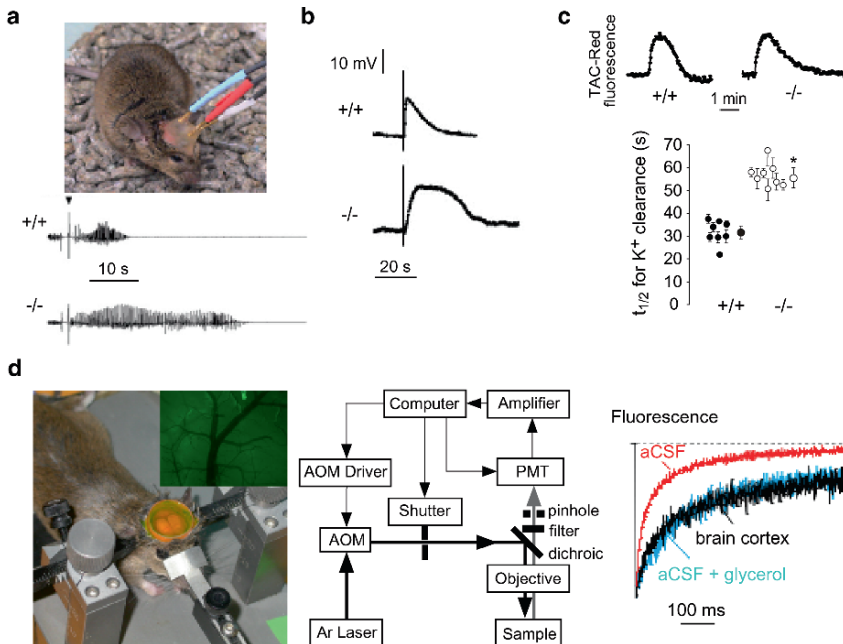


Fig. 3 Involvement of AQP4 in brain neuroexcitation. **(a)** Increased seizure duration in AQP4 null mice. *(top)* Bipolar electrodes implanted in the right hippocampus were connected to a stimulator and electroencephalograph recording system. *(bottom)* Representative electroencephalographic recordings in freely moving mice following electrically induced generalized seizures. **(b)** Delayed K^+ clearance in brain following electrically induced seizure-like neuroexcitation. Measurements done using K^+ -sensitive microelectrodes inserted into brain cortex in living mice. **(c)** Slowed K^+ clearance in brain ECS during cortical spreading depression measured using TAC-Red, a K^+ -sensitive fluorescent probe. *(top)* Representative data. *(bottom)* Half-times ($t_{1/2}$) for K^+ reuptake. **(d)** Expanded brain ECS in AQP4 null mice measured by cortical surface photobleaching. *(left)* Mouse brain surface exposed to FITC-dextran with dura intact following craniectomy and fluorescence imaging of cortical surface after loading with FITC-dextran (inset). *(middle)* Photobleaching apparatus. A laser beam is modulated by an acousto-optic modulator and directed onto the surface of the cortex using a dichroic mirror and objective lens. *(right)* In vivo fluorescence recovery in cortex of wildtype mouse shown in comparison to aCSF and 30% glycerol in a CSF. Taken from Binder et al. (2004b, 2006) and Padmawar et al. (2005)

mouse brain was stained with fluorescein-dextran by exposure of the intact dura after craniectomy (Fig. 3d, *left*), and diffusion detected by fluorescence recovery after photobleaching (Fig. 3d, *middle*). Diffusion was slowed \sim threefold in brain ECS relative to saline solutions (Fig. 3d, *right*), and significantly accelerated in AQP4 null mice, indicating an expanded ECS. ECS expansion in AQP4 deficiency was also shown utilizing a microfiberoptic epifluorescence photobleaching method to measure diffusion in deep brain structures (Zador et al. 2008). It remains unclear, however, whether ECS expansion in AQP4 deficiency could account quantitatively for the altered ECS K^+ dynamics, as well as the mechanisms involved in chronic ECS expansion in AQP4 deficiency.

5 AQPs and Eye Physiology

The eye expresses several AQPs at putative sites of fluid transport (Fig. 4a). The expression of MIP (major intrinsic protein, also referred to as AQP0) in lens fiber has been known for many years. Mutations in AQP0 in humans are associated with congenital cataracts (Berry et al. 2000). AQP1 is expressed in corneal endothelia and at sites of aqueous fluid production (ciliary epithelium) and outflow (trabecular meshwork). AQP3 is expressed in the conjunctival epithelium. AQP4 is expressed in Müller cells in retina, which support the electrically excitable hair cells, as well as in optic nerve. AQP4 is also expressed with AQP1 in non-pigmented ciliary epithelium. AQP5 is expressed in corneal epithelia and lacrimal gland. The expression pattern of AQPs provides indirect evidence for their involvement in intraocular pressure (IOP) regulation (AQP1 and AQP4), corneal and lens transparency (AQP0, AQP1 and AQP5), visual signal transduction (AQP4), tear film homeostasis (AQP3 and AQP5), conjunctival barrier function (AQP3) and tear formation by lacrimal glands (AQP5).

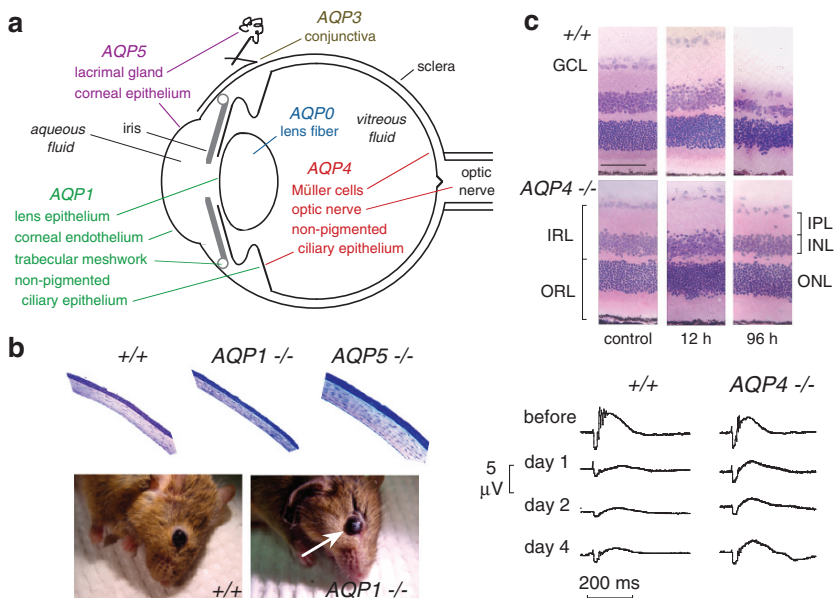


Fig. 4 Ocular phenotype in AQP deficient mice. **(a)** Sites of AQP expression in the eye. **(b)** (top) Stained plastic sections of corneas of mice indicated genotype showing epithelium (upper surface), stroma and endothelium. (bottom) Photographs of wildtype and AQP1 null mice at 40 min after a 10 min exposure of the corneal surface to distilled water showing corneal opacification in the AQP1 null mouse (white arrow). **(c)** (top) Retinal morphology in an ischemia-reperfusion model of retinal injury. Hematoxylin and eosin-stained retinal sections before and at 12 and 96 h after 60 min retinal ischemia in wildtype and AQP4 null mice. Note retinal swelling at 12 h and degeneration at 96 h. (bottom) Functional analysis by electroretinography. Representative electroretinograms before and at 1, 2 and 4 days after 45 min retinal ischemia in wildtype and AQP4 null mice. From Thiagarajah and Verkman (2002) and Da and Verkman (2004)

These possibilities have been examined systematically by phenotype analysis of AQP knockout mice. Interestingly, compared to wildtype mice that have a corneal thickness of 123 μm , corneal thickness was reduced in AQP1 null mice (101 μm) and increased in AQP5 null mice (144 μm) (Thiagarajah and Verkman 2002). Thickness measurements were made in fixed eyes (Fig. 4b, *top*), as well as by brightfield scanning confocal microscopy *in vivo*. After exposure of the external corneal surface to hypotonic saline the rate of corneal swelling was reduced \sim twofold by AQP5 deletion. After exposure of the corneal endothelial surface to hypotonic saline by anterior chamber perfusion, the rate of corneal swelling was reduced \sim fourfold by AQP1 deletion. Remarkably, though baseline corneal transparency was not impaired by AQP1 deletion, the recovery of corneal transparency and thickness after hypotonic swelling (10 min exposure of corneal surface to distilled water) was remarkably delayed in AQP1 null mice, with \sim 75% recovery at 7 min in wildtype mice compared to 5% recovery in AQP1 null mice (Fig. 4b, *bottom*). These data provide evidence for AQP1 involvement in active extrusion of fluid from the corneal stroma across the corneal endothelium. Water permeability has also been measured in conjunctiva, where it is significantly slowed in AQP3 knockout mice (Levin and Verkman 2004). Together with permeability data for cornea, a mathematical model of tear film osmolarity was developed, providing insights into the pathophysiology of dry eye disorders and possible roles of ocular surface AQPs.

The principal determinants of IOP are the rate of aqueous fluid production by the ciliary epithelium and the rate of fluid drainage (outflow) in the canal of Schlemm. As mentioned above, aqueous fluid production involves passive, near-isosmolar fluid secretion driven by active salt transport across the ciliary epithelium. Aqueous fluid drainage primarily involves pressure-driven bulk fluid flow in the canal of Schlemm. Using a modified micro-needle method to measure IOP, a small though significant reduction in IOP was found in mice lacking AQP1, with reduced aqueous fluid secretion, though unimpaired aqueous fluid drainage (Zhang et al. 2002). Whether larger differences in IOP will be found with AQP deficiency in models of glaucoma remains to be determined.

Like the AQP1-expressing corneal endothelium covering the corneal inner surface, the anterior surface of the lens is covered by an AQP1-expressing epithelium. Motivated by the marked impairment of AQP1 deletion on corneal transparency in an experimental model of corneal swelling, we tested the possibility that a lens AQP1 might serve a similar function (Ruiz-Ederra et al. 2006). Osmotic water permeability across lens epithelium was \sim threefold reduced in lenses from AQP1 null mice. Though AQP1 deletion did not alter baseline lens morphology or transparency, lens water content was significantly greater by \sim 4% in AQP1 null mice. *In vitro* and *in vivo* models were used to test for possible involvement of AQP1 in cataract formation. *In vitro*, following incubation of lenses in high glucose solutions, loss of lens transparency was greatly accelerated in AQP1-null lenses as measured by optical contrast analysis of transmitted grid images. *In vivo*, cataract formation was significantly accelerated in AQP1 null mice in a model of acetaminophen toxicity. The data suggested that AQP1 facilitates the maintenance of lens transparency and opposes cataract formation.

AQP4 is expressed in Müller cells in retina, where as mentioned above it appears to be involved in light signal transduction. We found evidence also for AQP4 involvement in retinal swelling (Da and Verkman 2004). Motivated by the protection against cytotoxic brain edema conferred by AQP4 gene deletion, the possibility was tested that AQP4 deletion in mice protects the retina in a transient ischemia-reperfusion model produced by 45–60 min IOP elevation to 120 mmHg. Retinal structure and cell number were remarkably preserved in AQP4 null mice, particularly in inner nuclear and plexiform layers of retina where Müller cells are concentrated (Fig. 4C). Retinal function and cell survival were also significantly improved in AQP4 deficient mice. By electroretinography, b-wave amplitude was reduced by ~75% at 1–4 days after ischemia in wildtype mice vs. less than 50% in AQP4 null mice (Fig. 4C). AQP4 deletion in mice is thus neuroprotective in a transient ischemia model of retinal injury, though the precise neuroprotective mechanism(s) remain to be established.

6 AQPs in Angiogenesis and Cell Migration

Phenotype analysis of AQP1 null mice led to discovery of AQP involvement in cell migration. Based on the expression of AQP1 in tumor microvessels (Endo et al. 1999), we tested the possible involvement of AQP1 in tumor angiogenesis (Saadoun et al. 2005a). We found that AQP1 deletion in mice reduces tumor growth following subcutaneous injection of melanoma cells (Fig. 5a), which was associated with increased tumor necrosis and reduced blood vessel formation within the tumor bed. In experiments designed to elucidate the mechanism of defective tumor angiogenesis in AQP1 deficiency, we found that cultured aortic endothelial cells from AQP1 null mice migrate more slowly towards a chemotactic stimulus compared with AQP1-expressing endothelial cells (Fig. 5b). Figure 5c shows increased movement of cells expressing AQP1. Interestingly, in migrating cells, AQP1 becomes polarized to the front end of cells (Fig. 5d) and is associated with increased turnover of cell membrane protrusions, suggesting an important role for AQPs at the leading edge of migrating cells.

Follow-up experiments showed that AQPs facilitate cell migration independent of AQP and cell types. AQP4 facilitates astrocyte cell migration (Saadoun et al. 2005b; Auguste et al. 2007), AQP3 facilitates migration of corneal epithelial cells (Levin and Verkman 2006) and epidermal cells (Hara-Chikuma and Verkman 2008a), and AQP1 facilitates the migration of cultured renal proximal tubule cells (Hara-Chikuma and Verkman 2006), B16F10 melanoma and 4T1 breast cancer cells (Hu and Verkman 2006). In addition to defective angiogenesis in AQP1 deficiency, other consequences of AQP-facilitated cell migration include AQP involvement in tumor spread, glial scar formation, and wound healing. We have obtained evidence for each of these processes: (a) AQP1 expression in tumor cells increases their migration across endothelial barriers, local invasiveness and metastatic potential (Hu and Verkman 2006); (b) AQP4 deletion in glial cells reduces their migration toward

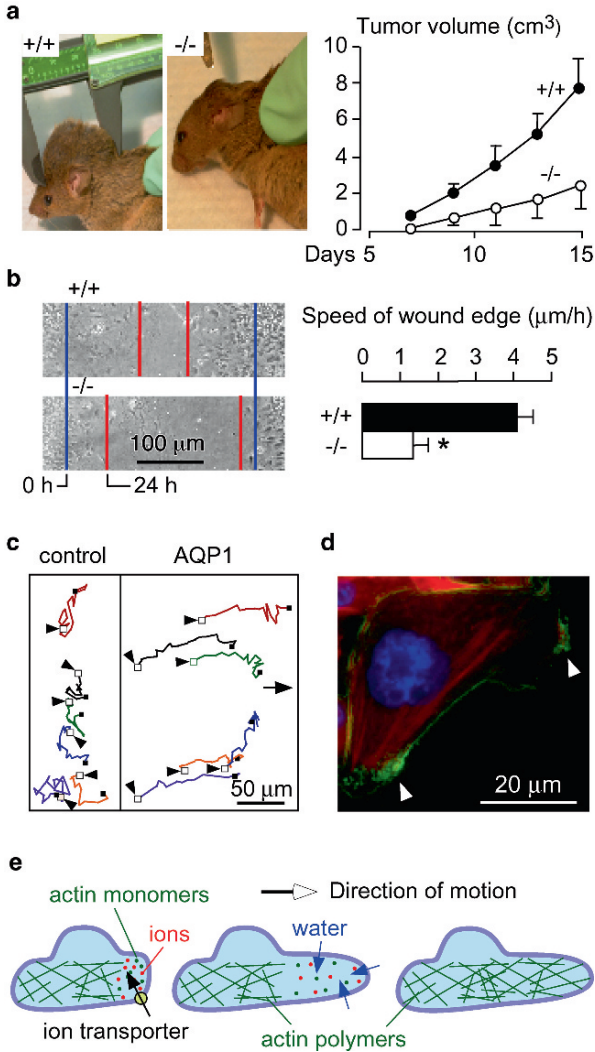


Fig. 5 Impaired tumor growth and endothelial cell migration in AQP1 null mice. **(a)** (left) Tumor in a wildtype vs. AQP1 null mouse, 2 weeks after subcutaneous injection of 10⁶ B16F10 melanoma cells. (right) Tumor growth data (ten mice per group, S.E., $P < 0.001$). **(b)** (left) Wound healing of cultured endothelial cells (initial wound edge blue, after 24 h red). (right) Wound edge speed ($n = 4$ per group, S.E., $*P < 0.01$). **(c)** Tracks of six migrating CHO cells expressing AQP1 vs. six non-AQP expressing control CHO cells, tracked for 4 h. Initial cell positions indicated by arrows. **(d)** AQP1 protein (green) polarization to lamellipodia (arrows) in a migrating CHO cell. **(e)** Proposed mechanism of AQP-facilitated endothelial cell migration: Actin de-polymerization and ion movements increase osmolality at the anterior end of the cell. Water entry increases local hydrostatic pressure, producing cell membrane expansion to form a protrusion. Actin re-polymerizes stabilizing the protrusion. Adapted from Saadoun et al. (2005a)

a wound *in vivo* (Auguste et al. 2007) and the rate of glial scar formation (Saadoun et al. 2005b); and (c) AQP3 deletion impairs closure of cutaneous wounds (Hara-Chikuma et al. 2005) and corneal wounds (Levin and Verkman 2006). Possible involvement of AQP-dependent cell migration in other processes, such as organ regeneration and leukocyte chemotaxis, remain to be tested.

The mechanisms by which AQPs enhance cell migration are under investigation. The enhanced cell migration found for multiple structurally different AQPs, independent of their modulation method (transfection, knock-out, RNA inhibition), suggests that AQP-facilitated transmembrane water transport is the responsible mechanism. One mechanism by which AQPs may accelerate cell migration is by facilitating rapid changes in cell volume, which accompany changes in cell shape as cells squeeze through the irregularly shaped extracellular space. Water flow across the cell membrane may also allow migrating cells to generate hydrostatic forces that 'push apart' adjacent stationary cells. This mechanism, however, does not account for the polarization of AQPs to the front end of migrating cells or for AQP enhancement of lamellipodial dynamics. These observations support a role for water movement into and out of the leading edge during cell migration, as was proposed previously (Condeelis 1993). According to this hypothesis, actin de-polymerization and ion influx increase cytoplasmic osmolality at the front end of the migrating cell (Fig. 5e). These localized changes in cytoplasmic osmolality drive water influx through the plasma membrane. Consistent with the idea that water flows into and out of migrating cells are reports that migration can be inhibited or accelerated by changing the osmolality of the extracellular medium. We proposed that water influx thus causes expansion of the adjacent plasma membrane by increased local hydrostatic pressure, which is followed by rapid actin re-polymerization to stabilize the cell membrane protrusion. Recent evidence shows that regional hydrostatic pressure changes within cells do not equilibrate throughout the cytoplasm on scales of 10 μm and 10 s (Charras et al. 2005) and could thus contribute to the formation of localized cell membrane protrusions. Direct measurements of water flow across the leading edge of migrating cells are needed for validation of these ideas.

7 Physiological Roles for Glycerol Transport by Aquaglyceroporins

For many years the physiological significance of glycerol transport by a subset of the AQPs, the aquaglyceroporins, was unclear. Phenotype studies of aquaglyceroporin knockout mice have addressed this question, producing a number of remarkable findings. There is now strong evidence for involvement of AQP3 in epidermal biology and cell proliferation and of AQP7 in adipocyte metabolism. A recent report on the phenotype of AQP9 null mice showed a subtle phenotype suggestive of impaired hepatic glycerol uptake (Rojek et al. 2007), though the mechanism remains to be established as does its proposed significance to diabetes.

7.1 AQP3 and Skin Function

The most superficial layer of skin is the stratum corneum (SC), which consists of terminally differentiated keratinocytes (corneocytes) that originate from actively proliferating keratinocytes in lower epidermis and contain a lamellar lipid layer (Fig. 6a). Hydration of the SC is an important determinant of skin appearance and physical properties and depends on a number of factors including the external humidity and its structure, lipid/protein composition, barrier properties and concentration of water-retaining osmolytes.

Phenotype analysis of AQP3 deficient mice has provided compelling evidence for a role of AQP3 in epidermal biology. AQP3 is expressed strongly in the basal layer of keratinocytes in mammalian skin (Fig. 6b, left). Figure 6b (right) shows reduced SC hydration in AQP3 null mice as measured by high frequency skin conductance (Ma et al. 2002), which is a linear index of SC water content. Exposure of mice to high humidity or occlusion increased SC hydration in wildtype, but not

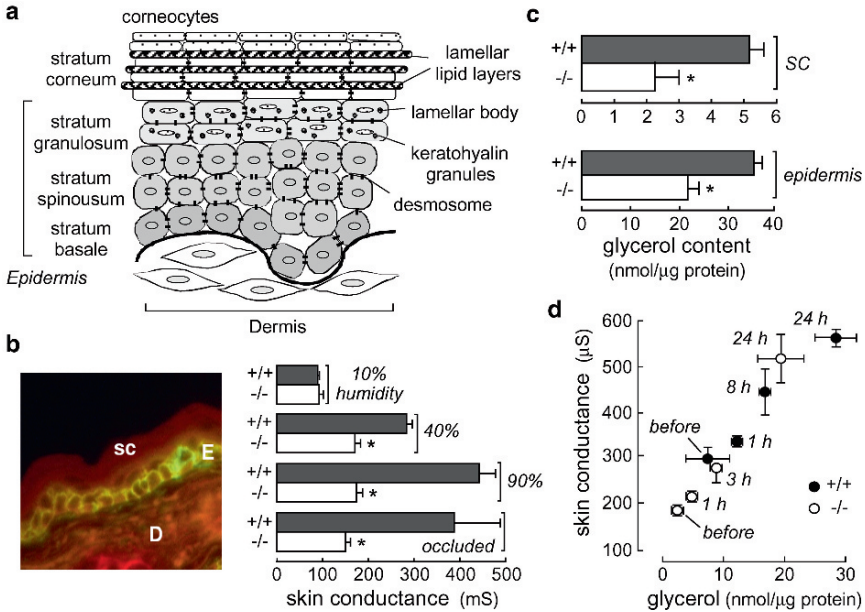


Fig. 6 Reduced skin hydration in AQP3 deficiency. (a) Schematic showing stratum corneum and epidermal layers. (b) (left) Immunofluorescence showing AQP3 in mouse epidermal cells. E epidermis; D dermis; sc stratum corneum. (right) High-frequency superficial skin surface conductance in dorsal skin of hairless wildtype and AQP3 null mice (S.E., 20 mice per group). Skin conductance measured after 24 h exposure to relative humidity of 10, 40, or 90%; * indicates a plastic occlusion dressing that prevents evaporative water loss (S.E., five mice per group). (c) Glycerol content measured in SC and epidermis (S.E., *P < 0.01). (d) Correlation between SC glycerol content and skin conductance for wildtype (filled circles) and AQP3 null (open circles) mice in a 90% humidity atmosphere for indicated times. Mice were given glycerol orally *ad libitum* as their only fluid source. From Hara et al. (2002), Ma et al. (2002) and Hara and Verkman (2003)

AQP3 null mice, indicating that water transport through AQP3 is not a rate-limiting factor in transepidermal water loss. If reduced SC hydration is related to a balance between evaporative water loss from the SC and water replacement through AQP3-containing basal keratinocytes, then preventing water loss by high humidity or occlusion should have corrected the defect in SC hydration in the AQP3 null mice. Further skin phenotype analysis indicated delayed barrier recovery after SC removal by tape-stripping in AQP3 null mice, as well as decreased skin elasticity and delayed wound healing (Hara et al. 2002).

Many types of experiments were done to investigate the mechanism by which AQP3 deficiency produces the pleiotropic defects in skin function. A systematic analysis of the ultrastructure and composition of the epidermis and stratum corneum in AQP3 deficient mice revealed reduced glycerol content in SC and epidermis (Fig. 6c), with normal glycerol in dermis and serum; suggesting reduced glycerol transport from blood into the epidermis in AQP3 deficiency through the basal keratinocytes. No significant differences in wildtype vs. AQP3 deficient mice were found in SC structure, cell turnover, lipid profile, protein content and the concentrations of amino acids, ions and other small solutes (Hara et al. 2002). From these observations it was postulated that reduced epidermal and SC glycerol content was responsible for the abnormal skin phenotype in AQP3 null mice. Because glycerol is a 'natural moisturizing factor', reduced SC glycerol is predicted to reduce SC hydration and skin elasticity; because of the biosynthetic role of glycerol in the epidermis, reduced epidermal glycerol is predicted to delay barrier recovery function and wound healing. In support of this hypothesis, it was found that glycerol replacement by topical or systemic routes corrected each of the phenotype abnormalities in AQP3 null mice (Hara and Verkman 2003). SC glycerol content and water content, as assessed by skin conductance, correlated well for mice placed in a 90% humidity atmosphere and given oral glycerol (Fig. 6d). Further, glycerol transport from blood into the epidermis and SC was found to be reduced in AQP3 deficiency, suggesting impaired glycerol transport into the epidermis and SC through the relatively glycerol impermeable basal keratinocyte layer resulting in reduced steady-state epidermal and SC glycerol content. These findings indicated an important role for AQP3 and glycerol in epidermal function, providing a rational scientific basis for the long-standing practice of including glycerol in cosmetic and skin medicinal preparations.

7.2 AQP3 and Cell Proliferation

We recently discovered a remarkable phenotype in AQP3 null mice – resistance to the development of skin tumors (Hara-Chikuma and Verkman 2008b). Our motivation for studying AQP3 and skin tumors was the strong expression of AQP3 in basal cells in human skin squamous cell carcinomas. Figure 7a shows one of many such examples. Also, we recently discovered proliferation defects in AQP3 knockout mice in normally AQP3-expressing cells in cornea (Levin and Verkman 2006), resulting in delayed healing of corneal wounds, in colon (Thiagarajah et al.

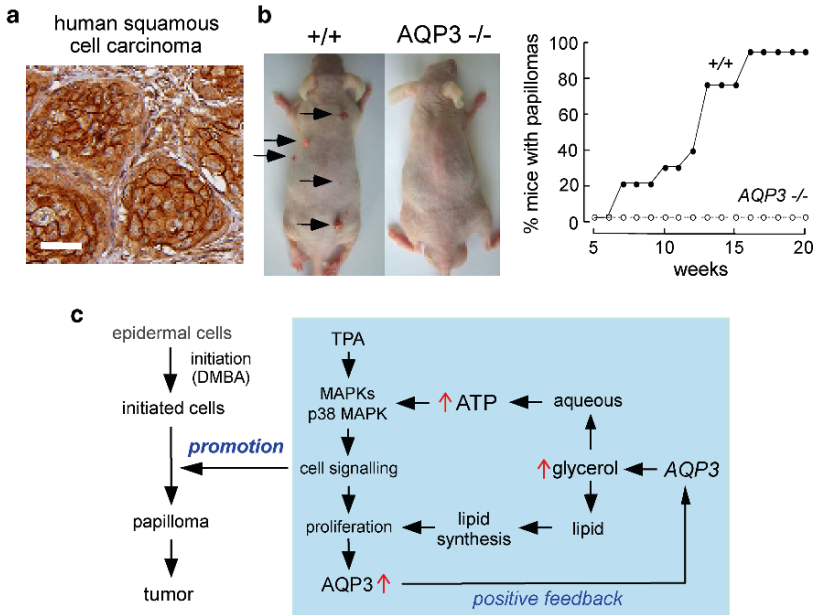


Fig. 7 AQP3 expression in human squamous cell carcinoma and protection against cutaneous papillomas in AQP3-null mice. **(a)** AQP3 immunostaining in human skin squamous cell carcinoma. Bar, 50 μ m. **(b)** (left) Dorsal skin of mice was treated with a single application of DMBA, followed by twice-weekly applications of TPA for 20 weeks. Representative photographs showing multiple papillomas in wildtype mouse but no papillomas in AQP3 null mouse. (right) Percentage of mice with papillomas. **(c)** Proposed cellular mechanism of AQP3-facilitated tumorigenesis. Adapted from Hara-Chikuma and Verkman (2008b)

2007), producing severe colitis in experimental models, and skin (Hara-Chikuma and Verkman 2008a), slowing cutaneous wound healing.

An established multistage carcinogenesis model was used to study skin tumor formation, which involves skin exposure to a tumor initiator and phorbol ester promoter. The remarkable phenotype finding, as shown in Fig. 7b was the absence of cutaneous papillomas in AQP3 knockout mice, whereas multiple tumors were produced in wild-type mice (Hara-Chikuma and Verkman 2008b). Experiments to establish the cellular mechanisms responsible for the impaired tumorigenesis phenotype showed impaired promoter-induced cell proliferation in AQP3-null or knock-down keratinocytes. AQP3-deficient keratinocytes had reduced content of glycerol, its metabolite glycerol-3-phosphate, and ATP, without impairment of mitochondrial function. Glycerol supplementation or AQP3 adenoviral infection (but not AQP1 adenoviral infection) corrected the defects in keratinocyte proliferation and reduced ATP generation. Further studies revealed correlations between cell proliferation and ATP and glycerol content. As diagrammed in Fig. 7c, we propose that AQP3-facilitated glycerol transport is an important determinant of epidermal cell proliferation and tumorigenesis by a mechanism in which cellular glycerol is a key

regulator of cellular ATP energy. The mechanism also shows glycerol biosynthetic incorporation into lipids, ATP-facilitated MAP kinase signaling and positive feedback in which cell proliferation increases AQP3 expression. It is not known whether this mechanism applies to non-epidermal, AQP3-expressing cells and to non-skin cancers. Our findings also raise potential concerns in the use of recently marketed cosmetics containing ingredients that increase epidermal AQP3 expression whose goal is to improve skin moisture and appearance.

7.3 *AQP7 and Fat Metabolism*

We discovered a remarkable phenotype in AQP7 null mice (Hara-Chikuma et al. 2005). Although wildtype and AQP7 mice grew at similar rates as assessed by mouse weight, AQP7 null mice had remarkably greater fat mass compared to wildtype mice as seen grossly (Fig. 8a, *top*). Fat mass from multiple sites was significantly elevated in both male and female AQP7 null mice at age 16 weeks. Epididymal fat mass was comparable in wildtype and AQP7 null mice until age 4 weeks, but became different as the mice aged (Fig. 8b). Histologically, adipocytes at 16 weeks were remarkably larger in AQP7 null mice than in wildtype mice (Fig. 8a, *bottom*), suggesting that the greater fat mass in the AQP7 null mice is a consequence of adipocyte hypertrophy. Adipocyte size was similar in young wildtype and AQP7 deficient mice.

The concentrations of glycerol and triglycerides in serum were unaffected by AQP7 deletion, though adipocyte glycerol and triglyceride concentrations were significantly elevated in AQP7 null mice (Fig. 8c). To investigate the mechanism for the progressive adipocyte hypertrophy in AQP7 deficiency, measurements were made of adipocyte plasma membrane glycerol permeability, glycerol release, lipolysis and lipogenesis. Plasma membrane glycerol permeability was measured from the initial uptake of ^{14}C -glycerol into isolated adipocytes from the younger wildtype and AQP7 null mice, where adipocyte size is comparable. ^{14}C -glycerol uptake was reduced by \sim threefold in AQP7 null mice compared to wildtype mice. Glycerol release was also significantly reduced in the AQP7 null mice, whereas lipolysis, as measured by free fatty acid release from isolated adipocytes, was similar in wildtype and AQP7 deficient mice. Also, lipogenesis was similar in the wildtype and knockout mice, as assayed from the incorporation of ^{14}C -glucose into triglycerides. From these results we proposed a simple mechanism for progressive TG accumulation in AQP7 deficient adipocytes (Fig. 8d). Reduced plasma membrane glycerol permeability in AQP7 deficiency results in an increase in steady-state glycerol concentration in adipocyte cytoplasm. Increased adipocyte glycerol concentration would then increase glycerol 3-phosphate and hence triglyceride (TG) biosynthesis. Similar conclusions about fat metabolism in AQP7 deficiency were reported independently (Hibuse et al. 2005), though with some relatively minor differences in phenotype findings compared to our results. From these data, it was speculated that AQP7 plays an important role in the pathogenesis of human obesity (reviewed in

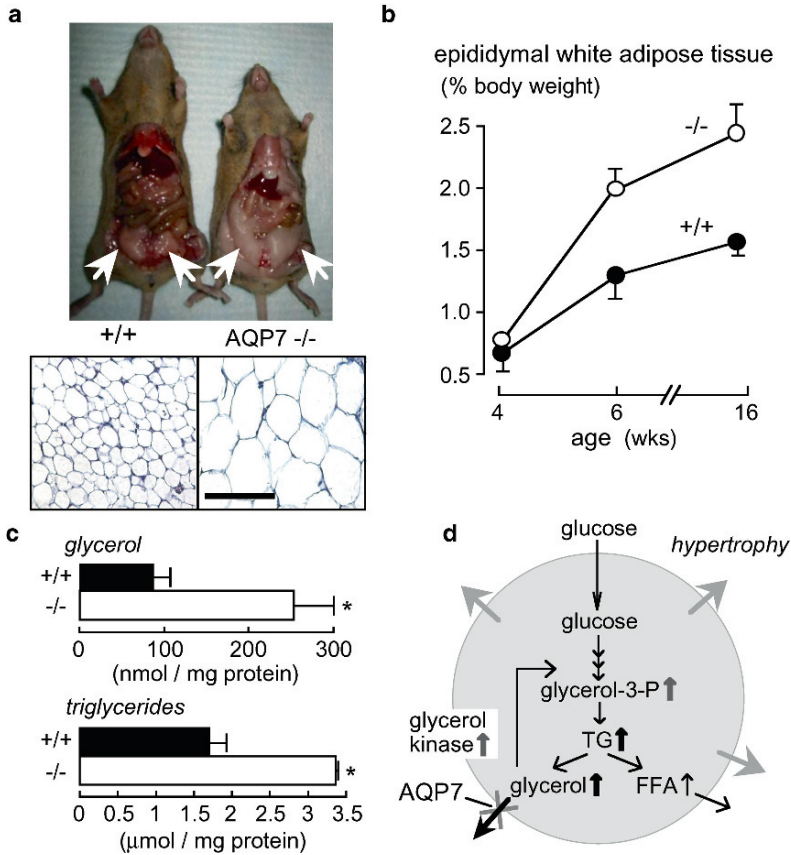


Fig. 8 Progressive fat accumulation and adipocyte hypertrophy in AQP7 deficiency. (a) (top) Photographs of mice showing increased gonadal fat in AQP7 null mice at age 16 weeks (white arrows). (bottom) Histology of gonadal fat (stained with hematoxylin and eosin). Bar, 100 μ m. (b) Age-dependent epididymal fat mass (S.E., six mice per group). (c) Glycerol and triglyceride content in adipocytes from mice of age 16 weeks (S.E., * $P < 0.01$). (d) Proposed mechanism for adipocyte hypertrophy in AQP7 deficiency. See text for explanations. From Hara-Chikuma et al. (2005)

Funahashi et al. 2006), though whether this is the case remains to be determined. Interestingly, a weak association of AQP7 polymorphisms with the risks of obesity and diabetes was reported (Prudente et al. 2007).

8 Summary and Perspective

The phenotype data on AQP-deficient mice suggests that AQP-facilitated water permeability is important: (a) when water movement is driven across a barrier by a continuous osmotic gradient (as in kidney collecting duct); (b) for active, near-isosmolar

fluid absorption/secretion (as in kidney proximal tubule and salivary gland); (c) for neural signal transduction (as in brain and inner ear); and (d) for cell migration (as in tumor angiogenesis). Aquaglyceroporin-facilitated glycerol transport is important in skin hydration and cell proliferation (AQP3) and adipocyte metabolism (AQP7). It is likely that additional new roles of AQPs will be discovered. Much work remains to be done in following up the mouse phenotype observations, in discovering new roles of AQPs in mammalian physiology and in developing clinical therapies based on the new insights emerging from the mouse phenotype analyses. Additional data are needed to establish a firm mechanistic basis for AQP involvement in migration, neural signal transduction and in clearance of excess brain water in vasogenic edema, and in the precise role of the aquaglyceroporins in metabolism and cell proliferation. Small-molecule modulators of AQP expression/function could have clinical applications in the therapy of congestive heart failure and hypertension, cytotoxic and vasogenic brain edema, epilepsy, obesity, cancer, glaucoma and other conditions.

Acknowledgments Supported by grants DK35124, EB00415, EY13574, HL59198, DK72517 and HL73856 from the National Institutes of Health and Research Development Program and Drug Discovery grants from the Cystic Fibrosis Foundation

References

- Amiry-Moghaddam M, Otsuka T, Hurn PD, Traystman RJ, Haug FM, Froehner SC, Adams ME, Neely JD, Agre P, Ottersen OP, Bhardwaj A (2003a) An alpha-syntrophin-dependent pool of AQP4 in astroglial end-feet confers bidirectional water flow between blood and brain. *Proc Natl Acad Sci U S A* 100:2106–2111
- Amiry-Moghaddam M, Williamson A, Palomba M, Eid T, de Lanerolle NC, Nagelhus EA, Adams ME, Froehner SC, Agre P, Ottersen OP (2003b) Delayed K⁺ clearance associated with aquaporin-4 mislocalization: phenotypic defects in brains of alpha-syntrophin-null mice. *Proc Natl Acad Sci U S A* 100:13615–13620
- Auguste KI, Jin S, Uchida K, Yan D, Manley GT, Papadopoulos MC, Verkman AS (2007) Greatly impaired migration of implanted aquaporin-4-deficient astroglial cells in mouse brain toward a site of injury. *FASEB J* 21:108–116
- Bai C, Fukuda N, Song Y, Ma T, Matthay MA, Verkman AS (1999) Lung fluid transport in aquaporin-1 and aquaporin-4 knockout mice. *J Clin Invest* 103:555–561
- Berry V, Francis P, Kaushal S, Moore A, Bhattacharya S (2000) Missense mutations in MIP underlie autosomal dominant ‘polymorphic’ and lamellar cataracts linked to 12q. *Nat Genet* 25:15–17
- Binder DK, Oshio K, Ma T, Verkman AS, Manley GT (2004a) Increased seizure threshold in mice lacking aquaporin-4 water channels. *Neuroreport* 15:259–262
- Binder DK, Papadopoulos MC, Haggie PM, Verkman AS (2004b) In vivo measurement of brain extracellular space diffusion by cortical surface photobleaching. *J Neurosci* 24:8049–8056
- Binder DK, Yao X, Sick TJ, Verkman AS, Manley GT (2006) Increased seizure duration and slowed potassium kinetics in mice lacking aquaporin-4 water channels. *Glia* 53:631–636
- Bloch O, Papadopoulos MC, Manley GT, Verkman AS (2005) Aquaporin-4 gene deletion in mice increases focal edema associated with brain abscess. *J Neurochem* 95:254–262
- Bloch O, Manley GT, Verkman AS (2006) Accelerated progression of kaolin-induced hydrocephalus in aquaporin-4 deficient mice. *J Cereb Blood Flow Metab* 26:1527–1537

- Charras GT, Yarrow JC, Horton MA, Mahadevan L, Mitchison TJ (2005) Non-equilibration of hydrostatic pressure in blebbing cells. *Nature* 435:365–336
- Chou CL, Ma T, Yang B, Knepper MA, Verkman AS (1998) Fourfold reduction of water permeability in inner medullary collecting duct of aquaporin-4 knockout mice. *Am J Physiol* 274:C549–C554
- Chou CL, Knepper MA, Hoek AN, Brown D, Yang B, Ma T, Verkman AS (1999) Reduced water permeability and altered ultrastructure in thin descending limb of Henle in aquaporin-1 null mice. *J Clin Invest* 103:491–496
- Condeelis J (1993) Life at the leading edge: the formation of cell protrusions. *Annu Rev Cell Biol* 9:411–444
- Da T, Verkman AS (2004) Aquaporin-4 gene disruption in mice protects against impaired retinal function and cell death after ischemia. *Invest Ophthalmol Vis Sci* 45:4477–4483
- Deen PM, Verdijk MA, Knoers NV, Wieringa B, Monnens LA, van Os CH, van Oost BA (1994) Requirement of human renal water channel aquaporin-2 for vasopressin-dependent concentration of urine. *Science* 264:92–95
- Endo M, Jain RK, Witwer B, Brown D (1999) Water channel (aquaporin 1) expression and distribution in mammary carcinomas and glioblastomas. *Microvasc Res* 58:89–98
- Funahashi T, Nagasawa A, Hibuse T, Maeda N (2006) Impact of glycerol gateway molecule in adipocytes. *Cell Mol Biol (Noisy-le-grand)* 52:40–45
- Hara M, Verkman AS (2003) Glycerol replacement corrects defective skin hydration, elasticity, and barrier function in aquaporin-3-deficient mice. *Proc Natl Acad Sci U S A* 100:7360–7365
- Hara M, Ma T, Verkman AS (2002) Selectively reduced glycerol in skin of aquaporin-3-deficient mice may account for impaired skin hydration, elasticity, and barrier recovery. *J Biol Chem* 277:46616–46621
- Hara-Chikuma M, Verkman AS (2006) Aquaporin-1 facilitates epithelial cell migration in kidney proximal tubule. *J Am Soc Nephrol* 17:39–45
- Hara-Chikuma M, Verkman AS (2008a) Aquaporin-3 facilitates epidermal cell migration and proliferation during wound healing. *J Mol Med* 86:221–231
- Hara-Chikuma M, Verkman AS (2008b) Prevention of skin tumorigenesis and impairment of epidermal cell proliferation by targeted aquaporin-3 gene disruption. *Mol Cell Biol* 28:328–332
- Hara-Chikuma M, Sohara E, Rai T, Ikawa M, Okabe M, Sasaki S, Uchida S, Verkman AS (2005) Progressive adipocyte hypertrophy in aquaporin-7 deficient mice: Adipocyte glycerol permeability as a novel regulator of fat accumulation. *J Biol Chem* 280:15493–15496
- Hibuse T, Maeda N, Funahashi T, Yamamoto K, Nagasawa A, Mizunoya W, Kishida K, Inoue K, Kuriyama H, Nakamura T, Fushiki T, Kihara S, Shimomura I (2005) Aquaporin 7 deficiency is associated with development of obesity through activation of adipose glycerol kinase. *Proc Natl Acad Sci U S A* 102:10993–10998
- Hu J, Verkman AS (2006) Increased migration and metastatic potential of tumor cells expressing aquaporin water channels. *FASEB J* 20:1892–1894
- King LS, Choi M, Fernandez PC, Cartron JP, Agre P (2001) Defective urinary-concentrating ability due to a complete deficiency of aquaporin-1. *N Engl J Med* 345:175–179
- Krane CM, Melvin JE, Nguyen HV, Richardson L, Towne JE, Doetschman T, Menon AG (2001) Salivary acinar cells from aquaporin 5-deficient mice have decreased membrane water permeability and altered cell volume regulation. *J Biol Chem* 276:23413–23420
- Levin MH, Verkman AS (2004) Aquaporin-dependent water permeation at the mouse ocular surface: in vivo microfluorimetric measurements in cornea and conjunctiva. *Invest Ophthalmol Vis Sci* 45:4423–4432
- Levin MH, Verkman AS (2006) Aquaporin-3-dependent cell migration and proliferation during corneal re-epithelialization. *Invest Ophthalmol Vis Sci* 47:4365–4372
- Li J, Verkman AS (2001) Impaired hearing in mice lacking aquaporin-4 water channels. *J Biol Chem* 276:31233–31237
- Li J, Patil RV, Verkman AS (2002) Mildly abnormal retinal function in transgenic mice without Muller cell aquaporin-4 water channels. *Invest Ophthalmol Vis Sci* 43:573–579

- Ma T, Yang B, Gillespie A, Carlson EJ, Epstein CJ, Verkman AS (1997) Generation and phenotype of a transgenic knockout mouse lacking the mercurial-insensitive water channel aquaporin-4. *J Clin Invest* 100:957–962
- Ma T, Yang B, Gillespie A, Carlson EJ, Epstein CJ, Verkman AS (1998) Severely impaired urinary concentrating ability in transgenic mice lacking aquaporin-1 water channels. *J Biol Chem* 273:4296–4299
- Ma T, Song Y, Gillespie A, Carlson EJ, Epstein CJ, Verkman AS (1999) Defective secretion of saliva in transgenic mice lacking aquaporin-5 water channels. *J Biol Chem* 274:20071–20074
- Ma T, Fukuda N, Song Y, Matthay MA, Verkman AS (2000a) Lung fluid transport in aquaporin-5 knockout mice. *J Clin Invest* 105:93–100
- Ma T, Song Y, Yang B, Gillespie A, Carlson EJ, Epstein CJ, Verkman AS (2000b) Nephrogenic diabetes insipidus in mice lacking aquaporin-3 water channels. *Proc Natl Acad Sci U S A* 97:4386–4391
- Ma T, Hara M, Sougrat R, Verbavatz JM, Verkman AS (2002) Impaired stratum corneum hydration in mice lacking epidermal water channel aquaporin-3. *J Biol Chem* 277:17147–17153
- Manley GT, Fujimura M, Ma T, Noshita N, Filiz F, Bollen AW, Chan P, Verkman AS (2000) Aquaporin-4 deletion in mice reduces brain edema after acute water intoxication and ischemic stroke. *Nat Med* 6:159–163
- Mhatre AN, Stern RE, Li J, Lalwani AK (2002) Aquaporin 4 expression in the mammalian inner ear and its role in hearing. *Biochem Biophys Res Commun* 297:987–996
- Moore M, Ma T, Yang B, Verkman AS (2000) Tear secretion by lacrimal glands in transgenic mice lacking water channels AQP1, AQP3, AQP4 and AQP5. *Exp Eye Res* 70:557–562
- Nielsen S, Nagelhus EA, Amiry-Moghaddam M, Bourque C, Agre P, Ottersen OP (1997) Specialized membrane domains for water transport in glial cells: high-resolution immunogold cytochemistry of aquaporin-4 in rat brain. *J Neurosci* 17:171–180
- Oshio K, Watanabe H, Song Y, Verkman AS, Manley GT (2005) Reduced cerebrospinal fluid production and intracranial pressure in mice lacking choroid plexus water channel aquaporin-1. *FASEB J* 19:76–78
- Padmawar P, Yao X, Bloch O, Manley GT, Verkman AS (2005) K^+ waves in brain cortex visualized using a long-wavelength K^+ -sensing fluorescent indicator. *Nature Meth* 2:825–827
- Pallone TL, Edwards A, Ma T, Silldorff EP, Verkman AS (2000) Requirement of aquaporin-1 for NaCl-driven water transport across descending vasa recta. *J Clin Invest* 105:215–222
- Papadopoulos MC, Verkman AS (2005) Aquaporin-4 gene disruption in mice reduces brain swelling and mortality in pneumococcal meningitis. *J Biol Chem* 280:13906–13912
- Papadopoulos MC, Manley GT, Krishna S, Verkman AS (2004) Aquaporin-4 facilitates reabsorption of excess fluid in vasogenic brain edema. *FASEB J* 18:1291–1293
- Papadopoulos MC, Saadoun S, Verkman AS (2008) Aquaporins and cell migration. *Pflugers Arch* 456:693–700
- Prudente S, Flex E, Morini E, Turchi F, Capponi D, De Cosmo S, Tassi V, Guida V, Avogaro A, Folli F, Maiani F, Frittitta L, Dallapiccola B, Trischitta V (2007) A functional variant of the adipocyte glycerol channel aquaporin 7 gene is associated with obesity and related metabolic abnormalities. *Diabetes* 56:1468–1474
- Rash JE, Yasumura T, Hudson CS, Agre P, Nielsen S (1998) Direct immunogold labeling of aquaporin-4 in square arrays of astrocyte and ependymocyte plasma membranes in rat brain and spinal cord. *Proc Natl Acad Sci U S A* 95:11981–11986
- Rojek AM, Skowronski MT, Füchtbauer EM, Füchtbauer AC, Fenton RA, Agre P, Frøkiaer J, Nielsen S (2007) Defective glycerol metabolism in aquaporin 9 (AQP9) knockout mice. *Proc Natl Acad Sci U S A* 104:3609–3614
- Ruiz-Ederra J, Verkman AS (2006) Accelerated cataract formation and reduced lens epithelial water permeability in aquaporin-1-deficient mice. *Invest Ophthalmol Vis Sci* 47:3960–3967

- Ruiz-Ederra J, Zhang H, Verkman AS (2007) Evidence against functional interaction between aquaporin-4 water channels and Kir4.1 K⁺ channels in retinal Müller cells. *J Biol Chem* 282:21866–21872
- Saadoun S, Papadopoulos MC, Hara-Chikuma M, Verkman AS (2005a) Impairment of angiogenesis and cell migration by targeted of aquaporin-1 gene disruption. *Nature* 434:786–792
- Saadoun S, Papadopoulos MC, Watanabe H, Yan D, Manley GT, Verkman AS (2005b) Involvement of aquaporin-4 in astroglial cell migration and glial scar formation. *J Cell Sci* 118:5691–5698
- Schnermann J, Chou CL, Ma T, Traynor T, Knepper MA, Verkman AS (1998) Defective proximal tubular fluid reabsorption in transgenic aquaporin-1 null mice. *Proc Natl Acad Sci U S A* 95:9660–9664
- Sohara E, Rai T, Miyazaki J, Verkman AS, Sasaki S, Uchida S (2005) Defective water and glycerol transport in the proximal tubules of AQP7 knockout mice. *Am J Physiol* 289:F1195–F1200
- Solenov E, Watanabe H, Manley GT, Verkman AS (2004) Sevenfold-reduced osmotic water permeability in primary astrocyte cultures from AQP-4-deficient mice, measured by a fluorescence quenching method. *Am J Physiol* 286:C426–C432
- Song Y, Verkman AS (2001) Aquaporin-5 dependent fluid secretion in airway submucosal glands. *J Biol Chem*
- Song Y, Fukuda N, Bai C, Ma T, Matthay MA, Verkman AS (2000a) Role of aquaporins in alveolar fluid clearance in neonatal and adult lung, and in oedema formation following acute lung injury: studies in transgenic aquaporin null mice. *J Physiol* 525(Pt 3):771–779
- Song Y, Yang B, Matthay MA, Ma T, Verkman AS (2000b) Role of aquaporin water channels in pleural fluid dynamics. *Am J Physiol* 279:C1744–C1750
- Song Y, Sonawane N, Verkman AS (2002) Localization of aquaporin-5 in sweat glands and functional analysis using knockout mice. *J Physiol* 541:561–568
- Thiagarajah JR, Verkman AS (2002) Aquaporin deletion in mice reduces corneal water permeability and delays restoration of transparency after swelling. *J Biol Chem* 277:19139–19144
- Thiagarajah JR, Papadopoulos MC, Verkman AS (2005) Non-invasive early detection of brain edema in mice by near-infrared light scattering. *J Neurosci Res* 80:293–299
- Thiagarajah JR, Zhao D, Verkman AS (2007) Impaired enterocyte proliferation in aquaporin-3 deficiency in mouse models of colitis. *Gut* 56:1529–1535
- Verbavatz JM, Ma T, Gobin R, Verkman AS (1997) Absence of orthogonal arrays in kidney, brain and muscle from transgenic knockout mice lacking water channel aquaporin-4. *J Cell Sci* 110:2855–2860
- Verkman AS (2007) Role of aquaporins in lung fluid physiology. *Resp Physiol Neurobiol* 159:324–330
- Verkman AS (2008) Dissecting the role of aquaporins in renal pathophysiology using transgenic mice. *Semin Nephrol* 28:217–226
- Verkman AS, Thiagarajah JR (2006) Physiology of water transport in the gastrointestinal tract. In: *Physiology of the gastrointestinal tract*. Johnson LR, Barrett K, Ghishan F, Manchant J, Said H, Wood J (eds.) vol. 4. New York, Academic Press, pp. 1827–1845
- Yang B, Brown D, Verkman AS (1996) The mercurial insensitive water channel (AQP-4) forms orthogonal arrays in stably transfected Chinese hamster ovary cells. *J Biol Chem* 271:4577–4580
- Yang B, Folkesson HG, Yang J, Matthay MA, Ma T, Verkman AS (1999) Reduced osmotic water permeability of the peritoneal barrier in aquaporin-1 knockout mice. *Am J Physiol* 276:C76–C81
- Yang B, Verbavatz JM, Song Y, Vetrivel L, Manley G, Kao WM, Ma T, Verkman AS (2000) Skeletal muscle function and water permeability in aquaporin-4 deficient mice. *Am J Physiol* 278:C1108–C1115
- Yang B, Song Y, Zhao D, Verkman AS (2005) Phenotype analysis of aquaporin-8 null mice. *Am J Physiol* 288:C1161–C1170
- Zador Z, Magzoub M, Jin S, Manley GT, Papadopoulos MC, Verkman AS (2008) Microfiber optic fluorescence photobleaching reveals size-dependent macromolecule diffusion in extracellular space deep in brain. *FASEB J* 22:326–332

- Zhang H, Verkman AS (2008) Aquaporin-4 independent Kir4.1 K⁺ channel function in brain glial cells. *Mol Cell Neurosci* 37:1–10
- Zhang D, Vetrivel L, Verkman AS (2002) Aquaporin deletion in mice reduces intraocular pressure and aqueous fluid production. *J Gen Physiol* 119:561–569

Part V
Towards Therapeutic Use of Aquaporins

Design, Synthesis and Assaying of Potential Aquaporin Inhibitors

Rose Haddoub, Michael Rützler, Aélig Robin, and Sabine L. Flitsch

Contents

1	Introduction	386
2	Assays for Aquaporins Inhibitors	386
2.1	Traditional Methods to Study Membrane Water Permeability	386
2.2	Intracellular Fluorophore Dilution Methods	388
2.3	Fluorescence Quenching	389
2.4	Potential of Traditional Approaches in HTS for AQP Inhibitors	389
2.5	Alternative Approaches	390
3	Known Inhibitors of AQPs	391
3.1	Transition Metals	392
3.2	Quaternary Ammonium Salts	394
3.3	Sulfonamide and Related Compounds	395
3.4	Phloretin	397
3.5	Recent Findings	398
4	Conclusion	399
	References	399

Abstract The aquaporin protein family performs fundamental tasks in the physiology of several organs in the human body. Their roles in several disorders known to involve water movement make them attractive targets for the development of novel drug therapies.

This chapter describes assays commonly used to study the water permeability across AQPs. It also describes the effect of some known inhibitors of aquaporins on water permeability, such as mercury, gold, silver, copper, phloretin, tetraethyl ammonium salts and acetazolamide compounds.

S.L. Flitsch (✉)

Manchester Interdisciplinary Biocentre (MIB) & The School of Chemistry,
University of Manchester, 131 Princess Street, M1 7DN Manchester, UK
Sabine.Flitsch@manchester.ac.uk

E. Beitz (ed.), *Aquaporins*, Handbook of Experimental Pharmacology 190,
© Springer-Verlag Berlin Heidelberg 2009

385

Abbreviations

AQP	aquaporin
AZA	acetazolamide
DMSO	dimethylsulfoxide
EZA	ethoxzolamide
GFP	green fluorescent protein
HTS	high throughput screening
RNA	ribonucleic acid
SPR	surface plasmon resonance
TMA	tetramethyl ammonium
TEA	tetraethyl ammonium
TPrA	tetrapropyl ammonium
TB	tetrabutyl ammonium
TPeA	tetrapentyl ammonium
TIRF	total internal reflection fluorescent

1 Introduction

Specific, high affinity inhibitors are important tools for studying aquaporins (AQPs) *in vivo* and promise treatment of several disorders such as stroke, traumatic injury and tumor-induced brain swelling, glaucoma and cystic fibrosis, which currently lack adequate medical treatment.

Discovering new AQP inhibitors is demanding, as the screening strategies frequently employed in the pharmaceutical industry to study ion channels, G-protein-coupled receptors and enzymes are in general not applicable to water channels. Also direct measurement of water movement through AQPs in the context of high throughput assays has been challenging. Methodologies used to evaluate cellular water transport through cell membranes can potentially be used to measure AQP function indirectly.

The methods described in this chapter have all been employed to measure water permeability and to identify several inhibitors.

2 Assays for Aquaporins Inhibitors

2.1 Traditional Methods to Study Membrane Water Permeability

Following the first functional characterization of an AQP in *Xenopus laevis* oocytes (Preston et al. 1992), oocytes were used in numerous studies to characterize water channel function including identification of presumed AQP inhibitors tetraethyl ammonium (TEA), acetazolamide (AZA) and chemically related compounds (i.e., Zhang

et al. 1993; Detmers et al. 2006; Brooks et al. 2000; Ma et al. 2004). In this system, heterologous protein expression is achieved through cytoplasmic injection of *in vitro* transcribed RNA. The initial experimental setup by Preston et al. (1992) consisted of a microscope attached to a video camera. Oocyte volume changes were induced by osmotic challenge and recorded for several minutes. In many cases oocytes expressing AQPs burst during the experiment.

Several improvements to the initial method have been suggested since (Meinild et al. 1998; Sogaard and Zeuthen 2007). Osmotic challenge in the original system was often accomplished by diluting oocyte bath-solution with distilled water. This crude way of reducing buffer osmolality may cause uncontrolled leakage of ions from the oocyte, resulting in a change of the effective osmotic gradient. Instead, bathing solution osmolality was changed by addition or removal of only one defined membrane-impermeable osmolyte such as mannitol. No change in membrane potential was observed when external osmolality was altered in this way indicating absence of ion fluxes (Meinild et al. 1998; Sogaard and Zeuthen 2007). Furthermore it was reported that *X. laevis* oocyte volume changes inaccurately describe water permeability if oocytes are monitored up until several minutes after an osmotic challenge (Sogaard and Zeuthen 2007). Consequently, water permeability and aquaporin function in *X. laevis* oocytes should only be calculated from initial osmotically induced volume changes (Meinild et al. 1998; Sogaard and Zeuthen 2007).

Following the first characterization of channel-like integral membrane protein of 28 kDa (CHIP28, now AQP1) in *X. laevis* oocytes (Zeidel et al. 1992), Van Hoek and Verkman (1992) purified recombinant AQP1 protein and incorporated it into lipid vesicles to provide further evidence for its function as a water channel. Utilizing a well-established method (for review see Verkman 2000), vesicles were rapidly exposed to a change in buffer osmolality and scattered light intensity was recorded to monitor vesicle volume change. Stopped flow light scattering allows the recording of volume changes with high temporal resolution of 0.5 ms. These experiments established that AQP1 did not require additional subunits for its basic function as a water pore. Furthermore it was concluded that AQP1 was not merely a regulator of an unknown protein facilitating water permeability in *X. laevis* oocytes. More generally speaking, this method allows for the study of AQP-function in the absence of other transmembrane transporters or channels that might alter experimentally applied osmotic gradients. It therefore seems well suited to investigate the specificity of presumptive AQP inhibitors to water channels because no unrelated properties of a host cell can obscure the results as in heterologous AQP expression systems.

Yang et al. used a stopped flow light scattering technique to investigate the effects of several putative inhibitors of AQP1 dependent water permeability in erythrocyte membranes (Yang et al. 2006). These authors also discussed potential pitfalls in studying AQP inhibitors even if lipid vesicles including purified AQPs are used. Some solutes such as DMSO can rapidly permeate lipid membranes, and the inhibitory effect of DMSO on water channels was first reported by Van Hoek et al. (1990). The interaction of DMSO with water permeability of brush border membrane vesicles from rat renal cortex was studied by measuring the kinetics of changes in scattered light intensity upon rapid osmotic perturbation using stopped-flow spectrophotometry. The inhibition was shown to be dose-dependent

and reversible. If DMSO is applied as an inhibitor, it may, depending on the direction of the osmotic gradient, diffuse against the overall osmotic gradient and thereby can reduce the total water flux by diminishing the applied osmotic gradient. This is predicted to affect rapid, aquaporin facilitated water permeability more than transmembrane water permeability and it may have contributed to the wrong assignment of DMSO as a general inhibitor of AQPs. We have found that DMSO inhibitory effects can be observed at 1–2% v/v which corresponds to ~150–310 mOsmol (M. Rützler measurement). These amounts of DMSO contribute to osmotic gradients at similar or larger levels than the total osmotic gradients that are typically employed in order to measure water movement in stopped-flow light scattering experiments or other water permeability measurements. Inhibitors applied at low-millimolar or lower concentrations should however not exhibit similar effects. Furthermore, if inhibitor concentrations are maintained pre- and post-osmotic challenge, no influence on the overall osmotic gradient should be observed, regardless of inhibitor membrane permeability.

A similar technique to stopped flow light scattering was used to identify gold and silver ions as inhibitors of plant aquaporins (Nodulins and plasma membrane integral proteins; PIPs) as well as AQPs in human red cell membranes (Niemiety and Tyerman 2002). In stopped flow fluorometry, membrane vesicles are loaded with high concentrations of a fluorescent dye. Vesicle volume decrease causes dye self-quenching if very high initial fluorophore concentrations are present. The process is not very well understood but may depend on dye dimerization, energy transfer to non-fluorescent dimers and collisional quenching interactions between dye monomers (Chen and Knutson 1988).

2.2 Intracellular Fluorophore Dilution Methods

Two strategies can be distinguished: in one variation a fluorescent protein is expressed within cells. Gao et al. (2005) established stable cell lines that express a fusion protein between AQP1 and Green Fluorescent Protein (GFP) to measure osmotic water permeability. Cells were exposed to dilution of culture media with distilled water and a time course of fluorescence intensity was recorded by confocal laser microscopy. A decrease of fluorescence intensity within an optical section following this osmotic challenge was interpreted as water entry and cell swelling. The slope of measured fluorescence decrease was compared between untreated cells and cells that had been pre-incubated with the known AQP1 inhibitor HgCl₂. As expected, the period following an osmotic challenge until fluorescence equilibration took place was prolonged by HgCl₂ treatment in a dose dependent manner. Furthermore, HEK293 cells that stably expressed cytoplasmic GFP were used as a control and similar to HgCl₂ treated GFP-AQP1 expressing cells these control cells showed slow fluorescence equilibration following osmotic challenge. This suggests validity of the method, which was utilized subsequently to verify previously observed inhibitory effects of acetazolamide on AQP1 facilitated water permeability (Gao et al. 2006).

Similarly, cell permeable fluorescent dyes have been used to determine cell volume changes and water permeability: typically, cells were loaded with a cell-permeable form of calcein. Quantum efficiency of this dye is minimally influenced by intracellular ion concentration (Allen and Cleland 1980; Kendall and MacDonald 1983). As described above for GFP expressing cells, water permeability was typically determined using confocal microscopy (Zelenina et al. 2002). The method was successfully used to identify nickel and copper as inhibitors of AQP3 as well as lead acetate as an activator of AQP4 (Zelenina et al. 2003; Gunnarson et al. 2005).

2.3 Fluorescence Quenching

In a study conducted on cultured confluent monolayers of hepatocytes a decrease of fluorescence intensity was observed along with cell shrinking (Wehner et al. 1995). These studies were conducted utilizing confocal microscopy, where cell shrinking should have increased the dye concentration within an optical section and thereby the measured fluorescence intensity. These observations were interpreted as a result of fluorescence self-quenching.

Systematic analysis of this behavior later showed a linear relationship between cell volume and calcein fluorescence intensity also in wide field microscopy (Hamann et al. 2002). Furthermore it was concluded that fluorescence intensity was quenched by cytosolic proteins and did not depend on dye self quenching. Partial confocality, due to high numerical aperture detection was not the reason for observed changes in fluorescence intensity (Solenov et al. 2004). This behavior of calcein and other fluorophors (Hamann et al. 2002) actually suggests that confocal microscopy and TIRF microscopy are less suited for detecting calcein fluorescence intensity changes than wide field microscopy: hypo-osmotic challenge i.e., causes cell swelling and consequently cytosolic dye dilution, which in theory should be recorded as a reduction in fluorescence intensity in confocal and TIRF microscopy, but not in wide field microscopy, because the overall amount of dye within the optical light path remains the same in this latter setup. At the same time increase in cell volume should cause fluorescence dequenching which should be observed as an increase in intensity in all three setups. In theory these effects thus should cancel out each other in confocal microscopy and TIRF microscopy and only the difference between dye-dilution related decrease in fluorescence intensity and dye-dequenching related increase in fluorescence intensity can be recorded. Cytosolic calcein quenching was observed over a wide range of intracellular dye concentrations (Solenov et al. 2004) suggesting that it will contribute to the observed signal in confocal microscopy and TIRF microscopy under most experimental conditions.

2.4 Potential of Traditional Approaches in HTS for AQP Inhibitors

Commercially available automated systems, which are designed for oocyte voltage clamp studies, can perform cytoplasmic injection of several thousand oocytes per

day. While such efforts have not been described, it is conceivable that the original assay by Preston et al. (1992) could be adapted to screen compound libraries in order to identify novel aquaporin blockers. However, suitable method for monitoring osmotic swelling of large numbers of oocytes has to be devised for such studies.

Currently available equipment for stopped flow light scattering is not suitable for high throughput screening of compound libraries. In order to identify novel AQP inhibitors other methods have to be employed initially, before inhibitor studies on purified water channels incorporated in lipid vesicles can provide independent confirmation in a largely inert environment.

The suitability of intracellular fluorophore dilution assays for high throughput identification of AQP inhibitors is limited at the moment because confocal microscopy or TIRF microscopy is required to detect fluorescence intensity changes. High throughput microscopy that facilitates TIRF detection and other advances in microscopy (for review see Oheim 2007) may however soon provide additional options for efficient identification of more potent and less toxic aquaporin inhibitors. Finally, monitoring calcein fluorescence quenching on plate readers may be feasible, which would make this method suitable for high throughput screening of chemical compound libraries. It is however unclear at this point if the small signal amplitudes observed in wide field microscopy can be detected on plate readers and if so, whether the signal to noise ratios will be sufficient to obtain a robust assay system.

2.5 Alternative Approaches

Several aquaporins including AQP1 facilitate enhanced cell migration, cell adhesion and cell proliferation (for review see Papadopoulos et al. 2007). Efficient assays to study these properties are established (Steinle et al. 2002; Lee et al. 2000) and were used by Verkman and co-workers to identify novel inhibitors of AQP1 dependent cell migration, adhesion and proliferation. These approaches have been patented for the identification of AQP1 inhibitors (international patent Nr. WO 2006/102483 A2) but could be used to identify blockers and activators of other AQPs, such as AQP3 and AQP4, which have similarly been described to facilitate cell migration and proliferation (Levin and Verkman 2006; Saadoun et al. 2005). It was suggested that AQP facilitated cell migration is a general phenomenon that is independent of AQP and cell type (Papadopoulos et al. 2007). This implies that similar assays as for AQP1 can be devised for most AQPs. A recent report however did not find enhanced migration in isolated, AQP4 expressing glioma cells (McCoy and Sontheimer 2007).

As a further alternative, high throughput identification of AQP inhibitors in yeast has been suggested (Daniels et al. 2006) and recently by Wu et al. (2007). In the first approach the plant aquaporin PvTIP3;1 was expressed in *Pichia pastoris*. In yeast a rigid cell wall protects cells from damage by hypotonic conditions. Daniels et al. removed the cell wall by enzymatic digest and stabilized the resulting spheroplasts in sorbitol-containing buffer. This hypertonic solution was diluted to various degrees subsequently and changes in absorbance at 600 nm were recorded. An increase in

absorbance was observed when wild type cells were shifted to hypotonic buffer, which is consistent with an increase in average cell volume. In contrast no increase in absorbance was observed for cells expressing PvTIP3;1. This was interpreted as partial lysis of the PvTIP3;1 expressing cells due to rapid, AQP facilitated swelling that exceeded the cells' capacities for volume regulation. It will be critical to standardize conditions of yeast growth and cell wall digestion to a degree that assay variability is acceptable before this type of assay can be used for the identification of novel AQP inhibitors by high throughput screening of chemical compound libraries. Another interesting approach was described by Wu et al. (2007). Deletion of the *S. cerevisiae* aquaglyceroporin Fps1 renders these yeast cells hypersensitive to methylamine. In wild-type cells methylamine, which enters through the unidirectional ammonium transporters Mep1-3 can escape through Fps1, while in Fps1 mutants toxic methylamine accumulates. If methylamine is properly titrated this results in yeast cell proliferation only if Fps1 is present, which can easily be measured, in a simple setup by absorbance reading of growing yeast cultures. Wu et al. furthermore demonstrated that Fps1 function can be replaced by other aquaporins that are permeable to methylamine i.e., *Plasmodium falciparum* AQP (*PfAQP*) as well as a mutant form of mammalian AQP1, which is normally a strict water channel. AQP-inhibitors are expected to block methylamine export and consequently to inhibit cell proliferation. Encouragingly, Wu et al. were able to identify 7 weak inhibitors of *PfAQP* and 2 weak inhibitors of the mutant AQP1 in a pilot screen of 167 compounds utilizing this novel approach. *PfAQP* inhibitors may be of medical interest; since this protein presumably facilitates glycerol uptake as well as ammonia release in the malaria parasite *P. falciparum*. Indeed, in a rodent malaria model, disruption of the *Plasmodium berghei* AQP gene leads to reduced proliferation of the parasite (Promeneur et al. 2007).

3 Known Inhibitors of AQPs

The physiological roles of aquaporins have been characterized primarily in water balance regulation. AQP1, AQP2, AQP3 and AQP4 knockout mice exhibit defects in urine concentration (Ma et al. 1998, 2000; Rojek et al. 2006). Deletion of AQP4, which is expressed at the blood–brain barrier (Nielsen et al. 1997), or deletion of proteins that facilitate its transport (Vajda et al. 2002) also protects mice from induced brain edema (Manley et al. 2000). These studies together with a series of parallel studies support the view that AQP4 is important in water transport across the blood brain barrier. Targeted gene deletion of aquaglyceroporins has linked these proteins to common metabolic diseases such as diabetes and obesity (Hara-Chikuma et al. 2005; Hibuse et al. 2005). Specific aquaporin blockers that are currently not available are urgently needed to enhance our understanding of the role that these ubiquitously conserved proteins play in mammalian physiology and pathophysiology.

3.1 Transition Metals

The first blockers of water permeability in AQP_s described in the literature were mercurial compounds. In order to provide evidence for functional water channels in erythrocytes inhibitors of the high water permeability of the red blood cell membrane were sought. Macey and Farmer (1970) found that treatment with mercurial sulfhydryl reagents such as *p*-CMBS (*p*-chloromercuribenzenesulfonate), chlormerodrin and mersalyl indeed reduced erythrocyte membrane permeability. A simple interpretation was that mercury reacted with sulfhydryl groups in proteins associated with water channels and resulted in closure of the channels.

Later, CHIP28 (now AQP1), an abundant protein in red cells membranes and renal proximal tubules (Smith and Agre 1991) was identified as the Hg²⁺-sensitive water channel in *X. oocytes* swelling assays (Preston et al. 1992). The amino acid sequence of CHIP28 contains four cysteines (87, 102, 152 or 189) and site-directed mutagenesis experiments demonstrated that mutation of cysteine 189 made AQP1 insensitive to Hg²⁺ inhibition.

Similar work was carried out using CHIP28k, a homologous protein of human erythrocyte CHIP28, which is found in the kidney proximal tubule and the thin limb of Henle (Zhang et al. 1993). Mutations of the four cysteins of CHIP28k confirmed that cysteine 189 is the site of action of mercurial sulfhydryl transport inhibitors. The aquaporin family of channels was therefore originally defined based on the inhibition of water transport in the red blood cell membrane by mercurial compounds. This selective inhibition subsequently allowed for AQP isolation, cloning and membrane transport characterization.

Mercury inhibition is thought to occur via covalent modification of cysteine residues within the water pore and in other regions of the protein causing either block or conformational changes leading to inhibition of water transport. Some studies have been carried out recently to understand the mechanism of inhibition in AQP1 (Savage and Stroud 2007). Using a mutant (T183C) of AQP Z, no conformational rearrangement of the protein occurred upon mercury binding, suggesting a steric inhibition mechanism.

Silver, as AgNO₃ or silver-sulfadiazine (Fig. 1) and gold (as HAuCl₄) have been tested as potential inhibitors of AQP_s (Niemietz and Tyerman 2002). The diameter of Ag⁺ ion (2.5 Å) matches the predicted AQP channel diameter of 2.8 Å. The Hg²⁺ ion is (2.2 Å), whereas the Au³⁺ ion is (2.7 Å).

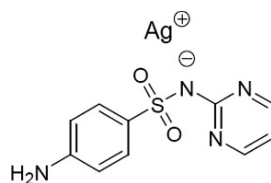


Fig. 1 Structure of silver sulfadiazine

Although the exact mechanism of action has not been discovered, silver and gold, as well as mercury, are thought to react with the sulfhydryl group of a cysteine residue in the vicinity of the NPA motif. The thiol moiety of cysteine has a pKa of around 8.5 and this value may go down to 6 when it is next to other amino acids. The thiolate function can coordinate transition metal ions and has also a strong nucleophile character which can react with the sulfonyl group of the silver-sulfadiazine. However, mercury-based inhibition is reversible in the presence of mercaptoethanol whereas silver inhibition is non-reversible, suggesting a different mechanism of action. Silver was found to inhibit osmotic shrinking of human red blood cells with an IC₅₀ of 3.9 μM in the case of AgNO₃ and 1.24 μM for silver sulfadiazine. Modulation of osmotic water permeability of human erythrocytes showed similar potency of mercury and silver, whereas gold ions were less efficient.

It is well documented that Ni²⁺ can regulate the activity of ion channels, (i.e., Gordon and Zagotta 1995; Zamponi et al. 1996; Perchenet and Clément-Chomienne 2001). Its inhibitory effect on human AQP3, AQP4 and AQP5 has been studied in a human lung cell line (Zelenina et al. 2003). Cells transfected with human AQP4 and AQP5 were insensitive to NiCl₂ but AQP3 was inhibited. Incubation with NiCl₂ caused rapid, dose-dependent and reversible reduction of AQP3 water permeability. A series of point mutations were introduced into the three extracellular loops of AQP3 in order to identify the molecular sites responsible for the Ni²⁺ sensitivity. Three residues (Trp128, Ser152 and His154) were shown to contribute to the blocking effect of Ni²⁺. Additionally, it was shown that AQP3 was sensitive to extracellular acidification (in the range from pH 5.5 to pH 7) as previously described for two others mammalian AQPs (AQP0 (Németh-Cahalan and Hall 2000) and AQP6 (Yasui et al. 1999)). Two other metals, zinc and cadmium, were also tested and had no effect on the water permeability of AQP3.

Furthermore copper was identified as a blocker of AQP3 water and glycerol permeability (Zelenina et al. 2004). This inhibition is reversible, rapid and specific. The same amino acids involved in the blocking effect of Ni²⁺ are also involved in the regulation of AQP3 by copper.

Most knowledge about the physiological function of AQPs has been gained from AQP knockout mouse models. It is however well known that in conventional gene knock-out approaches compensatory mechanisms may alleviate the conditions created by constitutive loss of a gene's function. For example confounding up-regulation of the UT-A urea transporter was found in UT-B gene-knockout mice (Klein et al. 2004).

In contrast to conventional gene-knockouts, "chemical knockout" by specific, small molecule inhibitors is an important alternative approach to study acute loss of specific protein functions in integrated systems. This approach has successfully been used to define the exact role of the urea transporter UT-B in renal urea handling and urinary concentration (Yang and Verkman 2002). Many of the described metal ion inhibitors of AQP function are highly toxic and with the exception of AQP3 inhibition by copper show hardly any specificity towards AQP subtypes. These substances are thus neither suited for *in vivo* pharmacological studies in animal models nor for treatment of human water imbalance disorders.

3.2 Quaternary Ammonium Salts

The search for alternative inhibitors began based on the hypothesis that moderate similarity between AQP1 and ion channels might suggest that inhibitors of ion channels could similarly affect AQPs. Indeed, Brooks et al. (2000) reported that tetraethyl ammonium chloride (TEA), a known blocker of potassium channels, inhibits AQP1 water permeability. Furthermore Ma et al. (2004) as well as Gao et al. (2006) described AQP1 inhibition by some carbonic anhydrase inhibitors like acetazolamide.

Tetraethyl ammonium is known as a pore-occluding blocker of voltage-gated potassium channels (Armstrong 1971), and cationic channels such as calcium-dependent K^+ channels (Latorre et al. 1982; Lang and Ritchie 1990). Brooks et al. (2000) tested ion channel blockers like tetramethyl-(TMA), tetraethyl-(TEA), tetrapropyl-(TPrA) ammonium and clofilium as potential inhibitors for AQP1 permeability (Fig. 2).

TEA at $100\mu\text{M}$ reduced the water permeability of human AQP1 expressed in *X.* oocytes with similar efficiency to mercury salt. The increasing of TEA concentrations up to 10 mM and the recovery of oocytes after multiple rinsing with saline solutions showed that the inhibition was dose dependant and reversible.

Several other tetralkyl ammonium salts were also tested against AQP1, AQP2, AQP3, AQP4 and AQP5-expressing oocytes in swelling assays in order to study the effect of the alkyl chain length on the inhibition properties (Detmers et al. 2006). At $100\mu\text{M}$, TEA showed inhibition of the water permeability of AQP1, AQP2, AQP4, whereas TPrA appeared to be specific for AQP1 (Fig. 4). In contrast, tetramethyl ammonium (TMA), as well as tetrabutyl ammonium (TB) and tetrapentyl ammonium (TPeA) chains, did not show any significant activity. The values of the P_f

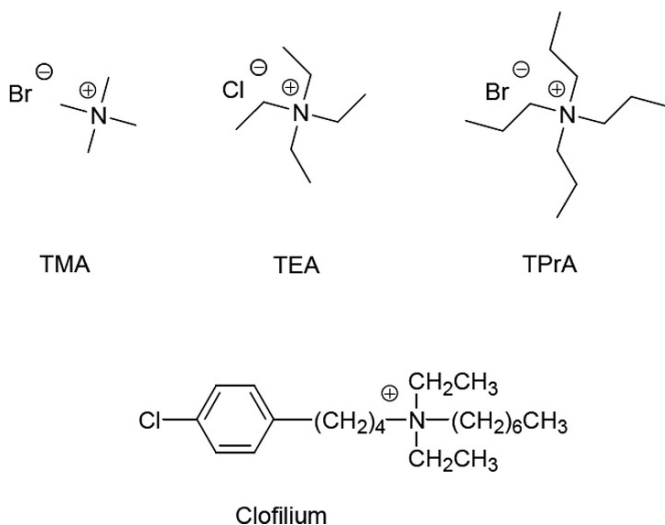


Fig. 2 Structures of TMA, TEA, TPrA, and Clofilium

showed that inhibition with 4 μM TEA was close to that of 100 μM TEA ($42 \pm 11\%$ and $40 \pm 14\%$ respectively). On the other hand, no inhibition was observed with 4 μM TPrA, thus indicating that TEA is a more potent inhibitor of AQP1 water permeation than TPrA. Finally, different IC_{50} values for AQP1, -2 and -4 were observed and indicated the potency of TEA to inhibit water permeation through AQP1 is much higher than for AQP2 and AQP4.

By analogy with potassium channel inhibition by TEA, it was suggested that AQP1 inhibition was due to the interaction between TEA and a tyrosine residue in the E loop of the protein. Indeed, when Tyr186 located near the mercury binding site Cys189, was mutated to a phenylalanine, the water permeability of the Y186F AQP mutant expressed in *X. oocytes* did not show any difference compared to the wild type AQP1 even in the presence of 100 μM TEA.

Sequence alignment of the amino acid sequences of the E loop of several AQPs showed that Tyr186 is conserved in AQP1, AQP2, and AQP4, which are all inhibited by TEA, whereas AQP3 and AQP5, which are not inhibited by TEA, have asparagine and phenylalanine residues at this position, respectively.

To address the question of whether AQP1 channels in native tissues are sensitive to TEA, as they are in *X. oocytes*, Yool et al. (2002) studied the water permeability of AQP1 channels in kidney and kidney derived-cells in the presence of TEA. TEA was found to inhibit the osmotically driven net movement of water across monolayers of Madin–Darby Canine Kidney (MDCK) cells expressing human AQP1 (1 mM TEA produced 34% block of osmotic water flux in MDCK cells). Also, TEA inhibited the water permeability in rat renal descending thin limbs of Henle's loops which express native AQP1, but not in ascending thin limbs which do not express AQP1.

Another study found that external TEA did not inhibit the cGMP-dependant AQP1 ionic conductance of AQP1 expressed in *X. oocytes*. This result suggests that the pathway of ions and water is different within the channel as well as their sensitivity to TEA.

The inhibition may be due to an interaction between TEA and amino acids located at the extracellular part of AQP1, especially the A-, C- and E-loops. The IC_{50} values of TEA for AQP1, -2 and -4 are in the micromolar region (1.4, 6.2 and 9.4 μM respectively), which indicated that TEA could be a lead compound for the development of reversible and specific AQP inhibitors. The molecular characterization of the binding site of TEA suggested perspectives for a rational approach toward more efficient and selective blockers of AQPs.

3.3 Sulfonamide and Related Compounds

Acetazolamide (AZA), an established pan-carbonic anhydrase (CA) inhibitor, acts through direct binding with Zn^{2+} and forms the carbonic anhydrase–acetazolamide complex. In 2004, it was shown that AZA inhibited osmotic water permeability through AQP1 expressed in *X. oocytes* (Ma et al. 2004). The relevance of AZA as an AQP1 blocker outside the *X.* expression has been demonstrated using embryonic

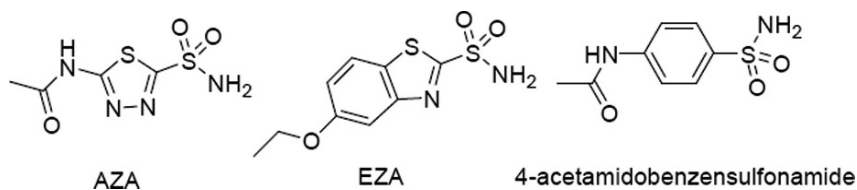


Fig. 3 Structures of AZA, EZA, and 4-acetamidobenzensulfonamide

kidney 293 (HEK293) cells transfected with pEGFP/AQP1 and by investigating the interaction between acetazolamide and AQP1 (Gao et al. 2006). Using SPR (Surface Plasmon Resonance) technique, the inhibition rate of AZA at 100 μ M was 39%. The binding assay showed that acetazolamide could directly interact with AQP1.

Due to sequence homology between AQP1 and AQP4, AZA was tested in an *in vivo* functional assay using *X. oocytes* expressing the Aquaporin 4-M23 isozyme (hAQP4b) (Huber et al. 2007). AZA showed 80% inhibition at 20 μ M and the apparent IC_{50} was found to be 0.9 μ M with a maximum inhibition of 85%. Two pan-carbonic anhydrase inhibitors similar to AZA, ethoxzolamide (EZA) and 4-acetamidobenzensulfonamide (Fig. 3) were also evaluated under the same conditions as potential AQP4 blockers. At 20 μ M, EZA showed an inhibition effect of 68% (similar to AZA) whereas 4-acetamidobenzensulfonamide showed a weak inhibition effect of 23%.

Due to their low toxicity, sulfonamide-containing carbonic anhydrase inhibitors are promising compounds which need to be optimized for a specific inhibition of AQP water channels.

The virtual docking studies of AZA and EZA using the BioMedCache/Active site software showed that both products have the same preferred conformation in the active site of ratAQP4. The docking scores are -63.666 and -67.042 kcal mol⁻¹ respectively. The final docked structure of AZA showed that the sulfonamide interacts with the guanidyl group of Arg-216 as well as with the carbonyl group of Gly-209. The acetamide moiety interacts also with the carboxyl of Asp-69. Several other hydrophobic interactions are also detected.

Clinically used anti-epileptic drugs (AEDS) are known to inhibit a number of carbonic anhydrase isoenzymes. From the hypothesis that some AEDS may have an inhibition effect on AQP4, 14 AEDS (Fig. 4) were screened *in silico* using a virtual docking into the ratAQP4b water channel (Huber et al. 2008a).

Based on their availability and docking scores, ten compounds were selected for *in vitro* assay in *X. oocytes* expressing the hAQP4b. Four of ten candidates, topiramate, zonisamide, phenytoin and lamotrigine were then selected for a dose dependant study. The IC_{50} was around 10 μ M. The correlation studies suggested that AEDS with a docking energy >50 kcal mol⁻¹ may have inhibitory effect on AQP4.

AEDS are known for their lack of specificity. They are therefore not useful drugs for *in vivo* use but they might give insight into the inhibition mechanism of AQP4. Furthermore, eighteen compounds with no significant anti-epileptic or carbonic anhydrase activity and sharing similar physico-chemical properties to known

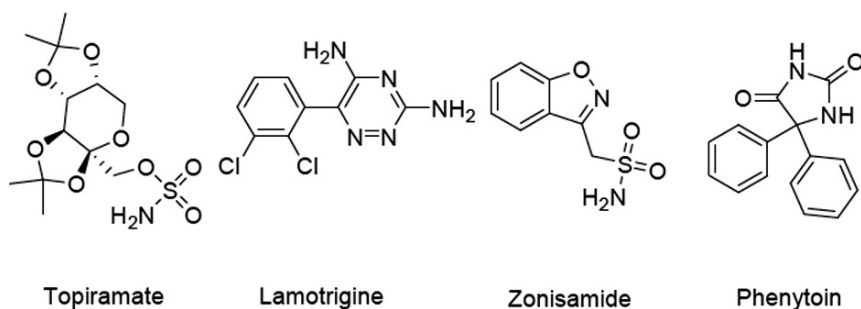


Fig. 4 Structures of some AEDS

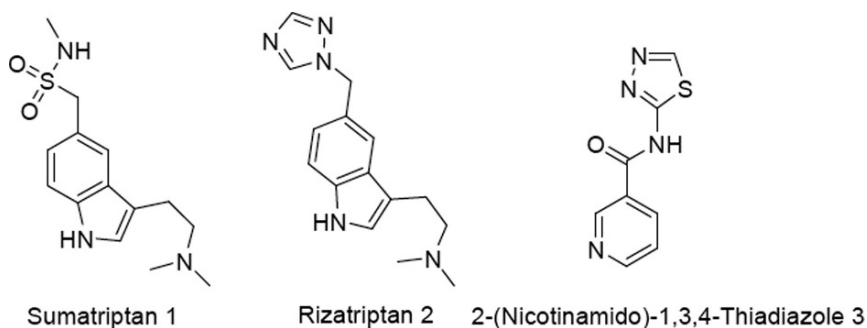


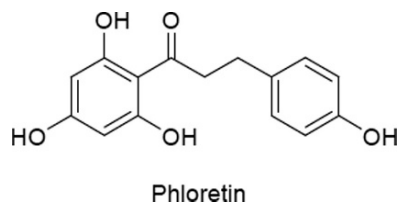
Fig. 5 Structures of sumatriptan 1, rizatriptan 2, and 2-(Nicotinamido)-1,3,4-thiadiazole 3

AQP4 inhibitor were selected. The inhibition values in *X. laevis* oocytes expressing hAQP4b were between 0 and 70% at 20 μ M (Huber et al. 2008b). Ten compounds in this library inhibited AQP4 in a statistically significant manner. Moreover, three compounds were selected for a dose dependant study: the 5-HT_{1B/1D} receptor agonists sumatriptan **1**, rizatriptan **2** and the 2-(Nicotinamido)-1,3,4-thiadiazole **3**, the IC₅₀ were 11, 2.9 and 3.1 μ M respectively (Fig. 5).

The docking of these 18 compounds into the water channel of ratAQP4b monomer showed that the best stabilized compounds are the one that can fit well into the hydrophobic channel and also have some interactions with polar residues. For example the 2-(Nicotinamido)-1,3,4-thiadiazole **3** was able to penetrate deeply into the water channel with a docking score of $-62.776 \text{ kcal mol}^{-1}$. In rizatriptan **2**, the C5 triazole substituent also penetrated into the water channel, whereas the indole and the C3 *N,N* dimethylaminoethyl substituent were located in the external region.

3.4 Phloretin

Phloretin has also been reported as a potential inhibitor of several AQPs (Tsukaguchi et al. 1998, 1999) (Fig. 6). At 0.1 mM phloretin inhibited the water permeability

Fig. 6 Structure of phloretin

of AQP9 expressed in *X. oocytes* as well as the permeabilities for glycerol, urea, mannitol, uracil, adenine and β -hydroxybutyrate. For oocytes expressing AQP3, water and urea permeability were partially inhibited by 0.1 mM phloretin, whereas the glycerol permeability remained unchanged (Tsukaguchi et al. 1998 and 1999).

However, phloretin was tested in an *in vitro* functional assay using *X. oocytes* expressing the human Aquaporin 4-M23 isozyme (hAQP4b) and found to have no effect on the water transport (Huber et al. 2007). Phloretin as an inhibitor of AQPs displays undesirable properties: it inhibits solute transporters as well as ion channels and thus exerts profound effects on osmotic gradients in multiple ways.

The virtual docking done by Huber et al. (2007) for Phloretin into the water channel of ratAQP4b indicated that the docking score is $-62.293 \text{ kcal mol}^{-1}$. Electrostatic interactions between the phenol group and Arg-216 and between the trihydroxyphenone and Asp-69 and His-151 were highlighted.

3.5 Recent Findings

Compounds with reported AQP1 inhibition activity, including Hg^{2+} , DMSO, Au^{3+} , Ag^+ , TEA and AZA were tested in two different assays in order to compare their potency for AQP1 (Yang et al. 2006). Water permeability was measured by stopped-flow light scattering in erythrocytes and volume marker dilution in epithelial cells.

Results obtained for AQP1 inhibition by the metal ions Ag^+ , Au^{3+} , Hg^{2+} and various other heavy metal ions were consistent with previous reports. However, TEA did not inhibit AQP1 water permeability in erythrocytes or AQP1-expressing epithelial cells at concentrations up to 10 mM. This result was explained by the fact that oocytes contain a TEA sensitive membrane protein or lipid component that interacts with AQP1. Also, apparent water transport may be influenced by non-specific effects of the high (10 mM) TEA concentrations such as block of K^+ channels and consequent altered basal cell volume.

AZA was previously reported to inhibit water permeability by $>80\%$ at $10 \mu\text{M}$ in *X. oocytes*, with IC_{50} $1 \mu\text{M}$, however no inhibition of AQP1 in erythrocytes or AQP1-expressing epithelial cells at concentrations of AZA up to 2 mM was detected by Yang et al. (2006).

Recent experiments by Sogaard and Zeuthen (2007), in agreement with Yang et al. (2006), did not observe effects of TEA and AZA on water AQP1 permeability

in an improved *X. laevis* oocyte system. It was suggested that the secondary effect of ion distribution across the membrane is very important and may be involved in the false positive results obtained previously.

4 Conclusion

Aquaporins are important targets for drugs that could be used to study aquaporin function. Knockout phenotypes of kidney aquaporins suggest that aquaporin blockers could function as diuretics and blockers of brain AQP4, could reduce fatal brain swelling (edema) after stroke or head trauma. Finally, AQP7 specific inhibitors could help to elucidate its function in glycerol transport and contribute to developing novel treatments of type II diabetes and obesity (Hara-Chikuma et al. 2005). Specific aquaporin blockers are currently not available. The atomic 3D structures of AQP0, AQP1 and AQP4 (from mammals), SoPIP2;1 (from plants) and AQPZ and GlpF (from bacteria) have however been determined and these structures can be exploited for rational design of drug candidates. Traditional HTS for AQP inhibitors is needed in parallel to provide appropriate starting points for molecular modeling approaches. Suitable methods have recently been described within international patent Nr. WO 2006/102483 A2. Novel substances that may inhibit AQP1 have been claimed within this patent and promise unique and powerful forms of future cancer chemotherapy through inhibition of angiogenesis (Saadoun et al. 2005). Furthermore recent technical advancements may provide to adopt several methods that have traditionally been employed in water permeability measurements for HTS for novel AQP inhibitors. Finally novel, yeast based screening methods are promising identification of *Pf*AQP inhibitors in the near future, which could function as a novel class of anti malarial drugs.

References

- Allen TM, Cleland LG (1980) Serum-induced leakage of liposome contents. *Biochim Biophys Acta* 597:418–426
- Armstrong CM (1971) Interaction of tetraethyl ammonium ion derivatives with the potassium channels of giant axons. *J Gen Physiol* 58:413–437
- Brooks HL, Regan JW, Yool AJ (2000) Inhibition of aquaporin-1 water permeability by tetraethyl ammonium: involvement of the loop E pore region. *Mol Pharmacol* 57:1021–1026
- Chen RF, Knutson JR (1988) Mechanism of fluorescence concentration quenching of carboxyfluorescein in liposomes: energy transfer to nonfluorescent dimers. *Anal Biochem* 172:61–77
- Daniels MJ, Wood MR, Yeager M (2006) In vivo functional assay of a recombinant aquaporin in *Pichia pastoris*. *Appl Environ Microbiol* 72:1507–1514
- Detmers FJ, de Groot BL, Muller EM, Hinton A, Konings IB, Sze M, Flitsch SL, Grubmuller H, Deen PM (2006) Quaternary ammonium compounds as water channel blockers. Specificity, potency, and site of action. *J Biol Chem* 281:14207–14214
- Gao J, Yu H, Song Q, Li X (2005) Establishment of HEK293 cell line expressing green fluorescent protein-aquaporin-1 to determine osmotic water permeability. *Anal Biochem* 342:53–58

- Gao J, Wang X, Chang Y, Zhang J, Song Q, Yu H, Li X (2006) Acetazolamide inhibits osmotic water permeability by interaction with aquaporin-1. *Anal Biochem* 350:165–170
- Gordon SE, Zagotta WN (1995) A Histidine residue associated with the gate of the cyclic nucleotide-activated channels in rod photoreceptors. *Neuron* 14:177–183
- Gunnarson E, Axehult G, Baturina G, Zelenin S, Zelenina M, Aperia A (2005) Lead induces increased water permeability in astrocytes expressing aquaporin 4. *Neuroscience* 136:105–114
- Hamann S, Kiilgaard JF, Litman T, Alvarez-Leefmans FJ, Winther BR, Zeuthen T (2002) Measurement of cell volume changes by fluorescence self-quenching. *J Fluoresc* 12:139–145
- Hara-Chikuma M, Sohara E, Rai T, Ikawa M, Okabe M, Sasaki S, Uchida S, Verkman AS (2005) Progressive adipocyte hypertrophy in aquaporin-7-deficient mice: adipocyte glycerol permeability as a novel regulator of fat accumulation. *J Biol Chem* 280:15493–15496
- Hibuse T, Maeda N, Funahashi T, Yamamoto K, Nagasawa A, Mizunoya W, Kishida K, Inoue K, Kuriyama H, Nakamura T, Fushiki T, Kihara S, Shimomura I (2005) Aquaporin 7 deficiency is associated with development of obesity through activation of adipose glycerol kinase. *Proc Natl Acad Sci U S A* 102:10993–10998
- Huber VJ, Tsujita M, Yamazaki M, Sakimura K, Nakada T (2007) Identification of arylsulfonamides as AQP4 inhibitor. *Bioorg Med Chem Lett* 17:1670–1273
- Huber VJ, Tsujita M, Nakada T (2008a) Identification of aquaporin 4 inhibitors using in vitro and in silico methods. *Bioorg Med Chem*. doi:10.1016/j.bmc.2007.12.038
- Huber VJ, Tsujita M, Kwee IL, Nakada T (2008b) Inhibition of Aquaporin 4 by antiepileptic drugs. *Bioorg Med Chem*. doi:10.1016/j.bmc.2007.12.040
- Kendall DA, MacDonald RC (1983) Characterization of a fluorescence assay to monitor changes in the aqueous volume of lipid vesicles. *Anal Biochem* 134:26–33
- Klein JD, Sands JM, Qian L, Wang X, Yang B (2004) Upregulation of urea transporter UT-A2 and water channels AQP2 and AQP3 in mice lacking urea transporter UT-B. *J Am Soc Nephrol* 15:1161–1167
- Lang DG, Ritchie AK (1990) Tetraethyl ammonium blockade of apamin-sensitive and insensitive Ca^{2+} activated K^{+} channels in a pituitary cell line. *J Physiol* 425:117–132
- Latorre R, Vergara C, Hidalgo C (1982) Reconstitution in planar lipid bilayers of a Ca^{2+} dependent K^{+} channel from transverse tubule membranes isolated from rabbit skeletal muscle. *Proc Natl Acad Sci U S A* 79:805–809
- Lee H, Goetzl EJ, An S (2000) Lysophosphatidic acid and sphingosine 1-phosphate stimulate endothelial cell wound healing. *Am J Physiol Cell Physiol* 278:C612–618
- Levin MH, Verkman AS (2006) Aquaporin-3-dependent cell migration and proliferation during corneal re-epithelialization. *Invest Ophthalmol Vis Sci* 47:4365–4372
- Ma T, Yang B, Gillespie A, Carlson EJ, Epstein CJ, Verkman AS (1998) Severely impaired urinary concentrating ability in transgenic mice lacking aquaporin-1 water channels. *J Biol Chem* 273:4296–4299
- Ma T, Song Y, Yang B, Gillespie A, Carlson EJ, Epstein CJ, Verkman AS (2000) Nephrogenic diabetes insipidus in mice lacking aquaporin-3 water channels. *Proc Natl Acad Sci U S A* 97:4386–4391
- Ma B, Xiang Y, Mu SM, Li T, Yu HM, Li XJ (2004) Effects of acetazolamide and anordiol on osmotic water permeability in AQP1-cRNA injected *Xenopus* oocyte. *Acta Pharmacol Sin* 25:90–97
- Macey RI, Farmer REL (1970) Inhibition of water and solute permeability in human red cells. *Biochim Biophys Acta* 211:104–106
- Manley GT, Fujimura M, Ma T, Noshita N, Filiz F, Bollen AW, Chan P, Verkman AS (2000) Aquaporin-4 deletion in mice reduces brain edema after acute water intoxication and ischemic stroke. *Nat Med* 6:159–163
- McCoy E, Sontheimer H (2007) Expression and function of water channels (aquaporins) in migrating malignant astrocytes. *Glia* 55:1034–1043
- Meinild AK, Klaerke DA, Zeuthen T (1998) Bidirectional water fluxes and specificity for small hydrophilic molecules in aquaporins 0–5. *J Biol Chem* 273:32446–32451

- Németh-Cahalan KL, Hall JE (2000) pH and calcium regulate the water permeability of aquaporin 0. *J Biol Chem* 275:6777–6782
- Nielsen S, Nagelhus EA, Amiry-Moghaddam M, Bourque C, Agre P, Ottersen OP (1997) Specialized membrane domains for water transport in glial cells: high-resolution immunogold cytochemistry of aquaporin-4 in rat brain. *J Neurosci* 17:171–180
- Niemietz CM, Tyerman SD (2002) New potent inhibitors of aquaporins: silver and gold compounds inhibit aquaporins of plant and human origin. *FEBS Lett* 531:443–447
- Oheim M (2007) High-throughput microscopy must re-invent the microscope rather than speed up its functions. *Br J Pharmacol* 152:1–4
- Papadopoulos MC, Saadoun S, Verkman AS (2007) Aquaporins and cell migration. *Pflugers Arch Eur J Physiol*. doi 10.1007/s00424-007-0357-5
- Perchenet I, Clément-Chomienne O (2001) External nickel blocks human Kv1.5 channels stably expressed in CHO cells. *J Membr Biol* 183:51–60
- Preston GM, Carroll TP, Guggino WB, Agre P (1992) Appearance of water channels in *Xenopus* oocytes expressing red cell CHIP28 protein. *Science* 256:385–387
- Promeneur D, Liu Y, Maciel J, Agre P, King LS, Kumar N (2007) Aquaglyceroporin PbAQP during intraerythrocytic development of the malaria parasite *Plasmodium berghei*. *Proc Natl Acad Sci U S A* 104:2211–2216
- Rojek A, Fuchtbauer EM, Kwon TH, Frokiaer J, Nielsen S (2006) Severe urinary concentrating defect in renal collecting duct-selective AQP2 conditional-knockout mice. *Proc Natl Acad Sci U S A* 103:6037–6042
- Saadoun S, Papadopoulos MC, Hara-Chikuma M, Verkman AS (2005) Impairment of angiogenesis and cell migration by targeted aquaporin-1 gene disruption. *Nature* 434:786–792
- Savage DF, Stroud RM (2007) Structural basis of aquaporin inhibition by mercury. *J Mol Biol* 368:607–617
- Smith BL, Agre P (1991) Erythrocyte Mr 28,000 transmembrane protein exists as a multisubunit oligomer similar to channel proteins. *J Biol Chem* 266:6407–6415
- Sogaard R, Zeuthen T (2007) Test of blockers of AQP1 water permeability by a high-resolution method: no effects of tetraethylammonium ions or acetazolamide. *Pflugers Arch Eur J Physiol*. doi 10.1007/s00424-007-0392-2
- Solenov E, Watanabe H, Manley GT, Verkman AS (2004) Sevenfold-reduced osmotic water permeability in primary astrocyte cultures from AQP-4-deficient mice, measured by a fluorescence quenching method. *Am J Physiol Cell Physiol* 286:C426–C432
- Steinle JJ, Meininger CJ, Forough R, Wu G, Wu MH, Granger HJ (2002) Eph B4 receptor signaling mediates endothelial cell migration and proliferation via the phosphatidylinositol 3-kinase pathway. *J Biol Chem* 277:43830–43835
- Tsukaguchi H, Shayakul C, Berger UV, Mackenzie B, Devidas S, Guggino WB, van Hoek AN, Hediger MA (1998) Molecular characterization of a broad selectivity neutral solute channel. *J Biol Chem* 273:24737–24743
- Tsukaguchi H, Weremowicz S, Morton CC, Hediger MA (1999) Functional and molecular characterization of the human neutral solute channel aquaporin-9. *Am J Physiol* 277:F685–F696
- Vajda Z, Pedersen M, Fuchtbauer EM, Wertz K, Stodkilde-Jorgensen H, Sulyok E, Doczi T, Neely JD, Agre P, Frokiaer J, Nielsen S (2002) Delayed onset of brain edema and mislocalization of aquaporin-4 in dystrophin-null transgenic mice. *Proc Natl Acad Sci U S A* 99:13131–13136
- Van Hoek AN, Verkman AS (1992) Functional reconstitution of the isolated erythrocyte water channel CHIP28. *J Biol Chem* 267:18267–18269
- Van Hoek AN, De Jong MD, Van Os CH (1990) Effects of dimethylsulfoxide and mercurial sulfhydryl reagents on water and solute permeability of rat kidney brush border membranes. *Biochim Biophys Acta- Biomembr* 1030:203–210
- Verkman AS (2000) Water permeability measurement in living cells and complex tissues. *J Membr Biol* 173:73–87
- Wehner F, Sauer H, Kinne RK (1995) Hypertonic stress increases the Na⁺ conductance of rat hepatocytes in primary culture. *J Gen Physiol* 105:507–535

- Wu B, Altmann K, Barzel I, Krehan S, Beitz E (2007) A yeast-based phenotypic screen for aquaporin inhibitors. *Pflugers Arch* 456:717–720
- Yang B, Verkman AS (2002) Analysis of double knockout mice lacking aquaporin-1 and urea transporter UT-B. Evidence for UT-B-facilitated water transport in erythrocytes. *J Biol Chem* 277:36782–36786
- Yang B, Kim JK, Verkman AS (2006) Comparative efficacy of HgCl₂ with candidate aquaporin-1 inhibitors DMSO, gold, TEA⁺ and acetazolamide. *FEBS Lett* 580:6679–6684
- Yasui M, Hazam A, Kwon TH, Nielsen S, Guggino WB, Agre P (1999) Rapid gating and anion permeability of an intracellular aquaporin. *Nature* 402:184–187
- Yool A, Brokl O, Pannabecker T, Dantzler W, Stamer D (2002) TEA block of water flux in AQP1 channels expressed in kidney thin limbs of Henle's loop and a kidney-derived cell line. *BMC Physiol* 2:1–8
- Zamponi GW, Bourinet E, Snutch TP (1996) Nickel block of a family of neuronal calcium channels: subtype- and subunit-dependent action at multiple sites. *J Membr Biol* 151:77–90
- Zeidel ML, Ambudkar SV, Smith BL, Agre P (1992) Reconstitution of functional water channels in liposomes containing purified red cell CHIP28 protein. *Biochemistry* 31:7436–7440
- Zelenina M, Zelenin S, Bondar AA, Brismar H, Aperia A (2002) Water permeability of aquaporin-4 is decreased by protein kinase C and dopamine. *Am J Physiol Renal Physiol* 283:F309–F318
- Zelenina M, Bondar AA, Zelenin S, Aperia A (2003) Nickel and extracellular acidification inhibit the water permeability of human aquaporin-3 in lung epithelial cells. *J Biol Chem* 278:30037–30043
- Zelenina M, Tritto S, Bondar AA, Zelenin S, Aperia A (2004) Copper inhibits the water and glycerol permeability of aquaporin-3. *J Biol Chem* 279:51939–51943
- Zhang R, van Hoek AN, Biwersi J, Verkman AS (1993) A point mutation at cysteine 189 blocks the water permeability of rat kidney water channel CHIP28k. *Biochemistry* 32:2938–2941

Aquaporin-1 Gene Transfer to Correct Radiation-Induced Salivary Hypofunction

Bruce J. Baum, Changyu Zheng, Ana P. Cotrim, Linda McCullagh, Corinne M. Goldsmith, Jaime S. Brahim, Jane C. Atkinson, R. James Turner, Shuying Liu, Nikolay Nikolov, and Gabor G. Illei

Contents

1	Introduction	403
2	Gene Transfer Vector: Construction and In Vitro Characterization	405
3	Pre-Clinical Model Testing	409
4	Toxicology and Biodistribution Studies	411
5	Clinical Protocol	415
	References	417

Abstract Irradiation damage to salivary glands is a common iatrogenic consequence of treatment for head and neck cancers. The subsequent lack of saliva production leads to many functional and quality-of-life problems for affected patients and there is no effective conventional therapy. To address this problem, we developed an in vivo gene therapy strategy involving viral vector-mediated transfer of the aquaporin-1 cDNA to irradiation-damaged glands and successfully tested it in two pre-clinical models (irradiated rats and miniature pigs), as well as demonstrated its safety in a large toxicology and biodistribution study. Thereafter, a clinical research protocol was developed that has received approval from all required authorities in the United States. Patients are currently being enrolled in this study.

1 Introduction

Each year, worldwide, ~500,000 individuals are diagnosed with a malignancy in the head and neck region.¹ Most of these patients will receive treatment that includes surgery ± chemotherapy and therapeutic irradiation (IR). While IR is quite

B.J. Baum (✉)

Molecular Physiology and Therapeutics Branch and Clinical Research Core,
National Institute of Dental and Craniofacial Research, NIH, Bethesda, MD 20892 USA
bbaum@dir.nidcr.nih.gov

¹ <http://www.oralcancerfoundation.org/>

effective as adjunctive therapy for the cancer, it can also damage adjacent normal tissues. Salivary glands are quite sensitive to IR. Indeed, IR leads to a dramatic loss of the fluid secreting salivary acinar cells, resulting in severe glandular hypofunction (a diminished production of saliva) in most patients (Vissink et al. 2003; Nagler and Baum 2003). The reason for this damage remains enigmatic, as salivary acinar cells are well differentiated and very slowly dividing, the opposite of the classical target cell for IR sensitivity. If patients have sufficient functional acinar tissue post-IR, it is possible to treat their salivary hypofunction with cholinergic drugs (Shiboski et al. 2007). However, most post-IR patients have salivary glands characterized by inadequate acinar cell mass with non-fluid secreting duct cells surviving and predominating (Vissink et al. 2003; Nagler and Baum 2003). There is no effective conventional therapy for these patients, a situation that led us to consider the use of gene therapy, i.e., in vivo gene transfer, as a therapeutic approach to repair damaged glands (Baum et al. 1999). The gene of choice was human aquaporin-1 (hAQP1).

The specific strategy we adopted is depicted in Fig. 1. This strategy was based on the understanding of salivary fluid secretion and salivary duct cell physiology available in 1991 (Baum 1993). In this figure, a surviving duct cell in an IR-damaged salivary gland is illustrated. We hypothesized that it would be possible for this cell to secrete fluid through the transfer of a gene encoding a functional, non-polarized water channel protein. Our hypothesis included a view that the duct cells could generate an osmotic gradient, lumen > interstitium, in the absence of any significant acinar cell secretion and the expression of a water channel in these normally water

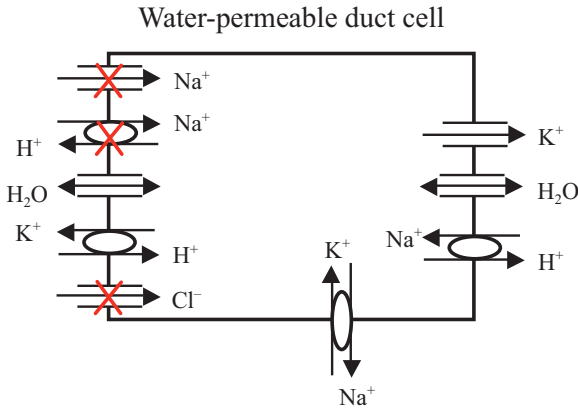


Fig. 1 Schematic diagram of the hypothesized mechanism for fluid secretion following AdhAQP1-mediated gene transfer to duct cells in an irradiated salivary gland. The surviving duct cell is presented in a simplified form, based on our understanding ~1991. The duct lumen is to the left and the interstitium is to the right. The three apical ion pathways with Xs will be inoperable in the absence of an isotonic primary secretion, which normally is made by acinar cells. We have hypothesized that duct cells could generate a KHCO₃ gradient (lumen > interstitium) enabling fluid to flow into the duct lumen following expression of the transgene hAQP1. This figure is modified from Vitolo and Baum (2002), and is based on the experiments presented in Delporte et al. (1997)

impermeant cells would in turn permit osmotically driven transepithelial fluid flow into the lumen. The specific hypothesis, in brief, is as follows. In the absence of an isotonic acinar cell secretion, most of the membrane transport proteins then-known to be present in the duct cell luminal membrane would be inactive owing to the low luminal concentrations of their respective substrates; these include the epithelial sodium channel, the cystic fibrosis transmembrane conductance regulator (i.e., a chloride channel) and the sodium/proton exchanger. However, a potassium/proton exchanger in the luminal membrane would be active and able to exchange intracellular potassium for a proton that could be generated in the lumen from the dissolution of CO₂ in the small amount of diffused water that normally should be present. The CO₂ would dissociate to yield the exchangeable proton and HCO₃⁻, resulting in a KHCO₃ osmotic gradient. As shown, the cDNA for hAQP1 has been transferred and it assumes a non-polarized distribution all around the plasma membrane. Water then would be able to flow across the duct cell into the lumen in response to the hypothesized KHCO₃ gradient. It is important to recognize that this hypothetical mechanism is still unproven, but the gene transfer strategy, as is presented below, has been successfully utilized in small and large animal pre-clinical models.

2 Gene Transfer Vector: Construction and In Vitro Characterization

To transfer the hAQP1 cDNA into duct cells we chose to use a first generation, serotype 5 adenoviral (Ad5) vector (Delporte et al. 1997). In earlier studies we showed Ad5 vectors were extremely efficient for in vivo gene transfer to rodent salivary glands (Mastrangeli et al. 1994). The AdhAQP1 vector was constructed (Delporte et al. 1997) and a schematic depiction of this vector is shown in Fig. 2. The vector consists of an Ad5 genome modified by a deletion in the E1 gene region, which is important to prevent replication, and a partial deletion in the E3 region. All other Ad5 genes remain in the vector. The transgene expression cassette was placed into the deleted E1 region via homologous recombination and includes a

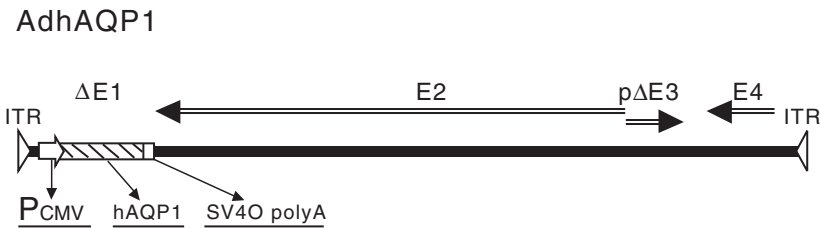


Fig. 2 Schematic diagram of AdhAQP1. *ITR* inverted terminal repeat; *Pcmv* cytomegalovirus promoter/enhancer; *hAQP1* human aquaporin-1 cDNA; *SV40 polyA* simian virus 40 polyadenylation signal; $\Delta E1$ deletion of adenoviral E1 sequences; *E2* adenoviral E2 genes; *pΔE3* partial deletion/modification of adenoviral E3 sequences; *E4* adenoviral E4 genes

cytomegalovirus promoter/enhancer to drive expression, the hAQP1 cDNA, and a simian virus-40 polyadenylation signal.

Initial studies of the function and potential utility of this vector were performed in vitro with several epithelial cell types (Delporte et al. 1997). As shown in the upper panel of Fig. 3, when compared to transduction with a control Ad5 vector, 293

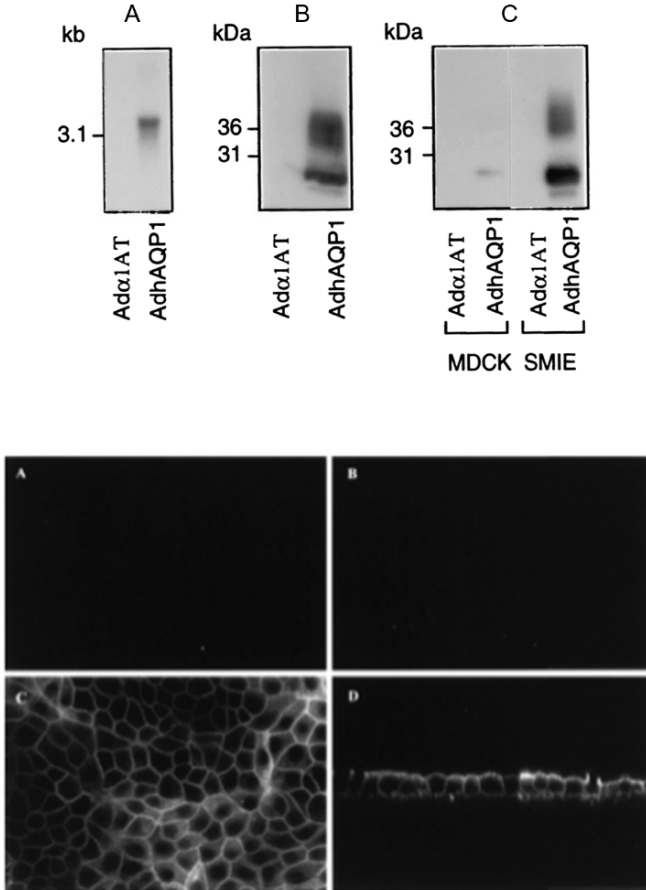


Fig. 3 Human aquaporin-1 expression in epithelial cells in vitro. *Upper panel:* (a) Northern blot using RNA from 293 cells transduced with either AdhAQP1 or a control vector, Adα1AT. (b) Western blot of crude membranes from 293 cells transduced with AdhAQP1 or the control vector. (c) Western blot of crude membranes from MDCK and SMIE cells transduced with AdhAQP1 or the control vector. Note that in the Western blots the monomeric non-glycosylated hAQP1 protein migrates at ~28 kDa, while multiple glycosylated forms are seen at slightly higher molecular weights. This figure originally was published as Fig. 1 in (Delporte et al. 1997). *Lower panel:* Localization of transgenic hAQP1 expressed in MDCK cells. Confluent MDCK cells were grown on filters and transduced for 24 h with either Adα1AT (a) and (b) or AdhAQP1 (c) and (d). Cell layers were then examined by confocal microscopy after immunofluorescent staining with an antibody to hAQP1. (a) and (c) are in the x-y plane, while (b) and (d) are in the x-z plane. This figure originally was published as Fig. 2 in (Delporte et al. 1997)

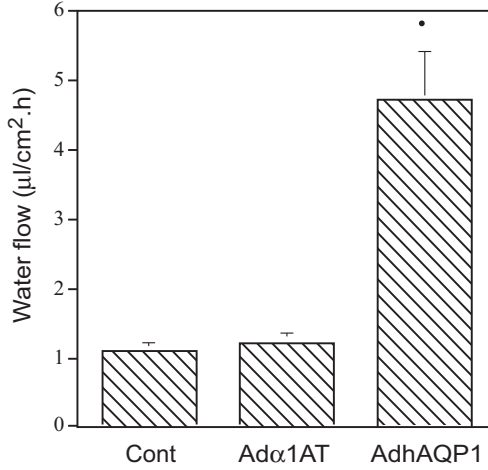


Fig. 4 Net fluid secretion rate of MDCK cells with and without transduction by AdhAQP1. Cells were either untreated (control, Cont), or transduced with either AdhAQP1 or a control vector, Adα1AT, and water flow measured in response to an apical (400 mosm) >basal (300 mosm) osmotic gradient. The results are expressed as water flow in microliters of fluid per cm² per hour and are mean values ± SEMs. This figure originally was published as Fig. 3 in (Delporte et al. 1997)

(human embryonic kidney), MDCK (canine kidney) and SMIE (rat submandibular gland) cells all begin to express hAQP1 after transduction with AdhAQP1. Furthermore, and essential for our hypothesis, the expressed hAQP1 assumes a non-polarized distribution in MDCK cells (Fig. 3, lower panel). Importantly, as shown in Fig. 4, the transgenic hAQP1 protein is functional and results in the net movement of fluid, from a basal to an apical direction, in response to an imposed osmotic gradient (apical 400 mosm; basal 300 mosm) (Delporte et al. 1997). The treatment of MDCK cells with an irrelevant vector had no effect on fluid movement (same as control cells), while treatment of cells with AdhAQP1 resulted in a ~fivefold increase in net fluid secretion (Delporte et al. 1997).

We further characterized the pharmacological properties of the AdhAQP1 vector using the SMIE cell line. As shown in Fig. 5, following transduction of cells at a MOI (multiplicity of infection) of 5, i.e. five infectious units (plaque-forming units, pfu)/cell, fluid movement across SMIE cell monolayers is linear for 15–30 min (Delporte et al. 1998). After 30 min, the transepithelial fluid movement across non-transduced cells was ~5µl cm⁻², while following transduction with AdhAQP1 this value was ~60µl cm⁻². As is shown in Fig. 6, osmotically obliged fluid movement across SMIE cells was AdhAQP1 dose dependent (Delporte et al. 1998). Fluid movement sharply increased at doses from 0.1, 0.5–1.0 MOI and began to plateau thereafter. Interestingly, significant fluid movement occurred at relatively low levels of hAQP1 expression in these monolayers, e.g., the amount of hAQP1 yielding ~50% of maximal fluid movement was <10% of the maximal hAQP1 protein expression observed.

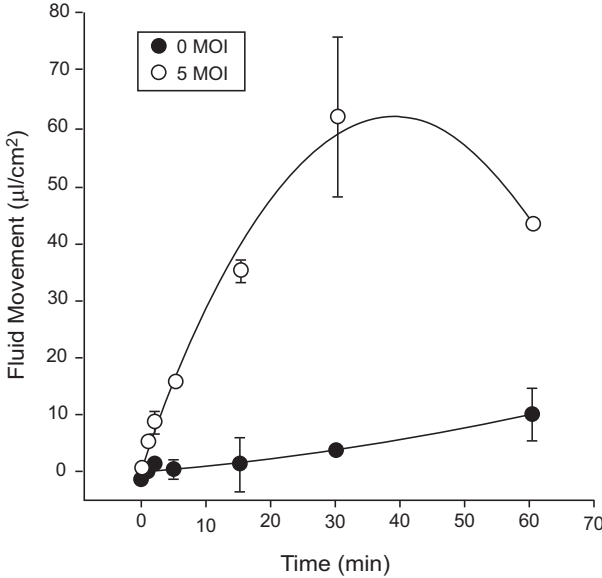


Fig. 5 Time course of fluid movement across SMIE cell monolayers. SMIE cells were transduced with AdhAQP1 (MOI = 5) or not, and after 24 h fluid movement was measured in response to an osmotic gradient as shown in Fig. 4. The results are expressed as water flow in microliters of fluid per cm² per hour and are mean values ± SEMs. This figure originally was published as Fig. 2 in (Delporte et al. 1998)

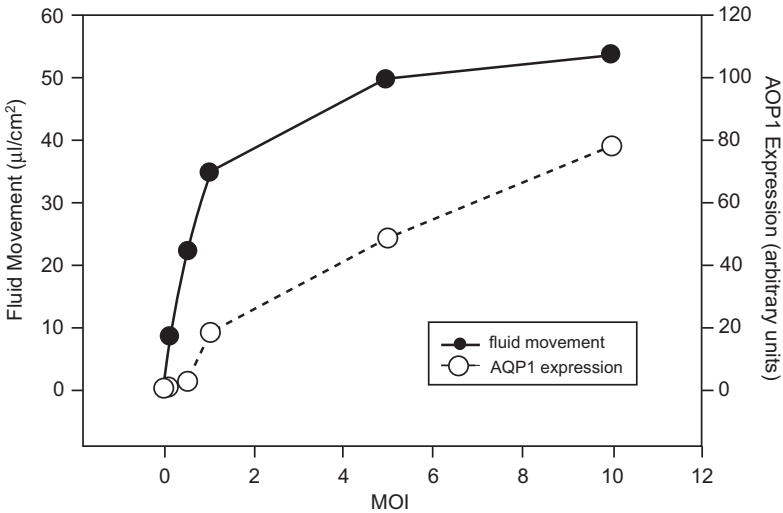


Fig. 6 Effect of vector concentration on fluid flow across SMIE cells. After reaching confluence, SMIE cell monolayers were transduced at the indicated MOI and fluid movement then measured for 15 min. Thereafter, crude membranes from each cell monolayer were prepared, electrophoresed and subjected to Western blotting with antibody to hAQP1. The films were scanned with a laser densitometer to quantify the amount of hAQP1 expressed (indicated in arbitrary units). This figure originally was published as Fig. 4 in (Delporte et al. 1998)

3 Pre-Clinical Model Testing

In order to determine if the AdhAQP1 vector was effective in restoring salivary flow to IR-damaged salivary glands, we used a rat IR model with which we previously had considerable experience (Nagler et al. 1998). Additionally, we knew that Ad5 vectors administered to rat salivary glands direct high levels of transgene expression in this tissue (Mastrangeli et al. 1994; Baum et al. 2002). For experimental convenience, we employed single radiation doses (either 17.5 or 21 Gray, Gy), rather than a fractionated scheme that is more typical of the clinical situation. Rodent salivary glands are considered relatively IR-resistant, so the IR doses used were high given the size of the animals (~300 g). A time line depicting the general experimental design of this study is shown in Fig. 7a. Animals were irradiated and then followed for either 90 (the 17.5 Gy group) or 120 (the 21 Gy group) days, providing moderate and severe IR damage models, respectively. At the appropriate time point animals were

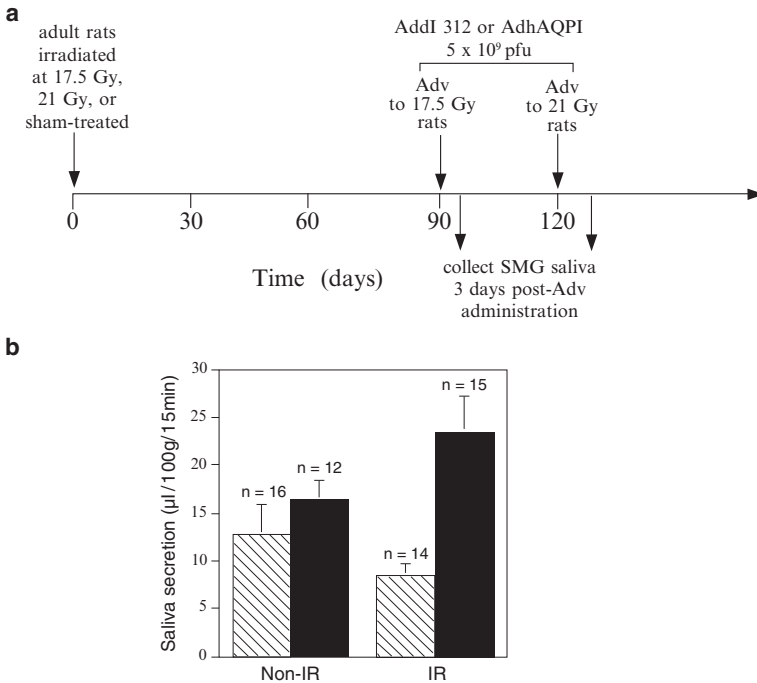


Fig. 7 (a) Time line of initial study of AdhAQP1 efficacy in irradiated rats. Rats were irradiated on day zero with either 17.5 Gy or 21 Gy, or sham-irradiated. After 90 (17.5 Gy) or 120 (21 Gy) days, AdhAQP1 or a control vector (Addl312) was administered to both submandibular glands and 3 days later saliva was collected. (b) Function of transgenic hAQP1 in vivo. Salivary flow rates obtained in animals irradiated (17.5 Gy) or not, and administered either AdhAQP1 or Addl312. Rats administered Addl312 are shown in the hatched bars, while rats administered AdhAQP1 are shown in the black bars. The results are expressed as saliva secretion in microliters per 100 g body weight per 15 min and are mean values ± SEMs. This figure originally was published as Fig. 4b in (Delporte et al. 1997)

Table 1 Effect of AdhAQP1 transduction on salivary secretion by rat submandibular glands after irradiation with 21 Gy

Experimental group	Add1312 (<i>n</i>)	AdhAQP1 (<i>n</i>)
Sham-irradiated	36.6 ± 6.8 (4)	28.4 ± 8.0 (6)
21 Gy irradiated	13.2 ± 3.7 (6)	30.6 ± 3.5 (9)

This table is modified from Table 1 of (Delporte et al. 1997). The data shown are salivary flow rates ($\mu\text{l}/100\text{ g}$ body weight per 15 min; mean \pm SEMs) for the number of rats in parentheses. Animals were either sham irradiated or their salivary glands were exposed to 21 Gy. Four months after irradiation, animals received 5×10^9 plaque forming units of either a control Ad5 vector (Add1312) or AdhAQP1 to each submandibular gland. Three days later saliva was collected

administered 5×10^9 pfu of the AdhAQP1 vector or a control Ad5 vector (Add1312, without any encoded transgene). The infectious dose used corresponds to $\sim 5 \times 10^{11}$ vector genomes and was delivered into both submandibular glands via intra-oral cannulation of the main excretory duct. After 3 days we collected whole saliva from each animal. The results were generally similar with both radiation groups, demonstrating administration of the AdhAQP1 vector increased salivary flow rate in the irradiated rats (Fig. 7b, Table 1). As shown in Fig. 7b, 17.5 Gy leads to a modest, $\sim 30\%$, decrease in salivary flow (control rats receiving IR plus the Add1312 vector) and administration of the AdhAQP1 vector to these rats resulted in a dramatic increase in salivary flow. As shown in Table 1, IR with 21 Gy leads to a marked decrease in salivary flow, $\sim 65\%$, in the Add1312 vector-treated rats. Conversely, salivary flow in rats receiving the AdhAQP1 vector was similar, independent of whether or not they were irradiated. Immunocytochemical examination of sections prepared from glands transduced with AdhAQP1 showed high levels of hAQP1 immunolabelling in both acinar and duct cells, (in this rat IR model many acinar cells survive IR treatment, but shrink in size (O'Connell et al. 1999a), somewhat unlike the situation in human glands). Nonetheless, these overall results strongly supported our original hypothesis that hAQP1 gene transfer could lead to a correction in salivary flow rates in irradiated animals. Interestingly, the $[\text{K}^+]$ in saliva was $\sim 40\%$ greater in samples collected from AdhAQP1-treated rats compared to that from rats treated with Add1312 (Delporte et al. 1997).

A critical step in the development of a gene therapy is demonstration of efficacy, and scaling, to a large animal model. Originally, for this purpose we conducted experiments in rhesus macaques, but the results were equivocal, likely because of the small number of animals available to us (five; including one control, with two animals in each of two dosage groups (O'Connell et al. 1999b)). Subsequently, we developed a more affordable, large animal salivary gland IR damage model using the miniature pig parotid gland (Li et al. 2005). In addition, we demonstrated that it was possible to scale the expression of an Ad5 vector-encoded reporter transgene (luciferase) between 20 g mice and ~ 25 –30 g miniature pigs (Li et al. 2004).

Consequently, we conducted an IR experiment in miniature pigs similar in general design to that used in rats (see Figs. 7a and 8a, and (Shan et al. 2005)).

We irradiated one miniature pig parotid gland with a single dose of 20 Gy, again for experimental convenience (Fig. 8a). Importantly, the IR dose used was slightly less than that used in rats, which were $\sim 1\%$ the size of the miniature pigs. Prior to IR we collected saliva twice from the parotid glands of each animal and normalized the average value to 100% secretion levels. We then irradiated the animals and followed them longitudinally for ~ 4 months (see Fig. 8a). Within 4 weeks average parotid salivary flow rates in irradiated glands had decreased by $\sim 60\%$ and by 16 weeks salivary flow was reduced by $\sim 80\%$ (Fig. 8b). Next, all animals were treated with either the AdhAQP1 vector or a control vector (for this study an Ad5 vector encoding luciferase). The maximum total vector dose administered to each parotid gland was 10^9 pfu, i.e., only 20% of the total vector dose used for rats. This dose, when normalized to the size of the targeted gland, is the same dose that we previously showed scaled from mice (Li et al. 2004). Three days after vector delivery, the 10^9 pfu AdhAQP1 dose resulted in a dramatic increase in parotid saliva flow rates, to $\sim 80\%$ of pre-IR control levels (Fig. 8b). Thereafter, flow rates began to decrease (at days 7 and 14), but on average still remained above those seen for glands receiving the control vector. Additionally, we showed that vector efficacy was dose-dependent, i.e., a 10^8 pfu/gland dose being without effect (Fig. 8c). When we examined formalin-fixed parotid gland sections by immunocytochemistry with an antibody directed at hAQP1, we saw high levels of hAQP1 immunolabelling only in duct cells. The gland sections also showed an apparent loss of acinar cells with replacement by connective tissue, as seen in humans. Although acinar cells were seen in the sections, none were transduced by vector. Interestingly, the $[K^+]$ in parotid saliva from animals transduced with the AdhAQP1 vector was decreased $\sim 40\%$ from the 16 week post-IR level to an average level approximating that seen prior to IR. This was different from what we expected, based on our hypothesis and the results of the rat study mentioned previously. However, the total amount of K^+ secreted by AdhAQP1-transduced glands was greater than that seen in the control glands. Although still unclear, this result may indicate an osmotic driving force operating in the transduced miniature pig duct cells different than we anticipated, or be reflective of a secretion arising only from the transduction of duct cells in these animals, i.e., unlike the mixed acinar and duct cell transduction seen in rats.

4 Toxicology and Biodistribution Studies

Based on the miniature pig experiments, it seemed that the AdhAQP1 vector could prove useful in human studies. Accordingly, it was imperative to conduct a detailed safety evaluation of this vector. We conducted such a study in male and female rats. The study conformed to the U.S. Food and Drug Administration's (FDA's) Good Laboratory Practice (GLP) guidelines (Zheng et al. 2006). Two hundred animals (equal number by gender) were divided into four dosage groups: zero vector (vehicle alone), 2×10^8 vector genomes, 8×10^9 vector genomes, or 2×10^{11} vector

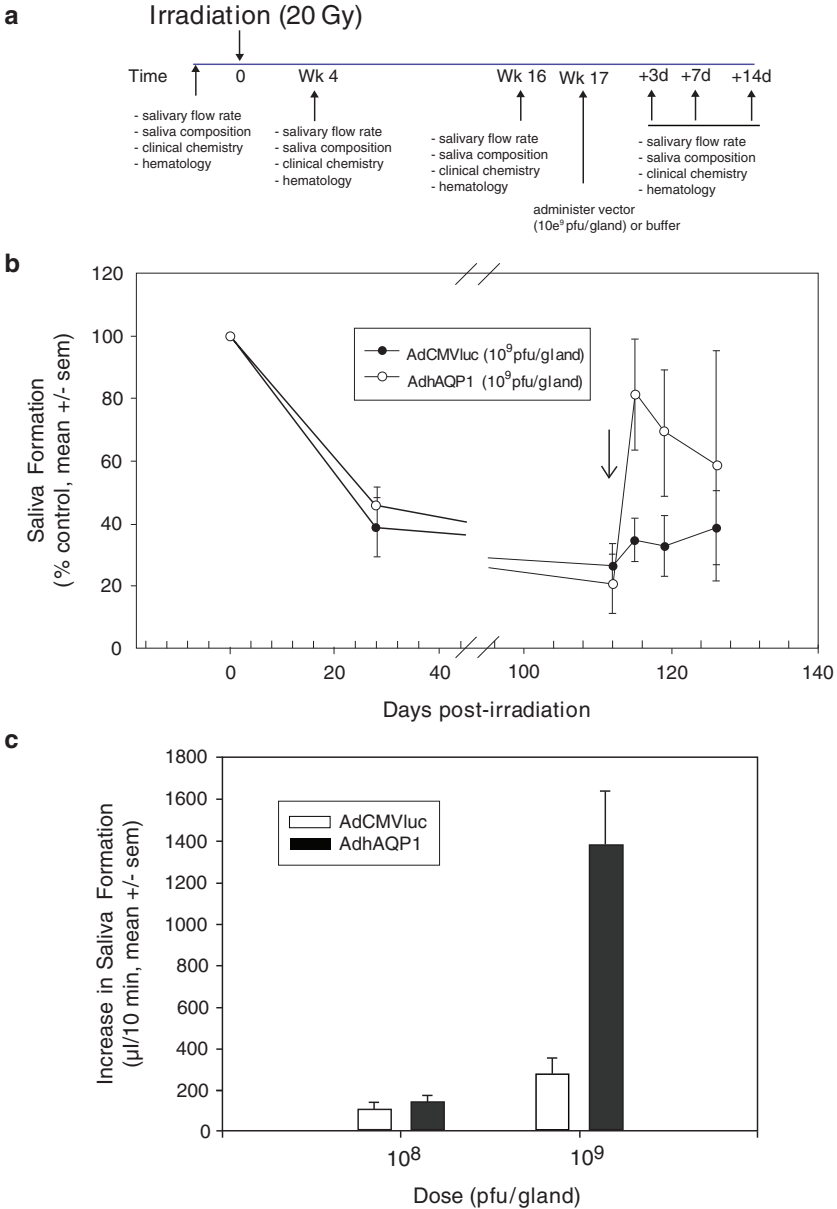


Fig. 8 The effect of AdhAQP1 vector administration on parotid salivary secretion in irradiated miniature pigs. **(a)** Time line of study. Animals (three separate cohorts) in these experiments were followed longitudinally. Either AdhAQP1, a control vector (AdCMVluc, encoding luciferase), or buffer was given as indicated. **(b)** Pattern of parotid salivary flow following irradiation and vector administration. Parotid salivary flow rates (in µl per 10 min; average of two measurements) prior to irradiation were normalized to 100% and data at other time-points are shown as a percentage of that initial value. The arrow indicates the time point when vectors were administered. **(c)** Effect of AdhAQP1 dose on parotid saliva secretion. All data shown are mean values ± SEMs. This figure originally was published as part of Fig. 1 in (Shan et al. 2005)

genomes. Vector was delivered to a single submandibular gland and thereafter, animals were evaluated on days 3, 15, 29, 57 and 92.

Administration of the AdhAQP1 vector led to no animal mortality or morbidities, and no adverse events were noted clinically (Zheng et al. 2006). Additionally, no neoplasms were detected in any animal studied. In male rats we observed vector-related chronic focal inflammatory lesions in the targeted gland, such as we had reported previously (Adesanya et al. 1996). Interestingly, this was not noted in female rats. Additionally, we observed some other minor gender related effects (in females) that were vector, but not dose, dependent. For example, in male rats we found no vector-associated alterations in multiple clinical chemistry and hematology parameters. Likewise, female rats did not show any changes in clinical chemistry values (Fig. 9); serum levels of alanine aminotransferase, creatine phosphokinase, lactate dehydrogenase and blood urea nitrogen were unaffected by vector treatment

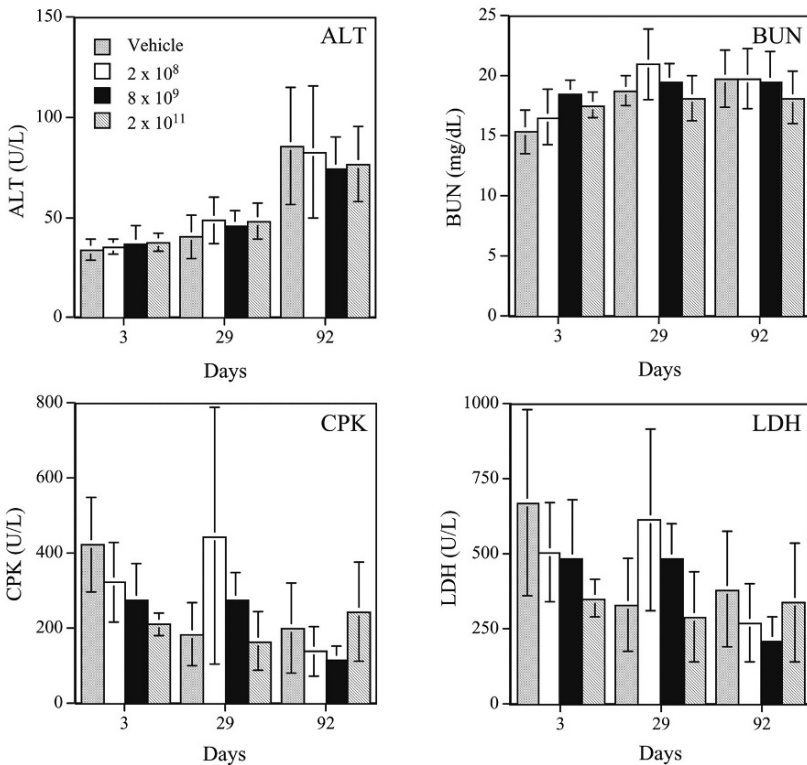


Fig. 9 Representative clinical chemistry results seen with female rats treated, or not, with various doses of AdhAQP1. ALT alanine aminotransferase (~liver damage); CPK creatine phosphokinase (~heart damage); BUN blood urea nitrogen (~kidney function); LDH lactate dehydrogenase (indicates general tissue damage). Data shown are mean values ± SD. Dosage groups are indicated (vector genomes of AdhAQP1 administered). This figure was published originally as Fig. 4 in (Zheng et al. 2006)

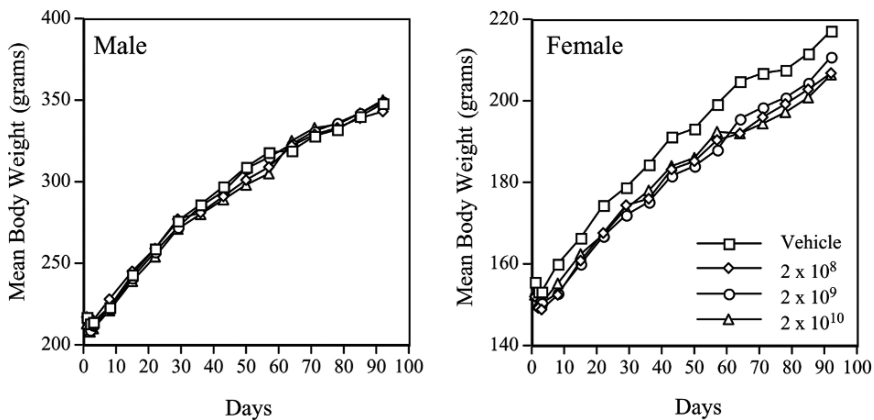


Fig. 10 Animal body weights during AdhAQP1 toxicology study. *Left panel:* Mean body weight in grams is depicted for all four groups of male rats over the time course of this study. *Right panel:* Mean body weight in grams is depicted for all four groups of female rats over the time course of this study. The animal study groups are as indicated (doses in vector genomes of AdhAQP1). This figure was published originally as Fig. 1 in (Zheng et al. 2006)

in female rats (Zheng et al. 2006). However, female rats displayed a small reduction in body weight (Fig. 10), which also was associated with a similarly small decrease in food consumption ((Zheng et al. 2006), not shown). Additionally, female, but not male, rats showed some evidence of persistent systemic inflammation (small increase in the total and segmented white blood cell number). While each of these gender related changes was quite small, it will be important to be attentive to possible gender differences in responses to AdhAQP1 administration in the clinical study described below.

We also conducted a detailed QPCR necropsy of all animals in order to determine AdhAQP1 vector biodistribution (Zheng et al. 2006). We sampled the following tissues for this study (Table 2): brain, left and right [the targeted gland] submandibular glands (separately), left and right parotid glands (separately), left and right sublingual glands (separately), buccal mucosa, palatal mucosa, tongue, floor-of-the-mouth mucosa, left and right mandibular lymph nodes (separately), spleen, heart, lung, small intestine, large intestine, kidney, liver, gonads (both testes and ovaries), blood and saliva. Three days after delivery of 2×10^{11} vector genomes of AdhAQP1, vector was detected primarily in the targeted right submandibular gland (Table 2). The median copy number in these samples was 2.24×10^3 copies μg^{-1} DNA. At later time points vector was found in \sim half of the targeted glands. Thus, following AdhAQP1 vector delivery to a single rat salivary gland, vector can persist in many animals for a long time, even though expression of the transgenic hAQP1 protein was not seen after day 15 (Zheng et al. 2006). Additionally, AdhAQP1 was frequently found in the right sublingual gland (days 3–57 the median value was 1.86×10^2 copies/ μg DNA), which is not surprising since sublingual glands can often share a common main excretory duct with submandibular glands. Furthermore, AdhAQP1 was never detected in any blood sample and only detected in a single

Table 2 Tissue distribution of AdhAQP1 in rats administered 2×10^{11} vector genomes in the right submandibular gland

Tissue	Day 3	Day 29	Day 92
Left parotid	0/10	0/10	0/10
Left SMG	4/10	1/10	3/10
Left SLG	0/10	0/10	1/10
Left mandibular lymph node	1/10	0/10	1/10
Right parotid	1/10	0/10	0/10
<i>Right SMG</i>	<i>9/10</i>	<i>4/10</i>	<i>4/10</i>
Right SLG	2/10	3/10	7/10
Right mandibular lymph node	2/10	0/10	1/10
Buccal mucosa	0/10	0/10	0/10
Floor-of-mouth mucosa	3/10	0/10	0/10
Palatal mucosa	0/10	0/10	0/10
Tongue	0/10	0/10	0/10
Brain	0/10	0/10	0/10
Spleen	2/10	0/10	1/10
Liver	1/10	0/10	0/10
Lung	2/10	0/10	0/10
Kidney	0/10	0/10	0/10
Gonads	0/10	0/10	0/10
Blood	0/10	0/10	0/10
Saliva	1/10	0/10	0/10

This table is modified from Table 2 of (Zheng et al. 2006). The data shown come from PCR-necropsies of experimental animals and represent the number of real time PCR-positive samples per total number of samples assayed. The target gland was the right submandibular gland, and these data are shown in italics. As is clear from the data, when the AdhAQP1 vector was administered to a single gland most of the vector was localized to that gland, and very little was found outside adjacent oral tissues

saliva sample on day 3. Also, only 5 of 90 non-oral samples tested positively in the sensitive QPCR assay used (Zheng et al. 2006). The limited biodistribution of the vector is consistent with the minimal toxicity indicated by clinical chemistry, hematology and pathology analyses. Finally, and quite importantly, QPCR assays showed no evidence for the generation of replication competent adenovirus in blood or saliva samples. Thus, in aggregate this GLP safety study showed that localized delivery of AdhAQP1 to rat salivary glands occurs without significant toxicity.

5 Clinical Protocol

In October of 2005, we submitted a clinical protocol, "Open-label, dose-escalation study evaluating the safety of a single administration of an adenoviral vector encoding human aquaporin-1 to one parotid salivary gland in individuals with irradiation-induced parotid salivary hypofunction", for initial review by our Institutional Review

Table 3 Dosage schedule for the AdhAQP1 clinical trial

Dosage group	Vector (genomes/gland)	Vector (genomes/ μ l)
1	4.8×10^7	1×10^5
2	2.9×10^8	5.8×10^5
3	1.3×10^9	2.6×10^6
4	5.8×10^9	1.2×10^7
5	3.5×10^{10}	0.7×10^8

This table shows the number of AdhAQP1 vector genomes to be administered to a single parotid gland in subjects ($n = 3$) in each of the five dosage groups approved for clinical study. The administered doses are presented as both the total dose to be administered (middle column) and the number of vector genomes to be administered per μ l infusate, i.e., assuming an infusate volume of 500 μ l (right column). Note that an additional three subjects can be enrolled if 1 of 3 subjects in a given dosage group experiences a dose-limiting toxicity. Also, if there are no adverse events in the three assigned subjects in the highest dosage group, an additional three subjects can be studied at that dose. Thus, a maximum of 21 patients can be studied under the approved clinical protocol. See website given in footnote 2 for additional information about this protocol

Board (IRB). The purpose of this clinical protocol is to test the safety of AdhAQP1, with some measures of efficacy, i.e., a Phase 1, dose escalation study, in adult patients with established IR-induced parotid gland hypofunction. The targeted tissue site for the AdhAQP1 vector in this protocol is a single parotid gland and safety is being monitored by measurements of an extensive battery of conventional clinical and immunological parameters. The primary outcome measure for biological efficacy is parotid gland salivary output, with secondary assessment of subjective improvements in symptoms of xerostomia. Five doses of vector are to be administered (Table 3), with three patients in each dosage group. A maximum of 21 patients can be enrolled, depending on the occurrence of protocol-related toxicities. Of note, the fourth dosage level (5.8×10^9 vector genomes) is roughly comparable, on per microliter infused basis, to the dose that was effective in increasing salivary flow in the miniature pig study described above. Additionally, the highest dose to be administered (3.5×10^{10} vector genomes) is a dose that has not been associated with any toxicity in previous clinical studies employing Ad5 vectors for other tissues, e.g., lung, heart, skin, tumors [e.g., (Harvey et al. 2002)]. It is also a dose that is 1,000 times lower than the dose (3.8×10^{13} vector genomes) that led to an Ad5 vector-related death in a clinical trial at the University of Pennsylvania in 1999 (Raper et al. 2003).

During the IRB review process the protocol was also submitted to the NIH Institutional Biosafety Committee and the NIH Recombinant DNA Advisory Committee. All of these review bodies gave approval to the submitted protocol, with minor modifications. The protocol was then submitted to the FDA as part of an Investigational New Drug (IND) application, which received approval, with some additionally required minor modifications, on August 30, 2006 (IND number 13,102). A

general description of the protocol can be found at the publicly accessible clinical trials.gov web site,² including detailed information on inclusion and exclusion criteria. Following the IND approval, a considerable amount of time was required to develop the operational infrastructure to conduct the trial. This included, in addition to staffing, extensive (and continuing) work with a Contract Research Organization (CRO) that helped us to develop all of the case report forms required, establishing a secure electronic database, developing and implementing a clinical specimen electronic tracking plan (a total of > 4,500 patient samples will be generated for testing) and establishing a study monitoring and protocol compliance plan. In addition, the CRO convened a Data and Safety Monitoring Board (DSMB) specifically to provide oversight of this study. The DSMB will examine all clinical safety data and all adverse event reports and will decide at each step whether escalation to the next higher dosage level is permissible.

Once the infrastructure was essentially established (~July 1, 2007), we were able to begin recruiting and pre-screening patients for eligibility to enroll in this protocol. As of the date of submission of this chapter (December 2007), we have pre-screened 43 individuals, of whom ~10% are initially eligible based on our conservative inclusion and exclusion criteria. These patients are then screened much more extensively. Each patient enrolled will be followed for one year and we expect the study will likely be completed in 2010.

Acknowledgments The authors' research is supported by the intramural research program of the National Institute of Dental and Craniofacial Research.

References

- Adesanya MR, Redman RS, Baum BJ, et al. (1996) Immediate inflammatory responses to adenovirus-mediated gene transfer in rat salivary glands. *Hum Gene Ther* 7:1085–1093
- Baum BJ (1993) Principles of saliva secretion. *Ann N Y Acad Sci* 694:17–23
- Baum BJ, Wang S, Cukierman E, et al. (1999) Re-engineering the functions of a terminally differentiated epithelial cell in vivo. *Ann N Y Acad Sci* 875:294–300
- Baum BJ, Wellner RB, Zheng C (2002) Gene transfer to salivary glands. *Int Rev Cytol* 213:93–146
- Delporte C, O'Connell BC, He X, et al. (1997) Increased fluid secretion after adenoviral-mediated transfer of the aquaporin-1 cDNA to irradiated rat salivary glands. *Proc Natl Acad Sci U S A* 94:3268–3273
- Delporte C, Hoque AT, Kulakusky JA, et al. (1998) Relationship between adenovirus-mediated aquaporin 1 expression and fluid movement across epithelial cells. *Biochem Biophys Res Commun* 246:584–588
- Harvey BG, Maroni J, O'Donoghue KA, et al. (2002) Safety of local delivery of low- and intermediate-dose adenovirus gene transfer vectors to individuals with a spectrum of morbid conditions. *Hum Gene Ther* 13:15–63
- Li J, Zheng C, Zhang X, et al. (2004) Developing a convenient large animal model for gene transfer to salivary glands in vivo. *J Gene Med* 6:55–63
- Li J, Shan Z, Ou G, et al. (2005) Structural and functional characteristics of irradiation damage to parotid glands in the miniature pig. *Int J Radiat Oncol Biol Phys* 62:1510–1516

² <http://www.clinicaltrials.gov/ct/show/NCT00372320?order=1>

- Mastrangeli A, O'Connell B, Aladib W, et al. (1994) Direct in vivo adenovirus-mediated gene transfer to salivary glands. *Am J Physiol* 266:G1146–1155
- Nagler RM, Baum BJ (2003) Prophylactic treatment reduces the severity of xerostomia following irradiation therapy for oral cavity cancer. *Arch Otolaryngol Head Neck Surg* 129:247–250
- Nagler RM, Baum BJ, Miller G, et al. (1998) Long-term salivary effects of single-dose head and neck irradiation in the rat. *Arch Oral Biol* 43:297–303
- O'Connell AC, Redman RS, Evans RL, et al. (1999a) Radiation-induced progressive decrease in fluid secretion in rat submandibular glands is related to decreased acinar volume and not impaired calcium signaling. *Radiat Res* 151:150–158
- O'Connell AC, Baccaglini L, Fox PC, et al. (1999b) Safety and efficacy of adenovirus-mediated transfer of the human aquaporin-1 cDNA to irradiated parotid glands of non-human primates. *Cancer Gene Ther* 6:505–513
- Raper SE, Chirmule N, Lee FS, et al. (2003) Fatal systemic inflammatory response syndrome in a ornithine transcarbamylase deficient patient following adenoviral gene transfer. *Mol Genet Metab* 80:148–158
- Shan Z, Li J, Zheng C, et al. (2005) Increased fluid secretion after adenoviral-mediated transfer of the human aquaporin-1 cDNA to irradiated miniature pig parotid glands. *Mol Ther* 11:444–451
- Shiboski CH, Hodgson TA, Ship JA, et al. (2007) Management of salivary hypofunction during and after radiotherapy. *Oral Surg* 103:Suppl: S66.e1–19
- Vissink A, Jansma J, Spijkervet FK, et al. (2003) Oral sequelae of head and neck radiotherapy. *Crit Rev Oral Biol Med* 14:199–212
- Vitolo JM, Baum BJ (2002) The use of gene transfer for the protection and repair of salivary glands. *Oral Dis* 8:183–191
- Zheng C, Goldsmith CM, Mineshiba F, et al. (2006) Toxicity and biodistribution of a first-generation recombinant adenoviral vector encoding aquaporin-1 after retroductal delivery to a single rat submandibular gland. *Hum Gene Ther* 17:1122–1133

Index

A

- Acetamide, 340
- Acetazolamide (AZA), 385, 386, 388, 394–396
- Acid, 301–303, 305, 306
- Acid-base regulation, 301
- Acidosis, 306
- Acinar cells, 254, 259, 306
- Activation energy, 78, 81, 87
- Acute promyelocytic leukemia (APL), 310, 311, 316, 317
- Adenine, 253
- Adenoviral vector, 405, 415
- AdhAQP1, 405–416
- Adhesion
 - fiber, 279–280, 287
 - molecule, 266–268, 279–280, 287
- Adipocyte, 371, 375–377
- “Ailing-1,” 311
- AKAPA, 134
- AKAP18 δ , 139, 140
- Akinase anchoring proteins (AKAPs), 133, 134, 138–143
- Alkalosis, 301, 306
- Alpha-MSH, 118
- Ammonia, 8, 70, 77, 78, 83–85, 88–89
- Ammonium, 327–329, 332–333, 339, 348, 351–353
- Ampullary crista, 173
- AmtB, 84
- AngII, 134
- Angiogenesis, 359, 369–371, 377
- Angiotensin, 105, 113, 116
- Anions, 8, 10
- Anion transport, 49
- Antimonite, 9, 77, 78, 83, 85
- Antimony, 309–311, 320
- AQP, 134, 312, 313
 - in the cochlea, vestibule and endolymphatic sac, 172
- AQP0, 6, 11, 14
- AQP1, 3–10, 12, 14–16, 18, 58–62, 64–67, 69–72, 78, 79, 82, 83, 85–89, 96–98, 100, 116–118, 121 161–163, 186–197, 254, 257–259, 403–417
 - immunoreactivity, in spiral ligament, 172, 173
- AQP2, 11–13, 16, 18, 133–150
 - expression in the inner ear, 174, 180
- AQP3, 8, 10–11, 18, 19, 253–255, 257
 - in the mouse inner ear, 174, 175
- AQP4, 16–18
 - in inner ear, 175–176
- AQP5, 12–13, 17–18, 186, 188–197
 - localized rat cochlear duct, 176
- AQP6, 8, 10
 - in cochlea, endolymphatic sac and vestibule, 176
- AQP7, 8, 9, 19, 252, 254–255, 260
 - glycerol transport, 219, 220, 222–224, 227
 - in the inner ear, 176–177
 - male infertility, 227, 228
 - male reproductive system, 226–229
 - mRNA and protein level, 226
 - tissue distribution, 220–221
 - urea transport, 220, 225–226
 - water transport, 219, 220, 224–225
- AQP8, 8, 13
 - in the inner ear, 177
- AQP9, 8, 9, 19, 20, 251–255
 - in epithelium of the endolymphatic sac, 177–178
- AQP10, 8
- AQP12A, 260

- AQP12B, 260
 AQP2 mutants, 146
 AQP2 S256A, 137, 146
 AQP2-S256D, 137
 AQPX, 252
 AQPX1, 252
 AQPX2, 252
 AQPZ, 329–331, 344, 350
 Aquaglyceroporin (AQPs), 32, 33, 37–40,
 251–254, 309, 310, 312–321
 Aquaporin 0, 265–287
 Aquaporins
 AQP2, 96–121
 AQP3, 96–100, 109, 111, 113, 114, 116–121
 AQP4, 97, 99, 119, 121
 AQP6, 87, 96, 99, 100
 AQP7, 97, 100
 AQP8, 97, 100
 AQP11, 97, 100
 Aquaporin 4 (AQP4), 159–167
 in central nervous system, 162–163
 in CSF production, 163
 in hemorrhagic stroke, 167
 in ischemic stroke, 160, 164, 165, 167
 Aromatic arginine (ar/R)
 motif, 344
 region, 328, 344–345, 347–348, 353
 restriction region, 343–346
 Aromatic residue/arginine, 38
 Arrhenius, 78, 81, 87
 ArsC, 312, 313
 Arsenic, 309, 310, 316
 Arsenic-rich soil, 310
 Arsenic trioxide, 310, 311, 315–317
 Arsenite, 9, 77, 78, 83–85, 255
 Artificial lipid bilayers, 338, 342
 As(III), 311–321
 As(OH)₃, 311–318
 As(V), 311, 313, 314, 316
 Assay, 77–85, 87–90
 Astrocyte, 159, 161–164
 Atomic force microscopy, 37, 41, 43
 ATRA, 317
 AVP, 133–136, 138–146, 149, 150
 AVP-AQP2 system in the inner ear, 178–180,
 182
- B**
- Bacteria, 79, 82
 Barrier
 electrostatic, 57, 63–64, 65, 73
 free energy, 65
 Biophysical assay, 82
- Blood brain barrier
 in ischemia, 165
 structure, 161
 Brain, 359, 360, 363–366, 369, 377
 Brain swelling. *See* cerebral edema
 Brattleboro rats, 99, 109, 113
- C**
- Ca²⁺, 277–278, 286
 Calcium, 134, 144–145
 Calmodulin, 273, 277–278
 Cancer, 360, 369, 375, 377
 CaR, 133, 145
 Carbon dioxide, 57, 65–67, 69–71
 Carboxy-termini, 253, 260
 Cataract
 aging, 272, 273, 287
 genetic, 265–287
 Cataractogenesis, 268, 272, 273, 287
 Cell migration, 359, 369–371, 377
 Cell proliferation, 359–360, 371, 373–375, 377
 Cerebellum, 306
 Cerebral edema
 cytotoxic, 160–161, 162, 164–167
 in hemorrhagic stroke, 163–165, 167
 in ischemic stroke, 160, 163–165
 vasogenic, 160–161, 162, 164–167
 CH₃As(OH)₂/MAs(III), 315
 Chemical gradient, 77, 79, 80
 CHIP28, 5, 6
 Cholera, 254
 Chromosome, 255, 256, 260
 CKII, 138
 Clinical, 403, 413, 415–417
 CO₂, 4, 9, 57, 65–67, 69–71
 Collapse, 180
 Collecting duct, 47, 49, 299, 300, 306
 Constriction, 38–40, 50
 Copper, 385, 389, 393
 COX2, 116
 Cyclosporin, 259
- D**
- Dexamethasone, 180, 181
 Diabetes insipidus, 98, 109–111, 113
 acquired, 110–111
 inherited, 109–110
 Differentiation, lens, 268–272, 280, 284
 Dimethylsulfoxide (DMSO), 386–388, 398
 Dipole orientation, 60
 Docking, 396–398
 Double KO mice, 258–259
 Drug-resistant, 320, 321
 Drugs, 385, 396, 399

Duodenum, 253–254, 256
 Dynamics, 33, 37, 39, 40, 50, 51
 Dynein, 143, 149
 Dystroglycan (DCG) complex, 163

E

Electron crystallography, 32, 33, 37, 41
 Electron microscopy, 257
 Endolymph, 171, 172, 174–178, 180–182
 Endolymphatic hydrops, 171, 172, 180–182
 Endolymphatic sac, 171–181
 Endoplasmic reticulum (ER), 257–259
 Enterochromaffin cells, 254–255
 ENU-induced point mutation, 256
 Epilepsy, 360, 377
 ER stress, 259
Escherichia coli, 329–331, 350
 Exchange protein directly activated by cAMP (Epac), 134, 144
 Extracellular Edema. *See* Vasogenic edema
 Eye, 360, 363, 367–369
 Ezrin-radixin-moesin (ERM), 143

F

F-actin, 134, 141–143, 145, 146, 149
 F-actin cytoskeleton, 134
 FDA, 411, 416
 Fibrocytes in the spiral ligament, 172, 173, 177
 Formamide, 339, 340
 Fps1, 83–85, 88
 Fps1p, 9, 313–315, 318
 Freeze fracture, 37, 41, 43

G

Gas permeation, 57, 65–67, 70
 Gas transport, 37, 50–51
 Gastrointestinal tract, 253–256
 Gating, 41, 48–49, 51, 302, 303, 306
 Gene
 deletion, 266, 280–282, 284, 285
 duplication, 255, 260
 family, 265, 267, 268, 284
 knockout, 98
 mutation, 266, 268, 272, 280, 281, 282–285
 therapy, 404, 410
 Gland, 359, 360, 363, 367, 377
 Glaucoma, 360, 368, 377
 Glial water channel. *See* Aquaporin 4 (AQP4)
 GlpF, 9, 57–59, 61–64, 67–73, 85, 86, 312, 313, 315
 Glucantime, 311, 318, 320

Glycerol, 32, 34–36, 38–40, 57, 58, 68–71, 73, 78, 81–84, 86–88, 90, 328–331, 340, 345, 347–348, 350–351, 353, 359, 360, 362, 366, 371–376
 Gold, 385, 388, 392, 393
 Golgi casein kinase (G-CK), 134, 137
 Green fluorescence protein (GFP), 303, 304
 Grothuss mechanism, 57, 63–64
 GTPases, 134, 142

H

hAQP3, 315
 hAQP7, 315
 hAQP9, 315
 hAQP10, 315
 H⁺-ATPase, 300–302, 306
 Henle's loop, 299
 Hensen's, Claudius cells, 175
 Hepatocytes, 351, 352
 High-throughput, 79, 82
 HL60, 317
 Hog1p, 314, 318
 Hsc70, 134, 145, 146
 Human African trypanosomiasis (HAT), 310, 320
 Hydrogen bonds, 58–61, 63, 64, 67–68, 72–73
 Hydrogen peroxide, 8, 77, 78, 83, 85
 Hydronium, 63, 65
 Hydrophobicity, solute, 58, 70–73
 Hypothalamus, 44

I

Inner ear fluid homeostasis, 171, 172, 176
 Inner medullary collecting duct (IMCD), 135, 136, 139–145
 Intercalated cells, 300–302
 Intermediate cells, of stria vascularis, 173
 Intracellular Ca²⁺, 144, 145
 Intracellular vesicles, 299–302, 306
 In vitro assay, 77, 78, 85, 89
 Inwardly rectifying potassium channel Kir4.1, 163
 Ion permeability, 302–303
 Irradiation (IR), 403, 404, 409, 410, 411, 412, 415, 416

J

Jejunum, 253–256
 Junction
 gap, 267, 280, 281
 thick, 267
 thin, 267, 279, 281

K

K562, 317
Kidney, 251, 252, 256–259, 299–301, 306,
360–363, 376, 377

L

Lacrimal Glands
AQPs expression, 185–190, 196
mechanisms, 190–194
morphology, 187
secretion and fluid transport, 190–194
Sjögren's syndrome, 194–197

Leishmania, 82, 83, 85, 311, 314, 318–320

Lens

accommodation, 266, 270, 287
beded filaments, 271, 280, 281
cataract, 265–287
connexins, 280–281
crystallins, 271, 280–282, 287
differentiation, 268–272, 280, 284
epithelia, 267–273, 275, 277, 278, 281
fibers, 265–270, 272–282, 284, 287
focus, 266, 268, 270, 277, 281, 285–287
microcirculation, 275, 277, 281, 287
proteins, 272, 280–282, 287
sutures, 270, 284

Leukemia, 310, 311, 316–318

Liposomes, 78–81, 84, 257

Lithium, 179, 180, 182

Lithium-induced NDI, 301

LmACR2, 314

LmAQP1, 83, 314, 319, 320

LmAQP α – δ , 319

Localization, 300, 302, 305, 306

Loop C, 34, 38, 42, 43, 44

M

Major intrinsic protein (MIP), 310, 312, 313

Malaria, 3, 19, 20

Mal-regulation of AVP-AQP2 system,
pathogenesis of Meniere's disease, 182

Mannitol, 339–340

Melarsoprol, 310, 320, 321

Membrane junctions, 41–45

Membrane permeability, 57, 65, 66–68, 70

Meniere's disease, 171–182

Mercuric chloride, 301

Mercury, 385, 392–395

Mercury-sensitive, 253

Metalloid, 309–321

Metastasis, 359, 371, 374

Methanothermobacter marburgensis,
329–331

Methylamine, 83–85, 88, 89

MethylAs(III) diglutathione (MAs(GS)₂), 316

Microfilaments, 141–143

Microtubules, 134, 143–144, 149

Mineralocorticoid, 180

Miniature pig, 403, 410–412, 416

MIP, 265–287

Mitochondria, 349, 351

Mitogen-activated protein kinase (MAPK),
310, 314, 318

Molecular dynamics simulation, 57–73

Motor protein, 134, 142, 143, 149

Multidrug resistance-associated protein 2
(MRP2), 316

Myosin Vb, 142, 149

N

Nephrogenic diabetes insipidus (NDI), 133,
134, 137, 139, 146–148, 150

Neurons, 257

Nickel, 389

Nitrate, 303, 306

NO, 4, 9–10

Non-obese diabetic mice, 196

NPA

boxes, 252, 253, 259, 267, 273

motifs, 32, 38, 41

repeat, 265, 267, 268

Null mice, 251, 252, 255–259

O

O₂, 67, 69–72

Obesity, 360, 375–377

Oocyte chamber, 335

Oocytes, 300–303, 305

Organ of Corti, 174, 176, 177

Orthogonal arrays, 37, 41, 43

Osmotic gradient, 79–81

Oxygen, molecular, 67

P

Pancreas, 259–260

AQPs expression, 185–190, 196

mechanisms, 190–194

morphology, 187

secretion and fluid transport, 193

Parotid, 410–412, 414–416

Parotid glands, 306

PDE4D, 139, 140

Pentostam, 311, 318–320

Perilymph, 172, 173, 180

Permeability, diffusive, 63

PFAQP, 83–85, 329–331, 340, 347, 350

PGE2, 134, 137, 149

pH, 275, 276–278, 286

- Phenotypic assay, 77, 79, 82–84, 88
 Phloretin, 385, 397–398
 Phosphodiesterase (PDE), 134, 137, 139–141
 Phosphorylation, 37, 47–49, 101–106, 108, 114
 AQP2, 102, 104, 105, 108
 prostaglandin E2, 104
 pH regulated anion channel, 303
 PKA, 133, 134, 136–140, 142, 144–146, 148, 149
 PKC, 138, 139, 145, 149
Plasmodium falciparum, 329–331, 350
 p38 MAPK, 318
 PML – RAR α , 317
 Polycystic kidneys, 251, 257
 Pore constriction, 78, 86
 Pore selectivity, 77–90
 Potential of mean force, 64, 66, 68–70, 72
 PPI and 2A, 134, 138
 Pre-clinical testing, 409–411
 Principal cells, 47, 299, 300
 Protein
 domains, 283
 interaction, 280–282, 287
 localization, 267
 mutations, 283
 Protein kinase A, 133, 134, 136–140, 142, 144–146, 148, 149
 Protein phosphatase 2B (PP2B), 138, 139
 Proteomics, 114
 Proton
 desolvation, 57, 65, 73
 exclusion, 57, 58, 63–65, 73, 89
 Proximal tubules, 257–259
 Pseudogene, 251, 255, 260
- R**
 Rab11, 142, 144
 Rab11-FIP2, 142
 Regulation of water permeability
 long-term, 98, 100
 short term, 98, 100
 Reissner's membrane, 174, 176, 177
 RhAG, 328, 352
 RhBG, 328, 352
 RhCG, 328, 352
 Rhesus (Rh) proteins, 327–328, 330, 332, 349, 352–353
 RhoA, 142, 143, 146, 149
 Rho family, 134, 142, 143
 Rho-GDI, 142
- S**
 Saccular membrane, 173
 Saccule, 174, 175, 177, 178
 Saliva, 306
 Salivary Glands
 AQPs expression, 185–190, 196
 mechanisms, 190–194
 morphology, 187
 secretion and fluid transport, 190–194
 Sjögren's syndrome, 194–197
 Salivary glands, 306, 403–405, 409, 410, 414, 415
 Salivary hypofunction, 403–417
 Sb(III), 312–314, 317–319, 321
 Sb(OH)₃, 315
 Sb(V), 314, 319
 Selectivity, 32, 37, 40, 57, 58, 64, 68–73, 302, 305
 Silicon, 77, 78
 Silver, 385, 388, 392–393
 Simulation, 57–73
 Single-file, 60, 62–63, 73
 Site-directed mutagenesis, 301–303
 Sjögren's syndrome, 185–197
 Skin, 359, 360, 372–375, 377
 Skin aquaporin-3, 207–214
 Skin aquaporins, 205–215
 Skin epidermis, 205–215
 Skin glycerol transport, 205–213
 Skin hydration, 208–211, 213–215
 SNARE, 47
 Spermatids, 351
 Spiral ligament, 172–174, 177
 Spiral prominence, 176
 stopped-flow, 80–82
 Stria marginal cells, 176
 Stria vascularis, 171, 173–179, 181
 Stroke
 hemorrhagic, 163–164, 167
 ischemic, 159–160, 163–165, 167
 Structure, 31–51, 303, 305, 306
 Sucrose, 258
 Superfamily, 252
 Swelling assay, 78, 80, 81, 87
- T**
 TaAmt1;1, 334, 335, 337, 342, 350
 TaTIP2;1, 329–331, 338, 347, 348
 TbAQPs, 320, 321
 Tetraethyl ammonium (TEA), 385, 386, 394–395, 398
 Tetramer, 34, 37, 38, 41–47, 50, 303
 The free-energy profile, 349
 Toxicology, 403, 411–415

Trafficking, 45–47, 49, 301, 303
Transmembrane helices, 38
Tritium aestivum, 329–331
Trypanosoma, 319, 320
Tunicamycin, 259
Type A intercalated cells, 300, 301

U

Unspliced form, 253–254
Urea, 58, 69–71, 78, 86–88, 327–354
Urea cycle, 328, 351
Urea transporters (UTs), 327, 330, 332, 352–353
Urine, 360–362
 concentration, 96, 98, 99, 109, 110, 115, 117, 118
 osmolality, 99, 115, 119, 121
 production, 98, 113
Utricle, 173, 174, 177

V

Vacuoles, 257–259
V2-antagonist (OPC-31260), 179–181
Vasopressin, 47, 96–111, 113–115, 118–121

Vasopressin V2 receptor, 100, 101, 109, 118, 119
Vesicles, 79, 81–82
Vesicular trafficking, 149
Vestibules, 38, 39
Voltage clamp, 302

W

Water, 31–33, 35–42, 44, 45, 47–51, 77–82, 85–88, 90
 channel, 65–68, 273–279, 284, 285, 287
 functional assay, 265, 267, 273, 275
 permeability, 59, 61–62, 68, 73
 permeation, 57, 59, 62, 63, 67, 73

X

Xenopus laevis oocyte, 78–80
Xenopus oocytes, 334, 335, 337–341
Xerostomia, 416
X-ray crystallography, 33, 43

Y

Yeast, 78, 79, 81–85, 87–89, 328, 338, 341